

https://dspace.org/

The total synthesis of 5-methoxy-3,4-dehydroxanthomegnin, dehydroherbarin lactone and 6-ferrocenyl-3,4-dihydroisochromene

Sumani, Jimmy Yaphet Ephet

2018

https://hdl.handle.net/10539/26737

Sumani, Jimmy Ephet Yaphet (2018) The total synthesis of 5-methoxy-3,4-dehydroxanthomegnin, dehydroherbarin lactone and 6-ferrocenyl-3,4-dihydroisochromene, University of the Witwatersrand, Johannesburg, <http://hdl.handle.net/10539/26737>

Downloaded from a DSpace repository. https://dspace.org/

The total synthesis of 5-methoxy-3,4-dehydroxanthomegnin, dehydroherbarin lactone and 6-ferrocenyl-3,4-dihydroisochromene

Jimmy Ephet Yaphet Sumani

A thesis submitted to the Faculty of Science

University of the Witwatersrand

Johannesburg

In fulfilment of the requirements for the Degree of Doctor of Philosophy

October 2018

Declaration

I, Jimmy Yaphet Ephet Sumani, hereby declare that the work presented in this thesis was carried out exclusively by myself under the supervision of Professor Charles de Koning. It is being submitted for the degree of Doctor of Philosophy at the University of the Witwatersrand, Johannesburg, South Africa. It has not been submitted before, in its totality or in parts thereof, for any degree or examination at any other University. The work not carried out in this study has been duly acknowledged.

_____

Jimmy E.Y. Sumani

October 2018

Abstract

Pyranonaphthoquinones, especially those with lactone functionality, are a class of naturally occurring compounds that exhibit a wide range of biological properties. For example, studies have shown that 10-hydroxy-5,7-dimethoxy-3-methyl-1*H*-naphtho-[2,3-*c*]-pyran-1,6,9-trione has a plethora of biological activities which includes, among others, cytotoxicity against McCoy cell lines and significant antibacterial property against *Helicobacter pylori*.

This PhD project describes the total synthesis of 7,9-dimethoxy-3-methyl-1*H*-benzo[*g*]isochromene-1,5,10-trione from simple starting materials in 14 steps in an overall percentage yield of 5%. The synthesis was achieved by subjecting the commercially available, 2,4-dimethoxybenzaldehyde, to a number of synthetic transformation protocols we have developed in our laboratory group. The key steps in the synthesis included the PIFA mediated methoxylation of the naphthalene nucleus that was constructed from the Stobbe condensation reaction and the palladium assisted Wacker oxidation reaction of the naphthoic acid intermediates.

We also successfully synthesized 10-hydroxy-5,7-dimethoxy-3-methyl-1*H*-benzo[*g*]isochromene-1,6,9-trione starting from 2,4,5-trimethoxybenzaldehyde in 15 steps in an overall percentage yield of 1%. This was achieved by employing the protocol we established during the synthesis of 7,9-dimethoxy-3-methyl-1*H*-benzo[*g*]isochromene-1,5,10-trione.

In the course of achieving the total syntheses of 7,9-dimethoxy-3-methyl-1*H*-benzo[*g*]isochromene-1,5,10-trione and 10-hydroxy-5,7-dimethoxy-3-methyl-1*H*-benzo[*g*]isochromene-1,6,9-trione a number of unexpected products were isolated and characterized.

The second part of the project was aimed at developing a methodology for coupling a ferrocene moiety to 3,4-dihydroisochromene and subjecting the resultant ferrocenyl 3,4-dihydroisochromene to oxidative demethylation protocols. Ferrocene coupled hybrid compounds are currently receiving a lot of attention because of their application in medicine.

For example, ferroquine is active against both chloroquine-sensitive and chloroquine-resistant *Plasmodium falciparum* strains.

The synthesis of 6-ferrocenyl-(±)-*trans*-3,4-dihydro-5,8-dimethoxy-1,3-dimethyl-6-vinyl-1*H*-isochromene was achieved starting from 2,5-dihydroxyacetophenone in 10 steps in an overall percentage yield of 10%. The key steps in this methodology involved the base mediated ring closing reaction which delivered (±)-*trans*-3,4-dihydro-5,8-dimethoxy-1,3-dimethyl-6-[(*E*)-1-propenyl]-1*H*-isochromene and the McMurray cross-coupling metathesis reaction which afforded 6-ferrocenyl-(±)-*trans*-3,4-dihydro-5,8-dimethoxy-1,3-dimethyl-6-vinyl-1*H*-isochromene.

The oxidative demethylation of 6-ferrocenyl-(±)-*trans*-3,4-dihydro-5,8-dimethoxy-1,3-dimethyl-6-vinyl-1*H*-isochromene to complete the total synthesis of 6-ferrocenyl-(±)-*trans*-3,4-dihydro-1,3-dimethyl-6-vinyl-1*H*-isochromene-5,8-dione was unsuccessful and an alternative protocol was developed which was aimed at coupling of ferrocene moiety to (±)-*trans*-6-bromo-3,4-dihydro-1,3-dimethyl-1*H*-isochromene-5,8-dione at the last step. This methodology did not yield the target molecule, 6-ferrocenyl-(±)-*trans*-3,4-dihydro-1,3-dimethyl-6-vinyl-1*H*-isochromene-5,8-dione. However, a number of potentially biologically important serendipitously obtained compounds were isolated.

The last part of this PhD project involved *in vitro* biological screening of 3 selected compounds synthesized in this project against the Gambian FCR-3 strain of *Plasmodium falciparum*. All the 3 compounds namely, (±)-*trans*-15-bromo-5,13-dimethoxy-2,4,10,12-tetramethyl-4,7,9,10,12,13-hexahydro-1*H*-7,13-methanopyrano[4',3':6,7]oxocino[2,3-*f*]isochromen-8(2*H*)-one, 3-(chloromethyl)-3,4-dihydro-5,7,10-trimethoxybenzo[*g*]isochromene-1,6,9-trione and *bis*[(±)-*trans*-3,4-dihydro-8-methoxy-1,3-dimethyl-1*H*-isochromen-5-yloxy]methane showed promising activity. (±)-*Trans*-15-bromo-5,13-dimethoxy-2,4,10,12-tetramethyl-4,7,9,10,12,13-hexahydro-1*H*-7,13-methanopyrano[4',3':6,7]oxocino[2,3-*f*]isochromen-8(2*H*)-one showed the best activity with an IC_{50} value of 0.0018 µM. This value was better than the activity shown by the reference compounds, quinine and dihydroartemisinin, which showed activity of 2.81 µM and 0.0061 µM, respectively, under the same assay conditions.

Dedication

I would like to dedicate this thesis to my mother, ***Mariah Magombo Sumani****, for being such a wonderful mother and the rock of our family. It is just a matter of time before God makes good of His words.*

Many thanks should go to the late ***Prof. Elizabeth Henry*** *who inspired me to take up the challenge of studying Chemistry. She inspired many students under her belt and will always be fondly remembered. May her soul rest in eternal peace.*

Acknowledgements

First and foremost, I would like to thank the almighty God for being God. There is no one like Him. I live in Him by Him for Him through Him and His mercies.

I wish to express my gratitude to my supervisor, Prof. Charles de Koning, for his support during the course of achieving this work.

The teaching and supporting staff in the Department of Chemistry at Wits University, in particular Professors: Joe Michael and Dean Brady and Doctors: Kennedy Ngwira (for a helping hand during the write-up), Maya Makhathin and Hendrick Henning are also acknowledged.

Many thanks should go to Prof. Moira Bode and Dr. Amanda Rousseau for coordinating testing of some of the compounds synthesized in this project against the wild-type HIV-1 and malaria parasite, respectively.

I am very grateful to Tickness Zgambo Banda, Woneckily Sumani Kuseni, Rev. Canon Captain Andrew Sumani, Grace Mwale Mpatse, Efridah Sumani and McDonald Chirwa for the support they rendered me during the course of my studies. It would not have been possible to complete this work without their unfettered support. They made unbearable situations bearable. Special and warm welcome to the 'new born', Hannah Annabel Sumani.

Prof. Andreas Lemmerer, Dr. Richard Mampa and Prof. Laurence Carlton are greatly indebted for unconditional assistance in analysing our results using x-ray crystallography and NMR spectroscopy.

The organic chemistry group at Wits University is greatly acknowledged for the support. In particular, Hannah Klein (for being so welcoming and teaching me laboratory protocols), Priya Pradeep, Venkatesh (a very good friend of mine), Tlabo, Siyanda, Donald, Charles, Memory, Kamogelo, Fatimah, Firoj, Somnath, Lydiah, Jean and all current group members.

Peter Wanyama Juma is greatly indebted for giving me a helping hand in putting together this thesis. The suggestions/recommendations and corrections he contributed to this thesis made a huge difference. Thank you very much.

Special thanks should go to the following people who have contributed significantly in making who I am today: Prof. John Daniel Kalenga Saka, Dr Norris Chokotho (The father of modern Organic Chemistry at Chancellor College, retired), Associate Prof. Maurice Monjerezi, Associate Prof. Timothy Tiwonge Biswick, Dr. Emmanuel Fabiano and Dr. Levis Eneya (Chancellor College, University of Malawi).

Dr Robert Luckay and Prof. H. G. Raubenheimer (Stellenbosch University) are greatly acknowledged for all the help they rendered me during my MSc studies. It is my honour to have met people like them.

Mr Ekenward V. Banda is greatly appreciated for his support during my secondary school days (Nkhota kota Sec. School). You made me fall in love with Bible Knowledge because of the way he presented it; He is an amazing teacher. I learnt a lot about the bible through him than I learnt from the church. What a pastor I had in him!

The love of my life, Esther Mkwanda, is greatly acknowledged for her love and care. It is my hope that we will continue this shared life as long as we live.

My vote of appreciation should also go to, William Sumani (Kamadya apa Kamajongolosi), Annie Chibophe, Thresa Msikuwanga, Evance Sumani, Rebecca Bendabenda and Chifuniro Fredrick Sumani. Specials thanks should go to pastor Bendabenda and pastor Kuseni for being great human beings.

Lastly, my appreciation should go to all the people who helped me in any small way without compromising their integrity. ***It is well with my soul***.

Abbreviations and full names

°C: degree celcius

2D: two-dimensional

AcOH: acetic acid

amu: atomic mass unit

aq: aqueous

CAN: ceric ammonium nitrate

CI_{50}: cytotoxicity index

cm^{-1}: wavenumber

CoA: coenzyme A

COSY: correlation spectroscopy

CQ: chloroquine

DEPT: distortionless enhancement by polarization transfer

DDQ: 2,3-dichloro-5,6-dicyanobenzoquinone

DHA: dihydroartemisinin

DMAP: 4-dimethylaminopyridine

DMF: *N*,*N*-dimethylformamide

DMSO: dimethyl sulfoxide

DMTHF: 2,5-dimethoxytetrahydrofuran

DNA: deoxyribonucleic acid

ED_{50}: effective dose

Et: ethyl

EtOAc: ethyl acetate

Et_2O: diethyl ether

EtOH: ethanol

FQ: ferroquine

FTIR: fourier transform infrared spectroscopy

HCl: hydrochloric acid

HIV: human immunodeficiency virus

HMBC: heteronuclear multiple-bond connectivities

HPLC: high performance liquid chromatography

HRMS: high resolution mass spectroscopy

hrs: hours

HSQC: heteronuclear single quantum correlation

Hz: hertz

IC_{50}: half-maximal inhibitory concentration

LDA: lithium diisopropylamide

Mp: melting point

MBC: minimal bactericidal concentration

Me: methyl

MeCN: acetonitrile

MeOH: methanol

MIC: minimal inhibitory concentration

min: minutes

mol: mole

MOM: methoxymethyl

MS: mass spectroscopy

MTPPBr: methyltriphenylphosphonium bromide

NAD: nicotinamide adenine dinucleotide

NADH: reduced nicotinamide adenine dinucleotide

NADPH: reduced nicotinamide adenine dinucleotide phosphate

n-BuLi: *n*-butyllithium

nM: nanomolar

NMP: *N*-methyl pyrrolidinone

NMR: Nuclear Magnetic Resonance

PCC: pyridinium chlorochromate

Pd/C: palladium on charcoal

PIFA: [*bis*(trifluoroacetoxy)iodo]benzene

RNA: ribonucleic acid

rt: room temperature

Salcomine: *N*,*N*-*bis*(salicylidene)ethylenediiminocobalt (II)

TBAF: *tetra*-(*n*-butyl)-ammonium fluoride

TBDMSCl: *tert*-butyldimethylsilyl chloride

TFA: trifluoroacetic acid

THF: tetrahydrofuran

TLC: thin layer chromatography

v: volume

w: weight

δ: Chemical shift

μL: microliter

Note to the reader:

The molar percentage in the schemes are given in italics to differentiate them from the percentage yields.

The numbering of the ORTEP diagrams is specific for a particular crystal structure and is not discussed in this thesis.

General representative molecular structures are given in cases where more than three compounds, with the same skeleton, were studied to limit the number of compounds reviewed in this thesis. This is mainly done in ***Chapter 3****.*

The cis/trans notation mainly as used in ***Chapter 4*** *is exclusively for the arrangement of the dimethyl groups of the pyran ring and does not apply to the double bond in structures where the two co-exists unless otherwise stated.*

The dimer ***trans-410*** *was also coded* ***JS-D*** *and the later code was used for biological testing alongside compounds coded* ***JS-QCl*** *and* ***JS-X10****.*

The numbering of the dimer ***JS-X10*** *was based on the name generated by the ChemDraw software and is different to the numbering adopted for the rest of the 3,4-dihydroisochromenes.*

The multiplicity of the signals (^{1}***H NMR spectra****) were assigned based on our observation and not on what one would expect based on theory.*

©2018

Jimmy E.Y. Sumani

All Rights Reserved

Table of contents

Declaration……..……..…….……..……..i

Abstract……..……..……..ii

Dedication……..……...……...iv

Acknowledgements……..…….…….…….....v

Abbreviations and full names…….……..vii

Note to the reader……..……..……xi

Table of contents……..…….xiv

Chapter 1: Introduction to pyranonaphthoquinones and isocoumarins…...1

1.0 Brief introduction to platinum and quinone based anticancer agents…….....1

1.1 Isocoumarins and 3,4-dihydroisocoumarins……....4

1.2 Biological activities of quinones and their modes of action……..…6

1.2.0 Radical based mechanism……...7

1.2.1 Bioreductive alkylation mechanism……..…….9

1.3 Biosynthesis of anhydrofusarubin lactone 32……10

1.4 Advantages of synthesizing plant based natural products and its history……..14

1.5 Isolation and biosynthesis of triacetic acid lactone 39…….……..15

1.6 Synthetic strategies towards assembling 2-pyranone ring systems…….....17

1.6.0 Synthesis of (*S*)-5,6-dihydro-4-methoxy-6-methylpyran-2-one ***S*-51**……..20

1.6.1 Synthesis of (*R*)-5,6-dihydro-4-methoxy-6-methylpyran-2-one ***R*-51**…….....20

1.7 Examples of natural products with isocoumarin and 3,4-dihydroisocoumarin groups.....21

1.7.0. Isolation and synthesis of mellein [(*R*)- and (*S*)-3,4-dihydro-8-hydroxy-3-methylisochromen-1-one] ***R*-15** and ***S*-15**…….21

1.7.1 Isolation and synthesis of 8-hydroxy-6-methoxy-3-methylisocoumarin **63**…….23

1.7.2 Isolation, bioactivity studies and synthesis of 6-*O*-methylreticulol (8-hydroxy-6,7-dimethoxy-3-methylisocoumarin) **69**……24

1.7.3 Isolation and bioactivity studies of semivioxanthin ***R*-77** and ***S*-77**…….....26

1.7.3.0 Synthesis of semivioxanthin ***rac*-77** using biomimetic protocol……....….27

1.7.3.1 Synthesis of enantiomerically pure semivioxanthin ***S*-77** using Staunton-Weinreb annulation…...…….28

1.7.4 Isolation, bioactivity studies and synthesis of vioxanthin ***R*-91**……...29

1.7.5 Isolation, bioactivity studies and synthesis of pigmentosin A ***R*-93**…….....….....30

1.7.6 Isolation and bioactivity studies of toralactone **98**……..…….....32

1.7.7 Isolation and bioactivity of eriocauline **101**…….33

1.7.8 Isolation and bioactivity studies of paepalantine (9,10-dihydroxy-5,7-dimethoxy-3-methyl-1*H*-naphtho[2,3-*c*]pyran-1-one) **102**…….33

1.7.9 Isolation and bioactivity studies of 8,8'-paepalantine dimer **104**…….35

1.7.10 Isolation and bioactivity studies of planifolin **105**…….36

1.8 Examples of natural products containing quinone functionalities……...37

1.8.0 Isolation, bioactivity studies and synthesis of semixanthomegnin ***R*-106**……37

1.8.1 Isolation, bioactivity studies and synthesis of (3*R*,3'*R*)-xanthomegnin ***R*-110** and luteosporin ***R*-111**……..38

1.8.2 Isolation of fusarubinoic acid (5,8-dihydro-1,4-dihydroxy-6-methoxy-5,8-dioxo-3-(2-oxopropyl)naphthalene-2-carboxylic acid) **31**……..40

1.8.3 Isolation of anhydrofusarubin lactone (5,10-dihydroxy-7-methoxy-3-methyl-1*H*-naphtho-[2,3-*c*]-pyran-1,6,9-trione) **32**……..41

1.8.4 Isolation of haemoventosin (3,4,6,9-tetrahydro-5,10-dihydroxy-7-methoxy-3*S*-methyl-l,6,9-trioxo-l*H*-naphtho-[2,3-*c*]pyran) ***S*-115**……42

1.8.5 Isolation and bioactivity studies of 5-methoxy-3,4-dehydroxanthomegnin (10-hydroxy-5,7-dimethoxy-3-methyl-1*H*-naphtho-[2,3-*c*]-pyran-1,6,9-trione) **34**……43

1.8.6 Isolation of viomellein ***R*-118**…….....44

1.8.7 Isolation of rubrosulphin **119** and viopurpurin **120**……..45

1.9 Lactones as synthetic intermediates for synthesis of other functionalities……..45

1.9.0 Synthesis of dehydroherbarin **121** using the Staunton-Weinreb annulation reaction as a key step……...46

1.9.1 Synthesis of enantiomerically pure thysanone **123** using the Diels Alder reaction as a key step……..……46

1.10 Justification for this PhD study…….48

1.11 Aim of the PhD project……...55

Chapter 2: Results and discussion……...……....57

2.0 Background to the attempted synthesis of paepalantine 102 and dehydroherbarin lactone 159……...57

2.1 Synthesis of dehydroherbarin lactone 159……..60

2.1.0 Synthesis of ethyl 4-acetoxy-6,8-dimethoxynaphthalene-2-carboxylate **170**……..60

2.1.1 Synthesis of allyl 4-(allyloxy)-6,8-dimethoxynaphthalene-2-carboxylate **172**……62

2.1.2 Synthesis of allyl 3-allyl-4-hydroxy-6,8-dimethoxynaphthalene-2-carboxylate **152**…….63

2.1.3 Synthesis of allyl 3-allyl-4-hydroxy-1,6,8-trimethoxynaphthalene-2-carboxylate **153**…….....64

2.1.4 Synthesis of allyl 3-allyl-1,4,6,8-tetramethoxynaphthalene-2-carboxylate **168**…...66

2.1.5 Synthesis of allyl 3-allyl-1,4-dihydro-6,8-dimethoxy-1,4-dioxonaphthalene-2-carboxylate **174**……..68

2.1.6 Attempted synthesis of 7,9-dimethoxy-3-methyl-1*H*-benzo[*g*]isochromene-1,510-trione **159**……...69

2.1.7 Synthesis of 1,4,6,8-tetramethoxy-3-[(*E*)-prop-1-enyl]naphthalene-2-carboxylic acid **175**……..70

2.1.8 Synthesis of 5,7,9,10-tetramethoxy-3-methyl-1*H*-benzo[*g*]isochromen-1-one **103**…….72

2.1.8.0 Proposed mechanism for inner-sphere Wacker oxidation reaction……..…74

2.1.8.1 Proposed mechanism for outer-sphere Wacker oxidation reaction……..77

2.1.8.2 Proposed mechanism for outer-sphere intramolecular Wacker oxidation reaction…….78

2.1.8.3 Proposed mechanism for inner-sphere intramolecular Wacker oxidation reaction…….79

2.1.8.4 Proposed mechanism for outer-sphere intramolecular Wacker oxidation reaction…….81

2.1.9 Synthesis of ethyl 4-hydroxy-6,8-dimethoxynaphthalene-2-carboxylate **198**……..84

2.1.10 Synthesis of ethyl 4-(allyloxy)-6,8-dimethoxynaphthalene-2-carboxylate **131**….85

2.1.11 Synthesis of ethyl 3-allyl-4-hydroxy-1,6,8-trimethoxynaphthalene-2-carboxylate **197**…….86

2.1.12 Synthesis of ethyl 3-allyl-1,4,6,8-tetramethoxynaphthalene-2-carboxylate **195**…87

2.1.13 Synthesis of 1,4,6,8-tetramethoxy-3-[(*E*)-prop-1-enyl]naphthalene-2-carboxylic acid **175**……..…89

2.1.14 Synthesis of 3-allyl-1,4,6,8-tetramethoxynaphthalene-2-carboxylic acid **167**…...90

2.1.14.0 Proposed mechanism for Pinnick oxidation reaction……..…...93

2.1.15 Synthesis of 5,7,9,10-tetramethoxy-3-methyl-1*H*-benzo[*g*]isochromen-1-one **103**……..……...94

2.1.15.0 Proposed mechanism for outer-sphere intramolecular Wacker oxidation reaction for terminal alkene……..…94

2.1.16 Synthesis of 7,9-dimethoxy-3-methyl-1*H*-benzo[*g*]isochromene-1,5,10-trione (dehydroherbarin lactone) **159**……..….97

2.1.17 Attempted synthesis of paepalantine **102**……...98

2.1.17.0 Proposed mechanism for oxidative demethylation using boron tribromide……...100

2.1.18 PIFA mediated oxidation of 9-*O*-methylpaepalantine **208**……...103

2.1.18.0 Proposed mechanism for PIFA mediated oxidative demethylation…….103

2.2 Concise synthesis of dehydroherbarin lactone 159……..108

2.2.0 Synthesis of 3-allyl-4-hydroxy-6,8-dimethoxynaphthalene-2-carboxylic acid **224**……...110

2.2.1 Synthesis of 3-allyl-4-(*tert*-butyldimethylsilyloxy)-6,8-dimethoxynaphthalene-2-carboxylic acid **227**……..112

2.2.2 Synthesis of 7,9-dimethoxy-3-methyl-1*H*-benzo[*g*]isochromene-1,5,10-trione **228**……...113

2.3 Synthesis of 5-methoxy-3,4-dehydroxanthomegnin 34……115

2.3.0 Synthesis of ethyl 4-hydroxy-5,6,8-trimethoxynaphthalene-2-carboxylate **234**…117

2.3.1 Synthesis of ethyl 3-allyl-4-hydroxy-5,6,8-trimethoxynaphthalene-2-carboxylate **235**……...119

2.3.2 Synthesis of ethyl 3-allyl-4-hydroxy-5,6,8-trimethoxynaphthalene-2-carboxylate **236**……...120

2.3.3 Synthesis of ethyl 3-allyl-4-hydroxy-1,5,6,8-tetramethoxynaphthalene-2-carboxylate **237**……120

2.3.3.0 Spectroscopic data analysis of compound **241**……..……126

2.3.3.1 Proposed mechanism for PIFA mediated *ortho* methoxylation……..…127

2.3.3.2 Proposed mechanism for 1,4-Michael-type addition…….132

2.3.4 Synthesis of 3-ally-5-ethoxy-4,6,8-trimethoxynaphthalene-2-carboxylic acid **248**……...134

2.3.5 Synthesis of 3-allyl-5,8-diethyl-1,4,6-trimethoxynaphthalene-2-carboxylic acid **253**……...136

2.3.6 Synthesis of ethyl 3-allyl-1,4,5,6,8-pentamethoxynaphthalene-2-carboxylate **230**……...137

2.3.7 Synthesis of allyl 4-(allyloxy)-5,6,8-trimethoxynaphthalene-2-carboxylate **256**...140

2.3.8 Synthesis of allyl 3-allyl-4-hydroxy-5,6,8-trimethoxynaphthalene-2-carboxylate **257**……...141

2.3.9 Synthesis of allyl 3-allyl-4-hydroxy-1,5,6,8-tetramethoxynaphthalene-2-carboxylate **259**…….....141

2.3.10 Synthesis of 5,6,7,9,10-pentamethoxy-3-methyl-1*H*-benzo[*g*]isochromen-1-one **229**……...142
42

2.3.10.0 Proposed mechanism for outer-sphere intermolecular and intramolecular Wacker oxidation reaction for terminal alkene……..…147

2.3.11 Synthesis of 3-(chloromethyl)-3,4-dihydro-5,7,10-trimethoxybenzobenzo[*g*]isochromene-1,6,9-trione **JS-QCl**……149

2.3.12 Synthesis of 5,6,7,9,10-pentamethoxy-3-methyl-1*H*-benzo[*g*]isochromen-1-one **229**……...151

2.3.13 Synthesis of 5,7,10-trimethoxy-3-methyl-1*H*-benzo[*g*]isochromene-1,6,9-trione **35**……154

2.3.14 Synthesis of 10-hydroxy-5,7-dimethoxy-3-methyl-1*H*-benzo[*g*]isochromene-1,6,9-trione (5-methoxy-3,4-dehydroxanthomegnin) **34**……..155

Chapter 3: Introduction to ferrocenyl hybrid molecules of biological importance……...159

3.0 Synopsis……159

3.1 History of malaria and mode of transmission……..159

3.2 Quinones with antimalarial activities……162

3.2.0 Antimalarial activity of Lawsone quinone analogues **272**, **273**, **274** and **275**……163

3.2.1 Antimalarial activity of Lawsone quinone amine analogues **276**, **277**, **278** and **279**……...165

3.2.2 Antimalarial activity of isopinnatal **280** and sterekunthal A **281**……...166

3.2.3 Antimalarial activity of pantalogin **282**……..166

3.2.4 Antimalarial activity of rufigallol **283**……167

3.3 Proposed mode of antimalarial action of quinones……..168

3.4 Ferrocene 288 and ferrocenium salts 290…….169

3.5 Organic ferrocene derivatives of biological importance…….171

3.5.0 Synthesis and biological application of ferrocenyl amines **298**…….172

3.5.1 Synthesis and biological application of ferrocenyl pyrimidines **299** and **301**…....173

3.5.2 Synthesis and biological application of ferrocenyl dihydroquinolinones **306**, **307** and **308**……176

3.5.3 Synthesis and biological application of ferrocenyl azamacrocyclic *bis*-quinoline **315**……...177

3.5.4 Synthesis and biological application of ferrocenyl pyrrolo[1,2-*a*]quinoxaline derivatives **324** and **325**……...178

3.5.5 Synthesis and biological application of ferrocenyl analogues of atovaquone **328**……...181

3.5.6 Synthesis and biological application of ferrocenyl indole **333**……...182

3.6 Tamoxifen 334 and ferrocifen 337 as anticancer agents…….183

3.6.0 Synthesis of ferrocenyl analogues of tamoxifen…….186

3.6.1 Proposed mode of action for ferrocifen…….……188

3.7 Chloroquine 351 and ferroquine 352……191

3.7.0 Synthesis of ferroquine……...193

3.7.1 Major differences between ferroquine **352** and chloroquine **351**……...194

3.8 Justification and aim of this study…….197

Chapter 4: Results and discussion…….…200

4.0 Background…….200

4.1 Synthesis of 6-ferrocenyl-(±)-*trans*-3,4-dihydro-5,8-dimethoxy-1,3-dimethyl-6-vinyl-1*H*-isochromene *trans*-367……..……202

4.1.0 Synthesis of 1-(5-allyloxy-2-methoxyphenyl)ethanone **370**……..202

4.1.1 Synthesis of 1-[2-allyl-3-(allyloxy)-6-methoxyphenyl]ethanone **373** and 1-(4-allyl-5-(allyloxy)-2-methoxyphenyl)ethanone **374**……..204

4.1.2 Synthesis of 1-(2,4-diallyl-3-hydroxy-6-methoxyphenyl)ethanone **375**……206

4.1.3 Synthesis of 1-(2,4-diallyl-3,6-dimethoxyphenyl)ethanol **377**……...207

4.1.4 Synthesis of (±)-*trans*-3,4-dihydro-5,8-dimethoxy-1,3-dimethyl-6-[(*E*)-1-propenyl]-1*H*-isochromene **378**……208

4.1.5 Synthesis of (±)-*trans*-3,4-dihydro-5,8-dimethoxy-1,3-dimethyl-6-vinyl-1*H*-isochromene…….....210

4.1.6 Synthesis of vinyl ferrocene **366**……213

4.1.7 Synthesis of ferrocenyl (±)-*trans*-3,4-dihydro-5,8-dimethoxy-1,3-dimethyl-6-vinyl-1*H*-isochromene ***trans*-367**……..213

4.1.8 Synthesis of 1-(2-allyl-3-hydroxy-6-methyoxyphenyl)ethanone **404**……228

4.1.9 Synthesis of 2-allyl-3-(1-hydroxyethyl)-4-methoxyphenol **406**…….231

4.1.10 Synthesis of (±)-*trans*-3,4-dihydro-8-methoxy-1,3-dimethyl-1*H*-isochromen-5-ol ***trans*-409**…….232

4.1.10.0 Assigning C-H protons and carbon atoms of *bis*[(±)-*trans*-3,4-dihydro-8-methoxy-1,3-dimethyl-1*H*-isochromen-5-yloxy]methane ***trans*-410**……235

4.1.10.1 Assigning non C-H carbon atoms of *bis*[(±)-*trans*-3,4-dihydro-8-methoxy-1,3-dimethyl-1*H*-isochromen-5-yloxy]methane ***trans*-410**……..…..236

4.1.10.2 The spectroscopic data analysis for (±)-*trans*-3,4-dihydro-8-methoxy-1,3-dimethyl-1*H*-isochromen-5-ol ***trans*-409**……...238

4.1.10.3 The spectroscopic data analysis of (±)-*trans*-5-(*tert*-butoxymethoxy)-3,4-dihydro-8-methoxy-1,3-dimethyl-1*H*-isochromene *trans*-411……..239

4.1.10.4 Proposed mechanism for the formation of *bis*[(±)-*trans*-3,4-dihydro-8-methoxy-1,3-dimethyl-1*H*-isochromen-5-yloxy]methane *trans*-410…….240

4.1.11 Acid hydrolysis of compounds ***trans*-410** and ***trans*-411**…….……246

4.1.12 Synthesis of 1-(2-allyl-3-*tert*-butyldimethylsilyloxy-6-methoxyphenyl)ethanol **423**……...247

4.1.13 Synthesis of (±)-*trans*-3,4-dihydro-8-methoxy-1,3-dimethyl-1*H*-isochromen-5-ol ***trans*-409**…….249

4.1.14 Synthesis of (±)-*trans*-6-bromo-3,4-dihydro-8-methoxy-1,3-dimethyl-1*H*-isochromen-5-ol ***trans*-425**……..251

4.1.14.0 Assigning C-H protons and carbon atoms of (±)-*trans*-6-bromo-3,4-dihydro-8- methoxy-1,3-dimethyl-1*H*-isochromen-5-ol ***trans*-425**…….……....252

4.1.14.1 Assigning non C-H carbon atoms for 6-bromo-3,4-dihydroisochromen-5-ol ***trans*-425**…….**....**252

4.1.15 Synthesis of (±)-*trans*-6-bromo-3,4-dihydro-1,3-dimethyl-1*H*-isochromene-5,8-dione ***trans*-383**……253

4.1.16 Synthesis of (±)-*trans*-15-bromo-5,13-dimethoxy-2,4,10,12-tetramethyl-4,7,9,10,12,13-hexahydro-1*H*-7,13-methanopyrano[4',3':6,7]oxocino[2,3-*f*]isochromen-8(2*H*)-one……255

4.1.16.0 Spectroscopic data analysis for proposed compound **JS-X10**…….258

4.1.16.1 Spectroscopic data analysis for proposed compounds **429**…….…….261

4.1.16.2 Proposed mechanism for the formation of dimer **JS-X10**……...263

4.1.16.2.0 Proposed ionic disconnection……263

4.1.16.2.1 Proposed mixed ionic-radical disconnection…….264

4.1.16.2.2 Proposed pure radical disconnection…….....271

Chapter 5: Preliminary biological testing of selected compounds……...273

5.0 Introduction…….273

5.1 Combination drug strategy……274

5.2 Justification of this PhD study……...275

5.3 The results and discussion for antimalarial activity……276

Chapter 6: Conclusion and Future Work…….282

6.0. Synthesis of pyranonaphthoquinones and future work……..282

6.1 Synthesis of ferrocenyl 3,4-dihydroisochromene and future work……290

6.2 Preliminary antimalarial screening of selected compounds……...295

6.3 Future biological screening of pyranonaphthoquinones and ferrocenyl pyranobenzoquinone…….296

Chapter 7: Experimental procedures……297

7.0 General Modus Operandi……...297

7.1 Thin layer chromatography, evaporation of solvents and cleaning of glassware……297

7.2 Purification of solvents and reagents……297

7.3 Chromatography procedures…….297

7.4 Spectroscopic methods……298

7.4.0 NMR spectroscopy…….298

7.4.1 Infrared spectroscopy…….298

7.4.2 High resolution mass spectroscopy……..……..299

7.5 Melting points……..299

7.6 Single crystal x-ray diffraction……..……299

7.7 Experimental section for the synthesis of dehydroherbarin lactone 159……...300

7.7.0 Synthesis of ethyl 4-acetoxy-6,8-dimethoxynaphthalene-2-carboxylate **170**……300

7.7.1 Synthesis of allyl 4-(allyloxy)-6,8-dimethoxynaphthalene-2-carboxylate **172**…..301

7.7.2 Synthesis of allyl 3-allyl-4-hydroxy-6,8-dimethoxynaphthalene-2-carboxylate **152**……...302

7.7.3 Synthesis of allyl 3-allyl-4-hydroxy-1,6,8-trimethoxynaphthalene-2-carboxylate **153**……...303

7.7.4 Synthesis of allyl 3-allyl-1,4,6,8-tetramethoxynaphthalene-2-carboxylate **168**….304

7.7.5 Synthesis of allyl 3-allyl-1,4-dihydro-6,8-dimethoxy-1,4-dioxonaphthalene-2-carboxylate **174**……305

7.7.6 Synthesis of 1,4,6,8-tetramethoxy-3-((*E*)-prop-1-enyl)naphthalene-2-carboxylic acid **175**……306

7.7.7 Synthesis of 5,7,9,10-tetramethoxy-3-methyl-1*H*-benzo[*g*]isochromen-1-one **103**……...307

7.7.8 Synthesis of ethyl 4-hydroxy-6,8-dimethoxynaphthalene-2-carboxylate **198**.....308

7.7.9 Synthesis of ethyl 4-(allyloxy)-6,8-dimethoxynaphthalene-2-carboxylate **131**….309

7.7.10 Synthesis of ethyl 3-allyl-4-hydroxy-6,8-dimethoxynaphthalene-2-carboxylate **197**……...……310

7.7.11 Synthesis of ethyl 3-allyl-4-hydroxy-1,6,8-trimethoxynaphthalene-2-carboxylate **196**……...310

7.7.12 Synthesis of ethyl 3-allyl-1,4,6,8-tetramethoxynaphthalene-2-carboxylate **195**……...311

7.7.13 Synthesis of 1,4,6,8-tetramethoxy-3-[(*E*)-prop-1-enyl]naphthalene-2-carboxylic acid **175**……....312

7.7.14 Synthesis of 3-allyl-1,4,6,8-tetramethoxynaphthalene-2-carboxylic acid **167**….313

7.7.15 Synthesis of 5,7,9,10-tetramethoxy-3-methyl-1*H*-benzo[*g*]isochromen-1-one **103**……...314

7.7.16 Synthesis of 7,9-dimethoxy-3-methyl-1*H*-benzo[*g*]isochromene-1,5,10-trione **159**……...315

7.7.17 Attempted synthesis of paepalantine **102**…….315

7.7.17.0 Method one: Synthesis of 10-hydroxy-5,7,9-trimethoxy-3-methyl-1H-benzo[g]isochromen-1-one (9-O-methylpaepalantine) **208**……...316

7.7.17.1 Method two: Synthesis of 7,9-dimethoxy-3-methyl-1*H*-benzo[*g*]isochromene-1,5,10-trione **159**……..……..316

7.7.18 Synthesis of 7,9-dimethoxy-3-methyl-1*H*-benzo[*g*]isochromene-1,5,10-trione **159**……...317

7.8 Concise synthesis of 7,9-dimethoxy-3-methyl-1*H*-benzo[*g*]isochromene-1,5,10-trione 159…….....318

7.8.0 Synthesis of 3-allyl-4-hydroxy-6,8-dimethoxynaphthalene-2-carboxylic acid **224**……...318

7.8.1 Synthesis of 3-allyl-4-(*tert*-butyldimethylsilyloxy)-6,8-dimethoxynaphthalene-2-carboxylic acid **227**……..318

7.8.2 Synthesis of 5-[(*tert*-butyldimethylsilyl)oxy]-7,9-dimethoxy-3-methyl-1*H*-benzo[*g*]isochromen-1-one **228**……...319

7.8.3 Synthesis of 7,9-dimethoxy-3-methyl-1*H*-benzo[*g*]isochromene-1,5,10-trione **159**……...320

7.9 Experimental work pertaining to the synthesis of 5-methoxy-3,4-dehydroxanthomegnin 34…….321

7.9.0 Synthesis of ethyl 4-acetoxy-5,6,8-trimethoxynaphthalene-2-carboxylate **233**….321

7.9.1 Synthesis of ethyl 4-hydroxy-5,6,8-trimethoxynaphthalene-2-carboxylate **234**…322

7.9.2 Synthesis of ethyl 4-(allyloxy)-5,6,8-trimethoxynaphthalene-2-carboxylate **235**..322

7.9.3 Synthesis of ethyl 3-allyl-4-hydroxy-5,6,8-trimethoxynaphthalene-2-carboxylate **236**……...323

7.9.4 Synthesis of ethyl 3-allyl-4-hydroxy-1,5,6,8-tetramethoxynaphthalene-2-carboxylate **237**……....324

7.9.5 Synthesis of ethyl 3-allyl-3-ethoxy-3,4-dihydro-5,6,8-trimethoxy-4-oxonaphthalene-2-carboxylate **242**……..325

7.9.6 Synthesis of ethyl 3-allyl-5,8-diethoxy-4-hydroxy-1,6-dimethoxynaphthalene-2-carboxylate **246**, ethyl 3-allyl-5-ethoxy-4-hydroxy-6,8-dimethoxynaphthalene-2-carboxylate **245** and ethyl 3-allyl-4-hydroxy-1,5,6,8-tetramethoxynaphthalene-2-carboxylate **237**……326

7.9.7 Synthesis of ethyl 3-allyl-5-ethoxy-4,6,8-trimethoxynaphthalene-2-carboxylate **247**……...328

7.9.8 Synthesis of ethyl 3-allyl-5,8-diethoxy-1,4,6-trimethoxynaphthalene-2-carboxylate **252**……...329

7.9.9 Synthesis of ethyl 3-allyl-4-hydroxy-1,5,6,8-tetramethoxynaphthalene-2-carboxylate **237**……330

7.9.10 Synthesis of ethyl 3-allyl-1,4,5,6,8-pentamethoxynaphthalene-2-carboxylate **230** ……....330

7.9.11 Synthesis of allyl 4-(allyloxy)-5,6,8-trimethoxynaphthalene-2-carboxylate **256**. ……331

7.9.12 Synthesis of allyl 3-allyl-4-hydroxy-5,6,8-trimethoxynaphthalene-2-carboxylate **257**……...332

7.9.13 Synthesis of allyl 3-allyl-4-hydroxy-1,5,6,8-tetramethoxynaphthalene-2-carboxylate **259**……333

7.9.14 Synthesis of allyl 3-allyl-1,4,5,6,8-pentamethoxynaphthalene-2-carboxylate **254** ……334

7.9.15 Synthesis of 5,6,7,9,10-pentamethoxy-3-methyl-1*H*-benzo[*g*]isochromen-1-one **229**……...335

7.9.16 Synthesis of 3-(chloromethyl)-3,4-dihydro-5,7,10-trimethoxybenzobenzo[*g*]-isochromene-1,6,9-trione **JS-QCl**…….....336

7.9.17 Synthesis of (2-allyl-1,4,5,7,8-pentamethoxynaphthalene-3-yl)methanol **269**…337

7.9.18 Synthesis of 3-allyl-1,4,5,6,8-pentamethoxynaphthalene-2-carboxylic acid **231** ……338

7.9.19 Synthesis of 5,6,7,9,10-pentamethoxy-3-methyl-1*H*-benzo[*g*]isochromen-1-one **229**……...339

7.9.20 Synthesis of 5,7,10-trimethoxy-3-methyl-1*H*-benzo[*g*]isochromene-1,6,9-trione **35** ……339

7.9.21 Synthesis of 10-hydroxy-5,7-dimethoxy-3-methyl-1*H*-benzo[*g*]isochromene-1,6,9-trione (5-methoxy-3,4-dehydroxanthomegnin) **341**……340

7.10 Experimental procedures for attempted synthesis of ferrocenyl (±)-*trans*-3,4-dihydro-1,3-dimethyl-6-vinyl-1*H*-isochromene-5,8-dione *trans*-368……341

7.10.0 Synthesis of 1-(5-allyloxy-2-hydroxyphenyl)ethanone **370**…….341

7.10.1 Synthesis of 1-(5-allyloxy-2-methoxyphenyl)ethanone **372**……342

7.10.2 Synthesis of 1-(2-allyl-3-(allyloxy)-6-methoxyphenyl)ethanone **373** and 1-(4-allyl-5-(allyloxy)-2-methoxyphenyl)ethanone **374**……..343

7.10.3 Synthesis of 1-(2,4-diallyl-3-hydroxy-6-methoxyphenyl)ethanone **375**……..344

7.10.4 Synthesis of 1-(2,4-diallyl-3,6-dimethoxyphenyl)ethanone **376**……..345

7.10.5 Synthesis of 1-(2,4-diallyl-3,6-dimethoxyphenyl)ethanol **377**…….345

7.10.6 Synthesis of (±)-*trans*-3,4-dihydro-5,8-dimethoxy-1,3-dimethyl-6-[(*E*)-1-propenyl]-1*H*-isochromene ***trans*-378**…….346

7.10.7 Synthesis of (±)-*trans*-3,4-dihydro-5,8-dimethoxy-1,3-dimethyl-1*H*-isochromanene-6-carbaldehyde ***trans*-364**……..347

7.10.9 Synthesis of (±)-*trans*-3,4-dihydro-5,8-dimethoxy-1,3-dimethyl-6-vinyl-1*H*-isochromene ***trans*-365**……348

7.10.10 Synthesis of vinyl ferrocene **366**……....349

7.10.11 Synthesis of ferrocenyl 3,4-dihydroisochromene ***trans*-367**……..350

7.10.11.0 Method one: Grubbs cross-metathesis reaction…….….350

7.10.11.1 Method two: McMurry cross-coupling metathesis reaction……...…350

7.11 Route two: Involving Heck-type cross-coupling reaction……...…..351

7.11.0 Synthesis of 1-(2-allyl-3-hydroxy-6-methoxyphenyl)ethanone **404**……351

7.11.1 Synthesis of 2-allyl-3-(1-hydroxyethyl)-4-methoxyphenol **406**……...352

7.11.2 Synthesis of (±)-*trans*-3,4-dihydro-8-methoxy-1,3-dimethyl-1*H*-isochromen-5-ol ***trans*-409**…….353

7.11.3 Hydrolysis of (±)-*trans*-5-(*tert*-butoxymethoxy)-3,4-dihydro-8-methoxy-1,3-dimethyl-1*H*-isochromene ***trans*-411**……..355

7.11.4 Hydrolysis of *bis*[(±)-*trans*-3,4-dihydro-8-methoxy-1,3-dimethyl-1*H*-isochromen-5-yloxy]methane ***trans*-410**…….....356

7.11.5 Synthesis of 1-(2-allyl-3-*tert*-butyldimethylsilyloxy-6-methoxyphenyl)ethanone **422**……...356

7.11.6 Synthesis of 1-(2-allyl-3-[(*tert*-butyldimethylsilyl)oxy]-6-methoxyphenyl)ethanol **423**……...357

7.11.7 Synthesis of (±)-*trans*-3,4-dihydro-8-methoxy-1,3-dimethyl-1*H*-isochromen-5-ol ***trans*-409**…….358

7.11.8 Synthesis of 1-(3-[(*tert*-butyldimethylsilyl)oxy]-6-methoxy-2-[(*E*)-prop-1-enyl)phenyl]ethanol **424**……..358

7.11.9 Synthesis of (±)-*trans*-6-bromo-3,4-dihydro-8-methoxy-1,3-dimethyl-1*H*-isochroman-5-ol ***trans*-425**……..359

7.11.10 Synthesis of (±)-*trans*-6-bromo-3,4-dihydro-1,3-dimethyl-1*H*-isochromene-5,8-dione……....360

7.11.11 Synthesis of (±)-*trans*-15-bromo-5,13-dimethoxy-2,4,10,12-tetramethyl-4,7,9,10,12,13-hexahydro-1*H*-7,13-methanopyrano[4',3':6,7]oxocino[2,3-*f*]isochromen-8(2*H*)-one **JS-X10**……...361

7.12 Biological evaluation of selected compounds……..362

Chapter 8: References…….……...363

Chapter 9: Appendices……..……..A1

A1 Appendices: 1D NMR spectroscopic data……..A1

A1.0 ^{1}H and ^{13}C NMR spectra of allyl ester **168**……..…A1

A1.1 ^{1}H and ^{13}C NMR spectra of naphthoquinone **174**……..……..A2

A1.2 ^{1}H and ^{13}C NMR spectra of lactone **103**……..……A3

A1.3 ^{1}H and ^{13}C NMR spectra of furanone **176**……..…….A4

A1.4 ^{1}H and ^{13}C NMR spectra of ethyl ester **195**……..……...A5

A1.5 ^{1}H and ^{13}C NMR spectra of carboxylic acid **167**……..……...A6

A1.6 ^{1}H and ^{13}C NMR spectra of pyranonaphthoquinone **159**……..……..A7

A1.7 ^{1}H and ^{13}C NMR spectra of 9-*O*-methylpaepalantine **208**……..…….A8

A1.8 ^{1}H and ^{13}C NMR spectra of carboxylic acid **227**…….……....A9

A1.9 ^{1}H and ^{13}C NMR spectra of lactone **228**……..……..A10

A1.10 ^{1}H and ^{13}C NMR spectra of ethyl ester **241**……..……...A11

A1.11 ^{1}H and ^{13}C NMR spectra of ethyl ester **242**…….....A12

A1.12 ^{1}H and ^{13}C NMR spectra of naphthol **245**……..…….A13

A1.13 ^{1}H and ^{13}C NMR spectra of naphthol **245**……..……..……...A134

A1.14 ^{1}H and ^{13}C NMR spectra of naphthol **246**……..……A15

A1.15 ^{1}H and ^{13}C NMR spectra of ethyl ester **252**…….A16

A1.16 ^{1}H and ^{13}C NMR spectra of ethyl ester **230**…….A17

A1.17 ^{1}H and ^{13}C NMR spectra of ethyl ester **254**…….A18

A1.18 ^{1}H and ^{13}C NMR spectra of carboxylic acid **231**…….A19

A1.19 ^{1}H and ^{13}C NMR spectra of lactone **229**……..A20

A1.20 ^{1}H and ^{13}C NMR spectra of lactone **260**……..A21

A1.21 ^{1}H and ^{13}C NMR spectra of pyranonaphthoquinone **JS-QCl**……..A22

A1.22 ^{1}H and ^{13}C NMR spectra of pyranonaphthoquinone **35**……...A23

A1.23 ^{1}H and ^{13}C NMR spectra of 5-methoxy-3,4-dehydroxanthomegnin **34**……..A24

A1.24 ^{1}H and ^{13}C NMR spectra of acetophenone **373**……...A25

A1.25 ^{1}H and ^{13}C NMR spectra of acetophenone **374**……...A26

A1.26 ^{1}H and ^{13}C NMR spectra of 3,4-dihydroisochromene carbaldehyde ***trans*-364**..A27

A1.27 ^{1}H and ^{13}C NMR spectra of vinyl 3,4-dihydroisochromene ***trans*-365**……...A28

A1.28 ^{1}H and ^{13}C NMR spectra of vinyl ferrocene **366**…….A29

A1.29 ^{1}H and ^{13}C NMR spectra of phenol **404**…….....A30

A1.30 ^{1}H and ^{13}C NMR spectra of phenol **405**……..A31

A1.31 ^{1}H and ^{13}C NMR spectra of ferrocenyl 3,4-dihydroisochrome ***trans*-367**.....A32

A1.32 ^{1}H and ^{13}C NMR spectra of symmetrical dimer ***trans*-410**……..A33

A1.33 ^{1}H and ^{13}C NMR spectra of isochromen-5-ol ***trans*-409**…….A34

A1.34 ^{1}H and ^{13}C NMR spectra of alcohol **424**……..A35

A1.35 ^{1}H and ^{13}C NMR spectra of bromoisochromen-5-ol ***trans*-425**……...A36

A1.36 ^{1}H and ^{13}C NMR spectra of bromoquinone ***trans*-383**……A37

A1.37 ^{1}H and ^{13}C NMR spectra of dimer **JS-X10**……..A38

B1 Appendices: Tabulated 2D NMR spectroscopic data……B1

B1.0 2D NMR spectroscopic data for ethyl ester **241**…….....B1

B1.1 2D NMR spectroscopic data for ketone **242**……B2

B1.2 2D NMR spectroscopic data for 3,4-dihydroiscoumarin **260**……..B3

B1.3 2D NMR spectroscopic data for quinone **JS-QCl**……...B4

B1.4 2D NMR spectroscopic data for dimer ***trans*-410**……B5

B1.5 2D NMR spectroscopic data for bromopyran ***trans*-383**……..B6

B1.6 2D NMR spectroscopic data for bromoquinone ***trans*-425**……..B7

B1.7 2D NMR spectroscopic data for dimer **JS-X10**……...B8

B1.8 2D NMR spectroscopic data for proposed dimer ***trans*-429**……B9

C1 Appendices: Crystallographic data……C1

C1.0 X-ray crystallographic data for 5,7,9,10-tetramethoxy-3-methyl-1*H*-benzo[*g*]isochromen-1-one **103**……C1

C1.1 X-ray crystallographic data for (*Z*)-3-ethylidene-46,8,9-tetramethoxynaphtho[2,3-*c*]furan-1(3*H*)-one **176**……..C3

C1.2 X-ray crystallographic data for 5-[(*tert*-butyldimethylsilyl)oxy]-7,9-dimethoxy-3-methyl-1*H*-benzo[*g*]isochromen-1-one **228**……..C5

C1.3 X-ray crystallographic data for ethyl 3-allyl-3,4-dihydro-3,5,6,8-tetramethoxy-4-oxonaphthalene-2-carboxylate **241**……...C7

C1.4 X-ray crystallographic data for 3-ethyl 3-allyl-5-ethoxy-4-hydroxy-6,8-dimethoxynaphthalene-2-carboxylate **248**……C9

C1.5 X-ray crystallographic data for 5,6,7,9,10-pentamethoxy-3-methyl-1*H*-benzo[*g*]isochromen-1-one **229**……..C11

C1.6 X-ray crystallographic data for *bis*[(±)-*trans*-3,4-dihydro-8-methoxy-1,3-dimethyl-1*H*-isochromen-5-yloxy]methane **JS-D** or ***trans*-410**…….C13

C1.7 X-ray crystallographic data for (±)-*trans*-15-bromo-5,13-dimethoxy-2,4,10,12-tetramethyl-4,7,9,10,12,13-hexahydro-1*H*-7,13-methanopyrano[4',3':6,7]oxocino[2,3-*f*]isochromen-8(2*H*)-one **JS-X10**..……..C15

Chapter 1: Introduction to pyranonaphthoquinones and isocoumarins

1.0 Brief introduction to platinum and quinone based anticancer agents

The emphasis of this chapter is on the review of some of the biologically important natural products which have been isolated from micro-organisms and higher plants among other sources. The importance of these products especially those with lactone functionalities is amplified by the fact that alternative drugs to the well-known anticancer drug, cisplatin **1** and its derivatives such as carboplatin **2** (**Figure 1.0**) are required. The platinum based drugs are still used in more than 50% of the treatment regimens for patients suffering from cancer.[1] Cisplatin is the most prominent member of this class and is known to be 70-80% effective in cases of testicular cancer and is also used in the treatment of ovarian cancer.[2]

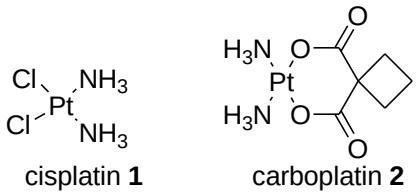


Figure 1.0: The molecular structures of cisplatin, *cis*-diamminedichloroplatinum (II), **1** and carboplatin, *cis*-diammine-1,1-cyclobutanedicarboxylatoplatinum (II), **2**.

Despite the tremendous success of platinum based drugs, they suffer from several drawbacks. For example, they are ineffective against platinum-resistant tumors such as mammary carcinoma and they have severe side-effects which include, among others, nephrotoxicity, renal impairment, neurotoxicity and ototoxicity (loss of balance/hearing).[3] Furthermore, as a consequence of its particular chemical structure, cisplatin **1** offers little possibility for rational improvements to increase its tumor-specificity and thereby reduce the undesired side effects.[4] These side effects led researchers from different parts of the world to turn their attention to natural products which are derived from micro-organisms and higher plants as an important source of biologically active compounds or lead compounds towards drug discovery.[5]

Among an array of naturally occurring and biologically important compounds, quinones occupy a prominent position because of their diverse application and are widely available in

nature.[6] Quinones are oxidized derivatives of aromatic compounds but they are not aromatic themselves despite being fully conjugated cyclic diketones. They are often readily synthesized from reactive aromatic compounds such as hydroquinones and catechols.[7] Quinones can behave as electrophilic Michael acceptors stabilised by conjugation.

In most cases, quinones are named after their corresponding aromatic analogues. Thus, benzene gives rise to *benzoquinone*, naphthalene to *naphthoquinone* and anthracene to *anthraquinone*. The compounds **3**, **4**, **5** and **6** in **Figure 1.1** are, therefore, named as 1,2-benzoquinone (*o*-benzoquinone), 1,4-benzoquinone (*p*-benzoquinone), 1,4-naphthoquinone (*p*-naphthoquinone) and 9,10-anthraquinone (*p*-anthraquinone), respectively.

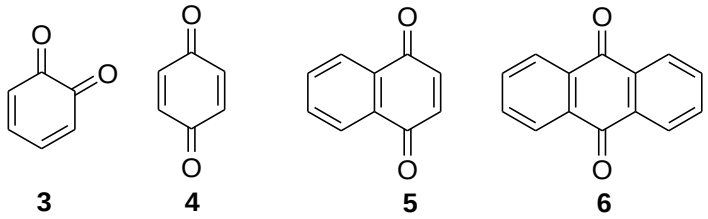
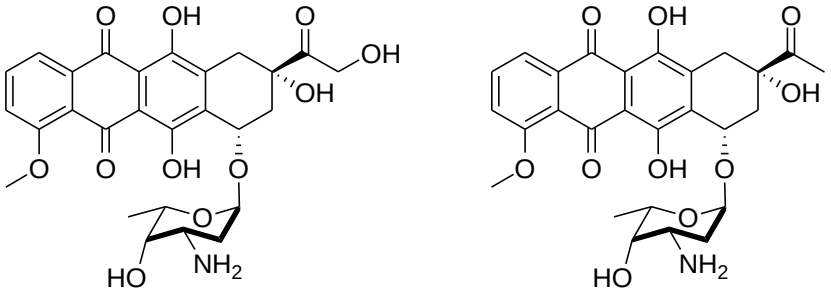


Figure 1.1: The molecular structures of *o*-benzoquinone **3**, *p*-benzoquinone **4**, *p*-naphthoquinone **5** and *p*-anthraquinone **6**.

There are many examples of natural products with the quinone moiety which are used in medicine or exhibit important anticancer activities. For example, doxorubicin **7** and daunorubicin **8** (**Figure 1.2**) are the best known members of the anthracycline antibiotics and are the most commonly used intercalating agents in the treatment of cancer. Doxorubicin **7** has a broad spectrum of antitumor activity and is particularly efficacious against solid tumors.[7] However, the clinical usefulness of anthracyclines is limited mainly by two major problems which are cumulative cardiotoxicity and the appearance of acquired resistance in most cases.[8] Nonetheless, this class of anticancer agents is better than the platinum based complexes as they are easily derivatized to reduce toxicity, improve specificity and increase their activity.[9]

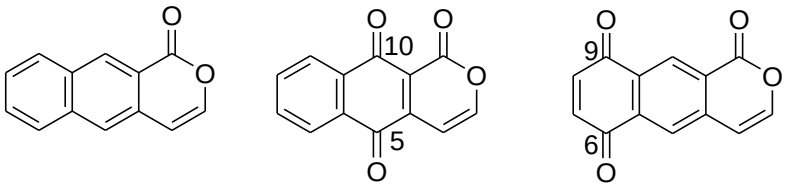


7 **8**

Figure 1.2: The molecular structures of anthraquinones, doxorubicin **7** and daunorubicin **8**.

Natural products that include a naphthopyranone (1*H*-naphtho[2,3-*c*]pyran-1-one) core structure **9** are widely dispersed in nature, having been isolated from a variety of sources including fungi, bacteria, algae, lichen and plants. They include pyranonaphthoquinones which have a quinone moiety in their structure and isocoumarins which have no quinone moiety.

The pyranonaphthoquinones are polysubstituted natural products which have a characteristic 1*H*-naphtho[2,3-*c*]pyran-5,10-dione **10** (or 1*H*-naphtho[2,3-*c*]pyran-6,9-dione **11**) framework sometimes with different types of functionalities.[10] The diketone functionality can either be at the 5,10-position or 6,9-position of the naphthalene ring system as shown in structures **10** and **11**, respectively (**Figure 1.3**).



9 **10** **11**

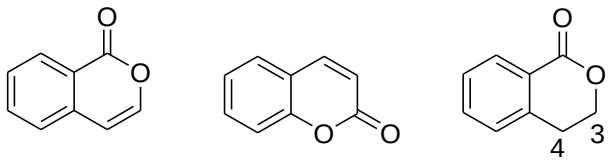
Figure 1.3: The basic molecular structures of isocoumarin **9** and pyranonaphthoquinones **10** and **11**.

The importance of isocoumarin and pyranonaphthoquinone based natural products is further exemplified by the fact that many active traditional medicine systems hinge on this group of compounds and have been used all over the world for thousands of years.[11] In fact, the World

Health Organization (WHO) estimates that approximately 80% of the world's inhabitants rely mainly on traditional medicine for their primary health care.[12]

1.1 Isocoumarins and 3,4-dihydroisocoumarins

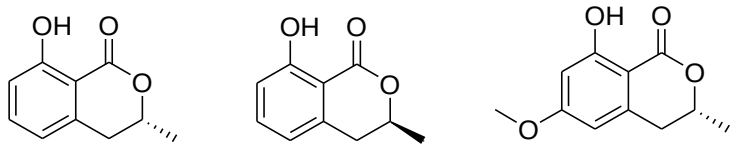
Isocoumarins are naturally occurring lactones that are found in higher plants, bacteria, fungi and insects among many other sources. They are examples of secondary metabolites and in simple terms they have a *δ*-pyranone ring as shown in structure **12**. Isocoumarins are structurally related to the coumarins which have the *α*-pyranone ring as shown in structure **13**, but with an inverted lactone ring. Isocoumarins exhibit a wide range of biological activities which includes, among others, anticancer, antibacterial, antifungal, anti-inflamatory, anti-angiogenic, anti-oxidative and anti-HIV activities.[13] This class of compounds is generally thought to be derived from the acetate pathway.[14] The 3,4-dihydroisocoumarins **14** are like isocoumarins in that they have a *δ*-pyranone ring but they have saturated (sp^3) carbon atoms at positions 3 and 4 of the pyranone ring as shown in **Figure 1.4**.



12 **13** **14**

Figure 1.4: The molecular structures of isocoumarin **12**, coumarin **13** and 3,4-dihydroisocoumarin **14**.

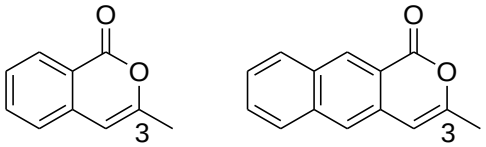
The IUPAC recognizes the naming of isocoumarins and 3,4-dihydroisocoumarins as 1*H*-isochromen-1-one and 3,4-dihydroisochromen-1-one, respectively. The majority of naturally occurring isocoumarins and 3,4-dihydroisocoumarins are given trivial names, which are derived from generic or specific names of source plant and fungi.[15] In some cases, the naming is based on a simple isocoumarin that is taken as a parent molecule. For example, (*R*)-(-)-mellein ***R*-15**, the 3,4-dihydro-8-hydroxy-3-methylisocoumarin, is taken as the parent compound for simple isocoumarins and thus, (*R*)-3,4-dihydro-8-hydroxy-6-methoxy-3-methylisocoumarin ***R*-16** is named as (*R*)-6-methoxymellein. Mellein is present in nature in both enantiomeric forms and the molecular structures of (*R*)-(-)-mellein ***R*-15**, (*S*)-(+)-mellein ***S*-15** and (*R*)-6-methoxymellein ***R*-16** are shown in **Figure 1.5**.



***R*-15** ***S*-15** ***R*-16**

Figure 1.5: The molecular structures of (*R*)-(-)-mellein ***R*-15**, (*S*)-(+)-mellein ***S*-15** and (*R*)-6-methoxymellein ***R*-16**.

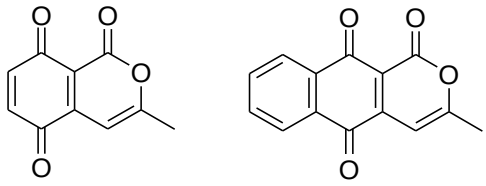
The isocoumarin and 3,4-dihydroisocoumarin functionality is present fused to a benzene, naphthalene or anthracene nucleus and can be substituted. In this thesis however, we will discuss the benzene and naphthalene based isocoumarins and 3,4-dihydroisocoumarins which have a methyl group at position 3 of the pyranone ring. The benzene or naphthalene ring system may or may not be substituted. The basic molecular structures of methyl substituted isocoumarins are shown in **Figure 1.6**.



17 **18**

Figure 1.6: The methyl substituted isocoumarins, 3-methyl-1*H*-isochromen-1-one **17** and 3-methyl-1*H*-benzo[*g*]isochromen-1-one **18**.

When the benzene or the naphthalene ring system has two ketone groups (diketone) at *ortho* or *para* positions to each other the compounds are generally known as pyranobenzoquinones and pyranonaphthoquinones, respectively. The basic molecular structures of *para*-pyranobenzoquinone and *para*-pyranonaphthoquinone are given in structures **19** and **20**, respectively (**Figure 1.7**).



19 **20**

Figure 1.7: The methyl substituted pyranoquinones, 3-methyl-1*H*-isochromene-1,5,8-trione **19** and 3-methyl-1*H*-benzo[*g*]isochromene-1,5,10-trione **20**.

Figures 1.6 and **1.7** show examples of methyl substituted isocoumarins and their oxidized analogues which has been done only for clarification purposes. The same examples apply for 3,4-dihydroisocoumarins, with the only difference being that in the case of the latter the double bond of the pyranone ring is saturated.

1.2 Biological activities of quinones and their modes of action

The detailed mechanism of action of bioactive quinones in biological systems is not fully understood but it is generally accepted that their interaction with biological systems may result from one or more of the three processes, namely:

i) A radical based mechanism generating highly toxic reactive oxygen species.

ii) A bioreductive alkylation-based mechanism involving reaction of quinone methides or other electrophilic side chains with vital cell compounds such as DNA, RNA and proteins.

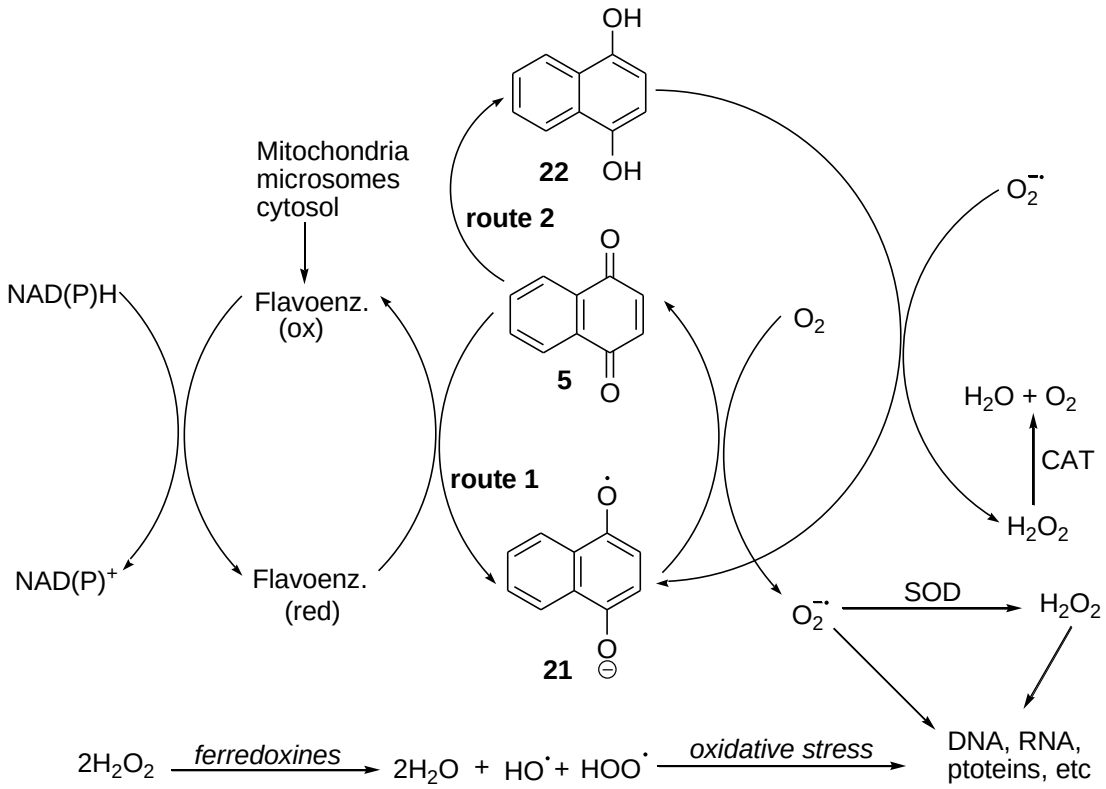
iii) An intercalation-based mechanism resulting from quinone insertion between two DNA base pairs causing disturbance in DNA transcription and replication by inhibition of DNA topoisomerase II.

These modes of action are not specific to types of quinones and may act in synergy for a particular molecule. It is also generally accepted that the biological activities of benzoquinones, naphthoquinones and pyranonaphthoquinones are related to a radical-based mechanism and/or bioreductive alkylation while those of anthraquinones are predicted to be

an intercalation based mechanism. In the following sections, we will discuss the first two and leave out the third mode of action which is prevalent in anthraquinones.

1.2.0 Radical based mechanism

At the core of many important energy conversion processes in biology are oxidation-reduction reactions in which electrons are transferred through the electron transport system. This process is particularly important in quinones because of their ability to accept one or two electrons to form the corresponding hydroquinones, radical anions or di-anion species.[16] Naphthoquinones can undergo metabolism *via* either a NADPH-quinone oxidoreductase (DT-diaphorase)-catalysed two-electron reduction to corresponding hydroquinones or a one-electron reduction catalysed by flavoenzymes such as NADPH-cytochrome P-450 reductase, NADH-cytochrome b_5 reductase or NADH-ubiquinone reductase to form semiquinone radicals (**Scheme 1.0**).[17]



Scheme 1.0: The bioreductive reactions of naphthoquinones through one-electron reaction (**route 1**) and two-electron reduction (**route 2**).

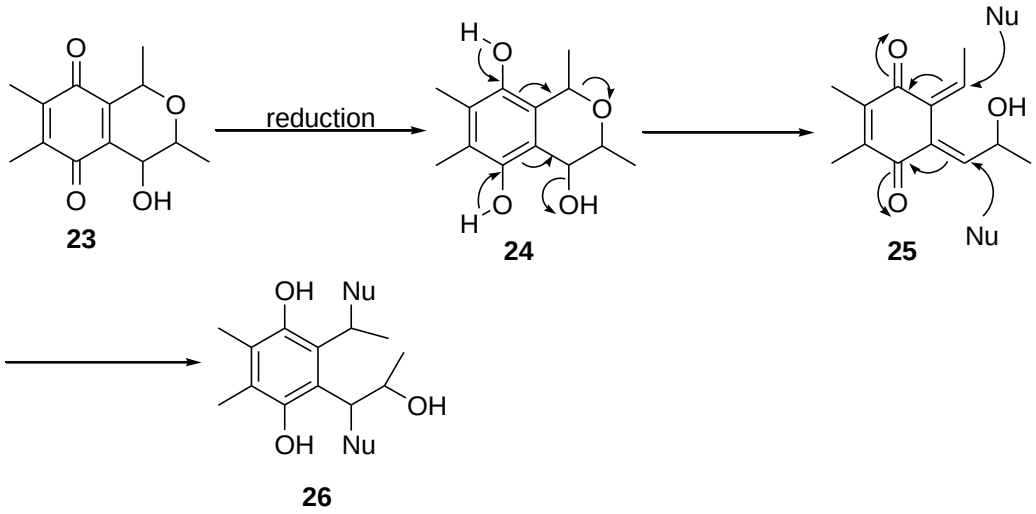
The one-electron reduction of quinones (**route 1**) has been suggested to result from the interaction of cellular electron transport systems (containing cytochromes and ferredoxines) which releases semiquinones as reversible products. For example, the one-electron reduction of naphthoquinone **5** by NADPH-cytochrome P-450 reductase flavoenzyme could generate the unstable seminaphthoquinone anion radical **21**. This process predominates under aerobic conditions found in healthy cells or in tumors with sufficient blood supply and the resultant seminaphthoquinone radical is readily auto-oxidised back to the original naphthoquinone **5** by molecular oxygen.[18] The auto-oxidation of the seminaphthoquinone **21** back to naphthoquinone **5** generates superoxide ion radicals ($O_2^{-\cdot}$) and is known as redox cycling because the re-generated naphthoquinone could undergo the same futile redox cycle.[19] The superoxide anion radicals are converted to hydrogen peroxide by superoxide dismutase (SOD) catalysed reaction. The resultant hydrogen peroxide is either broken down to water and molecular oxygen by catalase (CAT) or alternatively, is rapidly reacted with intracellular iron (II) ions *via* a Fenton-type reaction thereby generating highly reactive hydroxyl radicals ($HO^{\cdot}$).[20] The hydroxyl radicals primarily contribute to the cytotoxic effects of reactive oxygen species (ROS). ROS refers to superoxide anion radicals, hydroxyl radicals and hydrogen peroxide which are generated during energy conversion processes. The formation of a cascade of ROS triggers the oxidative stress responsible for irreversible cell damage leading to apoptosis or cell death.[21]

On the other hand, the two-electron reduction is believed to predominate under anaerobic conditions or inside anaerobic *loci* within a cell.[5a] This process results in reduction of naphthoquinone **5** (**route 2**) producing hydroquinone **22** which is more stable than seminaphthoquinone **21**.[22] The generation of less reactive hydroquinone reduces toxic, reactive and unstable quinones, by-passing the creation of toxic intermediates and thus sparing the cell from ROS formation. There is also a decrease in the concentration of the quinone available for one-electron reduction. This is generally true when this process involves excretion of hydroquinone after undergoing further metabolism to glucuronide and sulfate conjugate in what is generally known as detoxification process.[23] The hydroquinone could also react rapidly with superoxide anion radicals thereby generating less reactive hydrogen peroxide and seminaphthoquinone thus protecting the cell from the negative

consequences of superoxide anion radicals. This process may in some cases lead to oxidation of the hydroquinone back to the quinone which then undergoes the same futile oxidation-reduction process. Whether the two-electron reduction of a quinone leads to detoxification or activation of oxidative stress depends upon the rate of auto-oxidation of the formed hydroquinone.[24] If this rate is low under physiological conditions, conjugation may occur before oxidation. As a consequence, the two-electron reduction leads to detoxification and an increase in the oxidoreductase activity in tissues and is expected to decrease the toxicity of the quinone. If, however, the hydroquinone is rapidly oxidised, only a minor fraction may be conjugated before oxidation occurs, and hydroquinone formation would constitute an activation reaction. As a result, enhanced tissue levels of oxidoreductase would be expected to increase the toxicity of the quinone.[25]

1.2.1 Bioreductive alkylation mechanism

The term bioreductive alkylating agents was introduced in 1972 and refer to compounds that become potent alkylating agents after undergoing reduction *in vivo* resulting in formation of a quinone methide.[26] The methide may then alkylate DNA/RNA and/or other biomolecules resulting in potentially effective cancer-inhibitory drugs. For example, Sartorelli and Moore separately proposed that quinones which have a leaving group attached to the side chain like quinone **23** undergo *in vivo* reduction affording quinol **24** (**Scheme 1.1**). The cleavage of the pyran ring of this quinol delivers a highly reactive Michael acceptor, *bis*-quinone-methide system **25**. This process is followed by the reaction between the quinone methide **25** with biological nucleophile centres in DNA, RNA and biological molecules yielding hydroquinone **26**. This effectively affects the normal replication processes of cells and altering the normal activities of DNA and other biomolecules.



23 **24** **25** **26**

Scheme 1.1: Proposed bioreductive alkylation mechanism of quinone **23**, where *Nu* represents biological molecules.

1.3 Biosynthesis of anhydrofusarubin lactone 32

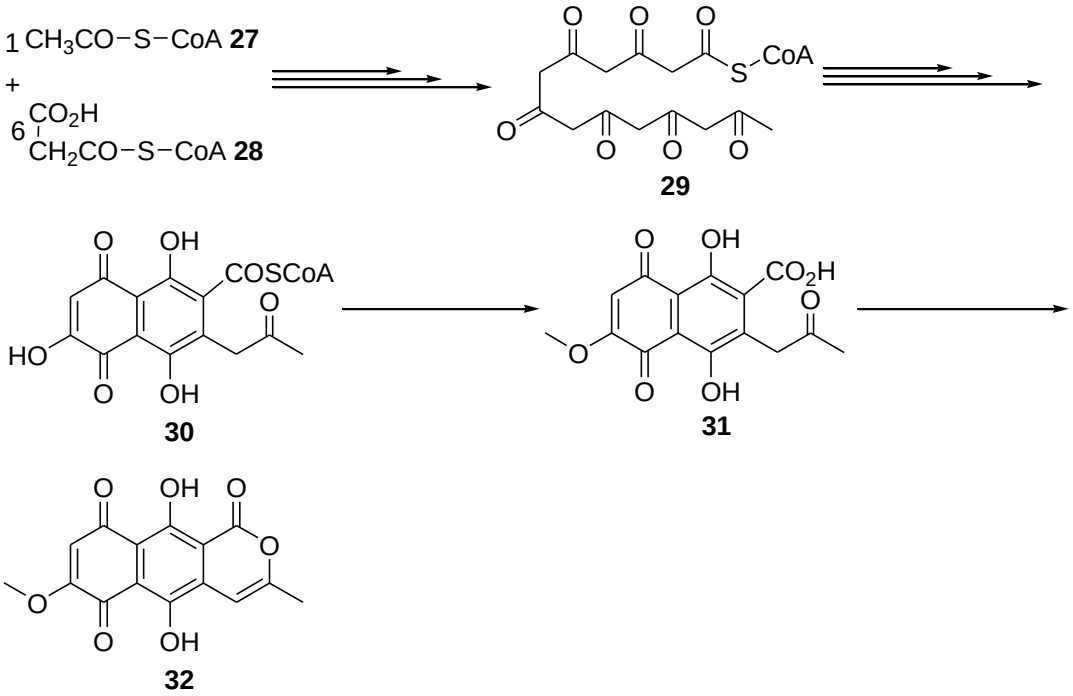
The secondary metabolites are derived principally from a few key intermediates of primary or intermediary metabolism, most often, phosphoenol pyruvate, acetyl coenzyme A, malonyl co-enzyme A, α-amino acids and shikimate by specific enzymes. Secondary metabolites have a distribution restricted, mostly, to a single major taxon and are more often a characteristic of specific botanical sources.[27] The polyketide pathway gives rise to several important plant metabolites, such as fatty acids, olefins, acetylenes and their branched derivatives and aromatics. Polyketide biosynthesis can involve the use of residues of a single, simple carboxylic acid subunit or a mixture of subunits. An important structural aspect of many polyketide-derived metabolites is the cyclic nature of the products, which often involves the formation of six-membered rings. Mechanistically, this process is the result of one or more intramolecular Aldol or Dieckmann cyclization reactions involving the oligoketide intermediate.

Anhydrofusarubin lactone is one example of many secondary metabolites produced by fungi. The structural similarities between quinones produced by fungi are attributed to their common biosynthetic origin, which is thought to be through the acetate-polyketide synthetase pathway. This class of quinone is believed to be formed from the variation of the number of

coenzyme A esters which results in a hypothetical polyketide chain that can fold and aromatize. The polyketide synthetase pathway also exists in a few plant species.[13]

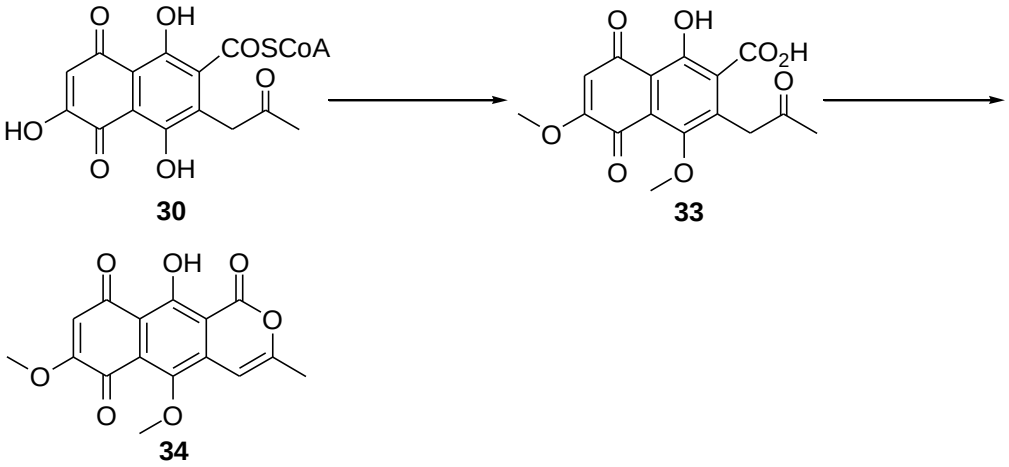
Detailed studies of the biosynthetic mechanism of quinones synthesized by fungi began in 1965 when ^{14}C-labelled acetate was used to show that the biosynthesis of 5-deoxyfusarubin by the fungus *Necteria haematococca* proceeds *via* the polyketide route.[28] This fungus is also responsible for the biosynthesis of anhydrofusarubin lactone and fusarubinoic acid.[29]

Anhydrofusarubin lactone is a heptaketide pyranonaphthoquinone and thus contains seven keto groups on the hypothetical polyketide chain (**Scheme 1.2**). It is believed that heptaketide is produced from a head-to-tail linear condensation of 1 acetyl coenzyme A unit **27** with 6 malonyl coenzyme A moieties **28**. The condensation reaction is followed by rotation and folding of the linear chain to produce a folded heptaketide **29**. The heptaketide **29** then undergoes further condensation and aromatization processes followed by the introduction of oxygen at the required positions yielding naphthoquinone **30**. This is followed by methylation of the non-hydrogen bonded hydroxyl group and the coenzyme A protein is then detached to give the fusarubinoic acid **31**. The intramolecular nucleophilic attack of the carboxylic acid on the ketone carbonyl carbon followed by dehydration of the resultant alcohol intermediate produces anhydrofusarubin lactone **32**. Impressively, the involvement of fusarubinoic acid **31** in the biosynthesis of pyranonaphthoquinones was predicted by Arsenault[30] 20 years before it was isolated from the culture medium of *N. haematococca* in 1988.[31]



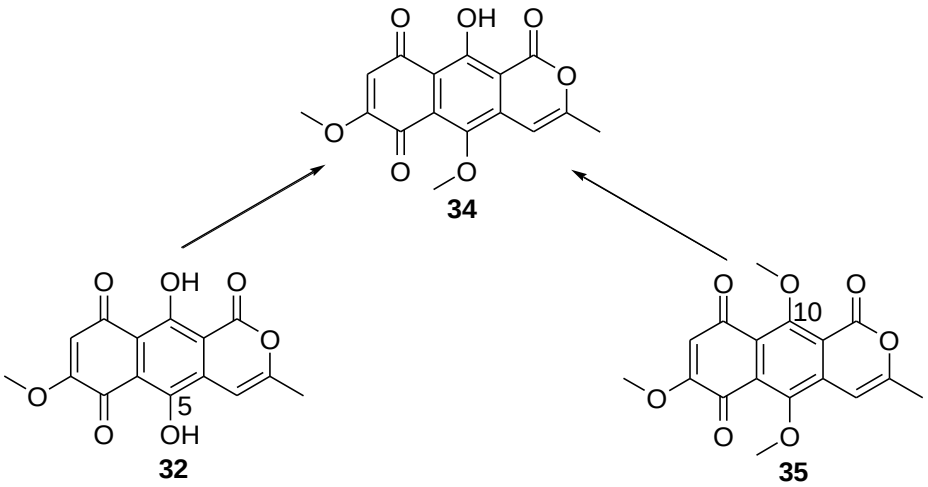
Scheme 1.2: Proposed route for the biosynthesis of anhydrofusarubin lactone **32** by the fungal genus *N. haematococca*.

A similar secondary metabolite, 5-methoxy-3,4-dehydroxanthomegnin **34**, is a pyranonaphthoquinone isolated from plants and its biosynthesis would, therefore, be predicted to be either through the acetate-polyketide or the mixed shikimate-polyketide pathway.[32] To the best of our knowledge, there are no studies that have been carried out to specifically elucidate the biosynthetic pathway of this biologically important metabolite but the two routes mentioned above should ultimately lead to the same quinone product with the methylation step being the only difference. Based on the foregoing discussion the biosynthesis of 5-methoxy-3,4-dehydroxanthomegnin **34** would be predicted to be by double methylation of naphthoquinone **30** by specific methylation enzymes to give a dimethyl naphthoquinone **33** (**Scheme 1.3**). The intramolecular nucleophilic attack of the carboxylic acid on the ketone group, followed by dehydration of the resultant intermediate would produce 5-methoxy-3,4-dehydroxanthomegnin **34** in basically the same way as for the synthesis of anhydrofusarubin lactone **32**.



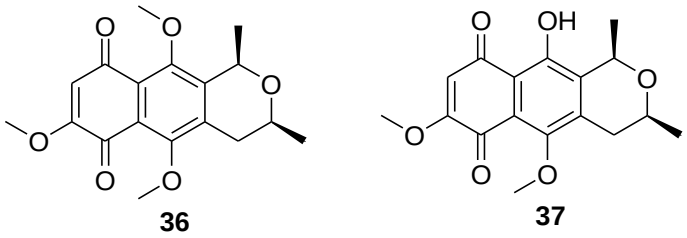
Scheme 1.3: Proposed biosynthesis of 5-methoxy-3,4-dehydroxanthomegnin from naphthoquinone **30**.

The other possible biosynthetic pathways which cannot be ruled out are the selective methylation or demethylation of pyranonaphthoquinones **32** or **35**, respectively, as depicted in **Scheme 1.4**. Anhydrofusarubin lactone **32**, which is a natural product, could be methylated at position 5 affording 5-methoxy-3,4-dehydroxanthomegnin **34**. In a similar fashion, pyranonaphthoquinone **35**, not a known natural product, could be selectively demethylated at position 10 yielding 5-methoxy-3,4-dehydroxanthomegnin **34**.



Scheme 1.4: Proposed biosynthesis of 5-methoxy-3,4-dehydroxanthomegnin **34** from anhydrofusarubin lactone **32** or its methylated analogue **35**.

Even though pyranonaphthoquinone **35** is not a known natural product, there is an example of a naturally available pyranonaphthoquinone, ventiloquinone *E* **36**, which was isolated from the root bark of *Ventilago maderaspatana*[33] and has similar arranged methoxy groups in its structure as depicted in **Figure 1.8**. In the same way, ventiloquinone *J* **37**[33] has a similar arrangement of methoxy groups to 5-methoxy-3,4-dehydroxanthomegnin **34**.

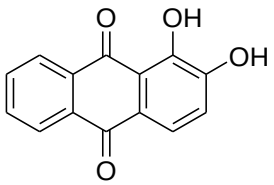


36 **37**

Figure 1.8: The molecular structure of ventiloquinone *E* **36** and ventiloquinone *J* **37**.

1.4 Advantages of synthesizing plant based natural products and its history

The synthesis of naturally occurring quinones began in 1868 when Graebe and Liebermann realised that alizarin **38** (**Figure 1.9**) was a dihydroxyanthraquinone and immediately sought its synthesis.[34] Alizarin is the principal pigment in the root of madder, *Rubia tinctorum*. Since then, the synthesis of naturally occurring quinones has advanced very slowly due, in part, to the complexity of building the highly oxygenated part of the molecule.



38

Figure 1.9: The molecular structure of alizarin **38**.

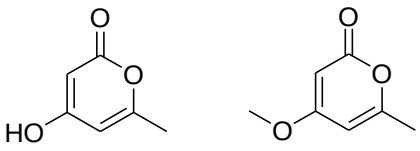
In the early natural product synthesis (pre-1950), most benzoquinones and naphthoquinones were synthesized from a precursor phenol by oxidation. This was followed, as required, by further modification of substituents. On the other hand, anthraquinones were obtained by condensation of substituted benzoic acids and cyclization of *o*-benzoylbenzoic acids, among others.[35]

The first advantage of synthesizing natural products is that there is no continual use of plant resources thereby saving some plants from extinction. After the initial isolation of plant based natural products subsequent studies on their biological activities have been carried out by isolating more metabolites from the same plants thereby continuing the destruction of the environment. The second advantage is that more often synthesis of compounds is cheaper than isolation and is not limited to certain geographical locations. The third advantage which we will highlight in this thesis is that there are cases where the correct structures of natural products or its absolute configuration have been confirmed or modified after their synthesis was accomplished. The fourth and probably the most important advantage of synthesizing natural products is that more often synthesis of natural products results in isolation of new unexpected compounds which are biologically important in themselves. The synthesis of most natural products involves linear multistep protocols and there are cases in which intermediates are more biologically active than the intended natural products.

1.5 Isolation and biosynthesis of triacetic acid lactone 39

Triacetic acid lactone (4-hydroxy-6-methyl-2*H*-pyran-2-one) **39** (**Figure 1.10**) is an example of a triketide which are very uncommon in nature. Just like most polyketides, triketides share at least four common enzymes which are acyl and malonyl transferases, an acyl carrier protein and the condensing enzyme 2-P-ketoacyl synthetase.[36] These enzymes are at the heart of constructing the end natural products from coenzymes.

Harris and co-workers[37] described isolation of triacetic acid lactone from cultures of *Penicillium patulum* NRRL strain 2159A and there are a few more examples of triacetic acid lactone isolation from nature.[38]



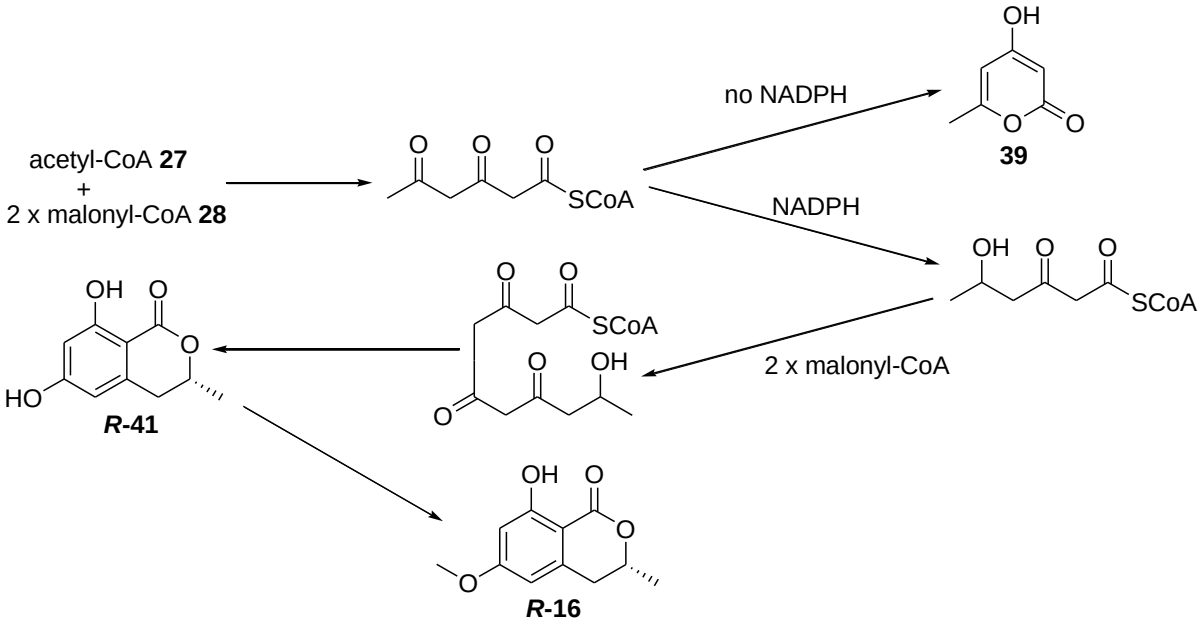
39 **40**

Figure 1.10: The molecular structures of triacetic acid lactone **39** and 4-methoxy-6-methyl-2*H*-pyran-2-one **40**.

This group of compounds is very important because the methylated form of triacetic acid lactone, 4-methoxy-6-methyl-2*H*-pyran-2-one **40**, is used extensively in Staunton-Weinreb annulation protocols as a Michael acceptor as explained later in the thesis. The alkoxy group is thought to increase the reactivity towards nucleophilic attack by orsellinates by stabilising the anion intermediate.[39] The other reason for increased reactivity is probably due to the fact that the alkoxy substituent is a better leaving group compared to a hydroxyl group and hence is easily eliminated.

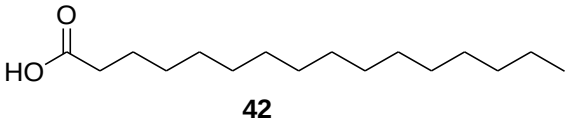
The pyranone ring system is widely present in the animal and plant kingdoms and possesses diverse pharmacological activities. Compounds with this ring system have been known for more than a century, but their versatility in organic synthesis to generate molecules of diverse functionality was recognised only after 1960.[40] The involvement of the pyranone ring system in different biological processes as biosynthetic intermediates and metabolites has made this scaffold an important chemical entity and has recently been reviewed by Donner.[41] Many of the 2-pyranone compounds have been used as precursors for the synthesis of pharmacologically active compounds such as HIV protease inhibitors, antifungals, cardiotonics, anticonvulsants, pheromones, antitumour agents and plant growth regulators.[42]

Kurosaki and co-workers reported the biosynthesis of triacetic acid lactone **39** alongside (*R*)-6-hydroxymellein ***R*-41** and their work was part of a review by O'Hagan[43] (**Scheme 1.5**). In this work, it was demonstrated that (*R*)-6-hydroxymellein ***R*-41**, which is a precursor to (*R*)-6-methoxymellein ***R*-16**, was produced when 1 mole of acetyl-CoA **27**, 2 moles of malonyl-CoA **28** and NADPH were incubated with homogenates of elicitor treated carrot roots.[44] In the absence of NADPH, triacetic acid lactone **39** was produced as a derailment product as shown in **Scheme 1.5**.[45]



Scheme 1.5: Biosynthetic pathway for the synthesis of triacetic acid lactone **39**.

Similarly, the fungal type I polyketide synthetase, 6-methylsalicylic acid synthetase (6-MSAS) from *Penicillium patulum* and the bacterial type I fatty acid synthetase B (FAS-B) from *Brevibacterium ammoniagenes* were shown to produce triacetic acid lactone **39** *in vitro* in the absence of NADPH by Hansen[46] and Richardson,[47] respectively, and afforded palmitic acid **42** (**Figure 1.11**) in the presence of NADPH.



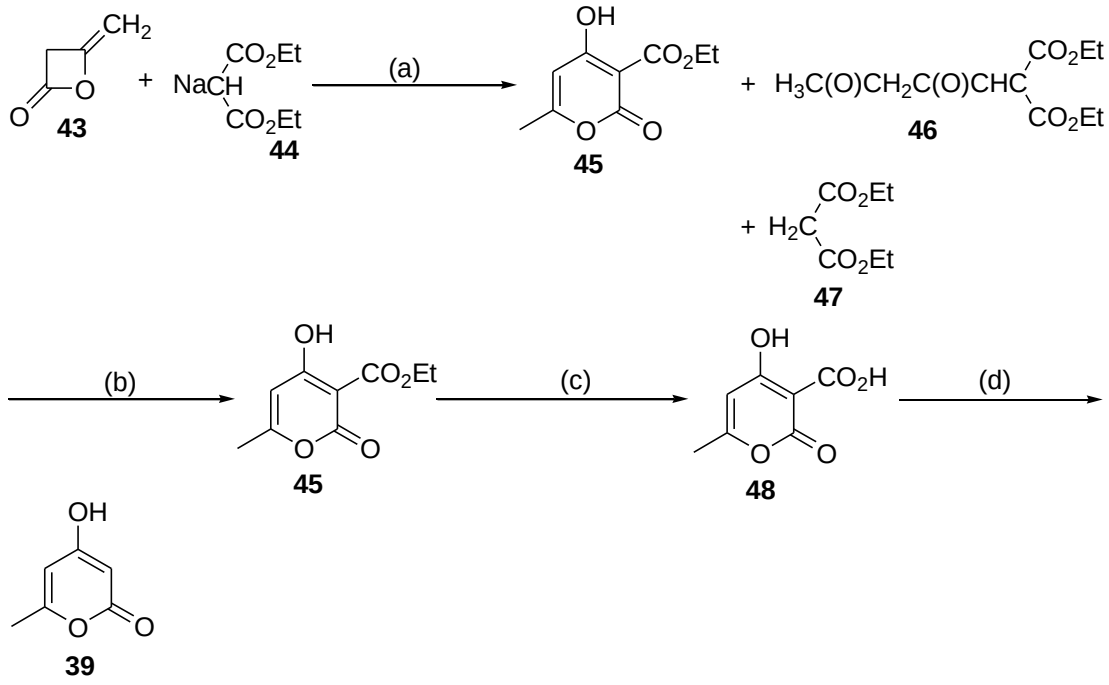
42

Figure 1.11: The molecular structure of palmitic acid **42**.

1.6 Synthetic strategies towards assembling 2-pyranone ring systems

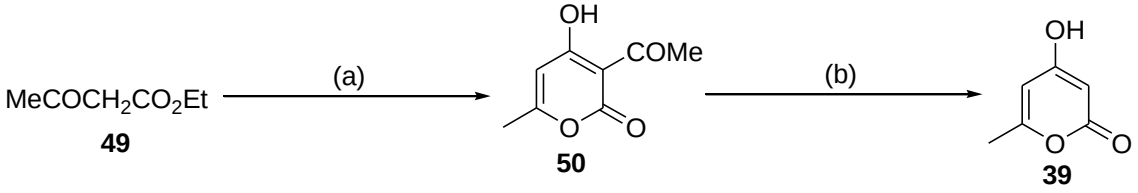
The synthesis of triacetic acid lactone **39** has also been accomplished in the laboratory using fairly simple procedures. For example, Suzuki and co-workers[48] reported the synthesis of triacetic acid lactone **39** by reacting diketene **43** with excess diethyl sodiomalonate **44** in tetrahydrofuran which afforded a mixture of pyranone ester **45**, dioxo diester **46** and diethyl malonate **47** (**Scheme 1.6**). To the surprise of the authors, the distillation of the diethyl malonate *in vacuo* effected cyclization of the dioxo diester **46** into a pyranone ester **45**. The

hydrolysis of the pyranone ester **45** followed by decarboxylation delivered the title compound **39**.



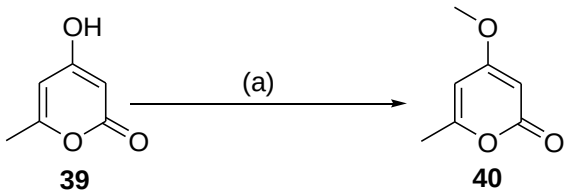
Scheme 1.6: *Reagents and conditions:* (a) (i) THF, -8 ^{o}C → rt (ii) aq. HCl (b) heat, 155 ^{o}C, 4 torr (c) (i) $Ba(OH)_2$, H_2O, 73 ^{o}C (ii) aq. HCl (d) heat, 155 ^{o}C, 5 min.

The most common and simple strategy for the synthesis of triacetic acid lactone **39** that has often been employed in laboratories is through the condensation-cyclisation of *β*-ketoesters. For example, O'Hagan demonstrated that ethyl acetoacetate **49** undergoes self-condensation in the presence of hydrogen chloride gas. This process is followed by cyclisation yielding 3-acetyl-4-hydroxy-6-methyl-2*H*-pyran-2-one **50**.[43] Deacetylation of intermediate **50** in sulfuric acid affords 4-hydroxy-6-methyl-2*H*-pyran-2-one **39** as shown in **Scheme 1.7**.



Scheme 1.7: *Reagents and conditions:* (a) HCl (g) (b) aq. H_2SO_4, heat.

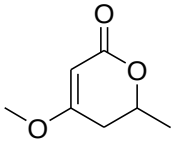
O-alkylation of triacetic acid lactone **39** is often accomplished by refluxing the pyranone in acetone with dimethyl sulfate and potassium carbonate as shown in **Scheme 1.8**.[46]



39 **40**

Scheme 1.9: *Reagents and conditions:* (a) Me_2SO_4, K_2CO_3, Me_2CO, reflux.

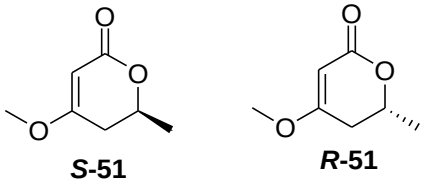
Closely related to 4-methoxy-6-methyl-2*H*-pyran-2-one **40** is 5,6-dihydro-4-methoxy-6-methylpyran-2-one ***rac*-51** (**Figure 1.12**) which is found in many natural products embedded into benzene, naphthalene or anthracene nuclei.



***rac*-51**

Figure 1.12: The molecular structure of 5,6-dihydro-4-methoxy-6-methylpyran-2-one ***rac*-51**.

Most natural products exist in an enantiomerically pure form. To mimic nature, lactones ***S*-51** and ***R*-51** (**Figure 1.13**), which are pure enantiomers of lactone ***rac*-51**, have been extensively applied in the Staunton-Weinreb annulation reaction for the synthesis of natural products.[49] Unlike lactone **39**, the hydroxyl form of lactone ***rac*-51** or its enantiomerically pure analogues (***S*-51** and ***R*-51**) have never been isolated in nature. There are many protocols that have been employed in the synthesis of 5,6-dihydro-4-methoxy-6-methylpyran-2-one as a racemate or a enantiomerically pure product.[39] Herein, we will highlight the protocols developed by Drochner and Müller in the synthesis of (*S*)-5,6-dihydro-4-methoxy-6-methylpyran-2-one ***S*-51** and (*R*)-5,6-dihydro-4-methoxy-6-methylpyran-2-one ***R*-51**.[50]

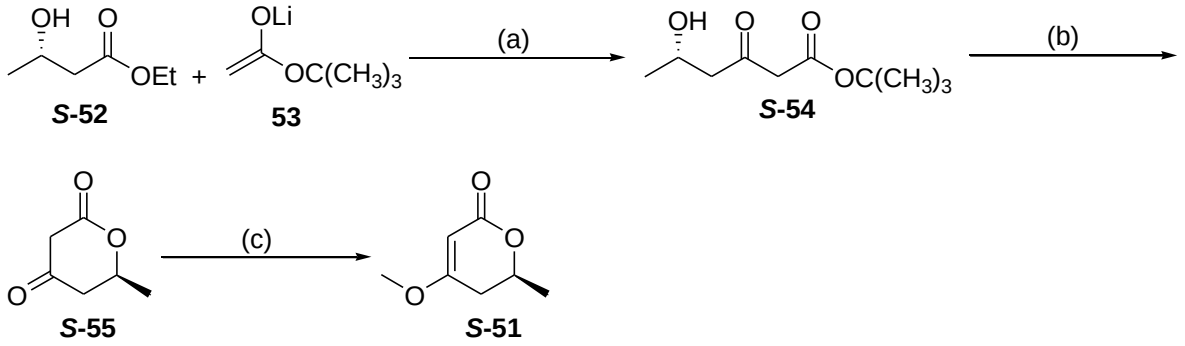


***S*-51** ***R*-51**

Figure 1.13: The molecular structures of (*S*)-5,6-dihydro-4-methoxy-6-methylpyran-2-one ***S*-51** and (*R*)-5,6-dihydro-4-methoxy-6-methylpyran-2-one ***R*-51**.

1.6.0 Synthesis of (*S*)-5,6-dihydro-4-methoxy-6-methylpyran-2-one *S*-51

In the first protocol, the synthesis of an important intermediate, *tert*-butyl (*S*)-5-hydroxy-3-oxohexanoate ***S*-54**, was achieved by Claisen condensation of *tert*-butyl acetate anion **53** and the commercially available ethyl (*S*)-3-hydroxybutanoate ***S*-52**. The resultant intermediate ***S*-54** was lactonized to pyran-2,4-dione ***S*-55** by hydrolysis with trifluoroacetic acid which was followed by *O*-methylation with dimethyl sulfate, affording the pure enantiomer of lactone ***S*-51** as shown in **Scheme 1.9**.

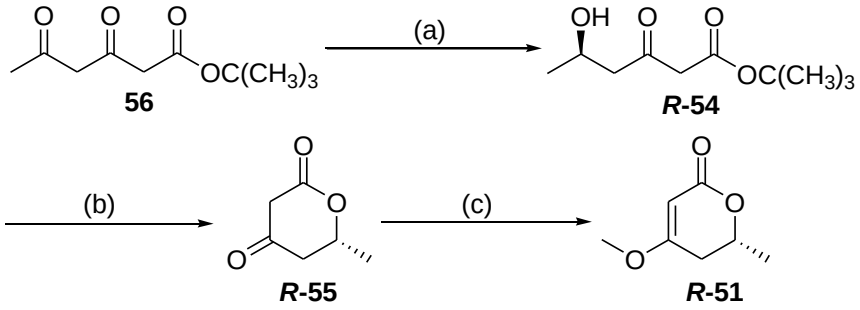


***S*-52** **53** ***S*-54** ***S*-55** ***S*-51**

Scheme 1.9: *Reagents and conditions:* (a) -78 ^{o}C, THF (b) TFA, CH_2Cl_2 (c) K_2CO_3, Me_2SO_4, Me_2CO, reflux.

1.6.1 Synthesis of (*R*)-5,6-dihydro-4-methoxy-6-methylpyran-2-one *R*-51

A slightly different protocol was employed by the same authors[50] in the synthesis of the (*R*)-isomer of lactone ***R*-51**. In this protocol, alcohol dehydrogenase from *Lactobacillus brevis* (*LB*ADH) was used for the regio- and stereo-selective enzymatic reduction of *tert*-butyl-3,5-dioxohexanoate **56** which afforded optically pure hydroxy ketone ***R*-54**. The (*R*)-hydroxy ketone ***R*-54** was then lactonized to pyran-2,4-dione ***R*-55** by hydrolysis with trifluoroacetic acid. The synthesis was completed by *O*-methylation of intermediate ***R*-55** using dimethyl sulfate which afforded lactone ***R*-51** as shown in **Scheme 1.10**.



Scheme 1.10: *Reagents and conditions:* (a) dehydrogenase (b) TFA, CH_2Cl_2 (c) K_2CO_3, Me_2SO_4, Me_2CO, reflux.

1.7 Examples of natural products with isocoumarin and 3,4-dihydroisocoumarin groups

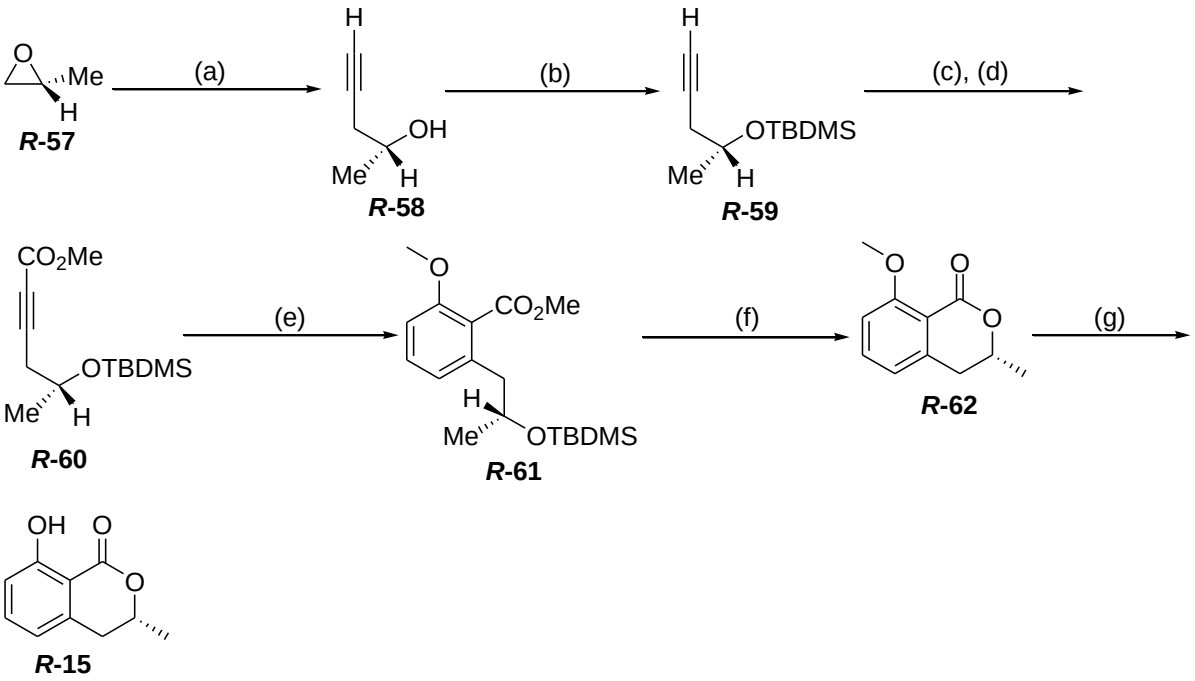
1.7.0. Isolation and synthesis of mellein [(*R*)- and (*S*)-3,4-dihydro-8-hydroxy-3-methylisochromen-1-one] *R*-15 and *S*-15

(*R*)-(-)-mellein ***R*-15** is regarded as a parent molecule of an extensive class of naturally occurring 3,4-dihydroisocoumarins which collectively display a wide range of biological activity.[14] For example, the defensive secretion of termites, Australian onerine ants, the mandibular gland secretion of *Camponotus herculeanus, C. lighiperda, C. pensylvanicus* (carpenter ants) and the male hair pencil of the oriental fruit moth, all contain (*R*)-(-)-mellein.[51] (*R*)-(-)-mellein was first isolated as a metabolite of *Aspergillus melleus*.[52] The other enantiomer, (*S*)-(+)-mellein ***S*-15**, was isolated from the marine fungus *Helicascus kanaloanus.*[53] Mellein of unspecified chirality was shown to exhibit antiviral activity as well as a distinct inhibiting activity on 3α-hydroxysteroid dehydrogenase (3α-HSD) and it was also reported to have toxic activity on coffee tree leaves and horse radish peroxidase.[54]

There are a number of procedures that have been reported in the literature for the total synthesis of both racemic and enantiomerically pure mellein[55] but in this thesis we will highlight the work carried out by Harte and co-workers.[56] These authors reported the synthesis of pure enantiomers of mellein by simply changing the chirality of the starting material, propylene oxide.

The commercially available (*R*)-propylene oxide ***R*-57** was treated with ethylenediamine complex of lithium acetylide which afforded (*R*)-pent-4-yn-2-ol ***R*-58** and silyl ether ***R*-59** upon silylation of the alcohol (**Scheme 1.11**). Metallation of intermediate ***R*-59** was followed

by exposure of the resultant acetylide anion to methyl chloroformate which delivered (*R*)-hexynoate ester ***R*-60**. The ester was then reacted with l-methoxy-l,3-cyclohexadiene, in the presence of trace amount of 2,3-dichloromaleic anhydride and *N*-phenyl-*β*-naphthylamine, which afforded a mixture consisting of benzoate ***R*-61** and unreacted ester ***R*-60**. The unreacted ester was separated from the mixture by filtration through a pad of silica gel followed by fractional distillation. Hydrolysis of the silyl ether group of benzoate ***R*-61** with subsequent lactonization of the secondary hydroxyl group afforded (*R*)-8-*O*-methylmellein ***R*-62** which is itself a natural product having been isolated from phytopathogen *Septoria nodorum*.[57] Finally, the demethylation of (*R*)-8-*O*-methylmellein ***R*-62** under acidic conditions delivered (*R*)-(-)-mellein ***R*-15** as depicted in **Scheme 1.11**.

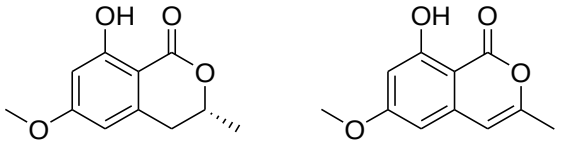


Scheme 1.11: *Reagents and conditions:* (a) $LiC{\equiv}CH{:}H_2N(CH_2)_2NH_2$ complex, DMSO, 0 °C → rt, 16 hrs (b) TBDMSCl, imidazole, DME, rt, 16 hrs (c) (i) *n*-BuLi, -78 °C, 30 min (d) $ClCO_2Me$, -78 °C → rt, 2 hrs (e) l-methoxy-1,3-cyclohexadiene, dichloromaleic anhydride, *N*-phenyl-13-naphthylamine, sealed tube, 185 °C, 26 hrs (f) *p*-TsOH, CH_2C1_2, rt, 25 hrs (g) HBr, AcOH, reflux, 4 hrs.

In a completely analogous fashion, Cotterill and co-workers reported transforming the commercially available (*S*)-propylene oxide ***S*-57** to (*S*)-(+)-mellein ***S*-15**.[58]

1.7.1 Isolation and synthesis of 8-hydroxy-6-methoxy-3-methylisocoumarin 63

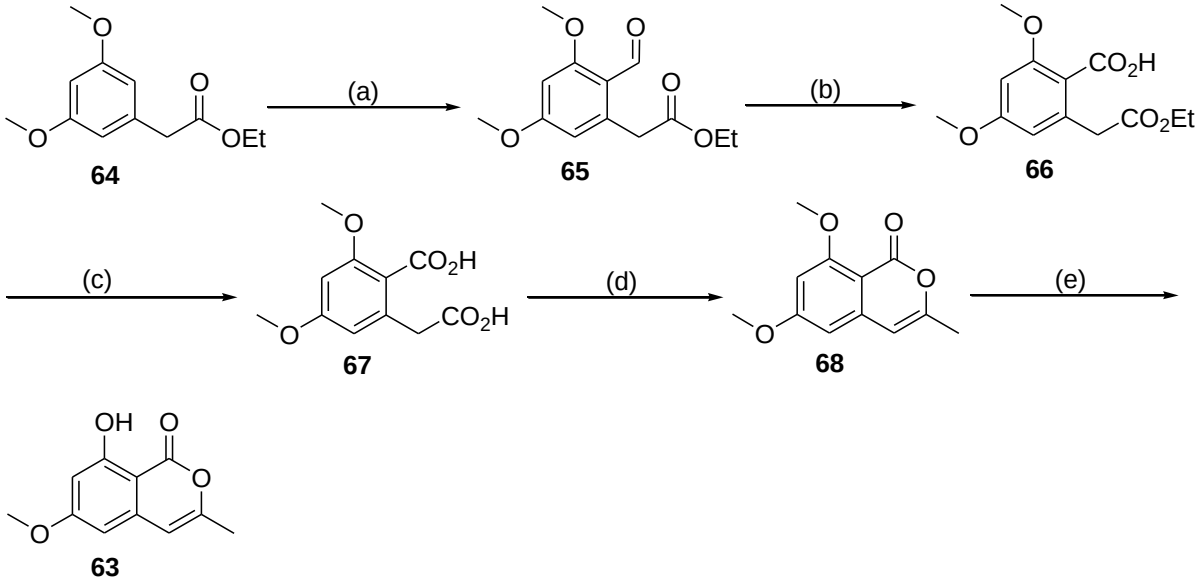
Similar to (*R*)-6-methoxymellein ***R*-16** is 8-hydroxy-6-methoxy-3-methylisocoumarin **63** which was isolated from the phytopathogenic fungus *Certacystis fimbriata* in 1969[59] and *Streptomyces mobaraensis* in 1971.[60] The structure of the compound was assigned on the basis of spectroscopic and degradation evidence. Unlike (*R*)-6-methoxymellein ***R*-16**, 8-hydroxy-6-methoxy-3-methylisocoumarin **63** has a double bond in its pyranone ring system as shown in **Figure 1.14**.



***R*-16** **63**

Figure 1.14: The molecular structures of 6-methoxymellein ***R*-16** and 8-hydroxy-6-methoxy-3-methylisocoumarin **63**.

The total synthesis of 8-hydroxy-6-methoxy-3-methylisocoumarin **63** was accomplished by Saeed and Rama.[61] The first step in the synthesis was achieved by subjecting ethyl 3,5-dimethoxyphenylacetate **64** to Vilsmeier Haack formylation conditions which afforded ethyl-2-formyl-3,5-dimethoxyphenylacetate **65** as shown in **Scheme 1.12**. The intermediate **65** was subsequently oxidised to ethyl 2-carboxy-3,5-dimethoxyphenylacetate **66** by potassium permanganate. The alkaline hydrolysis of ester **66** delivered 3,4-dimethoxyhomophthalic acid **67** and direct condensation of this acid with acetic anhydride yielded 6,8-dimethoxy-3-methylisocoumarin **68**. The final step in the protocol involved the selective demethylation of lactone **68** which delivered 8-hydroxy-6-methoxy-3-methylisocoumarin **63**.



Scheme 1.12: (a) $POCl_3$, 24 hrs, rt (b) $KMnO_4$, acetone (c) 5% aq. NaOH, MeOH, 1 hr (d) Ac_2O, reflux, 24 hrs (e) BCl_3, CH_2Cl_2, N_2 (g).

1.7.2 Isolation, bioactivity studies and synthesis of 6-*O*-methylreticulol (8-hydroxy-6,7-dimethoxy-3-methylisocoumarin) 69

6-*O*-methylreticulol **69** (**Figure 1.15**) is a naturally occurring isocoumarin isolated from an endophytic fungus which grows on the mangrove plant *Avicennia marina* in the Pearl River Estuary of Southern China. It is also a metabolite of fungus *Streptomyces mobaraensis* and S*treptoverticillium*.[62] There are also reports that isocoumarin **69** has also been found in liverworts *Wettsteinia schusterana* and *Wettsteinia inversa*.[63] The parent molecule, Reticulol **70**, is itself a natural product and was first isolated from *Streptomyces rubrireticulae*.[64] It was later found to co-exist with 6-*O*-methylreticulol **69** in *Streptomyces mobaraensis* and *Streptoverticillium* sp. NA-4803.[64] Reticulol **70** along with 6-*O*-methylreticulol **69** and 8-*O*-methylreticulol **71** (**Figure 1.15**) were isolated from a culture of *Actinomyces sp. Stamm K17/9*.[75]

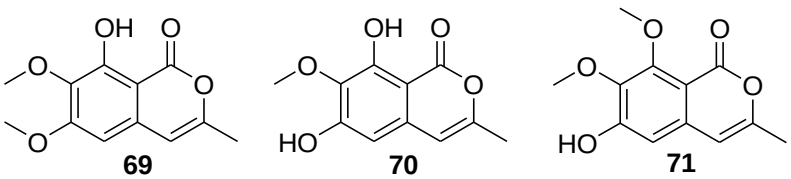
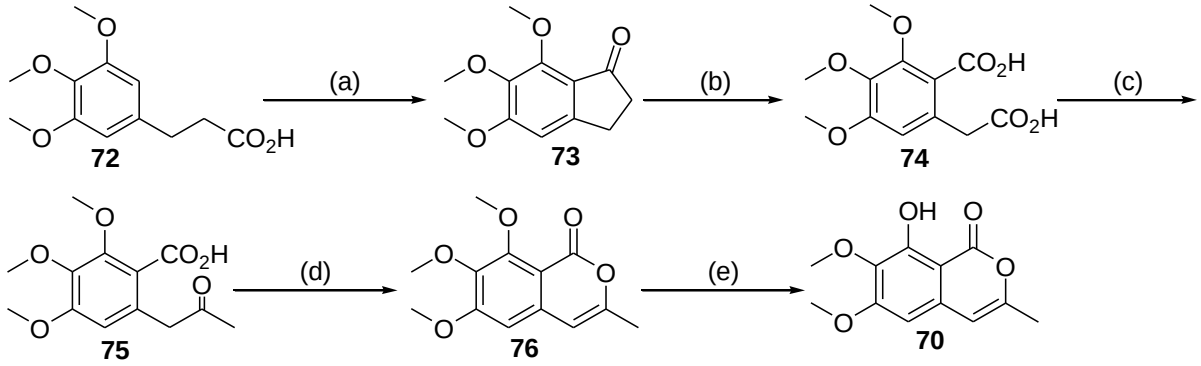


Figure 1.15: The molecular structures of 6-*O*-methylreticulol **69**, reticulol **70** and 8-*O*-methylreticulol **71**.

The majority of bioactivity studies have been carried out on reticulol **70**. Reticulol was reported to be an inhibitor of cyclic adenosine 3',5'-monophosphate phosphodiesterase[66] and an effective antitumor agent against melanoma B16F10.[67] It has also been reported that reticulol blocks the replication and/or transcription of DNA by inactivating topoisomerase I (Topo I) which is involved in tumor metastasis.[67] Reticulol **70** showed an inhibitory effect similar to that of camptothecin, which is a known Topo I inhibitor. In addition, the *in vivo* antitumor efficacy of reticulol was reported to be excellent at a concentration of approximately 10 mg/kg. In particular, a mixture of 5 mg/kg reticulol and 1 mg/kg doxorubicin (adriamycin) exhibited strong antitumor efficacy, which was not shown at a concentration of 1 mg/kg doxorubicin alone.[68]

The synthesis of 6-*O*-methylreticulol **69** was accomplished by Saeed and Ehsan.[68] In this protocol, the commercially available 3-(3,4,5-trimethoxyphenyl)propionic acid **72** was subjected to a cyclodehydration reaction using polyphosphoric acid (PPA) which afforded 5,6,7-trimethoxy-1-indanone **73** as depicted in **Scheme 1.13**. A toluene solution of indanone **73** and diethyl oxalate was then treated with a suspension of sodium methoxide which was followed by the addition of potassium hydroxide and 30% hydrogen peroxide. This concoction furnished 3,4,5-trimethoxyhomophthalic acid **74**. The reaction of homophthalic acid **74** with acetic anhydride in dry pyridine afforded 2,3,4-trimethoxy-6-(2-oxopropyl)benzoic acid **75** and cyclodehydration reaction of this intermediate yielded 6,7,8-trimethoxy-3-methylisocoumarin **76**. The regioselective demethylation of isocoumarin **76** using boron tribromide under mild conditions delivered 8-hydroxy-6,7-dimethoxy-3-methylisocoumarin **70**.



Scheme 1.13: *Reagents and conditions:* (a) PPA, 90 °C, 2 hrs (b) (i) $(EtO_2C)_2$, NaOMe, PhMe (ii) *30%* H_2O_2, KOH, MeOH (c) Ac_2O, pyridine, dry Et_2O, overnight, rt (d) Ac_2O, 2 hrs, reflux (e) BBr_3, dry CH_2Cl_2, -78 °C (20 min) then rt, 30 min.

1.7.3 Isolation and bioactivity studies of semivioxanthin *R*-77 and *S*-77

Semivioxanthin was first isolated from the culture filtrate of *Penicillium citreoveride* and its absolute configuration at *C*-3 of the pyranone ring was assigned as (*R*). This assignment was made on the basis of the correlation of its circular dichroism curve with that of (*R*)-mellein ***R*-15**.[69] The IUPAC name for (*R*)-semivioxanthin is given as (*R*)-3,4-dihydro-9,10-dihydroxy-7-methoxy-3-methylbenzo[*g*]isochromen-1-one. (*R*)-Semivioxanthin ***R*-77** (**Figure 1.16**) was also isolated from the *Aspergillus ochraceus LCJ11-102*, the endophytic fungus *Aspergillus sp. HS-05*, the leaves of *Huperzia serrata* and the capitulae of the plant *Eriocaulon buergerianum*.[70] Both of its enantiomeric forms occur in nature with the (*S*)-isomer ***S*-77** (**Figure 1.16**) isolated from the *Cryptospirosis abietina* which is the fungus responsible for stem canker of the Hinoki cypress in Japan and from a culture of *Penicillium janthinellum*.[71]

The (*S*)-semivioxanthin ***S*-77** showed abscisic activity against Hinoki cypress leaves and inhibited spore germination of the fungus *Cladosporium herbarum*.[72] Semivioxanthin (of unspecified stereochemistry) isolated from an unidentified marine-derived fungus showed immune stimulatory effects resulting from promotion of tumor necrosis factor (TNF)-α production through nuclear factor (NF)-κB and mitogen-activated protein kinase (MAPK) signalling pathways. Both enantiomers were reported to have antifungal and defoliant activity.[72]

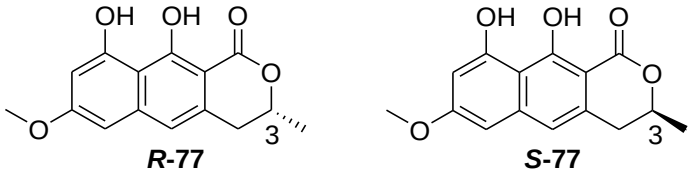
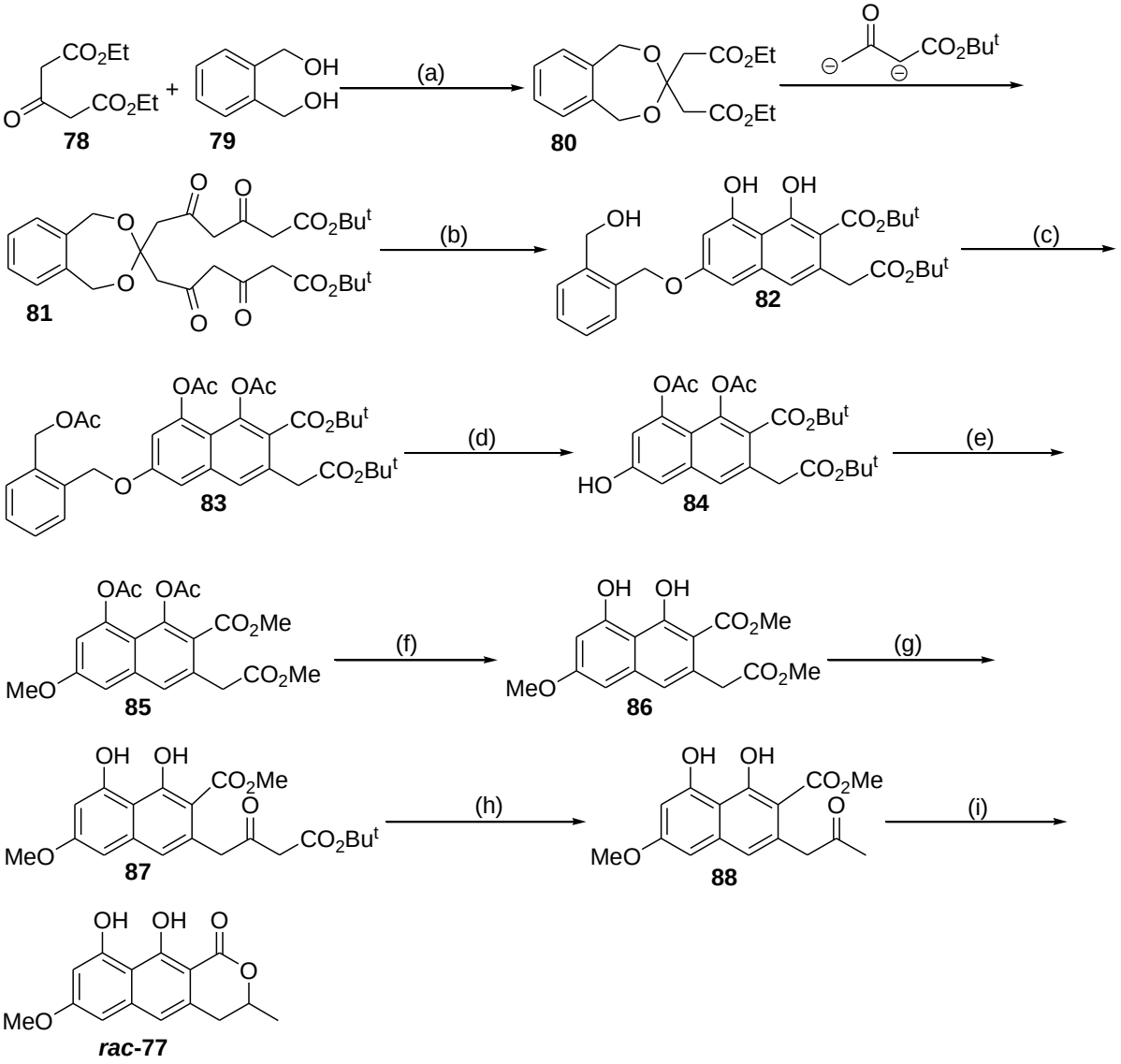


Figure 1.16: The molecular structures of (*R*)-semivioxanthin ***R*-77** and (*S*)-semivioxanthin ***S*-77**.

1.7.3.0 Synthesis of semivioxanthin *rac*-77 using biomimetic protocol

The first synthesis of racemate semivioxanthin ***rac*-77** was reported by Yamaguchi and co-workers[73] who used polyketide methodology to construct the naphthalene nucleus. In this protocol, diethyl 3-oxopentanedioate **78** was heated to reflux with diol **79** in the presence of toluene-*p*-sulfonic acid (PTS) in benzene which furnished ketal **80** (**Scheme 1.14**). The Claisen condensation of ketal **80** with *tert*-butyl acetoacetate dianion afforded the polyketide **81**. This was followed by the intramolecular condensation which was achieved by treating polyketide **81** with caesium acetate furnishing diester **82**. The acetylation of the three hydroxyl groups of this ester yielded intermediate **83**. The intermediate **83** was then subjected to selective deprotection by hydrogenation using palladium on charcoal which delivered naphthol **84**. The naphthol **84** was subsequently converted into the dimethyl ester by an ester exchange reaction which was accompanied by methylation of the resultant intermediate, affording naphthalene **85**. The successful methylation of the naphthol group of naphthalene **84** was followed by deacetylation of the two acetate groups which yielded naphthalenediol **86**. The selective Claisen condensation at the α-position of the naphthalenediol **86** with lithiated *tert*-butyl acetate gave the keto ester **87**. The successful condensation of intermediate **86** was followed by selective saponification of the *tert*-butyl ester and decarboxylation of the resultant carboxylic acid intermediate which yielded the methyl ketone **88**. Finally, the ketone intermediate was subjected to the ring forming reaction conditions using sodium borohydride which furnished racemic semivioxanthin ***rac*-77**.

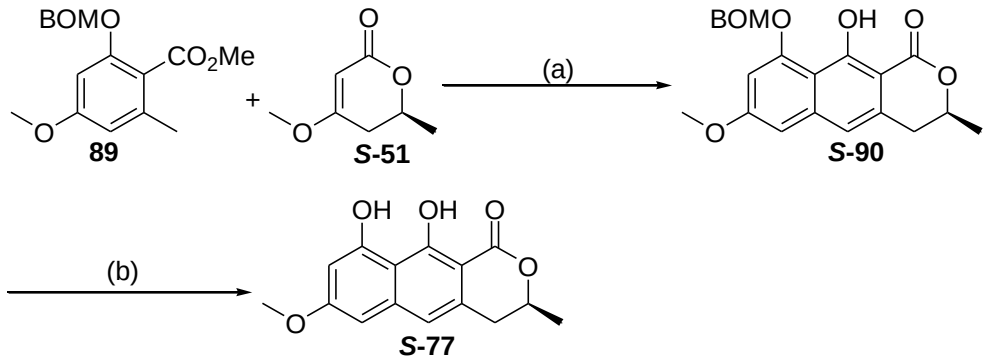


Scheme 1.14: *Reagents and conditions:* (a) PTS, benzene, reflux (b) $Ca(OAc)_2$ (c) Et_3N, Ac_2O (d) Pd/C, H_2 (g), EtOH, HCO_2H (e) (i) TFA (ii) CH_2N_2 (f) K_2CO_3, MeOH (g) LDA, $CH_3CO_2Bu^t$ (h) TFA, reflux (i) $NaBH_4$, MeOH.

1.7.3.1 Synthesis of enantiomerically pure semivioxanthin S-77 using Staunton-Weinreb annulation

Drochner and Müller reported the synthesis of both enantiomers of semivioxanthin in their single enantiomeric form using Staunton-Weinreb annulation reaction (tandem Michael-Dieckmann reaction) as a key step in the protocol.[50] The isocoumarin system of the (*S*)-enantiomer ***S*-77** was built up through the tandem Michael-Dieckmann reaction of orsellinate **89** with pyranone ***S*-51** (**Scheme 1.15**). In this methodology, orsellinate **89** was deprotonated

with lithium diisopropylamide (LDA) at -78 °C which afforded the corresponding toluate anion intermediate. The generated nucleophile attacked the pyranone ***S*-51** in an exclusively 1,4-addition which afforded an enolate intermediate. The enolate then attacked the carbonyl carbon of the methyl ester which led to the formation of the desired ring system ***S*-90**, after warming to room temperature. The selective cleavage of the benzyloxymethyl (BOM) group of intermediate ***S*-90** was achieved by hydrogenolysis with palladium on charcoal under a hydrogen atmosphere at ambient pressure which delivered (*S*)-semivioxanthin ***S*-77**. The same procedure was used with pyranone ***R*-51** replacing ***S*-51** which afforded (*R*)-semivioxanthin ***R*-77**.



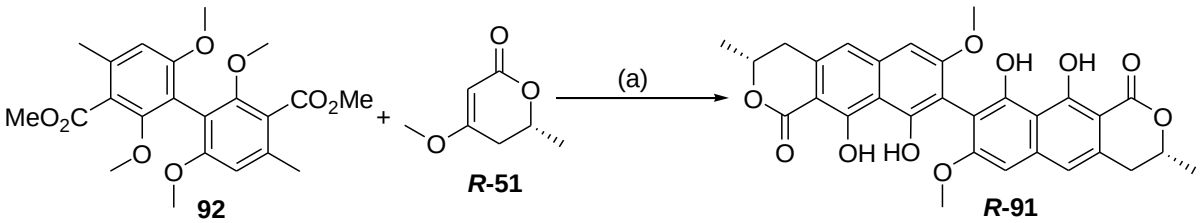
Scheme 1.15: *Reagents and conditions:* (a) (i) LDA, -78 ^{o}C → rt (ii) EtOH, THF (b) Pd/C, H_2 (g), rt.

1.7.4 Isolation, bioactivity studies and synthesis of (*R*)-vioxanthin *R*-91

The biarylic dihydronaphthopyranone (*R*)-vioxanthin ***R*-91** was first isolated by Blank and co-workers from the pathogenic fungus *Trichophyton violaceum*.[74] It was later isolated by Zeeck and co-workers from *Penicillium citreoviride* together with the monomeric compound (*R*)-semivioxanthin ***R*-77**.[69] Zeeck and co-workers determined the absolute configuration of the pyranone ring as (*R*) by comparison of its circular dichroism spectrum with that of (*R*)-mellein ***R*-15**. The stereochemistry of the compound was later confirmed by Bode and co-workers.[75] (*R*)-Vioxanthin has also been isolated from *Penicillium aurantiogriseum* obtained from cereal samples, *Aspergillus ochraceus* and the thermophilic fungus *Malbranchea pulchella var. sulfurea* isolated from compost.[76] There are several reports about the bioactivity of (*R*)-vioxanthin ***R*-91**. In a study by Teixeira on (*R*)-vioxanthin, paepalantine and 8,8'-paepalantine dimer, it was found that vioxanthin was the most potent against human

kallikrein 5 with an IC_{50} value of 53.7 µM, followed by the 8,8'-paepalantine dimer with an IC_{50} value of 72.9 µM. Paepalantine showed the least activity with an IC_{50} value of 367.4 µM.[76] Human kallikrein 5 and 7 (KLK5 and KLK7) are trypsin- and chymotrypsin-like serine proteases, respectively, and promising targets for the treatment of skin desquamation, inflammation and cancer.[76] In another study, (*R*)-vioxanthin ***R*-91** was shown to be highly active against Gram-positive bacteria and strictly anaerobic Gram-negative bacteria with an MIC range of 0.045-1.56 µg/mL.[41]

The synthesis of (*R*)-vioxanthin ***R*-91** was achieved by Zeeck and co-workers who used the dimeric orsellinate **92** in a typical tandem Michael-Dieckmann reaction as shown in **Scheme 1.16**. In this methodology, the dimeric orsellinate was condensed twice with the Michael acceptor ***R*-51**. This reaction was followed by selective demethylation of the resultant intermediate which delivered vioxanthin ***R*-91**.[69]

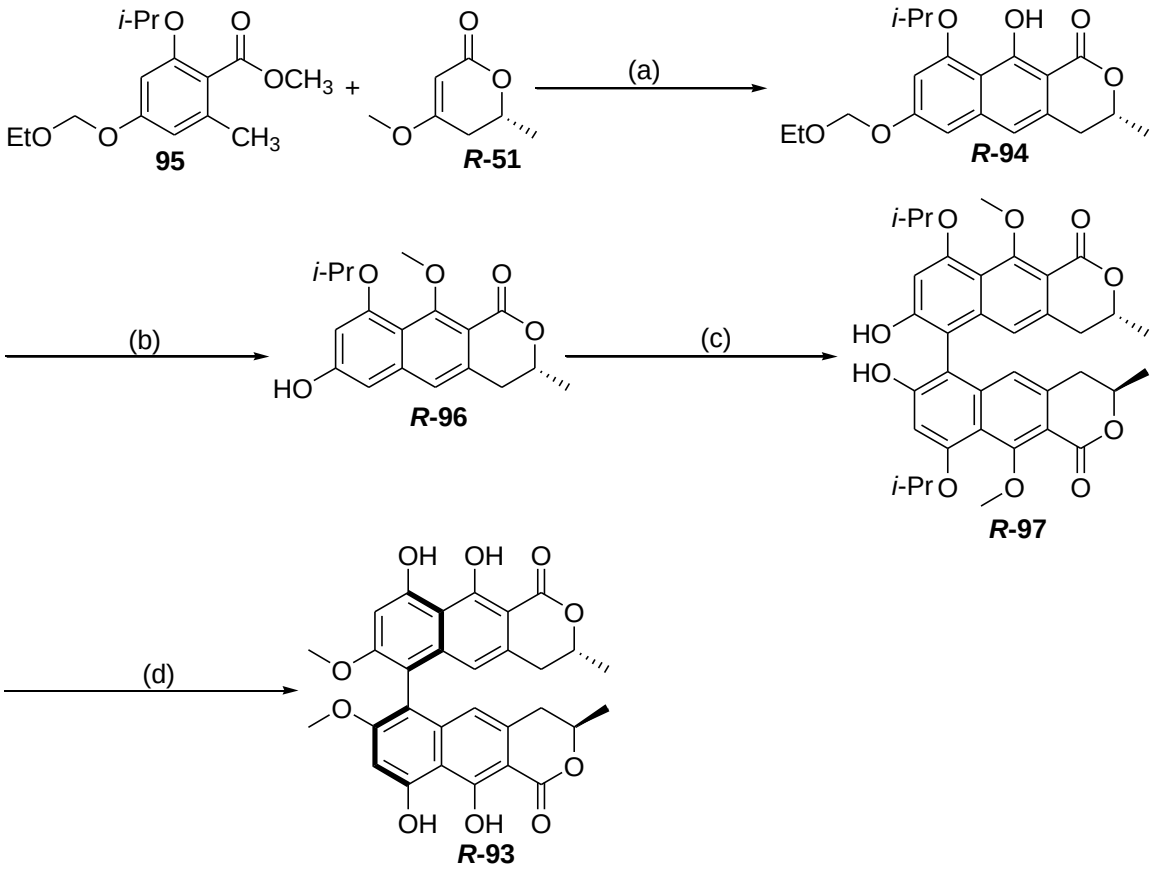


Scheme 1.16: *Reagents and conditions:* (a) (i) LDA, -78 ^{o}C → rt, THF (ii) BBr_3, CH_2Cl_2, rt.

1.7.5 Isolation, bioactivity studies and synthesis of pigmentosin A *R*-93

Pigmentosin A ***R*-93**, a 6,6'-binaphthopyranone, was isolated from the lichen *Hypotrachyna immaculata*[77] collected in Australia. The structure of the compound was established using 1D and 2D NMR spectroscopy. The regio-isomers, pigmentosin A ***R*-93** and (*R*)-vioxanthin ***R*-91**, were isolated as co-metabolites in the lichen *Hypotrachyna toiana* found in Malaysia.[78] The stereoselective synthesis of pigmentosin A by Grove and co-workers played a crucial role in establishing the absolute stereochemistry of this compound.[79] Preliminary biological studies by the same authors showed that the synthetic pigmentosin A ***R*-93** inhibited the growth of *Bacillus subtilis* with an MIC value of 20 µM. In addition, the *in vivo* studies of pigmentosin A in mice, administered in increasing doses, revealed that dimer ***R*-93** is significantly less toxic to mice than (*R*)-vioxanthin ***R*-91**.[79]

The synthesis of pigmentosin A ***R*-93** was reported alongside the synthesis of talaroderxine A and its diastereomer talaroderxine B. The key intermediate ***R*-94** was synthesized by a Staunton-Weinreb annulation reaction of a protected orsellinate ester **93**, with the requisite enantiomerically pure pyranone ***R*-51** (**Scheme 1.17**) The pyranone ***R*-51** was accessed by a variant of Ghosez's sulfone-epoxide annulation reaction. The choice of orsellinate ester **95** was in such a way that it delivered naphthol ***R*-96** with the naphthol substituent in the correct position to act as a handle in assembling the binaphthyl ring system ***R*-97** using a vanadium catalyst. The authors reported that the choice of the catalyst was crucial in ensuring that the correct configuration of the biaryl ring system was assembled. The last step in this protocol involved methylation and selective demethylation which delivered pigmentosin A ***R*-93**.

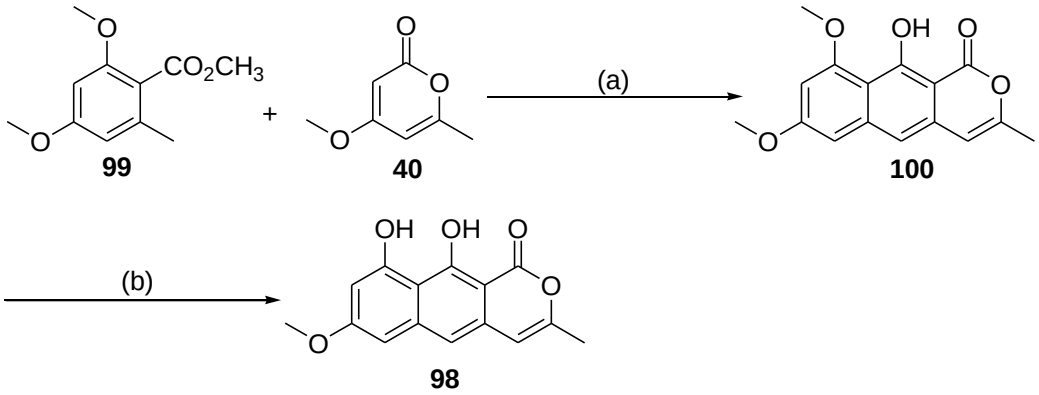


Scheme 1.17: *Reagents and conditions:* (a) (i) LDA, THF, -78 ^{o}C → 23 ^{o}C, overnight (ii) DDQ, benzene, 2 hrs (b) (i) K_2CO_3, Me_2SO_4, acetone, overnight (ii) 3 M aq. HCl, MeOH, 60 ^{o}C, 2 hrs (c) *20%* mole $VO(acac)_2$, CH_2Cl_2, 16 hrs (d) (i) Me_2SO_4, K_2CO_3, Me_2CO, reflux (ii) BCl_3, CH_2Cl_2, HPLC separation.

1.7.6 Isolation and bioactivity studies of toralactone 98

Toralactone **98** was first isolated in 1973 as a constituent of the seeds of *Cassia tora Leguminosae*.[80] It was later isolated from *Cassia obtusifolia Leguminosae* and was also found as a metabolite in a cultivated mycobiont of the *lichen Pyrenula sp*.[81] *Cassia tora Leguminosae* is widely distributed in tropical Asian countries and its seeds are reputed in oriental medicine as vision-improving, anti-asthenic, asperient and diuretic agents.[81a] *C. tora* seeds have also been shown to possess other biological and pharmacological activities such as antihepatotoxic, anti-allergic, antimutagenic, antifungal and radical scavenging activities.[82]

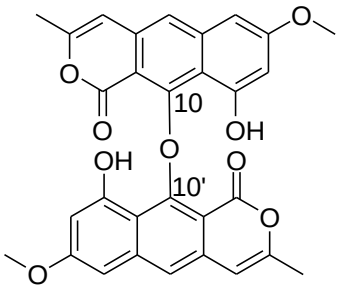
The first synthesis of toralactone was unexpectedly achieved by Staunton and co-workers in what has become to be known as the Staunton-Weinreb protocol.[83] In this methodology, the orsellinate **99** was deprotonated by lithium diisopropylamide and the resultant toluate anion was reacted with pyranone **40** in a tandem Michael-Dieckmann annulation reaction at low temperatures (**Scheme 1.18**). The reaction mixture was then warmed to room temperature and subjected to an acidic workup which afforded the desired 9-*O*-methyltoralactone **100**. The selective demethylation using boron tribromide afforded toralactone **98**. The versatility of this protocol was exemplified by Zhang and Yu who assimilated it in the synthesis of biologically important molecule, toralactone cassiaside C_2.[84]



Scheme 1.18: *Reagents and conditions:* (a) 2.0 equiv. LDA, THF, -78 °C → rt then aq. HCl (b) BBr_3, CH_2Cl_2, rt.

1.7.7 Isolation and bioactivity of eriocauline 101

The dimeric compound containing a pyranone skeleton, eriocauline **101** (**Figure 1.17**), is a yellow amorphous solid and a *C*-10/*C*-10' ether-linked dimer of toralactone. This compound was isolated from the dichloromethane extracts from capitulae of *Eriocaulon ligulatum* (VELL.) L. B. SMITH. *Eriocaulon ligulatum* is an ornamental flower exported to Europe, Japan and North America from Minas Gerais State in Brazil.[85] The structure of the compound was identified using spectroscopic methods (1D and 2D NMR spectroscopy and HRESI-MS) and whilst not possessing an asymmetric centre, the circular dichroism and specific rotation data of the compound suggested that it displayed atropisomerism.



101

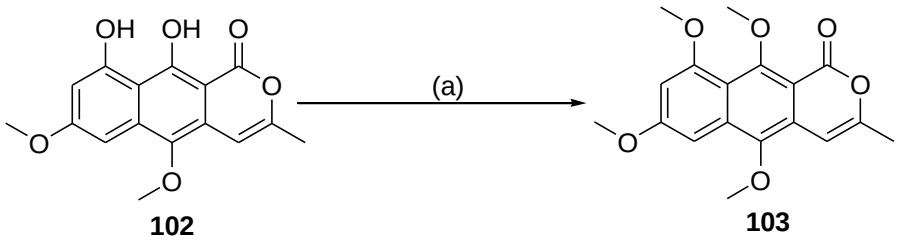
Figure 1.17: The molecular structure of eriocauline **101**.

The dichloromethane extract from *E. ligulatum*, in which there is a prevalence of eriocauline **101**, showed mutagenic activity (Ames test) against the TA98 strain of *Salmonella typhimurium*.[85] To the best of our knowledge, there is no report about the total synthesis of this compound.

1.7.8 Isolation and bioactivity studies of paepalantine (9,10-dihydroxy-5,7-dimethoxy-3-methyl-1*H*-naphtho[2,3-*c*]pyran-1-one) 102

The related monomer, paepalantine **102**, was first isolated from the methylene chloride extract of the capitulae of *Paepalanthus bromelioides* (Eriocaulaceae), a widespread species used in traditional medicine in some Brazilian regions.[86] This isocoumarin was later isolated from *Paepalanthus vellozioides*.[87] The structure of paepalantine **102** was established by means of the spectral data of the natural product and its derivatives. One such derivative was a methylated lactone **103** which was obtained by methylation of the naturally available

paepalantine **102** as shown in reaction **Scheme 1.19**. However, to the best of our knowledge, there is no report on the total synthesis of paepalantine **102**.



102 **103**

Scheme 1.19: *Reagents and conditions:* (a) Me_2SO_4, K_2CO_3, Me_2CO, reflux.

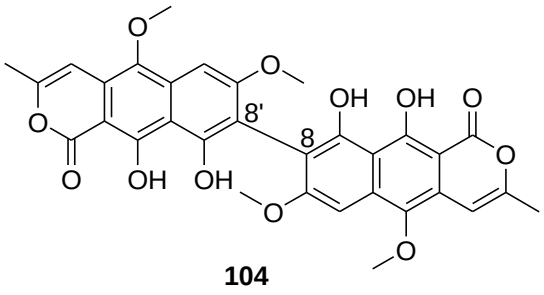
The bioactivity of paepalantine **102** has been extensively studied with the most recent research paper being published in 2017.[88] Vilegas and co-workers[86] reported that paepalantine **102** showed mutagenic activity against *Salmonella typhimurium* TA98, TA100 and TA102. The same authors also reported that paepalantine showed activity against Chinese hamster ovary (CHO) cell cultures, as well as cytotoxicity to McCoy cells. This isocoumarin is further reported to have shown antimicrobial activity in *in vitro* experiments with the minimum inhibitory concentrations (MIC) of 7.5, 7.5, 15 and 250 µg/mL against *Bacillus cereus* ATCC 14579, *Staphylococcus aureus* ATCC 6538, *S. epidermidis* ATCC 12228 and *Escherichia coli* ATCC 25922, respectively.[87] Paepalantine **102** also displayed potent cytotoxic activity *in vivo* in Wistar rat bone marrow cells and *in vitro* against human blood lymphocytes.[89] Furthermore, it showed preventative intestinal anti-inflammatory activity when tested in the trinitrobenzenesulfonic acid (TNBS) model of rat colitis. The activity was attributed to an improvement in the colonic oxidative status by preventing glutathione depletion. In addition, the intestinal anti-inflammatory effectiveness of this lactone was associated with an inhibition of colonic nitric oxide activity which is up regulated as a consequence of the inflammatory process.[90]

A more recent study by Damasceno and co-workers[88] revealed that paepalantine **102** exhibited significant antibacterial property against *Helicobacter pylori* with a minimum inhibitory concentration of 128 µg/mL and minimum bactericidal concentration (MBC) of 256 µg/mL. The *H. pylori* bacterium is one of the main causes of chronic gastritis, peptic ulcers and gastric cancer and is classified as a group 1 carcinogen by the International

Agency for Research on Cancer (IARC).[91] Scanning electron microscopy (SEM) revealed significant morphological changes in the bacterial cell as a response to a sub-micromolar concentration of paepalantine, which was said to be suggestive of a penicillin-binding protein (PBP) inhibition. These results were confirmed by computational studies which were carried out by the same authors when studying the binding modes for paepalantine in PBP binding sites.

1.7.9 Isolation and bioactivity studies of 8,8'-paepalantine dimer 104

8,8' Paepalantine dimer **104** (**Figure 1.18**) as the name suggests is a *C*-8/*C*-8' carbon-linked dehydro dimer of paepalantine. It was isolated from the methylene chloride extract of the capitulae of *Paepalanthus bromelioides* by chromatographic procedures and was identified by 1D and 2D NMR spectroscopy.[92]



104

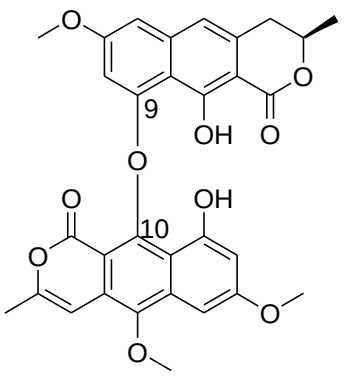
Figure 1.18: The molecular structure of 8,8'-paepalantine dimer **104**.

Coelho and co-workers reported that paepalantine dimer **104** is active against the McCoy cell line (ATCC CRL-1696) with an IC_{50} value of 55.9 µM in a colorimetric assay for toxicity.[92] In a study carried out by Teixeira and co-workers,[76] it was reported that the enzymatic inhibition assay of 8,8'-paepalantine dimer was active against human kallikrein 7 with an IC_{50} value of 112.4 µM. The docking studies by the same authors showed the competitive inhibition of this dimer with a K_i value of 12.2 µM. In a separate study, Devienne and co-workers reported assessing the anti-oxidant activity of dimer **104** alongside paepalantine **102** and (*R*)-vioxanthin ***R*-91** using isolated rat liver mitochondria and non-mitochondrial systems. It was found during this study that paepalantine **102** and 8,8'-paepalantine dimer **104** were effective at scavenging both 1,1-diphenyl-2-picrylhydrazyl ($DPPH^+$) and superoxide anion radicals ($O_2^{-\cdot}$) in non-mitochondrial systems. The scavenging property of the two

isocoumarins effectively protected the mitochondria from the *tert*-butylhydroperoxide-induced hydrogen peroxide accumulation and Fe(II)-citrate-mediated mitochondrial membrane lipid peroxidation, with almost the same potency as quercetin. The strong anti-oxidant action of paepalantine **102** and 8,8'-paepalantine dimer **104** were reproduced in liver hepatocellular carcinoma (HepG2) cells exposed to oxidative stress conditions induced by hydrogen peroxide.[93] The total synthesis of this dimer is yet to be achieved.

1.7.10 Isolation and bioactivity studies of planifolin 105

The ether bridged pyranonaphthoquinone, planifolin **105** (**Figure 1.19**), is a yellow solid which was isolated from a methylene chloride extract of the capitulae of *Paepalanthus planifolius* and its structure was determined by chemical and spectroscopic methods. *P. planifolius* Koern. (Eriocaulaceae) known as "sempre-viva" ("everlasting plant"), belongs to the sub-genus *Platycaulon*.[94] The molecule is made up of two monomeric portions of (*R*)-semivioxanthin ***R*-77** and paepalantine **102**, linked by an ether bond at the 9,10-position, respectively.



105

Figure 1.19: The molecular structure of planifolin **105**.

In a study to assess its cytotoxicity, planifolin showed significant *in vitro* cytotoxicity against McCoy cell lines with a cytotoxicity index (CI_{50}) value of 12.83 µg/mL. This value was better than the cytotoxicity index of cisplatin which was measured at 41.9 µg/mL under the same assay conditions.[95] It also showed mutagenic activity against *Salmonella typhimurium* strains TA100, TA98 and TA97a which was attributed to planifolin causing mutations by

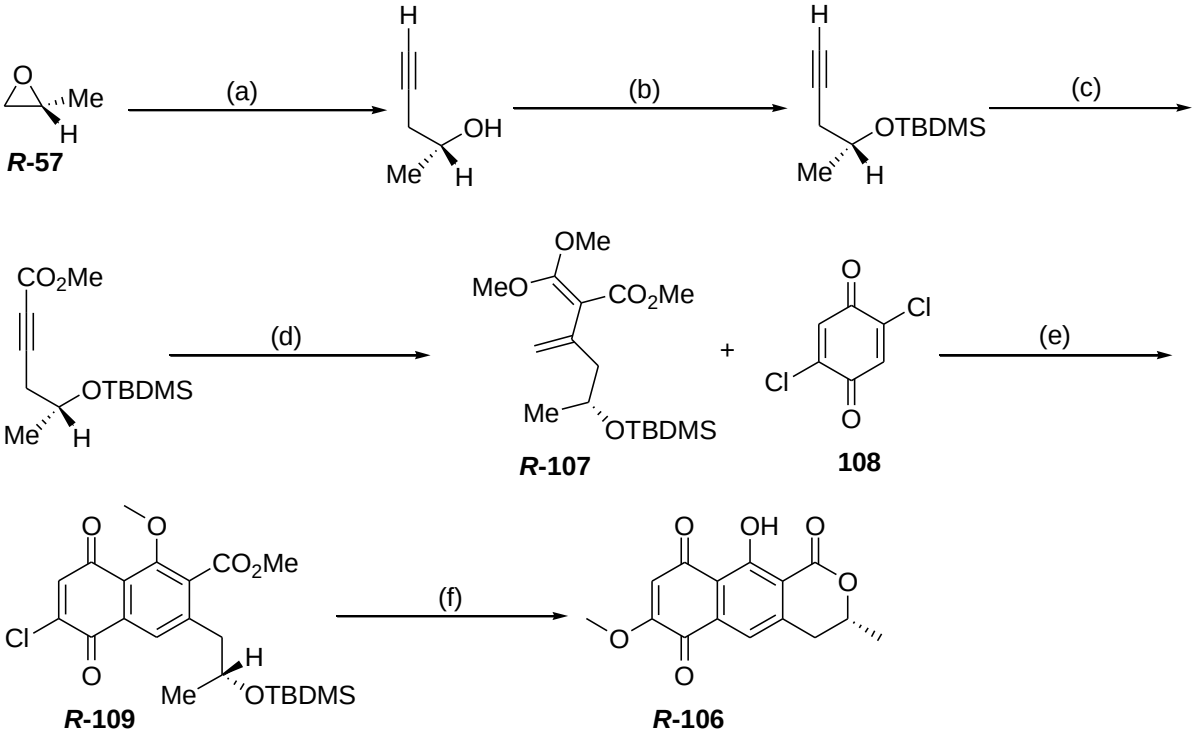
substitution, addition and deletion of bases in the DNA sequence.[95] To the best of our knowledge, there are no reports on the total synthesis of planifolin **105**.

1.8 Examples of natural products containing quinone functionalities

1.8.0 Isolation, bioactivity studies and synthesis of (*R*)-semixanthomegnin *R*-106

A simple natural product, (*R*)-semixanthomegnin ***R*-106**, was isolated as a metabolite in *Eriocaulon buergerianum* and it has recently been found in *Trichophyton megnini* and *Penicillium citreoviride*.[96] This pyranonaphthoquinone showed activity against a strain of *Staphylococcus aureus* with an MIC value of 64 μg/mL.[41]

Cotterill and co-workers[97] reported the total synthesis of (*R*)-semixanthomegnin starting from (*R*)-propylene oxide ***R*-57**. Some of the intermediates used in this protocol were similar to those used by the same authors in the synthesis of (*R*)-mellein ***R*-15** shown in **Scheme 1.11**. Thus, (*R*)-propylene oxide ***R*-57** was transformed over four steps to diene ***R*-107** which was then subjected to Diels-Alder cycloaddition reaction with 2,5-dichlorobenzoquinone **108** yielding, after aromatisation, the chloronaphthoquinone ***R*-109** (**Scheme 1.20**). The tandem nucleophilic substitution of the chloride substituent with a methoxide group, desilylation and lactonization afforded a lactone intermediate which upon demethylation with boron trichloride delivered (*R*)-semixanthomegnin ***R*-106**.



Scheme 1.20: *Reagents and conditions;* (a) $LiC{\equiv}CH{:}H_2N(CH_2)_2NH_2$ complex, DMSO, 0 ºC (b) TBDMSCl, imidazole, DMF, rt (c) (i) *n*-BuLi, THF, -78 ºC (ii) $ClCO_2Me$, -78 ºC, (d) $(MeO)_2C{=}CH_2$, sealed tube, 165 ºC, 24 hrs (e) 2,5-dichloro-1,4-benzoquinone, benzene, sealed tube, 145 ºC, 3 hrs (f) (i) NaOMe, MeOH, 0 ºC (ii) BCl_3, CH_2Cl_2, 0 ºC.

The synthesis of (*R*)-semixanthomegnin ***R*-106** was also achieved by semi-synthesis from (*R*)-semivioxanthin ***R*-77** by taking advantage of the hydrogen bonding between the naphthol OH with the carbonyl group. The hydrogen bonding allowed for exclusive oxidation of the naphthol OH at the right position that afforded the *para*-quinone ***R*-106**. This is shown in **Scheme 1.21** below.

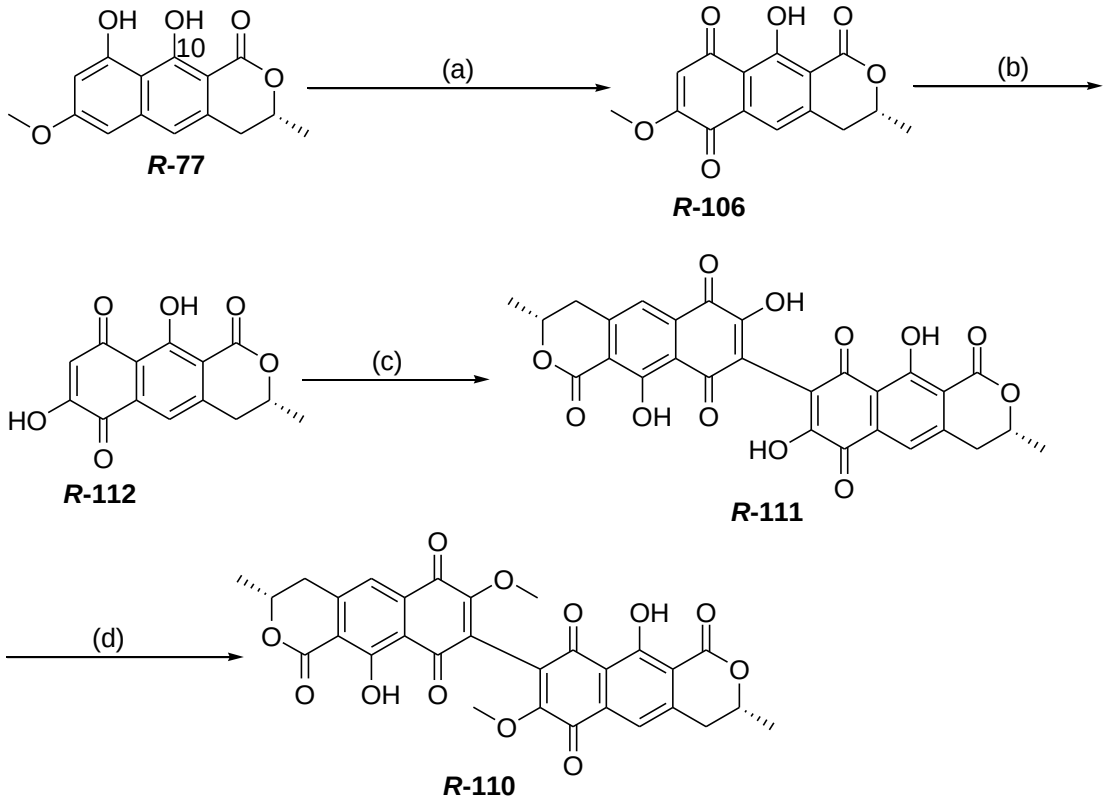
1.8.1 Isolation, bioactivity studies and synthesis of (3*R*,3'*R*)-xanthomegnin *R*-110 and luteosporin *R*-111

(3*R*,3'*R*)-Xanthomegnin ***R*-110**, a *C*-8/*C*-8' coupled dimer of (*R*)-semixanthomegnin ***R*-106**, was first isolated from the mould *Trichophyton megnini* Blanchard 1896[98] and was later isolated from various *Penicillium* and *Aspergillus* species.[99] The circular dichroism spectrum of the dimer ***R*-110** isolated from *P. citreoviride*, along with the ^{1}H NMR spectrum showed splitting of the hydroxyl signals, which indicated that the dimer essentially exists as a mixture

of atropisomers. This compound is one of a small group of metabolites used as taxonomic markers in various *Penicillium* species.[41] The biological studies indicated that (3*R*,3'*R*)-xanthomegnin inhibited the growth of *Bacillus subtilus* and showed potent antifungal activity. In addition, the bioactivity tests carried out on rat liver mitochondria showed it to be a strong uncoupler of oxidative phosphorylation.[100]

Luteosporin ***R*-111**, a fully demethylated dimer of (*R*)-semixanthomegnin ***R*-106**, is also a natural product having been isolated from *Microsporum cookie*.[101] It has recently been isolated from *Penicillium chermesinum*.[102] Bioactivity studies showed that luteosporin is a phospholipase A2 inhibitor.[102]

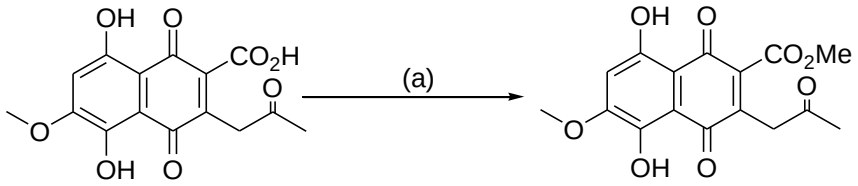
Zeeck and co-workers[69] synthesized (3*R*,3'*R*)-xanthomegnin from (*R*)-semivioxanthin ***R*-77**. This protocol led to the isolation of luteosporin *R*-111 as an intermediate (**Scheme 1.21**). The (*R*)-semivioxanthin ***R*-77** was oxidized to the corresponding (*R*)-semixanthomegnin ***R*-106** by taking advantage of hydrogen bonding at position 10, as explained before, which ensured regioselective oxidation. The demethylation of the resultant pyranonaphthoquinone ***R*-106** furnished a fully demethylated quinone ***R*-110**, which was then subjected to dimerization protocol affording luteosporin ***R*-111**. The selective methylation of luteosporin delivered the target dimer, (3*R*,3'*R*)-xanthomegnin ***R*-110**.



Scheme 1.21: *Reagent and conditions;* (a) $(KSO_3)_2NO$, Me_2CO, 0.1 M phosphate buffer, 2.5 hrs (b) $AlCl_3$, $CHCl_3$ (c) NaOH, H_2O, $K_2S_2O_8$, 95 ^oC, 1.5 hrs (d) CH_2N_2, ether.

1.8.2 Isolation of fusarubinoic acid (5,8-dihydro-1,4-dihydroxy-6-methoxy-5,8-dioxo-3-(2-oxopropyl)naphthalene-2-carboxylic acid) 31

Fusarubinoic acid **31** was isolated from the culture medium of *Nectria haematococca* strain 169 red mutant (Berk. and Br.) Wr. The structure of this naphthoquinone was established on the basis of MS and ^1H NMR spectroscopy determinations carried out on the isolate itself and on the methyl ester **113**.[31] Fusarubinoic acid **31** is considered as a candidate precursor in the biosynthesis of 5-deoxyfusarubin and anhydrofusarubin lactone **32** from the heptaketide as explained in **Section 1.3**. The methyl ester analogue of fusarubinoic acid **31**, naphthoquinone **113**, was synthesized by addition of a solution of diazomethane in diethyl ether to a solution of fusarubinoic acid and the resultant mixture was stirred at room temperature for 5 minutes which delivered quinone **113** as shown in **Scheme 1.22**.



31 **113**

Scheme 1.22: *Reagents and conditions;* (a) CH_2N_2, Et_2O, rt, 5 min.

Fusarubinoic acid does not belong to the group of pyranonaphthoquinones (naphthopyranones) and its inclusion in this review is solely on the basis that it is considered as an important intermediate in the biosynthesis of pyranonaphthoquinones as explained before.

1.8.3 Isolation of anhydrofusarubin lactone (5,10-dihydroxy-7-methoxy-3-methyl-1*H*-naphtho-[2,3-c]-pyran-1,6,9-trione) 32

Anhydrofusarubin lactone **32** (**Figure 1.20**), an amorphous dark purple powder, was isolated from a fungus of the genus *Necteria haematococca* and was first reported by Parisot and co-workers in 1983.[103] It was purified by preparative TLC after preliminary fractionation on an LH-20 Sephadex column. The availability of anhydrofusarubin **114** (**Figure 1.20**) was reported prior to isolation of anhydrofusarubin lactone **32** and played a crucial role in elucidation of its structure.

The spectrum of anhydrofusarubin lactone **32** showed no signal corresponding to the protons at *C*-1 found in the ^{1}H NMR spectrum of anhydrofusarubin **114**. In addition, the proton signal of one phenolic group is highly deshielded with respect to the phenolic protons of anhydrofusarubin **114**. This phenomenon is attributed to extensive hydrogen bonding of the phenol group at position 10 (**Figure 1.20**) of the lactone. Anhydrofusarubin lactone **32** has also been isolated from *Fusarium solani*.[104]

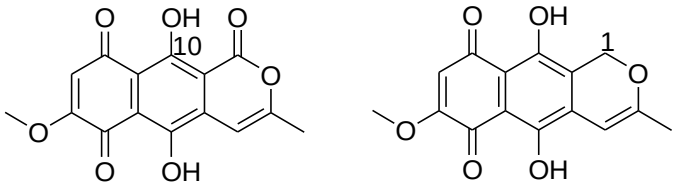


Figure 1.20: The molecular structure of anhydrofusarubin lactone **32** and anhydrofusarubin **114**.

1.8.4 Isolation of haemoventosin (3,4,6,9-tetrahydro-5,10-dihydroxy-7-methoxy-3*S*-methyl-l,6,9-trioxo-l*H*-naphtho-[2,3-*c*]pyran) *S*-115

The saturated enantiomerically pure analogue of anhydrofusarubin lactone **32**, haemoventosin ***S*-115** (**Figure 1.21**) is a red amorphous solid and was isolated in 1971 by Bruun and Lamvik from the lichen *Ophioparma ventosa* (L.) Norman [syn. *Haematomma ventosum* (L.) Massai. (Lecanoraceae)].[105] Bruun and Lamvik proposed a furanonaphthoquinone structure **116** for haemoventosin which was subsequently revised by Maksimov and co-workers in 1990 to the *o*-quinoid structure **117**. Maksimov and co-workers isolated haemoventosin from *Ophioparma lapponica* (Rasänen) Hafellner & R. W. Rogers (syn. *Haematomma lapponicum* Rasänen).[106] The structure proposed by Maksimov and co-workers was further revised by Rycroft and co-workers in 1995 to 3,4,6,9-tetrahydro-5,10-dihydroxy-7-methoxy-3*S*-methyl-l,6,9-trioxo-l*H*-naphtho-[2,3-*c*]pyran ***S*-115** on the basis of HMBC correlations observed in 2D NMR spectroscopy experiments and long-range δ_H/δ_D isotope effects observed in partial deuteriation experiments with 10-*O*-acetylhaemoventosin. The (*S*)-stereochemistry of 3,4-dihydropyranonaphthoquinone ***S*-115** was assigned after comparison of the circular dichroism spectrum of 10-*O*-acetylhaemoventosin with that of (*R*)-10-*O*-acetylsemixanthomegnin. The spectra were close to being mirror images of one another and therefore, haemoventosin ***S*-115** was proposed to possess (*S*)-stereochemistry at the *C*-3 position of the pyranone ring.[107]

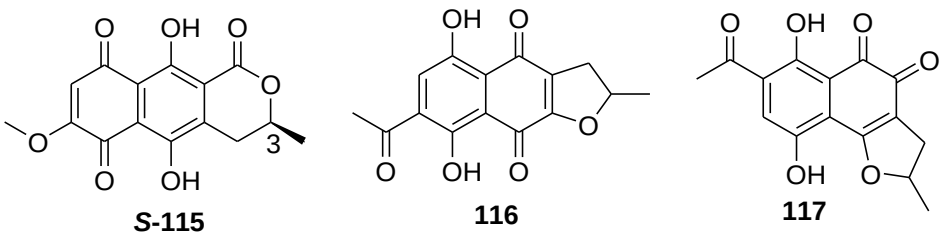
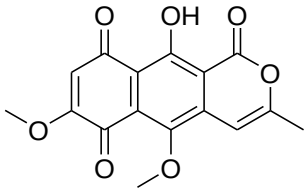


Figure 1.21: The molecular structure of haemoventosin ***S*-115** and incorrect structures **116** and **117** that were proposed for haemoventosin.

1.8.5 Isolation and bioactivity studies of 5-methoxy-3,4-dehydroxanthomegnin (10-hydroxy-5,7-dimethoxy-3-methyl-1*H*-naphtho-[2,3-*c*]-pyran-1,6,9-trione) 34

5-Methoxy-3,4-dehydroxanthomegnin **34** (**Figure 1.22**), an amorphous red powder, was isolated from the capitulae of *Paepalanthus latipes* a plant of the Eriocaulaceae family.[108] This species is widespread in the region of the Serra do Cipó, State Minas Gerais, in Brazil. Kitagawa and co-workers evaluated the *in vitro* cytotoxicity of the isolate on McCoy cell lines using the microculture MTT-tetrazolium assay and found that 5-methoxy-3,4-dehydroxanthomegnin **34** showed significant cytotoxic activity with a cytotoxicity index, CI_{50}, value of 35.8 μg/mL.[108] This value was better than the cytotoxicity of cisplatin which registered the CI_{50} value of 41.9 μg/mL under the same assay conditions. The activity of pyranonaphthoquinone **34** was increased 7 times (CI_{50} value of 5.9 μM) when tested together with ascorbic acid. The increase in activity was attributed to the hydrogen peroxide generated by ascorbate-driven 5-methoxy-3,4-dehydroxanthomegnin redox cycling.[109] This conclusion was reinforced by the observation that incubation of cells in the presence of quinone **34**/ascorbic acid/catalase resulted in an increase in McCoy cell survival. Catalase is an enzyme which destroys hydrogen peroxide which meant that its inclusion in the quinone/ascorbic acid mixture resulted in depletion of hydrogen peroxide.



34

Figure 1.22: The molecular structure of 5-methoxy-3,4-dehydroxanthomegnin **34**.

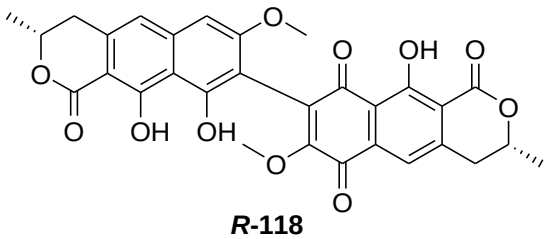
In a different study, pyranonaphthoquinone **34** showed significant cytotoxicity against murine mammary tumor cells (LM2) and lung adenocarcinoma cells (LPO7) with CI_{50} values of 74.6 and 6.2 μM against LM2 and LP07 cells, respectively. In contrast, cisplatin showed CI_{50} values of 168.4 and 4.34 μM for LM2 and LP07, respectively, under the same assay conditions. The reported results convinced the authors that pyranonaphthoquinone **34** is a promising candidate for the treatment of murine breast and lung cancer by immunomodulatory and antiproliferative activities.[110] Furthermore, 5-methoxy-3,4-

dehydroxanthomegnin showed anti-inflammatory activity which was demonstrated by suppression of nitric oxide (NO) generation on lipopolysaccharide-stimulated macrophages. More recently, Kitagawa and co-workers[111] reported that 5-methoxy-3,4-dehydroxanthomegnin **34** is a potent anti-*H. pylori* compound with an MIC value of 64 μg/mL and MBC value of 128 μg/mL. These results indicated that quinone **34** is a more potent anti-*H. pylori* compound compared to paepalantine **102** (see **Section 1.7.8**). The same authors[111] reported assessing the antioxidant activity of pyranonaphthoquinone **34** by noting its effect on the neutrophil oxidative burst using luminol- and lucigenin-amplified chemiluminescence. It was noted during these studies that 5-methoxy-3,4-dehydroxanthomegnin **34** decreased luminol- and lucigenin-amplified chemiluminescence, with ED_{50} values of 1.58 μg/mL and 5.4 μg/mL, respectively, reflecting an inhibitory effect on the oxidative burst.

1.8.6 Isolation of (*R*)-viomellein *R*-118

(*R*)-Viomellein ***R*-118** (**Figure 1.23**) is made up of (*R*)-semivioxanthin ***R*-77** and (*R*)-semixanthomegnin ***R*-106** connected by a *C*-8/*C*-8' carbon link. It was first isolated from *Aspergillus sulphureus* and its structure was established by spectroscopic analysis and comparison with (3*R*,3'*R*)-xanthomegnin.[99] (*R*)-Viomellein ***R*-118** has also been found in *A. ochraceus*, *A. melleus*, *Penicillium viridicatum*, *P. cyclopium* and *Nannizzia cajetani*, where it co-exists with other metabolites.[112]

Oxidative degradation of the dimer ***R*-118** and comparison of the circular dichroism spectrum of the resultant isocoumarin with that of (*R*)-mellein ***R*-15** established the absolute configuration for the dimer as (*R*).



***R*-118**

Figure 1.23: The molecular structure of viomellein ***R*-118**.

1.8.7 Isolation of rubrosulphin 119 and viopurpurin 120

Rubrosulphin **119** and viopurpurin **120** (**Figure 1.24**) are co-metabolites in *Aspergillus sulphureus*, *A. melleus* and *Penicillium viridicatum*, with viopurpurin also being obtained from *Trichophyton violaceum*.[74,99,113] The structure of rubrosulphin was established by spectroscopic analysis and confirmed by conversion of (*R*)-viomellein ***R*-118** to rubrosulphin **119** as explained later. On the other hand, the structure of viopurpurin **120** was established solely by spectroscopic analysis.

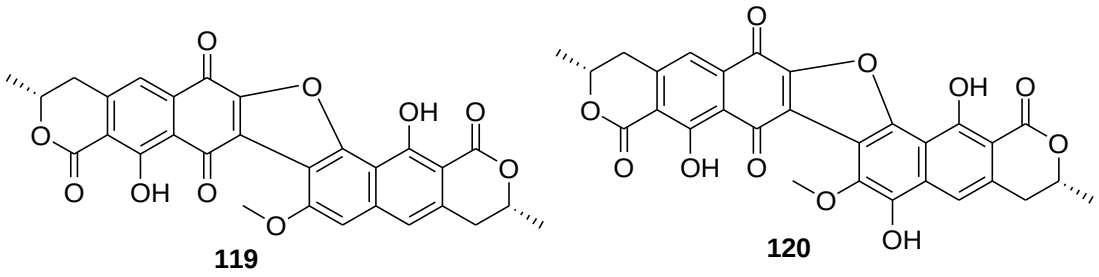
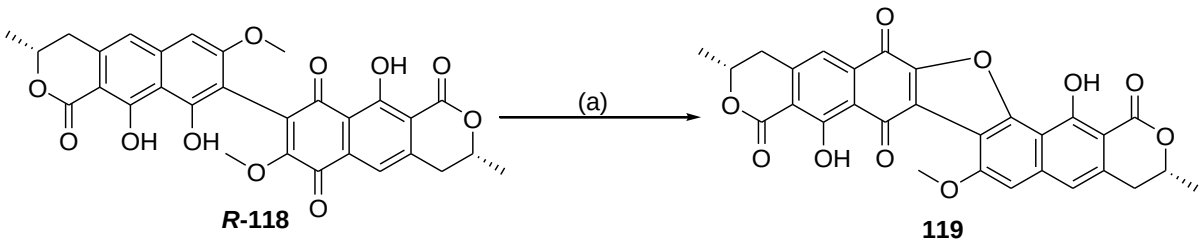


Figure 1.24: The molecular structures for rubrosulphin **119** and viopurpurin **120**.

Rubrosulphin **119** was synthesized by refluxing a solution of (*R*)-viomellein ***R*-118** in acetone with potassium carbonate as shown in **Scheme 1.23**.[99]



Scheme 1.23: *Reagents and conditions;* (a) K_2CO_3, acetone, reflux.

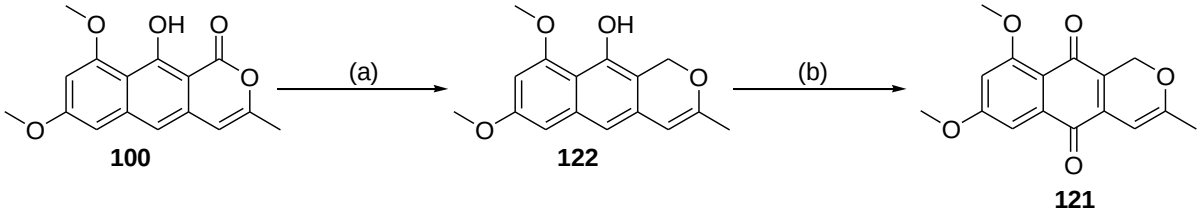
1.9 Lactones as synthetic intermediates for synthesis of other functionalities

The lactone functionality has received considerable attention as an intermediate towards the synthesis of natural products bearing other functionalities. This is the case because many researchers take advantage of the well-established methodologies such as the Staunton-Weinreb annulation and Diels Alder reactions to obtain intermediates in good yields *en route* to the synthesis of natural products.

1.9.0 Synthesis of dehydroherbarin 121 using the Staunton-Weinreb annulation reaction as a key step

One such example was the synthesis of a very important pyranonaphthoquinone, dehydroherbarin **121**, by Wadsworth and co-workers that was published in 2010.[114a] Dehydroherbarin is a natural product that was isolated from the dematiaceous fungus *Torula herbarum* and is often found on the dry leaves and twigs of *Felia microphylla*.[114b] In addition, it has been found in the endolichenic fungal strain, *Corynesspora* sp. BA-10763, which occurs in cavern beard lichen *Usnea cavernosa*.[115] Dehydroherbarin exhibits antimicrobial and anti-amoebic activity, as well as causing significant inhibition of both metastatic prostate (PC-3M) and breast (MDA-MB-231) cancers.[114b,115]

Wadsworth and co-workers[114a] took advantage of the well-established Staunton-Weinreb-annulation methodology which yielded the lactone intermediate **100** in a few steps (see **Scheme 1.18** for the synthesis of intermediate **100**). The pyranone **100** was reduced to pyran **122** by using diisobutylaluminum hydride (DIBAL-H) in toluene. The pyran intermediate was then oxidized by salcomine furnishing the target pyranonaphthoquinone **121** as shown in **Scheme 1.24**.



100 **122** **121**

Scheme 1.24: *Reagents and conditions;* (a) DIBAL-H (1.2 M in toluene), THF, rt, 48 hrs (b) O_2 (g), salcomine, CH_3CN, rt, 3 hrs.

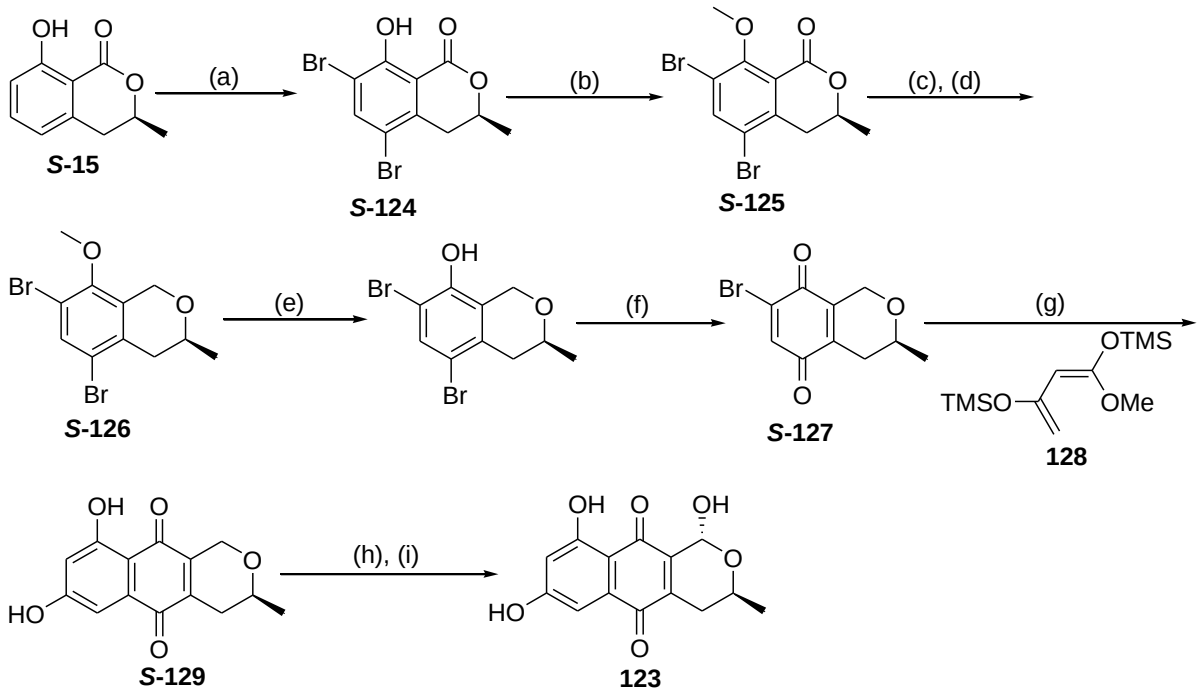
1.9.1 Synthesis of enantiomerically pure thysanone 123 using the Diels Alder reaction as a key step

Thysanone **123**, a yellow crystalline 3,4-dihydroisochromene quinone, was isolated from solid-state fermentations of the fungus *Thysanophora penicilloides* by chemists at Merck, Sharp & Dohme during a screening programme aimed at control and/or cure of the common cold.[116] The correct structure was elucidated by using the spectroscopic data and a single crystal x-ray analysis of the methyl acetal derivative. Thysanone **123** reportedly showed

potent activity against human rhinovirus (HRV) 3C-protease with an IC_{50} value of 13 μg/mL. HRV is one of a family of picornaviruses that are responsible for diseases such as polio, hepatitis A and foot-and-mouth disease. Its control is considered vital in the fight against these diseases.[117]

The absolute stereochemistry of this quinone was confirmed by Gill and Donner[118] who accomplished the total synthesis of enantiomerically pure thysanone using the Diels-Alder cycloaddition reaction as a key step.

In this protocol, (*S*)-mellein ***S*-51** was subjected to bromination and methylation reactions which furnished intermediates ***S*-124** and ***S*-125**, respectively (**Scheme 1.25**). The pyranone functionality of intermediate ***S*-125** was transformed into a pyran ring by treatment with diisobutylaluminium hydride. This was followed by exposure of the crude intermediate to sodium borohydride which afforded (*S*)-benzopyran ***S*-126**. The demethylation of intermediate ***S*-126** and oxidation of the resultant phenol delivered (*S*)-pyranobenzoquinone ***S*-127**. The Diels–Alder reaction between dienophile ***S*-127** with diene **128** afforded (*S*)-pyranonaphthoquinone ***S*-129**. The stereospecific hydroxylation of the pyran ring system of quinone ***S*-129** was accomplished by irradiating a carbon tetrachloride solution of bromine and ***S*-129** followed by treatment with aqueous tetrahydrofuran, furnishing thysanone **123**.

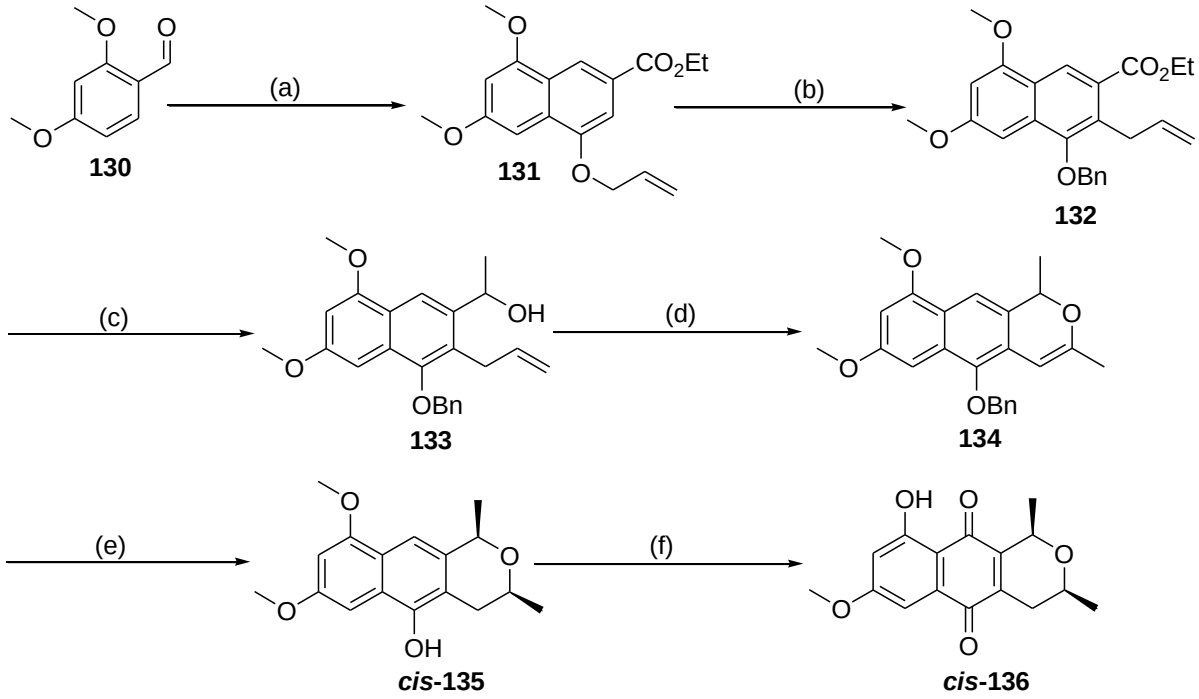


Scheme 1.25: *Reagents and conditions;* (a) NBS, DMF, rt, dark, 16 hrs (b) Me_2SO_4, K_2CO_3, Me_2CO, reflux, 1 hr (c) DIBAL-H, toluene, -70 °C (d) $NaBH_4$, THF, 30 °C, 1 hr (e) $(PhCH_2Se)_2$, $NaBH_4$, DMF, heat, 1 hr (f) CAN, MeCN-H_2O, rt, 30 min (g) toluene, heat, 3 hrs (h) Br_2, CCl_4, *hv*, 30 min (i) THF-H_2O, rt, 1 hr.

1.10 Justification for this PhD study

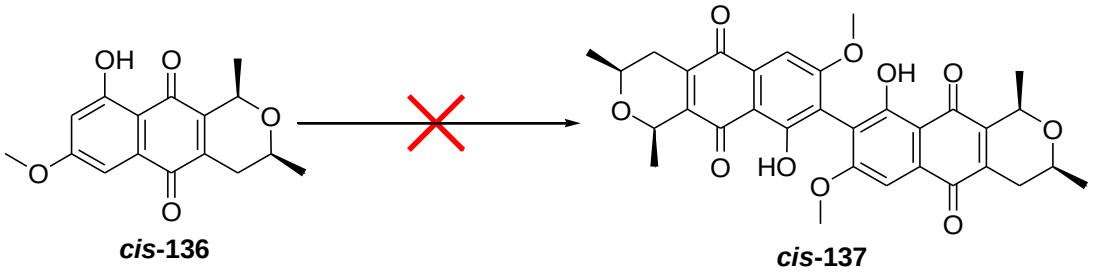
Over the years, a number of naphthoquinones has been synthesized in our laboratory. For example, in 2004 Mmutlane[119] under the supervision of de Koning accomplished the total synthesis of ventiloquinone L ***cis*-136**, a monomer of cardinalin 3 ***cis*-137**, as part of his PhD studies (**Scheme 1.26**). The key steps in the protocol were the Stobbe condensation reaction[120] which was followed by a naphthalene ring forming reaction. The Claisen rearrangement reaction[121] was employed in placing the allyl substituent at the *ortho* position to the alcohol functional group. A Wacker oxidation reaction delivered the isochromene which was subjected to naphthol oxidation to deliver the target compound. The first step towards accomplishing the total synthesis of pyranonaphthoquinone ***cis*-136** involved the construction of the naphthalene nucleus using Stobbe condensation of 2,4-dimethoxybenzaldehyde **130**. The allylated naphthalene **131** was then subjected to Claisen rearrangement reaction which allowed the placement of allyl group at *ortho* position to the ester group which delivered naphthalene **132** after further manipulation. The construction of the isochromene **134** was accomplished by an intramolecular Wacker oxidation reaction of

the benzyl alcohol **133**. The hydrogenation of the isochromene **134** was accomplished by using palladium on charcoal under a blanket hydrogen gas which also cleaved the benzyl ether group, affording naphthol precursor ***cis*-135**. The oxidation of the naphthol ***cis*-135** was accomplished by salcomine and selective demethylation was achieved using boron trichloride which furnished the natural product, ventiloquinone L ***cis*-136**.



Scheme 1.26: *Reagents and conditions; (*a) (i) diethyl succinate, *t*-BuOH, *t*-BuOK, reflux, 4 hrs (ii) NaOAc-Ac_2O, 130 °C, 4 hrs (iii) guanidine, EtOH-CH_2Cl_2, rt, 1 hr (iv) allyl bromide, K_2CO_3, Me_2CO, reflux, 16 hrs (b) (i) DMF, 170 °C, 12 hrs (ii) BnCl, KI, K_2CO_3, Me_2CO, reflux, 18 hrs (c) (i) $LiAlH_4$, THF, 0 °C → rt, 18 hrs (ii) PCC-Al_2O_3, CH_2Cl_2, rt, 8 hrs (iii) MeMgI, Et_2O-THF, 0 °C → rt, 8 hrs (d) (i) *10%* $PdCl_2$-$CuCl_2 \cdot H_2O$-DMF, rt, O_2 (g), 3 hrs (e) *10%* Pd/C, H_2 (g), CH_2Cl_2/dioxane, rt, 48 hrs (f) (i) 0.5 eq. salcomine, DMF, O_2 (g), rt, 18 hrs (ii) BCl_3, CH_2Cl_2, -78 °C.

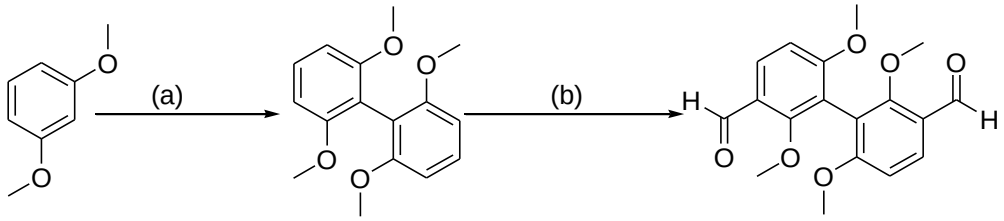
Having successfully synthesized ventiloquinone L ***cis*-136** attempts were made to synthesize cardinalin 3 ***cis*-137** which is a *C*-8/*C*-8'-dimer of ventiloquinone L, by a late stage coupling reaction of quinone ***cis*-136**, but the dimerization reaction was unsuccessful (**Scheme 1.27**). At this point a decision was made to utilize a bi-directional approach towards the total synthesis of cardinalin 3 and this formed the basis for a PhD study for Pelly and an MSc study for Govender.[122]



***cis*-136** ***cis*-137**

Scheme 1.27: Attempted dimerization of ventiloquinone L ***cis*-136** failed to deliver cardinalin 3 ***cis*-137**.

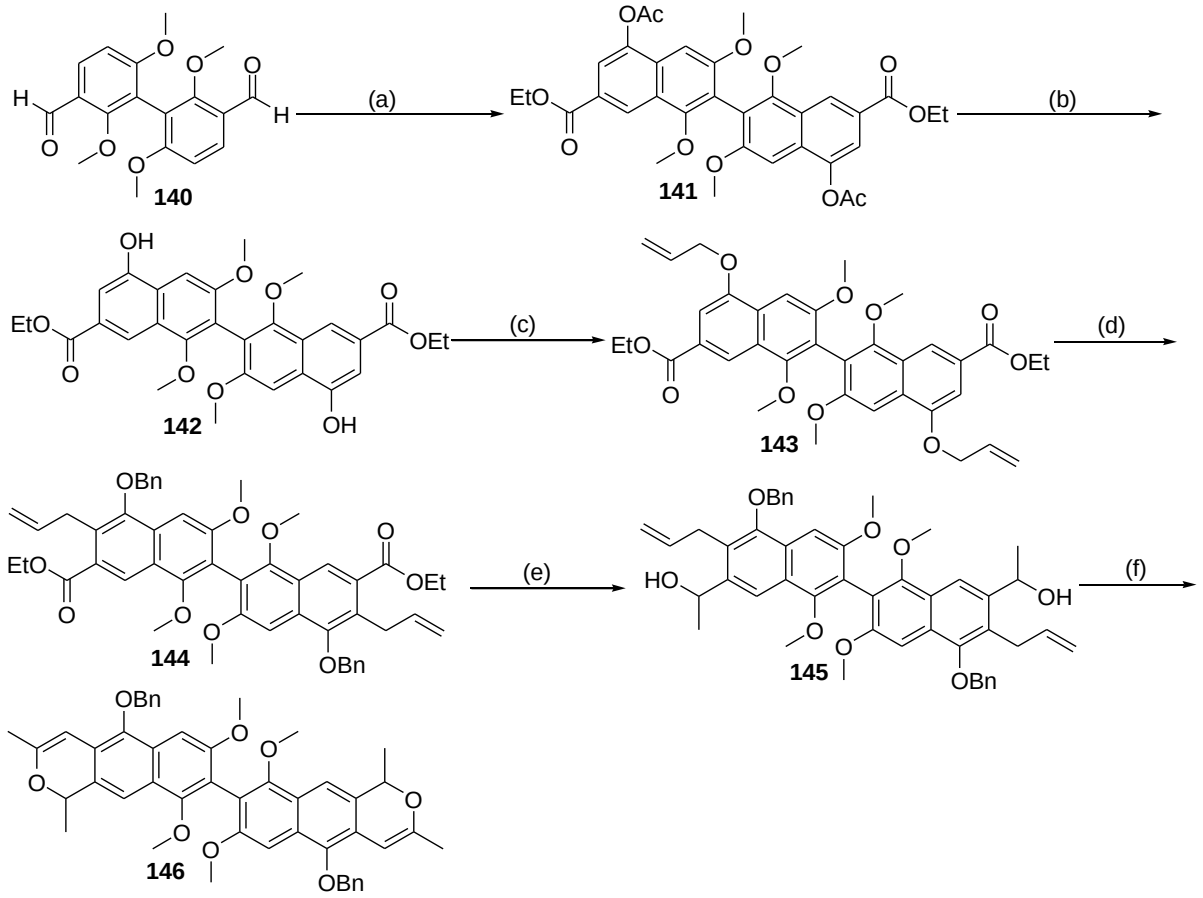
In this approach the dimerization of 1,3-dimethoxybenzene **138** was accomplished by an Ullmann-type coupling reaction which furnished *bis*-dimethoxybenzene **139**. The diformylation of the *bis*-dimethoxy benzene **139** afforded the required di-carbaldehyde **140** (**Scheme 1.28**) which was then subjected to the same protocol as used by Mmutlane.



138 **139** **140**

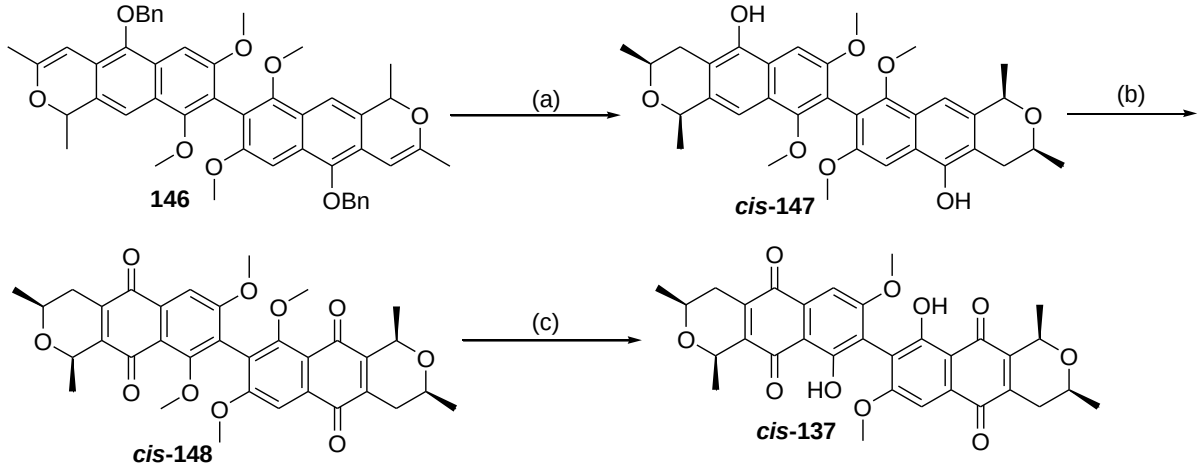
Scheme 1.28: *Reagents and conditions;* (a) (i) *n*-BuLi, CuI, THF, 0 ^{o}C, 3 hrs (ii) 2-iodo-1,3-dimethoxybenzene, pyridine, reflux, 72 hrs (b) $MeOCHCl_2$, CH_2Cl_2, $TiCl_4$, 0 ^{o}C.

Thus, the biaryl naphthalene ring system **141** was constructed by routine Stobbe condensation and naphthalene ring forming reactions. The selective deacetylation of *bis*-naphthalene **141** delivered biaryl naphthol **142**. The allylation of the dinaphthol delivered *bis*-allyl ether **143** which was then subjected to the Claisen rearrangement reaction and the resultant naphthol product was benzylated, affording biaryl naphthalene **144**. The double intramolecular Wacker oxidation was accomplished from the biaryl benzyl alcohol **145** which afforded *bis*-isochromene **146** as shown in **Scheme 1.29**.



Scheme 1.29: *Reagents and conditions;* (a) diethyl succinate, *t*-BuOK, *t*-BuOH, N_2 (g), reflux, 4 hrs (b) guanidine·HCl, *t*-BuOK, EtOH-CH_2Cl_2, rt, 1.5 hrs (c) allyl bromide, K_2CO_3, Me_2CO, reflux, 18 hrs (d) (i) DMF, microwave (200 W), 170 ^oC, 250 psi, 25 min (ii) BnCl, KI, K_2CO_3, Me_2CO, reflux, 18 hrs (e) (i) $LiAlH_4$, THF, 0 ^oC, 18 hrs (ii) PCC-Al_2O_3, CH_2Cl_2, rt, 8 hrs (iii) MeMgI-Et_2O-THF, rt, 18 hrs (f) *10%* $PdCl_2$, $CuCl_2·H_2O$-DMF, rt, O_2 (g), 18 hrs.

The naphthol precursor ***cis*-147** of cardinalin 3 was obtained by subjecting the intermediate **146** to hydrogenation conditions using palladium on charcoal under a blanket of hydrogen gas. The oxidation of the naphthol ***cis*-147** was accomplished by using salcomine which afforded 9-*O*-methylcardinalin 3 ***cis*-148** and selective demethylation was achieved using boron trichloride which delivered cardinalin 3 ***cis*-137**. This part of the protocol is shown in **Scheme 1.30**.

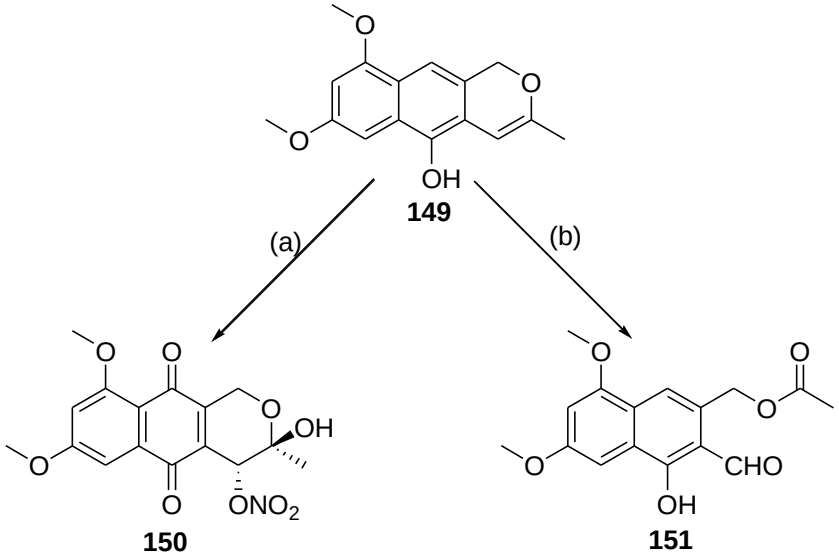


Scheme 1.30: *Reagents and conditions;* (a) *10%* Pd/C, H_2 (g), CH_2Cl_2-dioxane, rt, 48 hrs (b) salcomine, DMF, O_2 (g), rt, 18 hrs (c) BCl_3, CH_2Cl_2, 0 ^oC, N_2 (g), 15 min.

The synthesis of cardinalin 3 represented one of the finest achievements of our laboratory group and it led to other research groups synthesizing analogues of this dimer using this protocol as a reference point.[123]

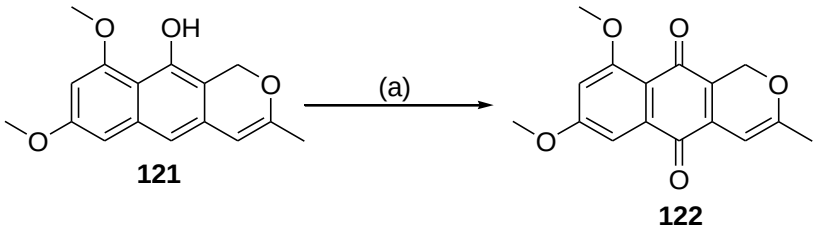
Pillay and co-workers in 2012[124] attempted to use the same combination of reaction steps to achieve the total synthesis of dehydroherbarin **121** but the attempted oxidation of the isochromene naphthol **149** resulted in oxidation of the pyran double bond which resulted in the isolation of compounds **150** and **151** from CAN-mediated oxidation and salcomine oxidation, respectively (**Scheme 1.31**).

The oxidation of the double bond was probably due to the fact that an enol ether **149** had a naphthol group in its proximity which may have allowed interaction between the oxidation reagents and the pyran double bond.



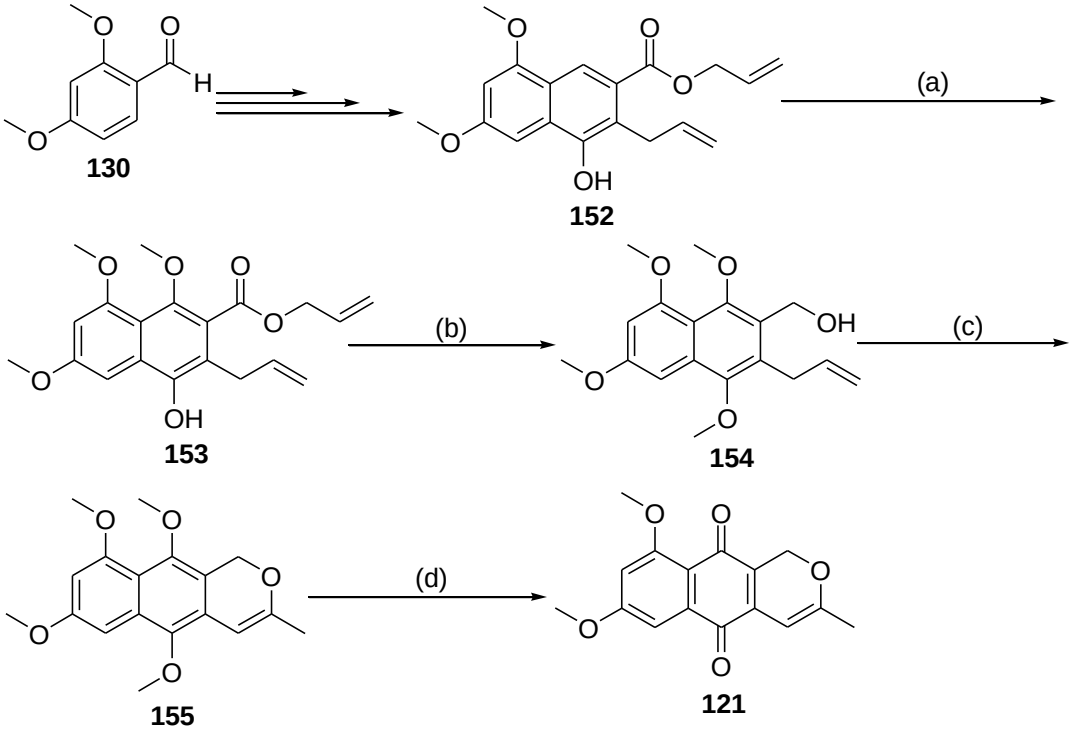
Scheme 1.31: *Reagents and conditions;* (a) CAN, H_2O/CH_3CN, rt, 30 min (b) salcomine, CH_3CN, O_2 (g), rt, 24 hrs.

Wadsworth and co-workers[114a] reported the synthesis of dehydroherbarin **121** using Staunton-Weinreb-annulation methodology as a key step as explained before. This methodology allowed the placement of the naphthol group far from the pyran enol ether and CAN-mediated oxidation of the isochromene naphthol **122** in this case did not result in the oxidation of the double bond and quinone **121** was obtained in good yield (**Scheme 1.32**).



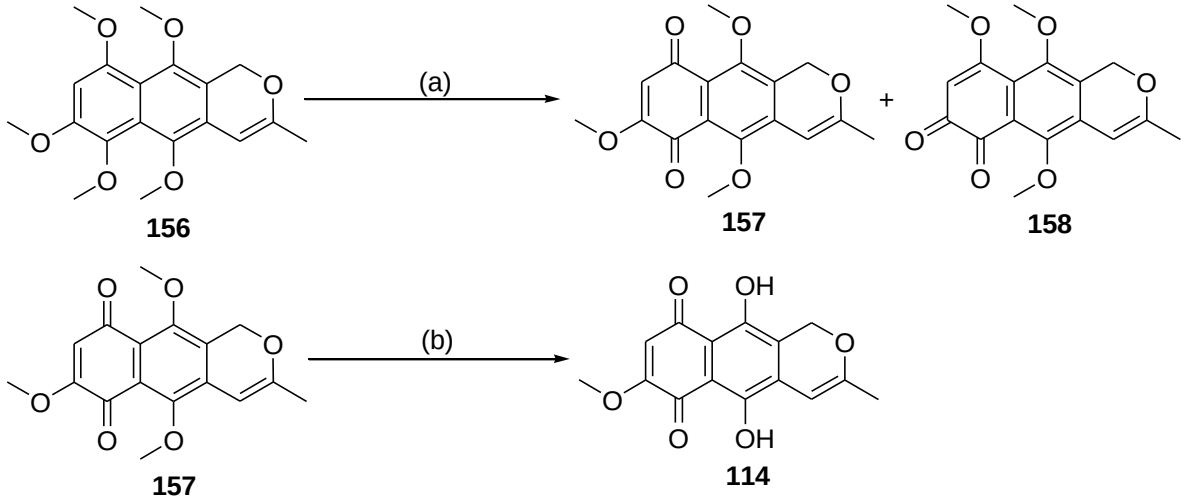
Scheme 1.32: *Reagents and conditions;* (a) CAN, H_2O/CH_3CN, rt, 30 min.

This observation necessitated modification of the protocol that was used by Mmutlane. The major difference was the inclusion of the PIFA mediated aromatic methoxylation step which allowed the placement of the methoxy group at the *para* position of the naphthalene ring system. The key steps for this protocol are shown in **Scheme 1.33**.



Scheme 1.33: *Reagents and conditions;* (a) (i) PIFA, MeOH, rt, 15 min (ii) NaOEt, EtOH, rt, 20 min (b) (i) K_2CO_3, Me_2SO_4, Me_2CO, reflux, 18 hrs (ii) $LiAlH_4$, Et_2O, rt, 2 hrs (c) cat. $PdCl_2$, $CuCl_2 \cdot 2H_2O$, DMF/H_2O, O_2 (g), rt, 2 hrs (d) PIFA, H_2O/CH_3CN, rt, 2 hrs.

Thus, 2,4-dimethoxyaldehyde **130** was subjected to a number of transformations which delivered naphthol **152**. The naphthol **152** was then subjected to PIFA mediated methoxylation and base promoted re-aromatization which afforded naphthol **153**. The difference between naphthol **152** and naphthol **153** was that naphthol **153** had an extra methoxy group in the naphthalene ring system. The methylation and reduction reactions of naphthol **153** delivered the required benzyl alcohol **154** which was then subjected to an intramolecular Wacker oxidation reaction affording isochromene **155**. The isochromene **155** was later subjected to oxidative demethylation which delivered the target quinone **121**. The successful synthesis of dehydroherbarin **121** using this methodology led to the synthesis of anhydrofusarubin **114** by the same authors as shown in **Scheme 1.34**.

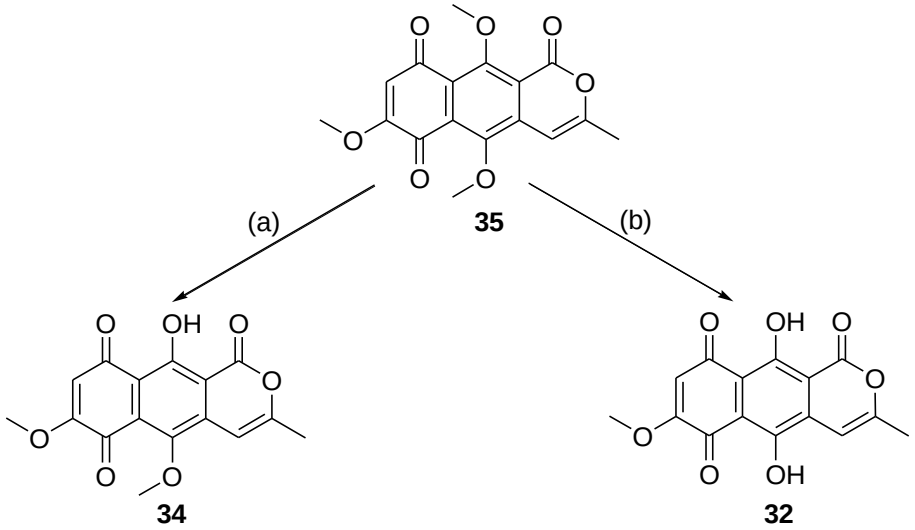


Scheme 1.34: *Reagents and conditions;* (a) AgO, *55%* aq. HNO_3, 1,4-dioxane (b) BCl_3, CH_2Cl_2, -78 °C.

The difference in this case was the use of silver (II) oxide with nitric acid for the oxidative demethylation of pyran **156** which led to the formation of both *para*-pyranonaphthoquinone **157** and *ortho*-pyranonaphthoquinone **158**. The two products were easily separated by column chromatography on silica gel and selective demethylation[125] of quinone **157** afforded pyranonaphthoquinone **114**.

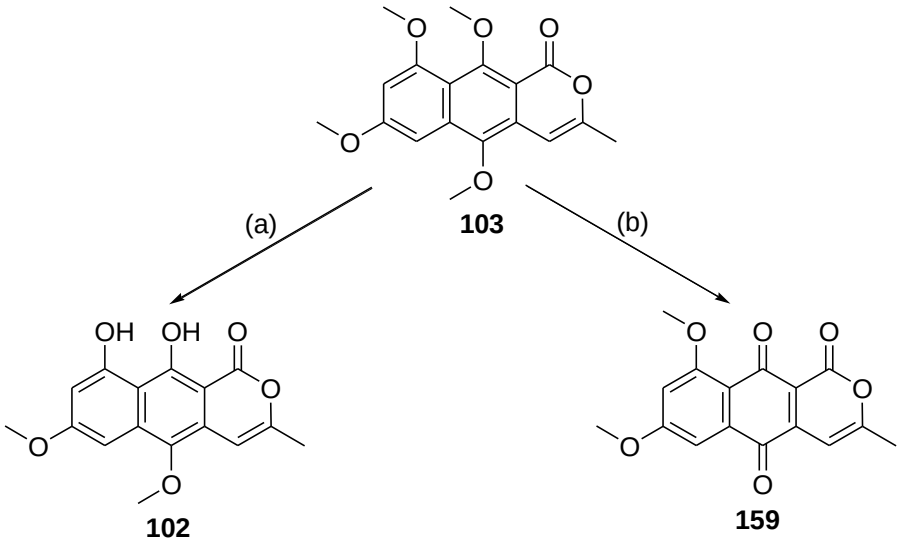
1.11 Aim of the PhD project

Despite the fact that there is a lot of literature on the biological activity of 5-methoxy-3,4-dehydroxanthomegnin lactone **34**, to the best of our knowledge, to date there has been no reported total synthesis of this natural product. We aimed at synthesizing pyranonaphthoquinone **34** starting from the appropriate commercially available simple starting material using modified protocols we have developed in our laboratory. The key intermediate in this synthesis, pyranonaphthoquinone **35**, could potentially lead to the synthesis of a similar natural product, anhydrofusarubin lactone **32** as shown in **Scheme 1.35**. Thus far intramolecular Wacker oxidation reactions have been carried out on alcohols in our laboratory and we were of the view that the target molecule **34** would afford us an opportunity to test the versatility of intramolecular Wacker oxidation methodology on a highly oxygenated carboxylic acid.



Scheme 1.35: *Reagents and conditions;* (a) 2.0 equiv. BCl_3, CH_2Cl_2, -78 °C (b) 4.0 equiv. BCl_3, CH_2Cl_2, -78 °C.

We envisaged that the synthesis of 5,7,9,10-tetramethoxy-3-methyl-1*H*-benzo[*g*]isochromen-1-one intermediate **103** could provide the required information to enable successful synthesis of pyranonaphthoquinone **34**. The successful synthesis of lactone **103** could further potentially lead to the first ever reported syntheses of both dehydroherbarin lactone **159** and paepalantine **102** as shown in **Scheme 1.36**.

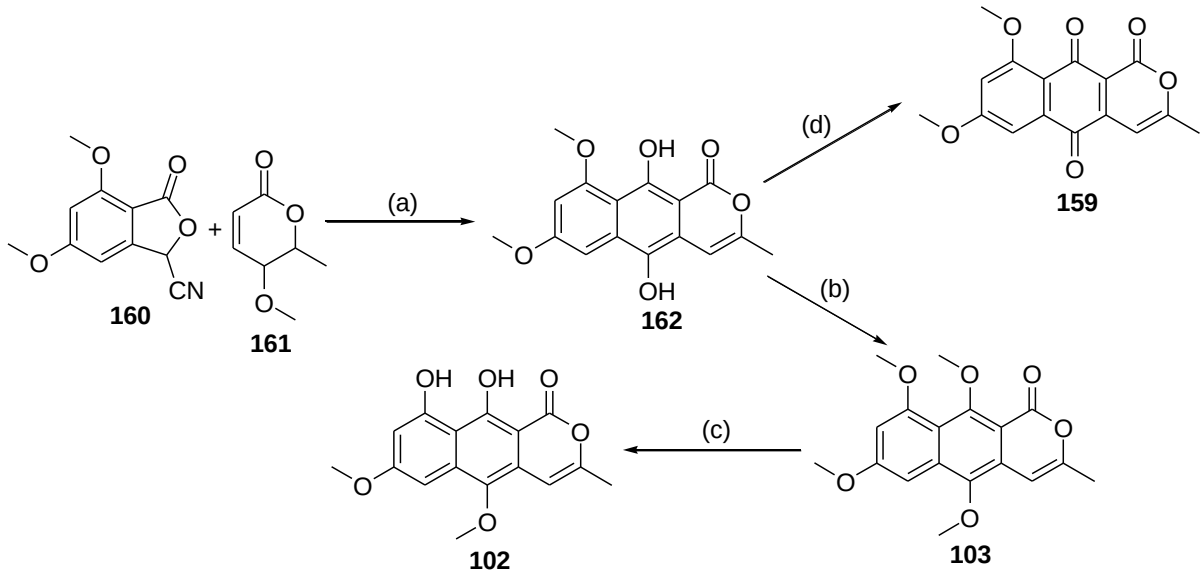


Scheme 1.36: *Reagents and conditions;* (a) BBr_3, CH_2Cl_2, -78 °C (b) AgO, *55%* aq. HNO_3, 1,4-dioxane.

Chapter 2: Results and discussion

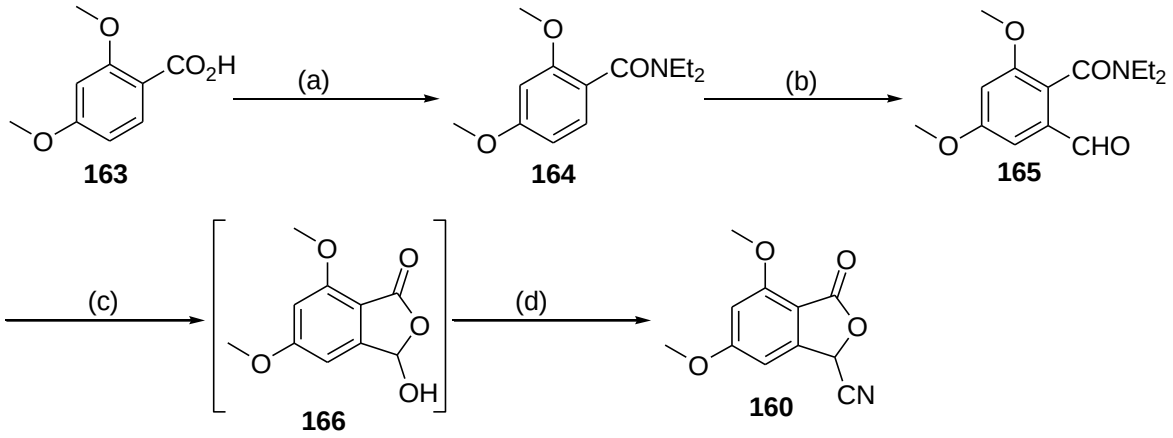
2.0 Background to the attempted synthesis of paepalantine 102 and dehydroherbarin lactone 159

Owing to interesting biological activities of paepalantine **102** as outlined in the introduction section, Mbala under the supervision of De Kimpe embarked on the synthesis of this lactone as part of his PhD studies.[126] Mbala identified 5,10-dihydroxy-7,9-dimethoxy-3-methyl-1*H*-benzo[*g*]isochromen-1-one **162** as a key intermediate towards the synthesis of paepalantine **102** and dehydroherbarin lactone **159** as shown in **Scheme 2.0**.[126] The reasoning behind this protocol was that dinaphthol **162** could be accessed through the Kraus annulation reaction involving 1,3-dihydro-4,6-dimethoxy-3-oxoisobenzofuran-1-carbonitrile **160** and 5,6-dihydro-5-methoxy-6-methylpyran-2-one **161**. It was thought that the methylation of dinaphthol lactone **162** followed by selective demethylation could potentially deliver paepalantine **102** and direct oxidation of dinaphthol lactone **162** could furnish dehydroherbarin lactone **159**, which was wrongly named as anhydrofusarubin lactone **32**. This will be explained in detail later.



Scheme 2.0: *Reagents and conditions:* (a) (i) LiO^tBu (ii) H_3O^+ (b) K_2CO_3, Me_2SO_4, Me_2CO (c) BBr_3, CH_2Cl_2 (d) cat. AcOH, CH_3CN/H_2O, *hv* (400 W).

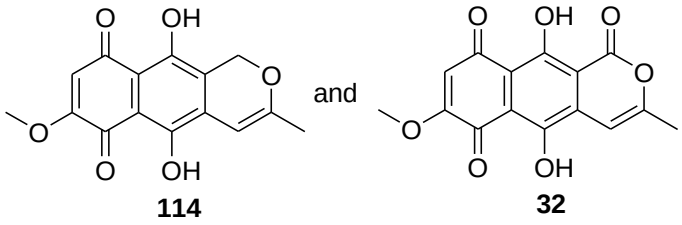
The cyanophthalide **160** was readily prepared from 2,4-dimethoxybenzoic acid **163** which was transformed to diethyl 2,4-dimethoxybenzamide **164** by acylation and substitution reactions. *Ortho*-lithiation of intermediate **164** followed by quenching the resultant carbanion with *N*,*N*-dimethylformamide afforded formylbenzamide **165**. The formylbenzamide was then heated to reflux under acidic conditions yielding 3-hydroxy-5,7-dimethoxyphthalide **166** which was subsequently converted to cyanophthalide **160** by reacting it with potassium cyanide and concentrated hydrochloric acid as shown in **Scheme 2.1**.[126]



Scheme 2.1: *Reagents and conditions:* (a) (i) 3 equiv. $SOCl_2$, PhMe, reflux, 2.5 hrs (ii) 3 equiv. Et_2NH, PhMe, 0 °C, 2 hrs (b) 1.1 equiv. *t*-BuLi, 20 min then 4.0 equiv. DMF, 12 hrs, THF, -78 °C → rt (c) *10%* aq. HCl, AcOH, reflux, 24 hrs (d) excess KCN, excess conc. HCl, H_2O, 0 °C → rt, 3 hrs.

However, the attempted synthesis of 5,6-dihydro-5-methoxy-6-methylpyran-2-one **161** was unsuccessful and with it the challenge for the first total synthesis of paepalantine **102** and dehydroherbarin lactone **159** remained unclaimed.

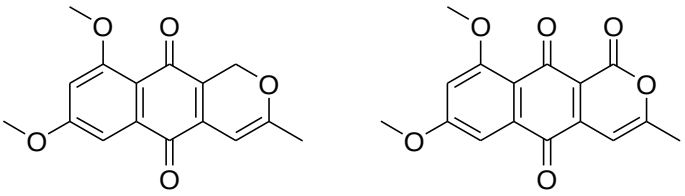
Mbala named pyranonaphthoquinone **159** as anhydrofusarubin lactone which is a name derived from anhydrofusarubin **114** (**Figure 2.0**) and has been given to pyranonaphthoquinone **32** in the literature.[103]



114 **32**

Figure 2.0: The molecular structures of anhydrofusarubin **114** and anhydrofusarubin lactone **32**.

Structurally related to anhydrofusarubin **114** is dehydroherbarin **121**[114b] which is depicted in **Figure 2.1**. On the basis of this naming system the correct name for pyranonaphthoquinone **159** would be dehydroherbarin lactone and not anhydrofusarubin lactone. A search for literature on dehydroherbarin lactone yielded no results except for the information which was presented in the thesis by Mbala.[126] This led us to believe that this lactone presented an interesting opportunity for its synthesis. Successful synthesis of pyranonaphthoquinone **159** would not only potentially lead to studies towards its biological activities in relation to anhydrofusarubin lactone **32** but would also provide valuable information regarding the methodology which could be assimilated in the synthesis of 5-methoxy-3,4-dehydroxanthomegnin **34**.



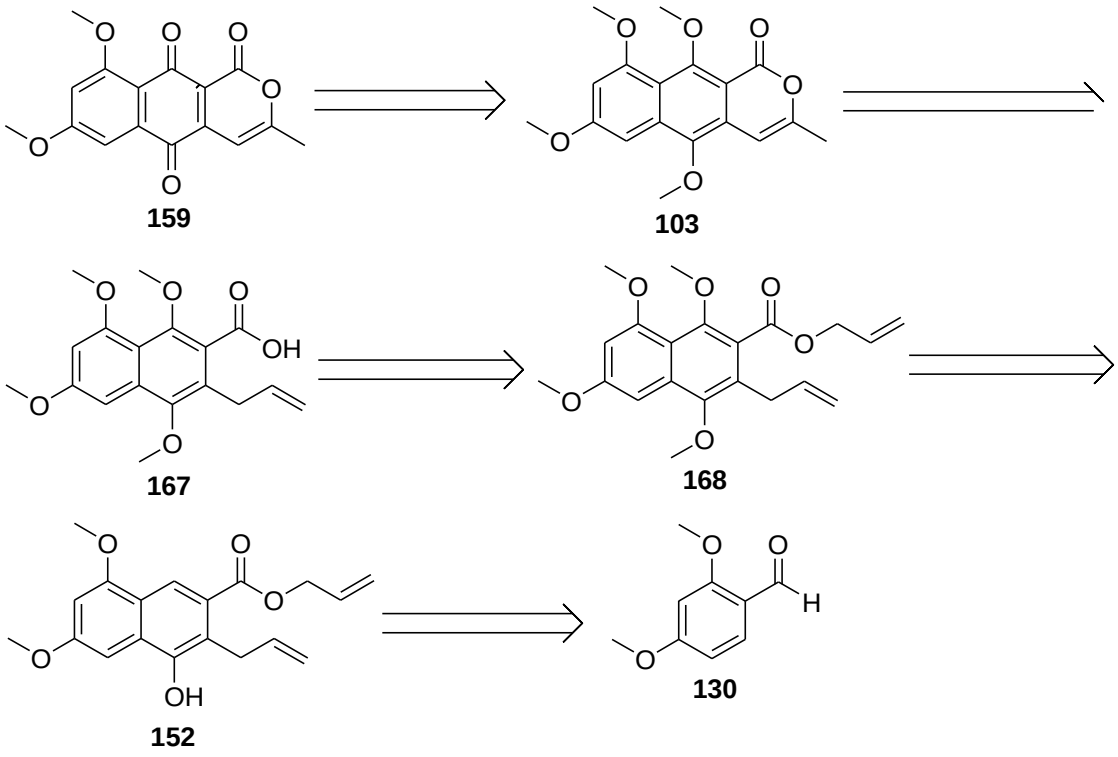
121 **159**

Figure 2.1: The molecular structures of similar pyranonaphthoquinones, dehydroherbarin **121** and dehydroherbarin lactone **159**.

Building on the work that has been carried out in our laboratory group, we thought that a modified synthetic protocol used by Mmutlane and Pillay would potentially lead to the synthesis of dehydroherbarin lactone **159**. To this end, the syntheses of some intermediates in our current protocol were previously achieved in our laboratory.[119,124,127]

We envisaged that the synthesis could be accomplished by subjecting aldehyde **130** to a number of transformations culminating to allyl ester **152** (**Scheme 2.2**). The ester **152** could

then be subjected to PIFA mediated methoxylation and methylation protocols furnishing tetraoxygenated naphthalene **168** which upon hydrolysis could afford carboxylic acid **167**. The Wacker oxidation reaction followed by oxidative demethylation could deliver lactone **103** and the target molecule **159**, respectively.



Scheme 2.2: Retrosynthetic analysis towards the synthesis of dehydroherbarin lactone **159**.

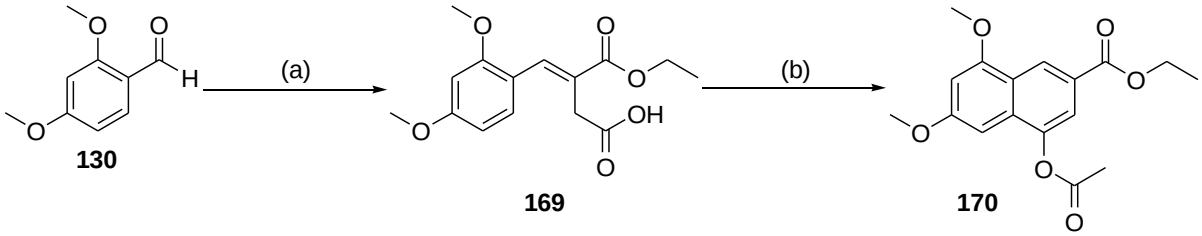
We also believed that the lactone intermediate **103** could offer us an opportunity to attempt the synthesis of paepalantine **102** by selective demethylation of this tetramethoxynaphthalene lactone as intimated by Mbala and shown in **Scheme 2.0** above.

2.1 Synthesis of dehydroherbarin lactone 159

2.1.0 Synthesis of ethyl 4-acetoxy-6,8-dimethoxynaphthalene-2-carboxylate 170

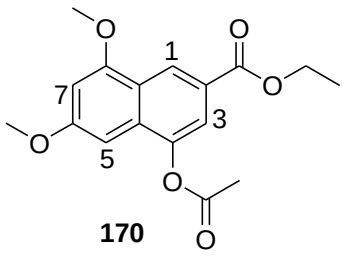
We commenced the synthesis by dissolving 2,4-dimethoxybenzaldehyde **130** and diethyl succinate in *tert*-butanol under nitrogen gas. Potassium *tert*-butoxide was subsequently added to the reaction mixture which was then heated to reflux for 4 hours. Acidification of the reaction mixture after 4 hours had elapsed led to the isolation of the carboxylic acid

intermediate **169** in a classic Stobbe condensation reaction. The acid intermediate **169** was immediately subjected to the naphthalene ring-forming conditions by heating it under reflux in acetic anhydride in the presence of sodium acetate at 130 ^{o}C for overnight. The reaction mixture was quenched by a highly exothermic protocol using methanol and the resultant crude product was passed through a short silica gel column. The isolated acidic product was washed with an aqueous solution of sodium hydrogen carbonate and purification by silica gel column chromatography afforded naphthalene **170** in 68% yield as shown in **Scheme 2.3**.



Scheme 2.3: *Reagents and conditions:* (a) (i) diethyl succinate, *t*-BuOK, *t*-BuOH, N_2 (g), reflux, 4 hrs (ii) *32%* aq. HCl (b) NaOAc, Ac_2O, N_2 (g), 130 °C, overnight, 68% (over two steps).

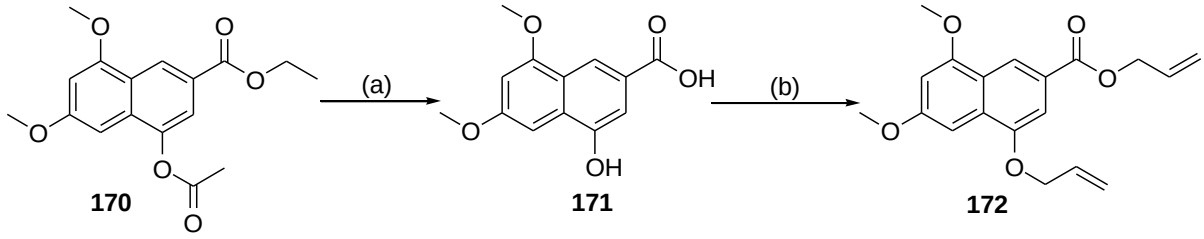
The ^{1}H NMR spectrum showed four signals in the aromatic/alkene region each integrating for 1 proton. The doublet signals at 8.78 ppm (1H, d, *J* = 1.6 Hz), 7.81 ppm (1H, d, *J* = 1.6 Hz), 6.64 ppm (1H, d, *J* = 1.9 Hz) and 6.51 ppm (1H, d, *J* = 1.9 Hz) were assigned to H-1, H-3, H-5 and H-7 protons, respectively. The signals at 4.42 ppm (2H, q, *J* = 7.3 Hz) and 1.42 ppm (3H, t, *J* = 7.3 Hz) were typical of the ethyl ester side chain protons. The singlet signal at 2.46 ppm (3H, s) was assigned to the methyl protons of the acetyl protecting group. The ^{13}C NMR spectrum showed signals at 170.1 ppm and 166.3 ppm which were assigned to the carbonyl carbon atoms of the acetyl substituent and ethyl ester, respectively. The signals at 61.0 ppm and 14.4 ppm were assigned to the carbon atoms of the ethyl side chain whereas the signal at 20.9 ppm was assigned to the methyl carbon atom of the acetyl protecting group. These signals confirmed the successful construction of the naphthalene skeleton of ester **170** with the desired substituent groups in place.



170

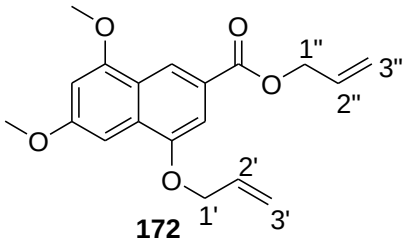
2.1.1 Synthesis of allyl 4-(allyloxy)-6,8-dimethoxynaphthalene-2-carboxylate 172

The next step was the double allylation of the naphthalene by replacing both the ester and acetyl substituents with allyl groups. This was achieved by charging a solution of naphthalene **170** in methanol into a round bottom flask to which an aqueous solution of sodium hydroxide was added while the reaction mixture was kept stirring. This mixture was then heated to reflux for 6 hours after which methanol was removed *in vacuo* and the aqueous medium residue was acidified to pH 4.0 using 32% aqueous hydrochloric acid. Ethyl acetate was then added to the acidic medium and the organic layer was separated. This procedure was repeated three times and the combined organic extracts were dried over magnesium sulfate and concentrated *in vacuo*. The crude product **171** was dissolved in acetone in a clean round bottom flask to which solid potassium carbonate and allyl bromide were added and the reaction mixture was refluxed for 18 hours. Column chromatography of the crude product on silica gel afforded diallylated naphthalene **172** in 86% yield as shown in **Scheme 2.4**.



Scheme 2.4: *Reagents and conditions:* (a) (i) KOH, MeOH/H_2O, reflux, 6 hrs (ii) *32%* aq. HCl (b) K_2CO_3, allyl bromide, Me_2CO, N_2 (g), reflux, 18 hrs, 86% (over two steps).

The ^{1}H NMR spectrum showed signals corresponding to the protons of the core naphthalene skeleton and methoxy groups but the signals due to the ethyl ester and acetyl group observed in the starting material were absent. The signal between 6.30-5.95 ppm (2H, m) was assigned to the inner vinylic protons of the two allyl groups ($ArOCH_2CH$=CH_2 (H-2') and $ArCO_2CH_2CH$=CH_2 (H-2")) whereas the signal between 5.59-5.24 ppm (4H, m) was assigned to the terminal vinylic protons of the two allyl groups ($ArOCH_2CH$=CH_2 (H-3') and $ArCO_2CH_2CH$=CH_2 (H-3")). A doublet signal at 4.87 ppm (2H, d, J = 5.6 Hz) was assigned to the allylic protons of the allyl ester group ($ArCO_2CH_2CH$=CH_2 (H-1")) and the last signal to be used for identification of

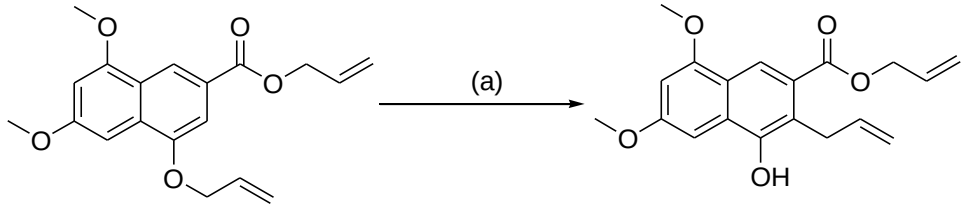


the successful double allylation was a doublet signal at 4.76 ppm (2H, d, J = 5.1 Hz) which was assigned to the allylic protons of the allyl ether group (ArOCH_2CH=CH_2 (H-1')). The ^{13}C NMR spectrum evidently showed the loss of the acetyl carbon signal which was prominent in the precursor compound at 170.1 ppm. It also showed four extra signals in the aromatic/alkene region corresponding to the four alkene carbon atoms of the two allyl groups. The signals at 133.3 ppm and 132.7 ppm were assigned to the inner vinylic carbon atoms of the allyl ether group (ArOCH$_2$*C*H=CH_2 (C-2')) and allyl ester group (ArCO_2CH_2*C*H=CH_2 (C-2")), respectively. Furthermore, the signals at 118.1 ppm and 117.5 ppm were assigned to the terminal vinylic carbon atoms of the allyl ether group (ArOCH$_2$CH=*C*H_2 (C-3')) and allyl ester group (ArCO_2CH_2CH=*C*H_2 (C-3")), respectively. The signals due to the allylic carbon atoms of the allyl ether (ArO*C*H$_2$CH=CH_2 (C-1')) and allyl ester (ArCO_2*C*H_2CH=CH_2 (C-1")) groups were evident at 69.2 ppm and 65.6 ppm, respectively.

Satisfied with the allylation step we were at this point set to attempt the thermal Claisen rearrangement reaction. The Claisen rearrangement reaction is tolerant to both solvent and solvent-free conditions[128] and *N*,*N*-dimethylformamide (DMF) is usually a solvent of choice but in our case we opted to perform this reaction under solvent free conditions.

2.1.2 Synthesis of allyl 3-allyl-4-hydroxy-6,8-dimethoxynaphthalene-2-carboxylate 152

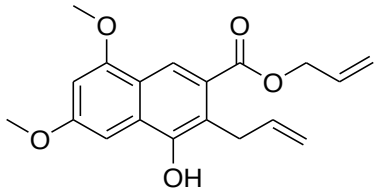
The diallyl naphthalene **172** was loaded neat in a round bottom flask equipped with a reflux condenser and a magnetic stirring bar. The flask was heated, under a blanket of nitrogen gas, at 180 ^{o}C in a silicon oil bath for 24 hours after which it was cooled to room temperature. The purification of the crude product by column chromatography on silica gel afforded naphthol **152** in 70% yield as shown in reaction **Scheme 2.5**. We noted that constant flow of water through the condenser and stirring of the reaction mixture was crucial in regulating the temperature of the reaction.



172 **152**

Scheme 2.5: *Reagents and conditions:* heat, 180 °C, N_2 (g), 24 hrs, 70%.

The ^{1}H NMR spectrum of naphthol **152** showed three aromatic proton signals which was one less than in the precursor allyl ester **172** corresponding to *C*-allylation. The D_2O exchangeable proton signal at 5.83 ppm was assigned to the naphthol proton of compound **152**. One group of the allylic protons shifted further upfield confirming that *C*-allylation had taken place. This signal was part of the broad singlet between 3.96-3.89 ppm (5H, br s). The ^{13}C NMR spectrum showed loss of a signal corresponding to the allylic carbon atom of the allyl ether group which was in the starting material at 69.2 ppm and a new signal at 31.6 ppm was assigned to the allylic carbon atom of the *C*-allyl group (Ar*C*H_2CH=CH_2).



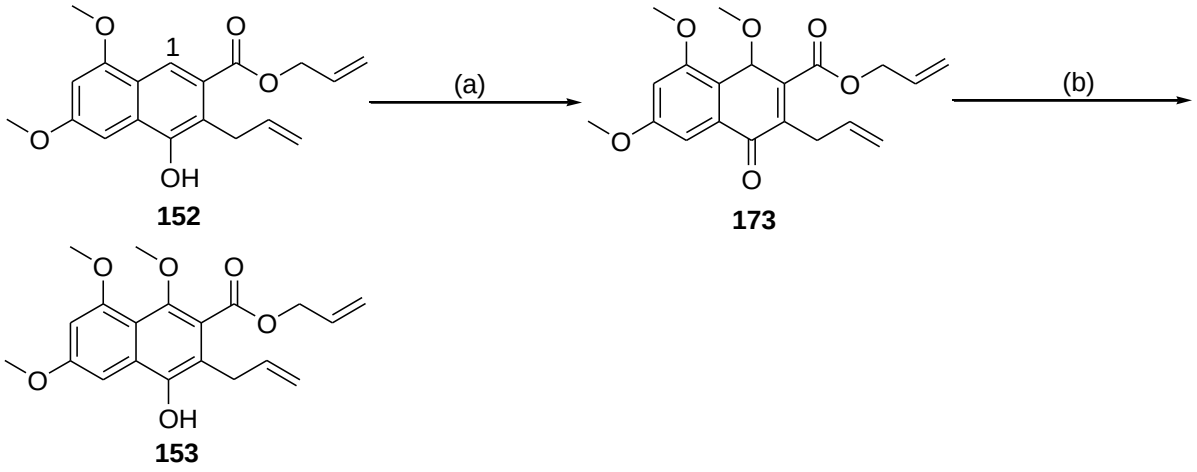
152

At this point we thought of introducing the methoxy group at the *para* position to the naphthol of the naphthalene core using PIFA mediated insertion of a methoxy substituent with subsequent re-aromatization.[129] The overall effect of this reaction is the substitution of a hydrogen atom of the naphthalene core with a methoxy substituent.

2.1.3 Synthesis of allyl 3-allyl-4-hydroxy-1,6,8-trimethoxynaphthalene-2-carboxylate 153

A solution of naphthol **152** in methanol was stirred at room temperature to which solid PIFA was added in one portion and stirring was continued for 15 minutes. The reaction mixture was quenched with a saturated aqueous solution of sodium hydrogen carbonate until effervescence stopped. The crude solid intermediate **173** was dissolved in ethanol in a clean round bottom flask equipped with a magnetic stirring bar and solid potassium *tert*-butoxide was added while vigorously stirring the reaction mixture and stirring was continued for a further 20 minutes. After this time had elapsed, the reaction mixture was quenched with a

saturated aqueous ammonium chloride solution and purification of the crude product by silica gel column chromatography delivered naphthol **153** in 58% yield as shown in reaction **Scheme 2.6**.



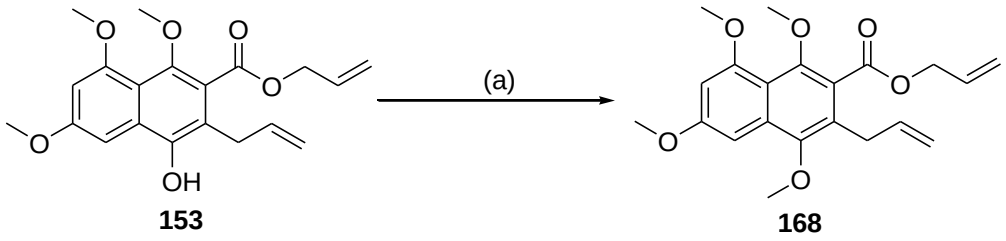
152 **173** **153**

Scheme 2.6: *Reagents and conditions:* (a) PIFA, MeOH, rt, 15 min (b) *t*-BuOK, EtOH, rt, 20 min, 58% (over two steps).

The ^{1}H NMR spectrum revealed loss of one aromatic proton (at position 1 of the naphthalene nucleus in the precursor compound **152**) and the naphthol proton signal shifted further downfield from 5.83 ppm in precursor naphthol **152** to 9.15 ppm in the tetraoxygenated naphthalene **153**. The two remaining aromatic proton signals at 7.27 ppm (1H, d, J = 2.5 Hz) and 6.75 ppm (1H, d, J = 2.5 Hz) showed typical *meta*-coupling with coupling constant of J = 2.5 Hz which strongly suggested that the successful PIFA mediated methoxylation substitution reaction took place at the *para* position to the naphthol group. The spectrum further showed a new signal corresponding to a new methoxy group between 3.90-3.19 ppm (making a total of 3 methoxy proton signals). The ^{13}C NMR spectrum confirmed the successful synthesis of the tetraoxygenated naphthalene **153** by showing a new signal corresponding to the methoxy carbon atom between 63.9-55.3 ppm (making a total of 3 methoxy carbon signals). We were pleased to have accomplished this transformation and the next step was to methylate the naphthol group of intermediate **153**.

2.1.4 Synthesis of allyl 3-allyl-1,4,6,8-tetramethoxynaphthalene-2-carboxylate 168

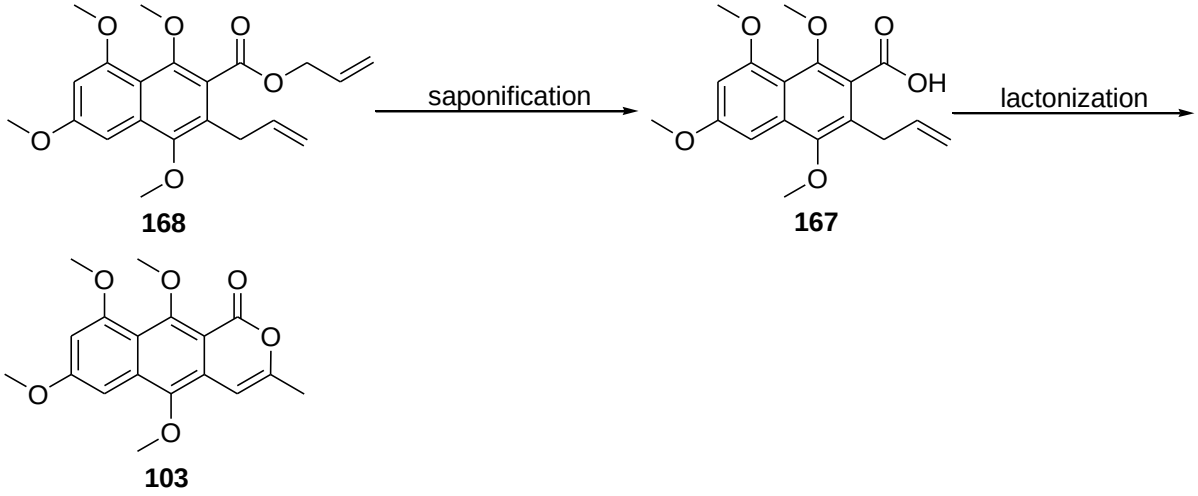
The naphthol group was methylated by dissolving compound **153** in acetone in a round bottom flask to which solid potassium carbonate and dimethyl sulfate were added. The resultant reaction mixture was heated to reflux for 18 hours. *Maximum care was exercised when handling dimethyl sulfate because of its carcinogenic effect*. The excess acid generated in the reaction as a by-product was neutralised with 25% aqueous ammonia solution and purification of the crude product by silica gel column chromatography furnished tetramethoxynaphthalene **168** (**Scheme 2.7**) in 92% yield. The successful methylation was confirmed by both ^{1}H and ^{13}C NMR spectroscopy.



Scheme 2.7: *Reagents and conditions:* (a) K_2CO_3, Me_2SO_4, Me_2CO, N_2 (g), reflux, 18 hrs, 92%.

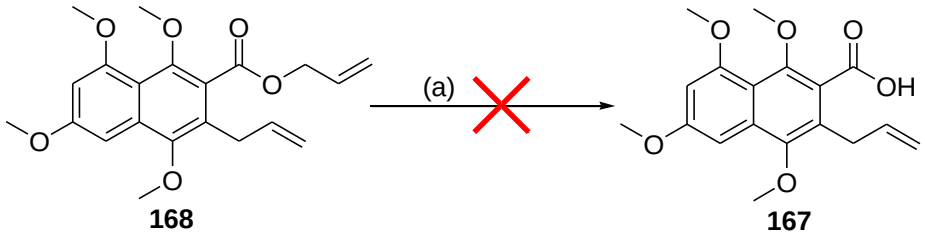
The ^{1}H NMR spectrum did not show the signal corresponding to the naphthol proton which was at 9.15 ppm in the precursor compound **153**. There was a new signal corresponding to aromatic methoxy protons making a total of 4 methoxy proton signals. Similarly, the ^{13}C NMR spectrum showed a new signal corresponding to the methoxy carbon atom attached to the aromatic ring making a total of 4 methoxy carbon signals.

At this point we were happy that the tetramethoxynaphthalene core was successfully constructed and we were nicely poised for saponification of the allyl ester to a corresponding carboxylic acid **167**. In our protocol, we had thought that allyl ester **168** could deliver acid **167** which could then be subjected to Wacker oxidation conditions to afford lactone **103** as depicted in **Scheme 2.8**.



Scheme 2.8: The proposed route towards the synthesis of lactone **103**.

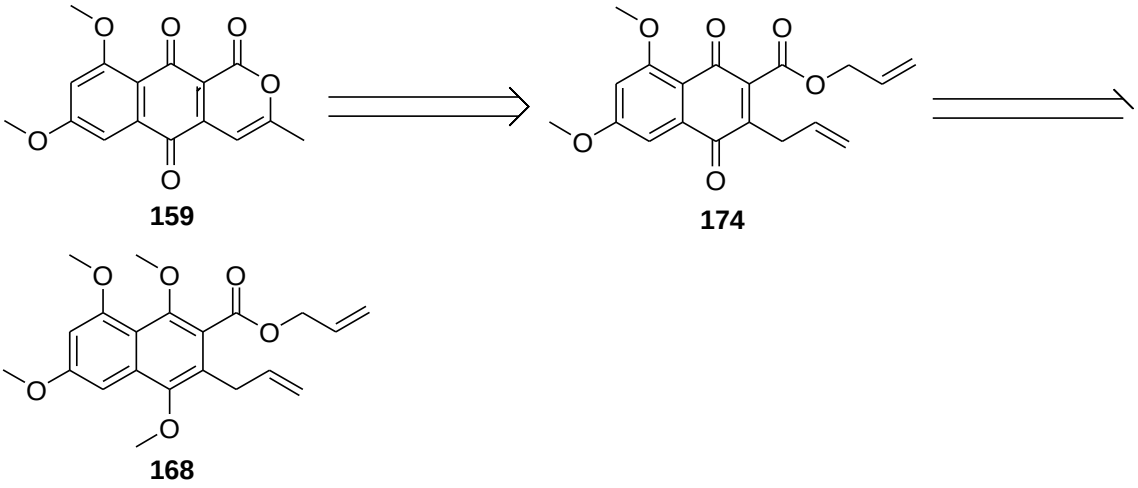
The saponification reaction was attempted and to our surprise this seemingly simple hydrolysis reaction proved very difficult to achieve. Deionised water was added to a solution of allyl ester **168** in methanol in a round bottom flask to which solid sodium hydroxide was added portion-wise while stirring the reaction mixture. The mixture was then stirred at room temperature for 2 hours and thereafter it was refluxed for 24 hours. The TLC plate of the reaction showed no consumption of the starting material and conversion to the corresponding naphthoic acid **167**. At this point more solid sodium hydroxide was added up to 12 mole equivalents and refluxed for a further 36 hours. Again, the TLC plate showed no spot corresponding to the carboxylic acid and the ^{1}H NMR spectrum of the recovered material indicated that it was unreacted allyl ester **168**. **Scheme 2.9** shows the reagents and conditions for the failed saponification of allyl ester **168** to a corresponding naphthoic acid **167**.



Scheme 2.9: *Reagents and conditions:* (a) NaOH, MeOH/H_2O, reflux, 62 hrs.

The related bases, potassium hydroxide and lithium hydroxide were also tried but with no success. At this point we thought that we could still obtain the target pyranonaphthoquinone

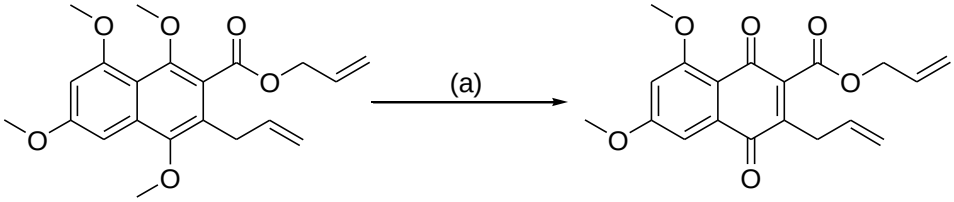
159 by oxidising the tetraoxygenated naphthalene **168** to a corresponding naphthoquinone **174** and subjecting the resultant naphthoquinone to Wacker oxidation conditions as shown in a retrosynthetic analysis (**Scheme 2.10**).



Scheme 2.10: Proposed new synthetic route encompassing naphthoquinone **174**.

2.1.5 Synthesis of allyl 3-allyl-1,4-dihydro-6,8-dimethoxy-1,4-dioxonaphthalene-2-carboxylate 174

The tetraoxygenated naphthalene **168** was dissolved in 1,4-dioxane and silver (II) oxide was added to the solution which was stirred in an open round bottom flask until a slurry was achieved. The 55% aqueous nitric acid was then added to the slurry drop-wise until all the silver (II) oxide dissolved.[130] After the reaction was complete, water was added to neutralise the excess acid and the product was extracted into dichloromethane. The crude reaction mixture was purified by column chromatography on silica gel affording the desired naphthoquinone **174** (**Scheme 2.11**) in 75% yield. Subjecting the tetraoxygenated naphthalene **168** to a CAN oxidation protocol[131] furnished the same naphthoquinone **174** in 60% yield. The IR spectrum of quinone **174** showed peaks at 1774 cm^{-1}, 1756 cm^{-1} and 1705 cm^{-1} corresponding to the carbonyl functional groups of the ester and diketone. The HRMS spectrum of the naphthoquinone further showed a molecular ion peak at 343.1172 amu which was in good agreement with the expected mass of 343.1182 amu for $C_{19}H_{19}O_6$.



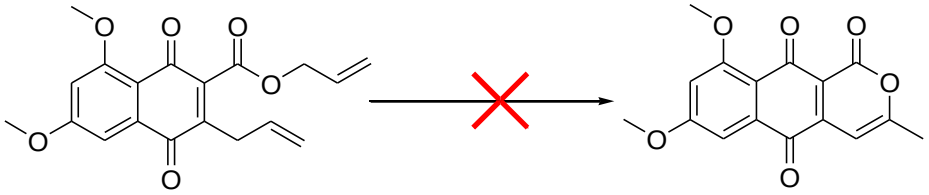
168 **174**

Scheme 2.11: *Reagents and conditions:* (a) AgO, *55%* aq. HNO_3, 1,4-dioxane, rt, 75%; or CAN, CH_3CN/H_2O, 30 min, rt, 60%.

The ^{1}H NMR spectrum of naphthoquinone **174** showed loss of two methoxy groups when compared to the ^{1}H NMR spectrum of the precursor compound and the signals due to the allyl alkene protons were all accounted for which meant that oxidation of the alkene double bonds did not take place. The ^{13}C NMR spectrum revealed the loss of two signals in the range of 64.0-55.0 ppm corresponding to loss of two aromatic methoxy groups and it further showed two signals at 184.5 ppm and 179.8 ppm corresponding to diketone carbonyl carbon atoms. Having succeeded in making the desired naphthoquinone **174** we were thrilled that we had only one step to potentially obtain the target compound, pyranonaphthoquinone **159**.

2.1.6 Attempted synthesis of 7,9-dimethoxy-3-methyl-1*H*-benzo[*g*]isochromene-1,5,10-trione 159

The naphthoquinone **174** was dissolved in *N*,*N*-dimethylformamide in a 2-neck round bottom flask equipped with a magnetic stirring bar and rubber septum. Copper chloride, water and catalytic amount of palladium chloride were added to the reaction mixture which was under a constant atmosphere of oxygen gas. The reaction was vigorously stirred for 48 hours after which column chromatography of the crude product did not yield the desired pyranonaphthoquinone **159**. **Scheme 2.12** shows the reagents and conditions of the failed palladium mediated lactonization of naphthoquinone **174**.



174 **159**

Scheme 2.12: *Reagents and conditions* (a) cat. $PdCl_2$, $CuCl_2 \cdot 2H_2O$, DMF/H_2O, O_2 (g), rt, 48 hrs.

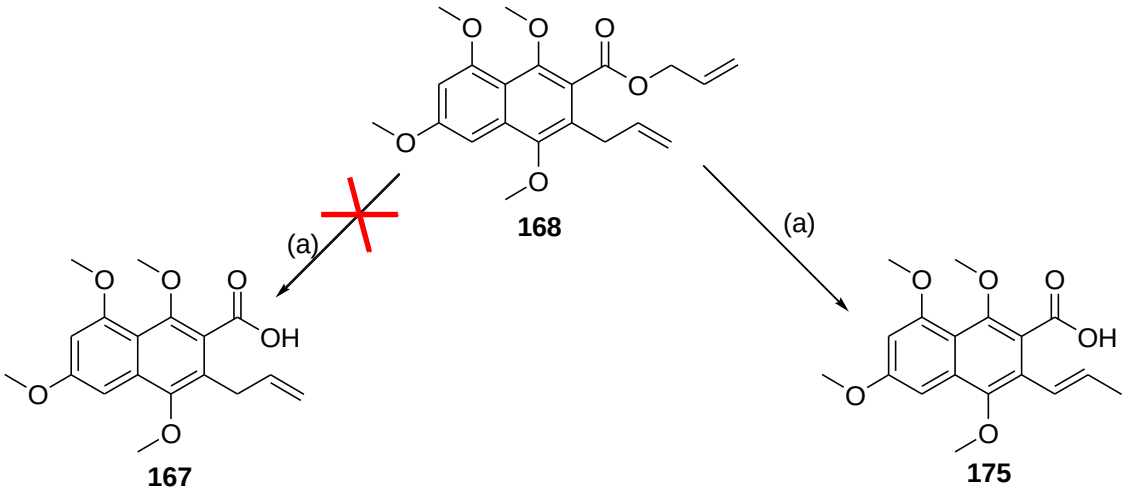
Despite appearing as one spot on the TLC plate which was different from the precursor compound, the ^1H NMR spectrum of the isolated compound revealed an uncharacterized impure material with no molecular ion peak corresponding to the target pyranonaphthoquinone **159** evident in the mass spectrum.

A literature search revealed that there is an array of metal-mediated methodologies which have been successfully deployed in deallylation of allyl esters.[132] Palladium is one of the metals which has been extensively employed for this reaction and its mechanism is thought to be through isomerization of the allyl double bond followed by cleavage of the allyl group.[134] The tetraoxygenated naphthalene **168** had both *O*-allyl and *C*-allyl substituents which meant that the *C*-allyl group could potentially be isomerized in the process of deallylation of the ester, but we thought that internalization of the *C*-allyl double bond would not pose challenges in subsequent steps.

2.1.7 Synthesis of 1,4,6,8-tetramethoxy-3-((*E*)-prop-1-enyl)naphthalene-2-carboxylic acid 175

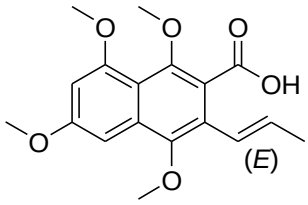
A mixture of allyl ester **168**, triphenylphosphine and morpholine were charged into a round bottom flask to which dry tetrahydrofuran was added. The catalytic amount of palladium acetate was then added and the reaction mixture was stirred for 12 hours at room temperature under the atmosphere of nitrogen gas. Purification of the crude product by column chromatography on flash silica gel afforded isomerized carboxylic acid **175** in 56% yield, instead of the desired acid **167** (**Scheme 2.13**) although this was not unexpected. The IR spectrum of acid **175** showed peaks at 3680 cm^{-1} and 1681 cm^{-1} corresponding to the hydroxyl and carbonyl functional groups of the carboxylic acid, respectively. In addition, the

HRMS spectrum showed a molecular ion peak at 333.1336 amu which was in good agreement with the expected mass of 333.1333 amu for $C_{18}H_{21}O_6$.



Scheme 2.13: *Reagents and conditions:* (a) cat. $Pd(OAc)_2$, PPh_3, morpholine, rt, N_2 (g), 12 hrs, 56%.

The ^{1}H NMR spectrum revealed loss of signals corresponding to loss of one *O*-allyl group.



The proton signals at 6.57 ppm (1H, dq, *J* = 16.1, 1.5 Hz) and 6.41 ppm (1H, dq, *J* = 16.1, 6.3 Hz) were assigned to (ArC*H*=CHCH$_3$) and (ArCH=C*H*CH$_3$), respectively. The large coupling constant of *J* = 16.1 Hz suggested that these protons were in a *trans*-configuration to each other and therefore, the configuration of the alkene was designated as *E*. The signal at 1.93 ppm (3H, dd, *J* = 6.4, 1.4 Hz) corresponded to the (ArCH=CHC*H*$_3$) protons. The ^{1}H NMR spectrum showed no signals corresponding to the desired carboxylic acid **167**. The ^{13}C NMR spectrum revealed loss of two signals in the aromatic/alkene region further confirming loss of one allyl group. The spectrum showed a signal at 170.7 ppm corresponding to the carbon atom of the carboxylic acid functional group.

The identity of the carboxylic acid was undeniably confirmed by single crystal x-ray crystallography and the ORTEP diagram is shown in **Figure 2.2**.

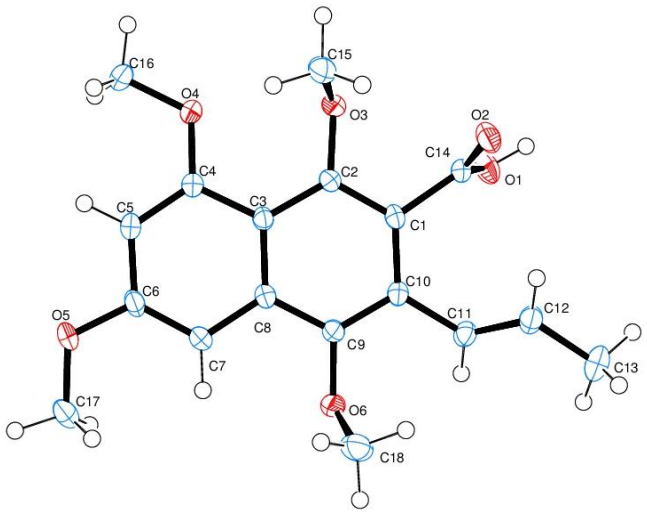


Figure 2.2: The ORTEP diagram of acid **175**. Thermal ellipsoids are shown at the 50% probability level.

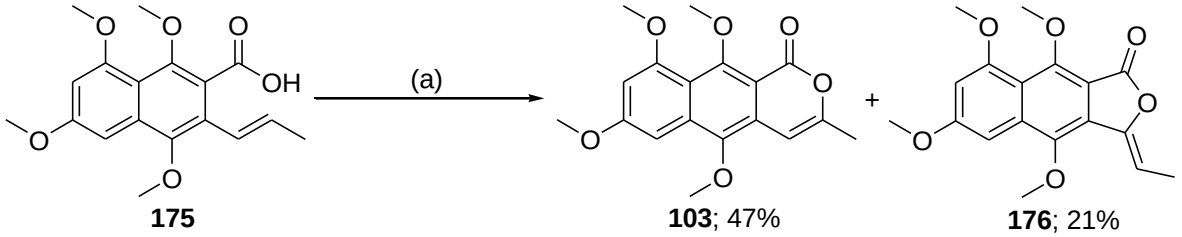
Satisfied that we had successfully synthesized the required carboxylic acid we were set to perform the Wacker oxidation reaction of the carboxylic acid **175**. A search for a precedent Wacker-type oxidation reaction involving a naphthoic acid yielded no results despite a plethora of reactions involving alcohol functional groups. Nonetheless we opted to use the normal Wacker oxidation reaction conditions.[135]

2.1.8 Synthesis of 5,7,9,10-tetramethoxy-3-methyl-1*H*-benzo[*g*]isochromen-1-one 103

The carboxylic acid **175** was dissolved in *N*,*N*-dimethylformamide in a 2-neck round bottom flask to which water, copper chloride and a catalytic amount of palladium chloride were added and the reaction mixture was vigorously stirred for 24 hours under a constant atmosphere of oxygen gas. The separation of the crude reaction mixture by silica gel column chromatography afforded lactone **103** and furanone **176** in 47% and 21% yields, respectively (**Scheme 2.14**). Despite having different R_f values, the two compounds proved difficult to separate even using flash silica gel as a stationary phase. Separation was fully achieved after chromatography using at least 3 repeated silica gel columns.

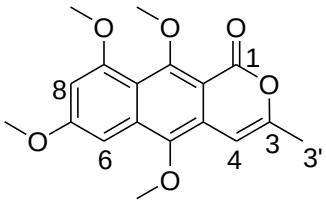
The IR spectrum of lactone **103** showed loss of a peak at 3460 cm^{-1} which was assigned to the hydroxyl functional group of the precursor acid and the peaks at 1689 cm^{-1} and 1603 cm^{-1}

were assigned to the carbonyl and alkene functional groups of the lactone, respectively. The HRMS spectrum of this isocoumarin further showed a molecular ion peak at 331.1181 amu which was in good agreement with the expected mass of 331.1176 amu for $C_{18}H_{19}O_6$.



Scheme 2.14: *Reagents and conditions:* (a) cat. $PdCl_2$, $CuCl_2 \cdot 2H_2O$, DMF/H_2O, O_2 (g), rt, 24 hrs.

The ^{1}H NMR spectrum of lactone **103** revealed loss of one alkene proton and the remaining proton showed a singlet signal. The signals at 6.98 ppm (1H, d, *J* = 2.3 Hz) and 6.51 ppm (1H, d, *J* = 2.3 Hz) corresponded to H-6 and H-8 protons, respectively which meant that the proton was not lost from the naphthalene portion of naphthoic acid **175**. The coupling constant of *J* = 2.3 Hz confirmed that H-6 and H-8 protons were *meta* to each other. The singlet signals at 6.48 ppm (1H, s) and 2.27 ppm (3H, s) were assigned to H-4 and H-3' protons, respectively. The ^{13}C NMR spectrum showed a signal at 160.0 ppm corresponding to the lactone carbon atom (C-1). The signals at 153.4 ppm and 19.8 ppm were assigned to C-3 and C-3' carbon atoms, respectively.



103

Vilegas and co-workers synthesized lactone **103** from paepalantine **102** by a methylation protocol as part of the structural elucidation process of paepalantine as explained in **Section 1.7.8**. The spectroscopic data presented here for lactone **103** was in agreement with the data presented by Vilegas and co-workers.[86]

The structure of lactone **103** was undoubtedly confirmed by x-ray crystal structure determination and the ORTEP diagram is shown in **Figure 2.3**.

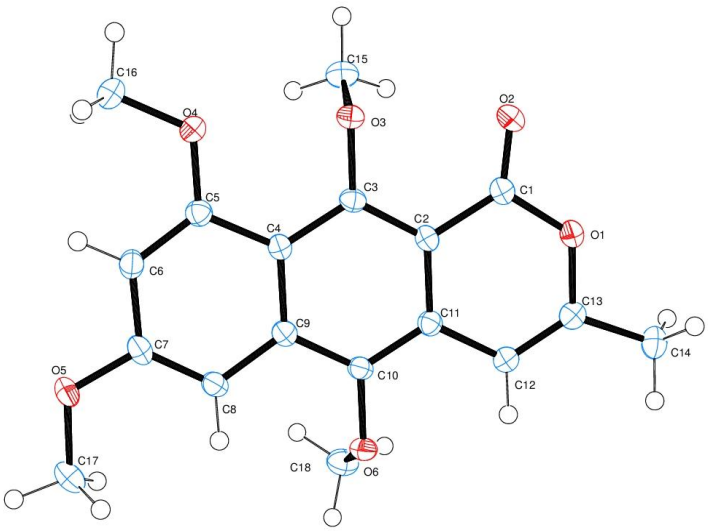


Figure 2.3: The ORTEP diagram of lactone **103**. Thermal ellipsoids are shown at the 50% probability level.

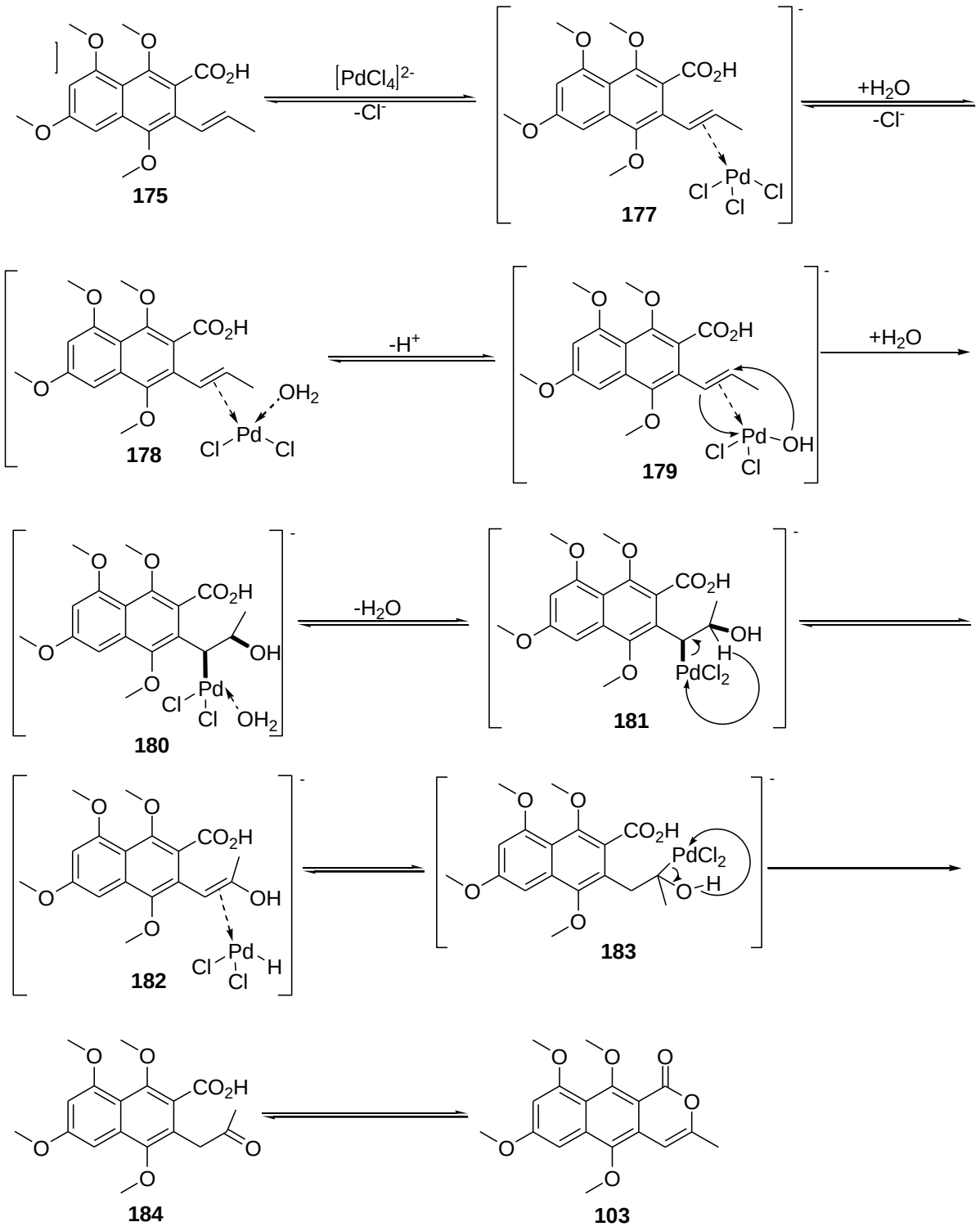
2.1.8.0 Proposed mechanism for inner-sphere Wacker oxidation reaction

The Wacker oxidation reaction mechanism is not fully understood but it is generally accepted that it proceeds by two different routes; namely the outer-sphere and the inner-sphere mechanistic pathways.[136] Depending on the prevailing reaction conditions the two mechanisms may be accessed by the reaction leading to the formation of products based on both pathways.

The inner-sphere mechanistic pathway is depicted in **Scheme 2.15**. The first step involves coordination of the palladium metal to the π-system of the allyl side chain of acid **175** thereby forming a palladium-alkene π-complex **177**. This process activates the alkene double bond for nucleophilic attack. One of the chloride atoms bonded to the palladium metal centre is then replaced by a water molecule leading to the formation of complex **178**. The loss of a proton from complex **178** delivers intermediate **179**. The complex **179** then undergoes *syn* addition of the hydroxyl group to one of the alkene carbon atoms to form a *cis*-(β-hydroxyalkyl)palladium complex **180**. This complex is decomposed by β-hydride elimination, as shown by curved arrows in complex **181**, affording the substituted enol **182**. The enol immediately undergoes a palladium-mediated tautomerization, *via* complex **183**, furnishing ketone **184**. Finally, the ketone reacts with the *ortho* positioned carboxylic acid

which is followed by a dehydration reaction affording pyranone ring-containing naphthalene **103**.

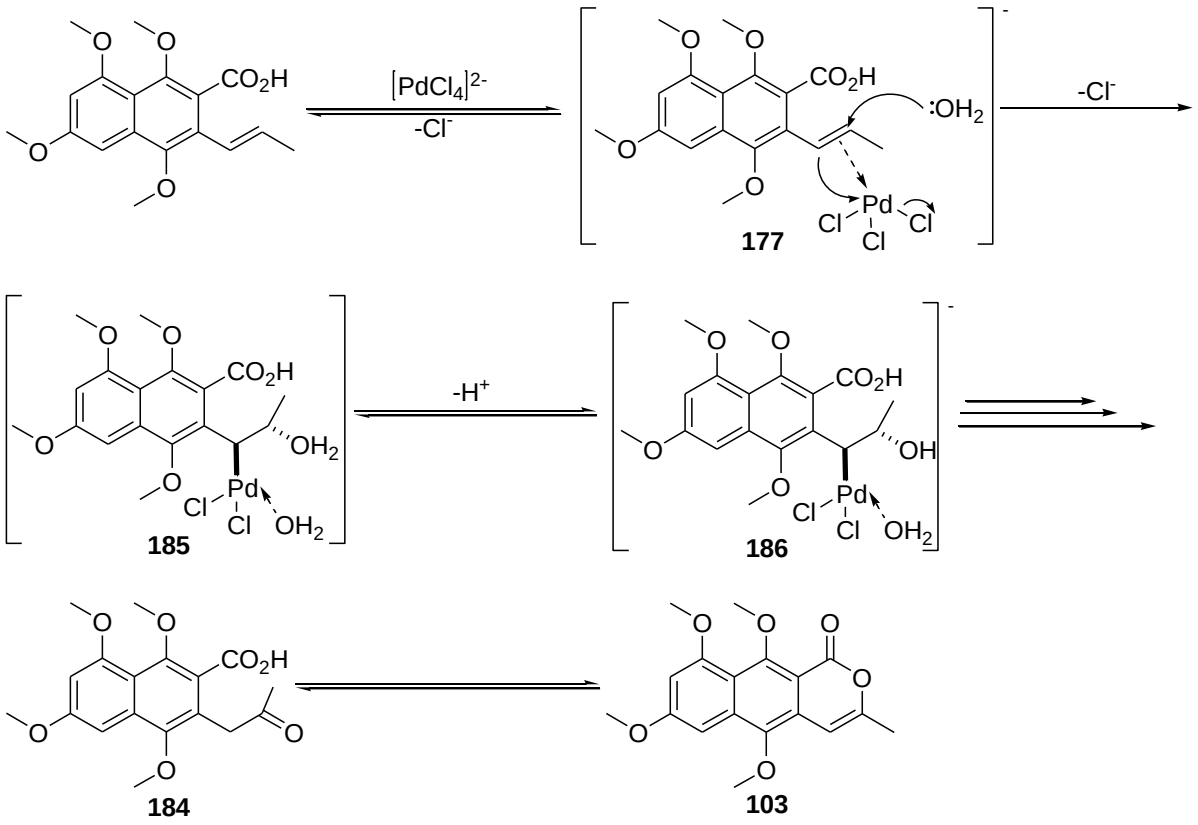
The palladium (0) catalyst in all Wacker oxidation reactions is regenerated to palladium (II) by copper (II) chloride and oxygen and re-enters the catalytic cycle.[137]



Scheme 2.15: Wacker inner-sphere mechanism for the formation of the 6-membered ring lactone **103**.

2.1.8.1 Proposed mechanism for outer-sphere Wacker oxidation reaction

In the outer-sphere pathway, the water molecule directly attacks the palladium-alkene π-complex **177** in an *anti*-nucleophilic fashion affording complex **185**. The loss of a proton from this complex delivers *trans*-(β-hydroxyalkyl)palladium complex **186**. The complex **186** then undergoes the same reaction sequences depicted in **Scheme 2.15** furnishing ketone **184** and cyclization affords lactone **103** as shown in reaction **Scheme 2.16**.



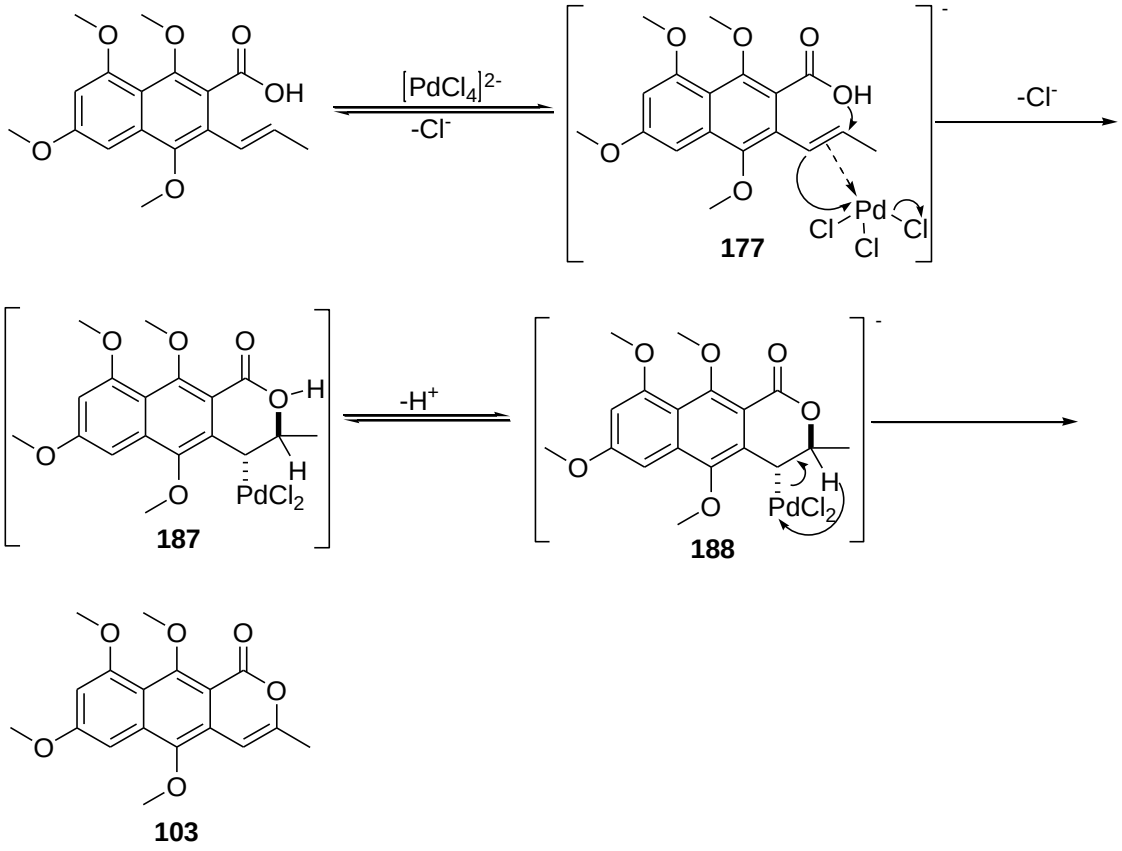
Scheme 2.16: Wacker outer-sphere mechanism for the formation of lactone **103**.

When a substrate has an internal nucleophile then it is expected that there will be competition between the water molecule and the internal nucleophile in attacking the palladium-alkene π-complex. In our laboratories, Pelly in her PhD thesis proposed that for substrates with an internal nucleophile like the one we had in our hands, it is most likely that the reaction proceeds by intramolecular Wacker oxidation reaction involving the internal nucleophile. This conclusion was reached after noting that no ketone intermediate species were isolated from the reaction mixture involving a substrate with an internal nucleophile.[122a] The same

observation was also made in our case in which despite isolating a small amount of the starting material, there was no evidence of any ketone products in the reaction mixture.

2.1.8.2 Proposed mechanism for outer-sphere intramolecular Wacker oxidation reaction

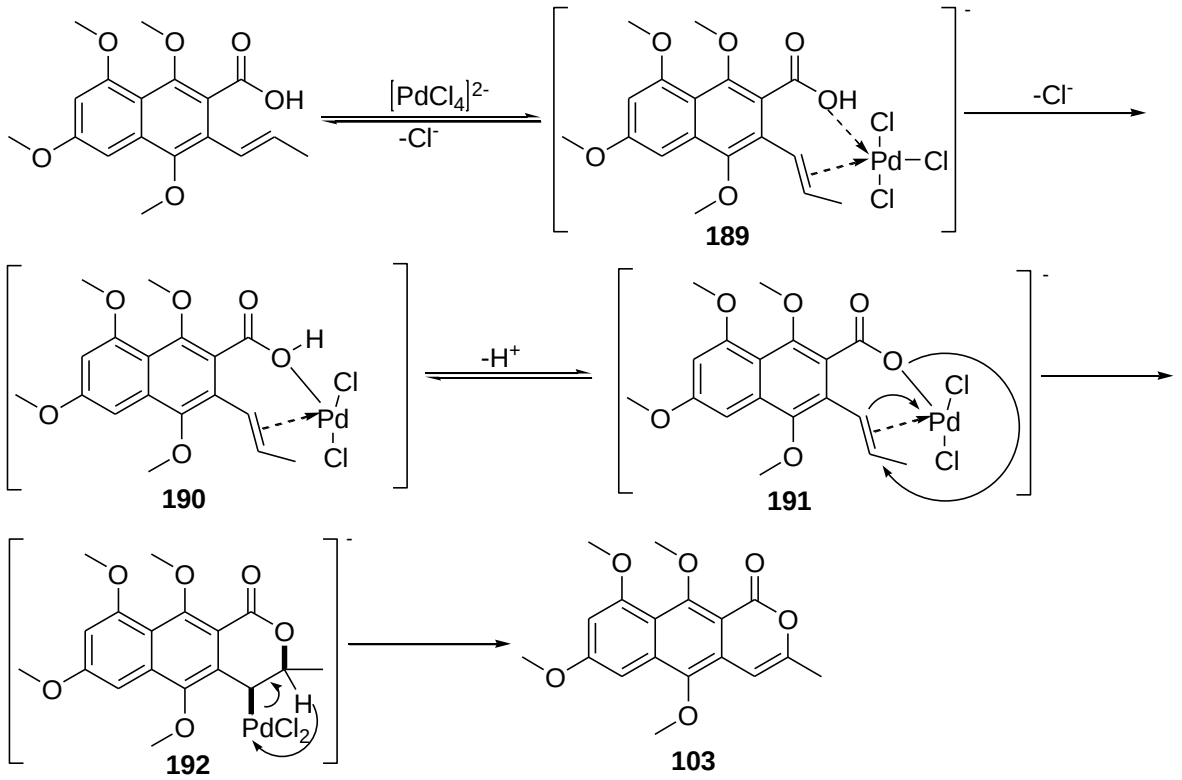
The outer-sphere pathway for an intramolecular Wacker oxidation reaction is depicted in **Scheme 2.17**. In this mechanism, the hydroxyl group of the carboxylic acid undergoes *anti*-intramolecular nucleophilic attack on the electrophilic palladium alkene π-complex **177** furnishing complex **187**. The loss of a proton from this complex affords a *trans*-complex **188**. The intermediate **188** then undergoes a typical β-hydride elimination delivering lactone **103**.



Scheme 2.17: Intramolecular Wacker outer-sphere mechanism for the formation of lactone **103**.

2.1.8.3 Proposed mechanism for inner-sphere intramolecular Wacker oxidation reaction

The inner-sphere intramolecular Wacker oxidation mechanism involves the coordination of the carboxylic acid functional group to the palladium metal centre as shown in complex **189** (**Scheme 2.18**). The coordinated hydroxyl group then attacks the metal centre which delivers complex **190**. The loss of a proton from this complex is followed by a *cis*-intramolecular nucleophilic attack on the electrophilic palladium alkene π-complex **191** which affords a *cis*-intermediate **192**. The β-hydride elimination shown by curved arrows in complex **192** yields lactone **103**. The mechanism for this reaction pathway is given in **Scheme 2.18**.

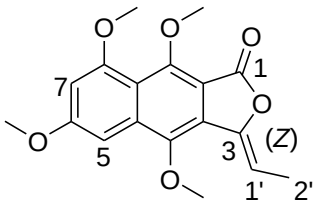


Scheme 2.18: Intramolecular Wacker inner-sphere mechanism for the formation of lactone **103**.

Having successfully identified and assigned various signals of lactone **103** to the corresponding protons and carbon atoms we turned our attention to identifying the second product from the reaction, pyranone **176**. Again the IR spectrum of this compound showed loss of a peak at 3680 cm^{-1} which was assigned to the hydroxyl functional group of the precursor acid **175**. The peaks at 1762 cm^{-1} and 1679 cm^{-1} in the product **176** were assigned to the carbonyl and alkene functional groups, respectively. The HRMS spectrum was largely

the same as that of lactone **103**. The ^{1}H NMR spectrum of furanone **176** revealed the loss of one alkene proton and the remaining proton showed a quartet multiplicity. The spectrum was fairly simple to solve due to the fact that there was only one manner in which the alkene proton could show a signal with a quartet multiplicity, which was by coupling to the methyl protons. This meant that in this case we had a 5-membered pyranone ring system unlike in compound **103** which had a 6-membered pyranone ring.

The ^{1}H NMR spectrum of furanone **176** showed proton signals at 7.02 ppm (1H, d, J = 2.3 Hz) and 6.56 ppm (1H, d, J = 2.3 Hz) corresponding to H-5 and H-7 protons, respectively. These signals showed a typical *meta*-coupling constant of J = 2.3 Hz which again meant that the proton was not lost from the naphthalene part of the precursor acid. The quartet signal at 5.92 ppm (1H, q, J = 7.3 Hz) was assigned to the H-1' proton and a doublet signal at 2.04 ppm (3H, d, J = 7.3 Hz) was assigned to the H-2' protons. The ^{13}C NMR spectrum showed signals at 164.8 ppm and 155.4 ppm corresponding to the furanone carbon atom (C-1) and alkene carbon atom C-3, respectively. The carbon signal at 11.7 ppm was assigned to C-2'.



176

The structure of furanone **176** was undoubtedly confirmed by x-ray crystal structure determination and the ORTEP diagram is shown in **Figure 2.4**. The crystal structure confirmed the configuration of the alkene as *Z*.

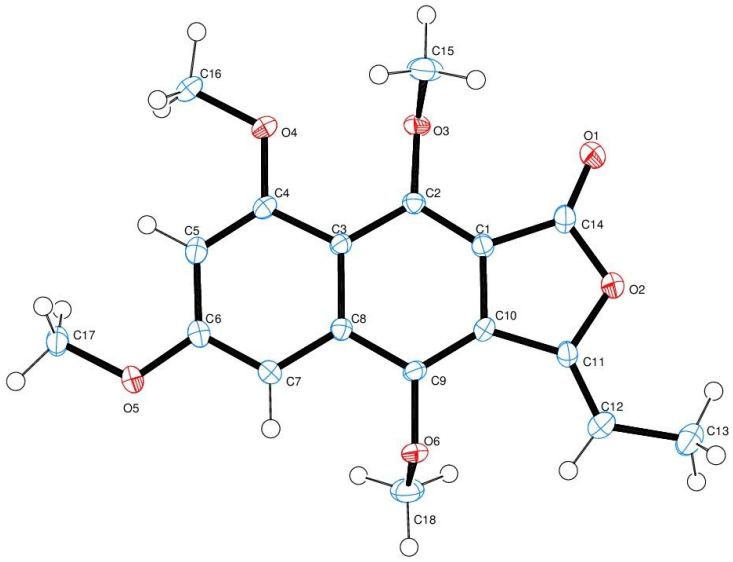
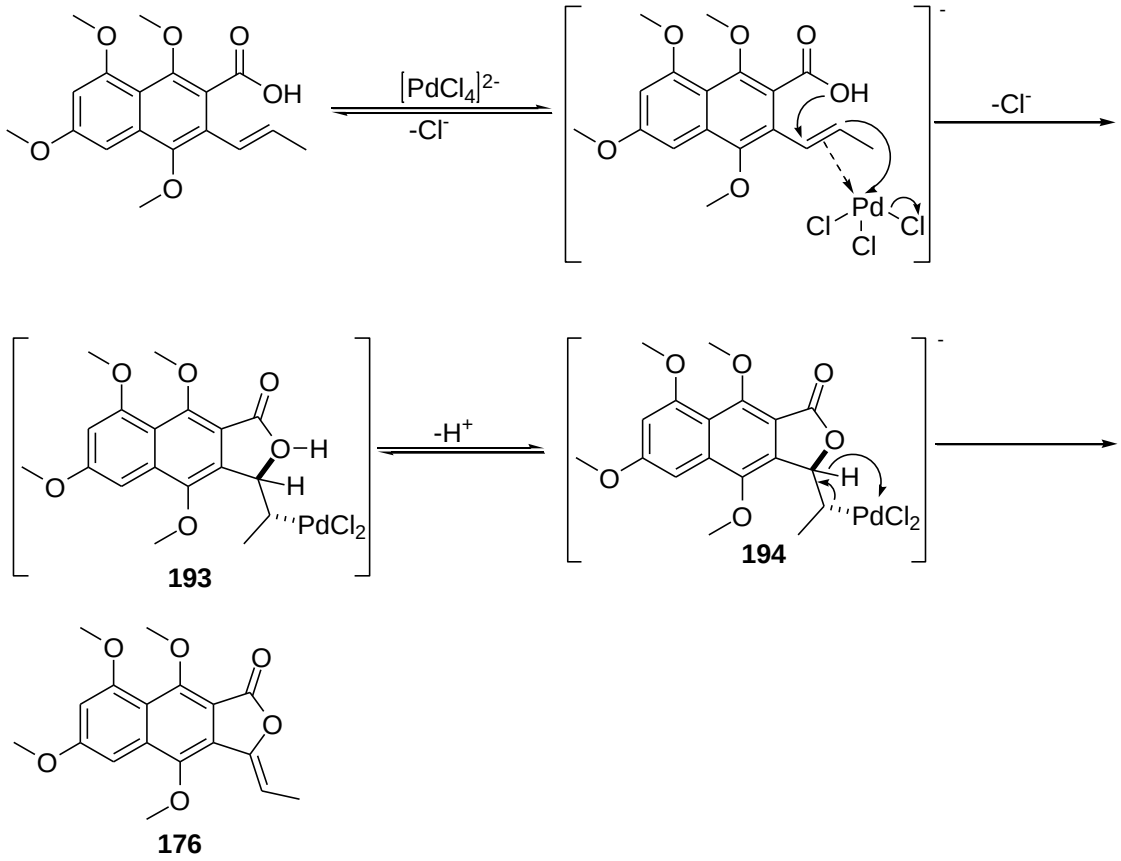


Figure 2.4: ORTEP diagram of furanone **176**. Thermal ellipsoids are shown at the 50% probability level.

The formation of the 5-membered pyranone ring could be analysed in the same way as the formation of the 6-membered pyranone ring. The Wacker oxidation reaction under our conditions follows Markovnikov's rule[138] in which nucleophilic attack is expected to take place at the more substituted carbon atom of the alkene. However, the substrate in our hands had the same substitution level at both carbon atoms of the alkene double bond. Nucleophilic attack on the inner carbon atom of the double bond furnished a 5-membered pyranone ring product as depicted in **Scheme 2.19** whereas nucleophilic attack on the outer vinylic carbon atom led to the formation of the 6-membered lactone ring as explained above.

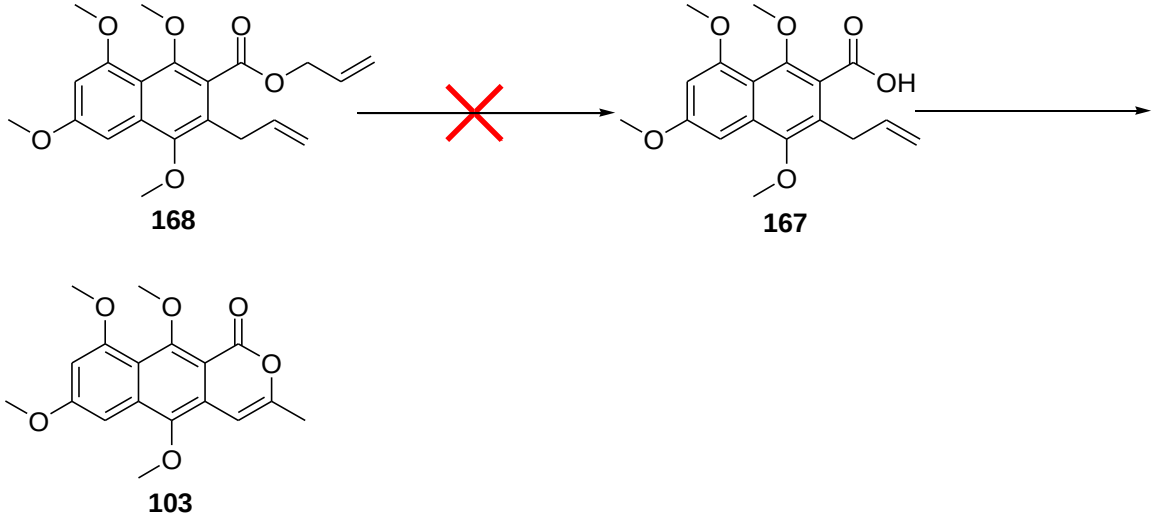
2.1.8.4 Proposed mechanism for outer-sphere intramolecular Wacker oxidation reaction

The outer-sphere mechanism for intramolecular Wacker oxidation reaction as depicted in **Scheme 2.19** involves the formation of the 5-membered ring palladium complex **193** and the deprotonation of this complex furnishes a *trans*-intermediate **194**. A typical *β*-hydride elimination reaction of complex **194** delivers furanone **176**.



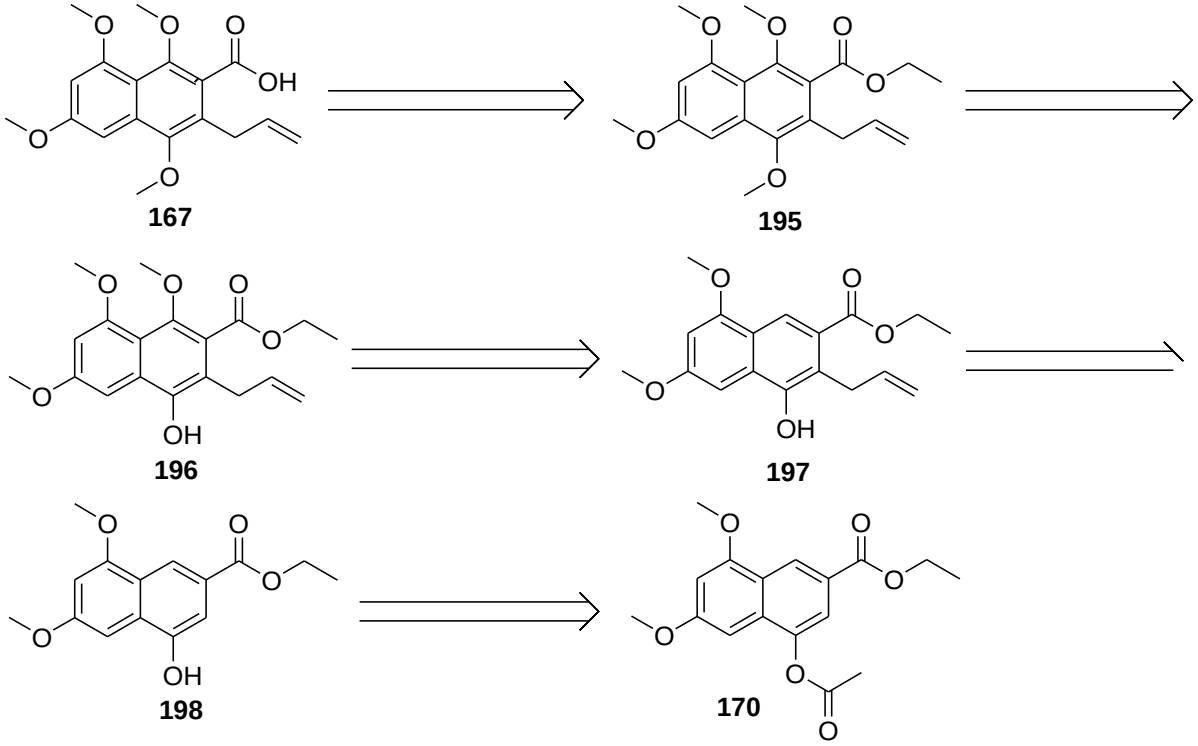
Scheme 2.19: Intramolecular Wacker outer-sphere mechanism for the formation of the furanone ring.

It was gratifying that we successfully synthesized an important precursor, lactone **103**, which we thought could potentially lead to the synthesis of both dehydroherbarin lactone **159** and paepalantine **102**. As much as we successfully completed the synthesis of the required lactone **103**, we were not pleased with the amount of effort it took to separate the two pyranone compounds **103** and **176**. Analysis of the proposed lactonization reaction mechanisms seemed to suggest that there was a high possibility that only a 6-membered lactone ring could be formed if naphthoic acid **167** was used for this reaction. A simple acid/base hydrolysis of allyl ester **168** did not possibly work because of the allyl groups which are known to require harsher conditions to effect hydrolysis.[139] In other words, to obtain lactone **103** as our only product we needed carboxylic acid **167** but simple hydrolysis of allyl ester **168** failed to deliver the required acid (**Scheme 2.20**).



Scheme 2.20: The failed acid/base hydrolysis of allyl ester **168**.

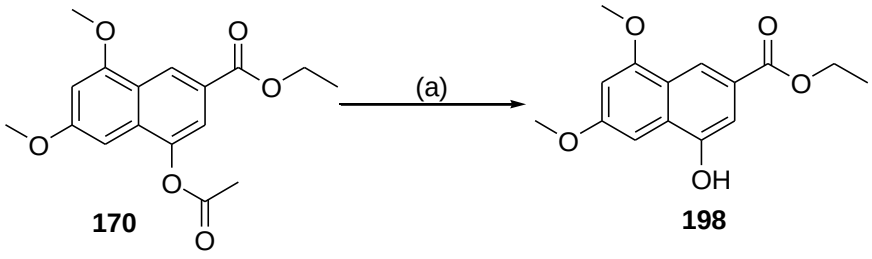
At this point we postulated that the ethyl or methyl ester of the tetraoxygenated naphthalene such as ester **195** might possibly not give us the same hydrolysis problems as the allyl ester **168**. The retrosynthetic analysis revealed that the ethyl equivalent of the allyl ester **168** could easily be synthesized by employing the same protocol we used for the synthesis of the allyl ester (**Scheme 2.21**). The only change in the protocol would be the selective cleavage of the acetyl protection group of naphthalene **170** which could furnish naphthol **198**. The monoallylation and Claisen rearrangement reactions could deliver naphthol **197**. PIFA mediated methoxylation of naphthol **197** could potentially lead to the synthesis of trimethoxynaphthalene **196**. The methylation of naphthol **196** could afford tetramethoxynaphthalene **195** which upon simple acid/base hydrolysis reaction could potentially deliver carboxylic acid **167**.



Scheme 2.21: Retrosynthetic analysis for the formation of acid **167**.

2.1.9 Synthesis of ethyl 4-hydroxy-6,8-dimethoxynaphthalene-2-carboxylate 198

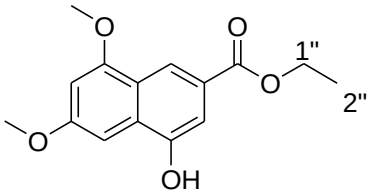
The synthesis commenced by dissolving naphthalene **170** in a 1% ethanolic solution of potassium hydroxide. The mixture was stirred at room temperature for 3 hours after which it was acidified with 32% aqueous hydrochloric acid and the crude reaction mixture was purified by column chromatography on silica gel yielding naphthol **198** in 88% (**Scheme 2.22**).



Scheme 2.22: *Reagents and conditions:* (a) (i) *1%* KOH in EtOH, rt, 3 hrs (ii) *32%* aq. HCl, 88%.

The ^{1}H NMR spectrum of naphthol **198** revealed loss of a singlet signal which was at 2.46 ppm in the precursor naphthalene **170** and was assigned to the methyl protons of the acetyl

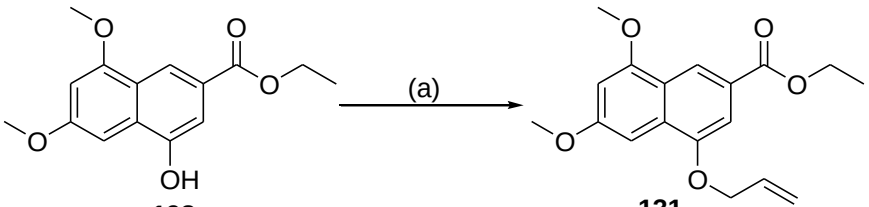
group. A new D_2O exchangeable signal at 9.13 ppm (1H, s) was typical of the naphthol proton. A quartet signal at 4.37 ppm (2H, q, *J* = 7.1 Hz) was assigned to the H-1" protons ($ArCO_2CH_2CH_3$) whereas a signal at 1.39 ppm (3H, t, *J* = 7.1 Hz) was assigned to the H-2" protons ($ArCO_2CH_2CH_3$). The ^{13}C NMR spectrum revealed loss of a signal which was at 170.1 ppm in the starting material and was attributed to the carbonyl carbon atom of the acetyl group. A signal at 167.2 ppm due to the ester carbonyl carbon atom was still visible alongside the signals at 61.2 ppm and 14.7 ppm for C-1" ($ArCO_2CH_2CH_3$) and C-2" ($ArCO_2CH_2CH_3$), respectively. These result confirmed successful selective deacetylation and at this point we were ready for selective allylation.



198

2.1.10 Synthesis of ethyl 4-(allyloxy)-6,8-dimethoxynaphthalene-2-carboxylate 131

Satisfied that we had successfully cleaved the acetyl group of the naphthalene core, we subjected the resultant naphthol **198** to a routine allylation reaction using allyl bromide and potassium carbonate which furnished allyl ether **131** in 87% yield as shown in **Scheme 2.23**. The loss of the naphthol proton was evident in the ^1H NMR spectrum and the signals due to the ethyl protons were noted which crucially indicated that the ethyl group was not lost during the allylation reaction.

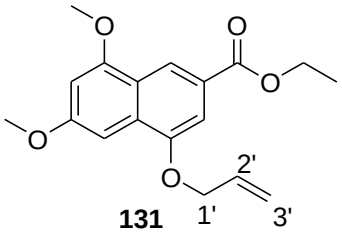


198 **131**

Scheme 2.23: *Reagents and conditions:* (a) K_2CO_3, allyl bromide, Me_2CO, reflux, 24 hrs, 87%.

A signal at 6.24 ppm (1H, ddt, *J* = 17.2, 10.4, 5.1 Hz) was assigned to the inner vinylic proton of the allyl group H-2' ($ArOCH_2CH=CH_2$) whereas the signal at 5.58 ppm (1H, dd, *J* = 17.3, 1.7 Hz) was assigned to one of the terminal vinylic protons H-3' ($ArOCH_2CH=CH_2$) which was in the *trans* position to the inner vinylic proton with a *trans*-coupling constant of *J* = 17.3 Hz. The signal at 5.35 ppm (1H, dd, *J* = 10.6, 1.5 Hz) was assigned to the remaining

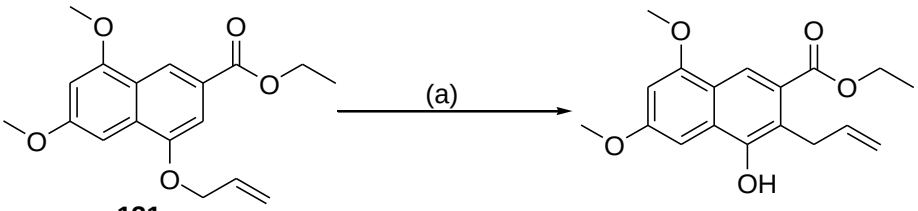
terminal vinylic proton H-3' ($ArOCH_2CH=CH_2$) which was in the *cis* position to the inner vinylic proton with a *cis*-coupling constant of J = 10.6 Hz. The doublet of triplets signal at 4.82 ppm (2H, dt, J = 4.9, 1.4 Hz) was assigned to the allylic proton H-1' ($ArOCH_2CH=CH_2$). The ^{13}C NMR spectrum revealed two new signals in the aromatic/alkene region corresponding to the two allyl alkene carbon atoms. The carbon signals at 134.5 ppm and 117.5 ppm were assigned to the C-2' and C-3' vinylic carbon atoms, respectively. The carbon signal at 69.8 ppm was typical of the ether allylic carbon atom C-1'.



131

2.1.11 Synthesis of ethyl 3-allyl-4-hydroxy-1,6,8-trimethoxynaphthalene-2-carboxylate 197

A routine neat Claisen rearrangement reaction of allyl ether **131** delivered the required *C*-allyl naphthol **197** (**Scheme 2.24**) in 69%. Successful formation of the product was confirmed by the loss of one aromatic proton in the ^1H NMR spectrum. The spectrum further revealed an upfield shift of the allylic proton signal at 4.82 ppm, which was for the *O*-allylic protons in the precursor allyl ether **131**, to 3.92 ppm (2H, d, J = 6.0 Hz) which was typical of the *C*-allylic protons. The exposed naphthol proton showed a D_2O exchangeable singlet signal at 5.65 ppm.



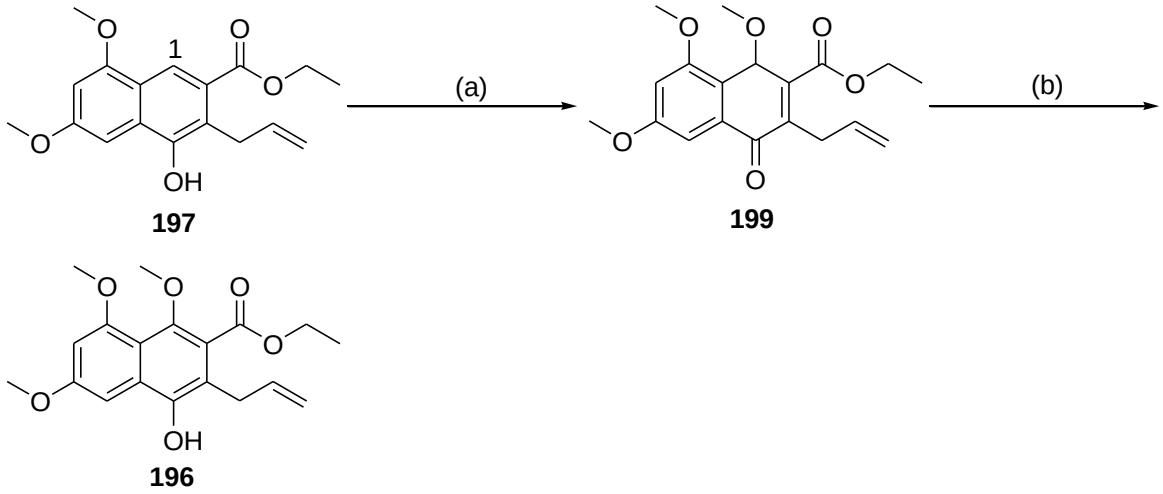
131 **197**

Scheme 2.24: *Reagents and conditions:* heat, 180 °C, N_2 (g), 24 hrs, 69%.

The ^{13}C NMR spectrum confirmed the successful Claisen rearrangement reaction by showing loss of a prominent *O*-allylic carbon signal at 69.8 ppm in the precursor compound. A new carbon signal at 31.8 ppm was assigned to the *C*-allylic carbon atom of the naphthol **197**.

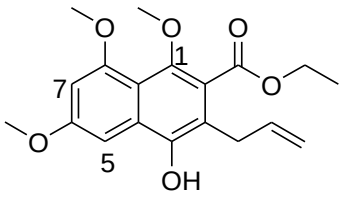
2.1.12 Synthesis of ethyl 3-allyl-1,4,6,8-tetramethoxynaphthalene-2-carboxylate 195

Satisfied that we had the desired substrate for the PIFA mediated insertion of the methoxy substituent we proceeded to carry out this reaction by subjecting naphthol **197** to a routine PIFA mediated insertion of a methoxy group. This reaction was immediately followed by re-aromatization of the presumed crude product **199** using potassium *tert*-butoxide (**Scheme 2.25**). The overall reaction resulted in an aromatic substitution reaction of a proton at *C*-1 of naphthol **197** with a methoxy substituent which delivered the tetraoxygenated naphthalene **196** in 60% yield.

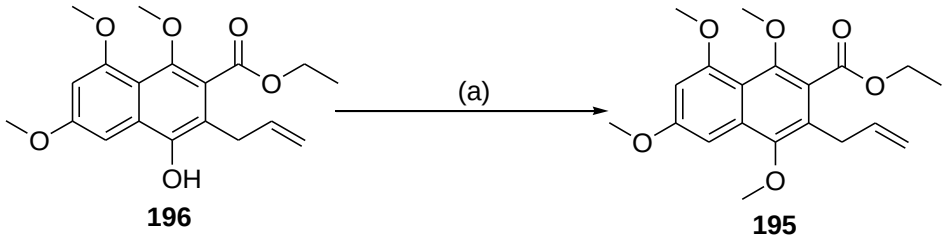


Scheme 2.25: *Reagents and conditions:* (i) (a) PIFA, MeOH, rt, 15 min (b) *t*-BuOK, EtOH, rt, 20 min, 60%.

Product formation was confirmed by the ^{1}H NMR spectrum which showed loss of one aromatic proton which was at 8.37 ppm in the precursor compound and was assigned to the proton *para* to the naphthol group (position 1). The two remaining signals at 7.08 ppm (1H, d, J = 2.2 Hz) and 6.53 ppm (1H, d, J = 2.2 Hz) corresponded to the H-5 and H-7 protons, respectively. These two protons showed a typical *meta*-coupling constant of J = 2.2 Hz indicating that methoxylation did not take place at positions 5 or 7 of the naphthalene nucleus. The spectrum further showed a new signal corresponding to the methoxy group attached to the aromatic carbon atom. Similarly, the ^{13}C NMR spectrum showed a new signal corresponding to the carbon signal of the methoxy group attached to the aromatic ring making a total of 3 methoxy carbon signals.



A routine methylation reaction of naphthol **196** using dimethyl sulfate and potassium carbonate (**Scheme 2.26**) afforded a tetramethoxynaphthalene **195** in 89% yield. The successful methylation reaction was confirmed by the ^{1}H NMR spectrum which showed the loss of the naphthol proton signal at 5.56 ppm in the precursor compound **196**. The presence of an additional methoxy group proton signal in the product, making a total of 4 methoxy group signals, was noted. The ^{13}C NMR spectrum confirmed the presence of an extra methoxy carbon signal, making a total of 4 aromatic methoxy signals.



Scheme 2.26: *Reagents and conditions:* (a) K_2CO_3, Me_2SO_4, Me_2CO, reflux, 24 hrs, 89%.

The successful methylation was further confirmed by crystallography and the ORTEP diagram of naphthalene **195** is given in **Figure 2.5**.

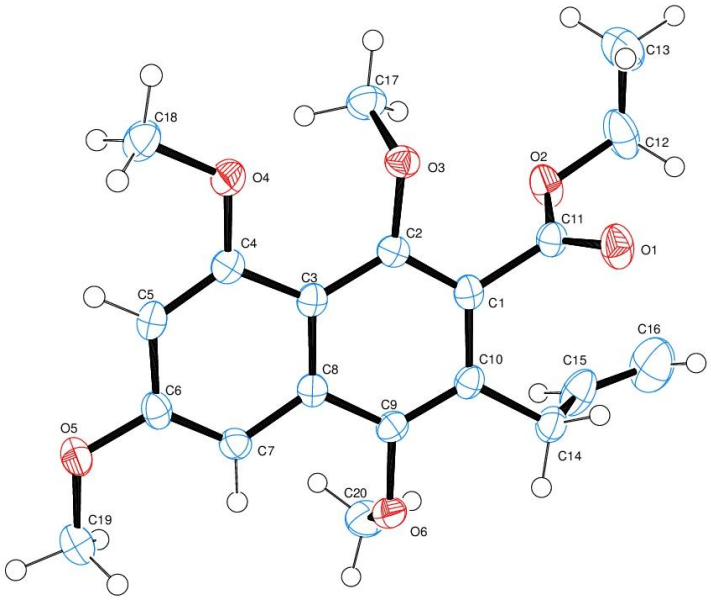
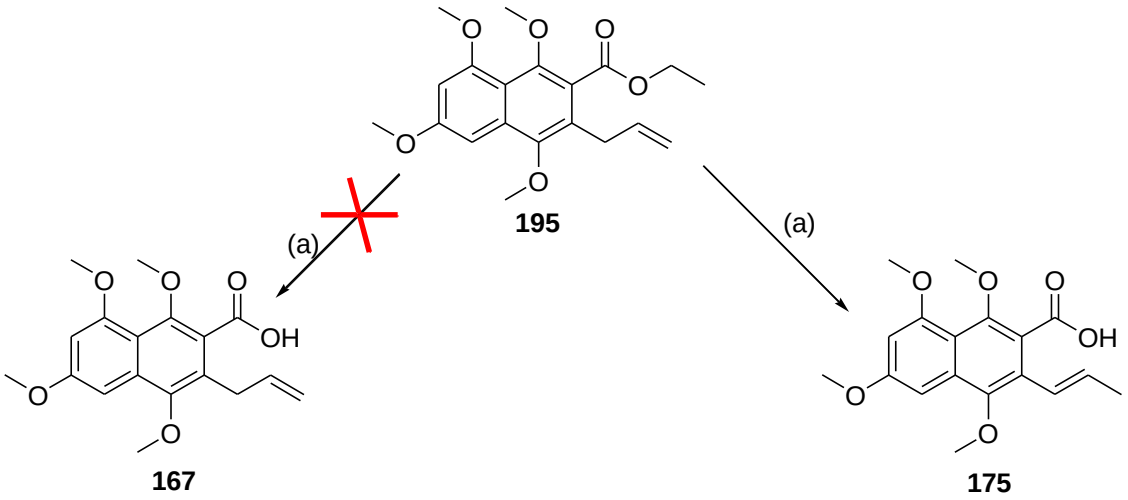


Figure 2.5: The ORTEP diagram of ester **195**. Thermal ellipsoids are shown at the 50% probability level.

2.1.13 Synthesis of 1,4,6,8-tetramethoxy-3-[(*E*)-prop-1-enyl]naphthalene-2-carboxylic acid 175

Satisfied with the results, we subjected ethyl ester **195** to base promoted saponification (**Scheme 2.27**) using sodium hydroxide as a base. To our surprise there was only a faint spot at the base of the TLC plate we believed corresponded to the carboxylic acid after monitoring the reaction for 24 hours. The reaction mixture was kept refluxing for a further 12 hours but there was no change in the intensity of the spot at the base of the TLC plate. At this point we decided to add potassium hydroxide to the reaction mixture and continued heating the reaction under reflux for a further 48 hours. The intensity of the spot corresponding to the carboxylic acid was more pronounced but there was still a faint spot on the TLC plate corresponding to the starting material.

At this point, the reaction mixture was acidified and the crude product was run through a short silica gel column and recrystallization from a hot solution of ethyl acetate and hexane afforded colourless crystals in 55% yield.



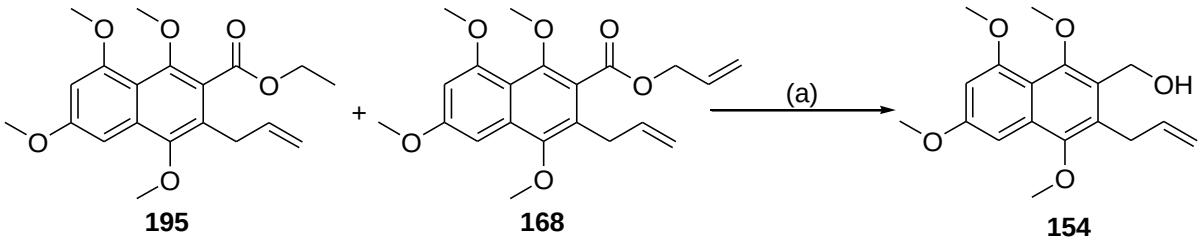
Scheme 2.27: *Reagents and conditions:* (a) (i) NaOH/KOH, MeOH/H_2O, reflux, 84 hrs (ii) *32%* aq. HCl, 55%.

The ^{1}H NMR spectrum showed loss of signals corresponding to the loss of the ethyl group. It further showed that the double bond of the *C*-allyl group had isomerized and all signals were similar to those the carboxylic acid **175** obtained from the palladium mediated deallylation

reaction. This meant that this reaction, again, delivered isomerized carboxylic acid **175** as opposed to the intended acid **167** as shown in **Scheme 2.27**.

2.1.14 Synthesis of 3-allyl-1,4,6,8-tetramethoxynaphthalene-2-carboxylic acid 167

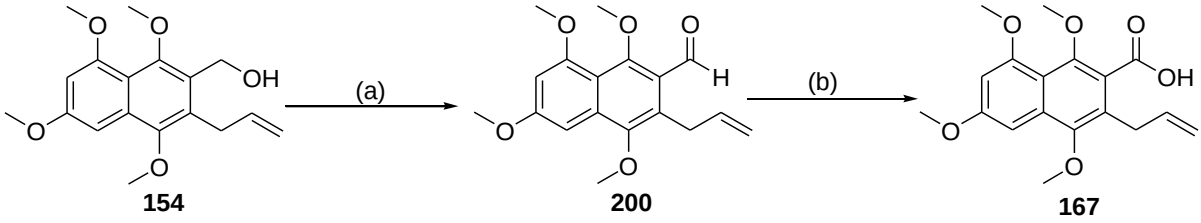
Frustrated by not obtaining the unisomerized carboxylic acid **167** using a one-step reaction protocol we were left with no option other than subjecting both esters **168** and **195** to a three-step reaction to obtain the required carboxylic acid as shown in **Schemes 2.28** and **2.29**. We envisaged that reduction of the two esters would give the same alcohol **154** which could then be oxidised to an aldehyde **200** and finally the aldehyde could be further oxidised to carboxylic acid **167** using Pinnick oxidation.[140] The mechanism for Pinnick oxidation should not result in isomerization of the allyl double bond.



Scheme 2.28: *Reagents and conditions:* $LiAlH_4$, THF, 0 $^oC \rightarrow$ rt, N_2 (g), 4 hrs (% yield not determined).

The two esters **168** and **195** were dissolved in dry tetrahydrofuran in a dry round bottom flask to which an equivalent amount of lithium aluminium hydride was added portion-wise and the resultant reaction mixture was stirred at room temperature for 4 hours. The presumed alcohol **154** was not purified apart from noting the differences in R_f values on the TLC plate. The crude alcohol **154** was oxidised to the corresponding aldehyde using pyridinium chlorochromate (PCC) adsorbed onto silica. The reaction was monitored by TLC and when all the alcohol was consumed the resultant crude aldehyde **200** was dissolved in 2-methyl-2-butene in a clean round bottom flask to which water, *tert*-butanol, sodium chlorite and monobasic sodium phosphate were added. The biphasic mixture was vigorously stirred at room temperature for 6 hours after which it was extracted into dichloromethane. The crude reaction mixture was purified by passing it through a silica gel column which was followed by recrystallization from a hot solution of ethyl acetate and hexane from which colourless

crystals were obtained in 60% yield (**Scheme 2.29**). The successful synthesis of the carboxylic acid **167** was confirmed by both ^{1}H and ^{13}C NMR spectroscopy. The IR spectrum of carboxylic acid **167** showed typical hydroxyl and carbonyl functional groups similar to carboxylic acid **175**. The HRMS spectrum of carboxylic acid **167** revealed essentially the same molecular ion peak as acid **175**.



154 **200** **167**

Scheme 2.29: *Reagents and conditions:* (a) PCC, silica, CH_2Cl_2, N_2 (g), 4 hrs (b) NaH_2PO_4, $NaClO_2$, H_2O, *t*-BuOH, 2-methyl-2-butene, 6 hrs, 60% over three steps (including the reduction step).

The ^{1}H NMR spectrum of carboxylic acid **167** revealed loss of signals due to the ethyl group and one allyl group available in esters **195** and **168**, respectively. The D_2O exchangeable signal at 10.82 ppm (1H, br s) was typical of carboxylic acid proton. The signal at 6.01 ppm (1H, ddt, J = 16.3, 10.1, 6.2 Hz) was assigned to the inner vinylic proton ($ArCH_2C\mathit{H}=CH_2$). The signal at 5.12 ppm (2H, dd, J = 2.8, 1.7 Hz) was assigned to the terminal vinylic protons ($ArCH_2CH=C\mathit{H}_2$) whereas the signal at 3.69 ppm (2H, d, J = 6.2 Hz) was assigned to the allylic protons ($ArC\mathit{H}_2CH=CH_2$). The ^{13}C NMR spectrum showed signals at 172.3 ppm and 31.6 ppm which were assigned to the carboxylic acid carbonyl carbon atom and the allylic carbon atom of the allyl group, respectively. The signal at 31.6 ppm was indicative of the unisomerized double bond of the propenyl substituent. The direct comparison of the spectra of the isomerized acid **175** with unisomerized acid **167** clearly showed the differences between the two carboxylic acids with acid **167** containing the allyl substituent whereas acid **175** contained a styrene substituent as shown in **Figure 2.6**.

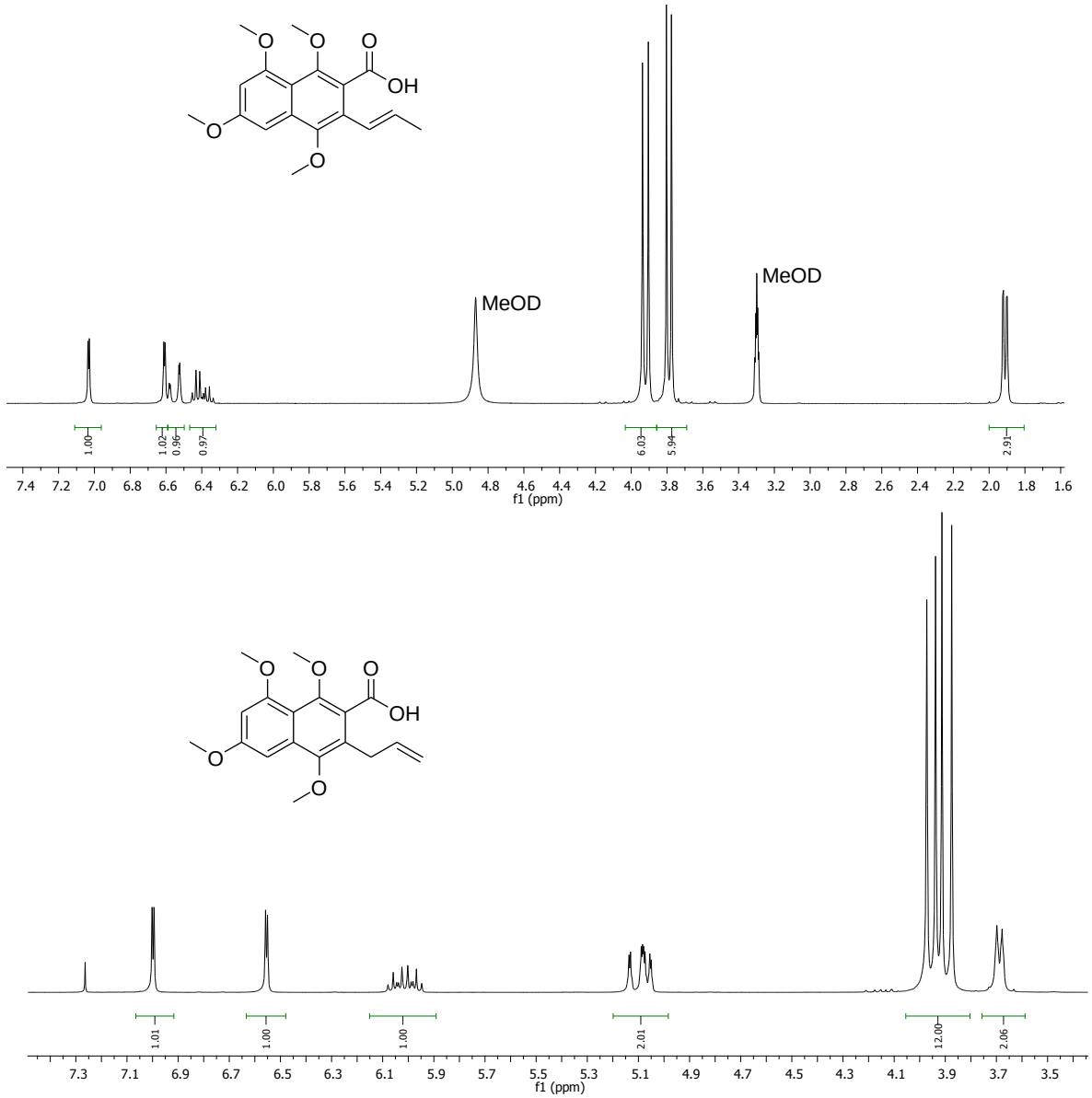


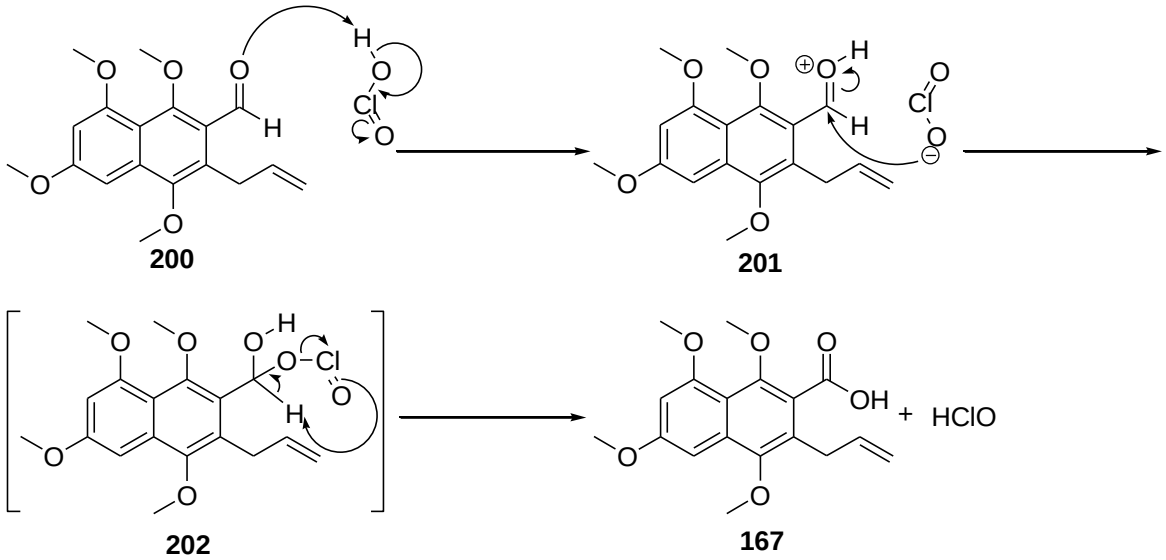
Figure 2.6: ^{1}H NMR spectra of carboxylic acids **175** (top) and **167** (bottom).

The top ^{1}H NMR spectrum in **Figure 2.6** clearly showed a doublet of doublets at 1.93 ppm integrating for 3 protons corresponding to the methyl group of the 2-propenyl substituent

whereas the bottom spectrum showed a doublet at 3.69 ppm integrating for 2 protons corresponding to the allylic protons of the 1-propenyl substituent.

2.1.14.0 Proposed mechanism for Pinnick oxidation reaction

The proposed Pinnick oxidation reaction mechanism involves chlorous acid as the active oxidant, which is known to be formed under acidic conditions from chlorite.[141] The chlorous acid protonates the aldehyde **200** to a corresponding protonated aldehyde **201** (**Scheme 2.30**). The intermediate **202** is produced from the nucleophilic attack of the conjugate base of chlorous acid on protonated aldehyde **201** and the resultant intermediate undergoes a pericyclic fragmentation reaction as shown by curved arrows in intermediate **202**. In this reaction, the aldehyde hydrogen is transferred to oxygen on the chlorine, with the chlorine group released as hypochlorous acid. This process furnished carboxylic acid **167** as the only organic acid.



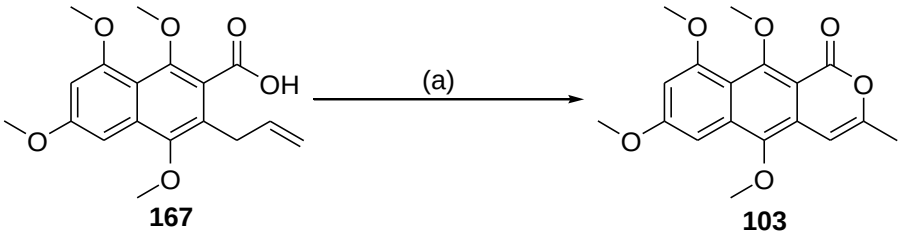
Scheme 2.30: Pinnick oxidation reaction mechanism for the formation of carboxylic acid **167**.

The hypochlorous acid by-product from the Pinnick oxidation reaction is in itself a reactive chemical that can destroy the sodium chlorite reactant or cause other undesired reactions with the organic materials. To prevent this interference, 2-methyl-2-butene was used as a scavenger which consumed the hypochlorous acid as it was formed and in the process produced halohydrin by-product.

At this point we were satisfied by the successful synthesis of the unisomerized carboxylic acid **167** which was our intended acid for the Wacker oxidation reaction.

2.1.15 Synthesis of 5,7,9,10-tetramethoxy-3-methyl-1*H*-benzo[*g*]isochromen-1-one 103

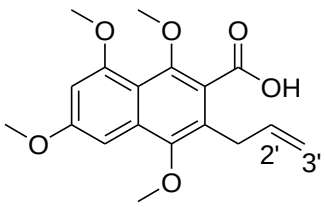
We finally subjected the carboxylic acid **167** to Wacker oxidation reaction conditions and we were very pleased when the TLC plate showed only one prominent spot. The reaction mixture was quenched after 24 hours and purification by column chromatography on silica gel furnished lactone **103** (**Scheme 2.31**) in 70% yield as the only product. The ^{1}H NMR spectrum confirmed the formation of lactone **103**.



Scheme 2.31: *Reagents and conditions:* (a) cat. $PdCl_2$, $CuCl_2{\cdot}2H_2O$, DMF/H_2O, O_2 (g), rt, 24 hrs, 70%.

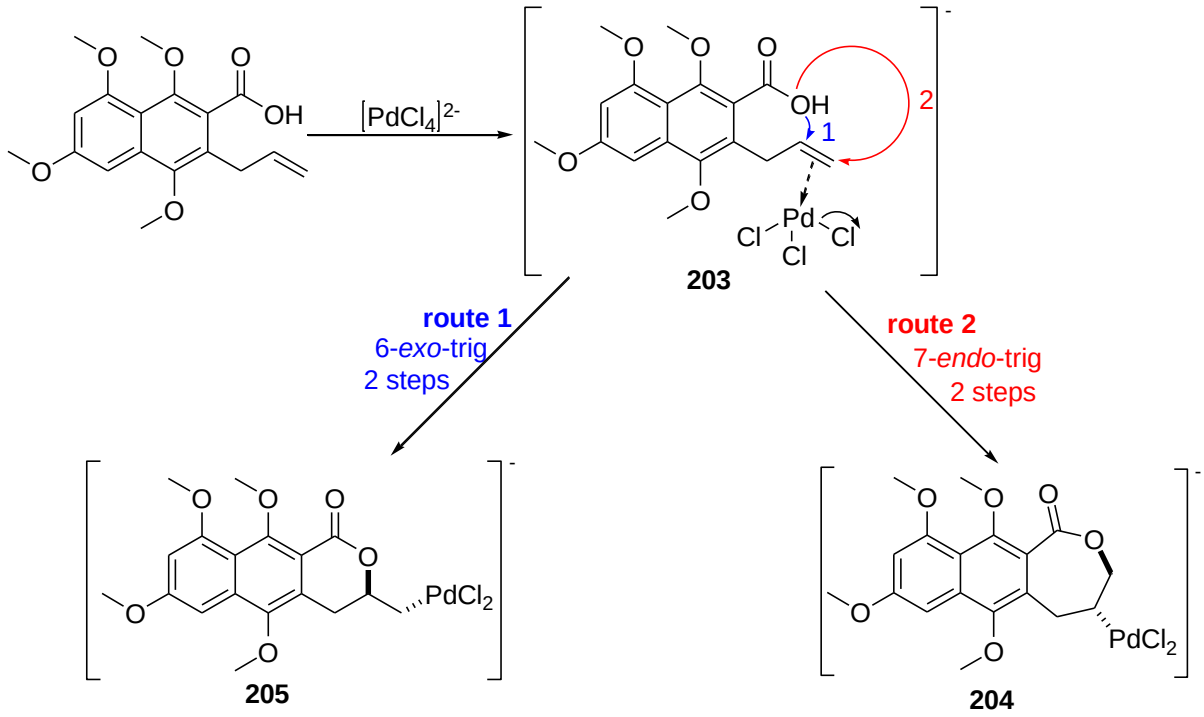
2.1.15.0 Proposed mechanism for outer-sphere intramolecular Wacker oxidation reaction for terminal alkene

If we consider the mechanistic pathways shown in **Schemes 2.17** and **2.19** the intermediate **177** was attacked on both ends of the alkene double bond leading to the formation of both 5- and 6-membered pyranone rings. The isomerization of the double bond leading to the formation of the 6-membered lactone ring took place at the end of the reaction after the hydroxyl group of the acid had already attacked one of the carbon atoms of the double bond. This implied that in the case of the terminal double bond there were only three possibilities after the initial coordination of the palladium metal to the alkene double bond.



The first possibility was that if the inner vinylic carbon atom ($ArCH_2\mathit{C}H{=}CH_2$, *C*-2') of the allyl group was more electrophilic than the terminal vinylic carbon atom ($ArCH_2CH{=}\mathit{C}H_2$, *C*-3') then the oxygen atom of the hydroxyl group would readily donate its electrons into a budding empty p orbital on *C*-2' and not on *C*-3'.

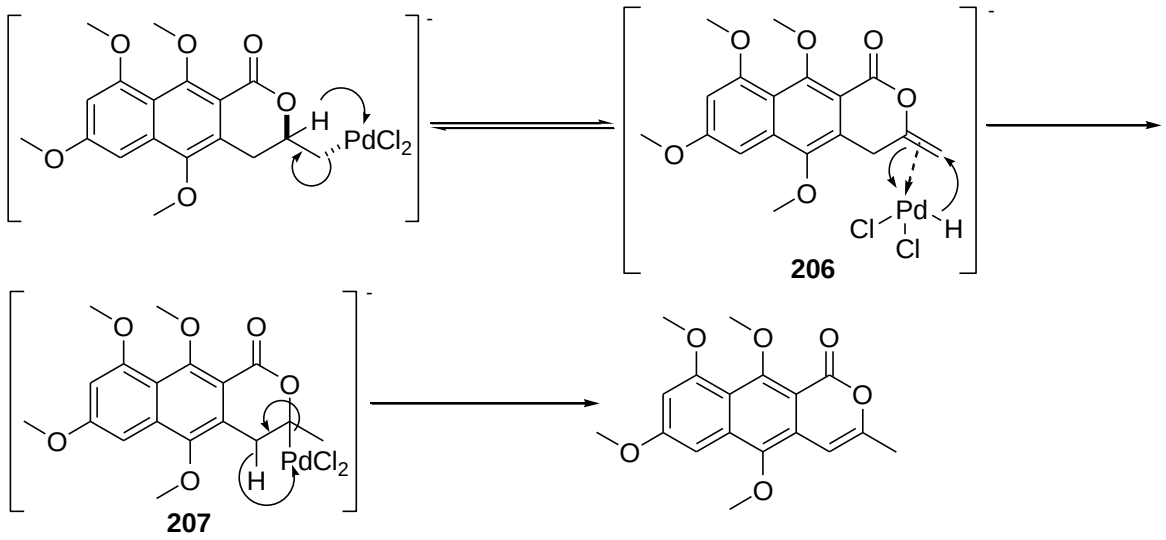
This attack would lead to the formation of the 6-membered lactone ring in a classic 6-*exo*-trig ring closing reaction. The second possibility was that if the *C*-3' carbon atom was more electrophilic than the *C*-2' carbon atom then the nucleophilic attack would take place on the *C*-3' carbon atom leading to the formation of the 7-membered ring lactone in a 7-*endo*-trig ring closing reaction. Finally, if the electrophilicity of the two carbon atoms were comparable then the mixture of products involving the above possibilities would be observed. The two independent possible routes are schematically represented by the intramolecular outer-sphere mechanistic pathway reaction steps depicted in **Scheme 2.32**.



Scheme 2.32: Two possible routes for the intramolecular nucleophilic attack on the palladium coordinated terminal alkene.

Much as both 6-*exo*-trig (**route 1**) leading to the formation of complex **205** and 7-*endo*-trig (**route 2**) leading to the construction of complex **204** are allowed reaction pathways by Baldwin rules, the 7-*endo*-trig product would come from the nucleophilic attack of the oxygen atom on a less substituted carbon. This route would most likely have a high energy transition state due to the fact that the coordination of the palladium metal on the alkene double bond withdraws electrons from the double bond such that the partial positive charge is

more stabilised by the secondary carbon atom compared to the primary carbon atom in accordance with Markovnikov's rule. Such an attack would also place a bigger palladium complex in a more sterically challenging environment. In theory, the transition state leading to the formation of the 6-membered ring should adopt more stable conformations compared to the transition state leading to the formation of the 7-membered ring and would therefore be of lower energy. These factors seemed to lead to the exclusive formation of the 6-membered lactone ring (**route 1**) as opposed to the 7-membered lactone ring (**route 2**). The rest of the mechanism proceeds as depicted in **Scheme 2.33**.



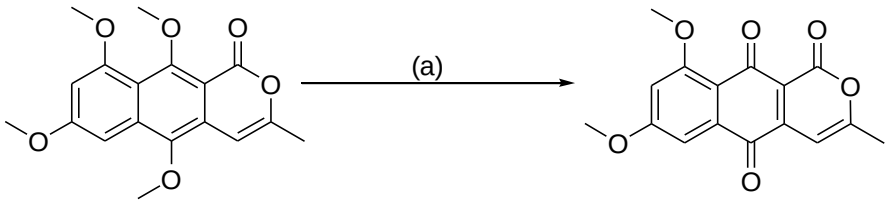
Scheme 2.33: Intramolecular Wacker oxidation involving 6-*exo*-trig reaction pathway.

One prominent feature of the intramolecular Wacker oxidation reaction of the terminal alkene **167** was the palladium mediated isomerisation of the less substituted alkene **206** to a more stable internal double bond. This process is mediated by the palladium catalyst through intermediate **207** as shown in **Scheme 2.33**.

Having synthesized enough 6-membered lactone ring precursor compound we were at this point in a good position to attempt the formation of dehydroherbarin lactone **159** by oxidative demethylation and the synthesis of paepalantine **102** by selective demethylation of lactone **103**.

2.1.16 Synthesis of 7,9-dimethoxy-3-methyl-1*H*-benzo[*g*]isochromene-1,5,10-trione (dehydroherbarin lactone) 159

To accomplish the oxidative demethylation reaction, lactone **103** was dissolved in 1,4-dioxane in a round bottom flask to which silver (II) oxide was added and the reaction mixture was stirred for 10 minutes under atmospheric conditions to achieve homogeneity. This was followed by drop-wise addition of nitric acid to the reaction mixture until all the silver (II) oxide dissolved. The reaction mixture was extracted into dichloromethane and attempted purification using silica gel column chromatography led to total decomposition of the product. Purification of the crude product was achieved by using semi-preparative C-18 reverse phase high pressure liquid chromatography (HPLC) using a reverse-phase C-18 column which delivered pyranonaphthoquinone **159** in 56% yield (**Scheme 2.34**).

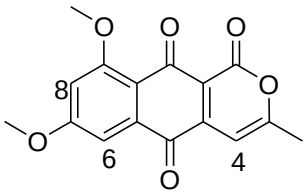


103 **159**

Scheme 2.34: *Reagents and conditions:* AgO, *55%* aq. HNO_3, 1,4-dioxane, rt, 56%.

The IR spectrum of quinone **159** showed peaks at 1782 cm^{-1}, 1762 cm^{-1} and 1705 cm^{-1} corresponding to the carbonyl functional groups. Furthermore, the HRMS spectrum showed a molecular ion peak at 301.0704 amu which was in good agreement with the expected mass of 301.0707 amu for $C_{16}H_{13}O_6$.

The ^{1}H NMR spectrum of pyranonaphthoquinone **159** showed loss of two sets of methoxy proton signals which were present in the precursor compound but all other proton signals were accounted for. The doublet proton signals at 7.23 ppm (1H, d, J = 2.1 Hz) and 6.80 ppm (1H, d, J = 2.1 Hz) were assigned to H-6 and H-8, respectively with a typical *meta*-coupling constant of J = 2.1 Hz. This meant that, as expected, there was no *meta*-oxidation of the lactone **103**. The proton signal at 6.69 ppm (1H, s) was ascribed to H-4 signifying that the double bond of the pyran ring was intact. The ^{13}C NMR

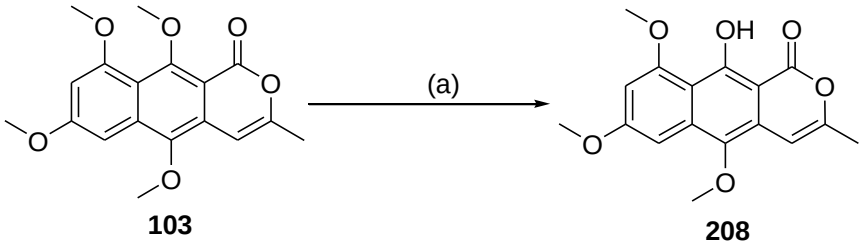


159

spectrum showed two new signals at 183.1 ppm and 178.1 ppm which were typical of *para*-quinone carbonyl carbon atoms. Crucially, the carbonyl signal of the lactone carbon atom resonated at 168.9 ppm which indicated that the lactone ring was still intact and did not open during the oxidation step.

2.1.17 Attempted synthesis of paepalantine 102

Satisfied that we had successfully synthesized dehydroherbarin lactone **159** we turned our attention towards synthesizing paepalantine **102** from precursor lactone **103** (**Scheme 2.35**). Lactone **103** was dissolved in dry dichloromethane in a 2-neck round bottom flask fitted with a rubber septum. The reaction mixture was cooled to -78 ^{o}C under a blanket of nitrogen gas and boron trichloride was added drop-wise *via* a syringe. The reaction mixture was allowed to warm to the room temperature and was stirred for two hours. After 2 hours had elapsed, the mixture was again cooled to -78 ^{o}C and boron trichloride was added for the second time. The reaction mixture was stirred at room temperature for a further 2 hours after which it was quenched with cold water. Purification of the crude product by column chromatography on flash silica gel yielded 9-*O*-methylpaepalantine **208** in 65% yield with no traces of paepalantine **102** being observed. The IR spectrum of naphthol **208** showed a broad peak at 3580 cm^{-1} corresponding to the hydrogen bonded hydroxyl functional group and the HRMS data showed a molecular ion peak at 317.1021 amu which was consistent with a predicted mass of 317.1020 amu for the formula $C_{17}H_{17}O_6$.



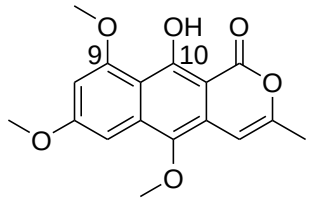
103 **208**

Scheme 2.35: *Reagents and conditions:* BCl_3, CH_2Cl_2, N_2 (g), -78 °C → rt, 65%.

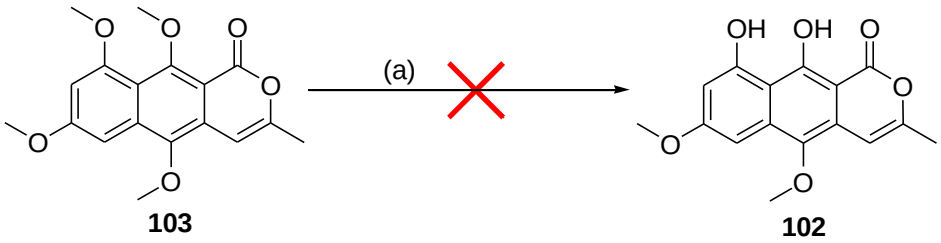
The ^{1}H NMR spectrum 9-*O*-methylpaepalantine **208** showed loss of one signal corresponding to one set of methoxy protons available in the precursor compound and the product showed a new signal at 12.79 ppm (1H, s) which was typical of the hydrogen bonded naphthol proton.

The signals corresponding to the aromatic protons were visible at 6.86 ppm (1H, d, J = 2.0 Hz) and 6.40 ppm (1H, d, J = 2.0 Hz). The singlet signal at 6.44 ppm (1H, s) was for the alkene proton and proved that the double bond was not chlorinated by boron trichloride. The ^{13}C NMR spectrum confirmed the loss of one aromatic methoxy carbon atom and the carbon signal at 167.7 ppm corresponded to the lactone carbonyl carbon atom.

These results were surprising because the methoxy group at position 9 was uncharacteristically resistant to cleavage by boron trichloride despite the use of at least four molar equivalents of the Lewis acid. The reaction was carried out in two stages in the hope that it would allow for proper coordination between the boron trichloride and the methoxy groups. The first two molar equivalents were expected to coordinate to the methoxy group at position 10 due to proximity to the carbonyl group and the second two molar equivalents were expected to coordinate to the methoxy group at position 9 of the lactone ring system which could eventually be cleaved by water. These results implied that there was no coordination between boron and the second methoxy group at position 9. Surprisingly, there was no evidence from the ^{1}H NMR spectroscopic data suggesting that the methoxy group at position 9 was out of plane which could have helped in explaining the lack of coordination to the boron reagent. Nevertheless, we thought of using a stronger Lewis acid, boron tribromide, to force the cleavage of the second methoxy group at this position but again we did not generate the desired paepalantine **102** but rather we obtained dehydroherbarin lactone **159** in a modest yield of 25%. The reagents and conditions for the failed demethylation of lactone **103** to a corresponding paepalantine **102** are shown in **Scheme 2.36**.



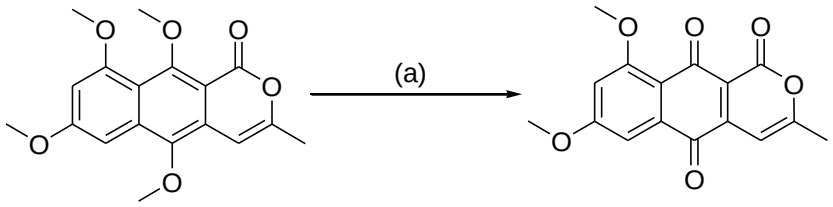
208



103 **102**

Scheme 2.36: *Reagents and conditions:* (a) BCl_3, CH_2Cl_2, N_2 (g), -78 °C → rt; or BBr_3, CH_2Cl_2, N_2 (g), -78 °C → rt.

The majority of the compound decomposed and the isolation of dehydroherbarin lactone **159** was surprising because the reaction was carried out strictly under a constant flow of dry nitrogen gas. The same results were obtained when 9-*O*-methylpaepalantine **208** (with one methoxy group already removed) was exposed to boron tribromide with dehydroherbarin lactone being the only compound which was isolated albeit in low yield. The schematic representation of the attempted demethylation protocol which delivered pyranonaphthoquinone **159** is shown in **Scheme 2.37**.



103 **159**

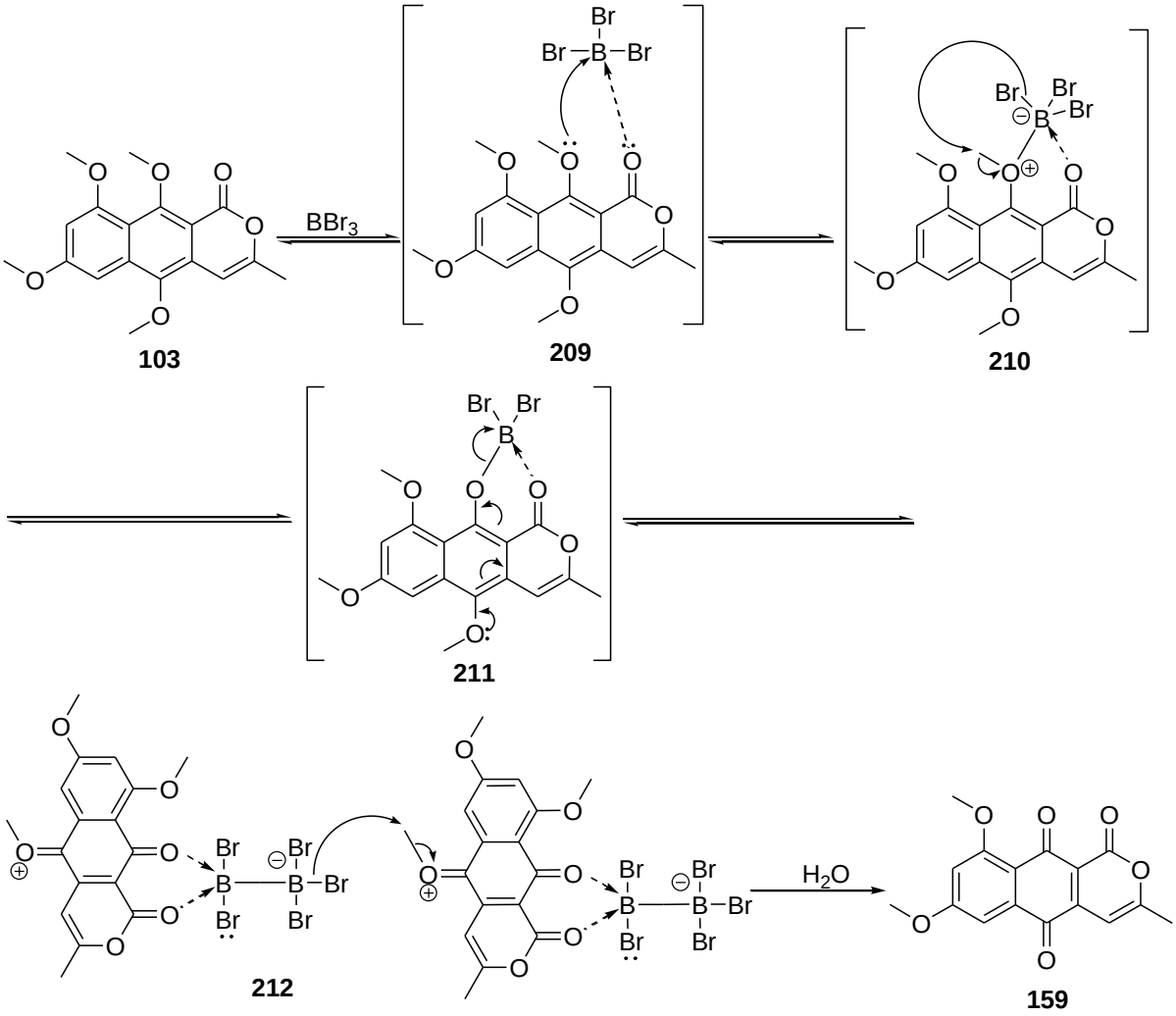
Scheme 2.37: *Reagents and conditions:* (a) BBr_3, CH_2Cl_2, N_2 (g), -78 °C → rt, 25%.

2.1.17.0 Proposed mechanism for oxidative demethylation using boron tribromide

Conceptually, demethylation of aromatic ethers by boron tribromide is thought to be through coordination of Lewis acid boron to the carbonyl oxygen atom which directs the adjacent methoxy group to donate electrons into the empty p orbital of the boron atom. This is followed by the loss of bromide as a free bromide ion in solution which goes on to attack the methyl group of the cationic intermediate thereby cleaving the C-O bond and the $ArOBBr_2$ adduct which undergoes hydrolysis upon aqueous work-up. However, recent computational studies by Kosak and co-workers[142] have shown that the mechanism involving free bromide ion in the solution leads to an increase in Gibbs free energy of the reaction such that it is not accessible by the reaction. These authors proposed that either bromide ion is coordinated to the unreacted boron tribromide or is lost together with the methyl group as MeBr in a unimolecular type of reaction pathway, both of which were found to be more favourable. We are aware that the same authors also proposed a bimolecular mechanism involving two methoxy groups coordinating to the same boron atom and we are of the view that in our case, such a system would not allow the two isocoumarin molecules to adopt an orthogonal arrangement thereby leading to unfavourable interactions which could likely lead to an

increase in Gibbs free energy. The proposed mechanistic pathway presented in **Scheme 2.38** represents a sandwiched mechanism by taking into consideration both the unimolecular and bimolecular mechanistic pathways as proposed by Kosak and co-workers[142] to suit the substrate in our hands. The sandwiched mechanism shown in **Scheme 2.38** does not change the overall mechanistic pathway of the reaction.

The first step involves coordination of boron tribromide to lactone **103** affording complex **209** and the methoxy oxygen next to the carbonyl group donates its electrons to the boron atom thereby forming complex **210**. One of the bromine atoms is then released from the complex as methyl bromide leading to the formation of complex **211**. This complex then undergoes PIFA-like mediated oxidation leading to the formation of complex **212**. The methyl group of the cationic intermediate is picked up by the bromine complex and hydrolysis of the resultant complex furnishes pyranonaphthoquinone **159**.



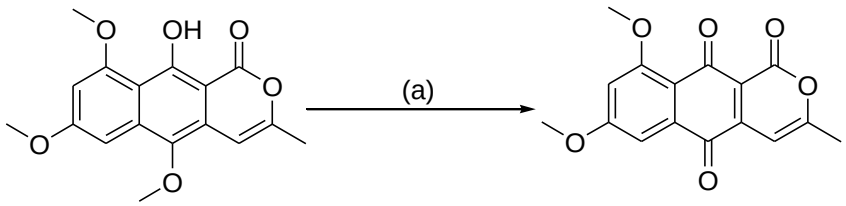
Scheme 2.38: Proposed mechanism for the oxidation of lactone **103** using BBr_3.

As discussed before, exposing 9-*O*-methylpaepalantine **208** to the same reaction conditions in the hope of demethylating the methoxy substituent at position 9 furnished the same results. This meant that, probably, the most energetically favourable route for both substrates **103** and **208** after the initial demethylation of the methoxy group at position 10 (in the case of **103**) was the oxidation to the corresponding pyranonaphthoquinone as opposed to demethylation of the second methoxy group. We also attempted a double demethylation reaction using ferric trichloride and aluminium powder but with no success.

2.1.18 PIFA mediated oxidation of 9-*O*-methylpaepalantine 208

When all these reactions failed to afford paepalantine **102** we turned our attention to the oxidation of 9-*O*-methylpaepalantine **208** to the corresponding pyranonaphthoquinone **159** using PIFA oxidation methodology. We wanted to test this reaction because there are numerous reports in the literature indicating that substrates with a methoxy group at the *para* position to a naphthol group are easily oxidised to the corresponding *para*-quinone[143] using PIFA in water/acetonitrile solvent system.

True to the reported literature, PIFA mediated oxidation of this precursor went smoothly and we obtained dehydroherbarin lactone **159** in a very high yield of 81% as shown in **Scheme 2.39**.



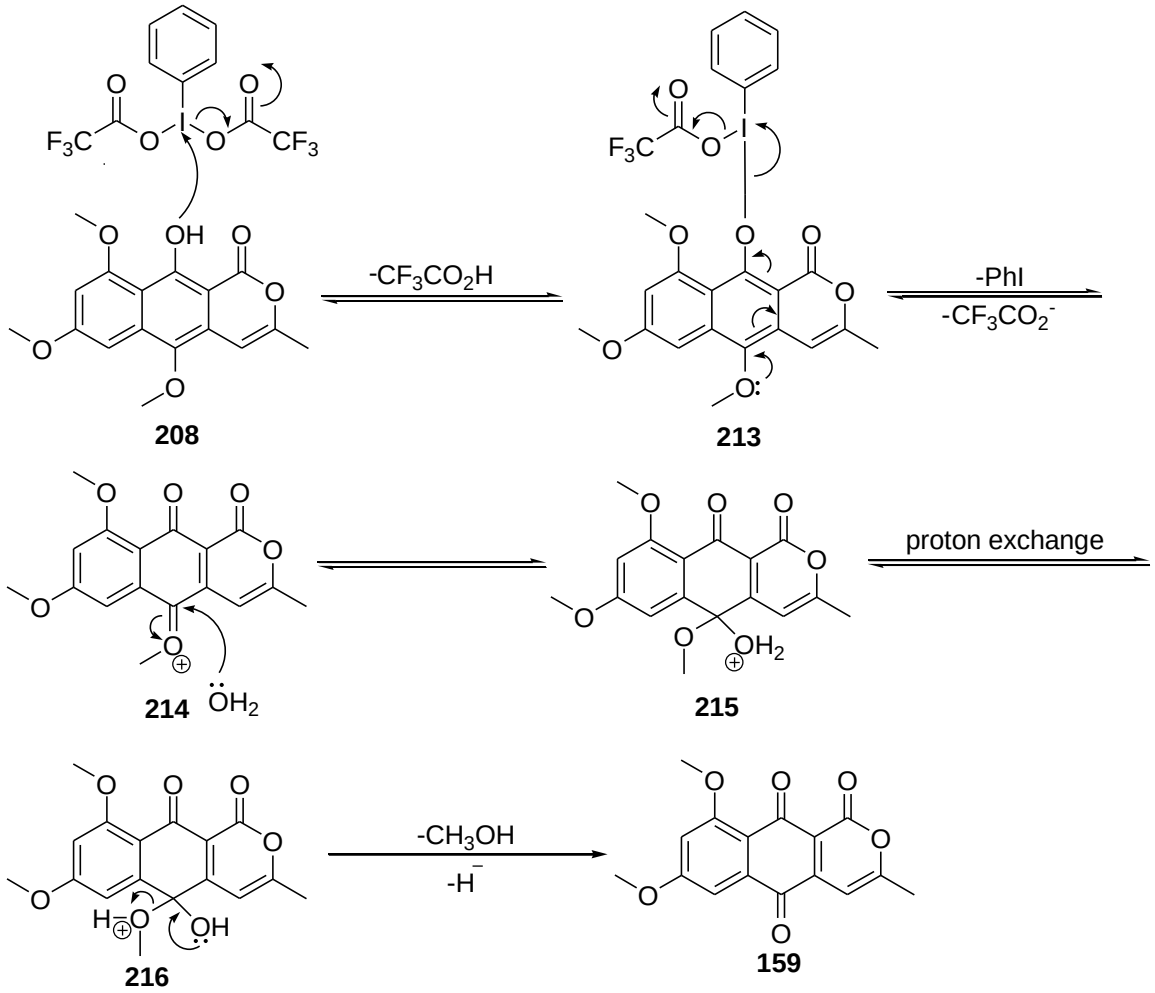
208 **159**

Scheme 2.39: *Reagents and conditions:* (a) PIFA, CH_3CN/H_2O, rt, 35 min, 81%.

The high yield is presumably due to better coordination between the naphthol group and the PIFA reagent compared to the coordination between the methoxy group and the PIFA reagent. The mechanism for this reaction is given in **Scheme 2.40** below.

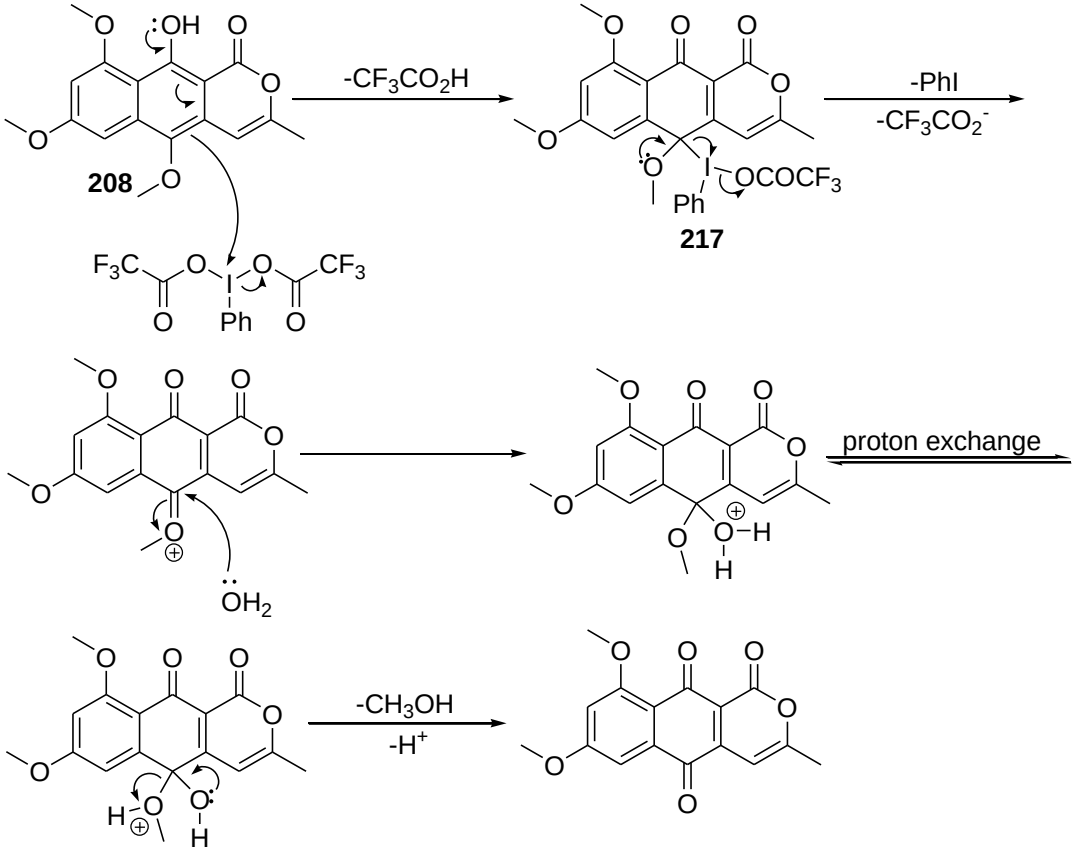
2.1.18.0 Proposed mechanism for PIFA mediated oxidative demethylation

The first step in the reaction is the typical activation of the naphthol **208** by PIFA to form complex **213** which goes on to form cationic intermediate **214**. The nucleophilic attack by a water molecule on the cation **214** delivers pyranonaphthoquinone **159** through intermediates **215** and **216**.



Scheme 2.40: Proposed mechanism for PIFA mediated oxidation of 10-hydroxy-5,7,9-trimethoxy-3-methyl-1*H*-benzo[*g*]isochromen-1-one **208**.

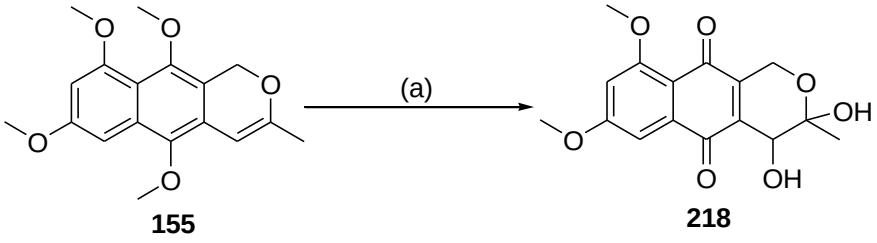
Or alternatively, the mechanism could involve the attack of PIFA on the naphthalene ring system which may be initiated by the nucleophilicity of the whole naphthalene ring to form complex **217**. This complex could then proceed in the same manner as the above mechanism as shown in **Scheme 2.41**.



Scheme 2.41: The proposed alternative mechanism for PIFA mediated oxidation of 9-*O*-methylpaepalantine **208**.

Pillay and co-workers[124] reported obtaining a 25% yield when pyran **155** was oxidized to a corresponding dehydroherbarin **121** using PIFA mediated oxidative demethylation. In our hands a faint spot corresponding to pyranonaphthoquinone **159** was obtained using TLC monitoring when the same protocol was used for oxidative demethylation of lactone **103**.

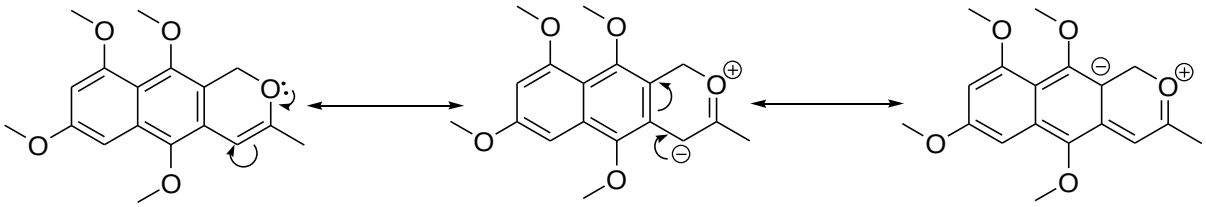
The same authors[125] reported very interesting results in which oxidative demethylation of compound **155** using PIFA in acetonitrile and water solution under high dilution conditions furnished a highly oxygenated pyran ring compound, dihydronaphthoquinone **218**, as the product as shown in **Scheme 2.42**.



155 **218**

Scheme 2.42: *Reagents and conditions:* (a) PIFA, CH_3CN/H_2O dilute conditions, rt, 15 min.

What was intriguing about this reaction was that it was only achieved under high dilution conditions and involved the oxidation of both the pyran double bond and the naphthalene ring system. The double bond of the pyran ring system was uncharacteristically susceptible to PIFA mediated oxidation which could probably be analysed in terms of species **219** and **220** (**Scheme 2.43**). These species are just two examples of several canonical forms involving isochromene **155** in solution. Much as their relative contributions to the stability of pyran **155** are not expected to be much, the oxidation results suggested that these species are better solvated under high dilution thereby making the pyran double bond more labile to a PIFA-mediated hydroxylation reaction.

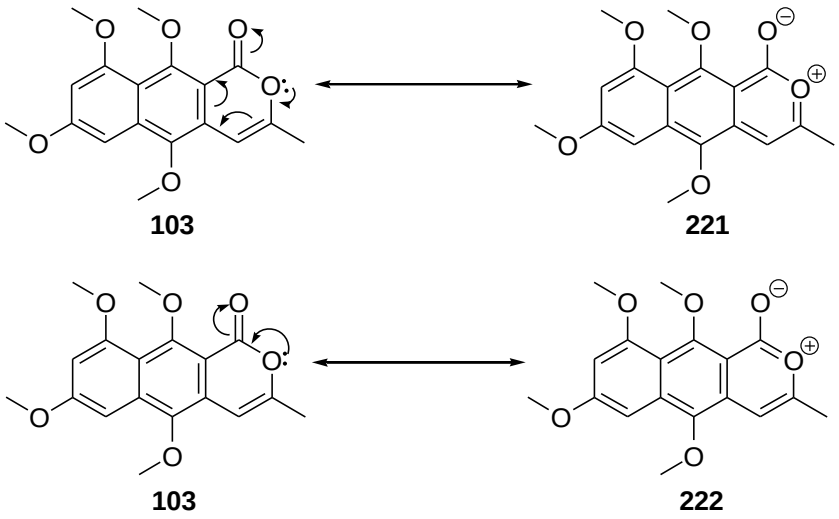


155 **219** **220**

Scheme 2.43: Two examples of resonance structures of isochromene **155**.

Attempted replication of the synthesis of a related dihydroxy-pyranonaphthoquinone lactone was unsuccessful with the substrate in our hands. The reason for failed PIFA mediated hydroxylation in our case could be due to differences in the nature of the double bond of the pyran ring in compound **155** and the pyranone ring in our substrate, lactone **103**. The contribution of the canonical forms **221** and **222** (**Scheme 2.44**) towards the stability of lactone **103** are expected to be higher compared to the contribution made by canonical forms **219** and **220** towards the stability of isochromene **155** in solution.

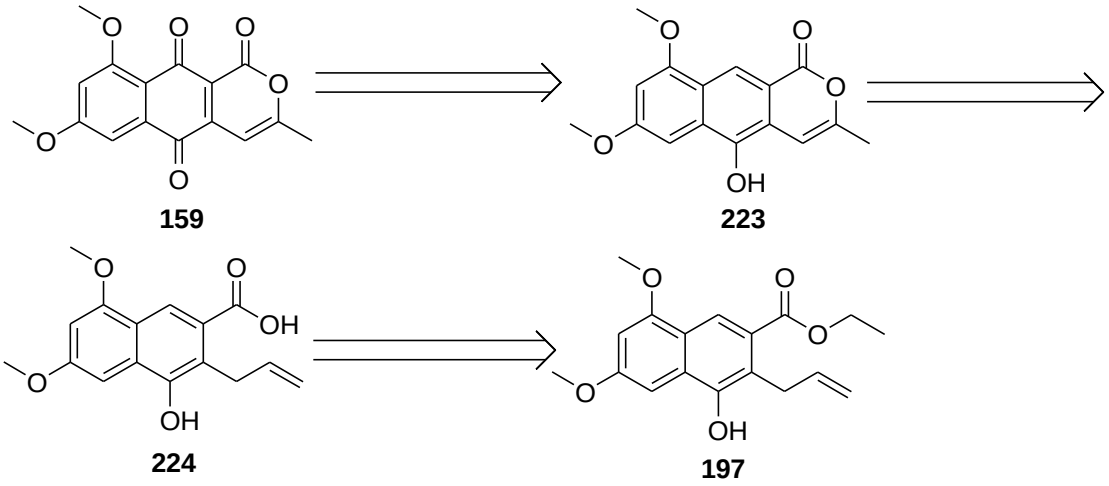
Pyranone rings are known to possess aromatic characteristics[40] but the contributions of the charged canonical forms towards the stability of the molecule are limited by charge separation.



Scheme 2.44: Two examples of resonance structures of lactone **103**.

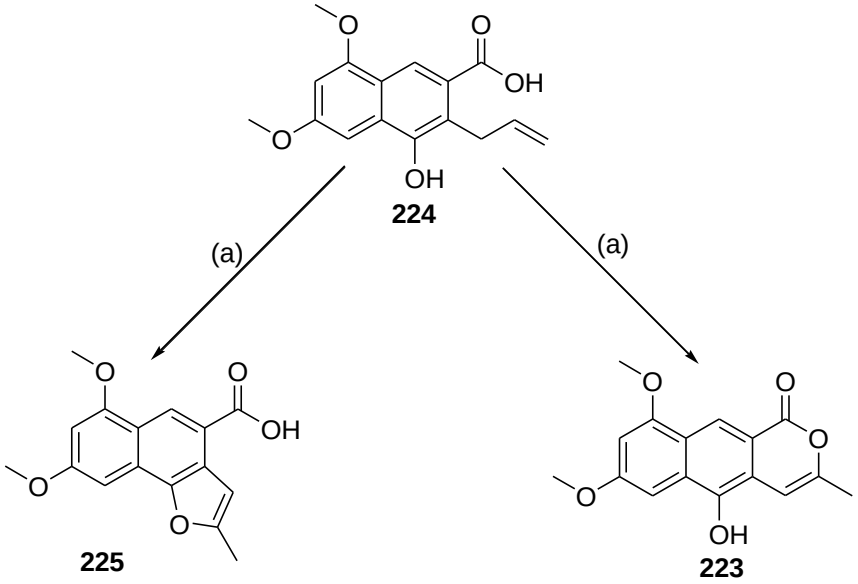
2.2 Concise synthesis of dehydroherbarin lactone 159

Despite being frustrated by not being able to complete the synthesis of paepalantine **102** we thought that the next positive step to take was to try to shorten the number of reaction steps that would be required to synthesize dehydroherbarin lactone **159**. We thought that by by-passing some synthetic steps involving protection groups we would be able to minimise the number of steps in the protocol we used to achieve the total synthesis of dehydroherbarin lactone **159**. The retrosynthetic analysis is shown in **Scheme 2.45**. We envisaged that the carboxylic acid **224** could be obtained by base promoted hydrolysis of naphthol **197** which could furnish lactone **223** upon lactonization and the oxidation of the lactone intermediate could potentially deliver pyranonaphthoquinone **159**.



Scheme 2.45: Retrosynthetic analysis for the synthesis of dehydroherbarin lactone **159**.

We thought that we could possibly achieve selective cyclization of carboxylic acid **224** to synthesize lactone **223** involving the acid group in the presence of the naphthol group as shown in **Scheme 2.46**. The cyclization of the naphthol group of carboxylic acid **224** could lead to the formation of the pyran **225**.



Scheme 2.46: Two possible cyclization routes for carboxylic acid **224**.

The formation of the two products are allowed by Baldwin rules[145] with lactone **223** formed from the 6-*exo*-trig and pyran **225** from 5-*exo*-trig cyclization reactions on the basis of mechanisms depicted in **Schemes 2.32** and **2.33**. The formation of intermediate **226** (**Figure 2.7**) precedes the formation of furan **225** before isomerization of the double bond.

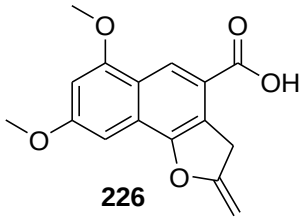
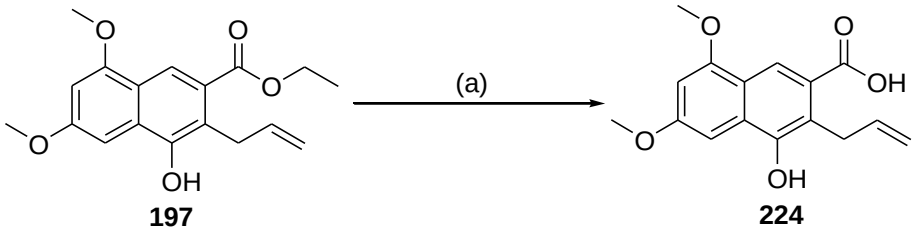


Figure 2.7: Proposed pyran intermediate **226** for 5-*exo*-trig cyclization.

In the case that both compounds **223** and **225** are formed we envisaged that separation of the two compounds would not pose a serious challenge because of the availability of the carboxylic acid group which may allow for the acid **225** to be apportioned in the aqueous layer while maintaining lactone **223** in the organic layer after a simple manipulation. We also anticipated that silica gel column chromatography may also be effective in separating the two compounds with the acid **225** being more polar than the pyranone **223**.

2.2.0 Synthesis of 3-allyl-4-hydroxy-6,8-dimethoxynaphthalene-2-carboxylic acid 224

The synthesis commenced by dissolving naphthol **197** in methanol and water in a round bottom flask to which excess solid sodium hydroxide was added while stirring the reaction mixture. The reaction mixture was stirred at room temperature for 5 hours and thereafter it was heated to reflux for 12 hours. The reaction mixture was cooled to room temperature, acidified with 32% aqueous hydrochloric acid, separated and purification of the crude product by silica gel column chromatography yielded naphthoic acid **224** as colourless crystals in 83% yield.



197 **224**

Scheme 2.47: *Reagents and conditions:* (a) (i) NaOH, MeOH/H_2O, rt for 5 hrs and reflux for 12 hrs (ii) *32%* aq. HCl, 83%.

The ^{1}H NMR spectrum of naphthoic acid **224** did not show signals related to the ethyl group of the precursor ester **197**. The proton signal between 6.22-6.07 ppm (1H, m) was ascribed to the inner vinylic proton. The signals at 5.22 ppm (2H, d, J = 13.2 Hz) for the terminal vinylic protons and 4.01 ppm (2H, d, J = 5.3 Hz) for the allylic protons indicated that there was no isomerization of the double bond. Even though there was no highly deshielded signal corresponding to the acid proton in the ^{1}H NMR spectrum, the ^{13}C NMR spectrum showed a signal at 173.0 ppm for the carboxylic acid carbonyl carbon atom which was in agreement with the resonances of the carbonyl carbon atoms of acids **167** and **175**. The successful synthesis of the carboxylic acid **224** was further confirmed by the crystal structure and the ORTEP diagram is shown in **Figure 2.8**.

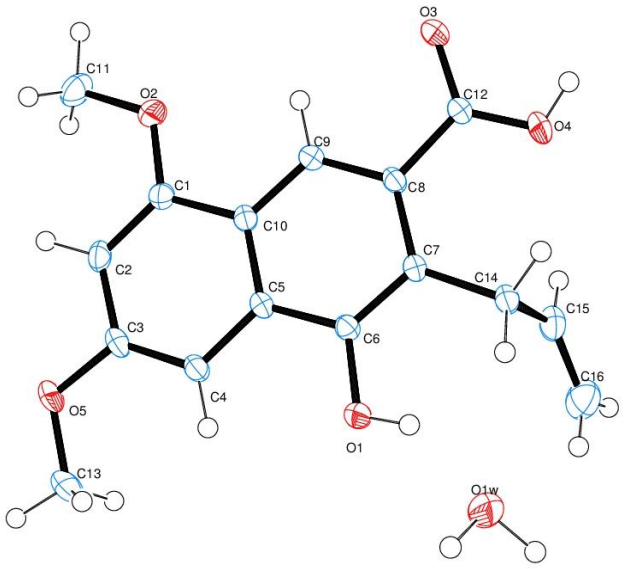
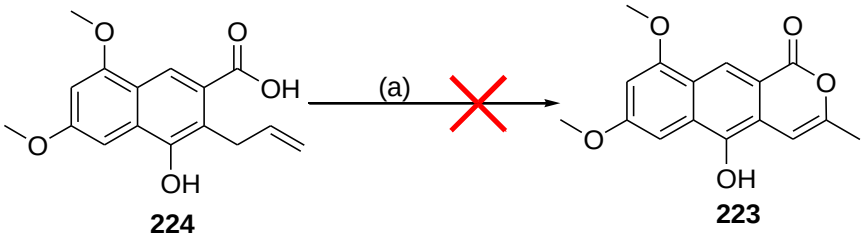


Figure 2.8: The ORTEP diagram of naphthoic acid **224**. Thermal ellipsoids are shown at the 50% probability level.

The acid **224** was charged into a 2-neck round bottom flask in *N*,*N*-dimethylformamide/water mixture and was subjected to a routine Wacker oxidation reaction but to our surprise the reaction did not take place after monitoring for 48 hours even after a progressive increase in the catalyst and copper chloride amounts in the reaction mixture. **Scheme 2.48** shows the conditions that were used for the failed Wacker oxidative lactonization of naphthoic acid **224**.

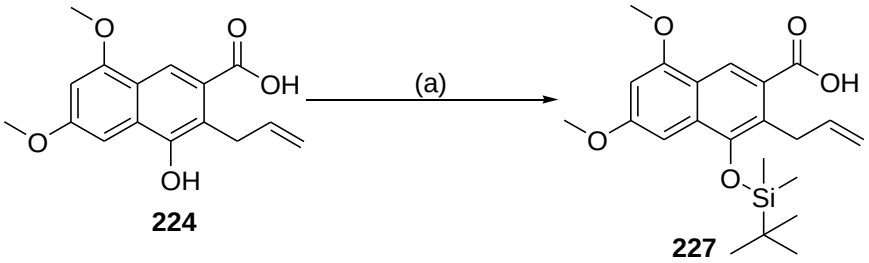


Scheme 2.48: *Reagents and conditions:* (a) cat. $PdCl_2$, $CuCl_2 \cdot 2H_2O$, DMF/H_2O, O_2 (g), rt, 48 hrs.

Analysis of the recovered material by ^1H NMR spectroscopy indicated that the double bond of the allyl group had not isomerized. At this point we thought that if the naphthol group was protected by a labile protecting group which could be easily removed after the Wacker oxidation it would still provide a short synthetic pathway to dehydroherbarin lactone **159**.

2.2.1 Synthesis of 3-allyl-4-(*tert*-butyldimethylsilyloxy)-6,8-dimethoxynaphthalene-2-carboxylic acid 227

The naphthoic acid **224** was dissolved in dichloromethane in a round bottom flask to which *tert*-butyldimethylsilyl chloride, imidazole and a catalytic amount of dimethylaminopyridine (DMAP) were added and the reaction was stirred at room temperature for 24 hours. The mixture was then washed with water and the crude product was purified by column chromatography on silica gel which furnished silyl protected acid **227** in 93% yield as shown in **Scheme 2.49**.



Scheme 2.49: *Reagents and conditions:* (a) TBDMSCl, imidazole, cat. DMAP, CH_2Cl_2, rt, 24 hrs, 93%.

The ^{1}H NMR spectrum of carboxylic acid **227** showed signals at 1.16 ppm (9H, s) and 0.26 ppm (6H, s) which were typical of silicon protecting groups for $ArOSi(CH_3)_2C(CH_3)_3$ and $ArOSi(CH_3)_2C(CH_3)_3$ protons, respectively. The ^{13}C NMR spectrum showed a signal at -2.9 ppm corresponding to the methyl carbon atoms directly bonded to the silicon atom ($ArOSi(CH_3)_2C(CH_3)_3$). The HRMS data showed a molecular ion peak at 403.1932 amu which was consistent with a predicted mass of 403.1935 amu for formula $C_{22}H_{31}O_5Si$.

The selectivity in the protection of the naphthol group in the presence of the carboxylic acid group was probably due to the fact that the silicon protecting group is very unstable when bonded to the carboxylic acid. The TLC plate showed two spots, one of which corresponded to the carboxylic acid **227** and the other spot with a higher R_f value presumably corresponded to protected acid product. The spot with higher R_f value was prominent within the first 6 hours of the reaction but became fainter with time. This spot was absent on the TLC plate after working up the reaction. The ORTEP diagram for the crystal structure of silyl protected carboxylic acid **227** is shown in **Figure 2.9**.

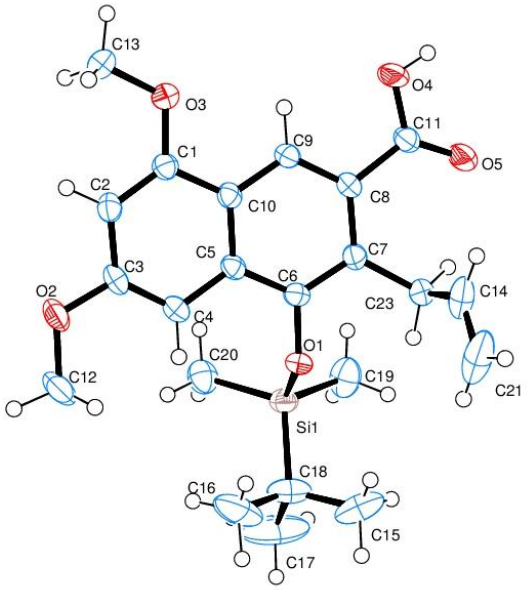
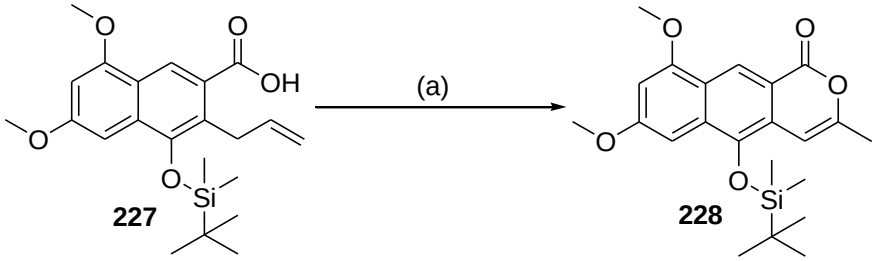


Figure 2.9: The ORTEP diagram of naphthoic acid **227**. Thermal ellipsoids are shown at the 50% probability level.

2.2.2 Synthesis of 7,9-dimethoxy-3-methyl-1*H*-benzo[*g*]isochromene-1,5,10-trione 228

The observed selectivity perfectly suited our aim and we proceeded to expose silyl protected naphthoic acid **227** to a routine Wacker oxidation reaction conditions which afforded lactone **228** in 73% yield (**Scheme 2.50**). The IR spectrum of the silyl protected lactone **228** did not show a peak corresponding to the hydroxyl function group of the carboxylic acid which was at 3620 cm^{-1} in the precursor compound and a typical carbonyl functional group of the pyranone ring was visible at 1739 cm^{-1}. The HRMS spectrum confirmed the mass of the molecule as 401.1789 amu which was in agreement with the predicted mass of 401.1779 amu for $C_{22}H_{29}O_5Si$.



Scheme 2.50: *Reagents and conditions:* cat. $PdCl_2$, $CuCl_2 \cdot 2H_2O$, DMF/H_2O, O_2 (g), rt, 24 hrs, 73%.

The ^1H NMR spectrum of lactone **228** revealed loss of the multiplet and doublet signals pertaining to the allyl group protons in the precursor acid **227**. The proton signal at 2.11 ppm (3H, s) for the methyl group compared favourably to the methyl proton signal of lactone **103**. The ^{13}C NMR spectrum showed signals at 26.0 ppm, 18.7 ppm and -3.2 ppm corresponding to $(ArOSi(CH_3)_2C(CH_3)_3)$, $(ArOSi(CH_3)_2C(CH_3)_3)$ and $(ArOSi(CH_3)_2C(CH_3)_3)$ carbon atoms of the silyl group. This meant that despite reports of desilylation under Wacker oxidation conditions[146] we did not lose the phenol silicon protecting group in our case. The ORTEP diagram for the crystal structure of lactone **228** is shown in **Figure 2.10**.

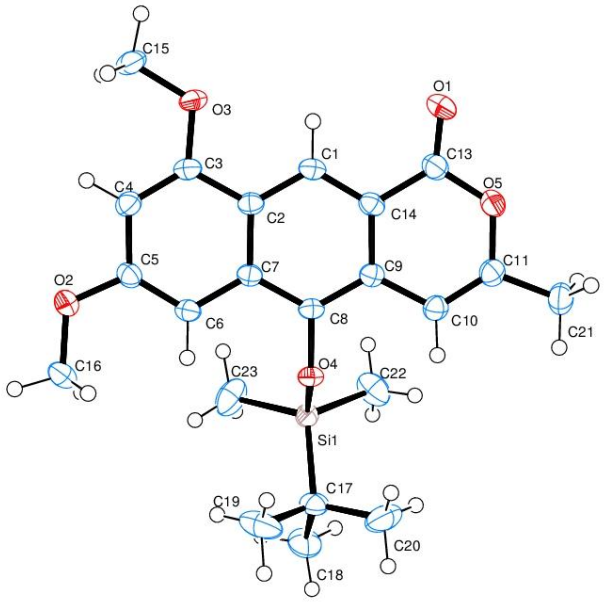
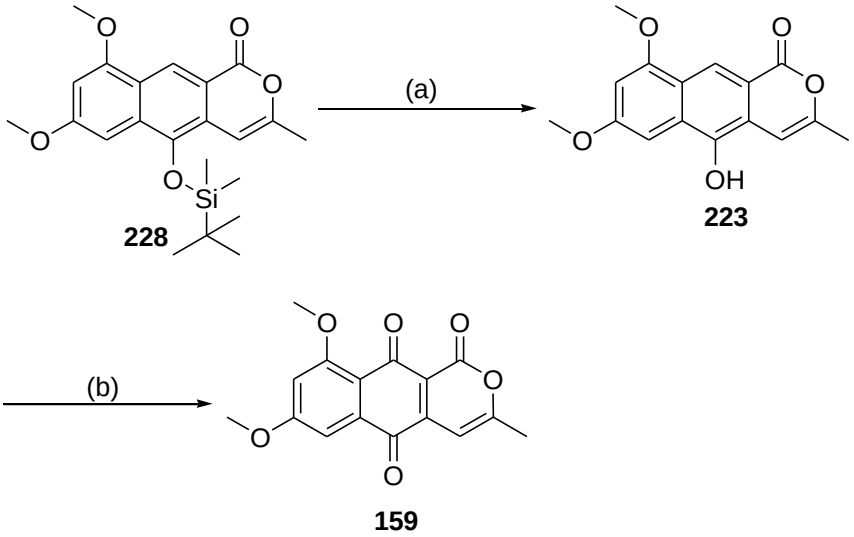


Figure 2.10: The ORTEP diagram of lactone **228**. Thermal ellipsoids are shown at the 50% probability level.

The next step was to remove the silicon protecting group which was achieved by dissolving lactone **228** in dry tetrahydrofuran to which *tetra*-butylammonium fluoride (TBAF) was added at 0 ^{o}C and the reaction mixture was allowed to warm up to room temperature and stirred for a further 24 hours. The crude product, presumably lactone **223**, was dissolved in acetonitrile in a round bottom flask to which aqueous solution of ceric ammonium nitrate was added. The reaction mixture was stirred at room temperature for 30 minutes and purification of the crude product delivered dehydroherbarin lactone **159** as a minor product in 10% yield and uncharacterizable orange amorphous solid compound as the major product.



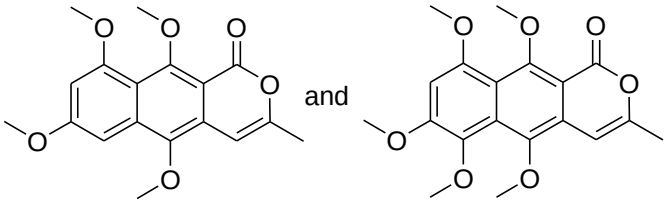
Scheme 2.51: *Reagents and conditions:* (a) TBAF, THF, 0 ^{o}C → rt, 24 hrs (b) CAN, CH_3CN/H_2O, 30 min, 10%.

Much as we managed to shorten the number of steps that led to the synthesis of dehydroherbarin lactone, the last step in the concise methodology gave poor yields. This was the case because the major product was the uncharacterizable orange amorphous solid compound. For the synthesis of 5-methoxy-3,4-dehydroxanthomegnin we opted not to employ this protocol.

2.3 Synthesis of 5-methoxy-3,4-dehydroxanthomegnin 34

Having successfully synthesized lactone **103** in the project involving the synthesis of dehydroherbarin lactone **159** we thought it was imperative to apply this methodology towards

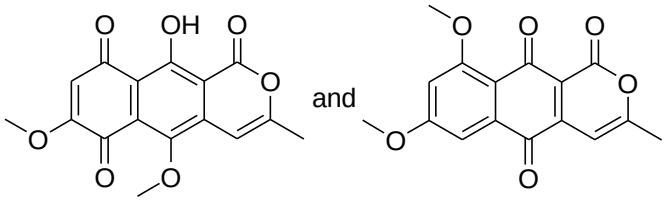
the synthesis of a potentially crucial intermediate **229** that could hold keys towards the synthesis of a structurally similar pyranonaphthoquinone, 5-methoxy-3,4-dehydroxanthomegnin **34**. The structures of the two lactones are shown in **Figure 2.11**.



103 **229**

Figure 2.11: Highlighting the similarities between lactones **103** and **229**.

In the same way, 5-methoxy-3,4-dehydroxanthomegnin **34** compared favourably with dehydroherbarin lactone **159** in that they both have the same pyranonaphthoquinone skeleton as shown in **Figure 2.12**.

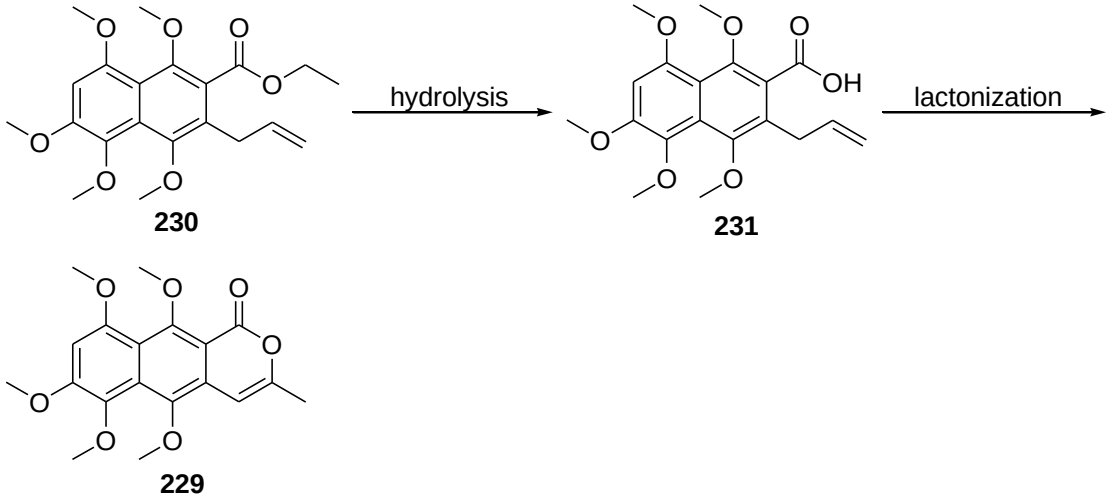


34 **159**

Figure 2.12: Highlighting the similarities between pyranonaphthoquinones **34** and **159**.

We postulated that up to this stage, we could use the same methodology to synthesize the pentaoxygenated lactone **229** which we thought could be an important precursor for the synthesis of pyranonaphthoquinone **34**. The differences in the oxygenation pattern of the two pyranonaphthoquinones could be taken care of by using a different starting material containing an extra oxygenated substituent.

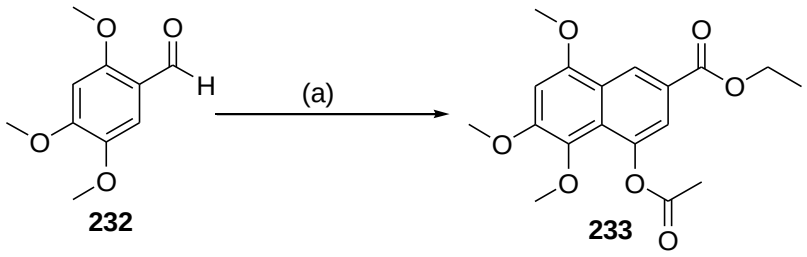
Thus, the same sequence of reactions was used for the synthesis of lactone **229**. Since the hydrolysis of the allyl ester **168** had proved very difficult in the first project we thought that the ethyl ester of this oxygenated naphthalene could provide us with the best opportunity to synthesize carboxylic acid **231** as shown in **Scheme 2.52**.



Scheme 2.52: Proposed route towards the synthesis of pentaoxygenated lactone **229**.

2.3.0 Synthesis of ethyl 4-hydroxy-5,6,8-trimethoxynaphthalene-2-carboxylate 234

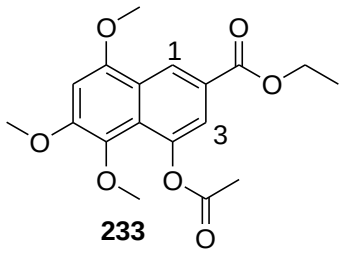
We commenced this part of the project by dissolving 2,4,5-trimethoxybenzaldehyde **232** in *tert*-butanol in a round bottom flask to which diethyl succinate and potassium *tert*-butoxide were added. The reaction mixture was heated to reflux for 4 hours after which the acidified crude product was extracted, dried and transferred into a clean round bottom flask charged with acetic anhydride and sodium acetate. The reaction mixture was again heated to reflux for overnight and purification of the crude product by silica gel column chromatography afforded naphthalene **233** in 68% yield.



Scheme 2.53: *Reagents and conditions:* (a) (i) diethyl succinate, *t*-BuOK/*t*-BuOH, reflux, N_2 (g), 4 hrs (ii) *32%* aq. HCl (iii) NaOAc/Ac_2O, 130 °C, N_2 (g), overnight, 68%.

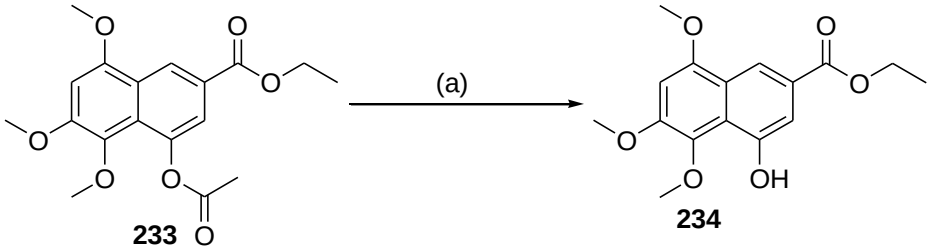
The identity of the product was confirmed by both ^1H and ^{13}C NMR spectroscopy. The ^1H NMR spectrum showed two doublet signals at 8.84 ppm (1H, d, J = 1.7 Hz) and 7.68 ppm (1H, d, J = 1.7 Hz) corresponding to *meta*-coupled protons and were assigned to H-1 and H-3

protons, respectively. The singlet aromatic proton signal in the starting material was faithfully reproduced at 6.69 ppm (1H, s). The ethyl ester group was confirmed by the presence of the quartet and triplet proton signals at 4.41 ppm (2H, q, J = 7.1 Hz) and 1.42 ppm (3H, t, J = 7.1 Hz), respectively. A singlet signal at 2.38 ppm (3H, s) was ascribed to the acetyl methyl protons. The ^{13}C NMR spectrum showed 10 independent signals in the aromatic/alkene region of the spectrum. The signals at 169.8 ppm and 166.1 ppm were assigned to the carbonyl carbon atoms of the acetyl and ester groups, respectively. The 10 carbon signals in the aromatic/alkene region in conjunction with the two *meta*-coupled protons proved that we had successfully constructed the naphthalene core.



233

Satisfied that the naphthalene core was in place we were ready to carry out selective deacetylation of the acetyl group while leaving the ethyl ester group intact. This was achieved by dissolving naphthalene **233** in a 1% ethanolic solution of sodium hydroxide and the reaction mixture was stirred at room temperature for 3 hours after which it was acidified and purified through silica gel column chromatography yielding naphthol **234** in 79% yield.



233 **234**

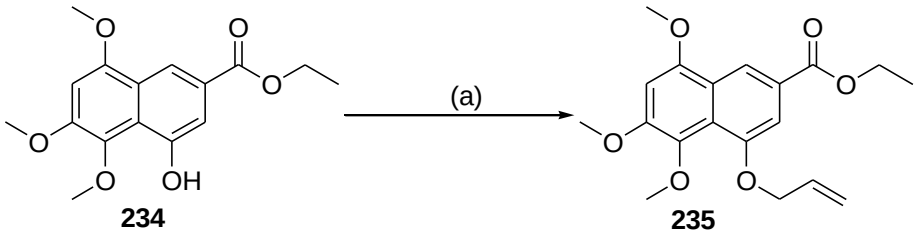
Scheme 2.54: *Reagents and conditions:* (a) (i) *1%* NaOH in EtOH, rt, 3 hrs (ii) *32%* aq. HCl, 79%.

The ^{1}H NMR spectrum of naphthol **234** showed a D_2O exchangeable singlet signal at 9.69 ppm (1H, s) consistent with the naphthol proton and loss of a singlet signal at 2.38 ppm was indicative of loss of the acetyl protecting group. This was confirmed by the ^{13}C NMR spectrum which showed loss of a carbon signal at 169.8 ppm which was visible in the precursor naphthalene **233** and was due to the carbonyl carbon atom of the acetyl protecting group. The signals corresponding to the ethyl group in both ^{1}H and ^{13}C NMR spectra were accounted for. The spectroscopic data proved beyond reasonable doubt that we had

successfully achieved selective deacetylation of the acetate group and at this point we were sure that selective allylation would be possible.

2.3.1 Synthesis of ethyl 3-allyl-4-hydroxy-5,6,8-trimethoxynaphthalene-2-carboxylate 235

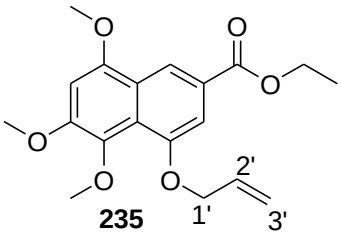
As expected, a routine allylation reaction using allyl bromide and potassium carbonate in acetone successfully delivered *O*-allyl ether **235** in 89% yield (**Scheme 2.55**). The excess allyl bromide was evaporated *in vacuo* after which the crude reaction mixture was purified by column chromatography on flash silica gel.



234 **235**

Scheme 2.55: *Reagents and conditions:* (a) K_2CO_3, allyl bromide, Me_2CO, N_2 (g), reflux, 24 hrs, 89%.

The ^{1}H NMR spectrum of allyl ether **235** showed loss of the signal at 9.69 ppm present in the precursor compound **234** which was attributed to the naphthol proton. The signal at 6.20 ppm (1H, ddt, *J* = 17.2, 10.5, 5.1 Hz) was consistent with the inner vinylic proton (H-2') of the allyl group whereas a signal at 5.60 ppm (1H, dd, *J* = 17.2, 1.6 Hz) was consistent with the terminal vinylic proton (H-3') in a *trans* position to the inner vinylic proton with a *trans*-coupling constant of *J* = 17.2 Hz. The signal at 5.33 ppm (1H, dd, *J* = 10.5, 1.6 Hz) was ascribed to the remaining terminal vinylic proton (H-3') which was in *cis* position to the inner vinylic proton with a typical *cis*-coupling constant of *J* = 10.5 Hz. The *geminal* coupling constant of the two terminal protons was measured at *J* = 1.6 Hz. The doublet signal at 4.71 ppm (2H, d, *J* = 5.1 Hz) was assigned to the allylic protons (H-1') of the allyl group. The ^{13}C NMR spectrum confirmed the successful allylation of naphthol **234** by showing two new signals in the aromatic/alkene region consistent with the two alkene carbon atoms of the allyl group. The signal at 63.9 ppm was consistent with *O*-allylic carbon atom (C-1'). Having successfully synthesized the *O*-allyl

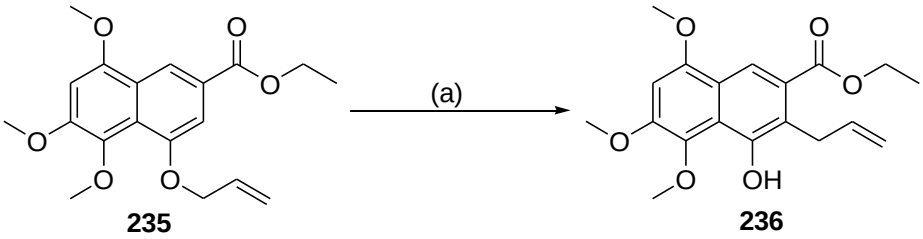


235

ether **235** we were at this stage nicely posed to perform the thermal Claisen rearrangement reaction to obtain the *C*-allyl naphthol.

2.3.2 Synthesis of ethyl 3-allyl-4-hydroxy-5,6,8-trimethoxynaphthalene-2-carboxylate 236

The *O*-allyl ether **235** was loaded neat into a round bottom flask equipped with a magnetic stirring bar and a reflux condenser and the flask was heated to 180 ^{o}C in a silicon oil bath under reflux conditions for 24 hours. After 24 hours, the reaction mixture was cooled to room temperature and the crude product was purified by column chromatography on silica gel yielding naphthol **236** in 71% yield as shown in **Scheme 2.56**.



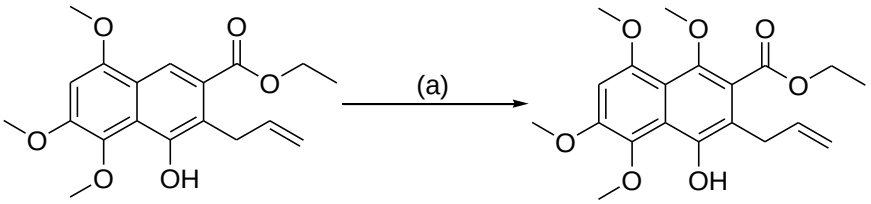
Scheme 2.56: *Reagents and conditions:* heat, 180 °C, N_2 (g), 24 hrs, 71%.

The ^{1}H NMR spectrum of naphthol **236** showed a D_2O exchangeable singlet signal at 10.09 ppm (1H, s) consistent with the naphthol proton. There was loss of 1 aromatic proton signal present in the precursor compound **235** which was consistent with *C*-allylation. The successful formation of naphthol **236** was confirmed by the ^{13}C NMR spectrum which revealed the disappearance of a signal at 63.9 ppm which was assigned to the *O*-allylic carbon atom in the precursor compound and the appearance of a signal at 30.1 ppm (Ar*C*H_2CH=CH_2) in the product which was consistent with the *C*-allylic carbon atom. Having successfully performed the *C*-2 allylation of the naphthalene moiety the stage was set for PIFA mediated insertion of the methoxy group on the naphthalene core.

2.3.3 Synthesis of ethyl 3-allyl-4-hydroxy-1,5,6,8-tetramethoxynaphthalene-2-carboxylate 237

The naphthol **236** was dissolved in methanol in a round bottom flask to which solid PIFA was added in one portion. The reaction mixture was stirred at room temperature for 15 minutes

after which it was quenched with saturated aqueous sodium hydrogen carbonate solution. The crude product was dissolved in ethanol in a clean round bottom flask to which excess 21% sodium ethoxide solution was added while the reaction mixture was vigorously stirred and stirring continued for a further 20 minutes. The reaction was then quenched with a saturated aqueous ammonium chloride solution and the crude product was purified by silica gel column chromatography delivering the desired pentaoxygenated naphthalene **237** in 52% yield (**Scheme 2.57**).



236 **237**

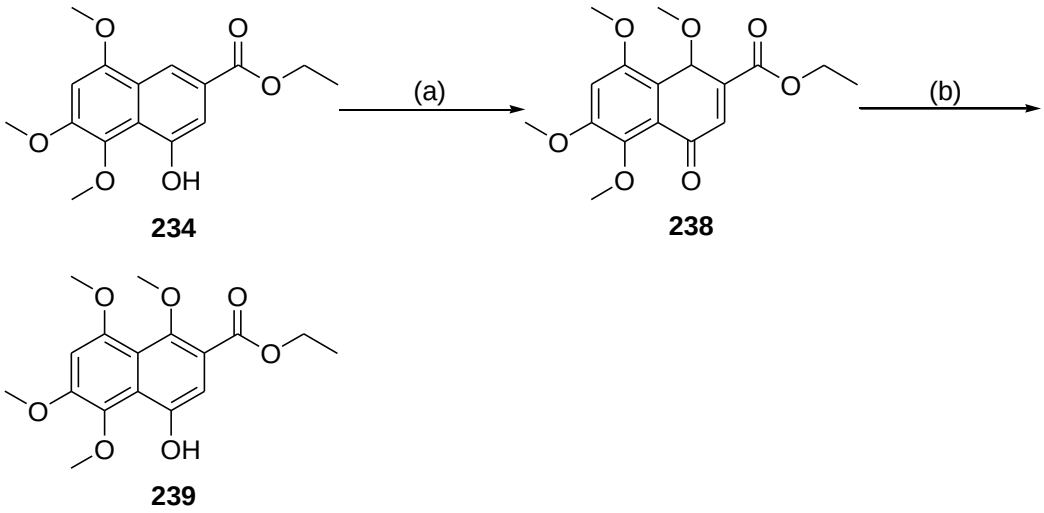
Scheme 2.57: *Reagents and conditions:* (a) (i) PIFA, MeOH, rt, 15 min, (ii) *21%* NaOEt, EtOH, rt, 20 min, 52%.

The ^{1}H NMR spectrum of naphthol **237** revealed loss of one proton signal in the alkene/aromatic region of the spectrum which was at 8.19 ppm in the precursor compound and appearance of a fourth signal typical of aromatic methoxy protons between 3.98-3.78 ppm consistent with the overall reaction which was substitution of the aromatic proton with a methoxy group. The ^{13}C NMR spectrum confirmed these findings by showing a new methoxy carbon signal together with the three others between 62.3-55.0 ppm.

Another fraction was separated from the same column in 10% yield and the ^{1}H NMR spectrum showed that this compound had a new signal corresponding to the methoxy carbon atom but the signal was upfield compared to the methoxy signals in the ^{1}H NMR spectrum of naphthol **237**. The spectrum further showed no signal corresponding to the naphthol proton which was at 10.20 ppm in the ^{1}H NMR spectrum of the pentaoxygenated naphthalene **237**. In addition, the ^{13}C NMR spectrum revealed fewer signals in the aromatic/alkene region of the spectrum (10 signals) when compared to naphthol **237** which showed a total of 12 signals in this area. The signal due to the carbonyl carbon of the ester functional group was accounted for but there was another carbonyl signal which was not typical of an ester group.

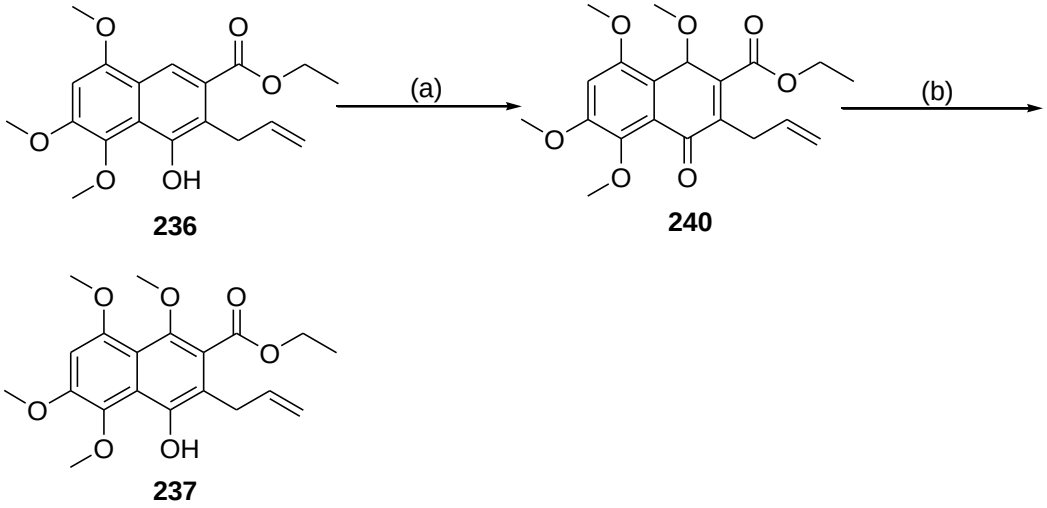
The IR spectrum showed peaks at 1708 cm^{-1} and 1698 cm^{-1} which were assigned to the carbonyl functional groups and the alkene functional group showed a peak at 1625 cm^{-1}. Furthermore, the HRMS spectrum showed a molecular ion peak at 377.1591 amu which was in good agreement with the expected mass of 377.1595 amu for $C_{20}H_{25}O_7$ which is the predicted formula for the ketone intermediate before re-aromatization.

Since PIFA mediated reaction of naphthol is thought to proceed *via* formation of the ketone intermediate and loss of aromaticity in one ring we thought that the new product was a result of incomplete re-aromatization of this intermediate and examination of signal multiplicity of the compound in the ^1H NMR spectrum together with the IR spectrum and HRMS data seemed to agree with that observation. Lonell and co-workers proposed that the formation of naphthol **239** from PIFA mediated methoxylation of naphthalene **234** went through ketone intermediate **238** as shown in **Scheme 2.58**.[129]



Scheme 2.58: *Reagents and conditions:* (a) PIFA, MeOH, rt, 15 min (b) EtOH, *t*-BuOK, rt, 20 min.

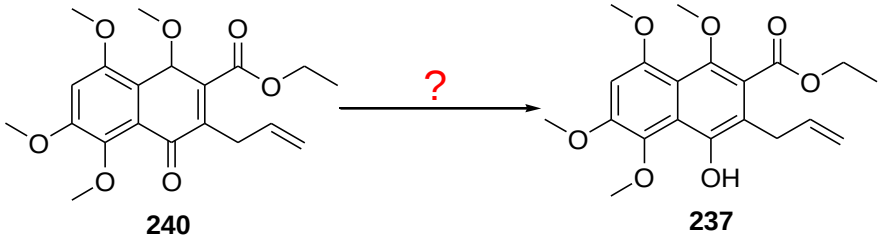
In our hands, the reaction would, therefore, proceed in a very similar manner as shown in **Scheme 2.59**. In other words, the naphthol **236** would be converted to the desired naphthol **237** containing an extra methoxy group *via* the ketone intermediate **240**.



Scheme 2.59: *Reagents and conditions:* (a) PIFA, MeOH, rt, 15 min (b) *21%* NaOEt, EtOH, rt, 20 min.

At this stage we thought that we probably did not expose the presumed intermediate **240** to the base, sodium ethoxide solution in this case, long enough to allow for a complete re-aromatization and we decided to redo the re-aromatization step as previously carried out albeit with longer reaction times. The presumed intermediate **240** was dissolved in ethanol solution and loaded into a dry round bottom flask. The sodium ethoxide solution was added to this mixture and stirred at room temperature for 30 minutes. The reaction mixture was then quenched and to our surprise the TLC plate showed a new spot which did not correspond to the desired naphthol **237**. The ^{1}H NMR spectrum showed one less methoxy group than in the starting material (presumed intermediate **240**) and surprisingly there were visibly two ethyl groups that appeared to be attached to a hetero atom presumably the oxygen atom. What was more surprising was that the carbonyl signal was still prominent in the ^{13}C NMR spectrum which meant that no re-aromatization reaction had taken place. The IR spectrum was similar to that of the precursor compound but the HRMS spectrum showed a molecular ion peak at 391.1748 amu which confirmed the expected increase in mass due to the ethyl group.

These results meant that the desired base re-aromatization shown in **Scheme 2.60** did not take place.



Scheme 2.60: Highlighting the desired base promoted re-aromatization step.

At this point, we thought that maybe by quenching the reaction mixture when the reaction was carried out in the beginning and re-exposing it to the base for the second time may have impacted on the way the reaction progressed and we decided to subject a new batch of the precursor naphthol **236** to the same PIFA mediated insertion of the methoxy group conditions and to allow the resultant ketone intermediate to be exposed to the base for a longer time. The new precursor naphthol **236** was reacted with PIFA as previously described and the intermediate was exposed to the base for 35 minutes instead of the literature period of 20 minutes. Comparison of the TLC plate of this batch with the old batch showed that the new batch (exposed to the base for 35 minutes) formed three products. One spot corresponded to the naphthol **237** and the other two spots were different from the R_f values of the ones we obtained before. The IR spectra of all three products showed the presence of a hydroxyl functional group. The HRMS data of the two unknown compounds showed molecular ion peaks at 361.1651 amu and 405.1908 amu for $C_{20}H_{25}O_6$ and $C_{22}H_{29}O_7$, respectively.

We were surprised by these results and we thought that a good starting point would be to review the spectroscopic data of the presumed intermediate **240** which we had obtained alongside the desired naphthol **237** in the very first PIFA reaction for naphthol **236**. Comparison of the major signals from presumed compound **240** (which was given a new code of **241**) and ChemDraw prediction of the *ortho*- and *para*-insertion of the methoxy group revealed that compound **241** contained the methoxy substituent adjacent to the carbonyl group as shown in **Table 2.0**.

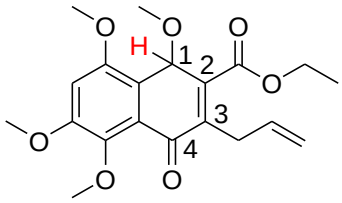
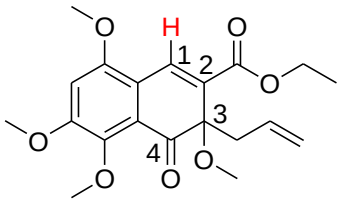
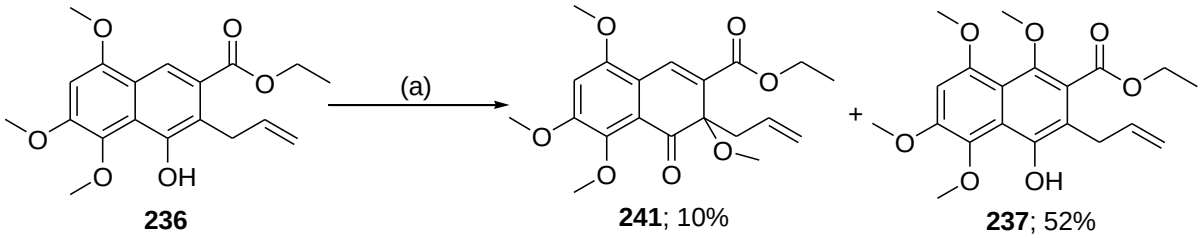
			Compound **241**
position	ChemDraw prediction for *para*-methoxy (ppm)	ChemDraw prediction for *ortho*-methoxy (ppm)	Experimental results for **241** (ppm)
C-1/H-1	65.1/4.81	137.2/7.89	132.4/8.09
C-2	142.4	131.8	128.9
C-3	143.1	89.3	85.0
C-4	183.1	197.7	198.2

Table 2.0: Comparison between ChemDraw predicted *ortho* and *para* methoxylation in relation to the experimental results

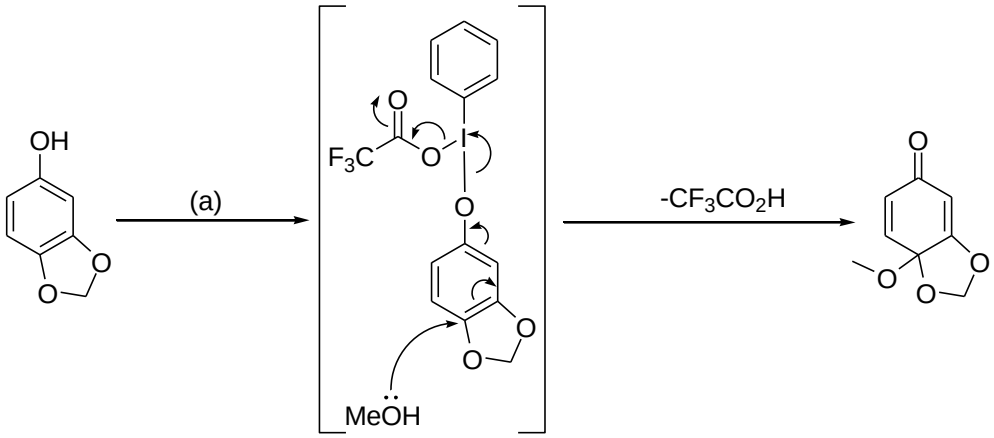
As surprising as these results may be, PIFA mediated insertion of the methoxy group is thought to proceed by coordination of the phenol or naphthol group to PIFA. Electronically, the effect felt at the *para* position to the coordinated naphthol group should be equally felt at the *ortho* position in a classic *ortho-para* activation. This means that the selectivity of the *para* position by PIFA reagent reported in the literature cannot be explained in terms of the electronic effect of the coordinated naphthol. There are some reagents which are known to direct the reaction at the *ortho* position by intramolecular transfer (coordination) but there cannot be such interaction between the PIFA reagent and the *para* position with respect to the coordinated OH group. In view of the foregoing discussion, the reported regioselectivity of the PIFA reagent would most likely be due to the steric interaction of the *ortho* position with the bulky PIFA group. The valid question would be: under what condition(s) would the steric interaction be reduced to allow for the insertion of the methoxy group at the *ortho* position albeit to a smaller extent? This question may not be easily answered but molecular studies

could shed more light in this regard. There are reports of PIFA mediated *ortho* reactions in the literature.[147] So the overall reaction for the first PIFA mediated methoxylation is shown in **Scheme 2.61**.



Scheme 2.61: *Reagents and conditions:* (a) PIFA, MeOH, rt, 15 min (b) *21%* NaOEt, EtOH, rt, 20 min.

Looking at the literature, the use of methanol as a nucleophile for the PIFA reaction was first reported by in 1987 Kita and co-workers who reported regioselective insertion of the methoxy group at the *para* position as shown in **Scheme 2.62**.[148]

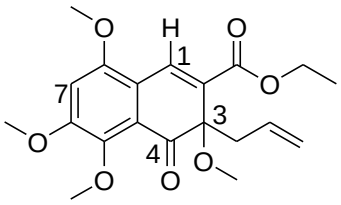


Scheme 2.62: *Reagents and conditions:* (a) PIFA, MeOH, rt, 30 min.

This reaction was then modified by Lonell and co-workers[129] in 2008 to allow for re-aromatization of the ketone intermediate such that the overall effect was the substitution of an aromatic hydrogen substituent with a methoxy group as shown in **Scheme 2.58** above.

2.3.3.0 Spectroscopic data analysis of compound 241

The ^{1}H NMR spectrum of ketone **241** showed two singlet signals at 8.09 ppm (1H, s) and 6.70 ppm (1H, s) which were consistent with H-1 and H-7 protons, respectively. The signal at 3.15 ppm (3H, s) was consistent with an alkyl methoxy group and was assigned to the methoxy group attached to *C*-3. The ^{13}C NMR spectrum showed a signal at 198.3 ppm which was consistent with the carbonyl carbon atom (C-4). The signal at 43.3 ppm was ascribed to the allylic carbon atom. It was of interest to note that this signal appeared uncharacteristically downfield compared to the normal *C*-allylic carbon atoms we had dealt with up to this point. The 2D spectroscopic data analysis for this compound is given in a tabulated form in A**ppendix B1.0**.



241

The formation of the *ortho* methoxylation product was later confirmed by crystal structure determination and the ORTEP diagram of compound **241** is given in **Figure 2.13**.

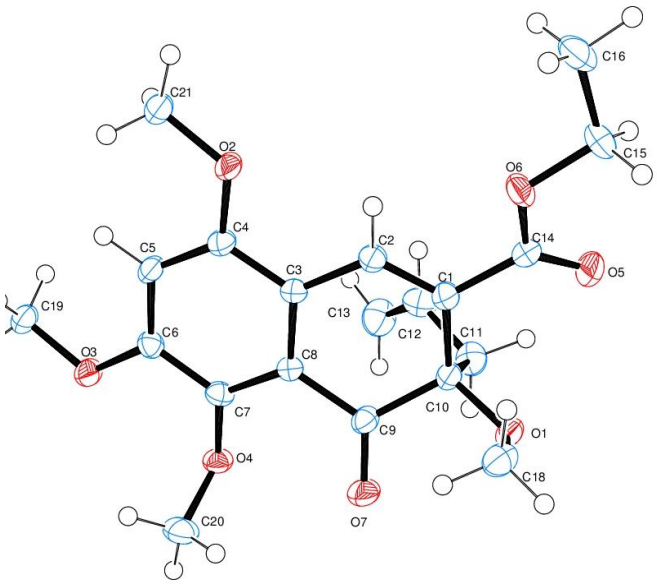
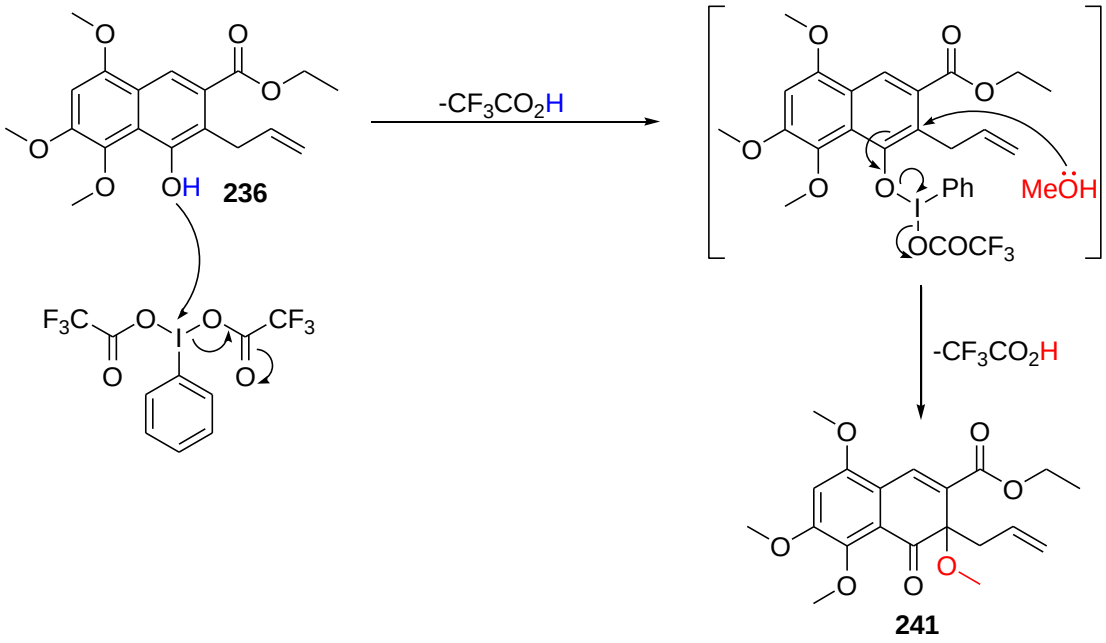


Figure 2.13: The ORTEP diagram of **241**. Thermal ellipsoids are shown at the 50% probability level.

2.3.3.1 Proposed mechanism for PIFA mediated ortho methoxylation

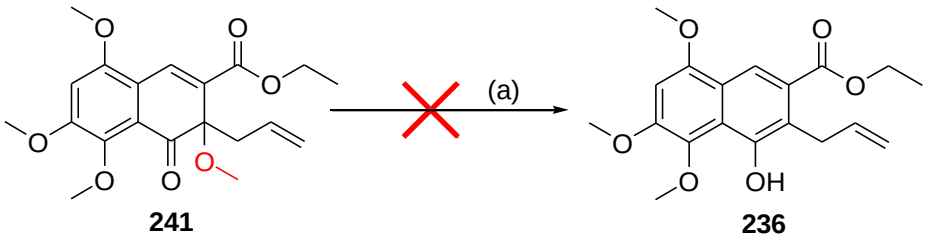
The proposed mechanism for the *ortho* methoxylation is shown in **Scheme 2.63**. The first step in the reaction is the typical coordination of the oxygen atom of the naphthol to the

iodine centre which is followed by loss of the proton from the naphthol. The methanol molecule is then added to the alkene double bond at the *ortho* position of the naphthol oxygen coordinated to the iodine which results in isolation of ketone **241**. When this result and that shown in **Scheme 2.58** are put into context we can safely conclude that the PIFA reagent activates both the *para* and *ortho* positions of the ring and selectivity which is normally observed in this reaction cannot be explained on the basis of electronic effects.



Scheme 2.63: Proposed mechanism for PIFA mediated *ortho* methoxylation of naphthol **236**.

At this point it is easy to explain why no re-aromatization (**Scheme 2.64**) was effected when compound **241** was exposed to the base even for longer times. The *ortho* insertion intermediate **241** lacked an enolizable hydrogen to initiate the re-aromatization process as required under mild basic conditions.



Scheme 2.64: The failed re-aromatization under mild basic conditions.

Having identified ketone **241** the next challenge was to figure out the nature of compound **242** which was obtained when we tried to re-aromatize ketone **241** by exposing it to excess sodium ethoxide for 30 minutes. As previously explained, it was clear from the ^{1}H NMR spectrum that one methoxy group was substituted by the ethoxy group (2 quartet and 2 triplet signals observed in the vicinity of each other) but the question we were left to answer was which one of the methoxy groups was replaced?

Again ChemDraw prediction proved very useful and the results are shown in **Table 2.1**. If the ethoxy group was attached to the sp^3 carbon at position 3 (*C*-3) then the methylene (*CH*$_2$) protons of the ethyl group would show signals more upfield compared to when attached to the aromatic ring. It was also expected that in such a scenario there would be no pronounced difference between the remaining 3 methoxy groups if they are all attached to the aromatic ring. The results clearly indicated that the ethoxy group substituted one of the methoxy substituents attached to the aromatic ring.

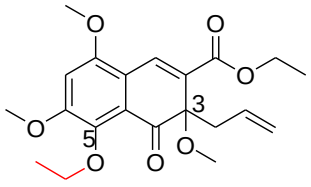
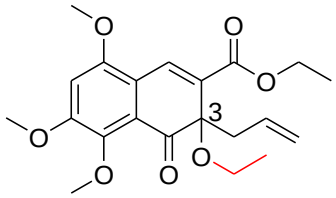
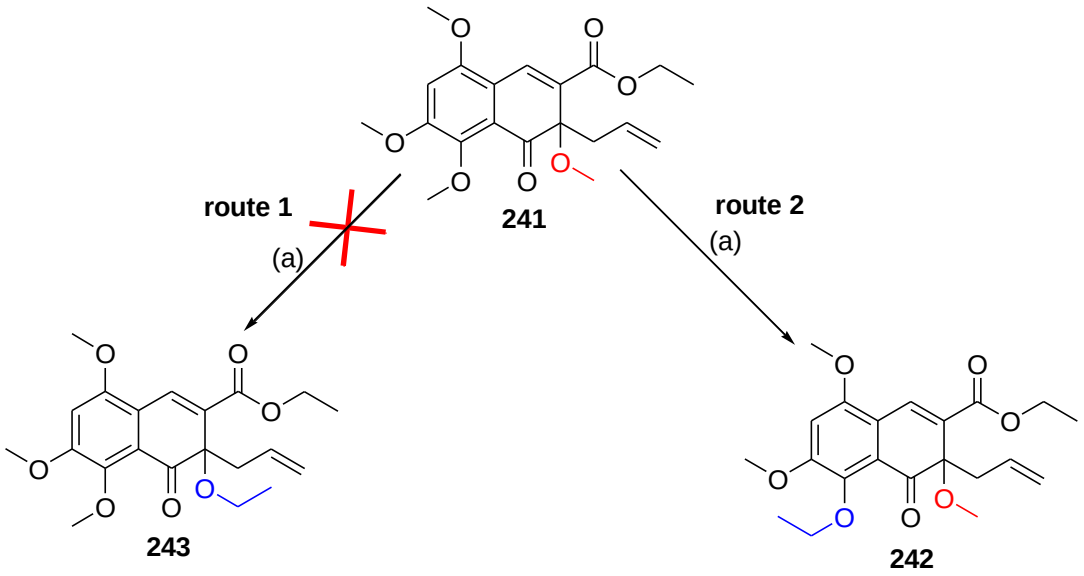
			Compound **242**
	Chemdraw prediction for aromatic methoxy substitution (ppm)	Chemdraw prediction for alkyl methoxy substitution (ppm)	Spectroscopic data
OCH_2CH_3	65.0	62.9	70.1
OCH_2CH_3	3.98	3.41	4.09-3.85 (part of m)
OCH_3	54.6 C(3)-OCH_3 and 56.3 for ArOCH_3	3 × ArOCH_3 = 56.2, 56.2, 56.3	53.6, 56.4, 56.3
OCH_3	3.24 for C(3)-OCH_3 and 3.73 for ArOCH_3	3.73 for ArOCH_3	3.15

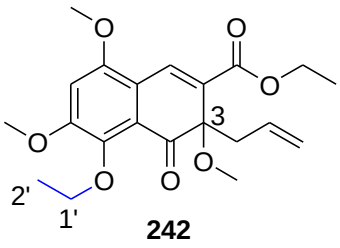
Table 2.1: Comparison between Chemdraw predicted resonances of nucleophilic substitution and experimental results

This meant that the reaction followed **route 2** as opposed to **route 1** as depicted in reaction **Scheme 2.65**.



Scheme 2.65: *Reagents and conditions:* (a) *21%* NaOEt, EtOH, 30 min, rt, 10%.

The ^{1}H NMR spectrum of the ketone **242** showed signals between 4.09-3.85 ppm (8H, m) corresponding to the protons of the two methoxy groups attached to the aromatic ring and the H-1' protons. A triplet proton signal at 1.43 ppm (3H, t, J = 7.0) was consistent with the H-2' protons. The ^{13}C NMR spectrum showed signals at 70.1 ppm and 15.5 ppm which were assigned to the C-1' and C-2' carbon atoms, respectively.



Pinpointing the exact methoxy group of the aromatic substituents which was involved in nucleophilic substitution reaction was the last outstanding question that needed to be addressed. A crystal structure determination would have offered a definitive answer as to the exact structure of compound **242** but efforts to grow suitable crystals from the oily product were not successful so we had to look for alternative methods. Painstaking analysis of the 2D spectroscopic data for compounds **241** and **242** amazingly offered sufficient information to pinpoint the methoxy group that was involved in the substitution reaction. The data revealed that the methoxy group at position 5 was involved in the substitution reaction and the 2D

spectroscopic data for compounds **241** and **242** are given in tabulated form in **Appendices B1.0** and **B1.1**, respectively. **Table 2.2** shows relative signals in ppm of O*C*H$_3$/Ar-*C* at positions 5, 6 and 8 for compounds **241** and **242**.

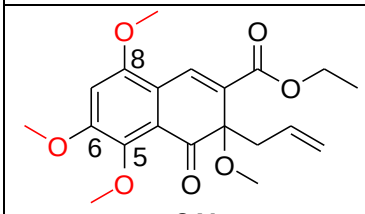
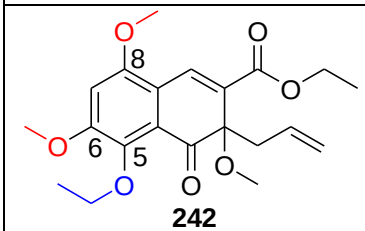
	O*C*H$_3$ 5/Ar-*C* (ppm)	O*C*H$_3$ 6/Ar-*C* (ppm)	O*C*H$_3$ 8/Ar-*C* (ppm)
 **241**	61.6/143.1	56.3 or 56.4/156.2	56.3 or 56.4/153.3
 **242**	O*C*H$_2$*C*H$_3$/Ar-*C* 70.1/142.3	56.3 or 56.4/156.5	56.3 or 56.4/153.3

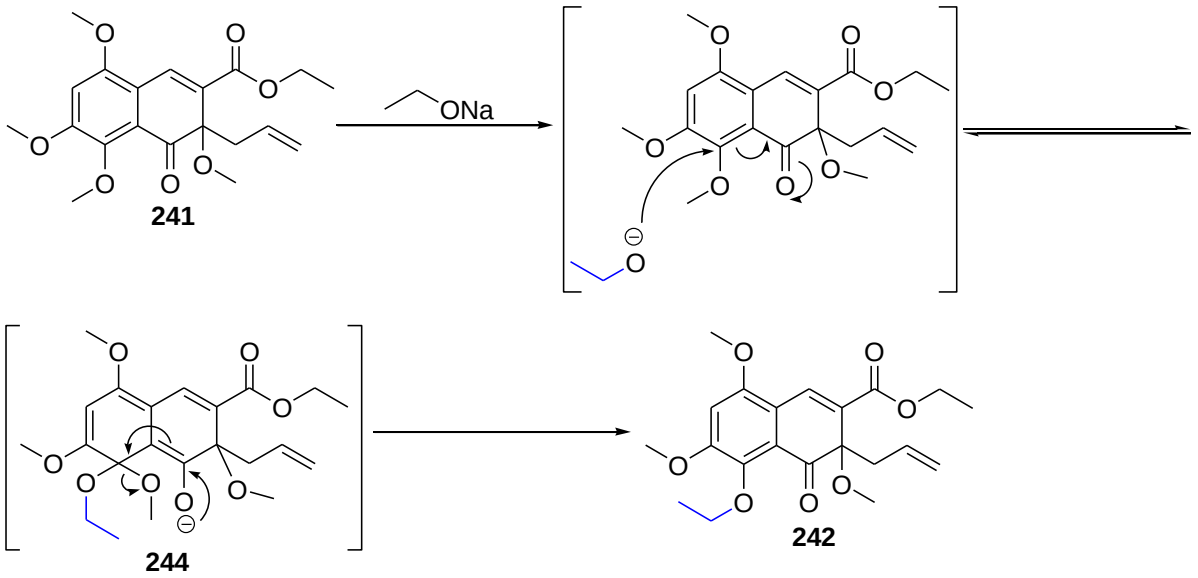
Table 2.2: Comparison of selected spectroscopic data for compounds **241** and **242**

We were unable to differentiate the methoxy signals at positions 6 and 8 due to the fact that the HSQC spectrum did not differentiate these protons from the corresponding carbon signals and we did not want to use inference which could not be fully supported by the data at hand. Nevertheless, the analysis perfectly suited our purpose and we were able to assign unambiguously the position of the ethoxy group on the naphthalene skeleton as 5 (see compound **242**).

This was one unusual case whereby almost all the carbon and proton signals of the two compounds correlated perfectly to each other. In most cases a small change in the compound brings a profound change in the magnetic properties of the resultant compound. The proposed mechanism for this substitution is shown in **Scheme 2.66**.

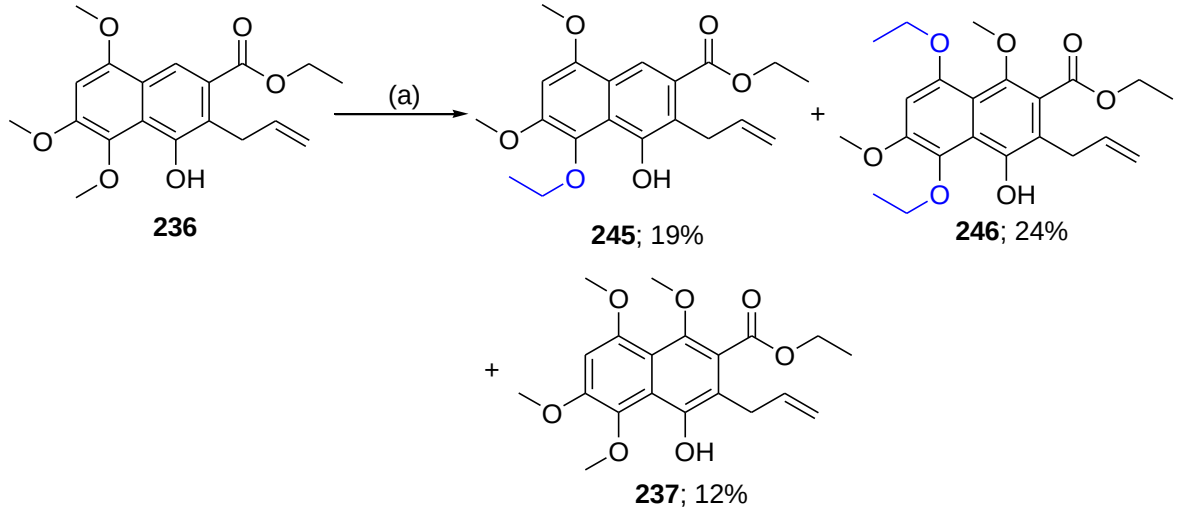
2.3.3.2 Proposed mechanism for 1,4-Michael-type addition

The ethoxide ion attacked the carbon atom of the aromatic ring of compound **241** holding the methoxy substituent at position 5 in a typical Michael-type addition reaction. We believed that the elimination of the methoxy group from the intermediate **244** was not connected to the stability of the resultant product or of the leaving group (methoxy group) but rather was more to do with statistical advantage the ethoxide ions had over methoxide ions. The reaction was carried out in the presence of much more sodium ethoxide as compared to the methoxide present in the reaction mixture which came from the compound itself.



Scheme 2.66: The proposed Michael-type substitution reaction.

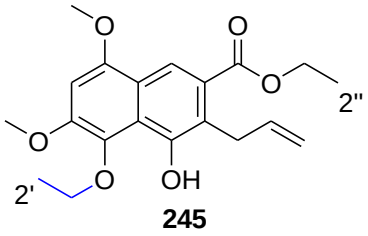
The discovery that ketone **242** was formed by the Michael type reaction proved very significant in solving the nature of the two unknown products which were obtained when the intermediate of the PIFA reaction was exposed to the base for 35 minutes which are shown in **Scheme 2.67**. In this case, the ketone intermediate had an enolizable hydrogen atom which led to a successful re-aromatization process.



Scheme 2.67: *Reagents and conditions:* (a) (i) PIFA, MeOH, rt, 15 min. (ii) *21%* NaOEt, EtOH, rt, 35 min.

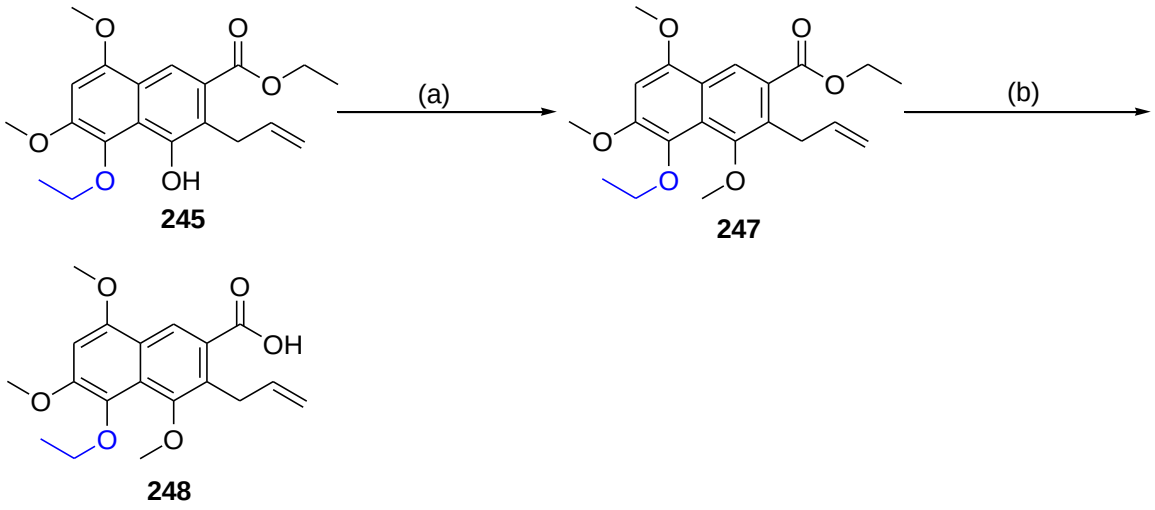
The top spot on the TLC plate (compound **245** which was isolated in 19% yield) showed two signals consistent with methoxy groups attached to the aromatic ring, a signal consistent with the naphthol proton and two signals consistent with the ethoxy groups. With the help of assignment of the NMR spectroscopy signals from compound **242** this compound was identified as naphthol **245**.

The ^{1}H NMR spectrum of naphthol **245** showed a signal at 10.25 ppm (1H, s) consistent with the naphthol proton. The two signals due to aromatic protons were at 8.20 ppm and 6.57 ppm indicating that the PIFA mediated insertion of the methoxy group was not successful. The signals at 1.45 ppm (3H, t, J = 6.4 Hz) and 1.41 ppm (3H, t, J = 6.4 Hz) compared favourably with the CH_3 protons of the two ethyl groups (C-2' and C-2"). The ^{13}C NMR spectrum showed 13 signals consistent with the naphthalene, alkene and ester carbonyl carbon atoms. Much as comparison of the signals due to the remaining methoxy groups of this compound with that of compound **242** gave a good indication of the position of the ethoxy group we thought that obtaining crystal structure of this compound would prove beyond reasonable doubt the position of the aromatic ethoxy group.



2.3.4 Synthesis of 3-ally-5-ethoxy-4,6,8-trimethoxynaphthalene-2-carboxylic acid 248

To achieve this, the carboxylic acid of naphthalene ester **245** was synthesized as shown in **Scheme 2.68** from which good crystals were grown for crystal structure determination. A routine methylation transformation of the naphthol group was accomplished by refluxing the acetone solution of naphthol **245** in dimethyl sulfate and potassium carbonate. The purification of the crude reaction mixture was accomplished by column chromatography on silica gel yielding compound **247** in 72% yield.



Scheme 2.68: *Reagents and conditions:* (a) (i) K_2CO_3, Me_2SO_4, Me_2CO, reflux, 24 hrs, 72% (b) NaOH, $MeOH/H_2O$, reflux, 24 hrs (% yield not calculated).

The ^1H NMR spectrum of naphthalene **247** revealed loss of the signal at 10.25 ppm which was assigned to the naphthol proton in the precursor compound and there was a new signal corresponding to the methoxy group. The ^{13}C NMR spectrum showed an additional signal corresponding to a methoxy group (making a total of 3 aromatic methoxy signals).

A routine base mediated hydrolysis of naphthalene **247** furnished the required carboxylic acid **248** and we were able to obtain crystals of this acid which were good enough for crystal structure determination. The crystal structure confirmed the position of substitution as position 5 and the ORTEP diagram of carboxylic acid **248** is given in **Figure 2.14**.

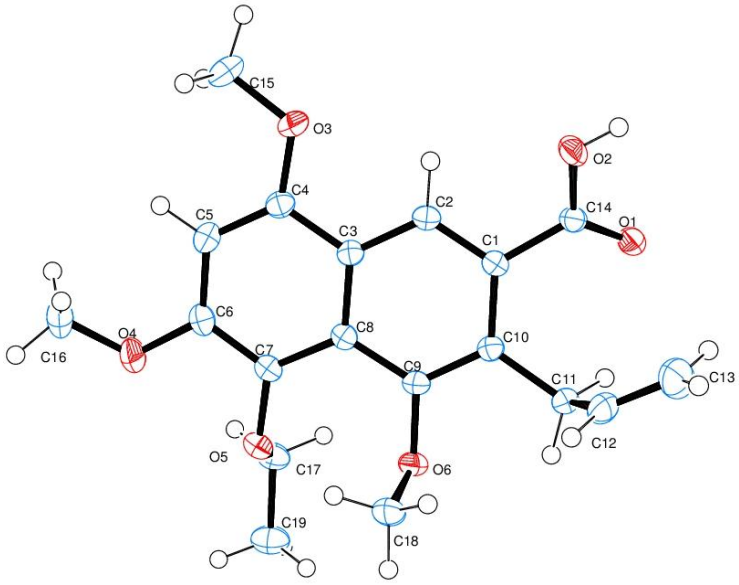
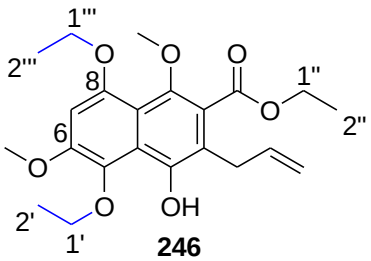


Figure 2.14 The ORTEP diagram of acid **248**. Thermal ellipsoids are shown at the 50% probability level.

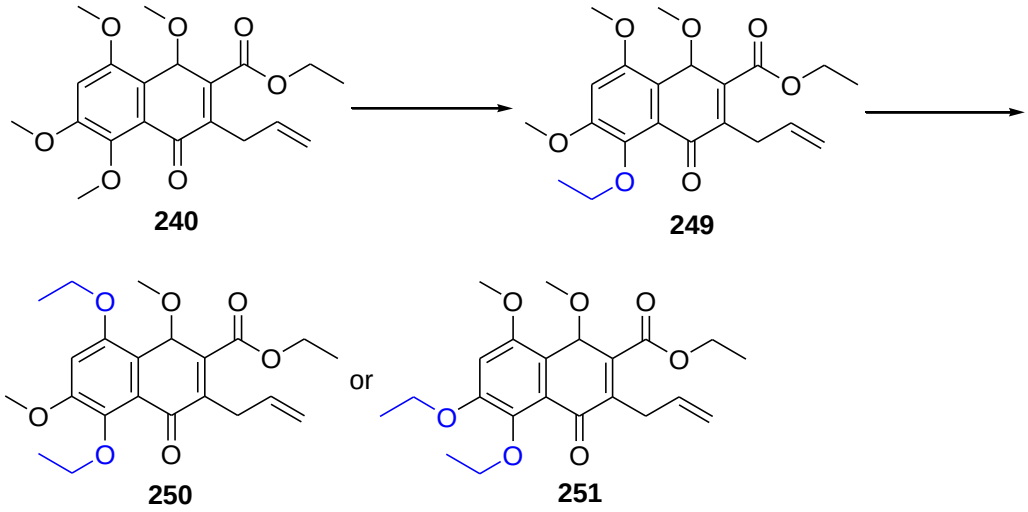
The mechanism for the formation of naphthol **245** could be explained in the same way as the formation of ketone **242** but in this case there was no insertion of the methoxy group. As explained before, the successful re-aromatization process of the ethyl substituted ketone intermediate was possible due to availability of the enolizable hydrogen atom.

The compound with two ethoxy groups was identified as naphthol **246**. The ^{1}H NMR spectrum clearly showed two quartet signals at 4.39 ppm (2H, q, J = 7.1 Hz) and 4.21 ppm (2H, q, J = 7.1 Hz) corresponding to the CH_2 protons (two sets of H-1' or H-1" or H-1'") of the ethyl groups. The third signal of the CH_2 ethyl protons was part of the multiplet signal between 4.05-3.86 ppm (8H, m) with the other signals being due to two sets of methoxy groups. There was also a multiplet signal between 1.48-1.30 ppm (9H, m) which was consistent with overlapping signals due to 3 sets of CH_3 protons (H-2' or H-2" or H-2'") of the ethyl groups.



246

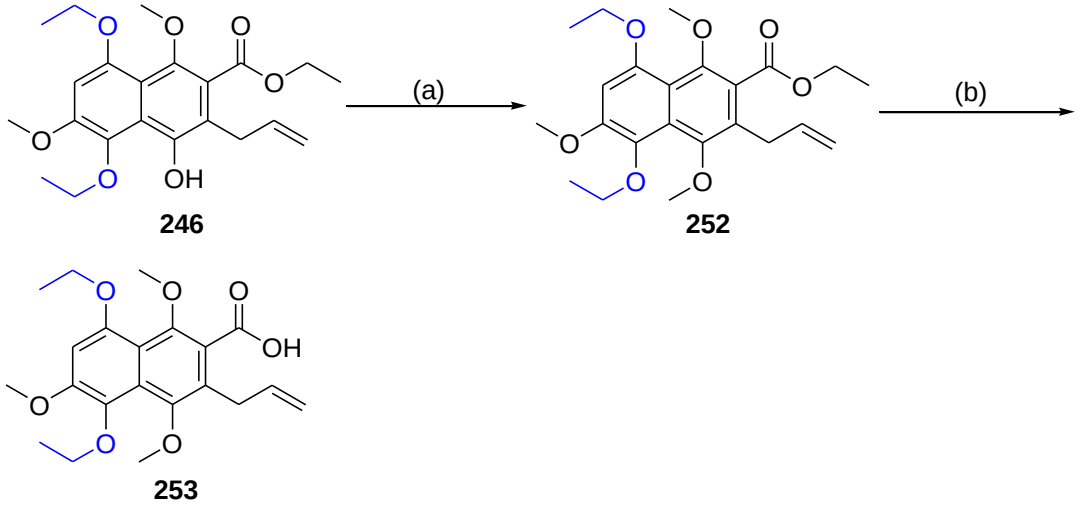
What was strange about this compound was that the mechanism for substitution of the methoxy substituent with the second ethoxy group (from intermediate **249**) was not very clear and it may as well be at position 6 (compound **251**). For the purposes of this discussion we assumed substitution at position 8 took place. **Scheme 2.69** shows the two possible double ethyl substituted intermediates **250** and **251**.



Scheme 2.69: *Reagents and conditions:* (a) *21%* NaOEt, EtOH, rt, 35 min.

2.3.5 Synthesis of 3-allyl-5,8-diethyl-1,4,6-trimethoxynaphthalene-2-carboxylic acid 253

In an attempt to grow crystals suitable for crystal structure determination we thought it was important to methylate naphthol **246**. A mixture of naphthol **246**, dimethyl sulfate and potassium carbonate in acetone was heated to reflux for 24 hrs. The crude reaction mixture was cooled to room temperature and purified by silica gel column chromatography affording pentaoxygenated naphthalene **252** in 78% yield (**Scheme 2.70**). The ^{1}H NMR spectrum of naphthalene **252** showed a new signal corresponding to an additional methoxy group attached to the naphthalene ring and there was loss of a signal corresponding to the naphthol proton. The ^{13}C NMR spectrum confirmed the successful methylation by showing a new signal corresponding to the methoxy carbon atom attached to the aromatic ring.

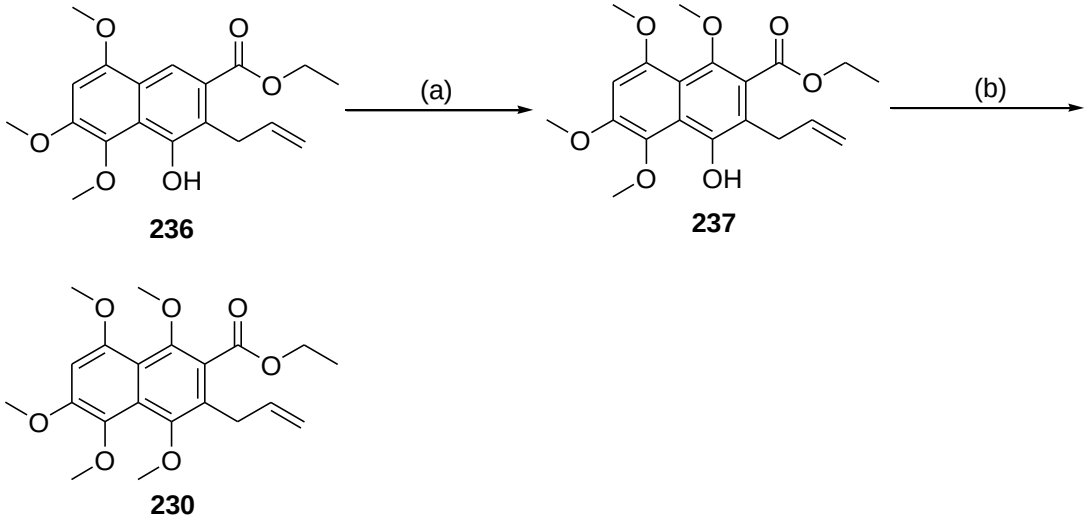


Scheme 2.70: *Reagents and conditions:* (a) K_2CO_3, Me_2SO_4, Me_2CO, reflux, 24 hrs, 78% (b) (i) $LiAlH_4$, Et_2O (ii) PCC, silica, N_2 (g) (iii) NaH_2PO_4, $NaClO_2$, H_2O, *t*-BuOH, 2-methyl-2-butene, (% yield not calculated).

The reduction of the ester group by lithium aluminium hydride was followed by oxidation to the corresponding aldehyde and finally, Pinnick oxidation afforded a carboxylic acid **253** but we were unable to grow crystals suitable for crystal structure determination as a result of only a small amount of the acid **253** being available.

2.3.6 Synthesis of ethyl 3-allyl-1,4,5,6,8-pentamethoxynaphthalene-2-carboxylate 230

At this point, we decided to proceed with the original project aim and a clean re-aromatization of the PIFA insertion intermediate was achieved using potassium *tert*-butoxide as a base instead of sodium ethoxide and there was no evidence of substitution products. The methylation of naphthol **237** furnished the corresponding methylated product **230** (**Scheme 2.71**) which was identified by loss of a signal corresponding to loss of a naphthol proton as well as formation of a new signal corresponding to a new methoxy group.



Scheme 2.71: *Reagents and conditions:* (a) (i) PIFA, MeOH, rt, 15 min (ii) *t*-BuOK, EtOH, rt, 20 min, 60% (over two steps) (b) K_2CO_3, Me_2SO_4, Me_2CO, reflux, 24 hrs, 83%.

The successful synthesis of ester **230** was further confirmed by crystal structure determination and the ORTEP diagram is given in **Figure 2.15**.

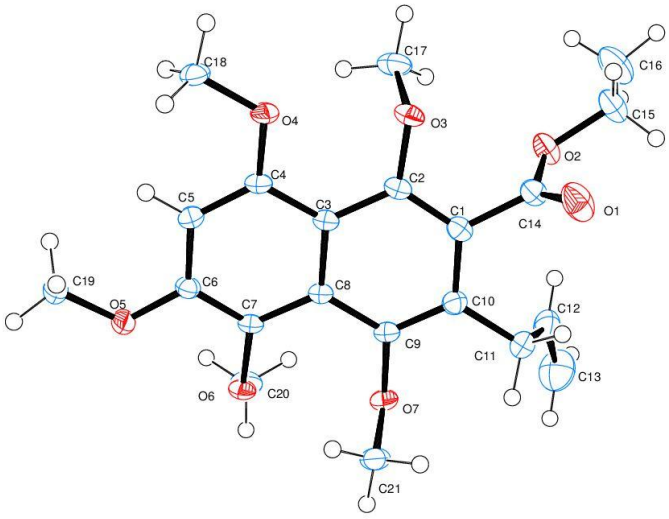
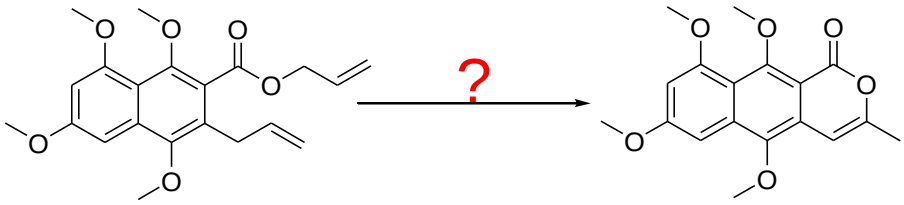


Figure 2.15: The ORTEP diagram of ester **230**. Thermal ellipsoids are shown at the 50% probability level.

Having successfully synthesized the pentaoxygenated naphthalene **230** we were surprised when the hydrolysis of ester **195** afforded the isomerized acid in the project involving the synthesis of dehydroherbarin lactone **159** which at this point was running concurrently with

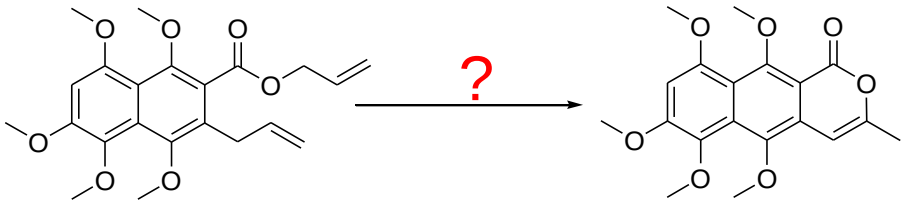
this project (see **Scheme 2.27** in **Section 2.1.12**). A small amount of ethyl ester **230** was hydrolysed using potassium hydroxide as a base and the ^{1}H NMR spectrum revealed the formation of the isomerized carboxylic acid as was the case with the tetraoxygenated naphthalene **195**. Dejected by these results we revisited the project involving the synthesis of dehydroherbarin lactone **159** and realized that we did not attempt subjecting allyl ester **168** to a tandem hydrolysis and cyclization reaction under Wacker oxidation conditions (**Scheme 2.72**). Unfortunately by that time we had already moved beyond this step in the synthesis of dehydroherbarin lactone **159** and we did not have the allyl ester **168** on which to test this reaction.



168 **103**

Scheme 2.72: *Reagents and conditions:* cat. $PdCl_2$, $CuCl_2 \cdot 2H_2O$, DMF/H_2O, O_2 (g), rt, 24 hrs.

The question we tried to address at that point was: *would subjecting allyl ester **254** to Wacker oxidation conditions deliver the required lactone intermediate **229** (**Scheme 2.73**) in the project involving synthesis of 5-methoxy-3,4-dehydroxanthomegnin **34**?*



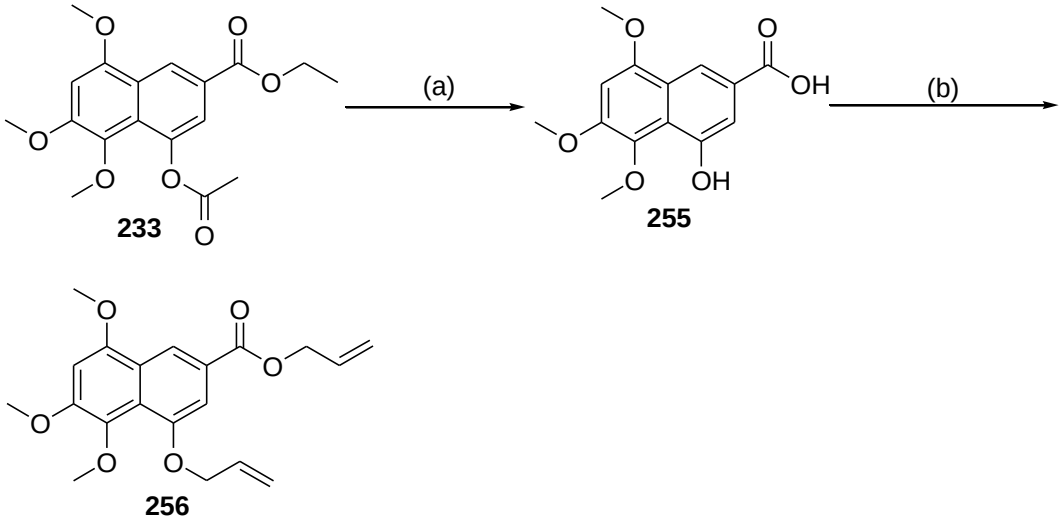
254 **229**

Scheme 2.73: *Reagents and conditions:* cat. $PdCl_2$, $CuCl_2 \cdot 2H_2O$, DMF/H_2O, O_2 (g), rt, 24 hrs.

The only way to find out the suitability of this reaction was to perform it so we devised a route in the same way allyl ester **168** was synthesized.

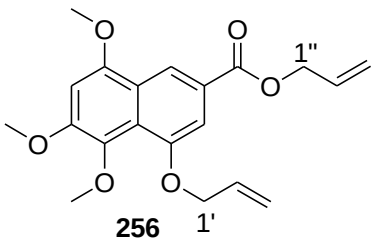
2.3.7 Synthesis of allyl 4-(allyloxy)-5,6,8-trimethoxynaphthalene-2-carboxylate 256

The new route towards the synthesis of allyl ester **254** commenced with a routine unselective saponification and deacetylation of tetra-oxygenated naphthalene **233** using sodium hydroxide solution in water and methanol. The crude product **255** was subjected to a double allylation reaction using excess allyl bromide and potassium carbonate in acetone yielding allyl ester **256** in 84% yield.



Scheme 2.74: *Reagents and conditions:* (a) (i) KOH, MeOH/H_2O, reflux, 6 hrs (ii) *32*% aq. HCl (b) K_2CO_3, allyl bromide, Me_2CO, reflux, 24 hrs, 84% (over 2 steps).

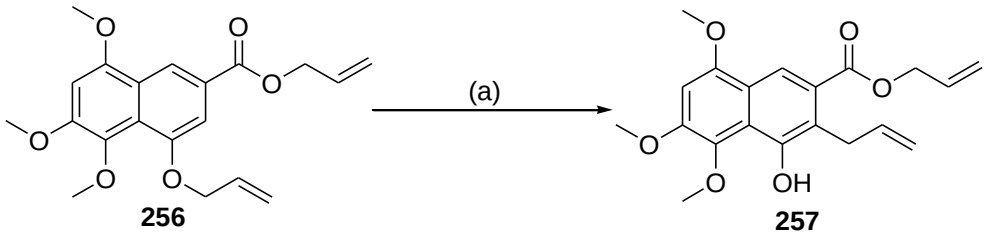
The successful allylation of both the carboxylic acid and the naphthol groups were confirmed by both the ^1H and ^{13}C NMR spectra. The ^1H NMR spectrum of naphthalene **256** showed a multiplet signal between 6.28-5.97 ppm (2H, m) corresponding to the inner protons of the two allyl groups ($ArCH_2CH$=CH_2 and $ArCO_2CH_2CH$=CH_2). The signal at 5.60 ppm (1H, dd, *J* = 17.2, 1.5 Hz) was attributed to one of the terminal vinylic protons of the allyl ester group ($ArCO_2CH_2CH$=CH_2) which was in a *trans* position to the inner vinylic proton with a typical *trans*-coupling constant of *J* = 17.2 Hz and the signal at 5.43 (1H, dd, *J* = 17.2, 1.4 Hz) was for the terminal vinylic protons of the allyl ether group ($ArCH_2CH$=CH_2) which was again in the *trans* position (*J* = 17.2 Hz) to the inner vinylic proton. The ^{13}C NMR spectrum showed signals at



70.4 ppm and 65.6 ppm corresponding to the allylic carbon atoms of the *O*-allyl ether (C-1') and *O*-allyl ester (C-1"), respectively.

2.3.8 Synthesis of allyl 3-allyl-4-hydroxy-5,6,8-trimethoxynaphthalene-2-carboxylate 257

A routine neat Claisen rearrangement reaction was carried out at 180 ^{o}C for 24 hours that delivered naphthol **257** as a yellow amorphous solid in 68% as shown in **Scheme 2.75**.

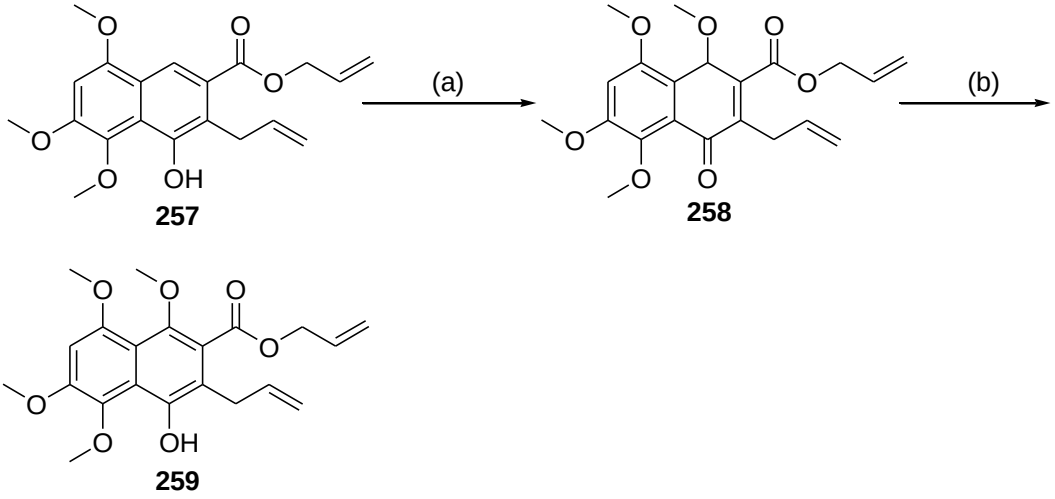


Scheme 2.75: *Reagents and conditions:* (a) heat, 180 ^{o}C, N_2 (g), 24 hrs, 68%.

The ^{1}H NMR spectrum of naphthol **257** showed loss of one signal in the aromatic/alkene region corresponding to the loss of one aromatic proton and a trademark naphthol proton signal was present at 10.08 ppm (1H, s). The ^{13}C NMR spectrum showed loss of a signal at 70.4 ppm which was attributed to the allylic carbon atom of the *O*-allyl ether in the precursor compound and there was a new signal at 30.0 ppm which was ascribed to the allylic carbon of the *C*-allyl group. These results clearly proved that the Claisen rearrangement reaction was successfully achieved and at this stage we turned our attention to the PIFA mediated insertion of the methoxy group.

2.3.9 Synthesis of allyl 3-allyl-4-hydroxy-1,5,6,8-tetramethoxynaphthalene-2-carboxylate 259

The routine PIFA reaction was carried out for 15 minutes and re-aromatization of the intermediate was achieved by using potassium *tert*-butoxide as a base. There was no indication of nucleophilic substitution products and the crude product was purified by column chromatography on flash silica gel yielding naphthalene **259** in 59% yield.

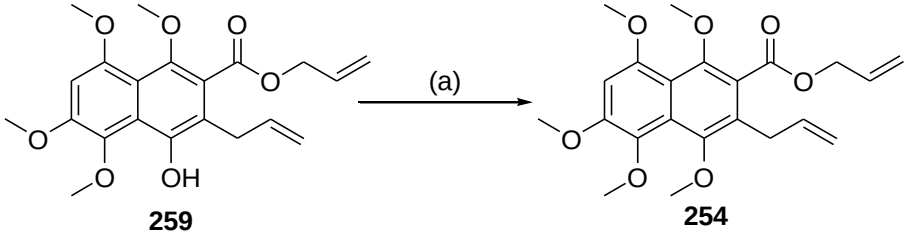


Scheme 2.76: *Reagents and conditions:* (a) PIFA, MeOH, rt, 15 min (b) *t*-BuOK, EtOH, rt, 20 min, 59% (over 2 steps).

The ^{1}H NMR spectrum of naphthol **259** showed loss of one proton signal in the aromatic/alkene region corresponding to the loss of one aromatic proton which was substituted by the methoxy group. The D_2O exchangeable proton signal at 10.21 ppm corresponding to the naphthol proton indicated that re-aromatization was successful and there was a new signal corresponding to an additional methoxy group attached to the aromatic ring.

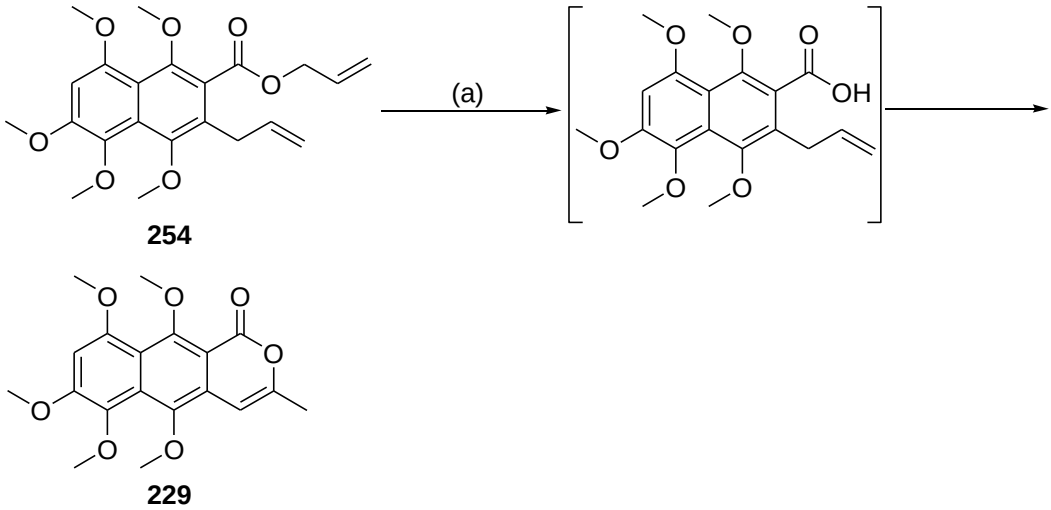
2.3.10 Synthesis of 5,6,7,9,10-pentamethoxy-3-methyl-1*H*-benzo[*g*]isochromen-1-one 229

A routine methylation reaction of naphthol **259** in acetone using dimethyl sulfate and potassium carbonate afforded allyl ester **254** in 91% yield (**Scheme 2.77**). The loss of the naphthol proton signal which was in the precursor compound was visible in the ^{1}H NMR spectrum and a new signal corresponding to the methoxy group was also noted. The ^{13}C NMR spectrum showed a new signal corresponding to an additional methoxy carbon atom attached to the aromatic ring. At this point we were pleased that we had successfully synthesized what we thought was a key intermediate towards a viable synthesis of lactone **229**.



Scheme 2.77: *Reagents and conditions:* (a) Me_2SO_4, K_2CO_3, Me_2CO, reflux, 24 hrs, 91%.

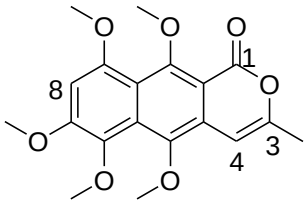
When the allyl ester **254** was subjected to a routine Wacker oxidation reaction it was noted by TLC analysis that the major composition of the reaction mixture after 12 hours corresponded to the starting material. At this point we decided to add more copper chloride and sodium chloride to the reaction mixture in the hope of facilitating *in situ* deallylation of the allyl ester group (**Scheme 2.78**). The formation of two new spots was visible on the TLC plate with the yellow bottom spot corresponding to the desired lactone **229** which was isolated in 36% yield. The IR spectrum of the lactone showed peaks at 1741 cm^{-1} and 1605 cm^{-1} which were typical of the carbonyl and alkene functional groups, respectively, and were similar to the peaks shown by lactone **103**. In addition, the HRMS spectrum showed a molecular ion peak at 361.1287 amu which was in good agreement with the expected mass of 361.1282 amu for $C_{19}H_{21}O_7$.



Scheme 2.78: *Reagents and conditions:* (a) cat. $PdCl_2$, $CuCl_2 \cdot 2H_2O$, DMF/H_2O, O_2 (g), rt, 48 hrs, 36%.

The ^{1}H NMR spectrum of lactone **229** revealed loss of all the signals which were attributed to the allyl ester group in the precursor compound **254**. It further showed two singlet signals corresponding to the aromatic/alkene protons and a singlet signal corresponding to a methyl group. These results were confirmed by the ^{13}C NMR spectrum which showed loss of signals corresponding to the allyl ester group which were visible in the precursor compound. There was also loss of a signal corresponding to the allylic carbon atom of the *C*-allyl group which was at 31.5 ppm in the diallyl ester **254**. These results were consistent with the expected results of the desired lactone **229**.

The signals in the ^{1}H NMR spectrum at 6.73 ppm (1H, s) and 6.57 ppm (1H, s) were consistent with protons H-8 and H-4, respectively. The proton signals corresponding to the five methoxy groups attached to the aromatic ring were accounted for and the singlet signal at 2.26 ppm (3H, s) was assigned to the protons of a methyl group attached to the carbon atom at position 3. The ^{13}C NMR spectrum showed a signal at 159.4 ppm which was assigned to the carbonyl carbon (C-1) of the lactone. The HSQC spectrum showed that the carbon signal at 96.9 ppm correlated to the H-8 proton whereas the signal at 97.4 ppm corresponded to the H-4 proton.



229

The ORTEP diagram for the crystal structure of lactone **229** is shown in **Figure 2.16**.

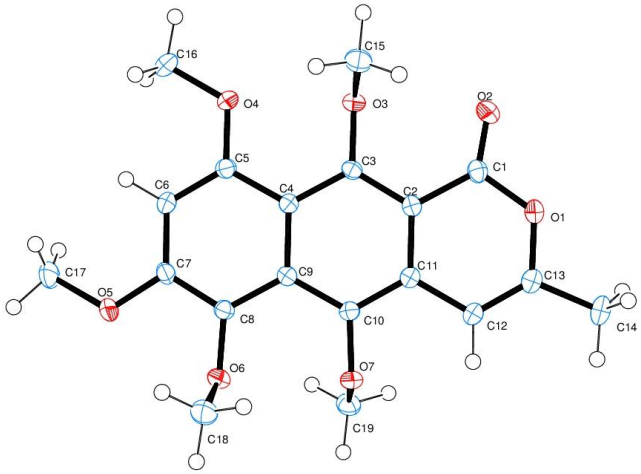
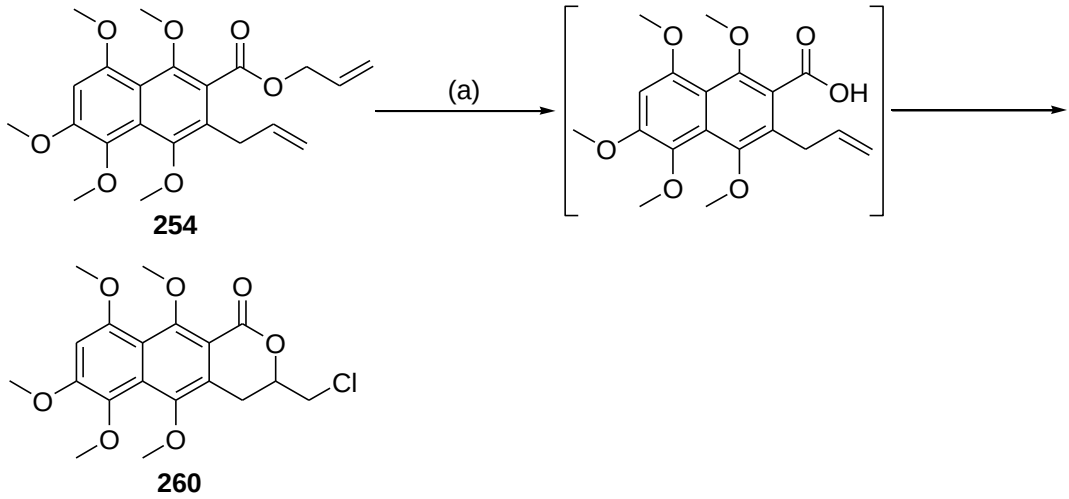


Figure 2.16: The ORTEP diagram for lactone **229**. Thermal ellipsoids are shown at the 50% probability level.

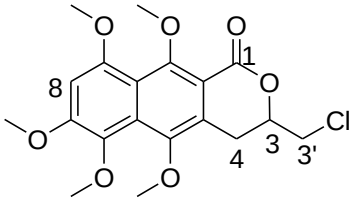
Having successfully identified the desired product we turned our attention to the top fluorescent spot which was obtained in 30% yield. The IR spectrum showed a peak corresponding to the lactone carbonyl functional group similar to that of lactone **229** but the alkene peak was absent.

^{1}H and ^{13}C NMR spectroscopy revealed that compound **260** did not have a similar pyranone ring to that in lactones **103** and **229**. A search on what has been carried out in our laboratory revealed that the multiplet and doublet of doublets signals were similar to the ones reported by Mmutlane.[119] This observation made us realize that we were dealing with a pyranone ring which had no double bond. The two distinct doublet of doublets signals were typical of a possible *pseudo*-chair conformation as reported by Mmutlane. All the signals corresponding to the methoxy groups were accounted for but there was a visible highly deshielded doublet which was part of the multiplet signal. This doublet signal appeared downfield compared to where we expected the methyl doublet of such systems to appear and the DEPT spectrum confirmed that it was due to a CH_2. Furthermore, the doublet signal integrated for 2 protons as expected. The 2D spectroscopic data analysis for this compound is given in a tabulated form in **Appendix B1.2**. The HRMS data gave the mass of the molecule as 397.1050 amu and predicted the formula as $C_{19}H_{22}ClO_7$. With this information at hand we were able to predict the structure of the 3,4-dihydroisocoumarin **260** (**Scheme 2.79**). Attempts to grow good crystals for structure determination for this lactone were unsuccessful.



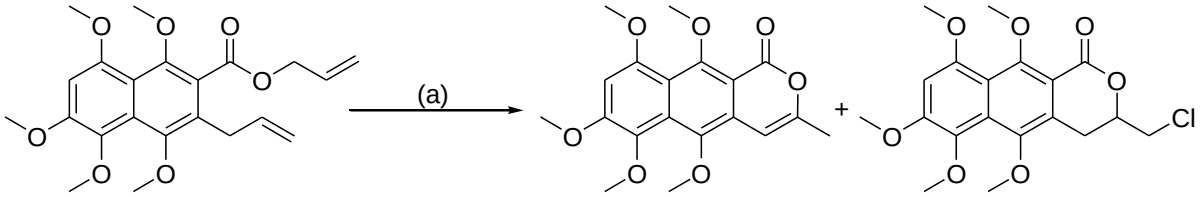
Scheme 2.79: *Reagents and conditions:* (a) cat. $PdCl_2$, $CuCl_2 \cdot 2H_2O$, DMF/H_2O, O_2 (g), rt, 48 hrs.

The ^{1}H NMR spectrum of lactone **260** showed a signal at 6.76 ppm (1H, s) consistent with the H-8 proton which was the only aromatic proton in the compound and the multiplet signal between 4.62-4.56 ppm (1H, m) was consistent with the H-3 proton. The multiplet signal between 3.88-3.69 ppm (8H, m) was attributed to the two methoxy groups and the H-3' protons. The signals at 3.53 ppm (1H, dd, *J* = 16.2, 2.8 Hz) and 3.00 ppm (1H, dd, *J* = 16.3, 10.8 Hz) were ascribed to the H-4 protons. The ^{13}C NMR spectrum showed a signal at 161.4 ppm which was typical of the carbonyl carbon atom of the lactone group. The HSQC spectrum revealed that carbon signals at 97.4 ppm and 76.2 ppm were correlated with the H-8 and H-3 protons, respectively. It further showed that the carbon signals at 44.4 ppm and 26.0 ppm were correlated with the H-1' and H-4 protons, respectively.



260

The overall reaction equation for the Wacker oxidation reaction of allyl ester **254** is given in **Scheme 2.80**.



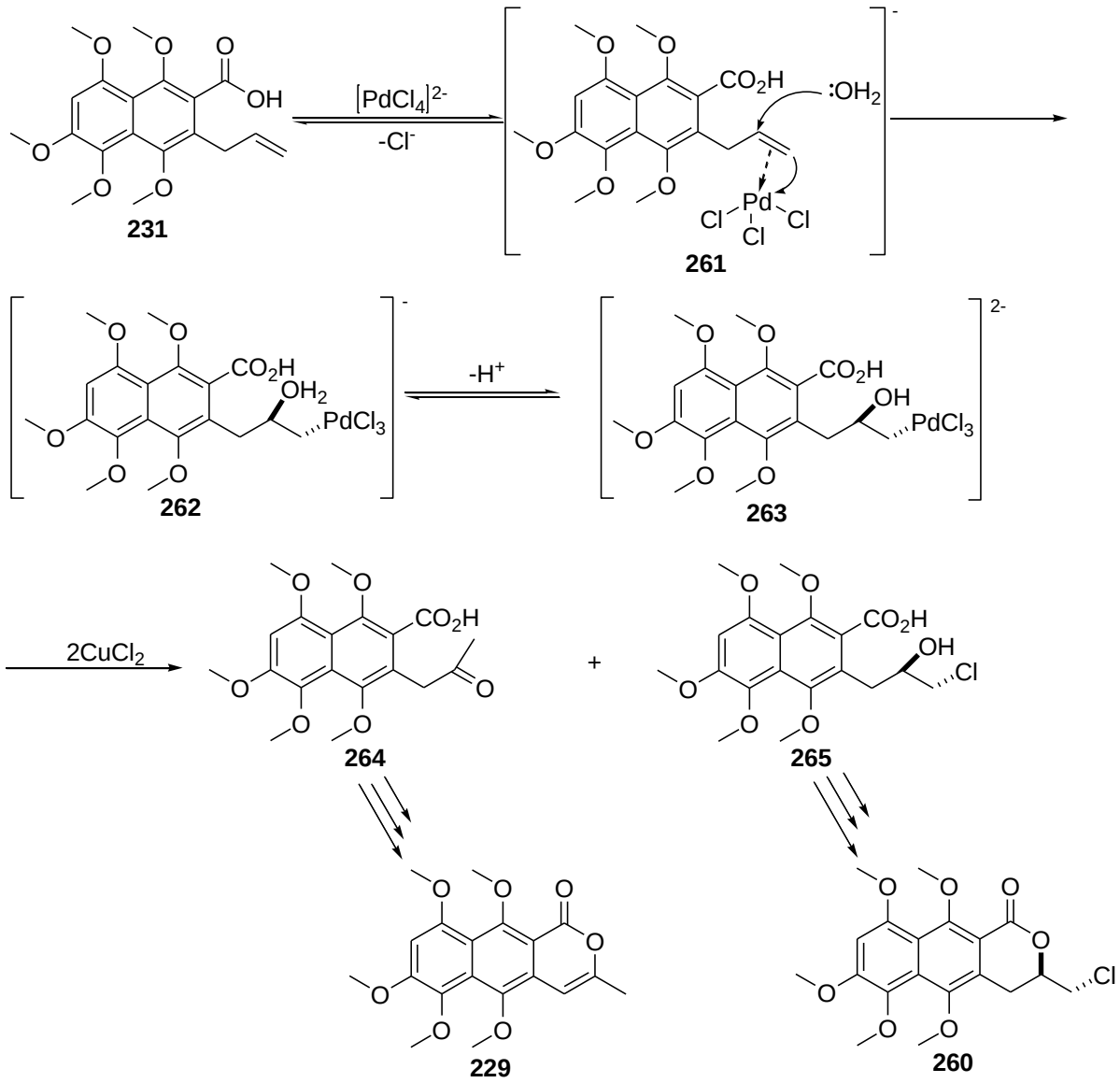
254 **229**; 36% **260**; 30%

Scheme 2.80: *Reagents and conditions:* (a) cat. $PdCl_2$, $CuCl_2{\cdot}2H_2O$, DMF/H_2O, O_2 (g), rt, 48 hrs.

The mechanism for the formation of lactones **229** and **260** shown in **Scheme 2.81** involved an *in situ* cleavage of the allyl ester group generating carboxylic acid **231** in the process. The addition of excess copper chloride and sodium chloride to facilitate the cleavage of the allyl ester group led to the increase in amounts of chloride ions in the reaction mixture. The high chloride ions and copper chloride concentrations led to the outer sphere rate limiting pathway being followed.[136a]

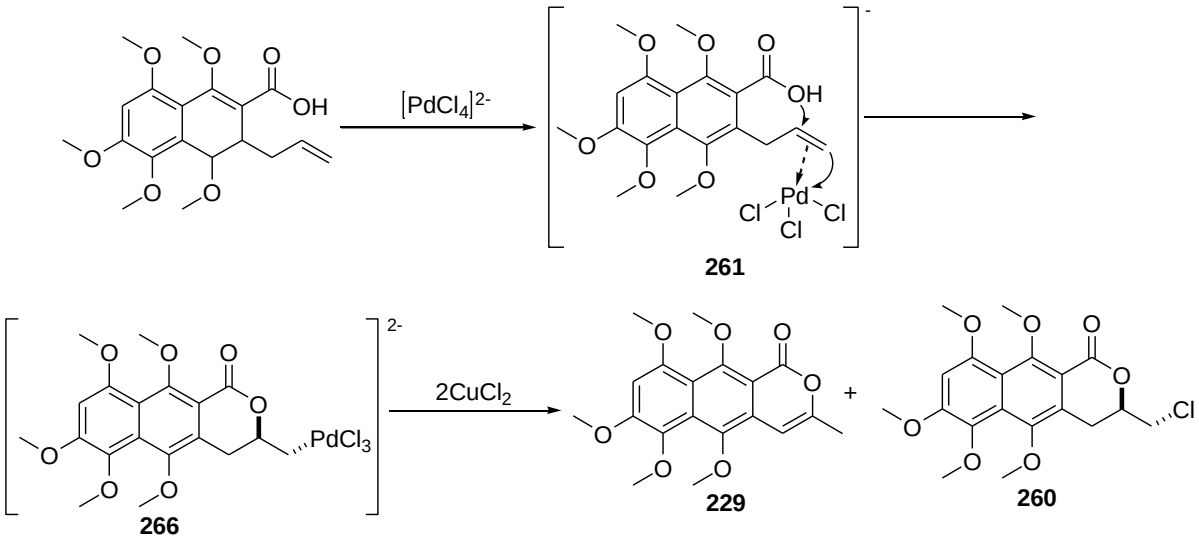
2.3.10.0 Proposed mechanism for outer-sphere intermolecular and intramolecular Wacker oxidation reaction for terminal alkene

In this mechanistic pathway, the first step is the formation of a η^2 π-complex between the Pd(II) metal and the alkene double bond of carboxylic acid **231**. This step is followed by the intermolecular nucleophilic attack of a water molecule on the more electrophilic carbon atom of the coordinated alkene **261**. This attack occurs in an *anti*-fashion which furnishes complex **263** through a loss of proton from intermediate complex **262**. The high concentration of chloride ions in the solution results in palladium metal being coordinated to purely chloride ions with no water molecules as shown in complex **263**. The aldehyde and chlorohydrin products are then eliminated from the intermediate complex **263** with the aldehyde **264** being a result of β-hydride elimination and chlorohydrin **265** by the interception of the copper chloride.[136a] The typical lactonization of ketone **264** and chlorohydrin **265** lead to the formation of lactones **229** and **260**, respectively.



Scheme 2.81: The proposed mechanism for the formation of lactones **229** and **260**.

Similarly, the intramolecular Wacker oxidation pathway under high concentration of chloride ions in the solution may have led to the formation of palladium metal complex **261** (**Scheme 2.82**). The formation of complex **261** is followed by the intramolecular nucleophilic attack of the hydroxyl group of the carboxylic acid on the activated alkene **261** which furnishes complex **266**. The *β*-hydride elimination followed by isomerization and interception of the copper chloride leads to the formation of lactones **229** and **260**, respectively.

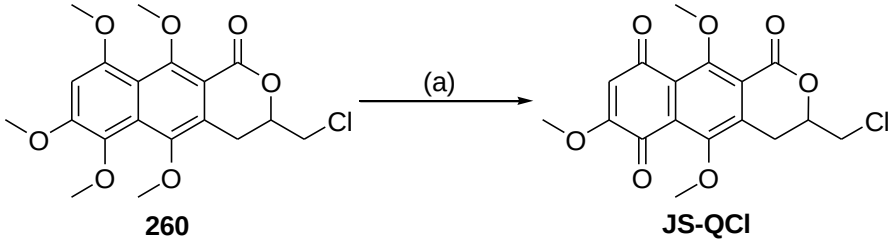


Scheme 2.82: The proposed intramolecular Wacker reaction pathway for the formation of lactones **229** and **260**.

Even though the separation of the two lactones proved very challenging we were happy with these results and we decided to proceed with the oxidation of lactone **260** to a corresponding pyranonaphthoquinone lactone **JS-QCl** with the aim of coming up with the synthetic analogues of 5-methoxy-3,4-dehydroxanthomegnin **34** and anhydrofusarubin lactone **32**.

2.3.11 Synthesis of 3-(chloromethyl)-3,4-dihydro-5,7,10-trimethoxybenzobenzo[*g*]iso-chromene-1,6,9-trione JS-QCl

A routine oxidative demethylation of 3,4-dihydroisocoumarin **260** using silver (II) oxide and nitric acid in 1,4-dioxane yielded a corresponding *para*-pyranonaphthoquinone **JS-QCl** in 60% yield. The IR spectrum of the quinone showed peaks at 1774 cm^{-1}, 1761 cm^{-1} and 1709 cm^{-1} corresponding to the carbonyl functional groups and 1689 cm^{-1} corresponding to the alkene functional group. In addition, the HRMS spectrum showed a molecular ion peak at 367.0584 amu which was in good agreement with the expected mass of 367.0579 amu for $C_{17}H_{16}ClO_7$.

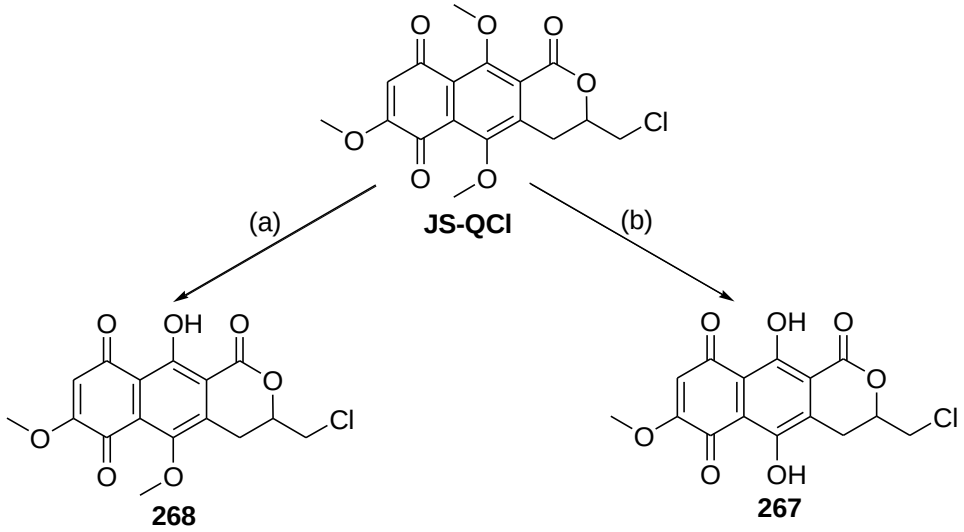


260 **JS-QCl**

Scheme 2.83: *Reagents and conditions:* AgO, *55%* aq. HNO_3, 1,4-dioxane, rt, 70%.

The product was confirmed by both ^{1}H and ^{13}C NMR spectroscopy. The ^{1}H NMR spectrum revealed loss of the signals which were prominent in the precursor compound corresponding to the loss of two methoxy groups. The aromatic proton signal which was at 6.76 ppm in the precursor compound shifted upfield to 6.08 ppm (1H, s) in the product **JS-QCl** and was assigned to the alkene proton of the pyranonaphthoquinone. The ^{13}C NMR spectrum showed two signals at 182.6 ppm and 178.9 ppm corresponding to the carbonyl carbon atoms of the *para*-pyranonaphthoquinone. The spectrum further revealed loss of two signals corresponding to the methoxy carbon atoms attached to the aromatic ring which were present in the starting material **260**.

Attempted selective demethylation (**Scheme 2.84**) of **JS-QCl** using 2 molar equivalents of the boron trichloride to obtain the synthetic analogue of 5-methoxy-3,4-dehydroxanthomegnin **34** (pyranonaphthoquinone **268**) and 4 molar equivalents of the boron trichloride to obtain a synthetic analogue of anhydrofusarubin lactone **32** (pyranonaphthoquione **267**) did not yield the desired results because of decomposition of the crude products during both normal and deactivated silica gel column chromatography.



Scheme 2.84: *Reagents and conditions:* (a) 2 mol. equiv. BCl_3, CH_2Cl_2, N_2 (g), -78 °C → 0 °C (b) 4 mol. equiv. BCl_3, CH_2Cl_2, N_2 (g), -78 °C → 0 °C.

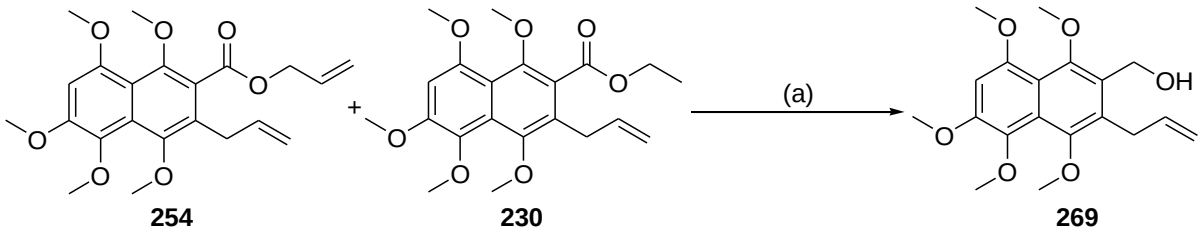
Nevertheless, it was satisfying that the crude products we obtained when 2 and 4 molar equivalents of boron trichloride were used resembled the red colour of the natural products 5-methoxy-3,4-dehydroxanthomegnin **34** and haemoventosin ***S*-115**.

2.3.12 Synthesis of 5,6,7,9,10-pentamethoxy-3-methyl-1*H*-benzo[*g*]isochromen-1-one 229

To build up more lactone intermediate **229** for the synthesis of 5-methoxy-3,4-dehydroxanthomegnin **34** we considered that it was better to employ a three-step reaction sequence involving reduction of esters to alcohol followed by oxidation to the carboxylic acid *via* a carbaldehyde. This protocol had the best chance of delivering unisomerized carboxylic acid **231** for the Wacker oxidation step as explained before. Unlike the protocol we used for the synthesis of carboxylic acid **167** (as explained in **Section 2.1.13**), we thought of separating alcohol **269** after the reduction step to reduce the amount of impurities in the carboxylic acid generated from the three-step reaction protocol.

A mixture of esters **230** and **254** was dissolved in dry tetrahydrofuran and a routine reduction using lithium aluminium hydride followed by column chromatography on flash silica gel yielded alcohol **269** in 80% yield. The IR spectrum of the pentamethoxynaphthalene **269** showed a broad peak at 3481 cm^{-1} corresponding to the alcohol functional group and the

HRMS spectrum showed a molecular ion peak at 349.1650 amu which was in good agreement with the expected mass of 349.1646 amu for $C_{19}H_{25}O_6$.

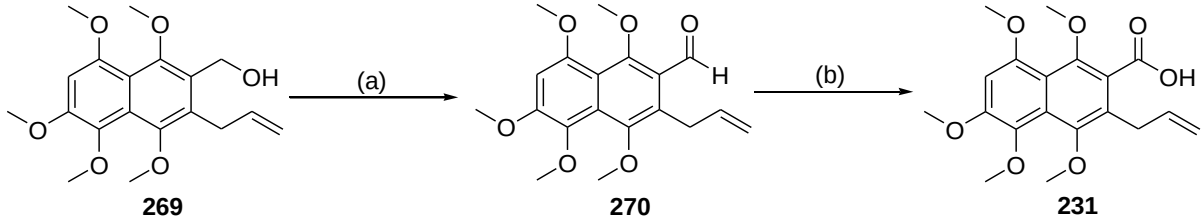


254 **230** **269**

Scheme 2.86: *Reagents and conditions:* $LiAlH_4$, THF, rt, N_2 (g), 4 hrs, 80%.

The ^1H NMR spectrum revealed loss of both the allyl and ethyl groups of the two esters **254** and **230**, respectively. A singlet signal at 4.81 ppm (2H, s) was assigned to the benzylic protons whereas the broad singlet signal at 2.46 ppm (1H, br s) corresponded to the alcohol proton. The signals due to the remaining allyl group (*C*-allyl group) were accounted for and showed that there was no isomerization as was expected. The ^{13}C NMR spectrum revealed a signal at 57.4 ppm corresponding to the benzylic carbon atom.

At this point the alcohol **269** was dissolved in dichloromethane and charged in a round bottom flask to which silica and pyridinium chlorochromate were added. The reaction mixture was stirred for 4 hours at room temperature (monitored by TLC), after which the presumed crude aldehyde **270** was dissolved in 2-methyl-2-butene, water and *tert*-butanol in a clean round bottom flask. Sodium chlorite and sodium hydrogen phosphate were added to the reaction mixture which was then stirred vigorously stirred for 6 hours (monitored by TLC). The crude reaction mixture was purified on normal silica gel column chromatography and recrystallized from hot ethyl acetate/hexane solution to obtain the acid **231** in 66% yield (**Scheme 2.87**). The IR spectrum of the acid showed peaks at 3680 cm^{-1} and 1692 cm^{-1} corresponding to the hydroxyl and carbonyl functional groups of the carboxylic acid. Furthermore, the HRMS data showed a molecular ion peak at 363.1440 amu which was consistent with a predicted mass of 363.1438 amu for the formula $C_{19}H_{23}O_7$.



Scheme 2.87: *Reagents and conditions:* (a) PCC, silica, 4 hrs, N_2 (g) (b) NaH_2PO_4, $NaClO_2$, H_2O, *t*-BuOH, 2-methyl-2-butene, 6 hrs, 66% (over 2 steps).

The ^{1}H NMR spectrum of carboxylic acid **231** revealed loss of a signal due to the benzylic protons and a new singlet signal at 10.80 ppm was typical of a carboxylic acid proton. Similarly, the ^{13}C NMR spectrum showed loss of a signal corresponding to the benzylic carbon atoms and there was a new signal at 172.4 ppm corresponding to a carbonyl carbon atom of the carboxylic acid. The allyl proton signals showed multiplicity which proved that naphthoic acid **231** contained an unisomerized allyl substituent.

The crystal structure of carboxylic acid **231** confirmed the formation of the unisomerized double bond of the allyl substituent and the ORTEP diagram is depicted in **Figure 2.17**.

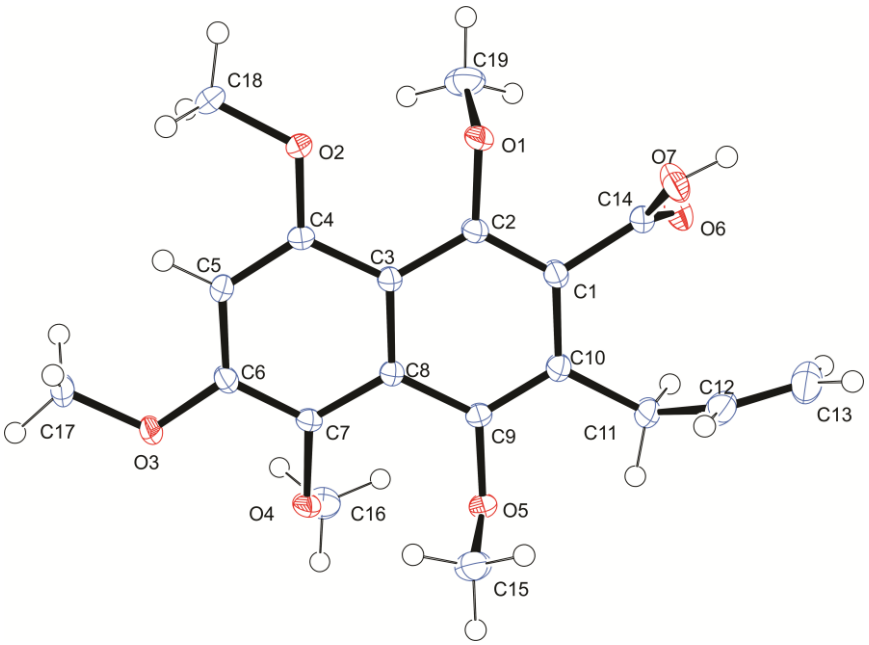


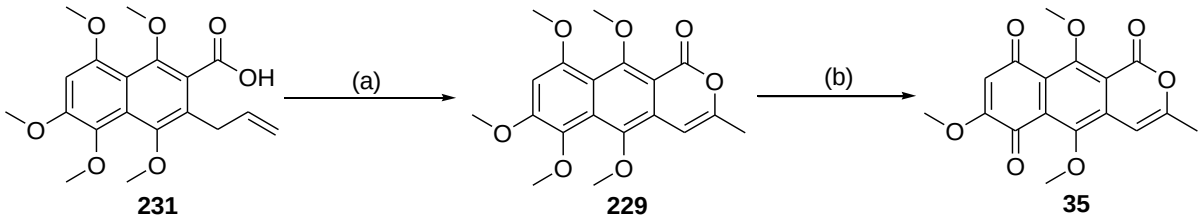
Figure 2.17: The ORTEP diagram of acid **231**. Thermal ellipsoids are shown at the 50% probability level.

At this point we were satisfied with the results we obtained for carboxylic acid synthesis and we moved on to subject the acid **231** to Wacker oxidation reaction.

2.3.13 Synthesis of 5,7,10-trimethoxy-3-methyl-1*H*-benzo[*g*]isochromene-1,6,9-trione 35

A routine Wacker oxidation reaction furnished the desired lactone **229** in 72% yield as the only product and the spectroscopic data matched well with those of lactone **229** we obtained when we subjected allyl ester **254** to Wacker oxidation reaction conditions.

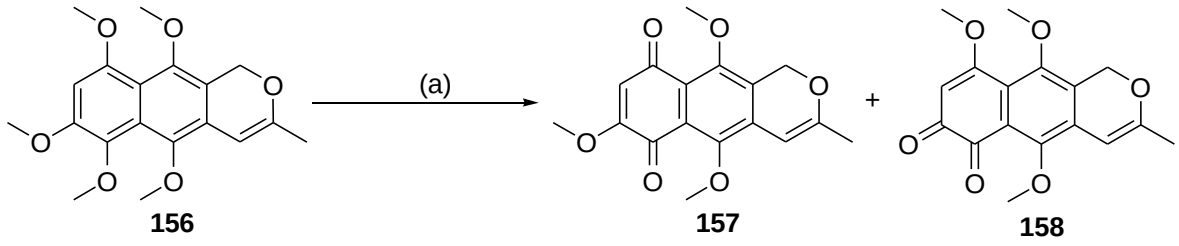
We were very happy with these results and we proceeded to effect oxidative demethylation using silver (II) oxide and nitric acid which furnished the corresponding *para*-quinone **35** in 75% yield (**Scheme 2.88**). The IR spectrum of the quinone showed peaks at 1788 cm^{-1}, 1762 cm^{-1} and 1712 cm^{-1} corresponding to the carbonyl functional groups and the peaks at 1693 cm^{-1} and 1606 cm^{-1} were ascribed to the alkene functional groups. In addition, the HRMS spectrum showed a molecular ion peak at 331.0814 amu which was in good agreement with the expected mass of 331.0812 amu for $C_{17}H_{15}O_7$.



231 **229** **35**

Scheme 2.88: *Reagents and conditions:* (a) cat. $PdCl_2$, $CuCl_2 \cdot 2H_2O$, DMF/H_2O, O_2 (g), rt, 24 hr, 72% (b) AgO, *55%* aq. HNO_3, 1,4-dioxane, rt, 75%.

The ^1H NMR spectrum revealed loss of two signals which were available in the precursor isocoumarin **229** corresponding to oxidation of two methoxy groups. The ^{13}C NMR spectrum showed two signals at 182.4 ppm and 178.9 ppm corresponding to the carbonyl carbon atoms of the pyranonaphthoquinone **35**. The spectrum further revealed loss of two signals corresponding to the methoxy carbon atoms attached to the aromatic ring. These results were in stark contrast to the results obtained by Pillay and co-workers[124] who reported obtaining both the *para*- and *ortho*-pyranonaphthoquinones (**157** and **158**) using a similar oxidative demethylation protocol of pyran **156** (**Scheme 2.89**).

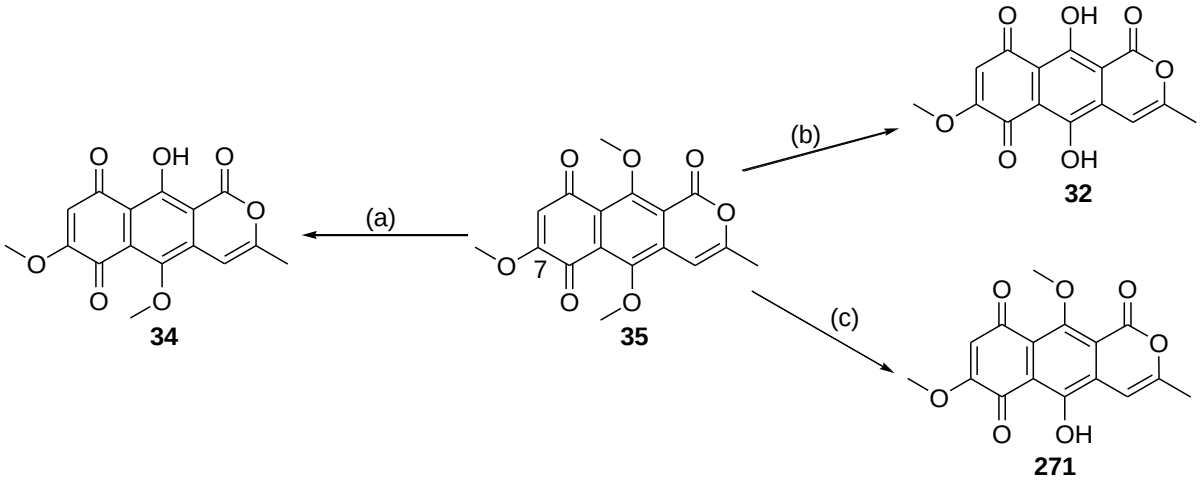


156 **157** **158**

Scheme 2.89: *Reagents and conditions:* AgO, *55%* aq. HNO_3, 1,4-dioxane, rt.

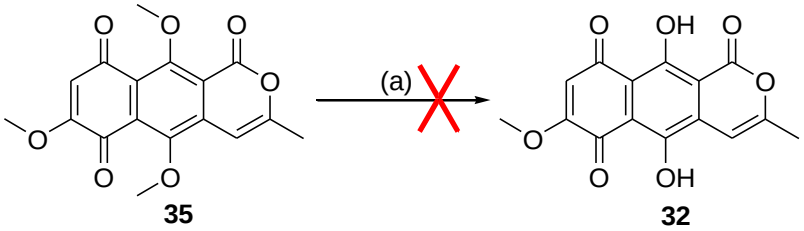
2.3.14 Synthesis of 10-hydroxy-5,7-dimethoxy-3-methyl-1*H*-benzo[*g*]isochromene-1,6,9-trione (5-methoxy-3,4-dehydroxanthomegnin) 34

At this point the stage was set to carry out selective demethylation reactions that could have potentially delivered two natural products **32** and **34**. According to the literature[150] 2 molar equivalents of boron trichloride are needed to remove 1 methoxy group next to the carbonyl group. Some authors believe that less than 1 molar equivalent per methoxy group is required when the compound does not have the carbonyl functional group.[151] In our case, we thought that if 2 molar equivalents were used then we could obtain a mixture of products namely 5-methoxy-3,4-dehydroxanthomegnin **34** (a natural product), 10-methoxy-3,4-dehydroxanthomegnin **271** (not a known natural product), anhydrofusarubin lactone **32** (a natural product) and the starting material pyranonaphthoquinone **35**. In such an event, we believed that hydrogen bonding would prove an important key to separation of these compounds. On the other hand if 4 molar equivalents were used (**Scheme 2.90**) then the understanding was that we could potentially obtain anhydrofusarubin lactone **32** as the only product. The methoxy group at position 7 can only be removed under very harsh conditions and to the best of our knowledge there is no report whereby this methoxy group was selectively removed using boron trichloride.



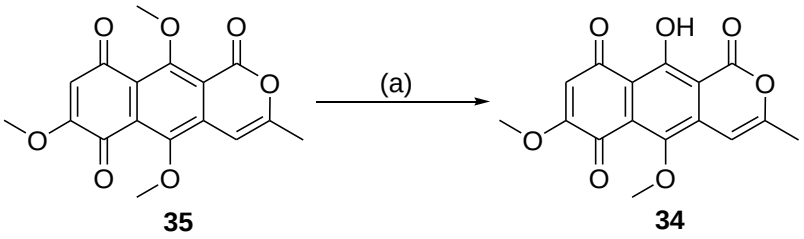
Scheme 2.90: Highlighting the 3 possible routes for demethylation of quinone intermediate **35**.

The pyranonaphthoquinone **35** was dissolved in dry dichloromethane and cooled to -78 ^{o}C after which 4 molar equivalents of boron trichloride was slowly added *via* a syringe. The reaction mixture was then slowly warmed to room temperature and stirred at this temperature for 4 hours. The reaction was quenched using cold water to obtain a crude product as a dark violet amorphous solid. Several different attempts to purify this compound by silica gel chromatography (normal and deactivated silica) did not yield any result. The natural product itself was purified using both Sephadex LH-20 and semi-preparative TLC chromatography[103] but in our hands we thought that the trace amount of Lewis acid used for demethylation was responsible for initiating decomposition when in contact with silica gel. Basic alumina was also used for chromatography but the components of the reaction did not move on the alumina charged column. When pure methanol was used, no separation took place and the ^{1}H NMR spectrum did not show signals corresponding to lactone **32**. The expected reaction when 4 molar equivalents of Lewis acid were used is shown in reaction **Scheme 2.91**. However, in our hands we were unable to isolate any characterizable quinone under the reaction conditions attempted presumably due to decomposition.



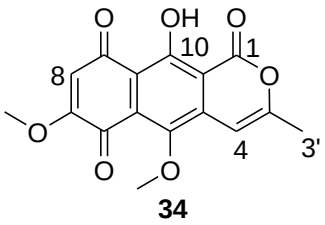
Scheme 2.91: *Reagents and conditions*: (a) 4 mol. equiv. BCl_3, CH_2Cl_2, N_2 (g), -78 °C → rt.

When compound **35** was subjected to the same demethylation protocol using 2 molar equivalents of boron trichloride we obtained 5-methoxy-3,4-dehydroxanthomegnin **34** in 20% yield as per the isolated mass of the compound (**Scheme 2.92**). The low percentage yield was attributed to the decomposition on silica gel. In the case of anhydrofusarubin lactone **32**, the decomposition was visibly immediately the crude product came into contact with the silica gel and continued to change to black as it was eluted. This was different in the case of 5-methoxy-3,4-dehydroxanthomegnin **34**, whereby decomposition was relatively slower as monitored in the same manner.



Scheme 2.92: *Reagents and conditions:* 2 mol. equiv. BCl_3, CH_2Cl_2, N_2 (g), -78 °C → rt, 20%.

The ^{1}H NMR spectrum of pyranonaphthoquinone **34** showed a signal at 14.57 ppm (1H, s) corresponding to the OH group attached to *C*-10. The signals at 6.67 ppm (1H, s) and 6.16 ppm (1H, s) were consistent with the H-8 and H-4 protons, respectively. The signals at 3.94 ppm (3H, s) and 3.88 ppm (3H, s) were consistent with methoxy groups attached to the sp^2 hybridised carbon atoms. The loss of one signal in this region was consistent with loss of one set of methoxy protons. Lastly, the singlet signal at 2.37 ppm (3H, s) was consistent with the methyl group protons and was assigned to the methyl protons attached to *C*-3'. The ^{13}C NMR spectrum showed the trade



mark signals at 189.3 ppm and 177.9 ppm consistent with two carbonyl carbon signals of the *para*-quinone. The carbon signal at 161.4 ppm was consistent with the carbonyl carbon atom of the lactone group (C-1). The loss of the carbon signal corresponding to one methoxy group when compared to the starting precursor was also visible in the region between 63.0-55.0 ppm. The remaining two methoxy groups were accounted for by the signals at 62.3 ppm and 56.9 ppm. The signal at 20.4 ppm was consistent with the signal of the methyl group carbon atom C-3'. The spectroscopic data was consistent with the reported data for this compound.[108] We did not carry out HRMS, IR and melting point analysis but nonetheless, this represents the first ever reported total synthesis of 5-methoxy-3,4-dehydroxanthomegnin **34**.

In conclusion, we successfully synthesized dehydroherbarin lactone **159** and 5-methoxy-3,4-dehydroxanthomegnin **34** from the commercially available aldehydes, 2,4-dimethoxybenzaldehyde **130** and 2,4,5-trimethoxybenzaldehyde **232**. The key steps in the syntheses were the PIFA mediated methoxylation which furnished naphthols with the required methoxy substituents and the Wacker oxidation reaction which delivered the required lactones in good yields. The major problem we encountered when carrying out the syntheses of pyranonaphthoquinones **159** and **34** was the decomposition of these quinones by silica gel column chromatography.

Chapter 3: Introduction to ferrocenyl hybrid molecules of biological importance

3.0 Synopsis

In this chapter we will briefly discuss malaria and highlight some of the natural and synthetic quinones that have shown activity against the malaria parasite. We will then discuss ferrocene coupled organic molecules of biological importance, giving methodologies for their synthesis and applications. Here we will highlight the diversity in biological applications of these compounds. The two most important ferrocene coupled organic compounds, ferrocifen and ferroquine, will be discussed in their own sections. This discussion will then lead us to link ferrocene coupled 3,4-dihydroisochromenes and their quinone analogues as potential important biological molecules.

3.1 History of malaria and mode of transmission

The term malaria originated from the Italian word *mala aria*, meaning "bad air" because initially malaria was thought to be caused by swamps and marshes, and was commonly referred to as "marsh fever".[152] The scientific consensus that micro-organisms are the causative agents of disease, together with the development of Louis Pasteur and Robert Koch's germ theory, encouraged the search for answers regarding the causative agents of malaria which at the time was believed to be transmitted either by air or water.[153] The causative agent of malaria was discovered in 1880 by Charles Louis Alphonse Laveran, when he compared infected blood from patients from Algeria with the blood of patients in the Roman Campagna (an area surrounding Rome) and noticed the same pigment within the parasites in both blood samples.[154] After this investigation, Laveran deduced that malaria was caused by a parasite and later, the Italian physician Giovanni Battista Grassi confirmed that the mosquito was the vector in transmitting the disease to humans.[153] Occasionally, transmission can occur by blood transfusion, organ transplantation, needle-sharing or congenitally from mother to foetus.[155]

Malaria is broadly distributed in tropical and sub-tropical countries worldwide where it causes almost 3 million deaths every year, mainly among children and pregnant women in Africa and South East Asia.[156] It is caused by single cell protozoan parasites of the genus *Plasmodium* of which *P. falciparum* is the most dangerous and accounts for 90% of all deaths from malaria. The most severe malaria episodes including cerebral malaria are due to *P. falciparum*. The 4 remaining malaria species that infect humans and cause the disease are *P. vivax, P. malariae, P. ovale,* and *P. knowlesi* of which *P. vivax* is a predominant threat to public health in Asia.[157] Malaria is a disease that can be treated in just 48 hours but if not treated, it quickly becomes life-threatening by increasing the inflammatory environment and disrupting the oxygen supply to vital organs, such as the brain.[158] The population at risk from this disease has increased because of the difficulties in eradicating the mosquito vector in the endemic regions and the emergence and spread of parasite resistance to almost all the commonly used antimalarial drugs.[159]

P. falciparum is spread by infected female mosquitoes of the *Anopheles* species which carries the parasite in its saliva. In humans, the sporozoites are injected by mosquitoes, when feeding on a blood meal, into the skin where they can remain for up to 6 hours.[160] A simplified life cycle of malaria parasites in humans is shown in **Figure 3.0**. For the sake of this discussion, we will concentrate on *P. falciparum* with no specific reference to different stages that are involved in the life cycle of the parasite from the vector to humans and back to the vector as depicted in **Figure 3.0**.

After the sporozoites are injected into the skin some of them leave the injection site and enter the lymphatic system and drain to the regional lymph nodes whereas the rest trickle into the bloodstream and move to the liver, resulting in multiple potential sites for sporozoite-host interaction.[161] This is in contrast to the traditional view that a feeding mosquito inoculates sporozoites from its salivary glands directly into the peripheral blood circulation of the host which ultimately results in the invasion of hepatocytes.[162] Despite relatively high numbers of sporozoites that leave the skin and travel to the liver, the capacity of each of these sporozoites to result in asexual erythrocytic-stage infections is low. The studies have shown that in humans, it takes the bites of five *P. falciparum*-infected mosquitoes to ensure 100%

infection.[163] In related studies, it was shown that it took the bites of six to eight infected mosquitoes to achieve 100% infection of inbred mice by intravenous administration of 20 sporozoites of *P. yoelii*.[164] The studies indicated that the majority of sporozoites inoculated by mosquitoes do not lead to productive infections.

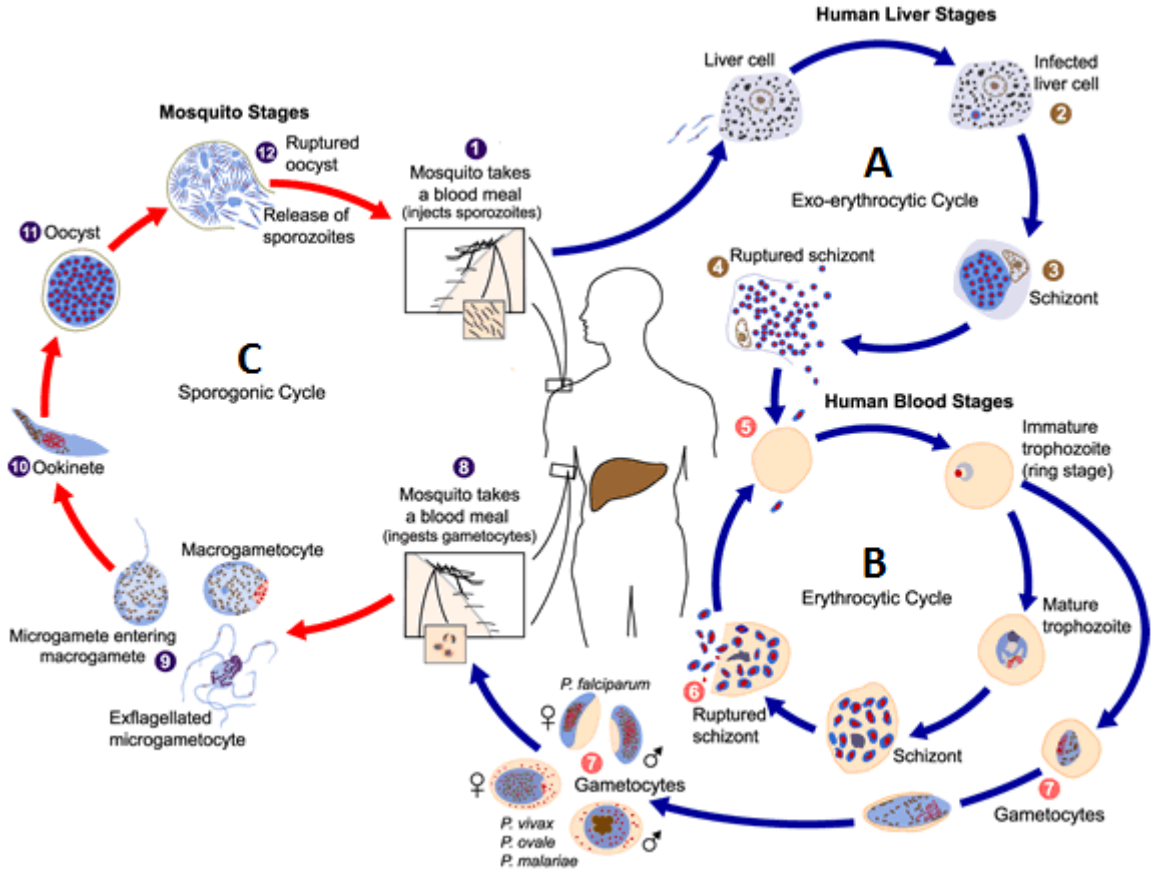


Figure 3.0: Depicting a simplified life cycle of malaria parasite in humans and mosquitoes.[165]

Once the hepatocytes are invaded by the parasites, the uninucleate sporozoites undergo a cycle of asexual amplification called schizogony that lasts between 2 to 10 days, depending on the species, with each exoerythrocytic schizont containing as many as 30,000 uninucleate merozoites.[162] The rupturing of mature exoerythrocytic schizonts releases merozoites into the bloodstream where they quickly invade red blood cells commencing the erythrocytic stage of the disease. The presence of the parasite in the bloodstream results in a sudden immune response causing fever which is one of the major symptoms of malaria.[166]

The invading merozoite carries with it to the interior of the red blood cell an enveloping membrane derived from the host cell and within an associated parasitophorous vacuole the parasite commences further asexual development. After maturation from the ring stage (immature trophozoite) to a trophozoite and then to a schizont, the parasite undergoes three to six mitotic divisions which yields between 6 to 36 merozoites within each erythrocytic schizont (ranges depend on the species). The schizonts rupture after 48 hours thereby releasing more merozoites into the bloodstream.[162,167] Some of these invade uninfected red blood cells and repeat the cycle of blood schizongony. In addition, when infection of new blood cells occurs, the parasites may also grow into immature gametocytes, which can be taken up in the blood meal of another feeding mosquito. The male gametocyte undergoes rapid nuclear division and produces a flagellated microgamete, which fuses with and fertilizes the female gametocyte forming a zygote. The zygote develops into an ookinete, which then sticks to the gut wall of the mosquito and moves to the outermost layer of the stomach to form an oocyst. The breakdown of the oocyst releases sporozoites, which migrate to the salivary glands of the mosquito to restart the parasite's life cycle.[162,167]

The reactions taking place in the acidic food vacuole and the by-products that are produced are of biological interest in the fight against the malaria parasite. This is the case because when the parasite digests methemoglobin (metHb) in the acidic food vacuole as a source of essential nutrients it produces reactive oxygen species and free heme (ferriprotoporphyrin IX(FeIII), FPIX) as toxic by-products. The heme moieties are neutralized by polymerization within or at the surface of lipids to form hemozoin as the major detoxification product; whereas the free radical species are detoxified by a vulnerable series of antioxidant mechanisms.[168] Tampering with the detoxification process and the fate of free radical species has been shown to lead to parasite death.

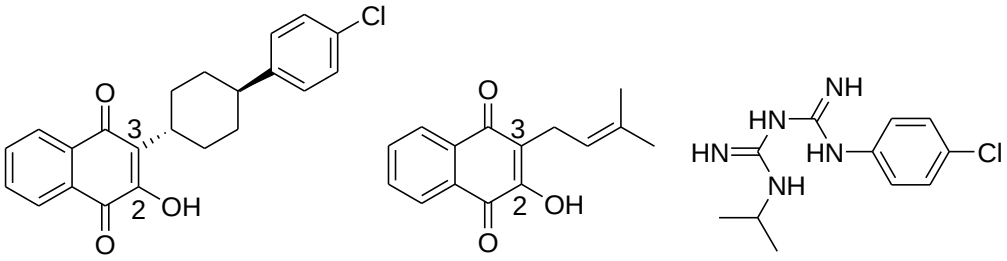
3.2 Quinones with antimalarial activities

Quinones, in particular 1,4-naphthoquinones, have long been known to display antimalarial activity in addition to a wide variety of other bioactivities.[169] Over the years, researchers have reported testing quinone molecules against malaria parasites to determine their efficacy. In this section we will highlight some of the quinones that have been tested against various

strains of *P. falciparum* and have shown good activity. Well-known anthraquinone antibiotics such as tetracycline and doxycycline have been used for antimalarial prophylaxis[170] for decades but they are not included in this review.

3.2.0 Antimalarial activity of Lawsone quinone analogues 272, 273, 274 and 275

The pioneering work by the separate research groups of Wendel[171] and Fieser[169b] on hydroxynaphthoquinones formed the basis for the development of the antimalarial drug atovaquone **272** from the lead compound lapachol **273**. Both atovaquone and lapachol have the same naphthoquinone moiety with a hydroxyl group at position 2 (**Figure 3.1**). The difference between the two compounds is that lapachol has a prenyl group at position 3; whereas atovaquone has a chlorinated benzene moiety linked *via* a cyclohexane ring to the naphthoquinone moiety at this position. The synthesis and antimalarial activities of atovaquone were first reported by Williams and Clark in 1998 and it remains the only clinical antimalarial agent in the class of naphthoquinones that is in use.[172]



272 **273** **274**

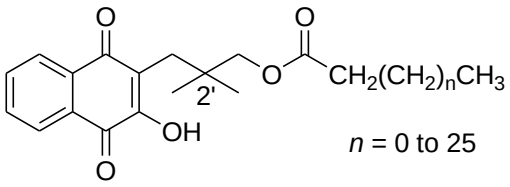
Figure 3.1: The molecular structures of atovaquone **272**, lapachol **273** and proguanil **274**.

Atovaquone **272** is a highly lipophilic drug and it acts selectively in sensitive parasites by affecting their mitochondrial electron transport and parallel processes, such as ATP and dihydro-orotate dehydrogenase, which both catalyse the synthesis of uridine monophosphate.[173] The overall effect of atovaquone is the inhibition of parasite respiration by binding to the cytochrome bc_1 complex. Currently, atovaquone is administered for prophylaxis and treatment of uncomplicated malaria in combination with proguanil **274** (**Figure 3.1**) as a synergistic partner under the trade name of Malarone.[174] This combination is effective in treating malaria with no evidence of the emergence of resistance prevalent in

atovaquone when used as a single agent.[175] Proguanil by itself has no effect on electron transport or mitochondrial membrane potential but it significantly enhances the ability of atovaquone **272** to collapse the electron transport or mitochondrial membrane potential when used in combination. This enhancement is observed at pharmacologically achievable doses and proguanil acts as a biguanide rather than as its active metabolite, cycloguanil (a parasite dihydrofolate reductase inhibitor) to enhance the atovaquone effect.[175]

Atovaquone **272** is also used as a prescription drug for the treatment of *Pneumocystis carinii* pneumonia (PCP), *Pneumocystis jirovecii* pneumonia (PJP) and toxoplasmosis which is caused by *Toxoplasma gondii*.[176]

More recently, Kongkathip and co-workers[177] described the synthesis of 26 novel naphthoquinone aliphatic esters (represented by the general compound **275** shown in **Figure 3.2**) of which 24 esters showed significant antimalarial activity against the 3D7 strain of *P. falciparum* with IC_{50} values in the range of 0.03-16.63 μM.



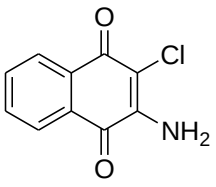
275

Figure 3.2: The general molecular structure of naphthoquinone aliphatic esters studied by Kongkathip and co-workers.

It was found in this study that the length of the aliphatic chain and the presence of *C*-2' substituents on the propyl chain had an impact on the activity of the compounds and most naphthoquinones showed no toxicity against normal Vero cell lines. It was also notable that the naphthoquinone aliphatic ester with *n* equal to 7 showed an IC_{50} value of 0.13 μM which was similar to an IC_{50} value showed by the compound with *n* equal to 17. The best activity was shown by compounds with *n* equal to 13 and 15 with IC_{50} values of 0.032 and 0.030 μM, respectively.

3.2.1 Antimalarial activity of Lawsone quinone amine analogues 276, 277, 278 and 279

Kapadia and co-workers[178] reported investigating eighteen compounds including several synthetic and natural naphthoquinones as potential antimalarial agents against *Plasmodium falciparum*. In this study, they found that 2-amino-3-chloro-1,4-naphthoquinone **276** (**Figure 3.3**) was the most potent antimalarial compound with an IC_{50} value of 0.18 μM against the W2 clone of *P. falciparum*. This value was slightly better than the activity shown by the reference compound, chloroquine, which showed an IC_{50} value of 0.23 μM under the same assay conditions. In addition, the same authors reported that 2-amino-3-chloro-1,4-naphthoquinone **276** was equally active against the D6 clone but no IC_{50} value was given.



276

Figure 3.3: The molecular structure of 2-amino-3-chloro-1,4-naphthoquinone **276**.

Carneiro and co-workers[179] modified the most active compound reported by Kapadia and co-workers (compound **276**) and reported the synthesis and *in vitro* evaluation for inhibitory activity of eighteen quinones and structurally-related oxiranes against the chloroquine-sensitive 3D7 clone of the human malaria parasite, *P. falciparum*. Of the tested compounds, it was found that 2-amino-1,4-naphthoquinone **277**, 2-(phenylamino)-1,4-naphthoquinone **278** and 2-(allyloxy)-1,4-naphthoquinone **279** (**Figure 3.4**) exhibited antiplasmodial activity with median inhibitory concentrations of 5.14, 6.30 and 5.18 μM, respectively. These compounds were generally less active than those reported by Kapadia and co-workers.

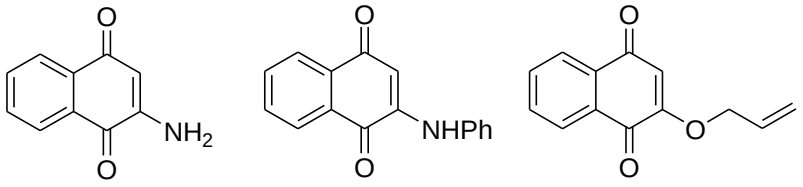


Figure 3.4: The molecular structures of 2-amino-1,4-naphthoquinone **277**, 2-(phenylamino)-1,4-naphthoquinone **278** and 2-(allyloxy)-1,4-naphthoquinone **279**.

3.2.2 Antimalarial activity of isopinnatal 280 and sterekunthal A 281

The root bark of *Bignoniaceae* trees is a source of a number of natural products and its extracts have been used extensively in African tribal medicine.[180] The activity of their components has been evaluated in a number of contexts.[187] For example, Houghton and co-workers reported that isopinnatal **280** (**Figure 3.5**) showed good activity against chloroquine-resistant and chloroquine-sensitive strains of *P. falciparum* with IC_{50} values of 0.76 and 1.55 µM, respectively.[182]

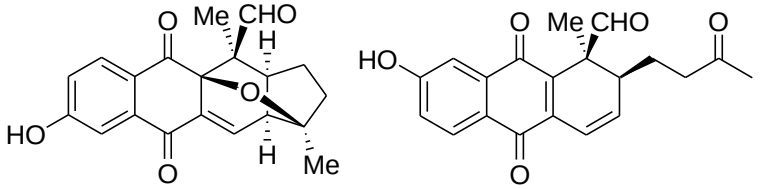
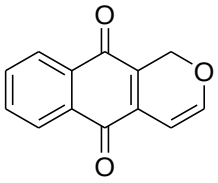


Figure 3.5: The molecular structures of isopinnatal **280** and sterekunthal A **281**.

In a separate study by Onegi and co-workers, the antiplasmodial activity of natural products isolated from *S. kunthianum* were assessed for their biological activity and it was found that the quinone, sterekunthal A **281** (**Figure 3.5**) was the most potent against the poW and Dd2 strains of *P. falciparum* with IC_{50} values of 3.8 and 1.2 µM, respectively.[183]

3.2.3 Antimalarial activity of pantalogin 282

Pentalongin **282** (**Figure 3.6**) is an unsubstituted, tricyclic 3,4-dehydro-pyranonaphthoquinone and was isolated from the roots of the Central East-African woody herb *Pentas longiflora* Oliv.[184]



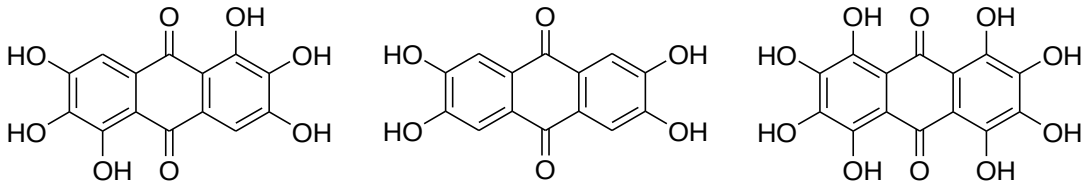
282

Figure 3.6: The molecular structure of pentalogin **282**.

The roots of this herb of which the pyranonaphthoquinone pentalogin **282** is the major compound are mixed with milk and used as a cure for malaria in Rwanda and Kenya, but causes acute diarrhoea in some cases.[185] The powder from the roots of *P. longiflora* is used by the traditional healers of the dispensary of traditional medicine of Curphametra (Butare, Rwanda) to treat the skin disease pityriasis versicolor. The roots of this herb are also eaten raw and used in Kenyan traditional medicine as a cure against tapeworm, itchy rash and acne.[186]

3.2.4 Antimalarial activity of rufigallol 283

One of the most famous polyhydroxyanthraquinones because of its historic synthesis is rufigallol **283** which is considered as one of the first organic compounds to be synthesized in the history of organic chemistry by Robiquet in 1836. Grimshaw and Haworth reported synthesizing this compound by dehydration of gallic acid.[187]



283 **284** **285**

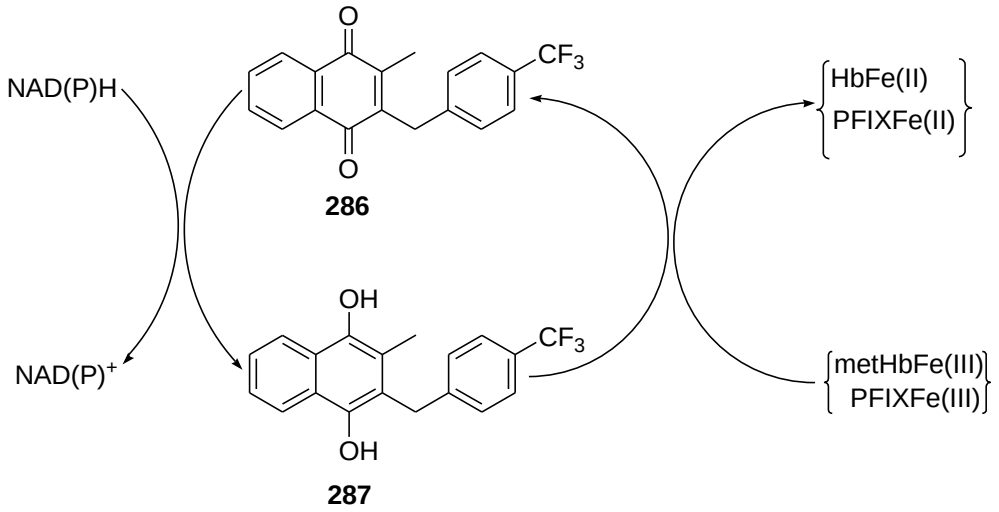
Figure 3.7: The molecular structures of rufigallol **283**, tetrahydroxyrufigallol **284** and octahydroxyrufigallol **285**.

Winter and co-workers reported screening a number of anthraquinones for inhibitory activity against the malaria parasites. It was found during this study that rufigallol **283** was the most potent of the anthraquinones that were tested producing *in vitro* antimalarial activity

equivalent to the activity of chloroquine that was used as a standard agent. The concentration of rufigallol **283** required to inhibit the growth of *P. falciparum* by 50% was measured at 35 nM whereas that of chloroquine standard was measured at 20 nM. The compound **283** was equally active against the W2 strain, which is the multi-drug resistant form of *P. falciparum*, but no IC_{50} value was given. The tetrahydroxyrufigallol **284** and octahydroxyrufigallol **285** (**Figure 3.7**) derivatives of rufigallol were moderately effective, exhibiting IC_{50} values of 0.300 µM and 0.800 µM, respectively.[188]

3.3 Proposed mode of antimalarial action of quinones

The antimalarial mode of action of quinones was proposed by Lanfranchi and co-workers using the antimalarial lead compound, 3-benzyl-menadione (benzylNQ) **286**, and is thought to involve a cascade of redox reactions in the parasite as depicted in **Scheme 3.0**.[158a]



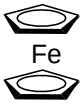
Scheme 3.0: Proposed mode of antimalarial action for 3-benzyl-menadione **286**.

The postulated bioactivation is thought to generate redox-active metabolites. For example, quinone **286** in oxidized form, is reduced by NADPH in glutathione reductase-catalyzed reactions within the cytosol of infected red blood cells. The hydroquinone **287**, which is the reduced of quinone **286** is capable of converting methemoglobinFe(III), the major nutrient of the parasite, into a very slowly digestible hemoglobinFe(II).[189] Consequently, the antimalarial lead compound, benzylNQ **286**, is suggested to perturb nutrient acquisition and the major

redox homeostasis of the targeted infected red blood cells,[158] resulting in arrest and death of the malaria parasite at the trophozoite stage (see **Figure 3.0**).

3.4 Ferrocene 288 and ferrocenium salts 290

Over the past decades, organometallic chemistry, which is classified as the chemistry studying chemical compounds containing at least one direct metal-carbon bond, was known mainly for its applications in catalysis rather than for applications in medicine.[190] The discovery of platinum based complexes as anticancer agents changed that perception and led to a steady growth of research into medicinal organometallic chemistry. In this regard, metallocenes occupy the most prominent place in the search for new metal based drugs. A metallocene is a compound typically consisting of two cyclopentadienyl anions (Cp, which is $C_5H_5^-$) bound to a metal center (M) in the oxidation state II, with the resulting general formula $(C_5H_5)_2M$. In general, metallocenes are known to exhibit a wide range of biological activities. Among them, ferrocene **288** (**Figure 3.8**) has attracted special attention because of its hydrophobicity, lipophilicity and non-toxicity. Ferrocene is also very stable towards moisture and air.[191] It is the first metallocene to be discovered and its particular structure was simultaneously elucidated by Wilkinson and Fischer in the early 1950s.[192] Ferrocene is comprised of a ferrous ion, Fe(II), coordinated to two cyclopentadienyl rings. The exceptional stability of this compound is attributed to the distribution of 18 electrons in the e_{2g} and a_{1g} non-bonding molecular orbitals.[193]

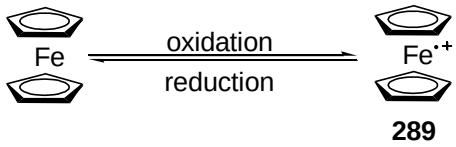


288

Figure 3.8: The molecular structure of ferrocene **288**.

In the bio-organochemistry realms, ferrocene has recently received tremendous interest due to the fact that it is easily derivatized and functionalized to form intermediates which are used in various synthetic reactions of biological importance. It also easily undergoes a reversible oxidation-reduction cyclic reaction by losing one electron to form a stable cationic radical

289 which can in turn accept one electron to regenerate the ferrocene compound as shown in **Scheme 3.1**.

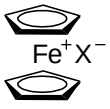


289

Scheme 3.1: The redox cycle of ferrocene.

This property offers ferrocenium cationic radical **289** the ability to act as a free radical scavenger under biological conditions which is particularly important in cancerous cells where there is build-up of superoxide anion radicals as well as hydroxide radicals. These radicals bind to DNA thereby causing damage during DNA replication. The removal of excess reactive oxygen species by the ferrocenium cationic radical reduces the damage done to the DNA and prevents the spread of cancerous cells.

The first studies on the antiproliferative effects of ferrocenyl complexes were carried out by Köpf-Maier and Neuse using ferrocenium salts **290** (**Figure 3.9**). This study showed that some ferrocenium salts possessed antineoplastic activity against Ehrlich ascites tumor (EAT) cell lines. This was significant because EAT cell lines are resistant to classical antitumor agents.[194] Subsequently, Osella and co-workers showed that the generation of reactive oxygen species, more specifically the hydroxyl radicals, by a Fenton-type reaction was responsible for cytotoxicity.[195] Ferrocene itself has no known medicinal application to date.

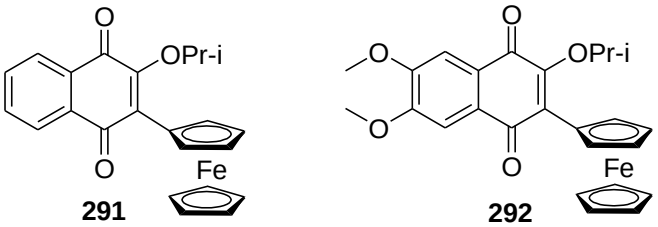


290

Figure 3.9: The general molecular structure of ferrocenium salt **290** where X^- is a counter ion.

Yucel and co-workers[196] demonstrated that the ferrocene moiety coupled to an organic molecule showed the same oxidation-reduction behaviour. These authors reported that the two ferrocenyl naphthoquinones **291** and **292** shown in **Figure 3.10** displayed two reversible

reduction processes involving seminaphthoquinone radical anion (Fc-snq$^{-\cdot}$)/naphthoquinone dianion (Fc-nq^{2-}) species and a one-electron oxidation process based on the ferrocenium/ferrocene (Fc^{+}-nq/Fc-nq) couple in dichloromethane. This observation was very instrumental in proving that the ferrocene moiety coupled to a quinone compound has the ability to initiate redox reactions involving the whole system as long as there is conjugation between the ferrocene and the remainder of the molecule.



291 **292**

Figure 3.10: The molecular structures of ferrocene coupled naphthoquinones **291** and **292** reported by Yucel and co-workers.

In the following section we will review some of the ferrocene based compounds which are currently being used to treat various diseases or are under investigation as potential drugs.

3.5 Organic ferrocene derivatives of biological importance

The term 'ferrocene derivatives' is sometimes used loosely to describe compounds that have either a ferrocene moiety datively coordinated or covalently bonded to an organic compound. However, in this thesis we will limit our discussion to those compounds that have an organic compound covalently bonded to the ferrocene moiety.

In recent years, ferrocene-containing biomolecules have attracted much attention for medicinal applications due to the ability of the ferrocene moiety to enhance the bioactivity, bioavailability, decrease toxicity and improve selectivity of the organic compounds in the resultant hybrid molecules. In some cases, ferrocene offers the new compound the ability to evade or reverse drug resistances prevalent in the parent molecule.[197]

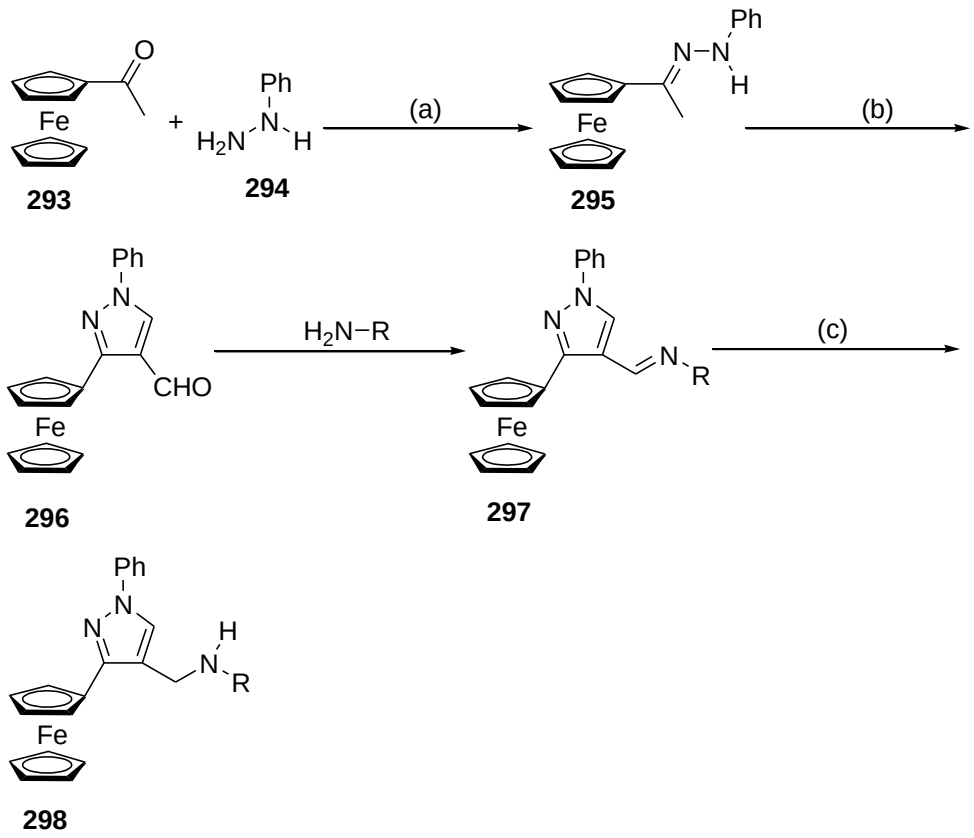
The two most important examples of ferrocene derivatives are ferrocifen and ferroquine which are used in cancer and malarial chemotherapy, respectively. These two biologically important compounds will be discussed separately in **Sections 3.6** and **3.7**, respectively. In

this section however, we will highlight some of the important examples of ferrocene derivatives that have shown potential or are already in use to treat a variety of diseases.

3.5.0 Synthesis and biological application of ferrocenyl amines 298

Damljanović and co-workers[198] reported screening ferrocenyl amines, represented by compound **298**, and the ferrocenyl imine intermediates, represented by compound **297**, for *in vitro* antimicrobial activity. The tests were carried out against eleven bacteria and three fungal/yeast strains, using disc diffusion and broth microdilution susceptibility assays. This study found that the ferrocenyl amines with *R* being *tert*-butyl and cyclohexyl substituents were the most active and showed reduction of bacterial and fungal growth comparable to or higher than that exhibited by tetracycline and nistatine which were used as positive controls. In general, ferrocenyl imines showed better activity against fungal strains compared to bacterial and yeast strains.

The synthesis of the compounds was achieved by condensation of 1*H*-3-ferrocenyl-1-phenylpyrazole-4-carboxaldehyde **296** with corresponding amines which afforded imine intermediates (represented by compound **297**, where *R* represents different alkyl groups) and reduction of the intermediates **297** with sodium borohydride delivered corresponding ferrocenyl amines (represented by compound **298**). 1*H*-3-Ferrocenyl-1-phenylpyrazole-4-carboxaldehyde **296** was synthesized by condensation of acetylferrocene **293** with phenylhydrazine **294** which was followed by intramolecular cyclization of the intermediate hydrazone **295** under Vilsmeier–Haack conditions as shown in **Scheme 3.2**.



Scheme 3.2: *Reagents and conditions:* (a) EtOH/reflux (b) 3 equiv. $POCl_3$, DMF, rt (c) $NaBH_4$, MeOH, where *R* stands for alkyl groups.

3.5.1 Synthesis and biological application of ferrocenyl pyrimidines 299 and 301

Amoebiasis is a formidable health problem present all over the world and is caused by *Entamoeba histolytica*.[199] The widespread resistance of *E. histolytica* to almost all chemotherapeutic agents currently in use is the major challenge in the fight against this disease. Parveen and co-workers[200] reported the synthesis of a series of 6-ferrocenyl-4-aryl-2-substituted piperidine and pyrrolidine derivatives which were evaluated for *in vitro* anti-amoebic activity against the HM1:IMSS strain of *E. histolytica* which is the causative pathogen for amoebiasis. All 16 compounds that were synthesized and tested exhibited activity with IC_{50} values in the range of 0.41-1.80 µM. A total of 10 ferrocenyl piperidine and pyrrolidine derivatives were more active than the reference drug metronidazole which showed the IC_{50} value of 1.80 µM, the same value as the remaining 6 ferrocenyl derivatives. It was also notable that all the ferrocenyl compounds were non-toxic to human kidney

epithelial (Graham) cells, unlike the reference drug which showed considerable toxicity. The ferrocenyl compound, 4-(4-chlorophenyl)-6-ferrocenyl-2-piperidin-1-yl-pyrimidine **300**, was the most active with an IC_{50} value of 0.41 µM.

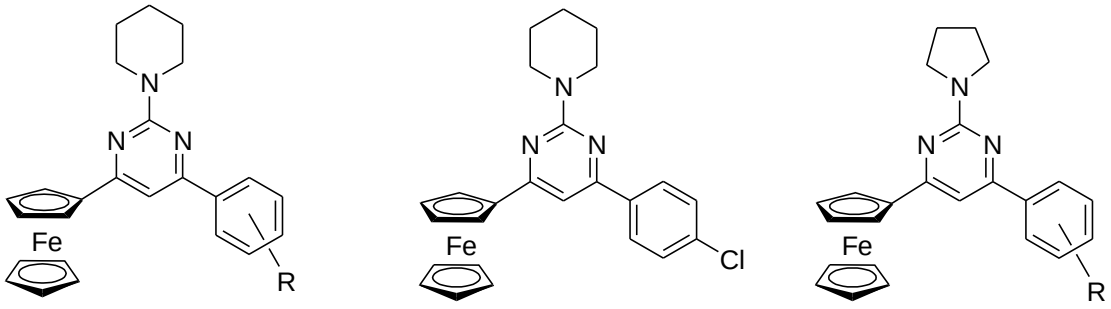
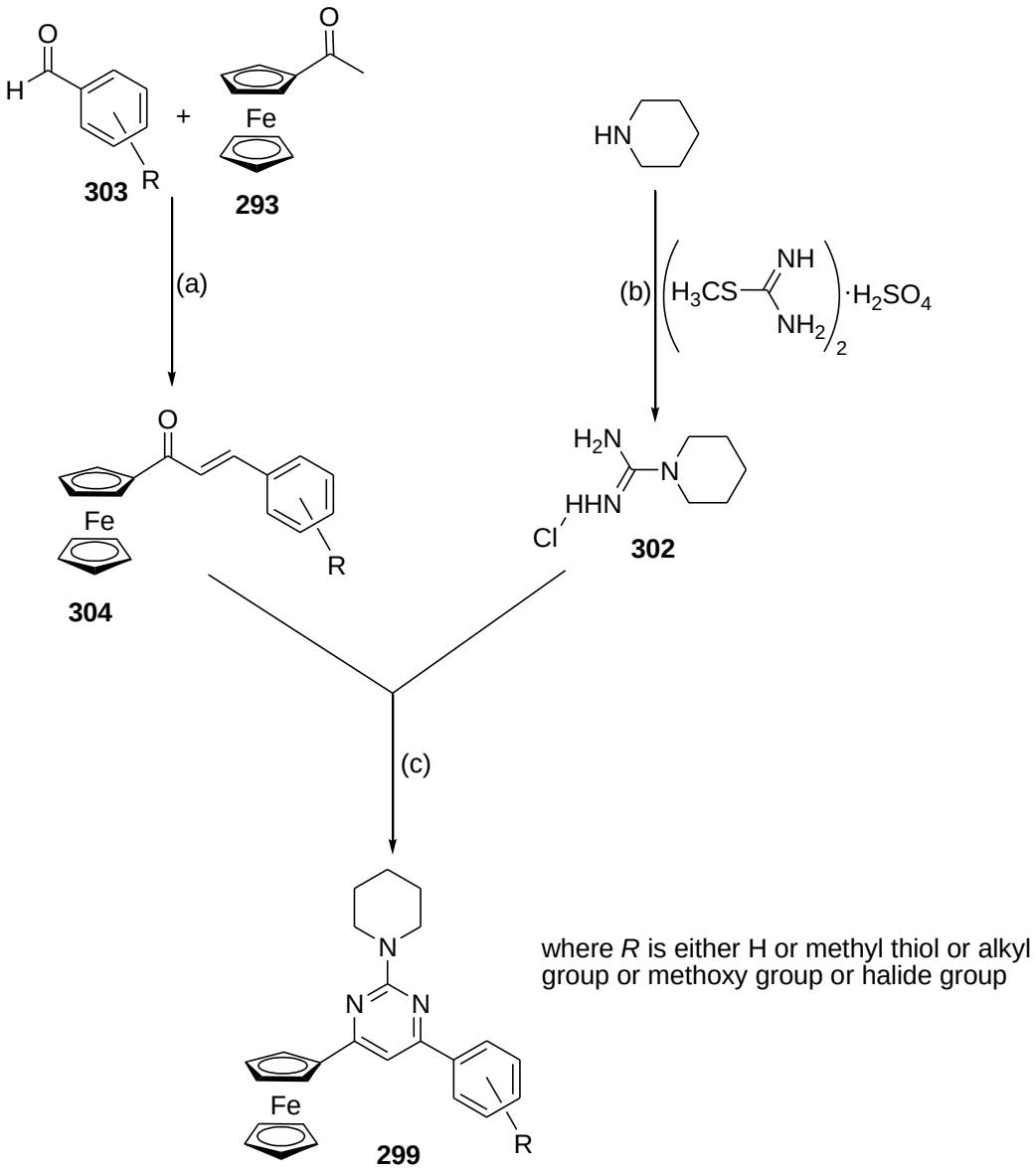


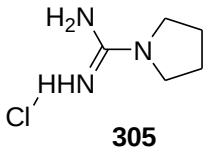
Figure 3.11: The general molecular structures of the ferrocenyl piperidine **299** and ferrocenyl pyrrolidine **301** derivatives and the most active compound **300**.

The first step in the synthesis of 6-ferrocenyl-4-aryl-2-substituted piperidines (represented by the general compound **299**) involved condensation of acetylferrocene **293** with substituted aromatic aldehydes **303** which gave ferrocenyl chalcones **304** with varying substituted phenyl groups. The ferrocenyl chalcones **304** were then reacted with deprotonated piperidine-1-carboxamidine hydrochloride **302** which delivered 6-ferrocenyl-4-aryl-2-piperidin-1-yl-pyrimidines **299** as shown in **Scheme 3.4**.



Scheme 3.4: *Reagents and conditions:* (a) *10%* aq. NaOH, MeOH, 0 ^{o}C → rt, 30 min (b) (i) H_2O, reflux, 15 min (ii) $BaCl_2$, reflux, 15 min (c) sodium isopropoxide, isopropanol, reflux, 8 hrs.

The same protocol was used for the synthesis of 6-ferrocenyl-4-aryl-2-pyrrolidin-1-yl-pyrimidines (represented by the general compound **301**) with pyrrolidine replacing piperidine as a starting material for the synthesis of pyrrolidine-1-carboxamidine hydrochloride intermediate **305** (**Figure 3.12**).

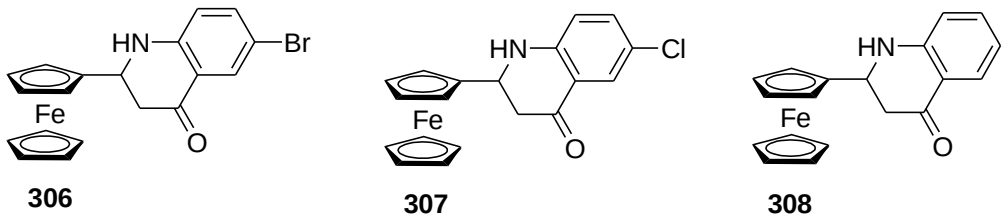


305

Figure 3.12: The molecular structure of pyrrolidine-1-carboxamidine hydrochloride intermediate **305**.

3.5.2 Synthesis and biological application of ferrocenyl dihydroquinolinones 306, 307 and 308

Pejović and co-workers[201] reported the synthesis of ferrocene containing 2,3-dihydroquinolin-4(1*H*)-ones. The electrochemical investigations, performed by cyclic voltammetry, showed that the compounds exhibited two oxidations and one reduction wave corresponding to one reversible redox pair and one irreversible oxidation event. The three compounds **306**, **307** and **308** (**Figure 3.13**) were screened for *in vitro* antimicrobial activity on a group of representative Gram-positive and Gram-negative bacteria and one human pathogen fungal strain. The compounds showed strong and unselective antimicrobial activities against all tested microorganisms with MIC values ranging from 0.01 to 10.0 µg/mL.



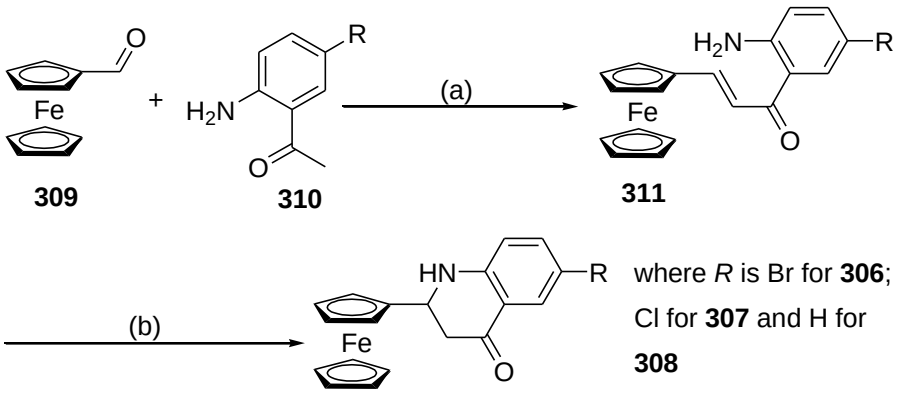
306 **307** **308**

Figure 3.13: The molecular structures of ferrocenyl 5-bromo-2,3-dihydroquinolin-4(1*H*)-one **306**, ferrocenyl 5-chloro-2,3-dihydroquinolin-4(1*H*)-one **307** and ferrocenyl 2,3-dihydroquinolin-4(1*H*)-one **308**.

The ferrocenyl compound **306** bearing the bromo-substituent was the most potent at inhibiting the growth of bacteria with MIC values lower than that shown by tetracycline although its anti-candidal activity was weaker than that of nystatin. Tetracycline and nystatin were used as positive controls for antibacterial and antifungal studies, respectively.

The synthesis of the compounds (**Scheme 3.5**) involved subjecting ferrocenecarboxyaldehyde **309** to a simple mixed aldol condensation with varying *o*-aminoacetophenones (represented by compound **310**) which afforded chalcone intermediates **311**. The chalcone intermediates

were then subjected to an intramolecular *aza* Michael-type addition which delivered the target compounds **306**, **307** and **308**. The *aza* Michael-type addition cyclization reaction was performed by either a solvent-free microwave (MW) irradiation (500 W/5 minutes) of a mixture of chalcones and montmorillonite K-10 or by using an acidic catalyst (a mixture of acetic and orthophosphoric acid).



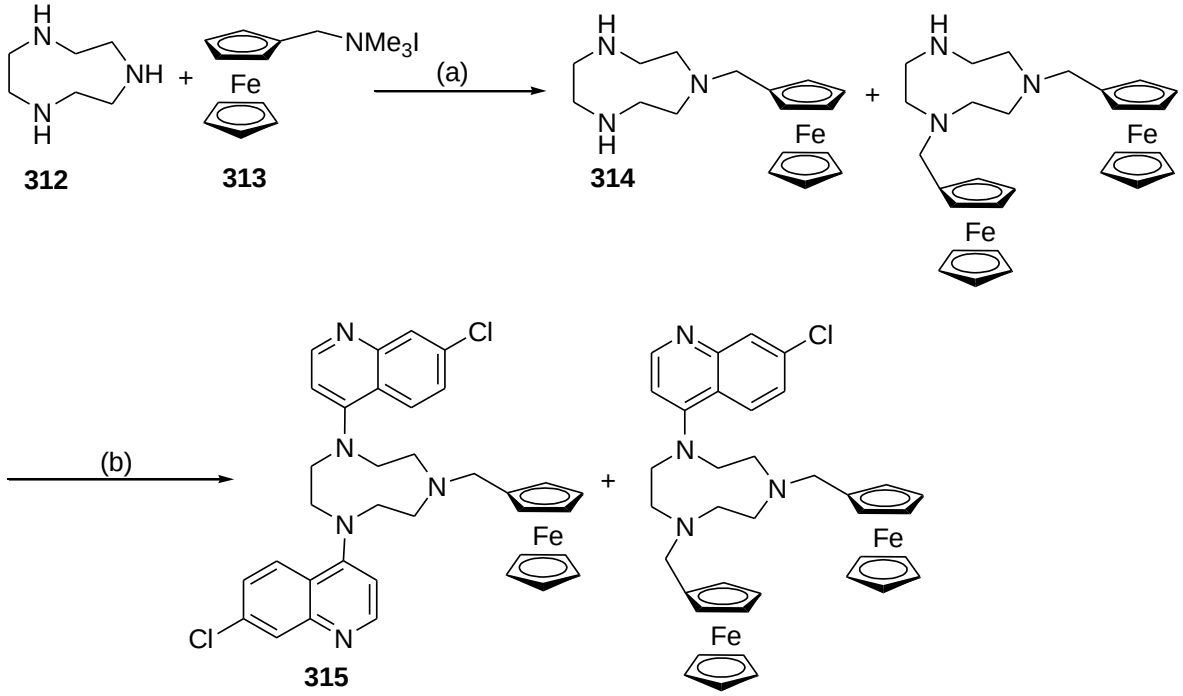
Scheme 3.5: *Reagents and conditions:* (a) NaOH (b) K-10, MW or $AcOH/H_3PO_4$, rt.

3.5.3 Synthesis and biological application of ferrocenyl azamacrocyclic *bis*quinoline 315

Biot and co-workers[202] reported the synthesis of ferrocenyl *bis*quinoline **315** from the commercially available *N*,*N*-dimethyl(ferrocenylmethyl)amine. The ferrocenyl azamacrocyclic *bis*quinoline **315** was tested for *in vitro* activity against the CQ-sensitive HB3 and the CQ-resistant Dd2 *P. falciparum* strains. The results revealed that the compound was active against both strains with IC_{50} values of 0.110 and 0.062 µM against HB3 and Dd2 *P. falciparum* strains, respectively. The authors attributed the activity of this compound to the presence of the ferrocene moiety in the molecule. The ferrocene moiety was thought to be involved in a one-electron redox system as well as offering the compound high lipophilicity. They also suggested that the ferrocene moiety may have led to a reduced affinity of the hybrid compound for the transporter gene responsible for resistance to chloroquine hence the high activity against the Dd2 strain compared to HB3 strain of *P. falciparum*.

The synthesis of *bis*quinoline was carried out as depicted in **Scheme 3.6**. The commercially available *N*,*N*,*N*-trimethyl(ferrocenylmethyl)ammonium iodide **313** was condensed with triazacyclononane **312** in deoxygenated water in the presence of potassium hydroxide which

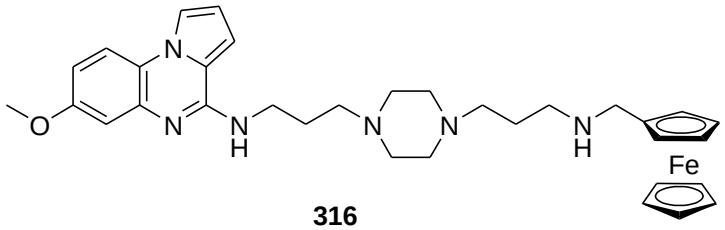
afforded ferrocenyl macrocycle **314** as one of the two major products which were not separated. Condensation of the mixture with 4,7-dichloroquinoline in *N*-methyl-2-pyrrolidinone delivered the required ferrocenyl *bis*quinoline **315** after separation.



Scheme 3.6: *Reagents and conditions:* (a) 5 equiv. K_2CO_3, H_2O, reflux, 3 hrs (b) 5 equiv. 4,7-dichloroquinoline, 2.5 equiv. K_2CO_3, NMP, 135 ^oC, 4 hrs.

3.5.4 Synthesis and biological application of ferrocenyl pyrrolo[1,2-*a*]quinoxaline derivatives 324 and 325

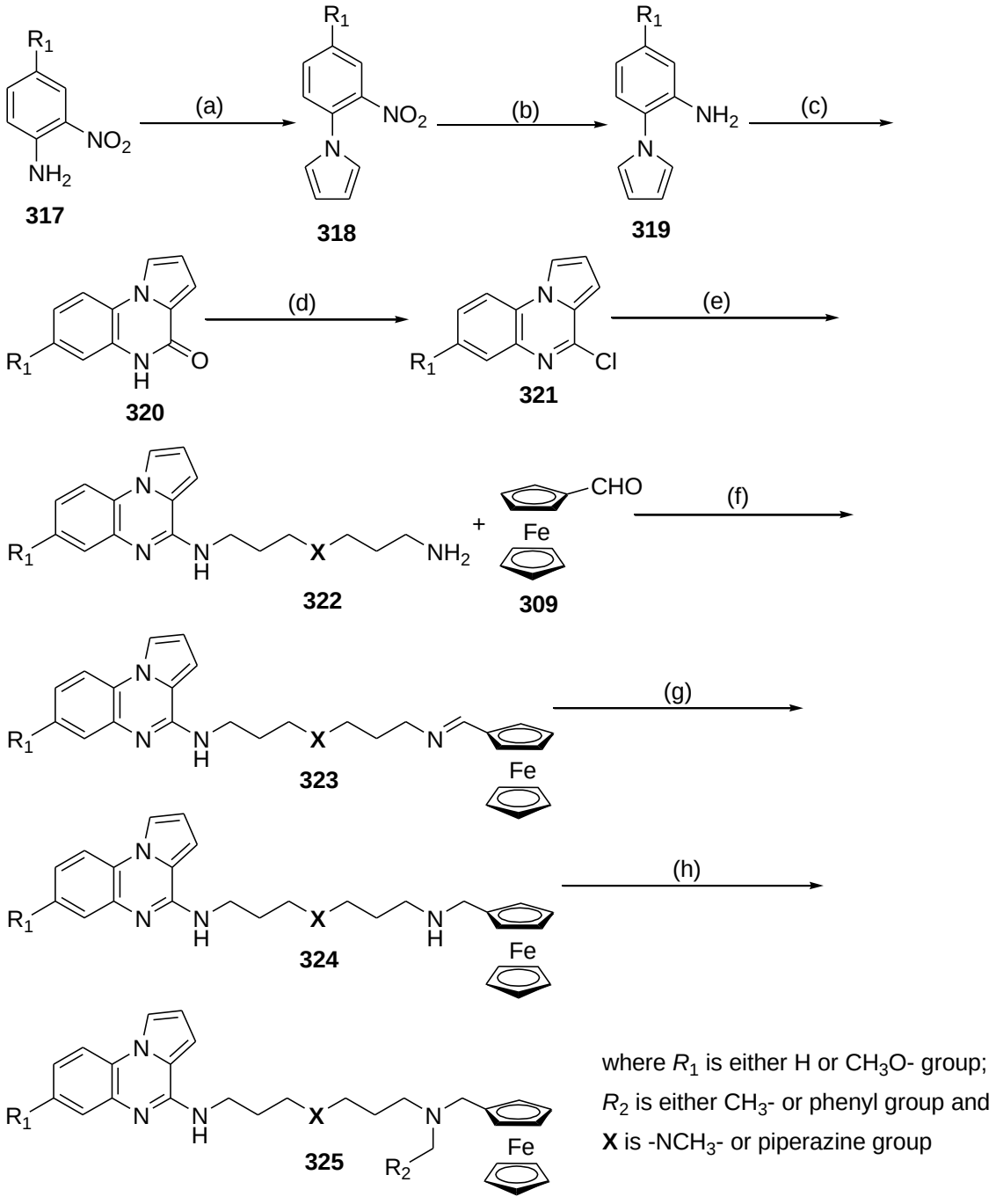
Guillon and co-workers[203] reported the synthesis of a series of pyrrolo[1,2-*a*]quinoxaline derivatives from various substituted nitroanilines which were tested for *in vitro* activity against the CQ-sensitive strain (F32) and the CQ-resistant strains (FcB1 and PFB) of *P. falciparum*. It was observed in this study that a methoxy group on the pyrrolo[1,2-*a*]quinoxaline nucleus and no substitution on the terminal *N*-ferrocenylmethylamine functionality enhanced the pharmacological activity of the compounds. The ferrocenyl compound **316** was the most active with IC_{50} values of 9.1, 16.6 and 22.2 nM against F32, FcB1 and PFB strains, respectively.



316

Figure 3.14: The molecular structure of ferrocene compound **316**.

The ferrocenyl pyrrolo[1,2-*a*]quinoxaline derivatives were synthesized from substituted 2-nitroanilines as shown in **Scheme 3.7**. The Clauson–Kaas reaction of anilines (represented by the general compound **317**) with 2,5-dimethoxytetrahydrofuran in acetic acid gave the pyrrolic derivatives **318**. The intermediates **318** were then reduced by sodium borohydride affording 1-(2-aminophenyl)pyrroles **319**. The cyclization between the amine and the *α*-carbon atom of the pyrrole ring was performed by reacting 1-(2-aminophenyl)pyrroles **319** with triphosgene in toluene which delivered lactams **320**. The lactams were subsequently chlorodehydroxylated with phosphorous oxychloride yielding chloroquinoxalines **321**. The intermediates **322** were obtained by coupling 4-chloropyrrolo[1,2-*a*]quinoxalines **321** to 1,3-*bis*(aminopropyl) piperazine or 1,3-*bis*(aminopropyl)methylamine using catalytic amounts of palladium acetate and the chelating ligand xantphos. The ferrocene carbaldehyde **309** was subsequently condensed with amines by heating to reflux in ethanol which delivered the ferrocenyl imines **323**. The reduction of the imines by sodium borohydride in methanol afforded 1-{*N*-(pyrrolo[1,2-*a*]quinoxalin-4-yl)-3-aminopropyl}-4[*N*-(ferrocenylmethyl)-3-aminopropyl]piperazines or methylamines analogues **324**. The resultant secondary amines were then subjected to reductive amination with sodium triacetoxyborohydride and acetaldehyde or benzaldehyde yielding ferrocenic pyrrolo[1,2-*a*]quinoxaline derivatives **325**.

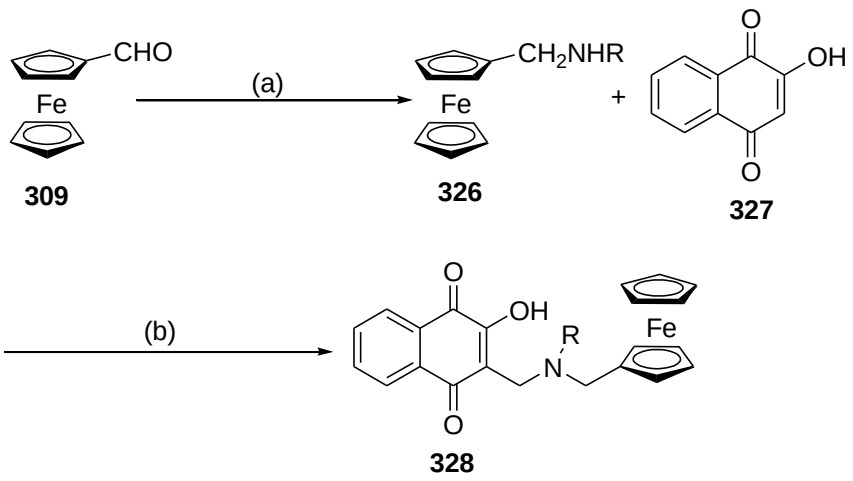


Scheme 3.7: *Reagents and conditions:* (a) DMTHF, reflux (b) $BiCl_3$, $NaBH_4$, EtOH (c) $CO(OCCl_3)_2$, toluene, reflux (d) $POCl_3$, reflux (e) **Method one:** xantphos, $H_2N–(CH_2)_3–$**X**$–(CH_2)_3–NH_2$, K_2CO_3, cat. $Pd(OAc)_2$, dioxane, reflux; **Method two:** $H_2N–(CH_2)_3–$**X**$–(CH_2)_3–NH_2$, 1-pentanol, reflux (f) EtOH, reflux (g) $NaBH_4$, MeOH, rt (h) $R_2–CHO$, $NaHB(OAc)_3$, CH_2Cl_2, rt.

3.5.5 Synthesis and biological application of ferrocenyl analogues of atovaquone 328

Baramee and co-workers[204] reported the synthesis of 14 ferrocenyl aminohydroquinone analogues of atovaquone (represented by ferrocenyl naphthoquinone **328**) from the Lawsone quinone **327**. The ferrocenyl compounds were tested for *in vitro* activity against *Toxoplasma gondii* and *Plasmodium falciparum*. The ferrocenyl atovaquone analogues with 6-8 carbon atoms in the aliphatic chain were significantly active against the atovaquone resistant strain of *T. gondii* (Ato^R) and the Dd2 CQ-resistant *P. falciparum* strain. This discovery was significant because *T. gondii* is increasingly receiving more attention for the reason that Toxoplasmosis is the most common cause of focal central nervous system abnormalities in immunocompromised patients with HIV or in transplant recipients. Currently, the drug of choice for the treatment of Toxoplasmosis is a combination of pyrimethamine and sulfadiazine which has toxic side effects such as bone marrow suppression and allergies in AIDS patients.[205]

The synthesis of ferrocenyl compounds **328** was accomplished by reductive amination of commercially available amines with ferrocene carbaldehyde **309** which afforded secondary ferrocenyl amine intermediates **326**. The ferrocenyl intermediates were then subjected to a Mannich reaction between Lawsone quinone **327**, ferrocenyl amines **326** and formaldehyde which delivered ferrocenyl compounds **328** with different alkyl (*R*) groups as shown in **Scheme 3.8**.

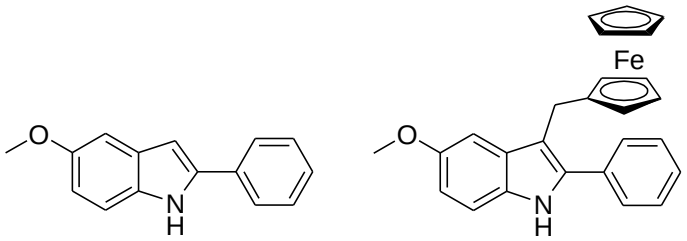


where *R* is -$(CH_2)_nCH_3$ for n= 1 to 11

Scheme 3.8: *Reagent and conditions:* (a) (i) RNH_2, *t*-BuMeO, reflux (ii) $NaBH_4$, MeOH (b) HCHO, EtOH, reflux.

3.5.6 Synthesis and biological application of ferrocenyl indole 333

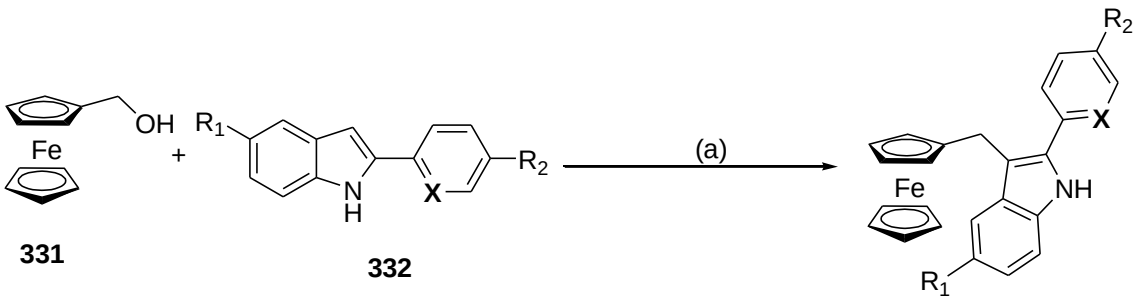
Other work on ferrocene hybrid molecules was carried out by Quirante and co-workers[206] who reported an interesting study which revealed that appending a ferrocene core to the 2-phenylindole scaffold increased the cytotoxicity of the resultant hybrid molecules. In this study all the ferrocene-indole hybrid molecules showed more activity than their purely organic parent indole compounds. For example, 3-ferrocenylmethyl-5-methoxy-2-phenyl-1*H*-indole **330** showed *in vitro* antiplasmodial activity with an IC_{50} value of 5.00 µM whereas the indole parent molecule, 5-methoxy-2-phenyl-1*H*-indole **329**, showed activity with IC_{50} value of 118 µM. The same results were reproduced when the compounds were tested for *in vitro* activities against the A549 human carcinoma cell line with the hybrid compounds showing more than 25-fold potency compared to their purely organic analogues.



329 **330**

Figure 3.15: The molecular structures for compounds **329** and **330**.

The ferrocenyl indole hybrid compounds were synthesized using a modified procedure of Boev and coworkers[207] as shown in **Scheme 3.9**. The 2-phenylindole derivatives **332** were reacted with ferrocene methanol **331** in dichloromethane in the presence of an aqueous solution of tetrafluoroboric acid (HBF_4) which delivered the target compounds **333**.



331 **332** **333**

where **X** is either H or N; R_2 is either H, F or Cl;
R_1 is either H, OCH_3, NO_2 or Cl

Scheme 3.9: *Reagents and conditions:* CH_2Cl_2, aq. HBF_4, rt, 1 hr.

3.6 Tamoxifen 334 and ferrocifen 337 as anticancer agents

Breast cancer is a malignant growth that begins in the tissue of the breast, usually the ducts and lobules and it occurs in both men and women although male breast cancer is rare.[208] It is the most common cancer among women and in general, the breast tumors can be divided into two groups that are distinguished by the presence [ER(+)] or absence [ER(−)] of the estrogen receptors (ER).[209] In the ER(+) cell lines, there are two receptor subtypes, ER_α and ER_β. Malignant breast tissue may express ER_α alone, a combination of ER_α and ER_β, no ER at all or in rare cases, ER_β alone. ER_β has been detected in the MDA-MB231 cell line which is taken as a standard ER_α-negative (ER−) cell line whereas ER_α is commonly found in the

MCF-7 cell line. About two-thirds of all cases belong to the ER(+) type, which is susceptible to hormone therapy by selective estrogen receptor modulators (SERMs).[210] SERMs are a set of chemically diverse compounds whose structures lack the steroid skeleton of estrogens but are still capable of interacting with the estrogen receptor-binding site. Like estrogens, SERMs operate by diffusing into the cell and binding to the receptor. This causes conformational changes and dimerization leading to direct interaction of the adducts with specific DNA promoter portions present on target genes.[211]

One of the most commonly used estrogen receptor modulators for the treatment of breast cancers is tamoxifen **334**[212] which exists in both *Z* and *E* configurations, with the *Z* isomer being the most strongly anti-estrogenic. Tamoxifen works by blocking estrogen from stimulating hormone-dependent breast cancer cells (MCF-7) by competitively binding to the estrogen receptors on tumors and other tissue targets thereby producing a nuclear complex that decreases DNA synthesis and preventing (pre)cancerous cells from dividing but does not necessarily cause cell death. Tamoxifen **334** in its original form is basically a prodrug,[213] with relatively little affinity for the estrogen receptor (ER) but is metabolized in the liver by the cytochrome P450 isoform CYP2D6 and CYP3A4 into active metabolites afimoxifen **335** (4-hydroxytamoxifen) and endoxifen **336** (*N*-desmethyl-4-hydroxytamoxifen). These active forms of tamoxifen have 30-100 times more affinity for the estrogen receptor than tamoxifen itself.[214] The active metabolites compete with estrogen in the body for binding to the estrogen receptors. Afimoxifene **335** is itself a selective estrogen receptor modulator and it was shown in a study conducted in France that rubbing afimoxifene on the cancerous skin was as effective as oral tamoxifen at slowing breast cancer growth.[215] On the other hand, *N*-desmethyl-4-hydroxytamoxifen **336** is a potent competitive aromatase inhibitor, and may also be involved in anti-estrogenic activity.

The drawback of tamoxifen is that it is susceptible to acquired resistance and a favourable response to the treatment is obtained in only one-third of patients over the long term (5+ years). It is also associated with side effects such as the increased risk of endometrial uterine cancer and blood clotting in the lungs.[216]

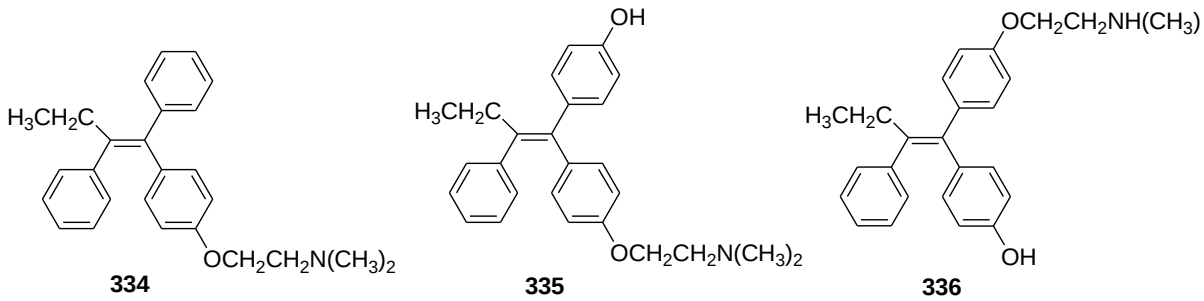


Figure 3.16: The molecular structure for tamoxifen **334**, afimoxifen **335** and endoxifen **336**.

As part of an effort to improve the efficacy and efficiency of tamoxifen, Jaouen and co-workers[217] reported the synthesis of ferrocifen **337** and hydroxyferrocifen **338** which are the ferrocene analogues of tamoxifen **334** and afimoxifen **335**, respectively. The only difference between tamoxifen **334** and ferrocifen **337** is that the phenyl group in tamoxifen is replaced by the ferrocene group in ferrocifen. The same difference is also observed in hydroxytamoxifen **335** and hydroxyferrocifen **338**.

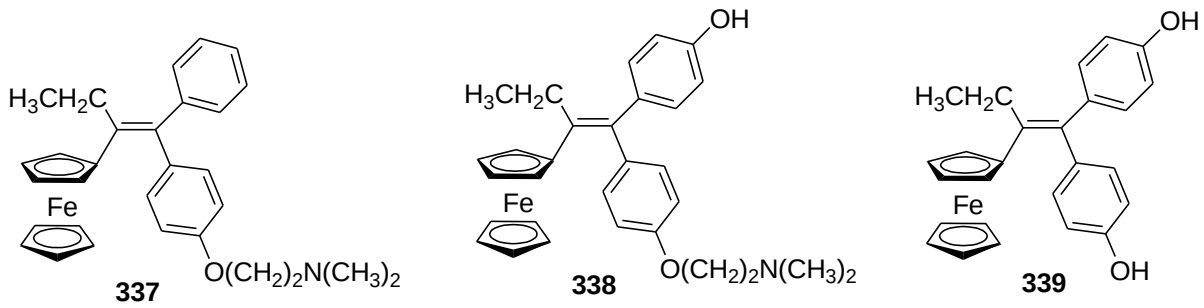


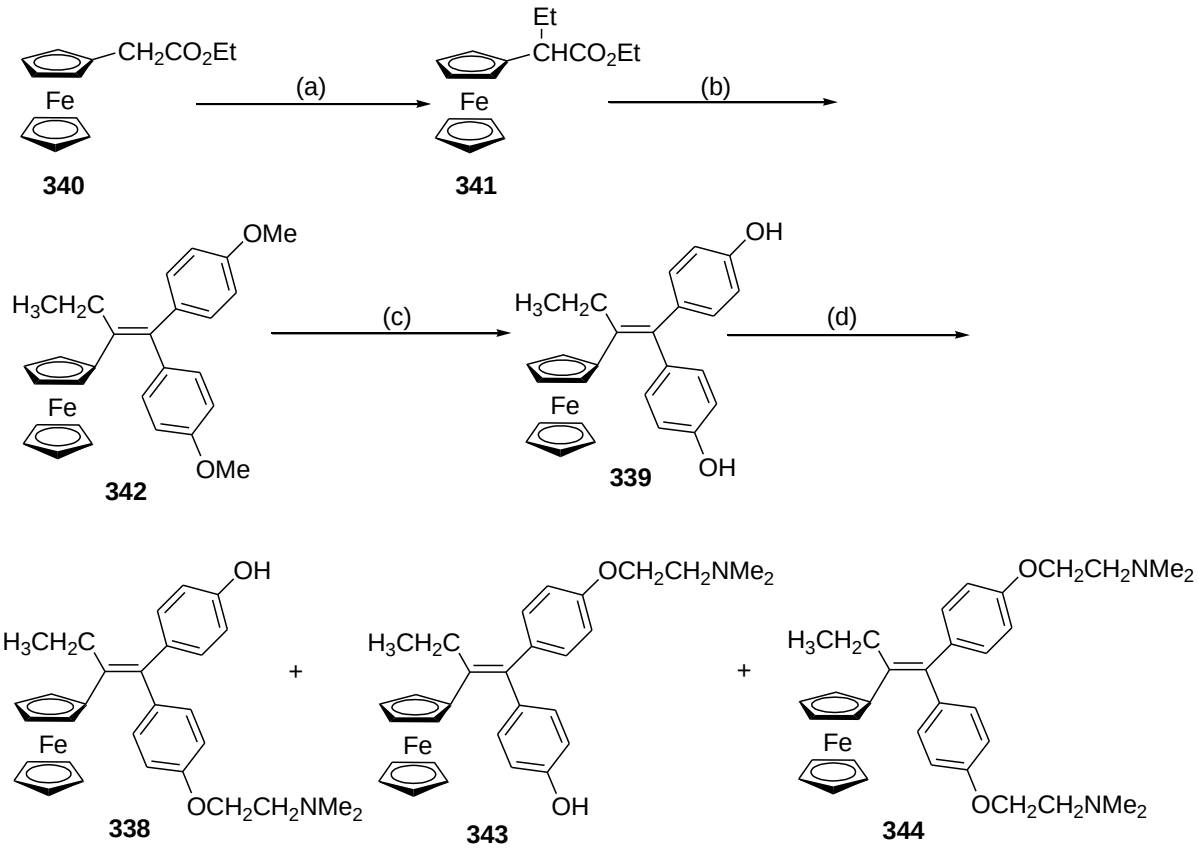
Figure 3.17: The molecular structures of ferrocifen **337**, hydroxyferrocifen **338** and ferrocenyl diphenol **339**.

The antiproliferative activity of the ferrocene analogues of tamoxifen were evaluated on MCF-7 and MDA-MB-231 cells lines and it was found during this study that all ferrocene analogues of tamoxifen showed comparable activity to that of afimoxifen on MCF-7 cells. The major difference in activity was observed on a hormone-independent cell line (MDA-MB-231) in which the ferrocene analogues of tamoxifen **334**, (ferrocifen **337**, hydroxyferrocifen **338** and ferrociphenol **339**) displayed a strong antiproliferative effect presenting remarkably low IC_{50} values of 0.8, 0.5 and 0.6 μM, for compounds **337**, **338** and **339**, respectively. The purely organic compounds (tamoxifen **334** and hydroxytamoxifen

(afimoxifen) **335**) were completely inactive.[218] The antiproliferative effect of ferrocenyl compounds **337**, **338** and **339** on both hormone-dependent and hormone-independent breast cancer cell lines is attributed to better membrane permeability and cytotoxicity caused by the redox properties of the appended ferrocene moiety. The production of reactive oxygen species is known to cause oxidative damage of DNA. What is interesting about this observation is that ferrocene by itself is not active against both the hormone-dependent and hormone-independent breast cancer cell lines.[195]

3.6.0 Synthesis of ferrocenyl analogues of tamoxifen

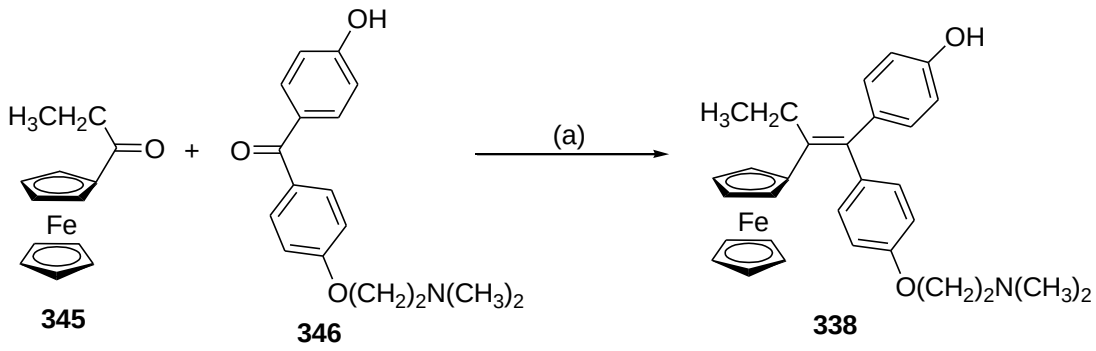
Two synthetic routes were developed to access the ferrocene hybrid molecules. The original synthesis of hydroxyferrocifen **338** (**Scheme 3.10**) involved ethylating the α-carbon atom of the ferrocene ester **340** using potassium *tert*-butoxide and the resultant nucleophile was rapidly reacted with iodoethane yielding ethyl 2-ethyl-2-ferrocenylacetate **341**. The ester **341** was then condensed with an organolithium reagent ($MeOC_6H_4Li$) and the acid promoted dehydration of the resultant alcohol intermediate afforded dimethylether alkene derivative **342** in both *Z*- and *E*-configurations. The unselective demethylation of alkene **342** was achieved by using boron tribromide which furnished the ferrocenyl diphenol **339**. The fixation of the amine chain to the diphenol **339** was achieved by treating the diphenol with (dimethylamino)ethyl chloride which delivered hydroxyferrocene **338** as one of the three products.[217a]



Scheme 3.10: *Reagents and conditions:* (a) (i) *t*-BuOK, Me_2SO (ii) EtI (b) (i) 2 × $MeOC_6H_4Li$, Et_2O (ii) H^+/H_2O (c) BBr_3, CH_2Cl_2 (d) (i) EtONa (ii) $Me_2NCH_2CH_2Cl$, aq. HCl.

This protocol had limitations, the first of which was the necessity to protect and then deprotect functional groups which were used in the reaction with lithium reagents.[219] It is generally accepted in linear organic synthesis that the longer the synthetic pathway the lower the overall percentage yield. The second limitation was lack of control in the last step to deliver a single product (formation of by-products **343** and **344** was observed).

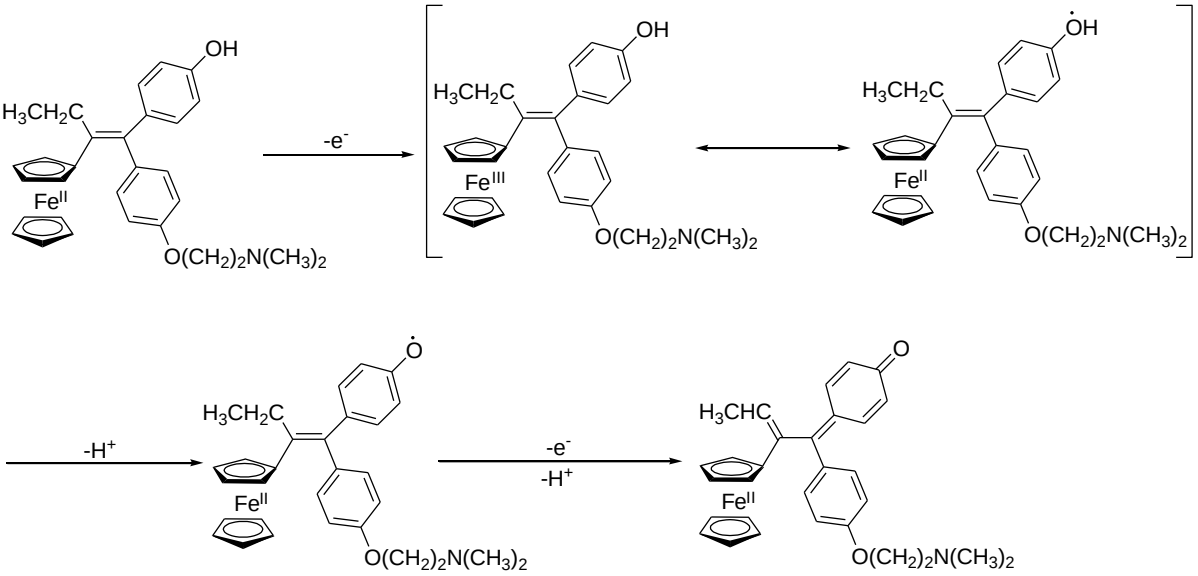
To overcome these limitations, the same authors decided to take advantage of a McMurry cross-coupling reaction which is tolerant to the phenol group to avert the need for methylation and demethylation steps.[217b] In this protocol, the ferrocenyl ketone **345** was condensed with diphenyl ketone **346**, which had an appropriately placed amine side chain, delivering hydroxyferrocifen **338** as shown in **Scheme 3.11**.



Scheme 3.11: *Reagents and conditions:* (a) $TiCl_4$/Zn, THF, reflux.

3.6.1 Proposed mode of action for ferrocifen

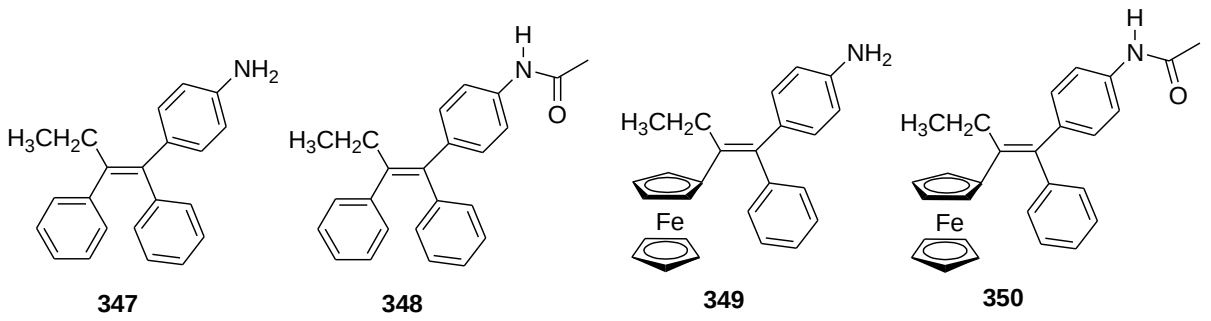
It has been hypothesized that the novel mechanism of action of the hydroxyferrocifen and its ferrocene derivatives involves the generation of a quinone methide owing to a conjugated redox ferrocenyl antenna. The ferrous ion of the ferrocene moiety is involved in a mild oxidation to a corresponding ferric ion which is then reduced back to the ferrous ion. This reversible redox property of ferrocene allows it to act as an intramolecular oxidant of a distant phenol group linked by a conjugated system thereby lowering the oxidation potential necessary for toxic quinone methide formation. The mechanism for the formation of the quinone methide is shown in **Scheme 3.12**. So far, there is no evidence linking the formation of the quinone methide in hydroxyferrocifen and its related ferrocene analogues to a bioreductive alkylation mechanism which is the major mode of action for quinones which have a leaving group attached to the side chain as discussed in **Section 1.2.1**.



Scheme 3.12: The proposed mechanism of activation of hydroxyferrocifen.

The mechanism depicted in **Scheme 3.12** was proposed on the basis of data generated by electrochemical experiments which supported the formation of a quinone methide in culture cells. Other investigators have shown that there is a correlation between the cytotoxicity of ferrocene derivatives of tamoxifen and the production of reactive oxygen species.[220]

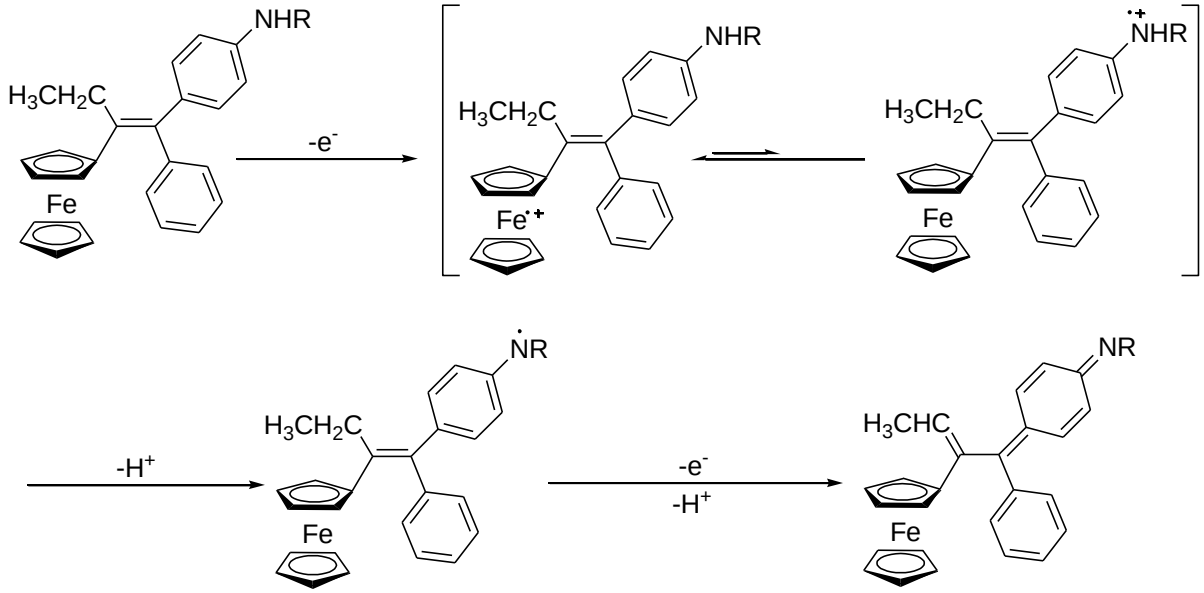
Pigeon and co-workers studied the importance of the phenol group in ferrocenyl analogues and found that compounds **347** and **348** with an amino and acetamide groups were active against hormone-dependent breast cancer cells lines but were not active against hormone-independent breast cancer cell lines more like tamoxifen and its non-ferrocene analogues.[221] The ferrocene analogues of compounds **347** and **348** (ferrocenyl compounds **349** and **350**) exhibited strong antiproliferative effects on both hormone-dependent and hormone-independent breast cancer cell lines. What was exceptional about compounds **349** and **350** was that they showed a dual estrogenic/cytotoxic activity on the MCF-7 cell line in which they were proliferative at low concentrations (0.10 μM) and antiproliferative at high concentrations (10 μM). The ferrocenyl compounds **349** and **350** were also antiproliferative on the MDA-MB-231 cell line with IC_{50} values of 0.8 μM for **349** and 0.65 μM for **350**.



347 **348** **349** **350**

Figure 3.18: The molecular structures of amine analogues of tamoxifen, compounds **347** and **348** and their ferrocenyl analogues **349** and **350**.

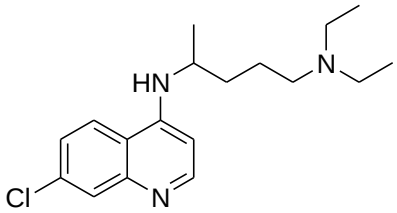
The electrochemical experiments suggested that ferrocenyl compounds **349** and **350** could be transformed to oxidized quinoid type species, analogous to what is observed for the ferrocene phenols depicted in **Scheme 3.12** above. The aniline substituents were hypothesized to be involved in the formation of quinone imines which were accessible *via* the same redox process triggered by the ferrocenyl antenna as shown in **Scheme 3.13**.



Scheme 3.13: Proposed mechanism of activation of ferrocenyl compounds **349** and **350**; where *R* is H for compound **349** and acetyl group for compound **350**.

3.7 Chloroquine 351 and ferroquine 352

Chloroquine (CQ) **351** (**Figure 3.19**) is one of the quinoline containing antimalarial drugs and was discovered in 1946 by German chemists.[222] It was once an elective chemotherapy against malaria and played an important role in both the treatment and prophylaxis of *P. falciparum* malaria in countries where transmission was and continues to be severe. As explained in **Section 3.1**, the malaria parasites generate free heme during degradation of methemoglobin but its accumulation within the digestive food vacuole is toxic to the same parasite. The digestive food vacuole occupies between 3-5% of the volume of the infected erythrocyte and the accumulation of the free heme reaches between the 200-500 µM concentration level and the malaria parasite deals with this problem by polymerizing the heme into non-toxic hemozoin (malaria pigment).[223]



351

Figure 3.19: The molecular structure of chloroquine **351**.

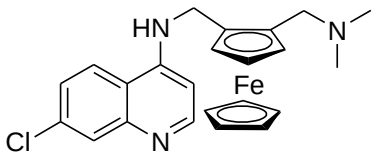
The molecular basis of the action of quinoline containing antimalarial drugs is not fully understood but it is thought to be by interfering with haemoglobin digestion in the blood stages of the malaria parasite's life cycle. This is achieved by impeding the detoxification of free heme in the parasite-infected red blood cell thereby disrupting the polymerization process of the heme into hemozoin. The disruption of the polymerization process results in accumulation of free heme in the parasite's food vacuole.[224]

In addition, chloroquine accumulates several thousand-fold inside the digestive food vacuole and binds to heme to form a FPIX-CQ complex which is equally highly toxic to the parasite. The formation of FPIX-CQ complex interferes with the polymerization of heme and/or the detoxification of the reactive oxygen species thereby disrupting the normal parasite membrane functions. The action of FPIX-CQ and ferriprotoporphyrin IX(FeIII) ultimately

results in parasite cell auto-digestion effectively killing the parasite with its own metabolic waste or a metabolic waste-chloroquine complex.[225]

Unfortunately, *P. falciparum* has developed resistance to chloroquine and other quinoline antimalarials in most affected areas.[226] Chloroquine resistance is thought to arise as a result of a decreased level of chloroquine uptake, due to an increased vacuolar pH or changes in a chloroquine importer or receptor gene. The emergence of quinoline drug resistance poses a major health problem to the endemic regions. To overcome this problem, Brocard and co-workers synthesized a ferrocene analogue of chloroquine named ferroquine (FQ) **352**. This work was inspired by the work of Jaouen on tamoxifen and its ferrocene analogues as discussed in **Section 3.6**. In ferroquine, a ferrocenyl group is covalently flanked by a 4-aminoquinoline nucleus and a basic alkylamine moiety. Biological studies showed that ferroquine exhibited excellent activity against malaria parasites, both *in vitro* and *in vivo*, with especially good activity against chloroquine-resistant parasites.

Ferroquine **352**, in contrast to other drugs, is the first organometallic antimalarial drug and is currently in development at Sanofi-Aventis. Studies have shown that the best activity is obtained when the ferrocene moiety is part of the basic chain as shown in **Figure 3.20**.



352

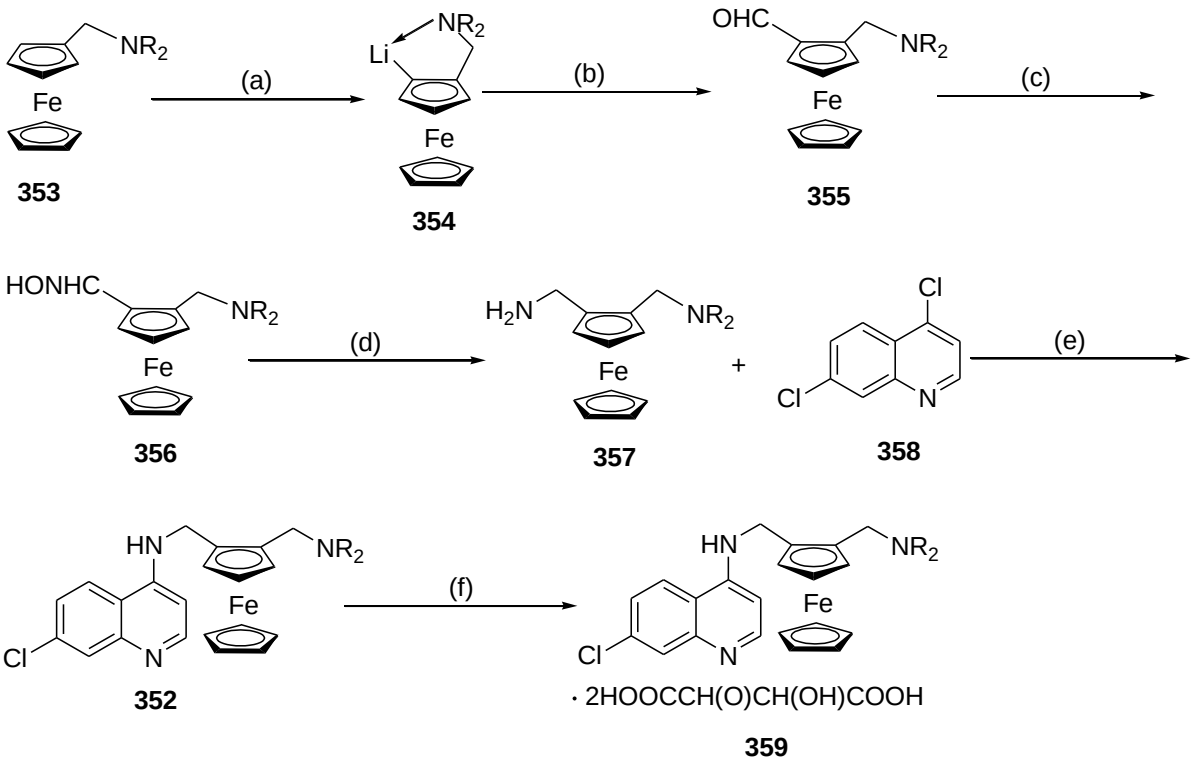
Figure 3.20: The molecular structure of ferroquine **352**.

The metabolic pathway of FQ was proposed based on experiments using animal and human hepatic models.[227] FQ is metabolized mainly *via* an oxidative pathway by cytochrome P450 isoforms 2C9, 2C19 and 3A4 into the major metabolites, mono-*N*-desmethyl FQ (loss of one methyl group) and di-*N*,*N*-desmethyl FQ (loss of two methyl groups). The 4-amino-7-chloroquinoline is also one of the degradation product and studies have shown that it has no antimalarial activity.[228] The major metabolites, mono-*N*-desmethyl FQ and di-*N*,*N*-desmethyl

FQ, were synthesized and tested against the CQ-susceptible strain 3D7 and the CQ-resistant strain W2. It was found that mono-*N*-desmethyl FQ was as active as ferroquine in both *in vitro* and *in vivo* studies in humans.[228b] The mono-*N*-desmethyl FQ was found to have a longer terminal half-life than FQ itself with an overall mean estimate of 31.4 days and its blood concentration exceeded that of FQ from approximately day 5 onwards.[228b] The di-*N,N*-desmethyl FQ was less active on both strains but remained more active than CQ on the CQ-resistant strain.

3.7.0 Synthesis of ferroquine

The original synthesis of ferroquine was reported by Biot and co-workers[229] in 1996. This protocol involved metallation of the commercially available *N,N*-dimethylferrocenylmethylamine **353** in the presence of *n*-butyllithium which afforded 2-[(*N,N*-dimethylamino)methyl]ferrocenecarboxyaldehyde **355** upon the formylation of the metallated intermediate **354** with *N,N*-dimethylformamide. The aldehyde **355** was then converted to the corresponding ferrocenyl amine **357** *via* the oxime **356** by reductive amination. The nucleophilic aromatic substitution reaction was achieved by condensation of amine **357** with 4,7-dichloroquinoline **358** in *N*-methyl-2-pyrrolidinone which delivered 7-chloro-4-[2-*N,N*-(dimethylaminomethyl)ferrocenylmethylamino]quinoline **352**. Finally, the conversion of free ferroquine **352** to the ammonium salt **359** was achieved by acidification of amine **352** with 2 molar equivalents of L-(+)-tartaric acid in acetone as shown in **Scheme 3.14**.



Scheme 3.14: *Reagents and conditions:* (a) *n*-BuLi, Et_2O (b) DMF, Et_2O (c) $NH_2OH.HCl$, NaOH, $EtOH/H_2O$ (d) $LiAlH_4$/THF (e) K_2CO_3, NMP (f) $(CH(OH)CO_2H)_2$, HCl/Me_2CO (where R_2 stands for *N*,*N*-dimethyl group).

3.7.1 Major differences between ferroquine 352 and chloroquine 351

A lot of progress has been made in elucidating the mechanism of action ferroquine but its full mode of action is still a subject of debate. It is thought that ferroquine behaves like chloroquine on chloroquine-susceptible parasites and uses a new mode of action on chloroquine-resistant parasites. Apart from the obvious structural differences between the two compounds, studies have shown that these compounds behave differently both *in vivo* and *in vitro*.

Ferroquine is able to overcome the chloroquine resistance problem, an important limitation for the control of *P. falciparum*. In addition, FQ has a good bioavailability and the i*n vivo* experiments performed on different murine *Plasmodium* species revealed that the curative dose of ferroquine (10 mg/kg/day for 4 days) remained unchanged, regardless of the susceptibility of the strain to chloroquine, and the means of administration (subcutaneously or orally). It is also less toxic than chloroquine and has the ability to maintain the capacity of

spleen cells to proliferate in response to different mitogens.[230] Furthermore, the results of both *in vitro* tests on field isolates and *in vivo* experiments on rodent models indicated that a potential resistance to ferroquine does not depend on gene polymorphism already involved in chloroquine resistance. This was shown on Cambodian isolates and extended to 15 *P. falciparum* laboratory strains, concerning the genes currently involved in drug resistance such as the *P. falciparum* chloroquine resistance transporter gene (*pfcrt*), the *P. falciparum* multidrug resistance-associated protein gene (*pfmrp*), the *P. falciparum* multidrug resistance protein 1 gene (*pfmdr1*), the *P. falciparum* Na+/H+ exchanger gene (*pfnhe1*) and the *P. falciparum* multidrug resistance protein 2 gene (*pfmdr2*).[231]

Ferroquine (FQ) is also able to form intramolecular hydrogen bonds as shown in structure **360** (**Figure 3.21**) which renders the molecule rigid. This property allows better interaction of the ferrocene core with the hydrophobic membranes and lipid bodies of the digestive food vacuole of the parasite. As a result, FQ is better suited in targeting the lipid site of hemozoin formation than chloroquine.[231b] The preferential localization of the ferroquine at the lipid-water interface prevents the conversion of heme into hemozoin by maintaining toxic free heme in the aqueous environment. The intramolecular hydrogen bonding also gives FQ a better permeability potential and it easily diffuses into the food vacuole compared to CQ. The intramolecular bonding is lost in favour of solvolysis once in the food vacuole which makes it difficult for FQ to diffuse out of the food vacuole. Substitution of the hydrogen on nitrogen atom 11 by a methyl group (compound **361**) prevents the formation of the hydrogen bonds and studies have shown that this substitution results in a reduction of the antimalarial activity in the resultant compound compared to the parent molecule, ferroquine.[232]

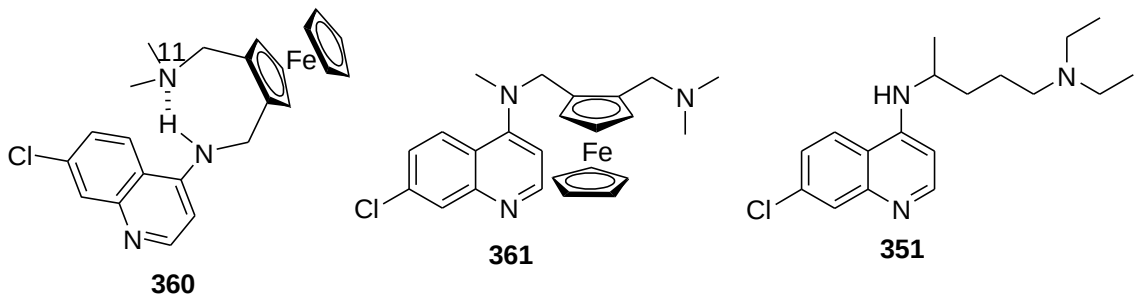
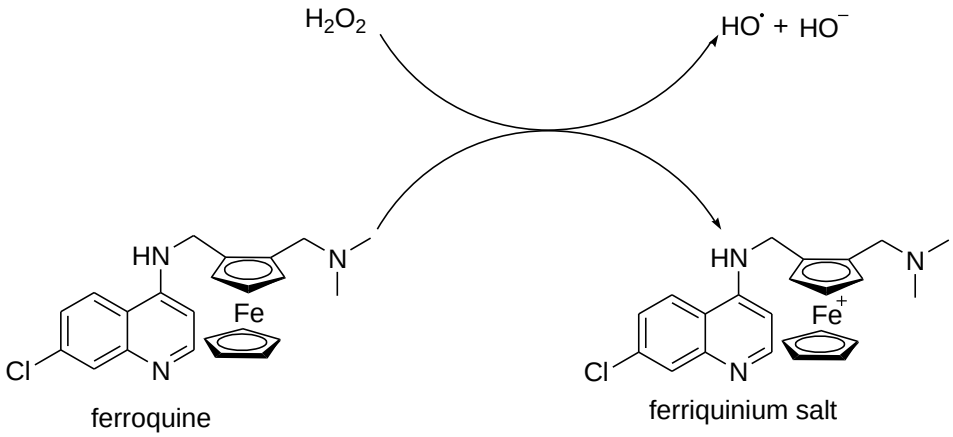


Figure 3.21: The intramolecular hydrogen bonding in ferroquine **360** which is not available in methyl ferroquine **361** and chloroquine **351**.

The other notable difference is that the basicity and lipophilicity of FQ and CQ are significantly different.[233] When protonated at the putative food vacuole pH of 5.2, the lipophilicity of FQ and CQ are similar with log *D* values of -0.77 and -1.2, respectively. However, there is a marked difference in lipophilicity at pH 7.4 with log *D* values of 2.95 and 0.85 for FQ and CQ, respectively. In addition, the p*K*a values of FQ are lower than those of CQ with p*K*a1 and p*K*a2 values of 8.19 and 6.99 for FQ and 10.03 and 7.94 for CQ, respectively. The lower p*K*a values of FQ are due to the presence of a strong intramolecular hydrogen bonds and the electron donating properties of the ferrocene moiety. The differences in p*K*a values influence the relative concentrations of each micro species at vacuolar pH and in the case of FQ the decreased accumulation arising from the less basic behaviour is compensated for by its strong *ß*-hematin inhibition. The neutral and mono-protonated forms of FQ are ten times more concentrated at the pH of the digestive food vacuole than those of CQ thereby profoundly influencing the inhibition of heme polymerization.[156b]

The other factor that needs to be considered is that a surplus of radicals is produced in infected red blood cells, causing an imbalance between pro-oxidant and anti-oxidant species. These excess radical species are not detected in healthy erythrocytes. The detoxification systems present in the parasite and also in the host cells are accelerated to counteract these radical species and create a new redox balance. Studies have shown that there is the presence of a small amount of hydrogen peroxide in the digestive food vacuole of the parasite.[234] This is notable because of the presence of Fe(II) cation in the structure of FQ which is known to undergo a reversible oxidation-reduction reaction. It has been shown that under oxidative

conditions of the digestive food vacuole of the parasite, FQ is capable of generating Fenton-like reactions leading to the production of ferriquinium salt and hydroxyl radicals as shown in **Scheme 3.15**.[234c]



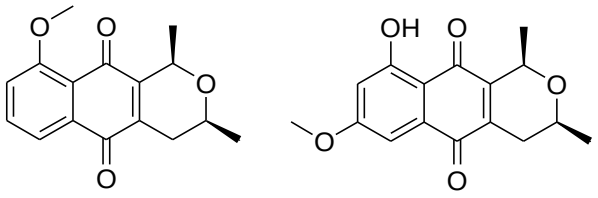
Scheme 3.15: The schematic representation of the oxidation of ferroquine into ferriquinium ion.

The generation of reactive oxygen species in the micromolar range is inadequate to affect the stability of FQ but is sufficient to move the delicate redox balance of the digestive vacuole, thereby contributing to the antimalarial activity of FQ. Comparatively, CQ is not able to produce hydroxyl radicals in the presence of hydrogen peroxide under vacuolar conditions.[235]

3.8 Justification and aim of this study

Quinones based on 3,4-dihydro-1*H*–naphtho[2,3-*c*]pyran that bear *cis* or *trans* methyl substituents at *C*-1 and *C*-3 in the heterocyclic pyran ring form an important class of biologically active natural products. The activities shown by compounds with this system are often as a result of them acting as bioreductive alkylating agents or due to the formation of reactive oxygen species. These comprises of such biologically important compounds as eleutherin ***cis*-362** (**Figure 3.22**) and its *C*-3 epimer, isoeleutherin ***trans*-363** (**Figure 3.23**) among others. Eleutherin ***cis*-362** and its *C*-3 epimer, isoeleutherin ***trans*-363** were isolated from the tubers of *Eleutherine bulbosa* (Iradaceae).[236] The methyl group at *C*-1 in both eleutherin and isoeleutherin adopts the more stable *pseudo*-axial position as such it is further away from the adjacent carbonyl group of the quinone. Eleutherin ***cis*-362** exhibits strong

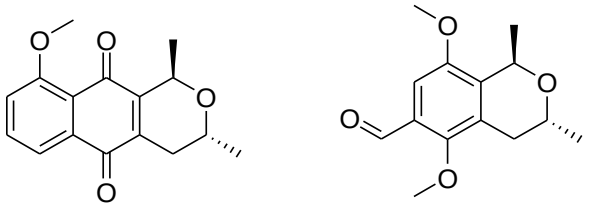
activity against *Pycococcus aureus* and *Streptococcus haemolyticus A*, and weak activity against *Bacillus subtilis*.[237] It is also reported to have a reversible inhibition of topoisomerase II by inducing religation and dissociation of the enzyme from DNA in the presence of ATP which is a property that is exploited in the anticancer agents. Extracts of *Eleutherine americana* of which eleutherin ***cis*-362** and isoeleutherin ***trans*-363** are the major constituents, is used to treat heart diseases such as angina pectoris.[238]



***cis*-362** ***cis*-136**

Figure 3.22: The molecular structures of eleutherin ***cis*-362** and ventiloquinone L ***cis*-136**.

As previously discussed, in our laboratory group, we successfully synthesized ventiloquinone L ***cis*-136** which has a similar pyran ring system to eleutherin ***cis*-362** (**Figure 3.22**). Two routes were devised in the total synthesis of this pyranonaphthoquinone and the intermediate (±)-*trans*-3,4-dihydro-5,8-dimethoxy-1,3-dimethyl-1*H*-isochromene-6-carbaldehyde ***trans*-364** was isolated in the route that did not deliver ventiloquinone L ***cis*-136**. The intermediate, 3,4-dihydroisochromene carbaldehyde ***trans*-364**, has the same pyran ring system as in isoeleutherin ***trans*-363** (**Figure 3.23**).

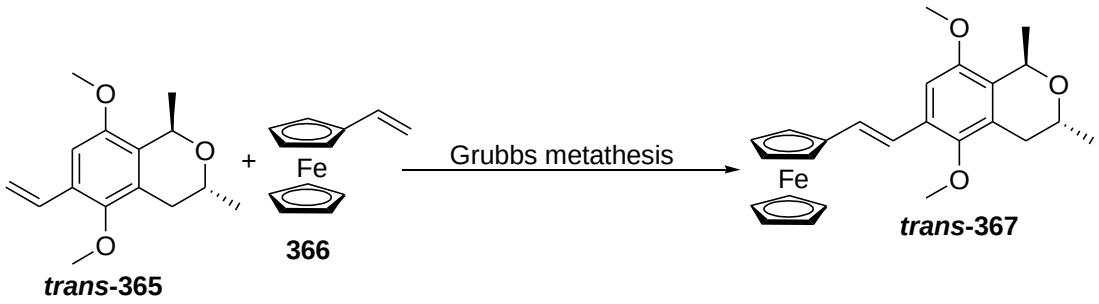


***trans*-363** ***trans*-364**

Figure 3.23: The molecular structures of isoeleutherin ***trans*-363** and 3,4-dihydroisochromene carbaldehyde ***trans*-364**.

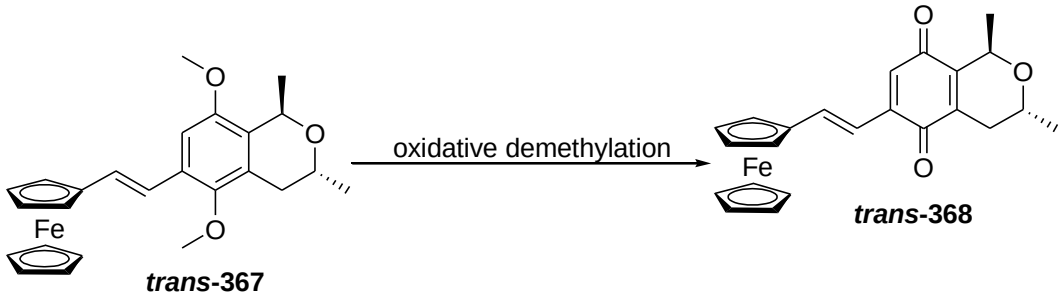
Even though numerous reports exist about bioactivity of ferrocene coupled compounds and also about quinones with a *cis*/*trans* 3,4-dihydro-1*H*–naphtho[2,3-*c*]pyran core, there is

limited information on ferrocene coupled pyranobenzoquinones. To the best of our knowledge, there are no studies in the literature that have reported coupling of the 3,4-dihydroisochromene ring system to the ferrocene moiety through a conjugated carbon bridge. With this in mind, a question at the heart of this research was to develop a methodology for coupling of a ferrocene moiety to a 3,4-dihydroisochromene nucleus as shown in **Scheme 3.16**. We intended to take advantage of the procedure we developed in our laboratory in the synthesis of intermediate ***trans*-364** and extend it to synthesize (±)-*trans*-3,4-dihydro-5,8-dimethoxy-1,3-dimethyl-6-vinyl-1*H*-isochromene ***trans*-365**. The Grubbs cross-metathesis[239] of alkenes ***trans*-365** and **366** could potentially deliver 6-ferrocenyl-(±)-*trans*-3,4-dihydro-5,8-dimethoxy-1,3-dimethyl-6-vinyl-1*H*-isochromene ***trans*-367** as shown in **Scheme 3.16**.



Scheme 3.16: The possible synthesis of ferrocene coupled 3,4-dihydroisochromene ***trans*-367**.

The ferrocene coupled 3,4-dihydroisochromene ***trans*-367** could then be oxidised to the corresponding 6-ferrocenyl-(±)-*trans*-3,4-dihydro-1,3-dimethyl-6-vinyl-1*H*-isochromene-5,8-dione ***trans*-368** as shown in **Scheme 3.17**.

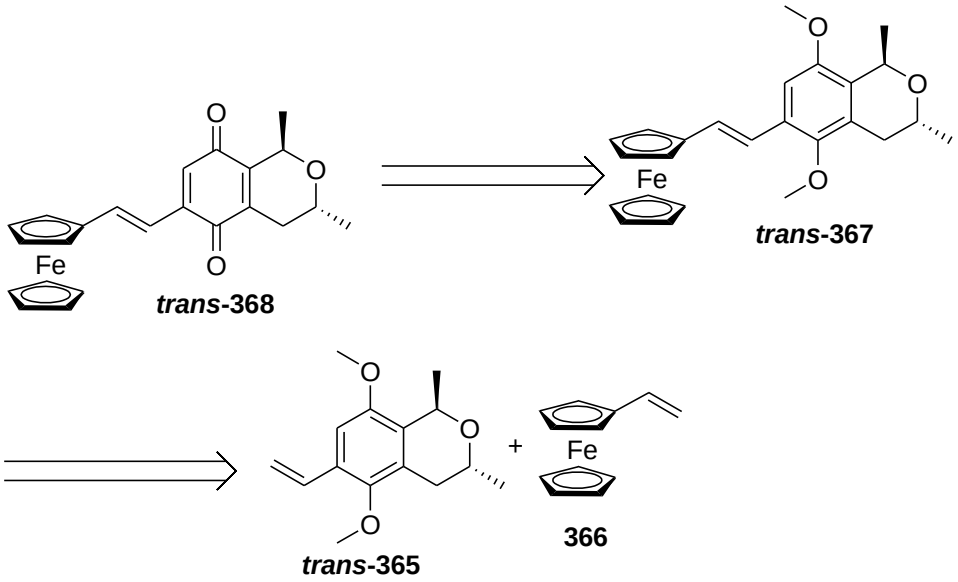


Scheme 3.17: The possible oxidative demethylation of ferrocenyl 3,4-dihydroisochromene ***trans*-367**.

Chapter 4: Results and discussion

4.0 Background

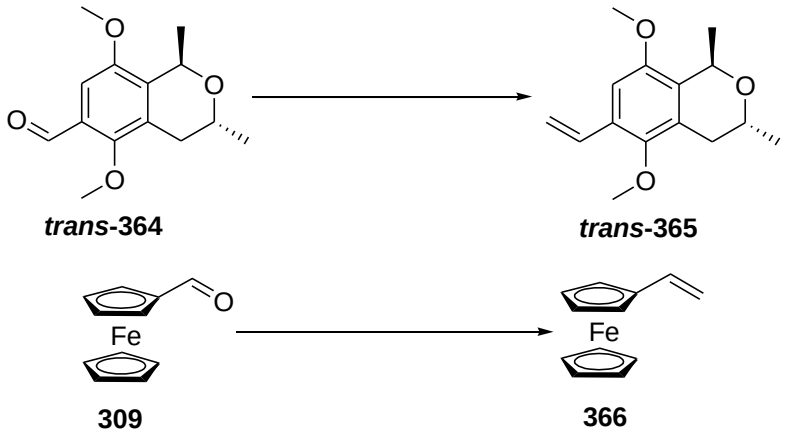
As discussed in **Chapter 3**, this part of PhD studies was aimed at developing a methodology which could be used in synthesizing ferrocene coupled 3,4-dihydroisochromenes from simple and commercially available starting materials. The retrosynthetic analysis revealed that we could achieve the synthesis of 6-ferrocenyl-(±)-*trans*-3,4-dihydro-5,8-dimethoxy-1,3-dimethyl-6-vinyl-1*H*-isochromene t***rans*-367** by performing a late stage Grubbs cross-metathesis reaction involving vinyl ferrocene **366** and (±)-*trans*-3,4-dihydro-5,8-dimethoxy-1,3-dimethyl-6-vinyl-1*H*-isochromene ***trans*-365** as shown in **Scheme 4.0**. The oxidative demethylation of ferrocenyl 3,4-dihydroisochromene ***trans*-367** could potentially deliver 6-ferrocenyl-(±)-*trans*-3,4-dihydro-1,3-dimethyl-6-vinyl-1*H*-isochromene-5,8-dione ***trans*-368**.



Scheme 4.0: Retrosynthetic analysis for the synthesis of ferrocenyl pyranobenzoquinone ***trans*-368**.

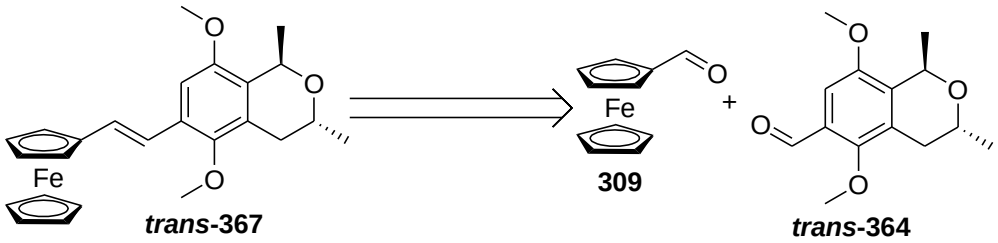
In our laboratory group, we have accomplished synthesis of a number of natural products. As discussed before, in one example, Mmutlane[119] achieved the total synthesis of ventiloquinone L ***cis*-136** from commercially available starting materials. Two different protocols were developed in which one protocol did not lead to the formation of ventiloquine L. As part of that methodology, (±)-*trans*-3,4-dihydro-5,8-dimethoxy-1,3-dimethyl-1*H*-isochromene-6-

carbaldehyde ***trans*-364** was isolated as one of the intermediates. We, therefore, thought that we could take advantage of this protocol to synthesize vinyl 3,4-dihydroisochromene ***trans*-365** by taking advantage of the Wittig reaction.[240] In the same way, the commercially available ferroaldehyde **309** could be transformed into vinyl ferrocene **366** (**Scheme 4.1**).



Scheme 4.1: *Reagents and conditions:* MTPPBr, *n*-BuLi, THF, 0 °C → rt.

Alternatively, a McMurry cross-coupling metathesis reaction[241] of the commercially available ferroaldehyde **309** and 3,4-dihydroisochromene carbaldehyde ***trans*-364** could deliver the same ferrocenyl 3,4-dihydroisochromene ***trans*-367** as shown in the retrosynthetic analysis **Scheme 4.2**.



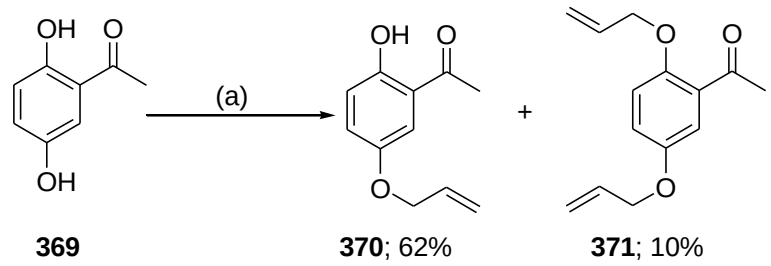
Scheme 4.2: Retrosynthetic analysis for the synthesis of ferrocenyl 3,4-dihydroisochromene ***trans*-367**.

As explained above, the 3,4-dihydroisochromene ***trans*-364** was constructed using the protocol previously developed in our laboratory starting from the commercially available 2,5-dihydroxyacetophenone **369**.[119]

4.1 Synthesis of 6-ferrocenyl-(±)-*trans*-3,4-dihydro-5,8-dimethoxy-1,3-dimethyl-6-vinyl-1*H*-isochromene *trans*-367

4.1.0 Synthesis of 1-(5-allyloxy-2-methoxyphenyl)ethanone 370

The first step towards the synthesis of intermediate ***trans*-364** was the monoallylation of 2,5-dihydroxyacetophenone **369** using allyl bromide and potassium carbonate as shown in **Scheme 4.3**. The starting material **369** was dissolved in acetone in a round bottom flask to which allyl bromide and potassium carbonate were added and the reaction mixture was heated to reflux for 24 hours under high dilution conditions. The solvent was removed *in vacuo* and the crude product was purified by column chromatography on silica gel yielding monoallyloxy phenol **370** as the major product in 62% yield.

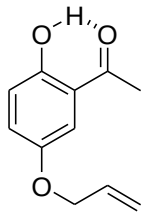


369 **370**; 62% **371**; 10%

Scheme 4.3: *Reagents and conditions:* (a) allyl bromide, K_2CO_3, Me_2CO, reflux, 24 hrs.

The phenol **370** was analysed using the ^{1}H NMR spectrum which showed a D_2O exchangeable signal at 11.86 ppm (1H, s) corresponding to the proton of the hydrogen bonded phenol group (**Figure 4.0**). The inner vinylic proton ($ArOCH_2C\mathit{H}=CH_2$) of the allyl group showed a multiplet signal between 6.13-5.98 ppm (1H, m). The doublet of quartets proton signal at 5.42 ppm (1H, dq, J = 17.3, 1.5 Hz) was assigned to one of the terminal vinylic proton ($ArOCH_2CH=C\mathit{H}_2$) which was in *trans* position to the inner vinylic proton with a *trans*-coupling constant of J = 17.3 Hz. The second doublet of quartets proton signal at 5.31 ppm (1H, dq, J = 10.5, 1.3 Hz) was assigned to the remaining terminal vinylic proton ($ArOCH_2CH=C\mathit{H}_2$) which was in *cis* position to the inner vinylic proton with a *cis*-coupling constant of J = 10.5 Hz. The allylic protons ($ArOC\mathit{H}_2CH=CH_2$) of the allyl side chain showed a doublet of triplets signal at 4.52 ppm (2H, dt, J = 5.3, 1.4 Hz). The ^{13}C NMR spectrum showed two new signals in the aromatic/alkene region and the signals were ascribed to the two alkene carbon atoms. The new carbon signal at 69.8 ppm was assigned to the *O*-

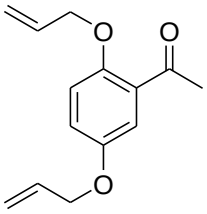
allylic carbon atom of the allyl group. These results confirmed that the monoallylation of the hydroquinone **369** was successful.



370

Figure 4.0: The molecular structure of monoallyloxy phenol **370** highlighting hydrogen bonding.

The minor product which was obtained in a modest yield of 10% was identified as a diallyl ether **371** (**Figure 4.1**) on the basis of the ^{1}H NMR spectrum. The diallyl ether **371** essentially had the same R_f value as the monoallyloxy phenol **370** but showed a blue spot under UV-light which appeared slightly above the yellow spot of the monoallyloxy phenol **370**. A substantial amount of the starting material was recovered and we noted that attempts to push this reaction to completion by addition of more allyl bromide only resulted in increased percentage yield of the diallyl ether **371**.

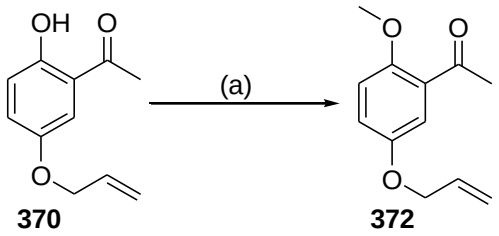


371

Figure 4.1: The molecular structure of diallyl ether **371** which cannot form hydrogen bonding.

The ^{1}H NMR spectrum of diallyl ether **371** did not show a D_2O exchangeable signal corresponding to the hydrogen bonded proton which was at 11.86 ppm in monoallyloxy phenol **370**. The multiplet signal between 6.15-5.94 ppm (2H, m) corresponded to two inner vinylic protons of two allyl ether groups (doubled in comparison to **370**). The remaining vinylic proton signals at 5.43 ppm (1H, dd, J = 5.4, 1.6 Hz), 5.38 ppm (1H, dd, J = 5.4, 1.6 Hz) and 5.34-5.22 ppm (2H, m) which integrated to a total of four protons were assigned to the terminal vinylic protons of the two allyl groups.

Satisfied that we had obtained the monoallyloxy phenol **370** the next step was methylation of the remaining phenol group. This was achieved by refluxing a solution of phenol **370** in acetone with dimethyl sulfate and potassium carbonate for 72 hours which delivered allyl ether **372** in 82% yield as shown in **Scheme 4.4**.



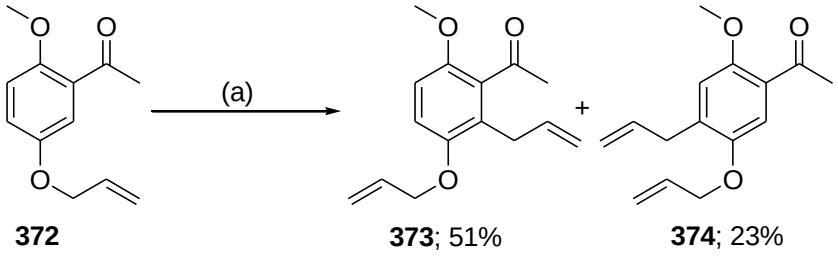
Scheme 4.4: *Reagents and conditions:* (a) Me_2SO_4, K_2CO_3, Me_2CO, reflux, N_2 (g), 72 hrs, 82%.

The identity of the product **372** was confirmed by the ^{1}H NMR spectrum which revealed loss of a signal at 11.86 ppm corresponding to the loss of the phenolic proton. The spectrum further showed a new singlet signal at 3.83 ppm (3H, s) corresponding to the methoxy protons bonded to the aromatic ring. Additionally, the ^{13}C NMR spectrum showed a signal at 56.3 ppm which corresponded to the methoxy carbon atom. At this point we were ready to carry out the Claisen rearrangement reaction and we followed the neat protocol we used in the synthesis of 5-methoxy-3,4-dehydroxanthomegnin **34** and dehydroherbarin lactone **159** as explained before.

4.1.1 Synthesis of 1-(2-allyl-3-(allyloxy)-6-methoxyphenyl)ethanone 373 and 1-(4-allyl-5-(allyloxy)-2-methoxyphenyl)ethanone 374

The thermal Claisen rearrangement was achieved by loading a neat sample of allyl ether **372** in a round bottom flask which was then heated to 170 ^{o}C in a silicon oil bath under a constant flow of dry nitrogen gas (**Scheme 4.5**). The temperature of the reaction was maintained by allowing a constant flow of water through a condenser which was connected to the reaction vessel. The progress of the reaction was followed by TLC and the development of two spots with lower R_f values than the starting material corresponding to the *C*-2-allylation and *C*-4-allylation products was noted. The crude product was passed through a short silica gel column to remove the tar after which the phenol intermediates were subjected to the same allylation protocol yielding two constitutional isomers **373** and **374** in 51% and 23% yields

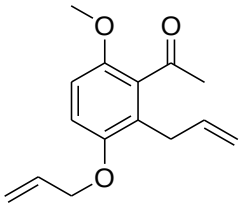
over two steps (Claisen rearrangement and allylation reactions), respectively. The isolation of the two constitutional isomers was surprising because they appeared as two close spots on the TLC plate but were easily separated on flash silica gel column chromatography.



372 **373**; 51% **374**; 23%

Scheme 4.5: *Reagents and conditions:* (a) (i) 170 °C, N_2 (g), 24 hrs (ii) allyl bromide, K_2CO_3, Me_2CO, N_2 (g), reflux, 24 hrs.

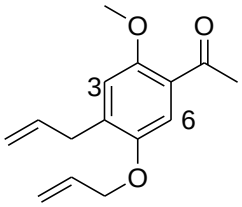
The ^{1}H NMR spectrum of allyl ether **373** showed two separate signals at 6.81 ppm (1H, d, *J* = 8.9 Hz) and 6.71 ppm (1H, d, *J* = 8.9 Hz) of doublet multiplicity with a typical *ortho*-coupling constant of *J* = 8.9 Hz corresponding to two aromatic protons *ortho* to each other. The multiplet signal between 6.12-5.77 ppm (2H, m) corresponded to the two separate inner vinylic protons of the *O*-allyl and *C*-allyl groups ($ArOCH_2CH{=}CH_2$ and $ArCH_2CH{=}CH_2$). The signal observed at 5.39 ppm (1H, dq, *J* = 17.3, 1.6 Hz) corresponded to the terminal vinylic proton of the allyl ether group ($ArOCH_2CH{=}CH_2$) which was in a *trans* position to the inner vinylic proton with a *trans*-coupling constant of *J* = 17.3 Hz whereas the signal observed at 5.24 ppm (1H, dq, *J* = 10.1, 1.0 Hz) corresponded to the remaining terminal vinylic proton of the allyl ether group which was in a *cis* position to the inner vinylic proton with a *cis*-coupling constant of *J* = 10.1 Hz. The signal due to the terminal vinylic protons of the *C*-allyl group ($ArCH_2CH{=}CH_2$) was observed between 5.05-4.85 ppm (2H, m). The signals observed at 4.48 ppm (2H, dt, *J* = 4.9, 1.6 Hz) and 3.35 ppm (2H, d, *J* = 6.3 Hz) were characteristic of allylic protons for *O*-allyl and *C*-allyl groups and were assigned as such, respectively. The ^{13}C NMR spectrum confirmed a successful Claisen rearrangement reaction by showing one new signal at 32.5 ppm corresponding to a *C*-allyl carbon atom ($ArCH_2CH{=}CH_2$). This signal was not present in the starting material.



373

The major difference which was noted between the two compounds was that the aromatic proton signals in allyl ether **373** coupled to each other as explained above whereas the aromatic proton signals of allyl ether **374** showed no coupling between them.

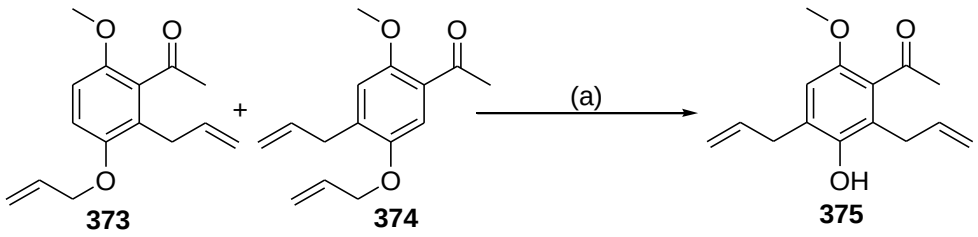
The ^{1}H NMR spectrum of allyl ether **374** showed two singlet signals at 7.31 ppm (1H, s) and 6.79 ppm (1H, s) corresponding to the two aromatic protons. The proton signal at 7.31 ppm corresponded to a highly deshielded proton which was *ortho* to the acetyl group of the ring (H-6). This proton was highly deshielded due to the anisotropic effect generated by the carbonyl functional group of the acetyl substituent. The signal at 6.79 ppm was assigned to the H-3 proton. The other signals were similar to the signals of allyl ether **373**.



374

4.1.2 Synthesis of 1-(2,4-diallyl-3-hydroxy-6-methoxyphenyl)ethanone 375

The typical thermal Claisen rearrangement reaction of the two allyl ethers **373** and **374** afforded the envisaged double *C*-allyl phenol **375** (**Scheme 4.6**) in 71% yield.

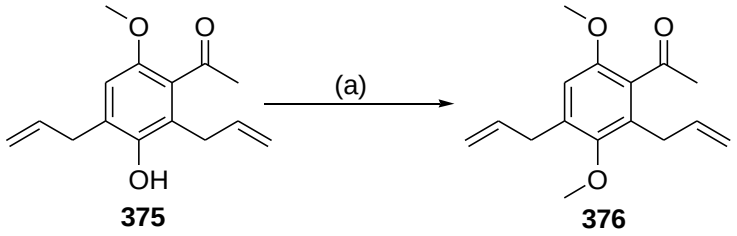


Scheme 4.6: *Reagents and conditions:* (a) 170 °C, N_2 (g), 24 hrs, 71%.

The ^{1}H NMR spectrum of the phenol **375** was largely identified by the presence of the D_2O exchangeable signal at 4.90 ppm (1H, s) corresponding to the phenol proton and the loss of one aromatic proton in the spectrum. The ^{13}C NMR spectrum revealed loss of the signals at 69.8 ppm and 69.4 ppm in the two precursor allyl ethers which were assigned to the *O*-allylic carbon atoms and the emergence of a new signal corresponding to the *C*-allylic carbon atom at 35.9 ppm. These results confirmed successful rearrangement of the *O*-allyl group to a *C*-allyl group.

4.1.3 Synthesis of 1-(2,4-diallyl-3,6-dimethoxyphenyl)ethanol 377

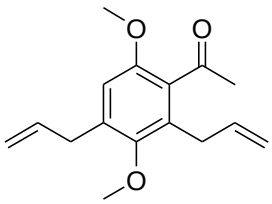
The next step in the sequence of reactions was the methylation of the diallyl phenol **375** which was achieved by heating the diallyl phenol **375** to reflux in acetone with dimethyl sulfate and potassium carbonate for 24 hours, which afforded dimethoxy phenol **376** (**Scheme 4.7**) as a colourless oil in 87% yield.



375 **376**

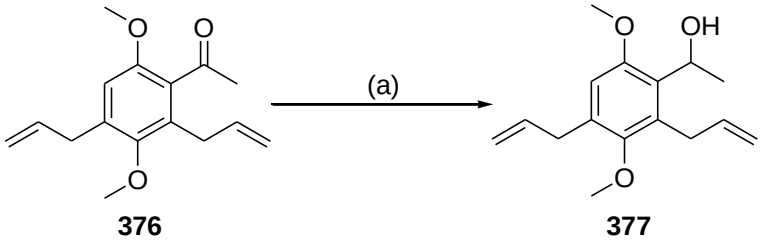
Scheme 4.7: *Reagents and conditions:* (a) Me_2SO_4, K_2CO_3, Me_2CO, N_2 (g), reflux, 24 hrs, 87%.

The ^{1}H NMR spectrum revealed loss of a signal at 4.90 ppm which was ascribed to the phenol proton in the precursor compound **375**. It further showed two singlet signals at 3.78 ppm and 3.68 ppm which integrated for 3 protons each and were assigned to the two methoxy protons bonded to the aromatic ring. One of the two signals was not observed in the precursor compound. The ^{13}C NMR spectrum showed two signals at 61.5 ppm and 55.8 ppm corresponding to two methoxy groups, one of which was for the new methoxy group. The product showed a higher R_f value compared to the starting material. These results confirmed the successful synthesis of diallyl acetophenone **376**.



376

Satisfied that we had obtained the intended double methylated *C*-allyl acetophenone **376** we decided to transform the carbonyl functional group of this ketone into an alcohol functional group. The acetophenone **376** was dissolved in freshly distilled dry tetrahydrofuran in a 2-neck round bottom flask which was under a constant flow of dry nitrogen gas. Lithium aluminium hydride was added to the reaction flask in two portions at 0 ^{o}C. The reaction mixture was then allowed to warm to room temperature and kept stirring for 4 hours. The reaction was quenched with cold water and purification of the crude reaction mixture by column chromatography on silica gel afforded the alcohol **377** as a viscous pale yellow oil in 71% yield as shown in **Scheme 4.8**.



376 **377**

Scheme 4.8: *Reagents and conditions:* (a) $LiAlH_4$, THF, N_2 (g), 0 $^oC \rightarrow$ rt, 4 hrs, 71%.

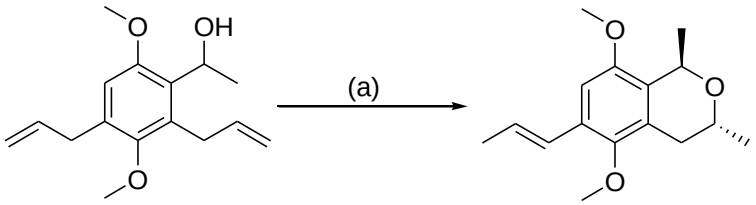
The ^1H NMR spectrum showed the presence of a quartet as part of the multiplet signal between 5.17-4.90 ppm (5H, m) which was assigned to the benzylic proton of the hydroxyethyl group (ArC*H*(OH)CH_3) and 2 pairs of the terminal vinylic protons (2 × $ArCH_2CH=CH_2$). The doublet signal at 1.52 ppm (3H, d, J = 6.7 Hz) was assigned to the terminal methyl protons of the hydroxyethyl group (ArCH(OH)CH_3). The ^{13}C NMR spectrum revealed loss of a signal at 199.3 ppm which was assigned to the carbonyl functional group carbon atom in the precursor compound **376** and the appearance of a signal at 67.3 ppm was characteristic of a benzylic hydroxymethylene group. The IR spectrum showed loss of a peak at 1715 cm^{-1} which was assigned to the carbonyl functional group in the precursor compound **376** and appearance of the peak at 3570 cm^{-1} which was assigned to the benzylic alcohol functional group of compound **377**. These results proved beyond reasonable doubt that we successfully reduced the ketone functional group of acetophenone **376** to the alcohol functional group.

At this point, we were satisfied with the progress that was made and we were ready to attempt one of the major steps towards the synthesis of an important intermediate, 3,4-dihydroisochromene carbaldehyde ***trans*-364**.

4.1.4 Synthesis of (±)-*trans*-3,4-dihydro-5,8-dimethoxy-1,3-dimethyl-6-[(*E*)-1-propenyl]-1*H*-isochromene 378

The alcohol **377** was dissolved in *N*-methylpyrrolidinone (NMP) and heated to 110 ^oC in an oil bath after which excess pure solid potassium *tert*-butoxide was added at that temperature and the reaction mixture was heated to reflux for a further 30 minutes. Thereafter, the reaction was quenched with cold water and the bulk of *N*-methylpyrrolidinone was distilled off under reduced pressure. Purification of the crude product by flash silica gel column

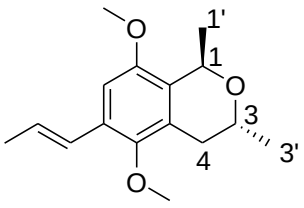
chromatography afforded propenyl 3,4-dihydroisochromene ***trans*-378** (**Scheme 4.9**) as colourless crystals in 63% yield. The double bond (propenyl substituent) on the other side of the 3,4-dihydroisochromene isomerized into a more stable styrene derivative as confirmed by the ^{1}H NMR spectrum.



377 ***trans*-378**

Scheme 4.9: *Reagents and conditions:* (a) *t*-BuOK, NMP, 110 °C, 30 min, 63%.

The ^{1}H NMR spectrum showed two separate doublet of quartets at 6.65 ppm (1H, dq, J = 15.9, 1.6 Hz) and 6.21 ppm (1H, dq, J = 15.9, 6.6 Hz) corresponding to the inner propenylic proton (ArC*H*=CHCH$_3$) and outer propenylic proton (ArCH=C*H*CH$_3$), respectively, which was indicative of the isomerization of one of the double bonds present in the starting material. The coupling constant between the two alkene protons was measured at J = 15.9 Hz which was indicative of *trans* configuration. The inner propenylic proton showed long range coupling to the ArCH=CHC*H*$_3$ protons with a small coupling constant of J = 1.6 Hz compared to the coupling constant of the outer propenylic proton which was measured at J = 6.6 Hz. A quartet signal at 5.06 ppm (1H, q, J = 6.5 Hz) and a multiplet signal between 4.13-3.95 ppm (1H, m) corresponded to H-1 and H-3 protons, respectively. The multiplet signal at 4.13-3.95 ppm was indicative of the *trans*-configuration of the 1,3-dimethylpyran system.[242] The proton signals at 2.83 ppm (1H, dd, J = 16.8, 3.2 Hz) and 2.38 ppm (1H, dd, J = 16.8, 10.8 Hz) were assigned to the H-4 *pseudo*-equatorial proton and H-4 *pseudo*-axial proton, respectively. These signals further confirmed the cyclic nature of the product because the two protons of the pyran ring system cannot interchange their positions due to the rigid nature of the ring and hence resonated at different magnetic fields. The proton signal at 1.91 ppm (3H, dd, J = 6.6, 1.6 Hz) was assigned to the methylinic protons (ArCH=CHC*H*$_3$) of the propenyl side chain. Lastly, the

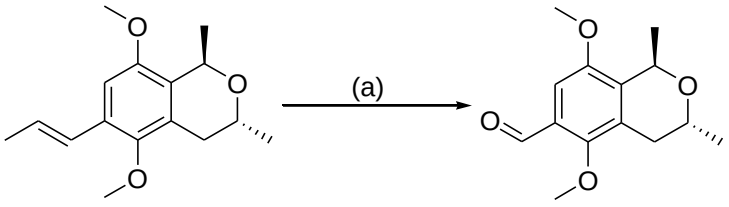


***trans*-378**

proton signals at 1.49 ppm (3H, d, *J* = 6.6 Hz) and 1.33 ppm (3H, d, *J* = 6.1 Hz) were assigned to the methylinic protons H-1' and H-3', respectively. Additionally, the ^{13}C NMR spectrum revealed loss of two signals in the aromatic/alkene region of the spectrum corresponding to loss of the double bond on the side where the pyran ring was formed. Finally, the IR spectrum showed loss of the peak at 3570 cm^{-1} which was present in the starting material corresponding to loss of the alcohol functional group. These results confirmed that we had successfully synthesized propenyl 3,4-dihydroisochromene ***trans*-378** and the next step was to attempt oxidation of the alkene double bond and Wittig reaction of the resultant aldehyde.

4.1.5 Synthesis of (±)-*trans*-3,4-dihydro-5,8-dimethoxy-1,3-dimethyl-6-vinyl-1*H*-isochromene

Two different methods were used to oxidise the alkene double bond of the 3,4-dihydroisochromene ***trans*-378** as shown in the reaction **Scheme 4.10**.



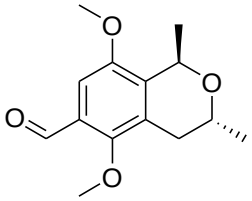
***trans*-378** ***trans*-364**

Scheme 4.10: *Reagents and conditions:* **Method one** (a) (i) O_3 (g), CH_2Cl_2, -78 °C (ii) N_2 (g), $(CH_3)_2S$, 68%; **Method two:** (a) cat. OsO_4, $NaIO_4$, H_2O, 1,4-dioxane, N_2 (g), rt, 13 hrs, 84%.

In the first protocol, the propenyl 3,4-dihydroisochromene ***trans*-378** was dissolved in dry dichloromethane in a round bottom flask to which 3 drops of Sudan (III) indicator was added. The reaction flask was cooled to -78 ^oC and ozone was bubbled through the reaction in an open flask until the indicator changed from a pink colour to colourless. Excess ozone was purged by passing dry nitrogen gas through the reaction vessel after which the reaction mixture was again cooled to -78 ^oC and treated with dimethyl sulfide. Column chromatography of the crude product afforded 3,4-dihyroisochromene carbaldehyde ***trans*-364** as cream-white fluffy needles in 68% yield.

In the second method, a mixture of a catalytic amount of osmium (VIII) oxide and propenyl 3,4-dihydroisochromene ***trans*-378** in 1,4-dioxane was stirred at room temperature for 30 minutes after which water and sodium periodate were added. The reaction mixture was stirred at room temperature for a further 12.5 hours and purification of the crude product by silica gel column chromatography afforded 3,4-dihyroisochromene carbaldehyde ***trans*-364** in 84% yield.

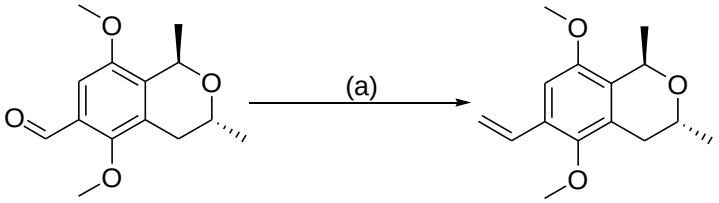
The presence of an aldehyde functional group was confirmed by ^{1}H NMR spectroscopy which showed a singlet signal at 10.32 ppm (1H, s) for the aldehyde proton with a corresponding signal at 189.4 ppm in the ^{13}C NMR spectrum for the carbonyl carbon atom. The ^{1}H and ^{13}C NMR spectra further revealed loss of proton and carbon signals corresponding to the alkene double bond and the methyl group of the propenyl side chain which were present in the precursor compound ***trans*-378**. All the signals corresponding to the pyran and aromatic rings were accounted for confirming that there was no oxidation of the aromatic ring which is sometimes possible during ozone mediated oxidation of alkene double bonds with an aromatic moiety.[243]



***trans*-364**

The spectroscopic data did not show any sign of epimerization of the pyran ring methyl groups. Lastly, the IR spectrum showed peaks at 2870 and 1685 cm^{-1} corresponding to aldehydic bond (O=C-H) and carbonyl functional group, respectively.

Having successfully synthesized intermediate ***trans*-364** we decided to transform part of this material into a vinyl 3,4-dihydroisochromene ***trans*-365** with the aim of performing the Grubbs cross-metathesis reaction with vinyl ferrocene **366**. This transformation was achieved by use of the Wittig reaction as shown in **Scheme 4.11**. A solution of 3,4-dihyroisochromene carbaldehyde ***trans*-364** was added to a round bottom flask containing a freshly made ylide and the mixture was stirred at room temperature for 18 hours. The crude product was purified by column chromatography on flash silica gel which afforded vinyl 3,4-dihydroisochromene ***trans*-365** in a high yield of 82%.

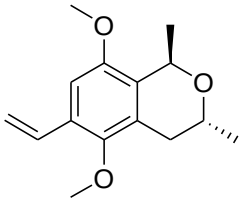


***trans*-364** ***trans*-365**

Scheme 4.11: *Reagents and conditions:* (a) MTPPBr, *n*-BuLi, THF, 0 ^{o}C → rt, 18 hrs, 82%.

The identity of the product was confirmed by both the ^{1}H and ^{13}C NMR spectroscopy. There was loss of a signal at 10.32 ppm in the ^{1}H NMR spectrum and the signal at 189.4 ppm in the ^{13}C NMR spectrum which were present in the starting material, implying the absence of the aldehyde group. Another notable feature was the appearance of new signals in the alkene/aromatic regions in both ^{1}H and ^{13}C NMR spectra.

A doublet of doublets signal at 6.99 ppm (1H, dd, J = 17.7, 11.1 Hz) in the ^{1}H NMR spectrum corresponded to the inner vinylic proton of the vinyl group (ArC*H*=CH_2) with coupling constants of J = 17.7 and 11.1 Hz indicating both *trans*- and *cis*-coupling to the terminal vinylic protons. A second doublet of doublets signal at 5.71 ppm (1H, dd, J = 17.7, 1.3 Hz) was assigned to one of the terminal vinylic protons (ArCH=CH_2) which was in *trans* position to the inner vinylic proton with a coupling constant of J = 17.7 Hz and a *geminal* coupling constant of J = 1.3 Hz. A third new signal in the alkene/aromatic region which appeared again as a doublet of doublets at 5.27 ppm (1H, dd, J = 11.1, 1.3 Hz) was assigned to the remaining terminal vinylic proton which was in a *cis* position relative to the inner vinylic proton with a typical *cis*-coupling constant of J = 11.1 Hz and a *geminal* coupling constant of J = 1.3 Hz. The corresponding signals at 131.7 ppm and 114.2 ppm in the ^{13}C NMR spectrum were assigned to the alkene carbon atoms.

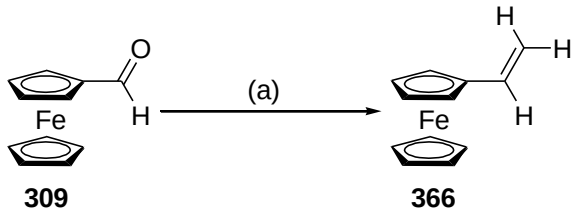


***trans*-365**

The IR spectrum revealed loss of the peak at 1685 cm^{-1} corresponding to the loss of the carbonyl functional group in the precursor compound and the new peak at 1595 cm^{-1} was attributed to the alkene functional group. The HRMS showed a molecular ion peak at 249.1487 amu which was in good agreement with the expected mass of 249.1485 amu for $C_{15}H_{21}O_3$.

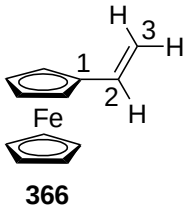
4.1.6 Synthesis of vinyl ferrocene 366

The next step was the transformation of the commercially available ferroaldehyde **309** to vinyl ferrocene **366** which was successfully achieved using the same Wittig protocol[240] as shown in reaction **Scheme 4.12**.



Scheme 4.12: *Reagents and conditions:* (a) MTPPBr, *n*-BuLi, THF, 0 ^{o}C → rt, 4 hrs, 85%.

The ^{1}H NMR spectrum showed a doublet of doublets signal at 6.43 ppm (1H, dd, J = 17.4, 10.8 Hz) which was consistent with H-2 proton. A doublet signal at 5.32 ppm (1H, d, J = 17.5 Hz) was assigned to one of the H-3 protons which was in *trans* position to the H-2 proton with a typical *trans*-coupling constant of J = 17.5 Hz and the last doublet signal at 5.01 ppm (1H, d, J = 10.6 Hz) was assigned to the remaining H-3 proton which was in a *cis* position to the H-2 proton with a typical *cis*-coupling constant of J = 10.6 Hz. The broad singlet signals at 4.34 ppm (2H, br s), 4.19 ppm (2H, br s) and 4.09 ppm (5H, br s) were assigned to the ferrocene protons. The ^{13}C NMR spectrum showed signals at 134.8 ppm and 111.2 ppm which were consistent with the alkene carbon atoms whereas the signal at 83.7 ppm was assigned to C-1. The spectroscopic data were in agreement with the spectroscopic data of vinyl ferrocene available on the Sigma Aldrich website as accessed on November 14, 2017.[244]

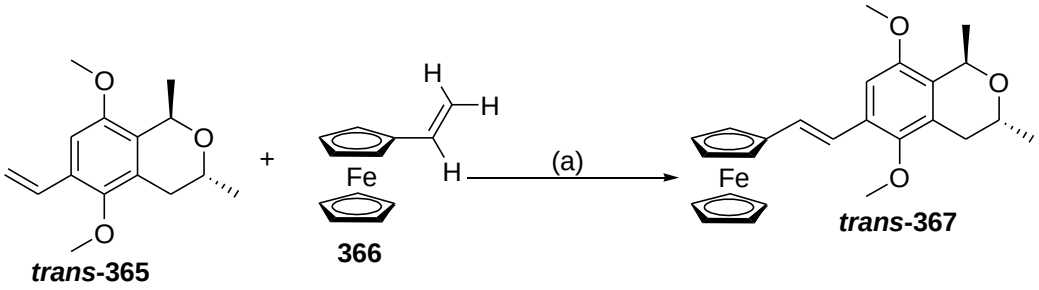


366

4.1.7 Synthesis of ferrocenyl (±)-*trans*-3,4-dihydro-5,8-dimethoxy-1,3-dimethyl-6-vinyl-1*H*-isochromene *trans*-367

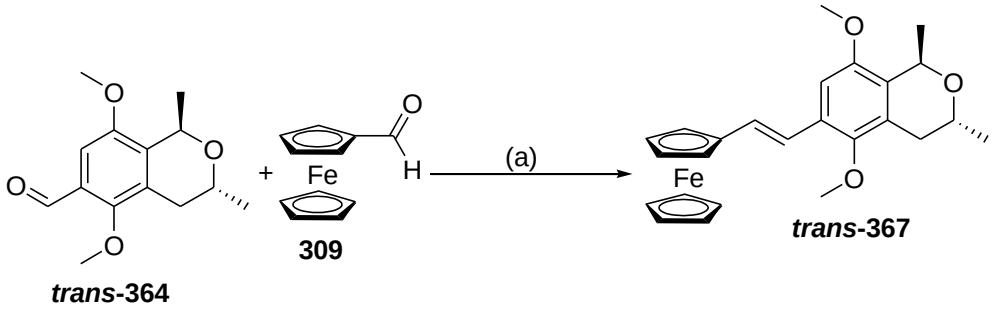
Having the two sets of intermediates in our hands we were at this stage ready to carry out the coupling reactions using Grubbs[239] and McMurry[241] cross-metathesis reactions for alkenes (***trans*-365** and **366**) and aldehydes (***trans*-364** and **309**), respectively. In the first protocol using Grubbs cross-metathesis reaction (**Scheme 4.13**), alkenes ***trans*-365** and **366** were

dissolved in dichloromethane in a round bottom flask to which Grubbs II catalyst was added while stirring the solution. The reaction mixture was heated to reflux for 18 hours under a blanket of nitrogen gas atmosphere. The reaction mixture was then cooled to room temperature and the solvent was removed *in vacuo*. Purification of the crude product by silica gel column chromatography afforded ferrocenyl 3,4-dihydroisochromene ***trans*-367** in 59% yield.



Scheme 4.13: *Reagents and conditions:* (a) Grubbs II, CH_2Cl_2, reflux, 59%.

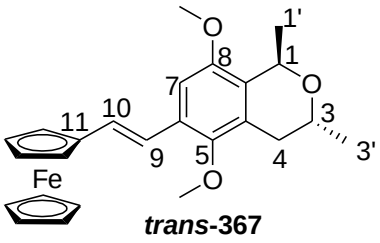
In the second methodology, a McMurray cross-coupling metathesis reaction (**Scheme 4.14**) was used to achieve coupling of ferroaldehyde **309** and 3,4-dihydroisochromene carbaldehyde ***trans*-364**. In this protocol, titanium tetrachloride was added to a suspension of zinc powder and the resultant mixture was heated to reflux for 2 hours. A solution of ferroaldehyde **309** and 3,4-dihydroisochromene carbaldehyde ***trans*-364** was then added to the reaction mixture and heated to reflux for a further 12 hours. Purification of the crude product by column chromatography on silica gel afforded ferrocenyl 3,4-dihydroisochromene ***trans*-367** in 70% yield.



Scheme 4.14: *Reagents and conditions:* (a) $TiCl_4$, Zn, THF, 12 hrs, 70%

Surprisingly, the McMurry cross-coupling reaction which we had initially thought would present us with challenges owing to the nature of the reagents afforded better yields of 70% compared to 59% that was obtained using the Grubbs cross-metathesis reaction.

The ^{1}H NMR spectrum showed two separate doublet signals at 6.50 ppm (1H, d, J = 11.9 Hz) and 6.37 ppm (1H, d, J = 11.9 Hz) and were assigned to H-10 and H-9 protons, respectively.



***trans*-367**

A quartet signal at 5.05 ppm (1H, q, J = 6.5 Hz) was consistent with the H-1 proton whereas a multiplet signal between 4.27-3.99 ppm (10H, m) was consistent with the 9 ferrocene protons and H-3 proton. The two singlet signals at 3.77 ppm (3H, s) and 3.54 ppm (3H, s) were typical of the methoxy protons of the aromatic ring. Furthermore, the two doublet of doublets signals at 2.86 ppm (1H, dd, J = 16.9, 3.2 Hz) and 2.42 ppm (1H, dd, J = 17.0, 10.8 Hz) were assigned to the H-4 protons and these signals were used to confirm that the 3,4-dihydroisochromene ring system maintained the same *pseudo*-chair conformation which was present in 3,4-dihydroisochromenes ***trans*-364** and ***trans*-365**. Finally, the two separate doublet signals at 1.50 ppm (3H, d, J = 6.6 Hz) and 1.36 ppm (3H, d, J = 6.1 Hz) were typical of the two methyl groups bonded to the pyran ring at *C*-3 and *C*-1 and were assigned to H-3' and H-1' protons, respectively.

To further confirm successful coupling of the two alkenes (and aldehydes), we thought that direct comparison of spectra for ferrocenyl 3,4-dihydroisochromene ***trans*-367** with the two individual starting alkenes (***trans*-365** and **366**) was significant as shown in **Figure 4.3**. What was of note was the presence of the pyran ring and ferrocene protons in the coupled product.

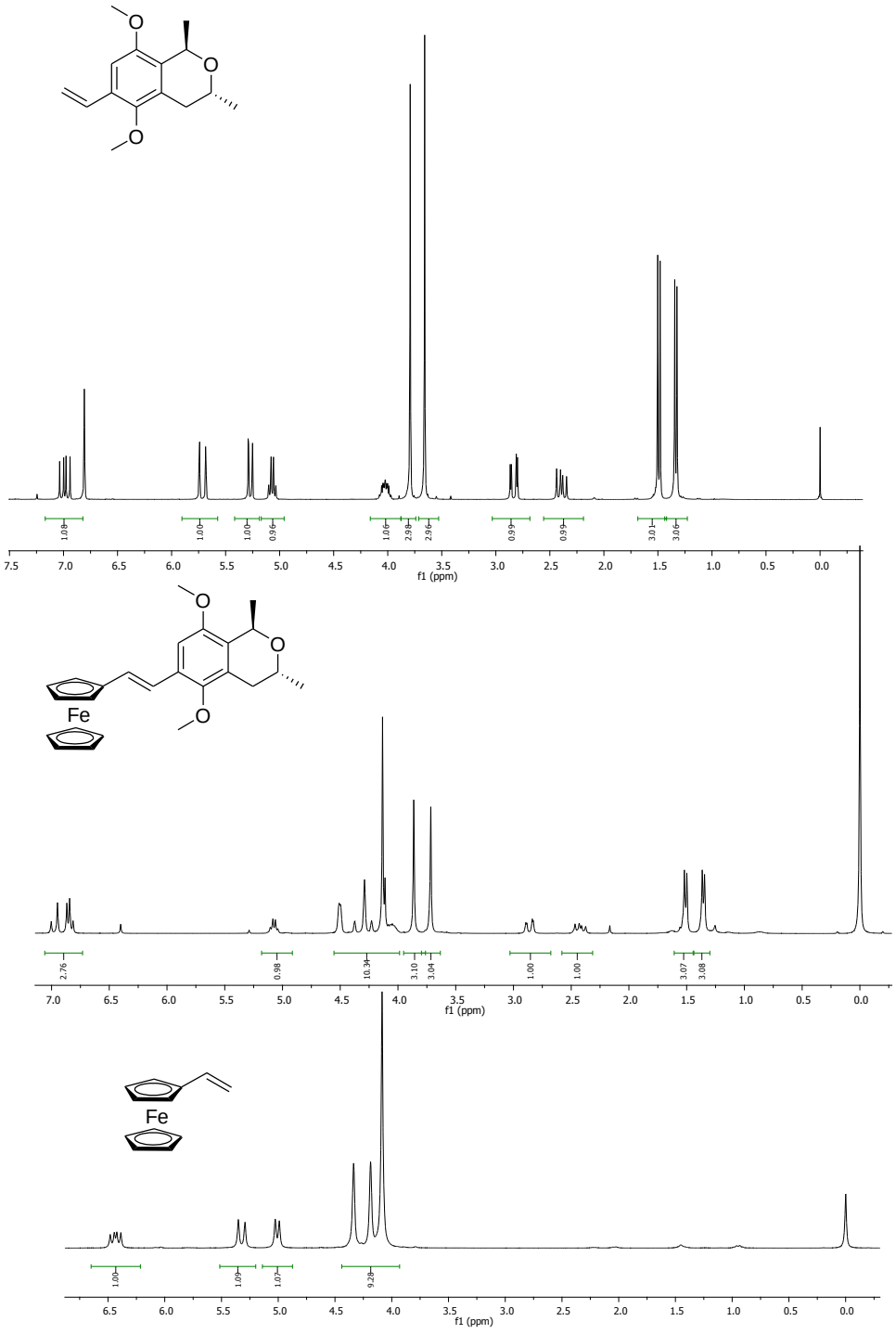


Figure 4.3: The ^{1}H NMR spectra of vinyl 3,4-dihydroisochromane ***trans*-365**, ferrocenyl 3,4-dihydroisochromene ***trans*-367** and vinyl ferrocene **366**.

Comparison of the ^{13}C NMR spectra of the three compounds (***trans*-365**, **366** and ***trans*-367**) as shown in **Figure 4.4** below further correlated the successful coupling of the vinyl

ferrocene **366** and vinyl 3,4-dihydroisochromene ***trans*-365**. Of note was the signal at 83.7 ppm which was indicative of the ferrocene carbon atom attached to the alkene carbon atom (C-11) in the ferrocenyl 3,4-dihydroisochromene ***trans*-367** and C-1 in the vinyl ferrocene **366**. The 8 carbon signals corresponding to the aromatic/alkene protons were accounted for as were the carbon atoms of the ferrocene and pyran ring system. In addition, the HRMS showed a molecular ion peak at 433.1464 amu which was in good agreement with the expected mass of 433.1461 amu for $C_{25}H_{29}O_3Fe$.

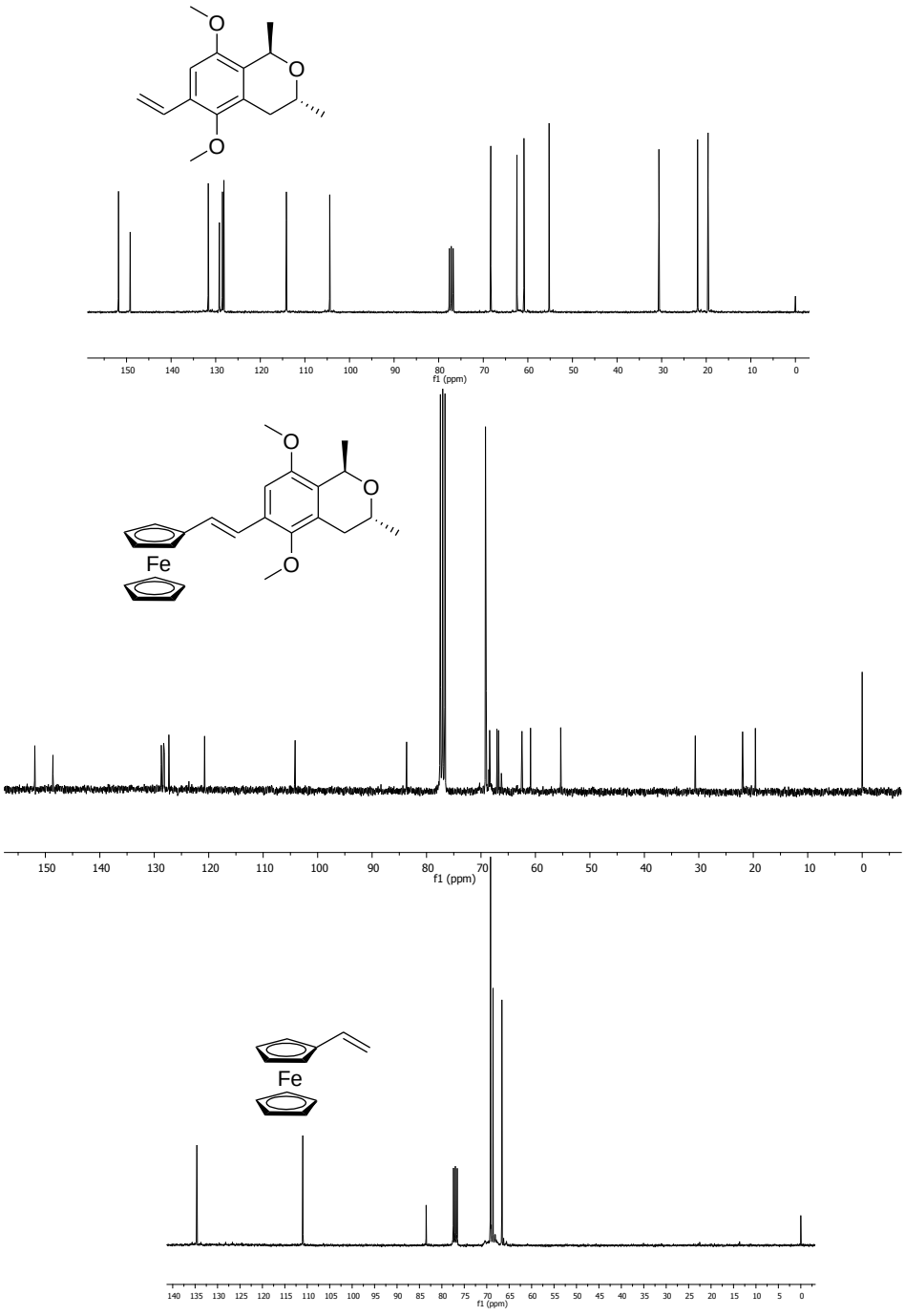
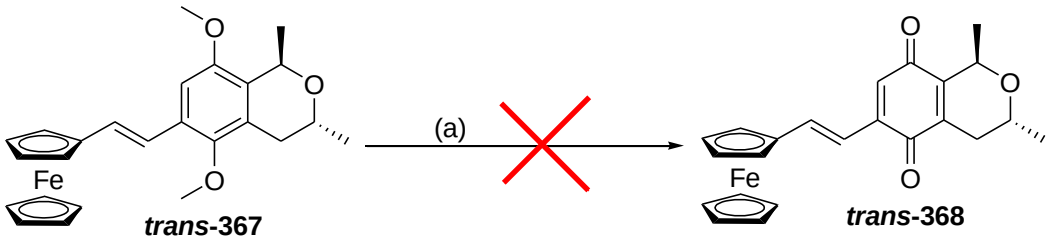


Figure 4.4: The ^{13}C NMR spectra of compounds ***trans*-365** (top), ***trans*-367** (middle) and **366** (bottom).

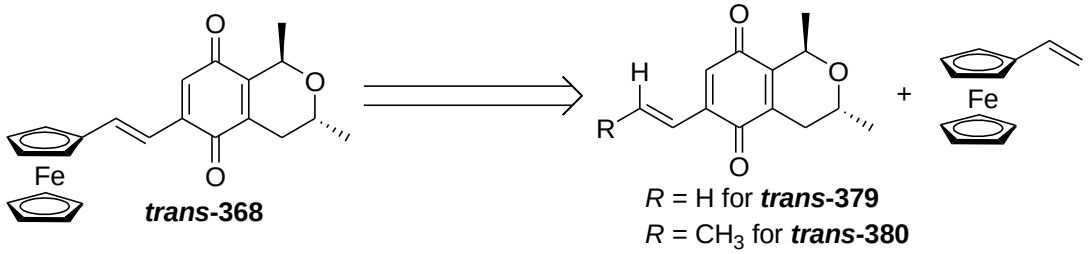
Excited by these results the stage was set for the final step which involved oxidative demethylation of the ferrocenyl 3,4-dihydroisochromene ***trans*-367**. We chose to carry out

this reaction using silver (II) oxide in the presence of nitric acid as we had successfully used this protocol in the synthesis of 5-methoxy-3,4-dehydroxanthomegnin **34**, dehydroherbarin lactone **159** and related compounds as discussed before but to our disappointment we did not isolate any identifiable product. The second reagent to be tested was the PIFA/acetonitrile/water combination which was chosen on the basis that it is generally considered a milder oxidation reagent. This system was successfully employed by Pillay[124] in our laboratory and was also used in this work as discussed in **Section 2.1.18** of **Chapter 2** but again it did not lead to isolation of the target compound, ferrocenyl pyranobenzoquinone ***trans*-368**. The CAN/acetonitrile/water oxidation methodology was also used to try to effect oxidative demethylation but this was again unsuccessful. **Scheme 4.15** shows the reagents and conditions that were employed in attempted demethylation of ferrocenyl 3,4-dihydroisochromene ***trans*-367**.



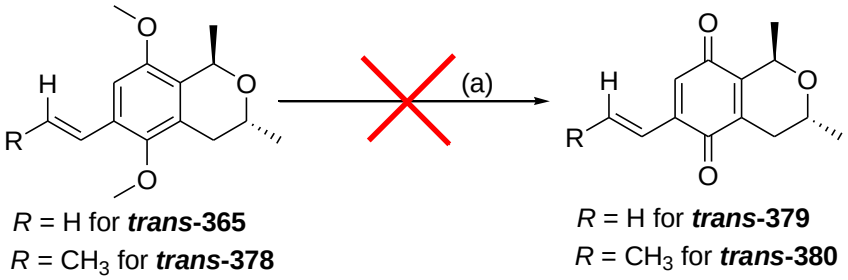
Scheme 4.15: *Reagents and conditions:* (a) AgO, *55%* aq. HNO_3, 1,4-dioxane, rt; or PIFA, CH_3CN/H_2O, rt, 25 min; or CAN, CH_3CN/H_2O, rt, 30 min.

At this point we thought that maybe even the milder oxidation conditions of PIFA/acetonitrile/water were probably too harsh which could have led to the cleavage of the labile double bond coupling the ferrocene moiety to the 3,4-dihydroisochromene resulting in decomposition of the substrate. Ferrocene is known for its electron donating effect which could make the ring extremely electron rich and controlling oxidation for such a system was probably the major challenge. To circumvent this problem we thought that the best way could be to oxidise alkenes ***trans*-365** and ***trans*-378** to the corresponding pyranobenzoquinones, ***trans*-379** and ***trans*-380**, in the hope that the Grubbs cross-metathesis reaction could deliver the final ferrocenyl pyranobenzoquinone ***trans*-368** as depicted in retrosynthetic analysis **Scheme 4.16**.



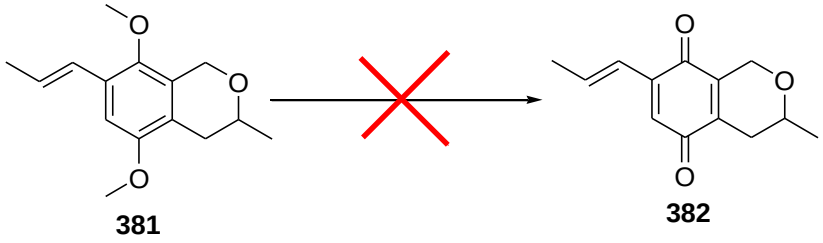
Scheme 4.16: *Reagents and conditions:* Grubbs II, toluene or CH_2Cl_2, reflux.

Subjecting both alkenes ***trans*-364** and ***trans*-378** to an array of oxidative demethylation reagents as used in attempted oxidation of the ferrocenyl 3,4-dihydroisochromene ***trans*-367** did not result in isolation of the corresponding quinones (**Scheme 4.17**). This was disappointing because it meant that the labile alkene double bond coupling the ferrocene moiety to the isochromane was not solely responsible for failure of the oxidative demethylation of ferrocenyl compound ***trans*-367**.



Scheme 4.17: *Reagents and conditions:* (a) AgO, *55%* aq. HNO_3, 1,4-dioxane, rt; or PIFA, CH_3CN/H_2O, 25 min, rt; or CAN, CH_3CN/H_2O, 30 min, rt.

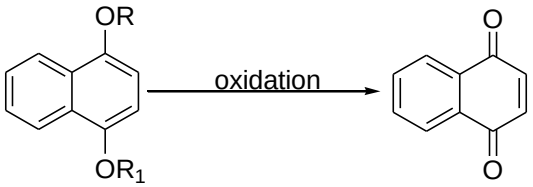
Similar results were obtained by Hugo[245] who reported that attempted oxidative demethylation of benzopyran **381** using either cerium (IV) ammonium nitrate or silver (II) oxide failed to deliver the corresponding benzoquinone **382** but instead led to decomposition of the substrate (**Scheme 4.18**).



381 **382**

Scheme 4.18: *Reagents and conditions:* (a) AgO, *55%* aq. HNO_3, 1,4-dioxane, rt; or CAN, CH_3CN/H_2O, 30 min.

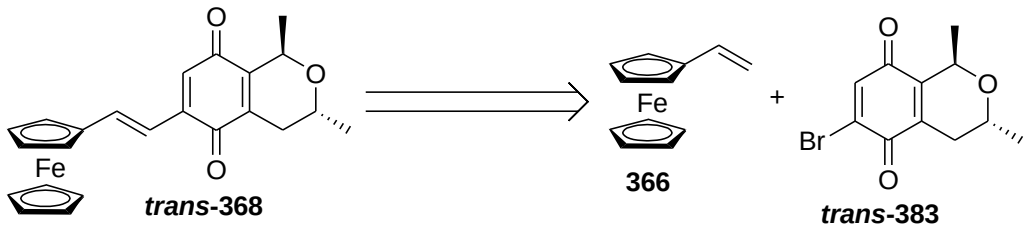
Our observation together with the results reported by Hugo[245] led us to believe that it was necessary to change the protective group strategy in favour of groups which could facilitate or at the very least not hinder the oxidation of the 2,4-dihydroisochromenes to the corresponding quinone analogues. One such strategy would be the use of a labile protecting group such as a silicon group which could deliver unprotected phenol in the penultimate step for simple air oxidation to afford the final ferrocenyl pyranobenzoquinone. Alternatively, one of the methoxy protection groups in 3,4-dihydroisochromene ***trans*-364** could be changed while maintaining the other methoxy group such that in the penultimate step we could have a phenol and methoxy group in a *para* position to each other. This is not as contradictory as it sounds because much as the hydroxyl group is expected to make the ring even more electron rich, it would also provide a selective handle for mild oxidative reagents to easily oxidise the ring into the quinone. There are literature reports of air oxidation of substrates with diphenol groups which are *para* to each other and the PIFA mediated oxidation of phenols (or naphthols) with a *para* methoxy group is shown in **Scheme 4.19**.[246]



Scheme 4.19: *Reagents and conditions:* air oxidation for *R*, R_1 = H and PIFA mediated oxidation for *R* = H and R_1 = CH_3.

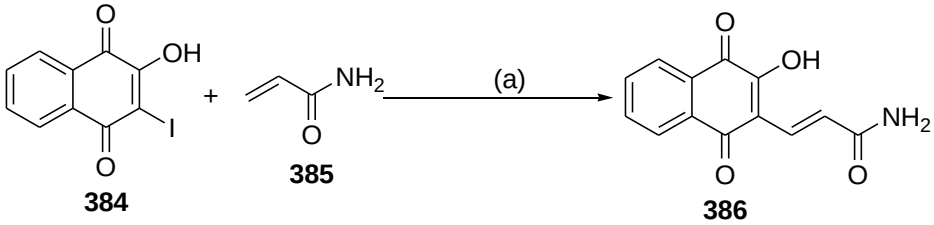
After going through the available literature we strongly felt that coupling the quinone to the ferrocene moiety at the last step offered a more promising route towards the synthesis of the

target compound ***trans*-368**. At this point we thought that intermediate ***trans*-383** could potentially be coupled to vinyl ferrocene **366** using a Heck-type cross-coupling reaction[247] as depicted in retrosynthetic analysis **Scheme 4.20**.



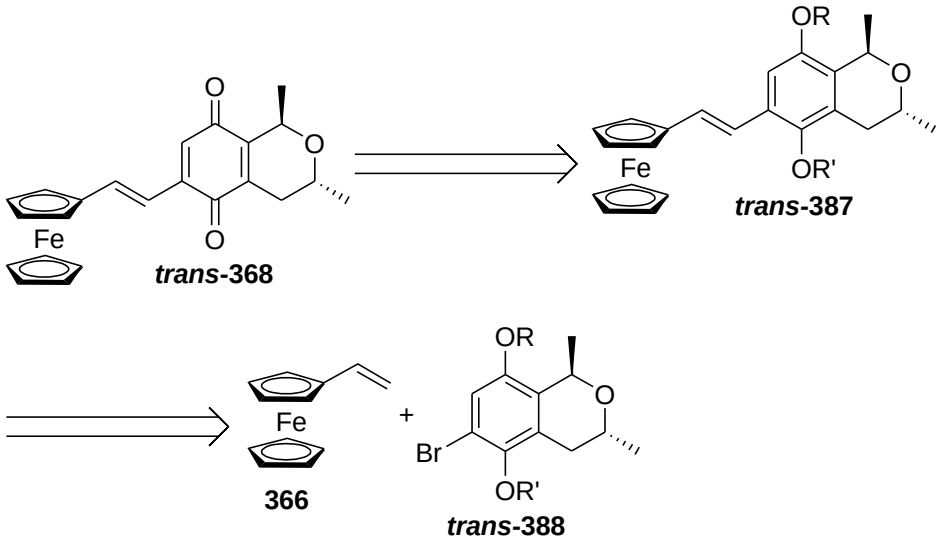
Scheme 4.20: Retrosynthetic analysis for the formation of ferrocenyl pyranobenzoquinone ***trans*-368** using Heck-type cross-coupling reaction.

There is literature precedence in which electron deficient alkenes were coupled to a quinone using a Heck-type cross-coupling reaction.[248] In all cases the products contained the *E* double bonds which, according to the authors, were clearly identifiable in the spectroscopic data and the best results were obtained when acrylamide **385** was used as a coupling partner of iodolawsone quinone **384** as shown in **Scheme 4.21**.



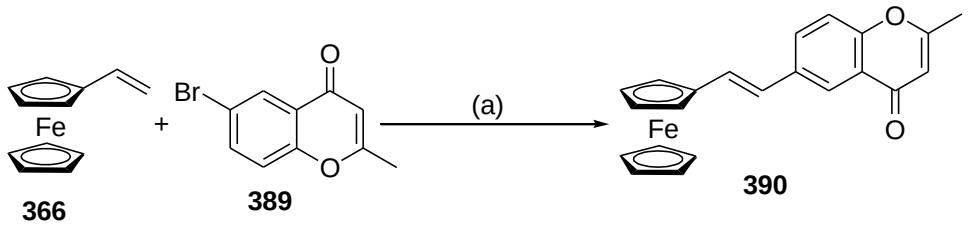
Scheme 4.21: *Reagents and conditions:* (a) cat. $Pd(OAc)_2$, K_2CO_3, H_2O, reflux.

If the coupling reaction depicted in retrosynthetic analysis **Scheme 4.20** did not work we could go one step back and attempt the coupling reaction at the penultimate stage. This could still potentially afford us an opportunity to synthesize the target compound ***trans*-368** as long as a labile protection group was used as explained above and shown in **Scheme 4.22** below.



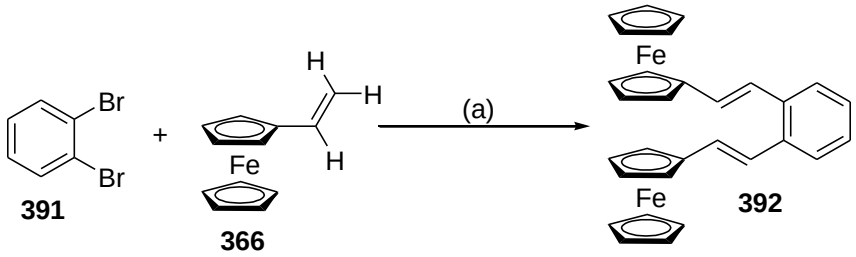
Scheme 4.22: Retrosynthetic analysis for the synthesis of the ferrocenyl pyranobenzoquinone ***trans*-368** through oxidation of ferrocenyl 3,4-dihydroisochromene ***trans*-387** with at least one labile protection group.

Again, there is literature precedence in which palladium catalysed phosphine-free Heck cross-coupling reaction of vinyl ferrocene **366** with bromochromone **389** was employed for the synthesis of ferrocenyl flavone **390** under solid-liquid phase-transfer conditions (potassium carbonate or sodium carbonate/tetrabutylammonium bromide) as shown in **Scheme 4.23**. This reaction was reported by Kowalski and co-workers.[249]



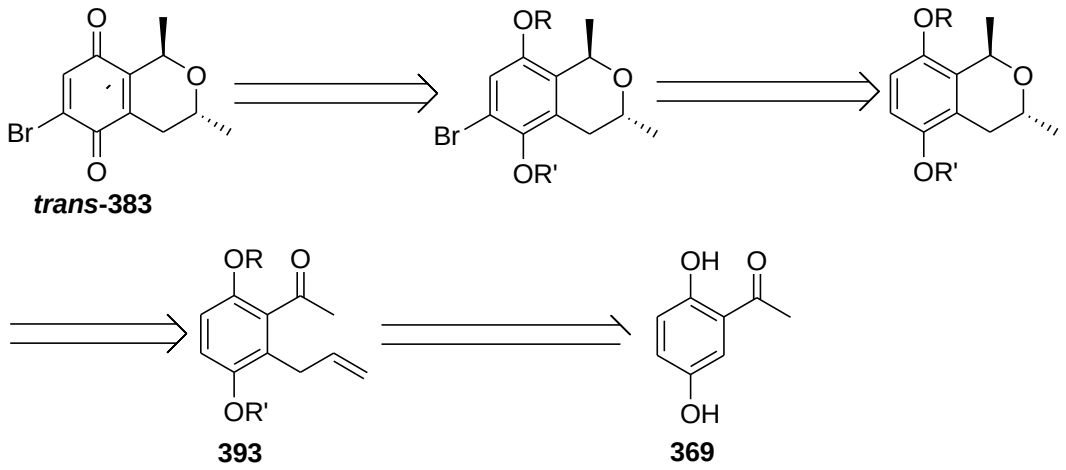
Scheme 4.23: *Reagents and conditions:* (a) cat. $Pd(OAc)_2$, K_2CO_3, BU_4NBr, DMF, 95 ^oC, 18 hrs.

A similar protocol was used by König and co-workers[250] who described a double Heck-coupling reaction of dibromobenzene **391** with vinyl ferrocene **366** which delivered di-ferrocenyl benzene **392** as shown in reaction **Scheme 4.24**.



Scheme 4.24: *Reagents and conditions:* (a) cat. $Pd(OAc)_2$, K_2CO_3, PPh_3, DMF, reflux, 24 hrs.

This approach was interesting and we quickly noted that starting from the same starting material, 2,5-dihydroacetophenone **369**, and using a modified Mmutlane protocol[119] we could synthesize the required bromo-3,4-dihydropyranobenzoquinone ***trans*-383** as shown in retrosynthetic analysis **Scheme 4.25**.



Scheme 4.25: Retrosynthetic analysis towards the synthesis of 6-bromo-3,4-dihydropyranobenzoquinone ***trans*-383**.

The retrosynthetic analysis depicted in **Scheme 4.25** above raised a number of interesting questions. One of which was whether it was possible to selectively obtain *C*-2-allyl Claisen rearrangement product **393** or at the very least successfully separate the *C*-2-allyl Claisen rearrangement product from the *C*-4-allyl Claisen rearrangement product shown in **Figure 4.5**.

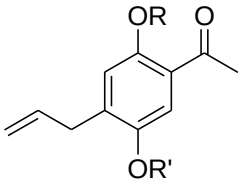
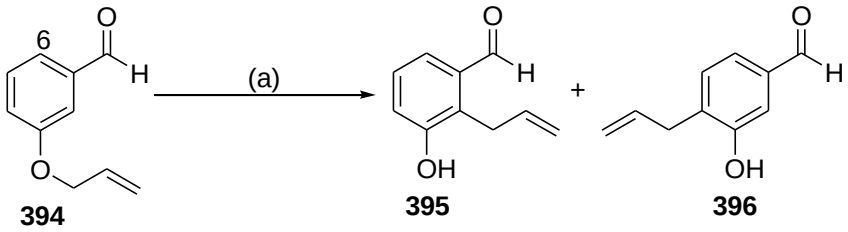


Figure 4.5: The molecular structure of *C*-4-allyl Claisen rearrangement product.

A search on what has been carried out in our laboratory group revealed that Mmutlane subjected allyl ether **394** (**Scheme 4.26**) under Claisen rearrangement conditions which afforded a chromatographically inseparable mixture of the *C*-allyl regio-isomers, 2-allyl-3-hydroxybenzaldehyde **395** and 4-allyl-3-hydroxybenzaldehyde **396** in equal amounts.[242]



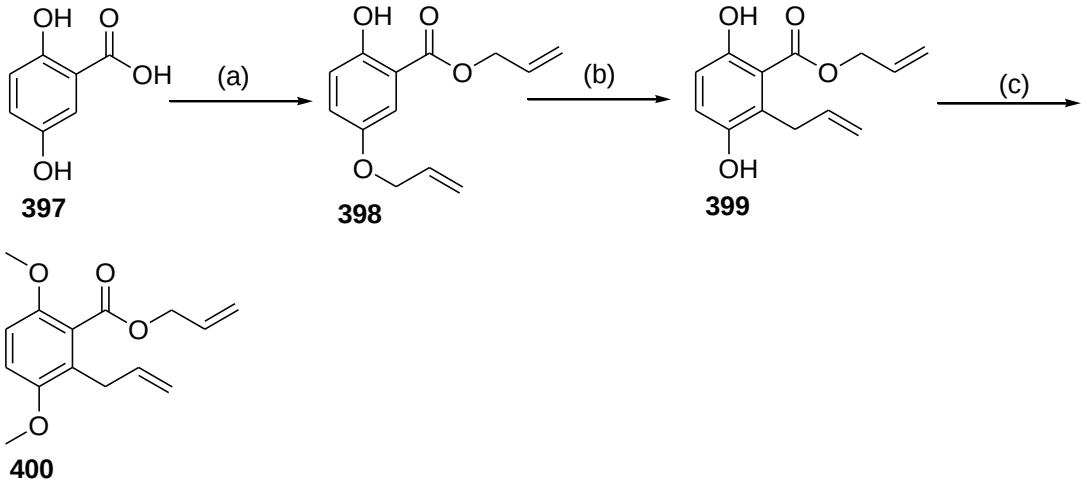
394 **395** **396**

Scheme 4.26: *Reagents and conditions:* (a) 170 °C, N_2 (g), 24 hrs.

To our delight, he also reported that fractional crystallisation of the mixture led to isolation of pure phenol **395** as a white crystalline solid. However, the excitement was short lived at the realisation that the substrate **394** did not have a phenol or a protected phenol group at position 6 which could have had a potentially profound effect on how the Claisen rearrangement reaction and separation of the resultant phenol product may have proceeded. Hydrogen bonding has a profound effect on the relative interaction between the stationary phase and the compound under separation.

Johnson[251] and Pelly[122a] reported exclusively obtaining the *C*-2-allyl Claisen rearrangement product **399** from phenol **398** (**Scheme 4.27**) which was obtained from the selective allylation of benzoic acid **397**. This was in line with what has been reported in the literature.[252a,b] Baker and co-workers[252a] attributed this phenomenon to the hydrogen bonding between the hydroxyl group and the neighbouring carbonyl group which is thought to produce a 6-membered ring intermediate in the transition state, thereby directing the rearrangement

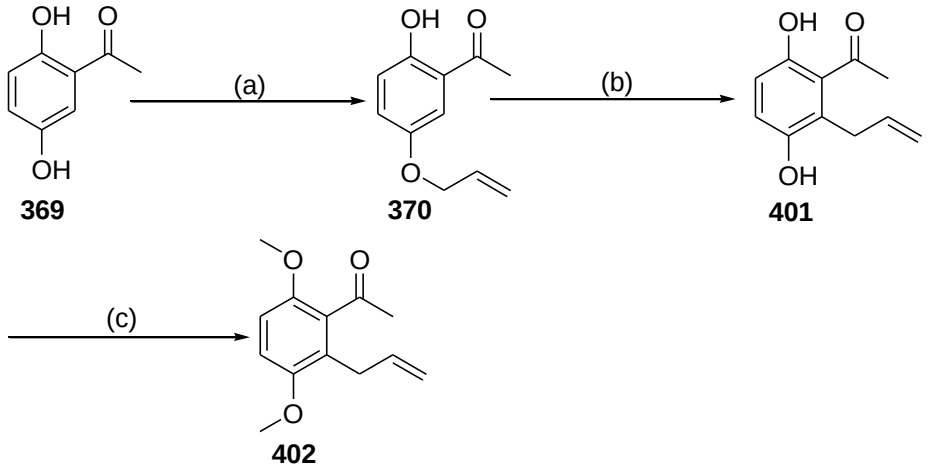
reaction to the *ortho* position of the allyl ester group. This protocol worked perfectly well in this case because the next step after the Claisen rearrangement reaction was the unselective methylation of the diphenol **399** which yielded allyl ester **400**. However, in our hands we aimed at protecting the two phenol groups using two different protection groups.



397 **398** **399** **400**

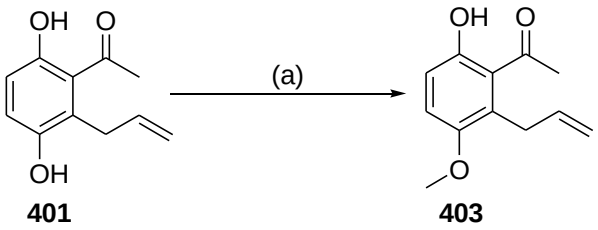
Scheme 4.27: *Reagents and conditions:* (a) K_2CO_3, allyl bromide, Me_2CO, reflux, 18 hrs (b) 170 °C, N_2 (g), 24 hrs (c) K_2CO_3, Me_2SO_4, Me_2CO, reflux, 18 hrs.

The most important correlation came from the paper Pillay and co-workers published which was titled: *"Wacker oxidation methodology for the synthesis of the benzo-fused acetal core of marticin"*.[253] In this paper, Pillay and co-workers reported synthesizing 1-(5-allyloxy-2-hydroxyphenyl)ethanone **370** from diphenol **369** which was then subjected to thermal Claisen rearrangement conditions yielding 1-(2-allyl-3,6-dihydroxyphenyl)ethanone **401** as the only product in a remarkable yield of 73%. The intermediate **401** was, however, unselectively methylated to 1-(2-allyl-3,6-dimethoxyphenyl)ethanone **402** as shown in reaction **Scheme 4.28**.



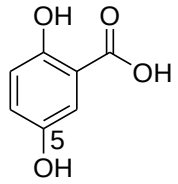
Scheme 4.28: *Reagents and conditions:* (a) K_2CO_3, allyl bromide, Me_2CO, reflux, 18 hrs (b) 170 °C, N_2 (g), 24 hrs (c) K_2CO_3, Me_2SO_4, Me_2CO, reflux, 18 hrs.

In our hands we found that there was very poor selectivity when we tried to selectively protect one phenol substituent (by taking advantage of hydrogen bonding) after the Claisen rearrangement step (**Scheme 4.29**) which was aimed at having two different oxygen protecting groups on the hydroquinone **401**.



Scheme 4.29: *Reagents and conditions:* (a) K_2CO_3, Me_2SO_4, Me_2CO, N_2 (g), reflux, 18 hrs.

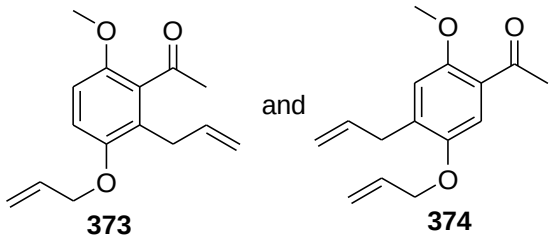
In synthesizing the monoallylated allyl ester **398** (**Scheme 4.27** above) from 2,5-dihydroxybenzoic acid **397**, Johnson[251] attributed the selectivity to both hydrogen bonding and steric effects around the phenol group at position 5 (**Figure 4.6** below). Once there is an allyl group at this position, the steric effect operates on both phenol groups as such the only difference in selectivity comes from the intramolecular hydrogen bonding which plays a significant role only when the reaction is carried out under very high dilution conditions.



397

Figure 4.6: The molecular structure of acid **397** highlighting position 5.

In the case of the protocol used by Mmutlane and repeated as part of this work, both *C*-2-allylation and *C*-4-allylation products were observed. Mmutlane highlighted the fact that once the hydrogen bonding was lost due to methylation, the selectivity at *C*-2-allylation and/or *C*-4-allylation is equally lost with it.[242] Much as Mmutlane did not attempt separation of the two constitutional isomers **373** and **374** (**Figure 4.7**) we thought that this was a good starting point in our case.



373 **374**

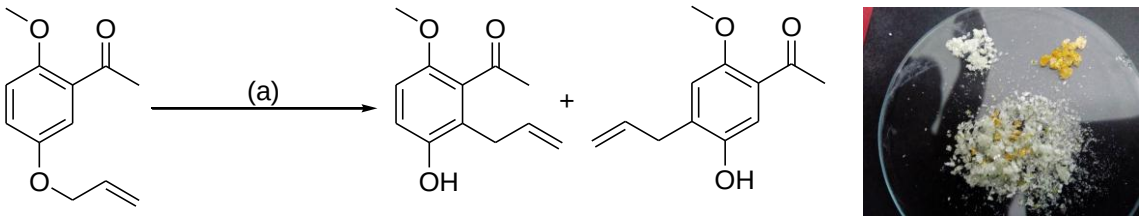
Figure 4.7: The molecular structures of allyl ethers **373** and **374**.

In this work, we were able to separate diallyl ethers **373** and **374** by column chromatography on flash silica gel (see **Section 4.1.1** above) which gave us the hope that we could possibly manage to separate out the constitutional isomers **404** and **405**.

4.1.8 Synthesis of 1-(2-allyl-3-hydroxy-6-methyoxyphenyl)ethanone 404

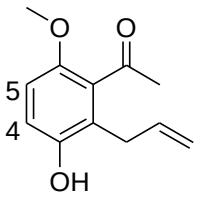
Having reviewed the information on the possibility of successful separation of two constitutional isomers **404** and **405**, we embarked on the separation of compound **404** by starting with running a short flash silica gel chromatographic column on the Claisen rearrangement product that was obtained in step 2 in the previous protocol (for synthesis see **Section 4.1.1** above) as shown in reaction **Scheme 4.30**. The mixture was concentrated *in vacuo*, heated to about 50 ^{o}C and left to slowly cool to room temperature and to our delight

white and orange crystals precipitated out of the solution. The *C*-2-allyl substituted acetophenone **404** appeared as colourless crystals and the *C*-4-allyl substituted acetophenone **405** as orange crystals in 56% and 20% yields, respectively. Crystals were physically separated by using tweezers and the spectroscopic techniques confirmed the identity of the crystals.



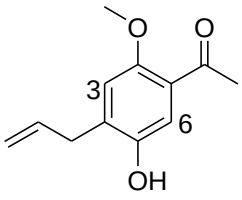
372 **404**; 56% colourless crystals **405**; 20% orange crystals

Scheme 4.30: *Reagents and conditions:* (a) 170 °C, N_2 (g), 24 hrs.



404

The ^{1}H NMR spectrum of 1-(2-allyl-3-hydroxy-6-methyoxyphenyl)ethanone **404** showed two separate doublet signals at 6.81 ppm (1H, d, *J* = 8.8 Hz) and 6.68 ppm (1H, d, *J* = 8.8 Hz) corresponding to two aromatic protons and were assigned to H-4 and H-5, respectively. The two signals showed a typical *ortho*-coupling constant of *J* = 8.8 Hz.



405

On the other hand, the ^{1}H NMR spectrum of 1-(4-allyl-5-hydroxy-2-methyoxyphenyl)ethanone **405** showed two singlet signals at 7.57 ppm (1H, s) and 7.13 ppm (1H, s) corresponding to the H-6 and H-3 protons, respectively. All other signals of the two compounds were largely the same.

The two compounds were unambiguously identified by their x-ray crystal structures and the ORTEP diagrams (at 50% ellipsoid) are shown in **Figure 4.8** for phenols **404** and **405**, respectively.

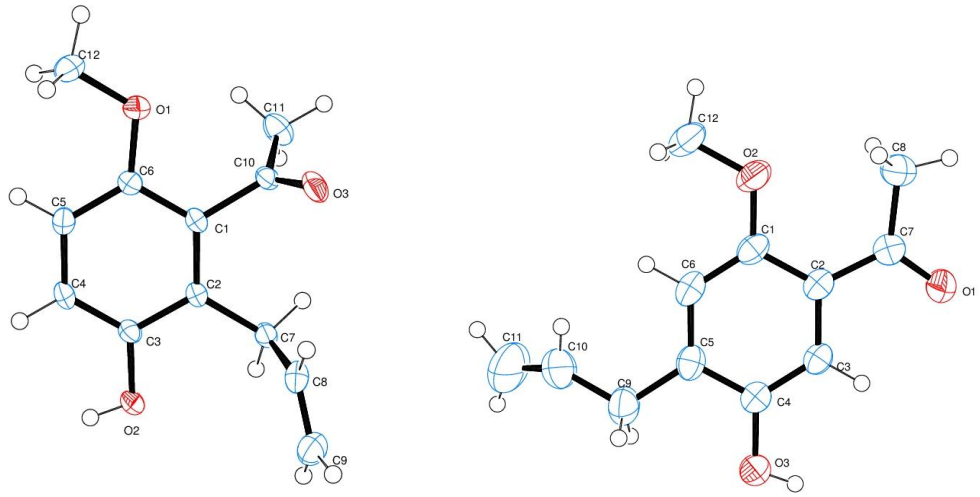
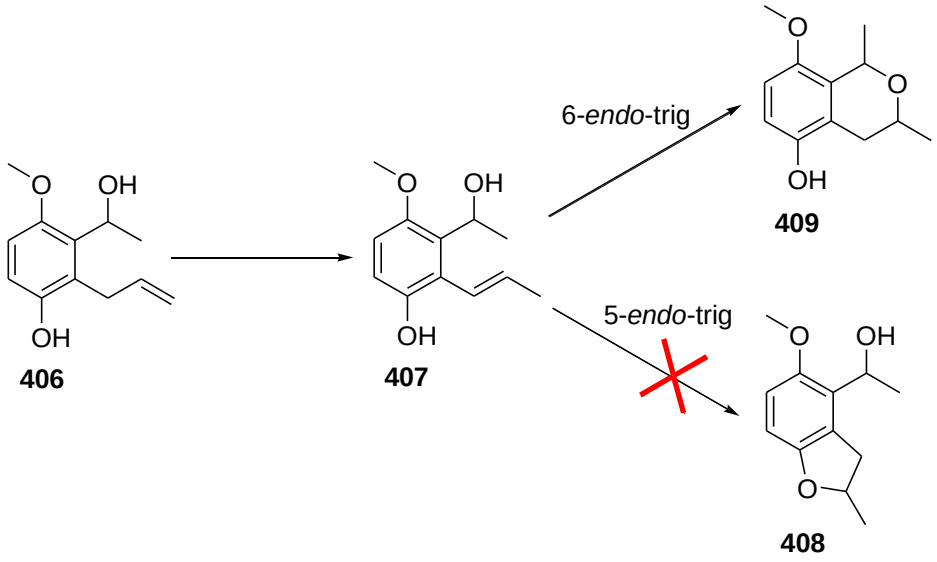


Figure 4.8: The ORTEP diagrams of allyl phenol **404** (left) and allyl phenol **405** (right). Thermal ellipsoids are shown at the 50% probability level.

Having successfully separated the two isomers we thought of proceeding with the reduction of the carbonyl group to a corresponding alcohol and performing the cyclization step without protecting the phenol group. Our reasoning behind this decision was that the two possible rings which could potentially be formed from the two OH groups (phenol OH and alcohol OH) would not be of the same size and therefore by taking advantage of Baldwin rules[145] we thought that we had a very good chance of synthesizing the intended intermediate **409** without the need to protect the free phenol. The Baldwin rules predict that the 6-*endo*-trig cyclization (leading to the formation of 3,4-dihydroisochromen-5-ol **409**) is favourable whereas the 5-*endo*-trig cyclization (leading to the formation of product **408**) is not favourable. Discrepancies and violations to the rules do exist but they are generally where the ring formation has no any other option other than to 'break' the rules.

Giles and co-workers[254] previously reported that ring cyclization of this nature under the mediation of potassium *tert*-butoxide is preceded by isomerization of the double bond. This meant that 3,4-dihydroisochromen-5-ol **409** would be as a result of 6-*endo*-trig ring cyclization as opposed to 6-*exo*-trig ring cyclization and similarly, product **408** would be as a result of 5-*endo*-trig ring cyclization and not 5-*exo*-trig reaction. This meant that effectively it was only the 6-*endo*-trig product which could result from precursor **407** as shown in **Scheme**

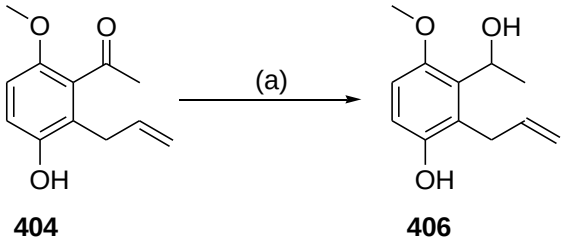
4.31. In this analysis we have ignored the influence of the relative acidity of the two OH groups because potassium *tert*-butoxide is a strong base which could deprotonate both labile alcohols without differentiating them (the base is used in excess of 3 mole equivalents).



Scheme 4.31: Two possible potassium *tert*-butoxide mediated cyclization pathways for phenol **406**.

4.1.9 Synthesis of 2-allyl-3-(1-hydroxyethyl)-4-methoxyphenol 406

Having convinced ourselves that this was a viable cyclization reaction pathway we proceeded to reduce the ketone using the previously used protocol involving lithium aluminium hydride in dry tetrahydrofuran to effect the transformation of the ketone **404** to alcohol **406** (**Scheme 4.32**). The identity of product **406** was confirmed by both the ^{1}H and ^{13}C NMR spectroscopy.



Scheme 4.32: *Reagents and conditions:* (a) $LiAlH_4$, THF, 0 $^{o}C \rightarrow$ rt, N_2 (g), 4 hrs, 77%.

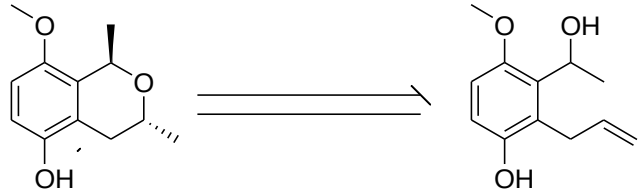
The ^{1}H NMR spectrum showed a multiplet signal between 5.13-4.91 ppm (3H, m) which corresponded to the two terminal vinylic protons ($ArCH_2CH=CH_2$) and the benzylic proton

(ArC*H*(OH)CH_3). The D_2O exchangeable signal at 4.25 ppm (1H, d, *J* = 10.9 Hz) was typical of the alcohol proton (ArCH(O*H*)CH_3) and finally the proton signal at 1.53 ppm (3H, d, *J* = 6.7 Hz) was ascribed to the methylinic proton of the hydroxyethyl side chain (ArCH(OH)C*H*$_3$). The ^{13}C NMR spectrum revealed the loss of the signal at 206.0 ppm in the starting material which was assigned to the carbonyl carbon atom and the new signal at 67.4 ppm was assigned to the carbon atom directly attached to the alcohol functional group (Ar*C*H(OH)CH_3). The IR spectrum confirmed the formation of the alcohol functional group by revealing the disappearance of the peak at 1714 cm^{-1} which was in the precursor compound **404** and was assigned to the carbonyl functional group. The disappearance of this peak corresponded to the appearance of the peaks at 3509 cm^{-1} and 3291 cm^{-1} in the product which were assigned to the two hydroxyl functional groups. The HRMS data for compound **406** was found to be 209.1171 amu which was in line with the calculated value of 209.1172 amu for $C_{12}H_{17}O_3$.

These results confirmed that we had successfully synthesised the required alcohol and at this point we were ready to carry out the next step which was to subject the alcohol **406** to the base promoted pyran ring forming reaction.

4.1.10 Synthesis of (±)-*trans*-3,4-dihydro-8-methoxy-1,3-dimethyl-1*H*-isochromen-5-ol *trans*-409

The solution of alcohol **406** in *N*-methylpyrrolidinone was heated to 110 ^oC in a silicon oil bath and solid potassium *tert*-butoxide was added to the reaction mixture at that temperature. The mixture was stirred for a further 30 minutes after which the reaction was quenched with cold water and extracted into dichloromethane. The majority of the solvent was distilled off under the reduced pressure and purification by column chromatography on flash silica gel afforded 3 products with R_f values (20% EtOAc/hexane) of 0.42 (3,4-dihydroisochromen-5-ol ***trans*-409**), 0.36 (dimer ***trans*-410** also coded **JS-D**) and 0.53 (3,4-dihydroisochromene ***trans*-411**) in 33 %, 26% and 14% yields, respectively. This was in stark contrast to the expected reaction as shown in retrosynthetic **Scheme 4.33**.



***trans*-409** **406**

Scheme 4.33: Retrosynthetic analysis for the formation of 3,4-dihydroisochromen-5-ol ***trans*-409**.

The ^{1}H NMR spectra of the 3 products were very similar and all of them showed loss of the signals due to the alkene protons in the alkene/aromatic region of the precursor alcohol **406** with a corresponding gain of proton signals in the alkyl region of the spectrum. The same observation was made in the ^{13}C NMR spectra which showed loss of two carbon signals in the alkene/aromatic region with corresponding gain of carbon signals in the aliphatic/alcohol region of the spectrum. This similarity was even more evident for the spectra of compounds with R_f values of 0.36 (dimer ***trans*-410**) and 0.42 (3,4-dihydroisochromen-5-ol ***trans*-409**) with the signals at 5.07 ppm (1H, s) and 6.19 ppm (1H, s) being the only difference apart from the minor differences in the chemical shifts. The ^{1}H NMR spectra of dimer ***trans*-410** and 3,4-dihydroisochromen-5-ol ***trans*-409** are shown in **Figure 4.9**.

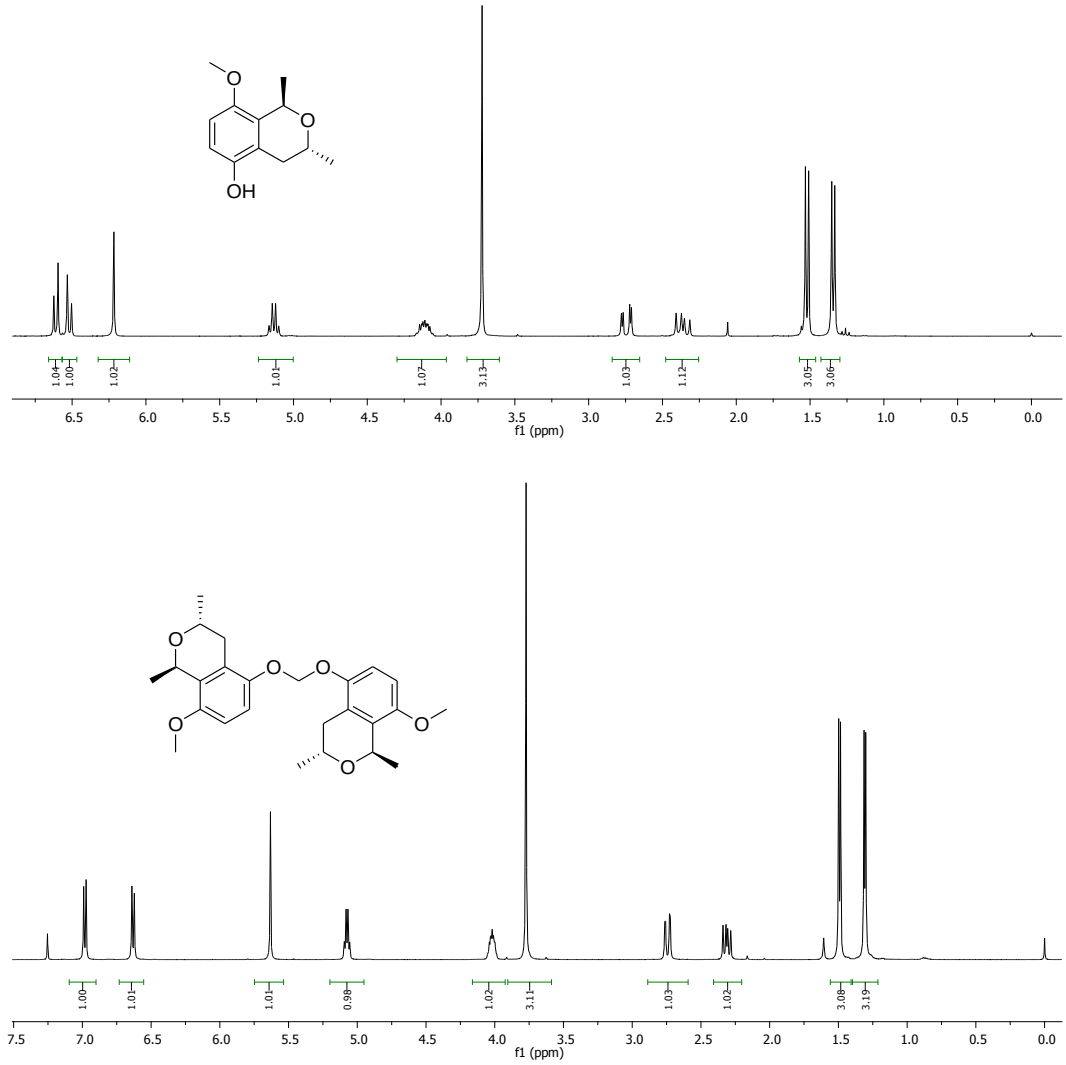
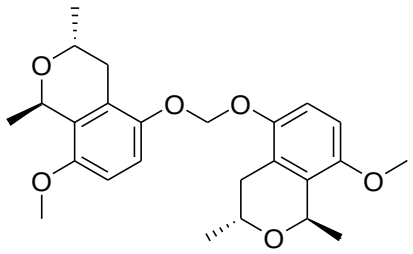


Figure 4.9: The ^{1}H NMR spectra of compounds ***trans*-409** (top) and ***trans*-410** (bottom).

At this point we figured out that if we could fully characterize two of the products we could easily determine the structure of the third product. We started with characterization of dimer ***trans*-410** (R_f value of 0.36). By analyzing the data obtained from the 1D and 2D NMR spectra, IR and HRMS spectra we were able to determine the identity of this compound as a

symmetrical dimer, *bis*((±)-*trans*-3,4-dihydro-8-methoxy-1,3-dimethyl-1*H*-isochromen-5-yloxy)methane ***trans*-410** shown in **Figure 4.10**. The 2D spectroscopic data for this compound are given in a table form in **Appendix B1.4**.

The IR spectrum showed no phenol stretching band which was present in the precursor compound which indicated that there was no phenol functional group in this product. The HRMS data showed a molecular ion peak at 429.2274 amu which was consistent with a predicted mass of 429.2272 amu for the formula $C_{25}H_{33}O_6$.

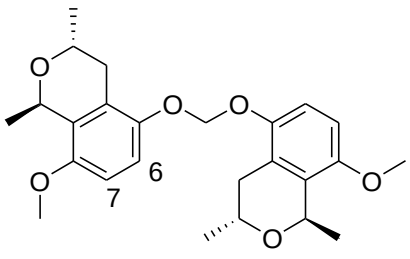


JS-D or ***trans*-410**

Figure 4.10: The molecular structure of dimer ***trans*-410**.

4.1.10.0 Assigning C-H protons and carbon atoms of *bis*[(±)-*trans*-3,4-dihydro-8-methoxy-1,3-dimethyl-1*H*-isochromen-5-yloxy]methane *trans*-410

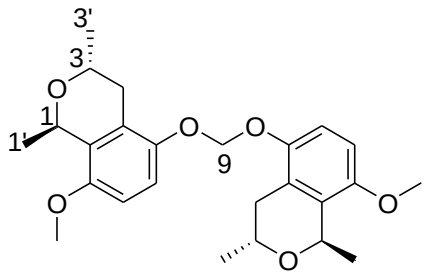
The ^{1}H NMR spectrum of ***trans*-410** showed two separate doublet signals at 6.98 ppm (1H, d, J = 8.8 Hz) and 6.63 ppm (1H, d, J = 8.9 Hz) with a typical *ortho*-coupling constant of J = 8.8 Hz and were assigned to H-6 and H-7, respectively. These protons were used as a starting point because the two aromatic protons in the starting material resonated in the same region and with the same multiplicity which made it easy to correlate these signals to the signals in the starting material. The ^{1}H-^{1}H COSY spectrum confirmed the interactions between the two protons. The HSQC spectrum revealed that the proton signal at 6.98 ppm correlated with the carbon nucleus resonating at 112.3 ppm and this signal was ascribed to C-6. The HSQC spectrum further revealed that the proton signal at 6.63 ppm correlated with the carbon signal at 107.5 ppm and this signal was assigned to C-7.



***trans*-410**

In addition, the proton signal at 5.63 (1H, s) was assigned to the H-9 proton and the HSQC spectrum revealed that it corresponded to the carbon signal at 92.4 ppm in the ^{13}C NMR spectrum and was assigned to C-9. However, the DEPT spectrum revealed that this signal was due to a methylenic (CH_2) carbon atom despite integrating for 1 proton (see ^{1}H NMR spectrum in **Figure 4.9** (the bottom spectrum) and **Appendix A1.31**) which meant that this was a centre of symmetry of a dimer.

The HSQC spectrum revealed that the quartet signal at 5.07 ppm (1H, q, J = 6.5 Hz) which was assigned to H-1 corresponded to the carbon nucleus resonating at 68.3 ppm and this signal was ascribed to C-1. A proton signal at 1.49 ppm (3H, d, J = 6.6 Hz) was assigned to H-1' on the basis of the ^{1}H-^{1}H COSY spectrum which showed interaction between these protons with the H-1 proton at 5.07 ppm. The HSQC spectrum further showed that the signal at 1.49 ppm correlated with the carbon nucleus resonating at 19.5 ppm and this signal was assigned to C-1'. In the same way, the multiplet signal between 4.07-3.96 ppm (1H, m) was assigned to H-3 and the HSQC spectrum revealed that this signal corresponded to the carbon signal at 62.2 ppm and was assigned C-3. The proton signal at 1.31 ppm (3H, d, J = 6.1 Hz) was ascribed to H-3' on the basis of its interaction with the multiplet signal between 4.07-3.96 ppm as revealed by the ^{1}H-^{1}H COSY spectrum. The HSQC spectrum showed that the carbon signal at 22.0 ppm correlated to this proton signal and was ascribed to C-3'. The proton signal at 3.77 ppm (3H, s) was indicative of the methoxy proton of the aromatic compound and using the HSQC spectrum we correlated this signal to a carbon signal at 55.4 ppm in the ^{13}C NMR spectrum.

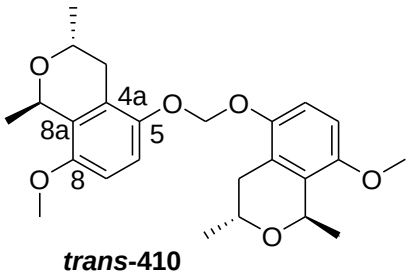


***trans*-410**

4.1.10.1 Assigning non C-H carbon atoms of *bis*[(±)-*trans*-3,4-dihydro-8-methoxy-1,3-dimethyl-1*H*-isochromen-5-yloxy]methane *trans*-410

Having unambiguously assigned all carbon signals of the spectrum by direct correlation using the HSQC spectrum we turned our attention to non-hydrogen bonded carbon atoms and we assigned them on the basis of correlation shown by the HMBC spectrum.

The HMBC spectrum revealed diagnostic long-range correlations between the proton signal at 5.43 ppm (H-9) and the carbon resonance at 148.4 ppm and this signal was assigned to C-5. The methoxy protons at 3.77 ppm showed correlation with the carbon signal at 150.7 ppm and this signal was ascribed to C-8. Furthermore, the proton signal at 1.49 ppm (H-1') revealed correlation with carbon signals at 68.3 ppm and 129.2 ppm and the signal at 129.2 ppm was assigned to C-8a. Lastly, the proton signal at 1.31 ppm (H-3') correlated with the carbon signal at 124.8 ppm and this signal was ascribed to C-4a.



***trans*-410**

The structure of the compound was later confirmed by obtaining the crystal structure as shown in the ORTEP diagram in **Figure 4.11**. The crystal structure also confirmed that the pyran ring maintained the methyl groups in the *trans*-configuration and the ring itself assumed the *pseudo*-chair conformation.

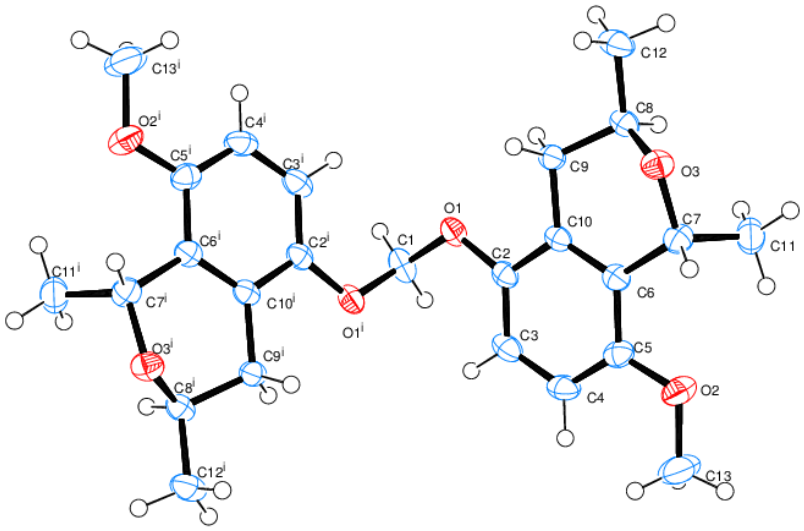
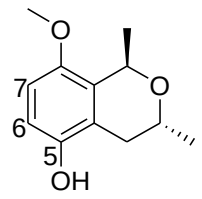


Figure 4.11: The ORTEP diagram of the dimer ***trans*-410**. Thermal ellipsoids are shown at the 50% probability level.

4.1.10.2 Spectroscopic data analysis for (±)-*trans*-3,4-dihydro-8-methoxy-1,3-dimethyl-1*H*-isochromen-5-ol *trans*-409

Having unambiguously assigned the signals for dimer ***trans*-410** we turned our attention towards identifying the remaining two compounds, ***trans*-409** and ***trans*-411**. The HSQC spectrum of compound ***trans*-409** showed that the proton signal at 6.19 ppm (1H, s) had no corresponding carbon signal and this signal was assigned to the phenol proton (ArO*H*) of the 3,4-dihydroisochromen-5-ol. The IR spectrum confirmed the presence of the phenol functional group which showed a broad peak at 3380 cm^{-1}.

The HMBC spectrum showed correlation between the proton signal at 6.19 ppm (ArO*H*) and the carbon signal at 147.5 ppm and this signal was assigned to C-5. The ^{1}H NMR spectrum of compound ***trans*-409** showed two signals at 6.61 ppm (1H, d, J = 8.7 Hz) and 6.52 ppm (1H, d, J = 8.7 Hz) which were typical of *ortho* coupled protons with a coupling constant of J = 8.7 Hz and the signals were assigned to H-6 and H-7 protons, respectively. These signals showed correlation to the carbon signals at 112.4 ppm and 108.0 ppm and the carbon signals were assigned to C-6 and C-7, respectively. The multiplet signal at 4.29-4.00 ppm (1H, m) was indicative of the *trans*-configuration of the 1,3-dimethylpyran system and was assigned to H-3.[242] Direct comparison of the rest of the signals in the ^{1}H NMR spectrum of 3,4-dihydroisochromen-5-ol ***trans*-409** with that of dimer ***trans*-410** showed that they were essentially the same and we concluded that the two compounds had the same pyran ring with the two methyl groups in a *trans* arrangement to each other and the ring assumed the same *pseudo*-chair conformation. The HRMS spectrum showed a molecular ion peak at 209.1178 amu which was the same as the expected mass for $C_{12}H_{17}O_3$.



***trans*-409**

The structure of the compound was later confirmed by the crystal structure as shown in the ORTEP diagram in **Figure 4.12** which also clearly showed the *pseudo*-chair conformation of the pyran ring and the *trans* arrangement of the two methyl groups at *C*-1 and *C*-3.

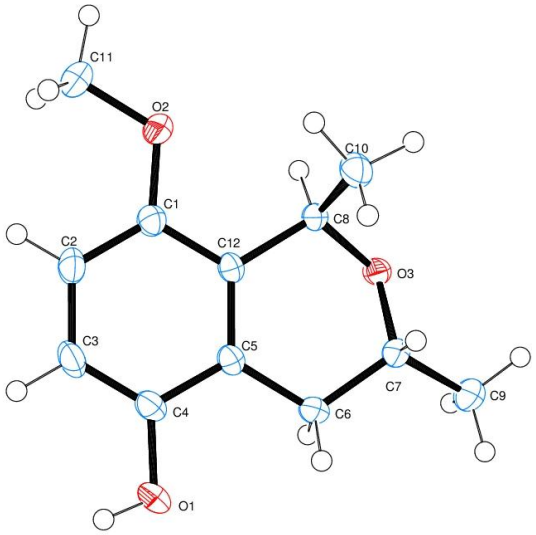
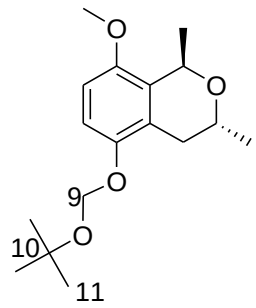


Figure 4.12: The ORTEP diagram of ***trans*-409**. Thermal ellipsoids are shown at the 50% probability level.

4.1.10.3 Spectroscopic data analysis of (±)-*trans*-5-(*tert*-butoxymethoxy)-3,4-dihydro-8-methoxy-1,3-dimethyl-1*H*-isochromene *trans*-411

Lastly, the ^{1}H NMR spectrum of compound ***trans*-411** showed a singlet signal at 5.22 ppm (2H, s) which was assigned to the ether proton H-9 (ArOC*H*$_2$OC(CH$_3$)$_3$) and the HSQC spectrum revealed that this signal correlated with the carbon signal at 88.4 ppm which was assigned to C-9. This signal was similar to the signal at 5.63 ppm of dimer ***trans*-410** which was assigned to H-9 but unlike for dimer ***trans*-410**, the ^{1}H NMR spectrum for compound ***trans*-411** revealed the ether linked *CH*$_2$ signal integrated for 2 protons as expected which meant that we were no longer dealing with a symmetrical dimer.

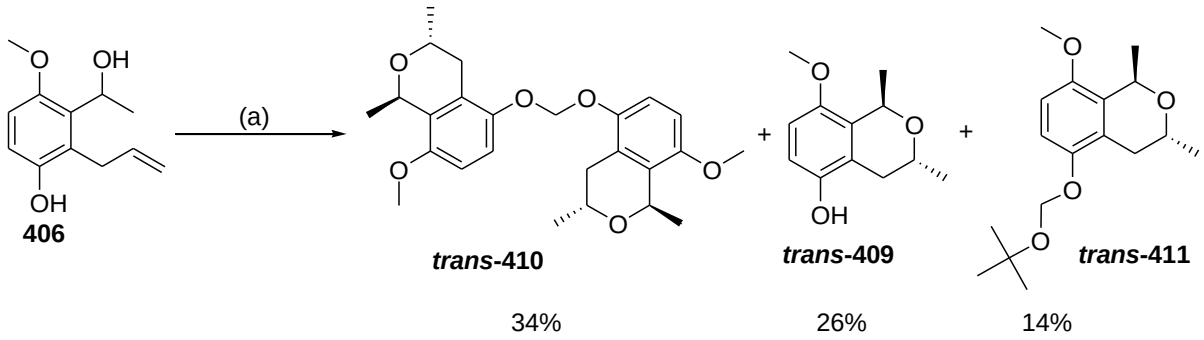


***trans*-411**

The proton signal at 1.29 ppm (9H, s) was assigned to 3 equivalent protons of a methyl group (ArOCH$_2$OC(C*H*$_3$)$_3$, H-11) on the basis that the signal correlated with one carbon signal at 28.6 ppm as shown by the HSQC spectrum and was assigned to C-11. The ^{13}C NMR spectrum further showed a signal at 75.3 ppm which did not have a corresponding proton in the HSQC spectrum and was ascribed to C-10. The signals due to the pyran ring were similar to the signals discussed above for compounds ***trans*-409** and ***trans*-410** which indicated that the *trans*

configuration and the *pseudo*-chair conformation of the pyran ring was also maintained in this compound. The IR spectrum of compound ***trans*-411** was similar to the IR spectrum of dimer ***trans*-410** with no peak corresponding to the phenol functional group. The HRMS spectrum confirmed the mass of the molecule as 295.1904 amu which was in agreement with the predicted mass of 295.1909 amu for $C_{17}H_{27}O_4$.

A complete reaction equation of unprotected phenol **406** with potassium *tert*-butoxide in *N*-methylpyrrolidinone at 110 ^{o}C is depicted in **Scheme 4.34**.



Scheme 4.34: *Reagents and conditions:* (a) *t*-BuOK, NMP, 110 °C, 30 min.

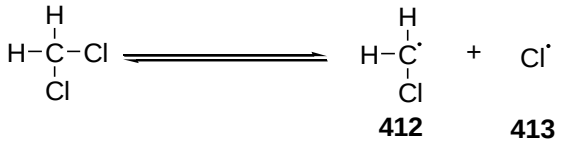
Even though we did not carry out mechanistic studies on the possible reaction pathways for formation of products ***trans*-410** and ***trans*-411** we thought it was important to shed more light on this reaction by proposing possible mechanistic pathways on the basis of the composition of the reaction mixture and the protocol that was followed. The actual mechanistic studies will be carried out in our laboratory at a later stage and these observations will be taken into consideration.

4.1.10.4 Proposed mechanism for the formation of *bis*((±)-*trans*-3,4-dihydro-8-methoxy-1,3-dimethyl-1*H*-isochromen-5-yloxy)methane *trans*-410

The mechanism for the formation of the pyran ring using this protocol is well documented[254] so the efforts here are meant to shed more light on the possible mechanistic pathway(s) for the formation of the methylene ether linkage in both products ***trans*-410** and ***trans*-411**.

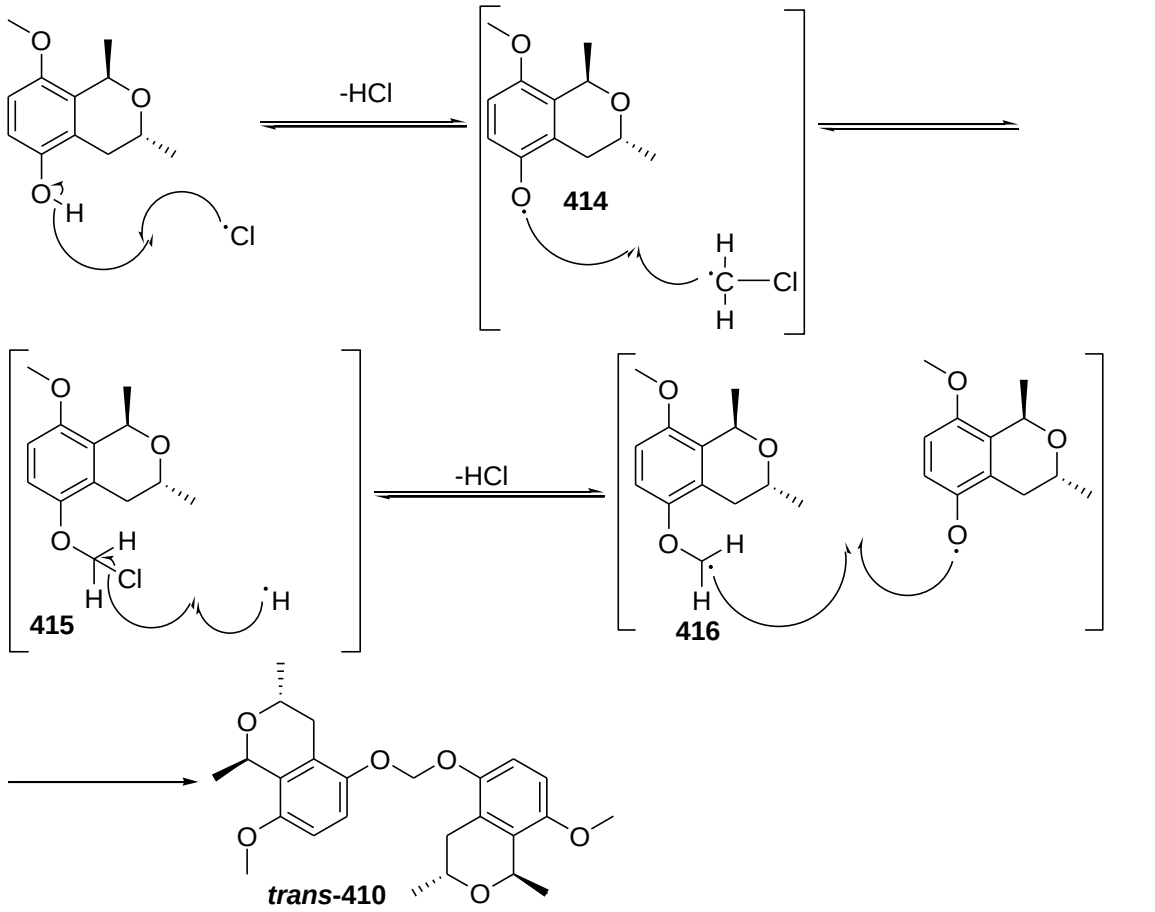
One of several possible ways the methylene ether linkage could be formed was through radical reaction involving the methyl group of the *N*-methylpyrrolidinone solvent. This was

unlikely owing to the fact that we did not isolate product(s) bonded to the solvent molecules and the ^{1}H NMR spectrum of the *N*-methylpyrrolidinone that was distilled off after the reaction did not show any evidence of alteration in its structural composition. However, the radical reaction may have involved generation of radicals from residual dichloromethane, which was used for partitioning, generated at high temperatures during the distillation of the *N*-methylpyrrolidinone solvent molecules. **Scheme 4.35** shows the possible thermal decomposition of dichloromethane at high temperatures (during the distillation of the *N*-methylpyrroldinone).



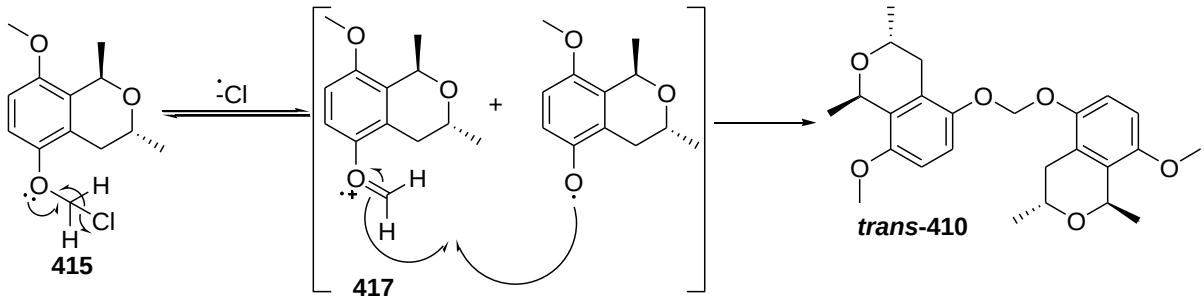
Scheme 4.35: Thermal decomposition of dichloromethane leading to formation of radicals **412** and **413**.

The chlorine **413** radical could then abstract a proton from 3,4-dihydroisochromen-5-ol ***trans*-409** resulting in formation of 3,4-dihydroisochromen-5-ol radical **414**. The reaction between radicals **414** and **412** could generate intermediate **415** which could possibly go on to form a dimer ***trans*-410** *via* intermediate **416** as shown in **Scheme 4.36**.



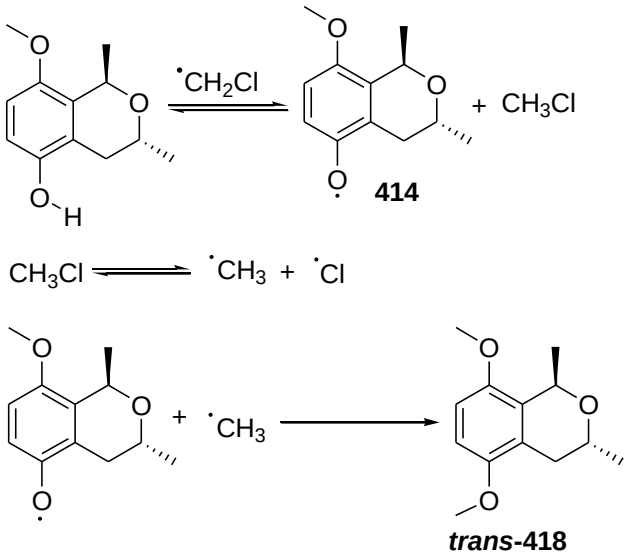
Scheme 4.36: Proposed mechanism for radical mediated dimerization of (±)-*trans*-3,4-dihydro-8-methoxy-1,3-dimethyl-1*H*-isochromen-5-ol ***trans*-409**.

There was also a possibility of intermediate **415** being involved in thermal decomposition to generate a cationic radical **417** which could undergo a dimerization reaction to deliver the dimer as shown in **Scheme 4.37**.



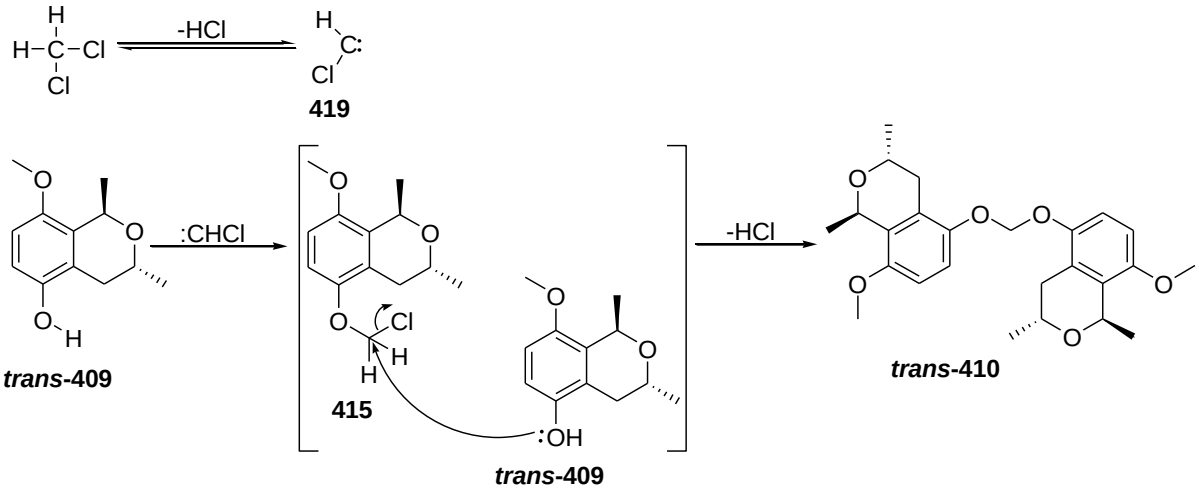
Scheme 4.37: Proposed mechanism *via* thermal decomposition of intermediate **415**.

The choice of the chlorine radical **413** abstracting a proton from the phenol ***trans*-409** was dictated by the fact that we did not isolate 3,4-dihydroisochromene ***trans*-418** as one of the products which could be formed if the chloromethane radical **412** was involved in this step as shown in **Scheme 4.38**.



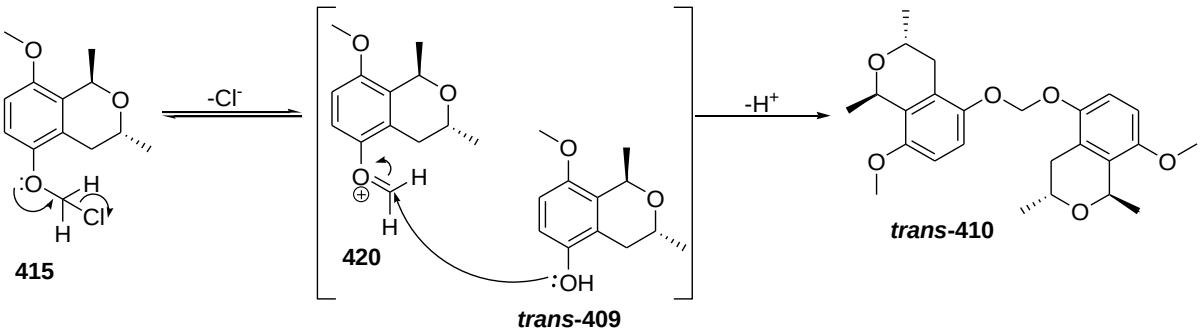
Scheme 4.38: The reaction equations for the possible formation of compound ***trans*-418**.

The second possible mechanistic pathway could be through a carbene-type of chemistry again involving residual dichloromethane. The α-elimination of the proton followed by loss of the chloride ion could generate carbene **419** which could then insert itself into the phenol O-H bond of 3,4-dihydroisochromen-5-ol ***trans*-409** affording intermediate **415**. There are literature reports of carbenes of this nature generated from carbanion intermediate.[255] The intermediate **415** could then undergo S_N2 type reaction to deliver the dimer ***trans*-410** as shown in **Scheme 4.39** below.



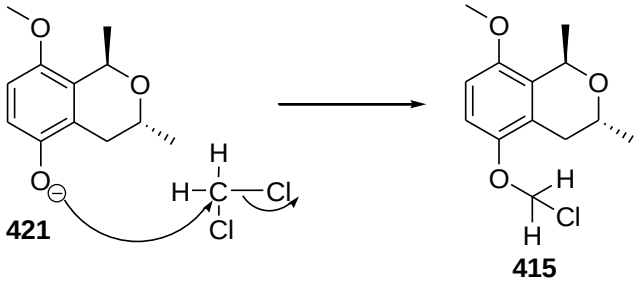
Scheme 4.39: Proposed mechanism for carbene mediated dimerization of ***trans*-409** through S_N2 type reaction.

Alternatively, the intermediate **415** could generate cation **420** which could then react with 3,4-dihydroisochromen-5-ol ***trans*-409** in a typical S_N1 type reaction to deliver the dimer ***trans*-410** as shown in reaction **Scheme 4.40** below.



Scheme 4.40: Proposed carbene mediated dimerization of phenol ***trans*-409** through S_N1 type reaction.

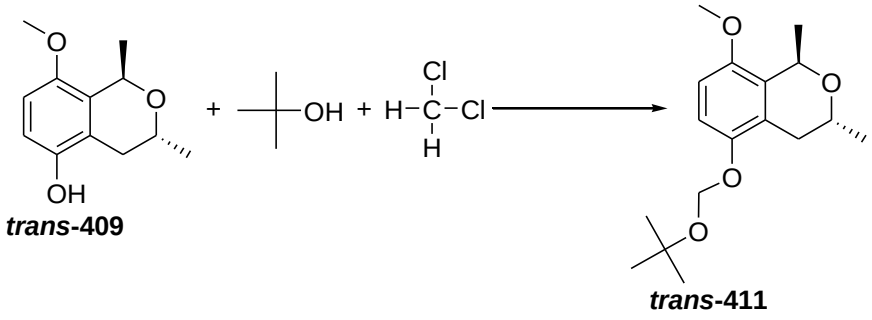
The third possibility involving the formation of carbanion **421** which could go on to attack the dichloromethane at high temperatures to form an important intermediate **415** as shown in **Scheme 4.41** below was not considered as a viable mechanistic pathway due to the fact that dichloromethane was used for extraction after the reaction had been quenched with cold water.



Scheme 4.41: Proposed anionic mechanistic pathway for the formation of intermediate **415**.

The fact that some of the intermediates were the same in the above proposed mechanistic pathways meant that there was also a possibility of combined radical/ionic/carbene mechanistic pathways. All of the above possibilities will be taken into consideration in our laboratory when studying the mechanistic pathway for this reaction.

The formation of the *tert*-butoxyl product ***trans*-411** could be analysed in the same way with *tert*-butanol reacting in place of the second molecule of 3,4-dihydroisochromen-5-ol ***trans*-409**. The general reaction equation for the formation of compound ***trans*-411** is depicted in **Scheme 4.42** below.



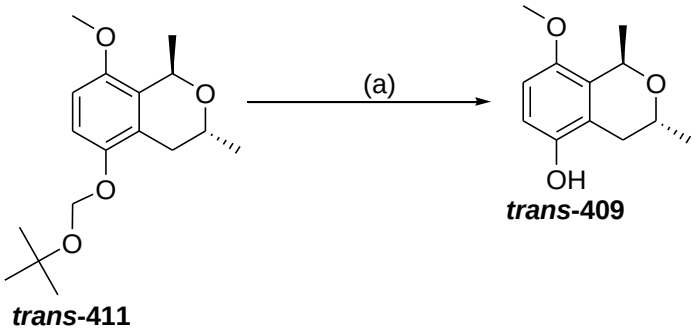
Scheme 4.42: The possible reaction equation for the formation of ***trans*-411**.

The three products synthesized from the unprotected phenol involved the favourable 6-*endo*-trig ring cyclization and there was no evidence of product(s) relating to the unfavourable 5-*endo*-trig ring cyclization. This meant that the Baldwin rules were faithfully abided to by this reaction even though we did not foresee the possibility of dimerization of the 3,4-dihydroisochromen-5-ol ***trans*-409**.

At this point we were inquisitive to study the cyclization reaction with the phenol protected by the silicon protection group which was chosen due to the fact that its cleavage does not generally involve harsh conditions. We wanted to investigate if silyl protected phenol would lead to dimerization. Before we embarked on this study we first completed hydrolysis of compounds ***trans*-410** and ***trans*-411** to regenerate monomer ***trans*-409**.

4.1.11 Acid hydrolysis of compounds *trans*-410 and *trans*-411

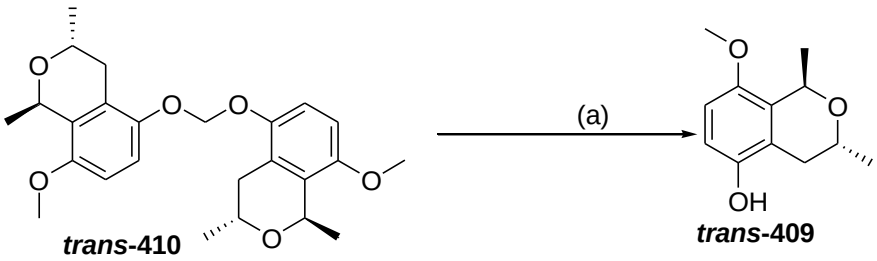
The acid hydrolysis of compound ***trans*-411** was achieved by heating under reflux the methanol solution of 3,4-dihydroisochromene ***trans*-411**, to which 32% aqueous hydrochloric acid was added, for 12 hours (**Scheme 4.43**). The crude product was purified by column chromatography on silica gel yielding 3,4-dihydroisochromen-5-ol ***trans*-409** in 84% yield. The successful hydrolysis was confirmed by ^{1}H NMR spectroscopy and there was no sign of epimerization of the 1,3-dimethyl pyran ring in the product.



***trans*-411** ***trans*-409**

Scheme 4.43: *Reagents and conditions:* (a) *32%* aq. HCl, MeOH, reflux, 12 hrs, 84%.

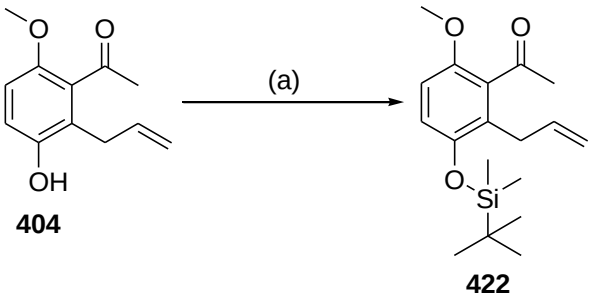
Subjecting dimer ***trans*-410** to the same acidic conditions using 32% aqueous hydrochloric acid did not lead to hydrolysis of the dimer and the starting material was recovered. After a number of mineral acids were tried we found that the hydrolysis reaction went smoothly when the dimer was heated to reflux for 24 hours in a mixture of methanol and trifluoroacetic acid (**Scheme 4.44**) which yielded 3,4-dihydroisochromen-5-ol ***trans*-409** in 90% yield. The pyran ring was stable under these conditions and again the ^{1}H NMR spectrum of phenol ***trans*-409** did not show signs of epimerization of the pyran ring.



Scheme 4.44: *Reagents and conditions:* MeOH, TFA, reflux, 18 hrs, 90%.

4.1.12 Synthesis of 1-(2-allyl-3-*tert*-butyldimethylsilyloxy-6-methoxyphenyl)ethanol

1-(2-Allyl-3-hydroxy-6-methoxyphenyl)ethanone **404** was subjected to a routine silicon protection protocol which delivered the desired compound **422** in 93% yield.



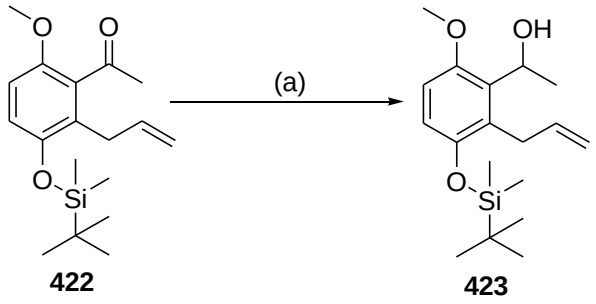
Scheme 4.45: *Reagents and conditions:* (a) TBDMSCl, imidazole, cat. DMAP, CH_2Cl_2, rt, 24 hrs, 93%.

The successful protection of the phenol group of compound **404** was confirmed by ^{1}H NMR spectroscopy which revealed the disappearance of a signal at 5.40 ppm corresponding to the phenol proton in the starting material. The proton signal at 0.78 ppm (9H, s) was typical of the silicon protection group *tert*-butyl protons ($ArOSi(CH_3)_2C(CH_3)_3$) and the proton signal at 0.00 ppm (6H, s) was assigned to the methyl protons directly bonded to the silicon atom ($ArOSi(CH_3)_2C(CH_3)_3$). The HSQC spectrum revealed that the carbon signal at 25.8 ppm and -4.2 ppm corresponded to the proton signals at 0.78 ppm and 0.00 ppm and were assigned to *tert*-butyl carbon atoms of the silicon group ($ArOSi(CH_3)_2C(CH_3)_3$) and the carbon atoms of the two methyl groups directly bonded to the silicon atom ($ArOSi(CH_3)_2C(CH_3)_3$), respectively.

The IR spectrum of ketone **422** showed loss of a broad peak at around 3240 cm^{-1} which was due to the phenol functional group in the precursor compound **404** and the HRMS showed a

molecular ion peak at 321.1880 amu which was in good agreement with the expected mass of 321.1886 amu for $C_{18}H_{29}O_3Si$.

These results confirmed that we had successfully protected the phenol group and we proceeded to reduce the ketone functional group to the corresponding alcohol using lithium aluminium hydride under the blanket of nitrogen gas. The identity of the product **423** was confirmed by both ^{1}H NMR and ^{13}C NMR spectroscopy.



422 **423**

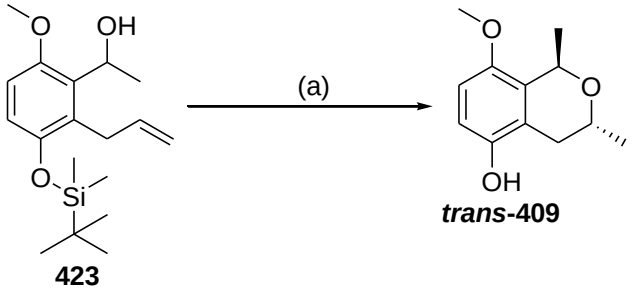
Scheme 4.46: *Reagents and conditions:* (a) $LiAlH_4$, THF, 0 $^oC \rightarrow$ rt, N_2 (g), 4 hrs, 89%.

The ^{1}H NMR spectrum of alcohol **423** showed a new signal at 1.31 ppm (3H, d, J = 6.7 Hz) which was assigned to the β-methylinic protons (ArCH(OH)CH_3) of the hydroxyethyl side chain. The D_2O exchangeable proton signal at 3.81 ppm (1H, d, J = 11.1 Hz) did not have a corresponding carbon resonance in the HSQC spectrum and was assigned to the secondary alcohol proton (ArCH(O*H*)CH_3). The multiplet signal between 4.94-4.57 ppm (3H, m) was assigned to the benzylinic proton (ArC*H*(OH)CH_3) and the terminal vinylic protons (ArCH_2CH=CH_2). The ^{13}C NMR spectrum revealed loss of the signal at 205.3 ppm which was assigned to the carbonyl carbon atom in the starting material and a new signal at 67.5 ppm was typical of the benzylinic carbon atom bonded to the alcohol group (Ar*C*H(OH)CH_3). The signals due to the silicon protection group protons and carbon atoms in the starting material were faithfully reproduced in the secondary alcohol **423** which indicated that we did not lose this group in the course of reducing the ketone **422**.

The IR spectrum of alcohol **423** showed loss of a peak at 1703 cm^{-1} which was due to the carbonyl functional group in the precursor compound **422** and a new signal at 3562 cm^{-1} in the product was due to the alcohol functional group.

4.1.13 Synthesis of (±)-*trans*-3,4-dihydro-8-methoxy-1,3-dimethyl-1*H*-isochromen-5-ol

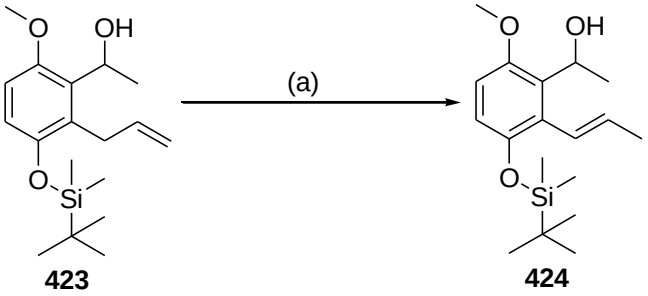
Satisfied that we had our protected alcohol in place we went on to expose the alcohol **423** in *N*-methylpyrrolidinone to potassium *tert*-butoxide at 110 ^{o}C as previously carried out and we obtained phenol ***trans*-409** in 70% yield as the only product (**Scheme 4.47**).



Scheme 4.47: *Reagents and conditions:* (a) *t*-BuOK, NMP, 110 °C, 30 min, 70%.

The first observation we noted in the ^{1}H NMR spectrum was the absence of the signals corresponding to the silicon protection group which indicated that the group was lost in the course of the reaction. The ^{13}C NMR spectrum correlated this observation. The second observation was that there were no traces of compounds ***trans*-410** and ***trans*-411** even when the crude product was compared by TLC.

Giles and co-workers,[254] as previously explained, had shown that this reaction passes through two major stages which are isomerization of the alkene double bond and ring cyclization. At this point we thought it was imperative to estimate the stage at which the oxygen silicon protection group was lost. When performing the next batch of the reaction we decided to draw out a small amount of the reaction mixture at 4 minutes after the addition of the base. The drawn reaction mixture was quenched in the same way as previously carried out. The TLC plate showed a major spot with similar R_f value to the starting material and there was no spot corresponding to 3,4-dihydroisochromen-5-ol ***trans*-409**. The crude reaction mixture was purified on flash silica gel column chromatography and analysed using ^{1}H and ^{13}C NMR spectroscopy.

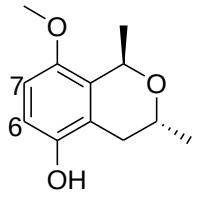


423 **424**

Scheme 4.48: *Reagents and conditions:* (a) *t*-BuOK, NMP, 110 °C, 4 min, (% yield not calculated).

Analysis of the ^{1}H NMR spectrum revealed that what we thought was the starting material was in fact the isomerized alcohol **424** (**Scheme 4.48**). The proton signal at 6.74 ppm (1H, dq, J = 11.2, 1.5 Hz) was assigned to the inner propenylic proton (ArC*H*=CHCH$_3$) whereas the proton signal at 6.11 ppm (1H, dq, J = 11.2, 6.8 Hz) was assigned to the outer propenylic proton (ArCH=C*H*CH$_3$). The doublet of doublets at 1.67 ppm (3H, dd, J = 6.8, 1.7 Hz) was ascribed to the allylic protons (ArCH=CHC*H*$_3$). There was no evidence of signals due to the unisomerized alkene in the ^{1}H NMR spectrum which probably meant that at this stage all the starting material had already isomerized to a more stable internal double bond. The signals due to the silicon protecting group were all accounted for which confirmed that the group was not lost during the initial isomerization step.

Nevertheless, we were very satisfied that the silicon protection group was lost in the course of the reaction (**Scheme 4.47**) because in any case, we would have carried out the deprotection step before attempting bromination to ensure selective bromination at position 6 and not 7 of 3,4-dihydroisochromen-5-ol ***trans*-409** (**Figure 4.13**).



***trans*-409**

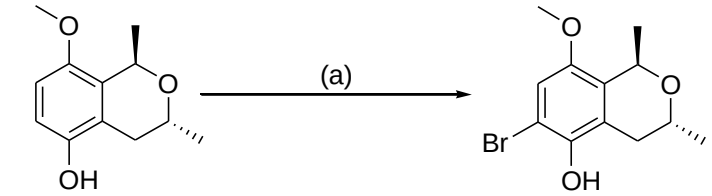
Figure 4.13: The molecular structure of phenol ***trans*-409** highlighting positions 6 and 7.

There is literature precedence for brominating the *ortho* position to the phenol group as opposed to the *ortho* position to the methoxy group of the aromatic ring.[256] This is due to the

electron donating effect of the phenol substituent by resonance being is much stronger compared to the electron donating effect of the methoxy group.

4.1.14 Synthesis of (±)-*trans*-6-bromo-3,4-dihydro-8-methoxy-1,3-dimethyl-1*H*-isochromen-5-ol *trans*-425

The bromination of 3,4-dihydroisochromen-5-ol ***trans*-409** was carried out using the protocol reported by Deore and co-workers.[256b] The 3,4-dihydroisochromen-5-ol was dissolved in acetic acid in a 2-neck round bottom flask to which sodium acetate was added under a blanket of nitrogen gas. A solution of bromine was added and the reaction mixture was stirred at room temperature for 30 minutes after which it was quenched using saturated sodium hydrogen carbonate solution. The crude product was purified by silica gel column chromatography affording the intended product ***trans*-425** (**Scheme 4.49**) in 59% yield. The 6-bromo-3,4-dihydroisochromen-5-ol ***trans*-425** was fully characterized to ensure that bromination took place at position 6 of phenol ***trans*-409** (**Figure 4.13**) and that there was no epimerization of the pyran ring. This decision was made because we were unable to grow good crystals for crystal structure determination which could have easily confirmed the position of bromine on the phenol moiety. The 2D spectroscopic data for this compound are given in a table form in **Appendix B1.5**.

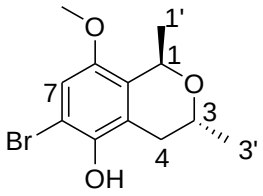


***trans*-409** ***trans*-425**

Scheme 4.49: *Reagents and conditions:* (a) Br_2, AcOH, NaOAc, 30 min, 59%.

4.1.14.0 Assigning C-H protons and carbon atoms of (±)-*trans*-6-bromo-3,4-dihydro-8-methoxy-1,3-dimethyl-1*H*-isochromen-5-ol *trans*-425

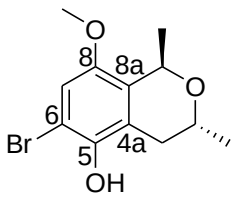
The ^{1}H NMR spectrum revealed loss of one aromatic proton and the remaining proton appeared as a singlet signal at 6.56 ppm (1H, s) and was assigned to H-7. The HSQC revealed that this proton signal correlated with the carbon signal at 109.0 ppm and the carbon signal was ascribed to C-7. The D_2O exchangeable proton signal at 5.16 ppm (1H, s) did not show correlation to any carbon signal in the HSQC spectrum and was assigned to the phenol proton. The signal at 5.10 ppm (1H, q, *J* = 6.4 Hz) was assigned to H-1 and a doublet signal at 1.54 ppm (3H, d, *J* = 6.6 Hz) was assigned H-1' on the basis of correlation shown by the ^{1}H-^{1}H COSY spectrum. The HSQC spectrum showed that H-1 and H-1' protons correlated with the carbon signals at 68.3 ppm and 19.5 ppm and the signals were assigned to C-1 and C-1' carbon atoms, respectively. The two separate doublet of doublets at 2.81 ppm (1H, dd, *J* = 17.1, 3.4 Hz) and 2.39 ppm (1H, dd, *J* = 17.1, 10.9 Hz) were typical of the H-4 protons. The HSQC spectrum revealed that these protons correlated with the same carbon signal at 30.6 ppm and this carbon atom was ascribed to C-4. The multiplet signal between 4.19-3.99 ppm (1H, m) was typical of the H-3 proton and the proton signal at 1.36 ppm (1H, d, *J* = 6.1 Hz) was assigned to H-3' on the basis of correlation shown by the ^{1}H-^{1}H COSY spectrum. In addition, the HSQC spectrum showed that H-3 and H-3' protons correlated to the carbon signals at 62.3 ppm and 22.0 ppm and these signals were assigned to C-3 and C-3', respectively. Lastly, the proton signal at 3.77 ppm (3H, s) was assigned to the methoxy group which correlated to the carbon signal at 55.6 ppm. This meant that there was no bromination or epimerization of the pyran ring system.



***trans*-425**

4.1.14.1 Assigning non C-H carbon atoms for 6-bromo-3,4-dihydroisochromen-5-ol *trans*-425

The HMBC spectrum showed correlation between the proton signal at 3.77 ppm (methoxy proton) with the carbon signal at 149.6 ppm and this signal was assigned to C-8. The proton signal at 1.54 ppm (H-1') correlated with a carbon nucleus resonating at 129.7 ppm and this carbon signal was assigned to C-8a. The proton signal at 1.36 ppm (H-3')

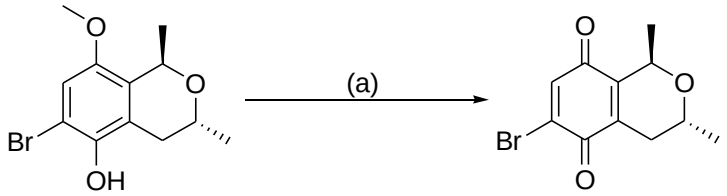


***trans*-425**

showed correlation with the carbon signals at 123.1 ppm and 123.0 ppm and was assigned to C-4a. The signal was somehow split into a doublet. The phenol proton signal at 5.16 ppm showed correlation with carbon signals at 144.2 ppm, 123.0 ppm and 123.1 ppm and the signal at 144.2 ppm was ascribed to C-5. The fact that the signal at 6.56 ppm (H-7) correlated with a carbon signal at 68.3 ppm (C-1) but not the carbon signal at 30.6 ppm (C-4) together with the observation that there was no correlation between the proton signals at 2.81 ppm and 2.39 ppm (H-4) with the carbon signal at 109.0 ppm confirmed that bromination took place at position 6 of the ring. The carbon atom holding the bromine substituent resonated at 119.9 ppm and was assigned to C-6.

4.1.15 Synthesis of (±)-*trans*-6-bromo-3,4-dihydro-1,3-dimethyl-1*H*-isochromene-5,8-dione *trans*-383

Satisfied that we had the desired 6-bromo-3,4-dihydroisochromen-5-ol ***trans*-425** the next step in the sequence of reactions was to oxidize phenol ***trans*-425** to a corresponding 6-bromo-3,4-dihydropyranobenzoquinone ***trans*-383**. A solution of phenol ***trans*-425** in 1,4-dioxane was oxidised to a corresponding *p*-benzoquinone using silver (II) oxide and nitric acid. Purification of the crude reaction mixture by column chromatography on silica gel yielded *p*-pyranobenzoquinone ***trans*-383** (**Scheme 4.50**) in 73% yield.



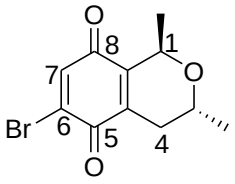
***trans*-425** ***trans*-383**

Scheme 4.50: *Reagents and conditions:* (a) AgO, *55%* aq. HNO_3, 1,4-dioxane, rt, 73%.

There was a minor epimerization from the initial *trans* configuration to *cis* configuration which was undeniably visible in both the ^{1}H and ^{13}C NMR spectra. The epimerization increased greatly when the reaction was left for extended periods indicating that it was most likely the quinone product ***trans*-383** which was epimerizing as opposed to the reaction intermediate(s). We felt that the quinone product presented us with an opportunity to reconfirm the position of the bromine substituent in the starting material. This was even more

crucial when one of the products for attempted silylation reaction had a bromine substituent at position 7 as opposed to position 6. This reaction will be fully discussed in **Section 4.1.16**. The 2D spectroscopic data for 6-bromo-3,4-dihydropyranobenzoquinone ***trans*-383** are given in a table form in **Appendix B1.6**.

The ^{1}H NMR spectrum of quinone ***trans*-383** revealed the absence of the phenol proton signal which was at 5.16 ppm in the starting material and the methoxy carbon signal at 55.6 ppm in the ^{13}C NMR spectrum was also absent indicating the possibility that oxidation took place. The proton signal at 7.22 ppm (1H, s) was assigned to H-7 and it showed correlation to a carbon signal at 138.0 ppm (C-7) in the HSQC spectrum. The proton signals due to the pyran ring were largely unchanged except for small signals corresponding to the *cis* product. The ^{13}C NMR spectrum showed new signals at 183.2 ppm and 178.6 ppm indicating a typical *para*-quinone as explained in previous sections. The HMBC spectrum showed that the proton signal at 4.83 ppm (1H, q, J = 6.7 Hz) corresponding to H-1 correlated with a carbon signal at 183.2 ppm and this signal was assigned to C-8. In addition, the signal at 2.64 ppm (1H, dd, J = 19.2, 3.2 Hz) and 2.18 ppm (1H, ddq, J = 19.2, 10.0, 2.2 Hz) for H-4 protons correlated strongly with a carbon signal at 178.6 ppm but only weakly with a carbon signal at 183.2 ppm and the signal at 178.6 ppm was assigned to C-5.



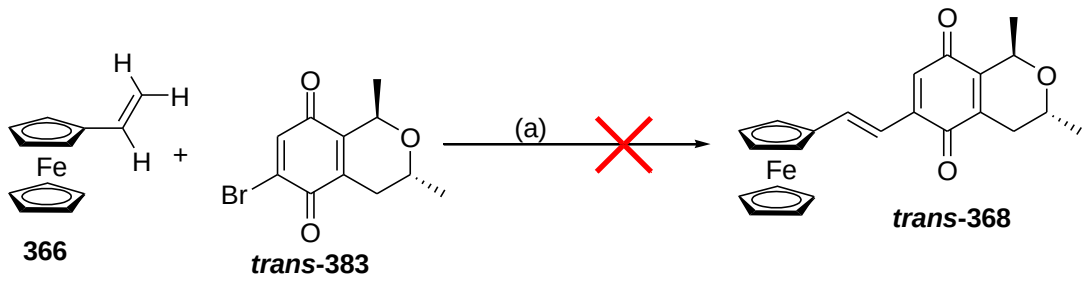
***trans*-383**

The HMBC spectrum further showed that there was correlation between the H-7 proton and a carbon signal at 66.9 ppm (C-1) in the ^{13}C NMR spectrum but not with a signal at 30.2 ppm (C-4). Conversely, there was no correlation between the H-4 proton signals to a carbon signal at 138.0 ppm. These facts were further proof that this proton was on position 7 and not 6 which in turn proved that bromination took place at position 6 of the phenol ***trans*-409**.

The IR spectrum did not show a peak at 3610 cm^{-1} which was in the precursor phenol corresponding to the alcohol functional group but rather showed peaks at 1774 cm^{-1} and 1753 cm^{-1} corresponding to the carbonyl functional groups of the diketone. Additionally, the HRMS spectrum showed a molecular ion peak at 270.9970 amu which was in good agreement with the expected mass of 270.9964 amu for $C_{11}H_{12}O_3{}^{79}Br$.

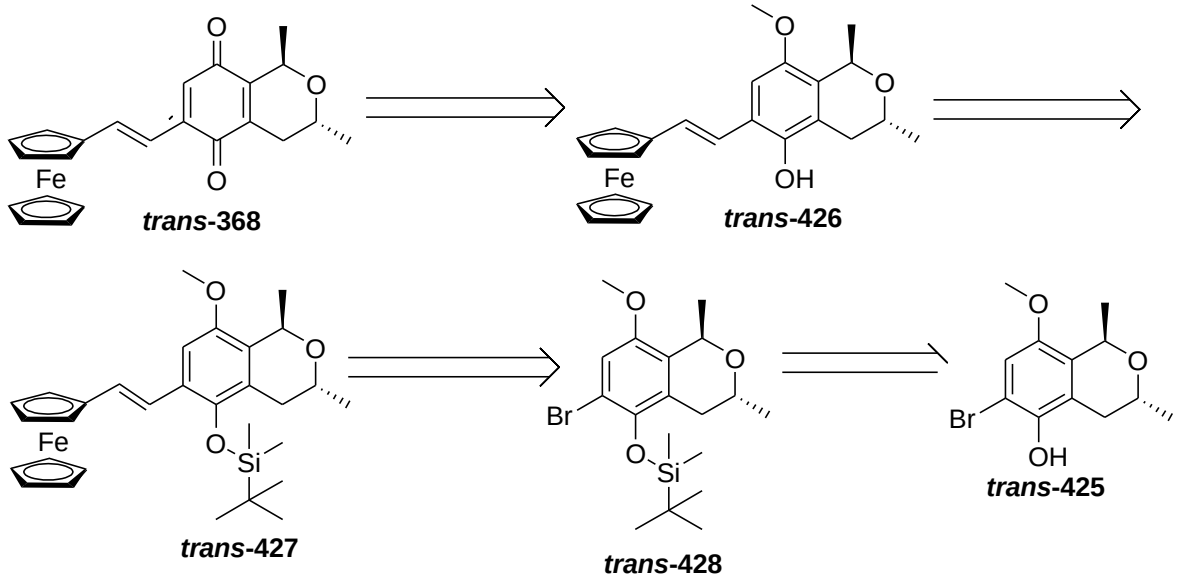
4.1.16 Synthesis of (±)-*trans*-15-bromo-5,13-dimethoxy-2,4,10,12-tetramethyl-4,7,9,10,12,13-hexahydro-1*H*-7,13-methanopyrano[4',3':6,7]oxocino[2,3-*f*]isochromen-8(2*H*)-one

With the quinone in hand and having already synthesized vinyl ferrocene **366**, our main effort at this stage was directed towards coupling the two intermediates to obtain the target compound, ferrocenyl 3,4-dihydropyranobenzoquinone ***trans*-368**. The vinyl ferrocene **366** and quinone ***trans*-383** (5:1 ratio, respectively) were dissolved in tetrahydrofuran in a round bottom flask after which water, palladium acetate and potassium carbonate were added while stirring. The mixture was heated to reflux for 4 hours (monitored by TLC) after which it was allowed to cool to room temperature, separated, dried over magnesium sulfate and filtered. Purification of the crude residue by column chromatography did not yield the target compound ***trans*-368** (**Scheme 4.51**) but rather an uncharacterizable compound despite the crude reaction mixture showing a clear new spot on the TLC plate which was different from the two starting materials.



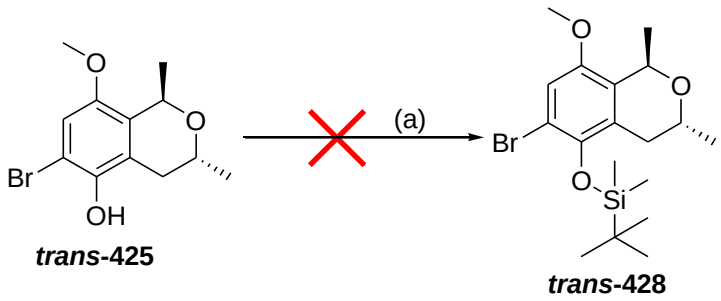
Scheme 4.51: *Reagents and conditions:* cat. $Pd(OAc)_2$, K_2CO_3, THF, PPh_3, reflux, 2 hrs.

Frustrated by these results we thought that protecting the phenol group and subjecting the *ortho*-brominated intermediate ***trans*-428** to Heck cross-coupling reaction could potentially afford ferrocene coupled intermediate ***trans*-427** which could be desilylated delivering ferrocenyl 3,4-dihydroisochromen-5-ol ***trans*-426**. The intermediate ***trans*-426** (**Scheme 4.52**) could easily be oxidised to ferrocenyl quinone ***trans*-368** as already discussed.



Scheme 4.52: The retrosynthetic analysis for the formation of ***trans*-368** through ferrocenyl phenol ***trans*-426**.

When bromophenol ***trans*-425** was subjected to a routine silicon-protection protocol we did not isolate silyl protected 3,4-dihydroisochromene ***trans*-428** (**Scheme 4.53**). The TLC plate showed several spots none of which corresponded to the starting material. Despite repeated silica gel column chromatography and recrystallization we could only manage to purify one component sufficiently for it to be characterized by spectroscopic techniques at our disposal. **Scheme 4.53** shows the reagents and conditions for the failed silylation of bromophenol ***trans*-425**.



Scheme 4.53: *Reagents and conditions:* (a) TBDMSCl, imidazole, cat. DMAP, DMF, rt, 72 hrs.

The ^{1}H and ^{13}C NMR spectroscopy revealed very complicated spectra but we were able to figure out that it was a dimer based on four different shielded doublet signals in the ^{1}H NMR spectrum which were consistent with the methyl groups of the pyran ring in the starting

material. The ^{1}H NMR spectrum further revealed 2 sets of signals typical of the *pseudo*-axial and *pseudo*-equatorial protons of which only 1 set was present in the precursor bromophenol ***trans*-425**. The spectrum showed 1 aromatic proton indicating loss of 1 aromatic proton on one half of the 3,4-dihydroisochromen-5-ol moiety. Furthermore, the two methoxyl groups resonated at very different chemical shifts indicating that they were in two completely different magnetic as well as chemical environments. There were also, surprisingly, two highly deshielded doublet signals each integrating for 1 proton with a coupling constant of *J* = 3.9 Hz. In addition, there was no signal corresponding to the phenol group which was confirmed by the IR spectrum which showed no hydroxyl functional group stretching peak. The ^{13}C NMR spectrum showed one carbonyl carbon signal at 191.54 ppm which was confirmed by the IR spectrum which showed a peak at 1763 cm^{-1} corresponding to the carbonyl functional group. The ^{13}C spectrum further revealed that there were 8 signals in the alkene/aromatic region which meant that 4 aromatic signals were lost. The loss of 4 signals in the aromatic/alkene region corresponded to the gain of 1 carbonyl signal and 3 alkyl carbon signals. The HMRS data showed a molecular ion peak at 493.1226 amu with a predicted formula of $C_{24}H_{30}{}^{79}BrO_6$. This value was in agreement with a calculated value of 492.1220 amu for $C_{24}H_{30}{}^{79}BrO_6$. These data led to two possible predicted structures namely dimers **429** and **JS-X10** as shown in **Figure 4.14**.

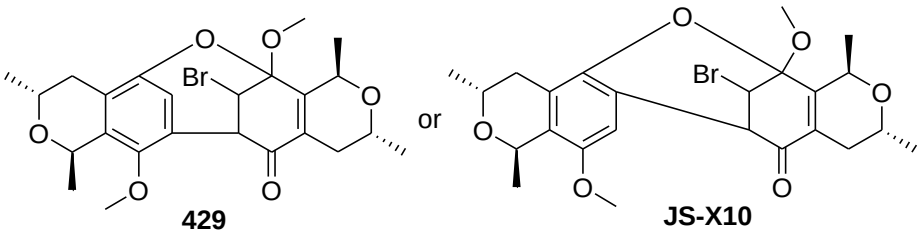


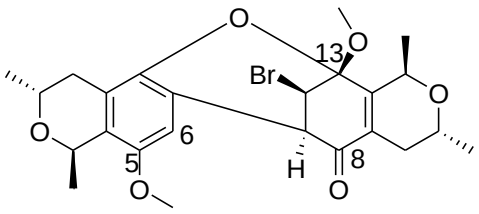
Figure 4.14: The molecular structure of 2 possible compounds, **429** and **JS-X10**.

Due to the nature of the structures in **Figure 4.14**, prediction of the protons and carbon atoms signals using ChemDraw software (effectively used previously) proved less significant and HSQC, COSY, DEPT and HMBC spectra were fully analysed and used in assigning the signals to the corresponding atoms. We felt that this was very important because the compound showed interesting preliminary biological results as will be discussed in **Chapter 5**. The studies into the biological importance of this compound are ongoing in our laboratory

group. The 2D spectroscopic data for **JS-X10** is shown in a tabulated form in **Appendix B1.7**.

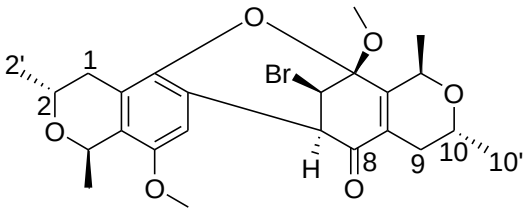
4.1.16.0 Spectroscopic data analysis for proposed compound JS-X10

The ^{1}H NMR spectrum showed a signal at 6.42 ppm (1H, s) which was assigned to the H-6 proton as the only aromatic proton and using both the HSQC and DEPT spectra, a carbon signal at 105.8 ppm in the ^{13}C NMR spectrum correlated to this proton and was assigned C-6. A proton signal at 3.73 ppm (3H, s) was typical of the methoxy protons of the aromatic ring (ArOCH_3) and a carbon signal at 55.6 ppm in the ^{13}C NMR spectrum was assigned to this methoxy carbon atom on the basis of the HSQC spectrum. A proton signal at 3.53 ppm (3H, s) was assigned to the only remaining methoxy group which was attached to an sp^3 hybridised carbon atom and the signal at 48.4 ppm in the ^{13}C NMR spectrum was assigned to this methoxy group on the basis of correlation shown by the HSQC spectrum. The signal at 191.5 ppm in the ^{13}C NMR spectrum was unequivocally assigned to C-8. The HMBC spectrum showed correlation between the signals at 3.73 ppm and 3.53 ppm to the carbon signals at 150.5 ppm and 98.3 ppm, respectively. The signal at 150.5 ppm was therefore assigned to C-5 and the signal at 98.3 ppm was assigned to C-13.



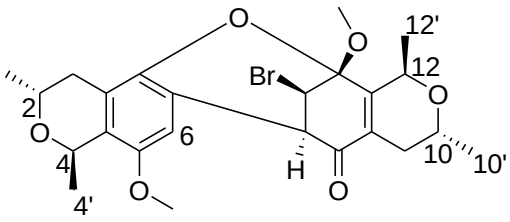
JS-X10

The four signals which appeared as doublet of doublets each at 2.71 (1H, dd, *J* = 17.4, 3.6 Hz), 2.46 (1H, dd, *J* = 18.3, 4.0 Hz), 2.29 (1H, dd, *J* = 17.4, 10.6 Hz) and 1.75 ppm (1H, dd, *J* = 18.3, 10.6 Hz) in the ^{1}H NMR spectrum were typical of the pyran ring protons in the *pseudo*-equatorial and *pseudo*-axial positions of the ring as previously discussed. Using the HSQC spectrum we were able to correlate the signals at 2.71 ppm and 2.29 ppm to a carbon signal at 29.9 ppm and the signals at 2.46 ppm and 1.75 ppm to a carbon signal at 29.2 ppm. The HMBC spectrum showed a strong correlation between the proton signal at 2.46 ppm and the carbon signal at 191.5 ppm (C-8) but there was no correlation between the proton signals at 2.71 ppm and 2.29 ppm to this carbon signal.



This led to assigning H-9 and C-9 to the signals at 2.46 ppm and 29.2 ppm, respectively. This meant that the signal at 2.71 ppm in the ^{1}H NMR spectrum and 29.9 ppm in the ^{13}C NMR spectrum were assigned to H-1 and C-1, respectively. At this point the ^{1}H-^{1}H COSY spectrum would have given us the headway by separating the H-2 (and H-2') to the H-10 (and H-10') but unfortunately there was no visible interactions between these pairs of protons. Nevertheless the HSQC spectrum showed that the 4 separate doublets in the ^{1}H NMR spectrum at 1.60 ppm (3H, d, J = 6.6 Hz), 1.48 ppm (3H, d, J = 6.6 Hz), 1.33 ppm (3H, d, J = 6.1 Hz) and 1.19 ppm (3H, d, J = 6.1 Hz) correlated to the carbon signals in the ^{13}C NMR spectrum at 20.6 ppm, 19.3 ppm, 22.0 ppm and 21.6 ppm, respectively. Additionally, the HMBC spectrum showed that the proton signal at 1.33 ppm correlated with the signals at 29.9 ppm and 61.9 ppm. The HSQC spectrum showed that the signal at 61.9 ppm corresponded to a multiplet between 4.14-3.89 ppm (3H, m) and these facts led to assignment of a signal at 1.33 pm and one of the multiplet protons between 4.14-3.39 ppm to H-2' and H-2, respectively and the signals at 22.0 ppm and 61.9 ppm in the ^{13}C NMR spectrum to C-2' and C-2 carbon atoms, respectively.

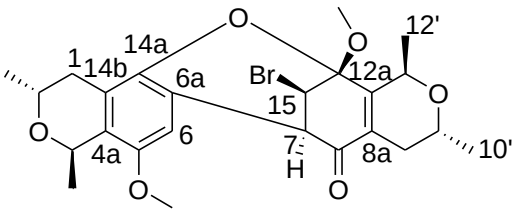
In the same way, the HMBC spectrum showed that the signal at 1.19 ppm correlated with the carbon signals at 29.2 ppm and 62.0 ppm. Furthermore, the HSQC spectrum showed that the signal at 62.0 ppm corresponded to a multiplet between 4.14-3.89 ppm. Combining these facts led us to assign a signal at 1.19 pm and one of the multiplet protons between 4.14-3.39 ppm to H-10' and H-10 protons, respectively and the signals at 21.6 ppm and 62.0 ppm in the ^{13}C NMR spectrum to C-10 and C-10' carbon atoms, respectively.



Even though both H-10 and H-2 protons were part of the multiplet signal between 4.14-3.89 ppm and the individual signals generated by them would not be individually correlated to the carbon atoms bonded to them at this stage, they were very useful in identifying the remaining protons in the pyran ring. A signal at 5.03 ppm (1H, q, J = 6.6 Hz) showed correlation to a carbon signal at 61.9 ppm but not to the carbon signal at 62.0 ppm and was assigned to H-4 protons. Using the HSQC spectrum we assigned a signal at 68.1 ppm in the ^{13}C NMR

spectrum to C-4 carbon atom. At this point the ^{1}H-^{1}H COSY interaction alongside the HSQC spectrum were used to assign a signal at 1.48 ppm in the ^{1}H NMR spectrum to H-4' protons and a signal at 19.3 ppm to C-4' carbon atom. The remaining quartet signal at 4.66 ppm (1H, q, J = 6.8 Hz) was assigned to H-12 protons and a doublet signal at 1.60 ppm was assigned to H-12' protons on the basis of the ^{1}H-^{1}H COSY correlation. The HSQC spectrum was therefore used to assign carbon signals at 67.7 ppm and 20.6 ppm to C-12 and C-12' carbon atoms, respectively. These assignments were further confirmed by the painstaking analysis of the HMBC spectrum.

At this point we turned our attention to the two unusual doublet signals one of which was at 4.71 ppm (1H, d, J = 3.9 Hz) and the other one was part of a multiplet signal between 4.14-3.89 ppm in the ^{1}H NMR spectrum. The signal at 4.71 ppm correlated with a carbon signal at 67.7 ppm which was not the case with all the protons involved in the multiplet signal between 4.14-3.89 ppm. Conversely, the multiplet protons correlated with the carbon signal at 105.8 ppm (assigned to C-6 with H-6 proton) which was not the case with a proton signal at 4.71 ppm. Since we already identified the other two protons as H-2 which was 5 bonds away from H-6 and H-10 which was 6 bonds away from H-6, this correlation must have come from a doublet signal of the multiplet. These two observations alongside the HSQC spectrum were used to assign a signal at 4.71 ppm in the ^{1}H NMR spectrum and a signal at 45.1 ppm in the ^{13}C NMR spectrum to H-15 proton and C-15 carbon atom, respectively. This implied that the doublet signal in the multiplet was due to H-7 proton and the signal at 55.3 ppm in the ^{13}C NMR spectrum was due to C-7 carbon atom. These assignments were consistent with the analysis of the HMBC spectrum.



Having unambiguously assigned all important proton and carbon signals the remaining carbon atoms, with no protons attached to them, were assigned on the basis of the HMBC spectrum. The signals at 149.5 ppm and 130.0 ppm in the ^{13}C NMR spectrum were assigned to C-12a and C-8a carbon atoms, respectively, by analysing the correlation of H-12' and H-15 protons which interacted with a carbon signal at 149.5 ppm but not at 130.0 ppm and H-10' protons which correlated with a carbon signal at 130.0 ppm but not with a signal at 149.5

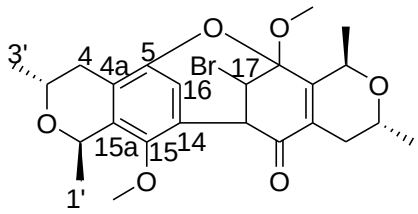
ppm. Having also isolated the signal of the multiplet due to H-7 proton, we were able to determine that it showed correlation to the carbon signal at 130.0 ppm but not with a signal at 149.5 ppm.

The carbon signals at 143.5 ppm and 114.3 ppm in the ^{13}C NMR spectrum were assigned to C-14a and C-6a, respectively on the basis of correlation shown between a carbon signal at 143.5 ppm with H-1 but not with a signal at 114.3 ppm. Likewise, there was correlation between a carbon signal at 114.3 ppm and a proton signal at H-7 but this proton did not show any correlation with a carbon signal at 143.5 ppm.

Finally, the carbon signals at 130.4 ppm and 123.7 ppm in the ^{13}C NMR spectrum were assigned to C-14b and C-4a, respectively on the basis of correlation between H-6 and the carbon signal at 130.4 ppm which was not replicated with a carbon signal at 123.7 ppm. This was further confirmed by a weak interaction of the proton signals at 1.33 ppm and 1.48 ppm to the carbon signals at 123.7 ppm and 130.4 ppm, respectively.

4.1.16.1 Spectroscopic data analysis for proposed compounds 429

Much as the spectroscopic data obtained for this reaction step matched compound **JS-X10** we felt that it was still imperative that we analyse the data with respect to proposed compound

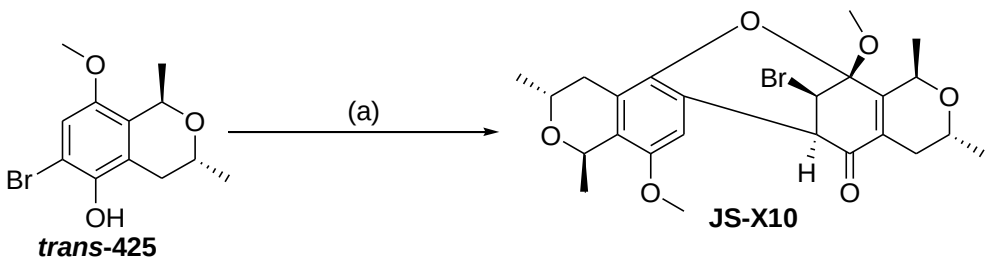


429. The only difference between compounds **429** and **JS-X10** was the connectivity between the two 3,4-dihydroisochromene moieties on the side of the aromatic ring. Based on this fact, we thought that it was prudent to concentrate our spectroscopic data analysis for this compound on the aromatic side. The table showing ^{1}H-^{13}C and ^{1}H-^{1}H correlations is presented in **Appendix B1.8**.

The HMBC spectrum showed correlated between a proton signal at 3.73 ppm (3H, s, ArOC*H*$_3$) and the carbon signal at 150.49 ppm and this carbon signal was ascribed to C-15. The proton signal at 6.42 ppm (H-16) showed correlation to the carbon signals at 150.5 ppm, 143.5 ppm, 130.4 ppm and 114.3 ppm. Likewise, the proton signal at 4.71 ppm (H-17) showed correlation to a carbon signal at 114.3 ppm whereas the proton signals at 2.71 ppm

(H-4) and 2.29 ppm (H-4) showed correlations to carbon signals at 143.5 ppm, 130.4 ppm and 123.7 ppm.

On the basis on the above analysis as simplified below, the carbon signal at 143.5 ppm was assigned to C-5 on the basis of correlation it showed with H-4 proton but this proton did not show correlation to a carbon signal at 114.3 ppm. Likewise, there was correlation between a carbon signal at 114.3 ppm with H-17 proton signal but this proton did not show any correlation with a carbon signal at 143.5 ppm and the carbon signal at 114.3 ppm was assigned to C-14. The carbon signals at 130.4 ppm and 123.7 ppm in the ^{13}C NMR spectrum were assigned to C-15a and C-4a, respectively on the basis of correlation between H-16 and a carbon signal at 130.4 ppm which was not replicated with a signal at 123.7 ppm. The assignment of the carbon signals at 130.4 ppm and 123.7 ppm were not fully in agreement with the observed weak interaction of the protons at 1.33 ppm (H-3') and 1.48 ppm (H-1') to the signals at 123.7 ppm and 130.4 ppm, respectively. This marked the only observable difference between compound **429** and **JS-X10** which meant that **JS-X10** was the unknown compound we isolated as shown in reaction **Scheme 4.54**.



Scheme 4.54: *Reagents and conditions:* (a) TBDMSCl, imidazole, cat. DMAP, DMF, rt, 72 hrs, 30%.

A great deal of effort was directed towards growing crystals of this compound to identify the compound undeniably. Ultimately, we were able to grow crystals good enough for x-ray crystal structure determination which confirmed the structure as that of **JS-X10** as shown in **Figure 4.15**.

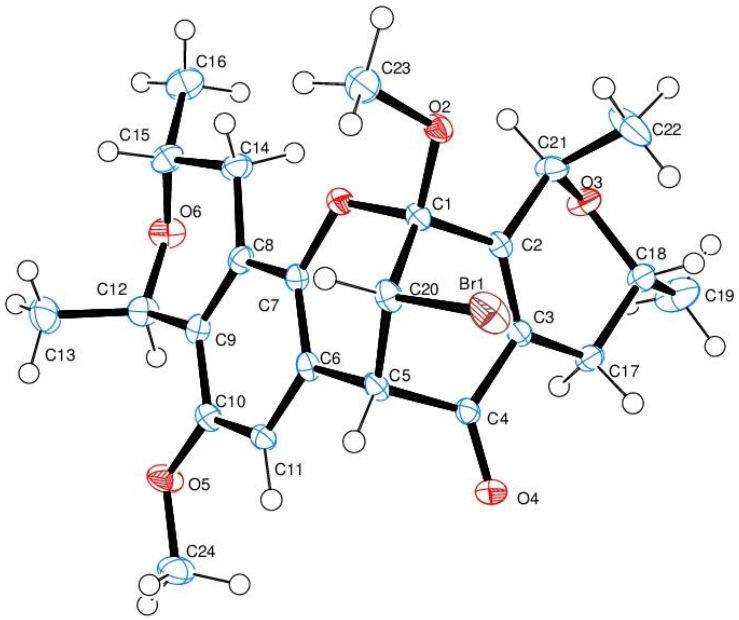


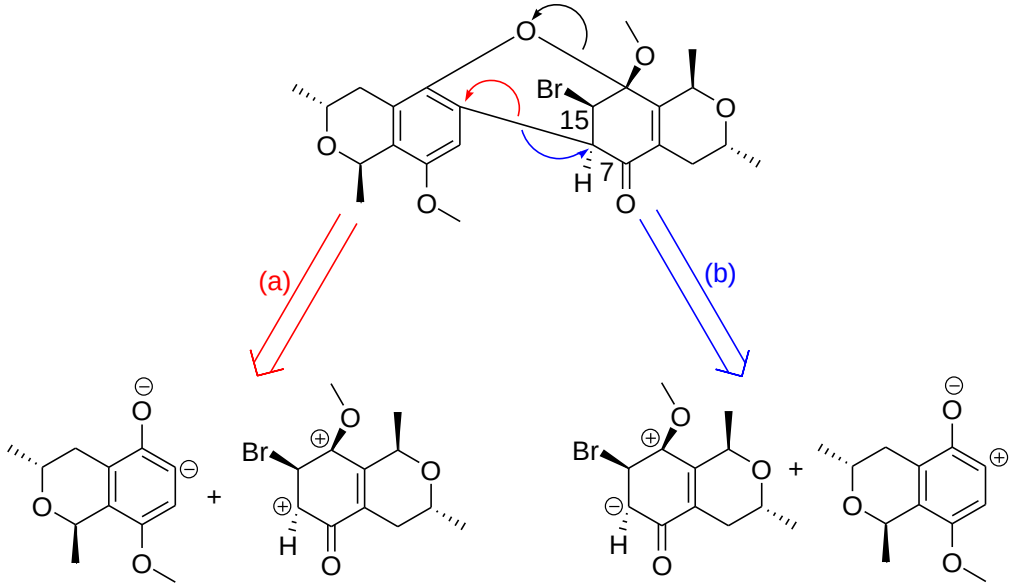
Figure 4.15: The ORTEP diagram for **JS-X10**. Thermal ellipsoids are shown at the 50% probability level.

4.1.16.2 Proposed mechanism for the formation of dimer JS-X10

Efforts to understand the mechanistic pathway for this reaction are underway in our laboratory and the proposed mechanisms discussed here are merely to offer some insights into this reaction. The exact mechanistic pathway can only be deduced from a combination of theoretical studies using computational methods and experiments tailored at eliminating competing potential pathways. The major point to consider was that the reaction was carried out under basic conditions and the substrate, ***trans*-425**, had an acidic phenol proton.

4.1.16.2.0 Proposed ionic disconnection

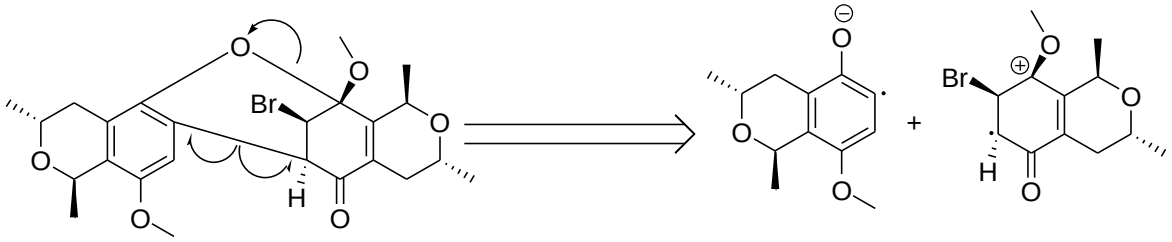
The retrosynthetic analysis shown in **Scheme 4.55** assumed an ionic mechanistic pathway. The crystal structure of the dimer **JS-X10** revealed that the H-Br was added in a *trans*-fashion across the *C*-7 and *C*-15 bond and the bromine was added to a less substituted carbon atom in a typical anti-Markovnikov addition. These facts convinced us that we were not dealing with a purely ionic reaction.



Scheme 4.55: Disconnection of the dimer **JS-X10** resulting from purely ionic synthons.

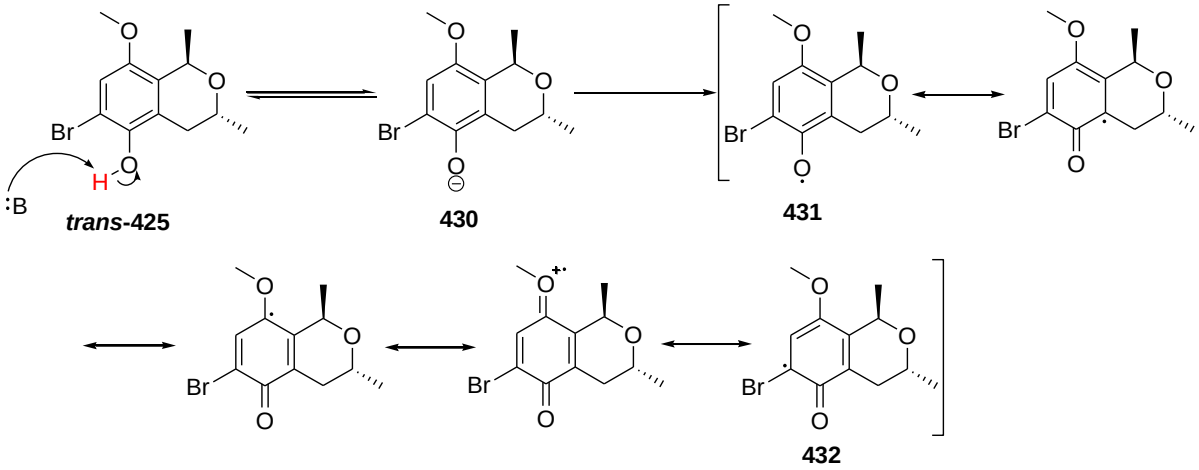
4.1.16.2.1 Proposed mixed ionic-radical disconnection

There are a total of 3 possible ways the dimer **JS-X10** could be disconnected to involve both ionic and radical mechanistic pathways. If the ether linkage was formed from the ionic reaction and the C-C linkage from the radical reaction then there could be only one way that this could be achieved as shown in **Scheme 4.56**. One of the synthons shown in **Scheme 4.56** is a typical Pummerer ketone.[257]



Scheme 4.56: Disconnection of the dimer resulting from radical-ionic synthons.

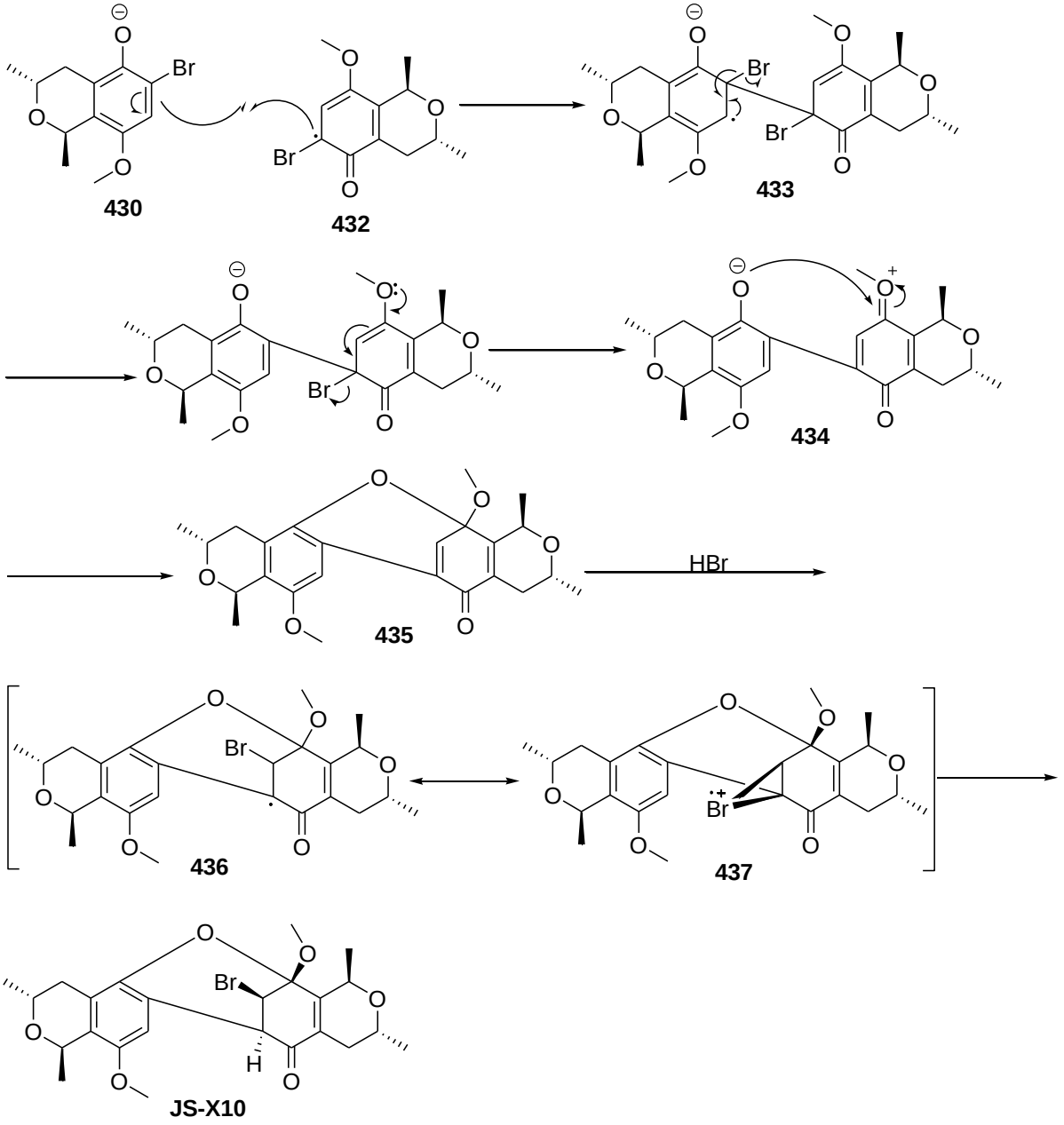
Under basic reaction conditions the first step could involve the deprotonation of bromophenol ***trans*-425** which could go on to generate anion **430** and the anion could generate reactive radicals. The generated radical would be highly stabilized by conjugation as shown in **Scheme 4.57**.



Scheme 4.57: The formation of radical intermediate from anion **430** under basic conditions.

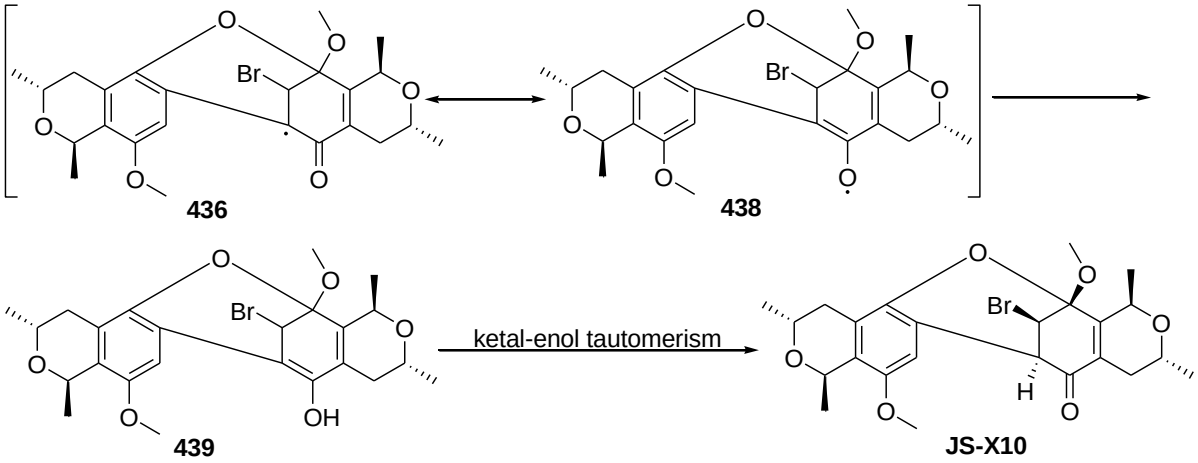
The next step could involve the attack of the radical **432** on the anion **430** to generate radical anion intermediate **433**. The loss of the two bromine atoms by a combination of radical and ionic reactions would generate intermediate **434**. The intermediate **434** could then be attacked by the phenoxide ion in a typical nucleophilic addition to generate intermediate **435**. The last step could involve radical addition of the H-Br across the double through the bromonium radical **437** yielding the dimer **JS-X10**. The choice of the alkene double bond attacked by the bromine radical for the anti-Markovnikov addition and the face of attack by the hydrogen radical on the bromonium radical could be dictated by the steric factors. The full reaction mechanism is shown in reaction **Scheme 4.58** below.

The choice of the anion **430** as a reaction partner of radical **432** was dictated by the fact that under basic condition there should be excess anion molecules in the reaction mixture such that the generated radicals quickly reacted with the anion **430** as opposed to bromophenol ***trans*-425**.



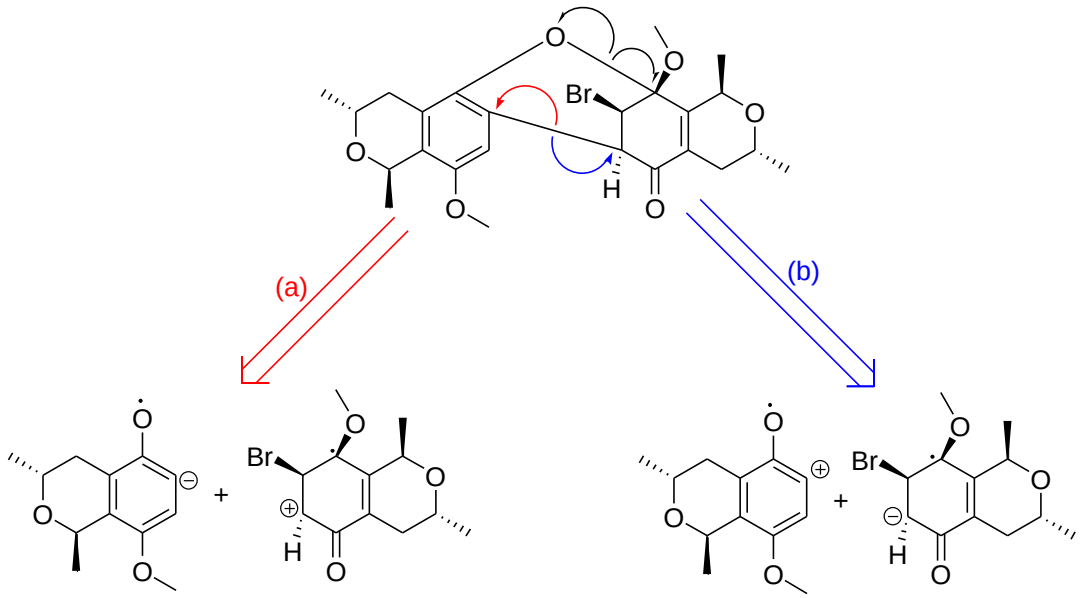
Scheme 4.58: The proposed radical-ionic reaction mechanism for the formation of dimer **JS-X10**.

The dimer **JS-X10** could also be formed from a third canonical form of the radical intermediate **436**, radical intermediate **438**, which was not included in **Scheme 4.58** above for clarity purposes. The intermediate **438** could acquire a hydrogen radical to form enol **439** which could undergo the bromine mediated ketal-enol tautomerism to deliver the dimer **JS-X10** as shown in reaction **Scheme 4.59**.



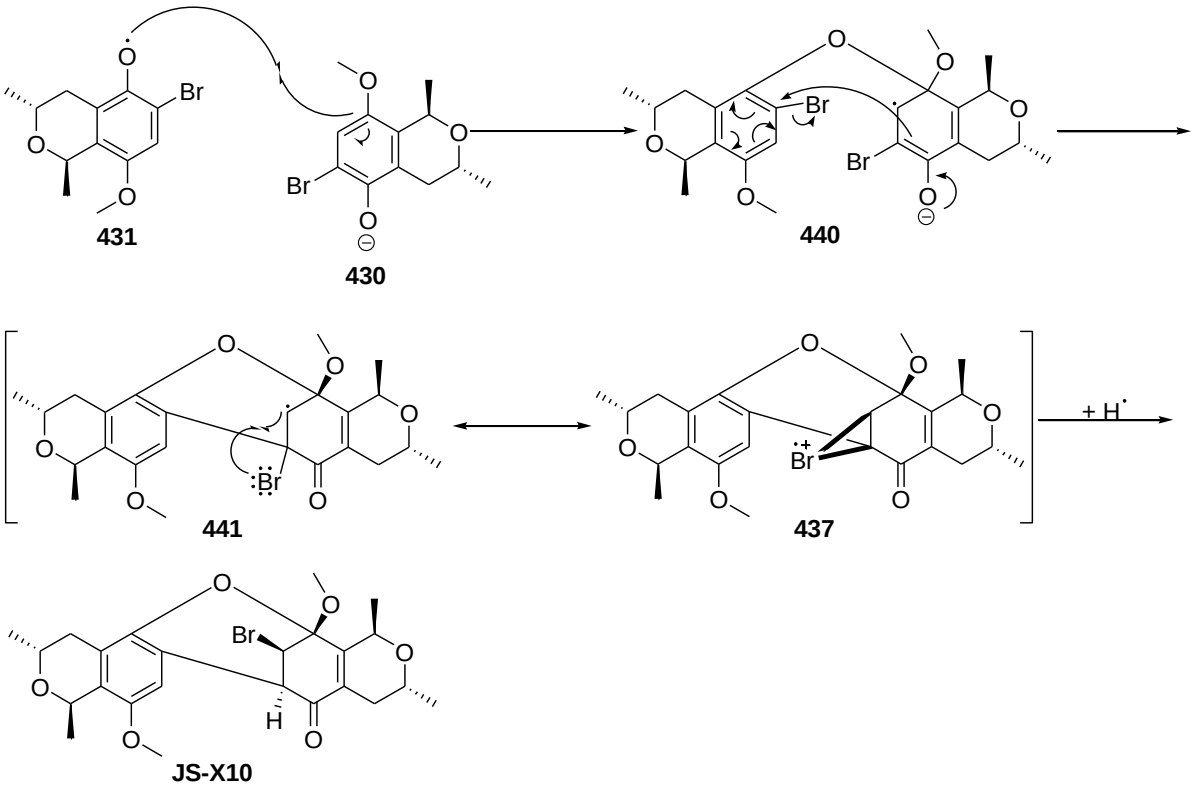
Scheme 4.59: Showing the bromine-mediated ketal-enol tautomerism of intermediate **439**.

If on the other hand, the ether linkage was formed from the radical reaction and the C-C linkage from the ionic reaction then there could be two possible ways in which this could be achieved as shown in **Scheme 4.60**. Route (a) would be as a result of bromine leaving as a cation which requires reversed polarities between the bromine and the carbon atom. Such a disconnection is very unlikely to result in assembly of dimer **JS-X10** because of the need for unusual umplong synthons. This meant that route (b) was the only viable disconnection.



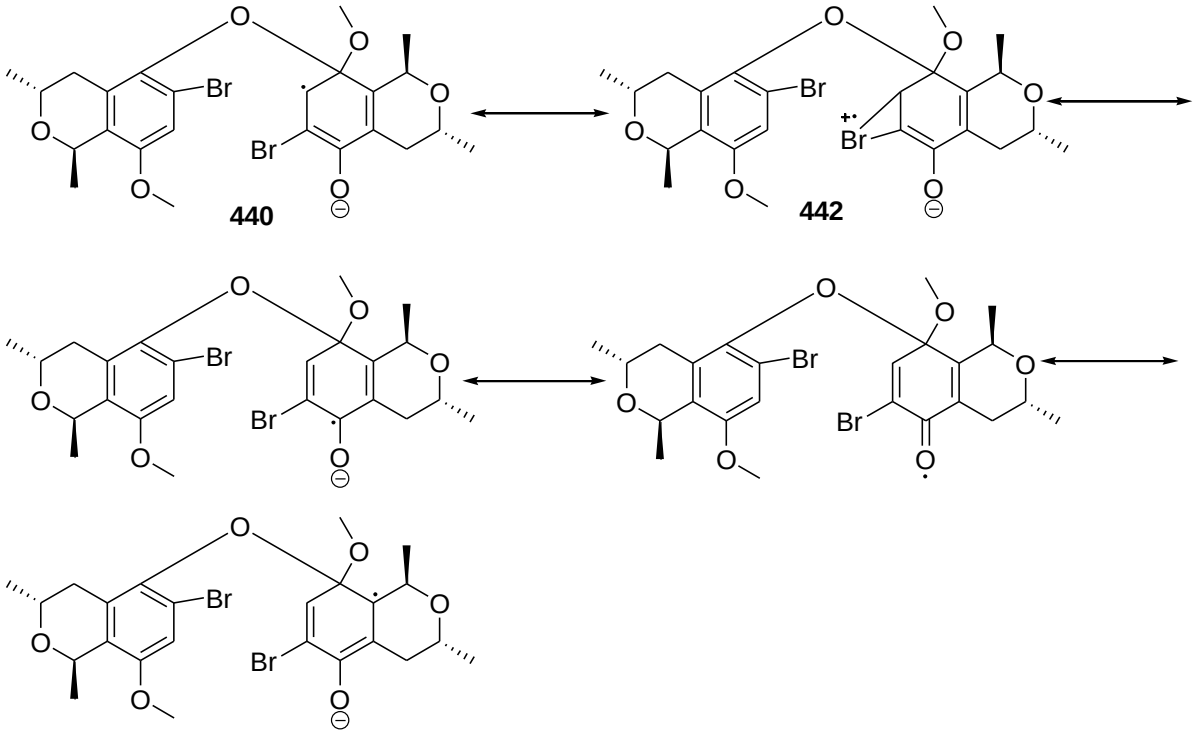
Scheme 4.60: Disconnection of the dimer **JS-X10** resulting from radical/ionic synthons.

If route (b) was followed, the first step of the mechanism would still involve the generation of the radical intermediates as shown in **Scheme 4.57** above. The attack on phenoxide ion **430** by radical **431** would generate the radical intermediate **440**. The nucleophilic attack of the phenoxide ion would lead to the formation of the radical intermediate **441** and one of its canonical forms **437** could then pick up the hydrogen radical to deliver the dimer **JS-X10** as presented in **Scheme 4.61**.



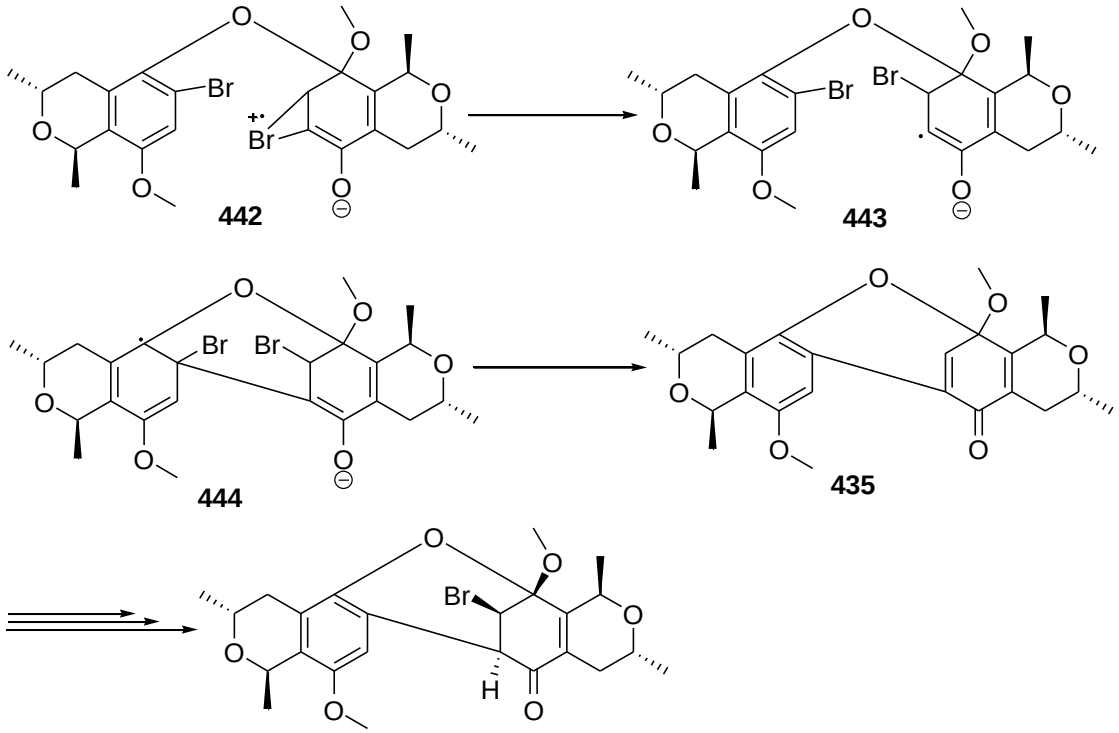
Scheme 4.61: Proposed mixed radical/ionic mechanism starting with the formation of ether linkage.

The choice of the intermediate **440** reacting by the typical nucleophilic aromatic reaction in the presence of a radical may seem odd but there is literature precedence of stabilized radicals which are not as reactive as free radicals. The radical in intermediate **440** (**Scheme 4.61** above) is stabilized by 5 canonical forms as depicted in **Scheme 4.62** whereas the phenoxide ion is stabilized by 2 resonance forms (which are not shown in this thesis for clarity purposes).



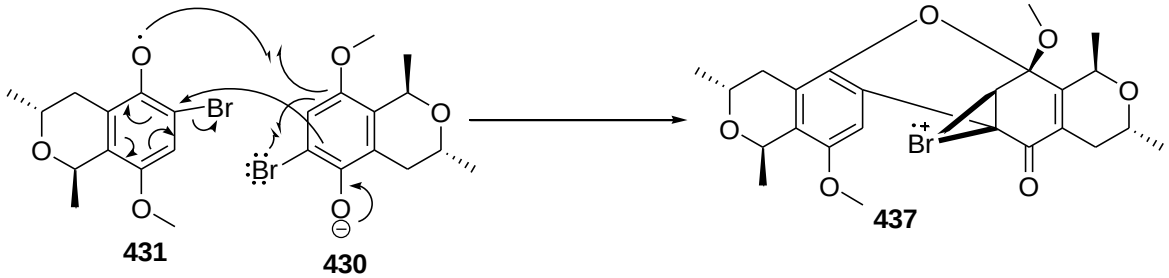
Scheme 4.62: Possible canonical forms of radical anion intermediate **440**.

If the theoretical studies would show that this is not the case then one of the canonical forms of **440** (**Scheme 4.61**) could be involved in the formation of the dimer **JS-X10**. For example, the canonical form **442** could be involved in dimerization reaction which could potentially afford dimer **JS-X10** as shown in **Scheme 4.63** below. The grey area for this mechanistic pathway was the 1,2-bromine shift of the intermediate **442** which generates intermediate **443**. This shift would involve the breaking of the stronger bond between Br-C(sp^2) in the presence of the weaker bond Br-C(sp^3). The shift was also not supported by the conjugation but for an intermediate anion with multiple double bonds there may be other factors at play. If it is assumed that the formation of radical intermediate **443** was a viable reaction step, then once it was formed it would react very quickly to form intermediate **444**. The radical in intermediate **443** would be very reactive because it would be in sp^2 orbital and therefore not stabilized by conjugation. The intermediate **444** could then lose both bromine atoms to form intermediate **435**. The intermediate **435** could react in the same way as shown in **Scheme 4.58** above.



Scheme 4.63: Proposed mechanism for the formation of dimer **JS-X10** through 1,2-bromine shift.

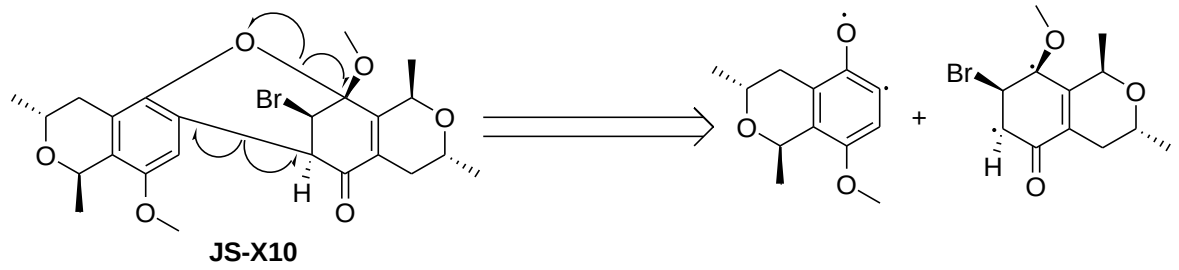
In a study by Saeed and co-workers[258] they found that there was no pronounced difference in reaction enthalpies between the formation of ether-linked and carbon-linked dimers for the first step in radical dimerization of 2-bromophenol and 2-chlorophenol. This means that there was a possibility of a concerted reaction involving a radical intermediate **431** and anion intermediate **430** as shown in reaction **Scheme 4.64**. The intermediate **437** could then undergo reaction sequence as previously discussed and shown in **Scheme 4.58**.



Scheme 4.64: The proposed reaction mechanism involved a concerted reaction between radical **431** and anion **430**.

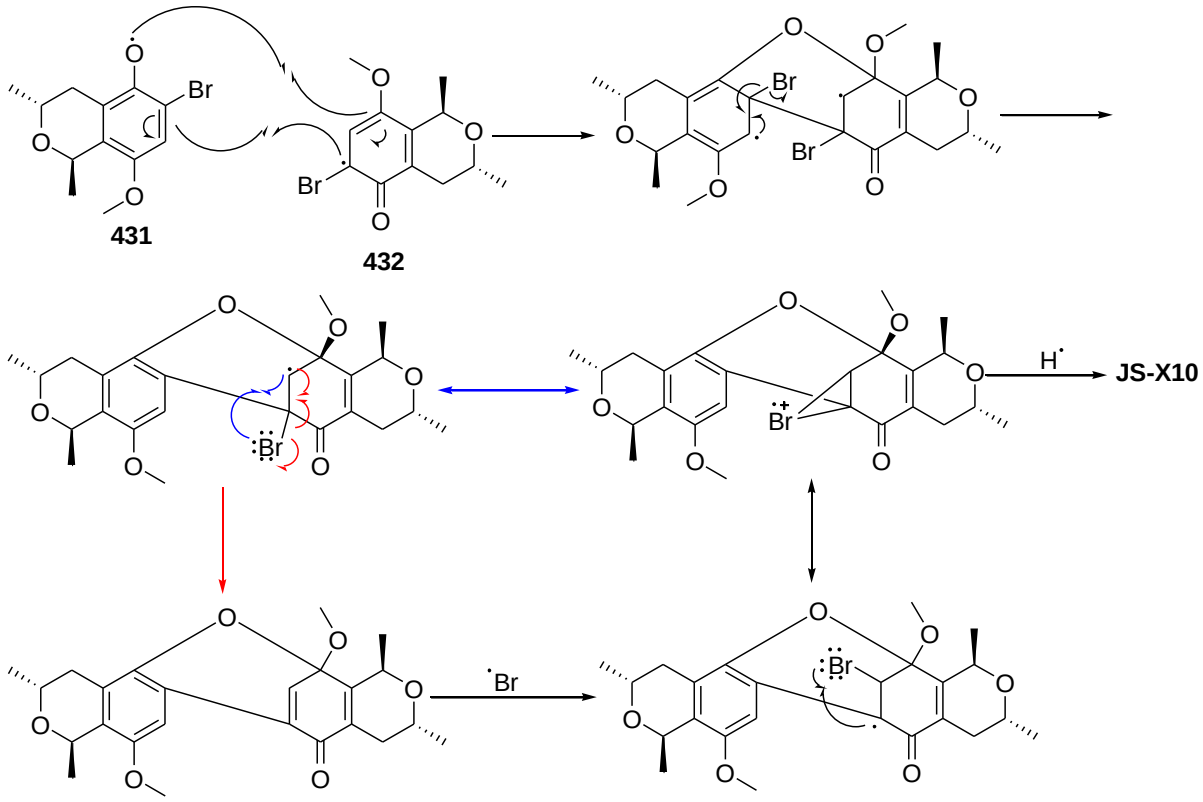
4.1.16.2.2 Proposed pure radical disconnection

There is only one way to disconnect bonds C-C and C-O of **JS-X10** to give radical synthons as shown in **Scheme 4.65**.



Scheme 4.65: Disconnection of the dimer **JS-X10** resulting from purely radical synthons.

The purely radical mechanism is highly unlikely under our conditions because radicals are very reactive and they would probably react with the anions (which were in excess) immediately when they are formed. The radicals generated in this case would be highly stabilised by conjugation such that there is a high possibility that their half-lives would be far much higher than normal free radicals. The reaction mechanisms discussed above for the mixed radical/ionic mechanisms would be applicable but with the anion step replaced by the radical step. In this thesis, we will give one example involving concerted reaction of radical intermediates **431** and **432**. The concerted reaction was chosen because it encompasses both routes i.e. the route involving the formation of the ether linkage as the first step as well as the route involving the formation of the C-C linkage as the first step. What was of note was that both routes (mechanisms not shown here) and concerted pathway led to the formation of intermediates that we have already encountered in the case of the combined radical/ionic with a radical replacing the anion as shown in **Scheme 4.66**.



Scheme 4.66: Proposed concerted mechanism for purely radical reaction.

In conclusion, we have successfully developed an effective design for synthesis of ferrocene coupled 3,4-dihydroisochromene which could be utilized in preparation of a variety of related analogue compounds. The versatility and applicability of our methodology for coupling of ferrocene moiety to isocoumarins and 3,4-dihydroisocoumarins based natural products will continue to be investigated in our laboratory.

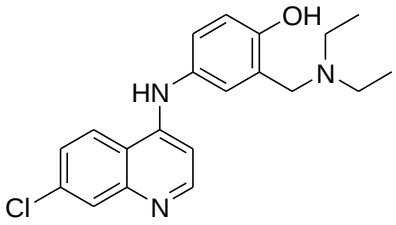
Chapter 5: Preliminary biological testing of selected compounds

5.0 Introduction

Some years ago, malaria was almost eliminated from many areas of the world through a combination of drug treatments and vector control interventions.[259] However, the rapid emergence and spread of drug resistance of the *P. falciparum* to almost all the commonly used antimalarial drugs in 1980s coupled with failure in eradicating the mosquito vector in the endemic regions using treated nets reversed the gains that were made in the fight against this disease by the discovery of chloroquine and its derivatives. For example, *P. falciparum* chloroquine resistance was first detected in Gabon in the 1980s and spread rapidly reaching between 90-100% *in vitro* resistance.[260] The *P. falciparum* resistance to quinine, sulfonamide-pyrimethamine combination, mefloquine, halofantrine and artemisinin and its derivatives were also reported in Gabon.[261] This meant that the population at risk from malaria increased drastically and the fight against the disease remained a major challenge especially in Southeast Asia and sub-Saharan Africa.

Reversing drug resistance usually takes a very long time as was highlighted by Chim and co-workers. These researchers reported that despite the use of chloroquine to treat *P. falciparum* infections in Cambodia being abandoned at the beginning of the 1980s, the data obtained between 2001 and 2003 indicated that the CQ-resistant phenotype was still common in this country. This demonstrated that resistance is stable over a long period of time and that a return to susceptibility may require many years.[262]

The antimalarial agent amodiaquine **445** (**Figure 5.0**) is effective against both CQ-susceptible and QC-resistant strains of *Plasmodium falciparum*. However, the clinical use of this drug is limited for long-term treatments due to adverse side effects which include hepatotoxicity and agranulocytosis among others.[263]



445

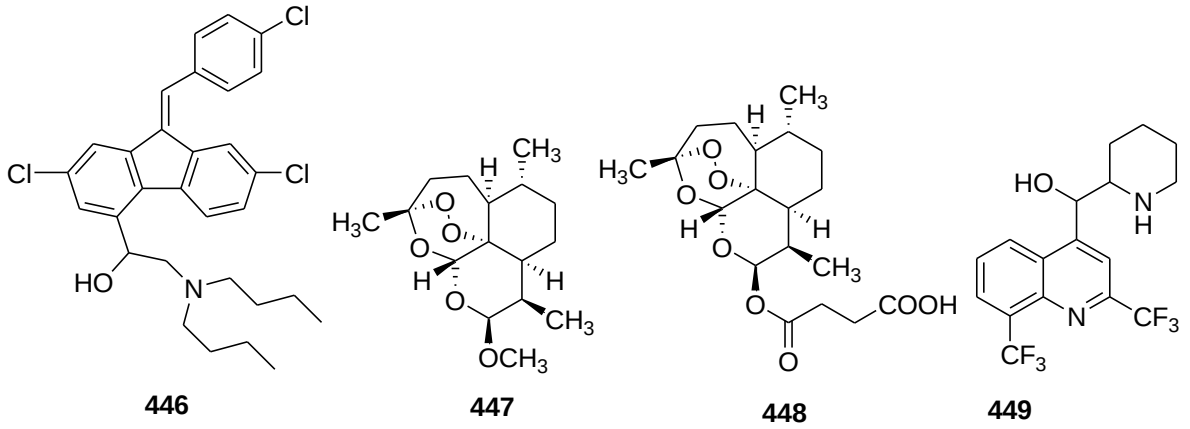
Figure 5.0: The molecular structure of amodiaquine **445**.

5.1 Combination drug strategy

To avoid the spread of resistance, Peters was among the first researchers to demonstrate that a drug combination strategy could be beneficial in the treatment of malaria. He showed that a combination of antimalarial drugs could delay the selection of resistant mutants.[264] As discussed before, the combination of atovaquone and proguanil not only resulted in improvement of efficacy in the resultant drug (Malarone) but also evaded the resistance prevalent in atovaquone when used alone. However, Malarone is very expensive such that it is normally only used by tourists visiting endemic areas as a prophylaxis.[265]

The drug combination strategy has found success in artemisinin based drugs which are the only fully effective class of antimalarial drugs used in large scale. Artemisinin and its derivatives when used alone are thermally unstable which limit their use in countries where access to the treatment is difficult and WHO recommends the use of short acting artemisinin based drugs in combination with long acting quinoline based drugs as the first-line therapy for *falciparum* malaria.[266]

For example, coartem, which is a combination of artemether and lumefantrine (**Figure 5.1**), is the first artemisinin based combination fixed-dose therapy prequalified by the WHO since 2004 and is used worldwide for *P. falciparum* malaria.[263,267] In Cambodia, a mefloquine-artesunate (**Figure 5.1**) combination is currently used as the first-line treatment for uncomplicated *P. falciparum* malaria.[268]



446 **447** **448** **449**

Figure 5.1: The molecular structures of lumefantrine **446**, artemether **447**, artesunate **448** and mefloquine **449**.

Much as the artemisinin combination therapies have retained the same level of efficacy (about 98% cure rate), there are numerous reports of delayed clearance of *P. falciparum* after artemisinin combination therapy administration in Southeast Asia region, specifically near the Thai-Cambodia border which could herald the onset of clinical resistance to combination drugs. The clearance time for *P. falciparum* has increased from the initial 30 hours to 72 hours when treated with artemisinin based drugs.[269] These observations have triggered a concerted search for new drugs that could be deployed if artemisinin resistance were to spread.

5.2 Justification of this PhD study

The introduction of the artemisinin-based combination therapies may have clawed back the gains that were made before the parasite acquired resistance to chloroquine but the reports about delayed clearance of the parasite to combination drugs and resistance to artemisinin is a worrying situation.[270] Many of the therapies currently in development use known antimalarial pharmacophores (for example, aminoquinolines and/or peroxides) which are chemically modified to overcome the liabilities of their parent molecules.[271] Although these compounds may become important in the treatment of malaria, it would be preferable to discover chemotypes with novel mechanisms of action. It is in this spirit that selected compounds we synthesized in this PhD project as shown in **Figure 5.2** were tested against the CQ-resistant Gambian FCR-3 strain of the *P. falciparum*. In our laboratory group, malaria research is

coordinated by Rousseau and the testing of the compounds presented in here was carried out under her supervision.

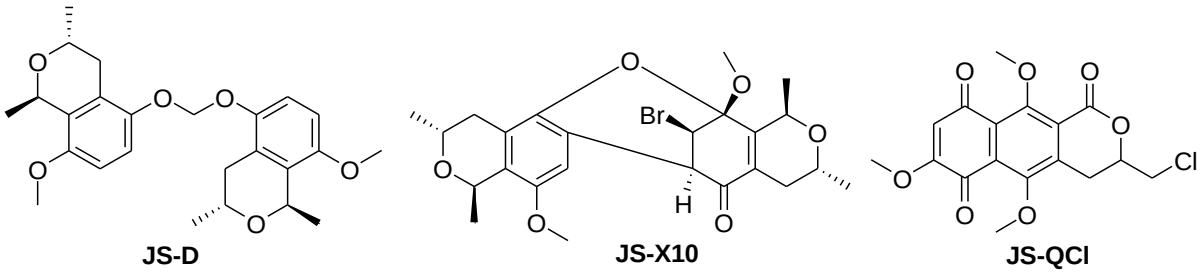


Figure 5.2: The molecular structures of symmetrical dimer **JS-D**, unsymmetrical dimer **JS-X10** and pyranonaphthoquinone **JS-QCl**.

The tests were carried out by Prof. R. van Zyl at the University of Witwatersrand School of Pharmacy and Pharmacology, South Africa and dihydroartemisinin **450** and quinine **451** (**Figure 5.3**) were used as positive controls.

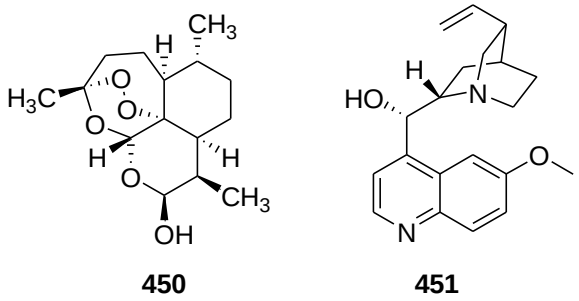


Figure 5.3: The molecular structures of dihydroartemisinin **450** and quinine **451**.

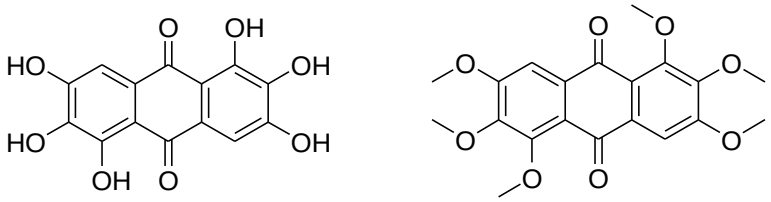
5.3 The results and discussion for antimalarial activity

The results of the biological activities for compounds **JS-X10**, **JS-QCl** and **JS-D** are shown in **Table 5.0**. The dimer **JS-X10** showed the best antimalarial activity with an IC_{50} value of 0.0018 µM which was followed by compound **JS-QCl** which displayed an IC_{50} value of 11.06 µM. The dimer **JS-D** was the least active compound of the three with an IC_{50} value of 64.02 µM.

Compound	IC_{50} (μM)	Number of runs
JS-D	64.02 ± 11.86	3
JS-QCl	11.06 ± 2.59	3
JS-X10	0.0018 ± 0.0004	3
Quinine	2.81 ± 0.57	3
DHA	0.0061 ± 0.0011	3

Table 5.0: Results of *in vitro* antimalarial assay for compounds **JS-X10**, **JS-QCl** and **JS-D** against the Gambian FCR-3 strain of *P. falciparum*.

The biological activity displayed by compound **JS-QCl** (IC_{50} value of 11.06 μM) was very promising considering that methylated quinones are known to be less active compared to their demethylated analogues. This was demonstrated in the case of rufigallol **283** in which the methylated analogue, compound **452**, showed less activity by more than 142-fold. The parent molecule, rufigallol **283**, showed activity against *P. falciparum* with an IC_{50} value of 0.035 μM whereas the methylated rufigallol **452** showed activity of 5.00 μM.[188]



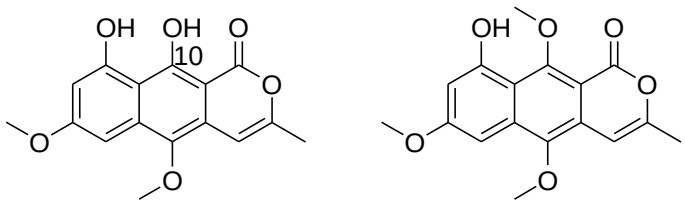
283 IC_{50} = 0.035 μM

452 IC_{50} = 5.00 μM

Figure 5.4: The molecular structures and IC_{50} values of rufigallol **283** and its methylated analogue **452**.

In another case, Varanda and co-workers in 1997[87] proposed that methylating paepalantine **102** may decrease its cytotoxic property, a suggestion which was backed by Tavares and co-workers in 1999.[89] This proposition was confirmed by Devienne and co-workers[9] who demonstrated that methylation of paepalantine **102** at position 10 resulted in a compound, 10-

O-methylpaepalantine **453** (**Figure 5.5**), that was much less cytotoxic compared to the parent compound **102**.



102 **453**

Figure 5.5: The molecular structures of paepalantine **102** and 10-*O*-methylpaepalantine **453**.

The foregoing discussion seems to suggest that there is a good chance that demethylating **JS-QCl** could lead to analogues with better antimalarial activity.

As mentioned before, the unsymmetrical dimer **JS-X10** showed the best preliminary antimalarial activity with the IC_{50} value of 0.0018 µM. To put the antimalarial results we obtained in perspective, **Table 5.1** shows the comparative results of biological activities for ferroquine **352** (FQ), chloroquine **351** (CQ), methotrexate (MT), mefloquine **449** (MQ) and dihydroartemisinin (DHA) **450** against the same Gambian FCR-3 strain of *P. falciparum*. The dimer **JS-X10** compares favourably with dihydroartemisinin **450** (the most active form of artemisinin derivatives) which indicated that at the very least **JS-X10** has a potential of being a lead compound towards antimalarial drug discovery.

Compound	IC_{50} (nM)
CQ[b]	477.5
MT[a]	230
MQ[c]	62.1
FQ[b]	11.5
DHA[a]	6.1
JS-X10[a]	1.8
DHA[c]	1.4

Table 5.1: The biological activities of different drugs (or potential drugs) against the Gambian FCR-3 strain of *P. falciparum*; *Key: a = this work, b = Ref* [232]*, c = Ref* [273].

The fact that dihydroartemisinin **450** showed less activity under our conditions (IC_{50} value of 6.1 nm) compared to the activity reported by Delhaes and co-workers[273] (IC_{50} value of 1.4 nm) means that the activity reported for dimer **JS-X10** under our assay conditions may be underestimated.

In a different study both compounds **JS-X10** and **JS-QCl** were shown to be non-toxic against human embryonic kidney cell lines (HEK293) at the concentration of greater than 100 µM.

The most prominent and unique features of the dimer **JS-X10** are highlighted in red in **Figure 5.6**. The pyran ring system (highlighted in blue) may be useful in combination with the functionalities highlighted in red but it does not appear to be very important on its own as exemplified by the dimer **JS-D** which has the same dimeric pyran ring system but did not show good activity.

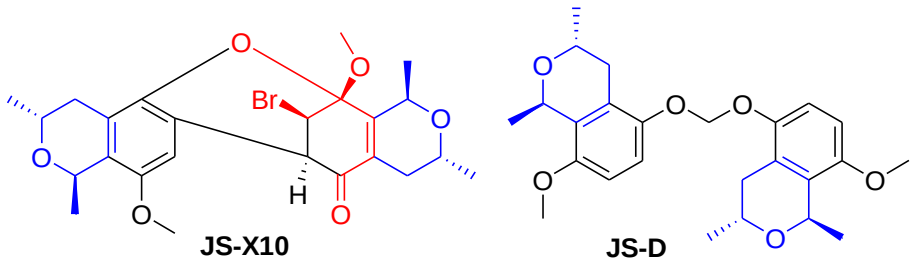
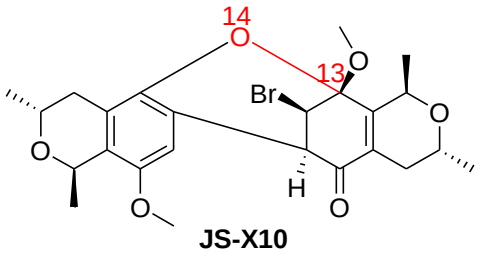


Figure 5.6: The molecular structures of two dimeric compounds **JS-X10** and **JS-D** with similar pyran rings.

Comparison of dimer **JS-X10** with compounds which are currently in use as antimalarial agents does not seem to reveal its possible mode of action and no studies were carried out in our preliminary biological studies to determine its possible mode of action. However, we suspect that radical cleavage of the bond between O-14 and C-13 could be involved in facilitating the binding of the resultant radical species to the heme, more like the peroxide drugs, thereby interfering with the detoxification process of the parasite.[274] As discussed in **Chapter 3**, studies have shown that the digestive food vacuole of the parasite has a small but significant amount of hydrogen peroxide which could initiate the cleavage of a labile bond between O-14 and C-13 at the vacuolar pH.



The availability of multiple functionalities in dimer **JS-X10** suggests that this compound could potentially belong to the group of drugs which have multiple targets (pleiotropic drugs) as opposed to the group of drugs that have single specific proteins or enzymes as their main target. The historical evidence on the development and evolution of resistance to classical antimalarial drugs has shown that the mode of action of a drug influences its useful therapeutic life (UTL). UTL is commonly used to refer to the time period a drug remains efficacious after its initial introduction for large-scale clinical use to the time it is no longer pharmacologically judicious to be administered to patients owing to resistance. Drugs that target single and specific targets such as antimalarial atovaquone are more often rendered ineffective within a short time of their clinical use whereas drugs with multiple targets such as aminoquinolines and peroxides have generally long useful therapeutic lives.[275]

In conclusion, the preliminary antimalarial activity shown by **JS-X10** and **JS-QCl** are very encouraging thus providing an excellent starting point to develop unsymmetrical pyran

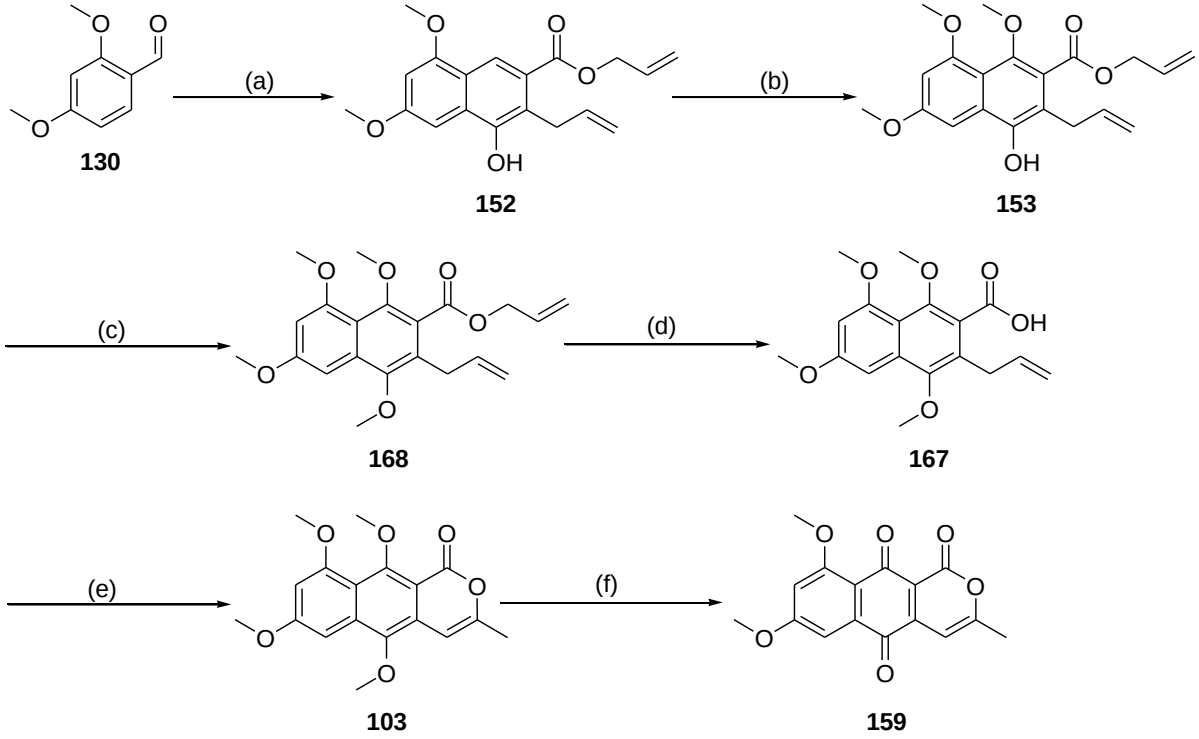
dimers and chlorinated pyranonaphthoquinones as novel antimalarial agents. The studies in this regard are on-going in our laboratories.

Chapter 6: Conclusion and Future Work

6.0. Synthesis of pyranonaphthoquinones and future work

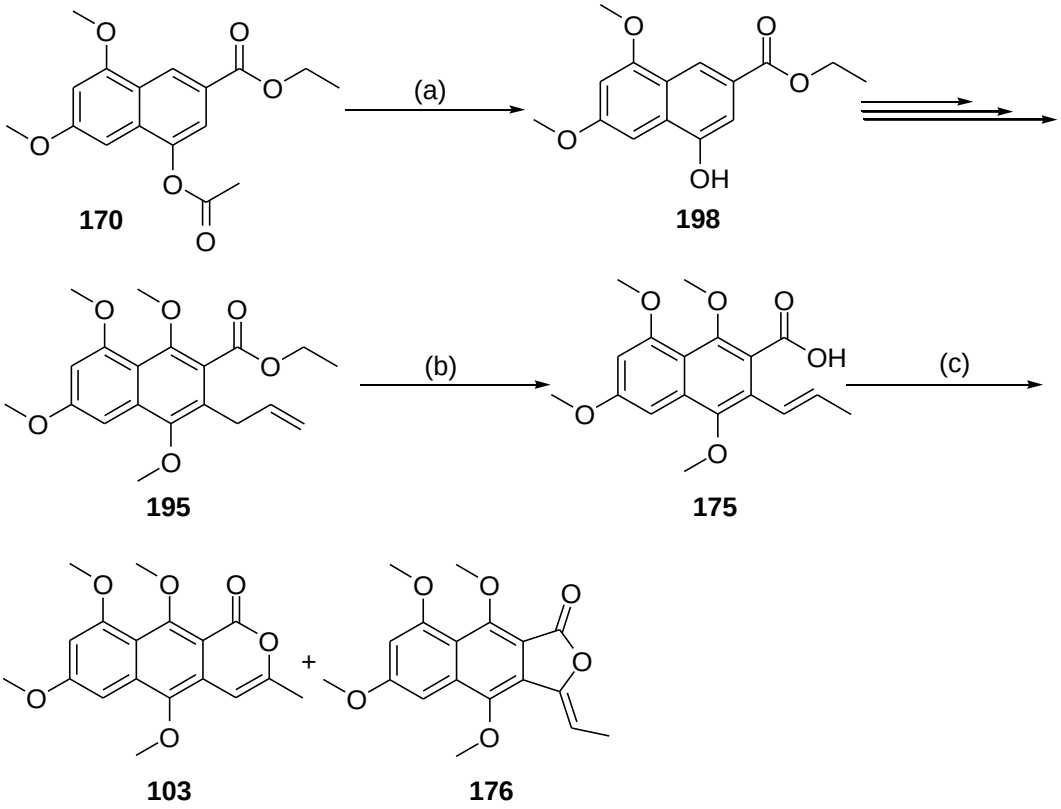
New synthetic methodology for the synthesis of highly oxygenated pyranonaphthoquinones was successfully developed in this PhD project. The synthesis of dehydroherbarin lactone **159** was achieved from the commercially available 2,4-dimethoxybenzaldehyde **130** in 14 steps in an overall yield of 5% as shown in reaction **Scheme 6.0**.

The key steps in the synthesis were the PIFA mediated methoxylation of the naphthol **152** which delivered the tetra-oxygenated allyl ester **168** after the methylation of naphthol **153** and the Wacker oxidation of the carboxylic acid **167**. The oxidative demethylation of lactone **103** using silver (II) oxide delivered dehydroherbarin lactone **159**. The pyranonaphthoquinone **159** was purified using semi-preparative C-18 reverse phase HPLC because of decomposition by silica gel column chromatography.



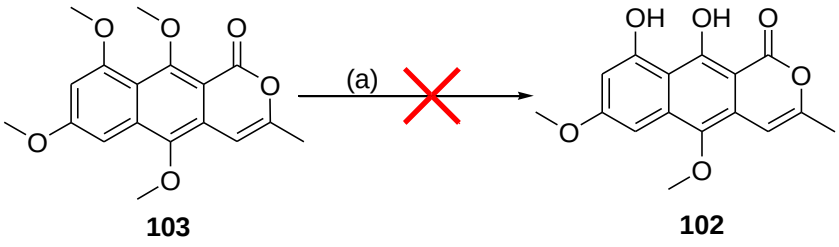
Scheme 6.0: *Reagents and conditions*: *(*a) (i) diethyl succinate, *t*-BuOH, *t*-BuOK, reflux, 2 hrs (ii) NaOAc-Ac_2O, 130 °C, 12 hrs, 68% (iii) NaOH, MeOH/H_2O, reflux, 6 hrs (iv) *32%* aq. HCl (v) allyl bromide, K_2CO_3, Me_2CO, reflux, 16 hrs, 86% (vi) 180 °C, 24 hrs, 70% (b) (i) PIFA, MeOH, rt, 15 min (ii) NaOEt, EtOH, rt, 20 min, 58% (c) K_2CO_3, Me_2SO_4, Me_2CO, reflux, 18 hrs, 92% (d) (i) $LiAlH_4$, Et_2O, 0 $^oC \rightarrow$ rt, 2 hrs (ii) PCC, silica, N_2 (g) (iii) NaH_2PO_4, $NaClO_2$, H_2O, *t*-BuOH, 2-methyl-2-butene, 60% (e) cat. $PdCl_2$, $CuCl_2 \cdot 2H_2O$, DMF/H_2O, O_2 (g), rt, 24 hrs, 70% (f) AgO, *55%* HNO_3, 1,4-dioxane, 56%.

In the course of synthesizing dehydroherbarin lactone **159**, furanone **176** was isolated as an unexpected product of the Wacker oxidation reaction of the isomerized carboxylic acid **175** as shown in **Scheme 6.1**. In this case, the selective deacylation of naphthalene **170** afforded naphthol **198** which was then subjected to a series of transformations yielding ethyl ester **195**. The base mediated saponification of ethyl ester **195** afforded the isomerized carboxylic acid **175** and the Wacker oxidation reaction of this acid delivered lactone **103** and furanone **176**.



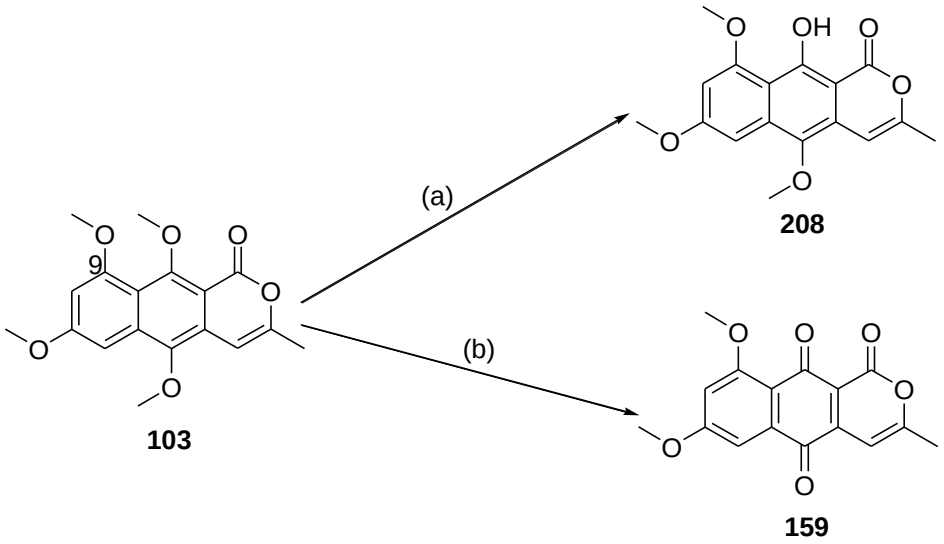
Scheme 6.1: *Reagents and conditions*: *(*a) (i) diethyl succinate, *t*-BuOH, *t*-BuOK, reflux, 2 hrs (ii) NaOAc-Ac_2O, 130 °C, 12 hrs (iii) *1%* NaOH in EtOH, rt, 6 hrs (iv) HCl (aq) (b) KOH, MeOH/H_2O, reflux, 72 hrs (c) cat. $PdCl_2$, $CuCl_2 \cdot 2H_2O$, DMF/H_2O, O_2 (g), rt, 24 hrs.

As discussed before, Mbala in his PhD thesis proposed that successful synthesis of lactone **103** could potentially lead to the synthesis of a biologically important isocoumarin, paepalantine **102** by performing boron tribromide mediated demethylation reaction of lactone **103**. **Scheme 6.2** shows the suggested reaction conditions proposed by Mbala which did not deliver the desired paepalantine **102**.



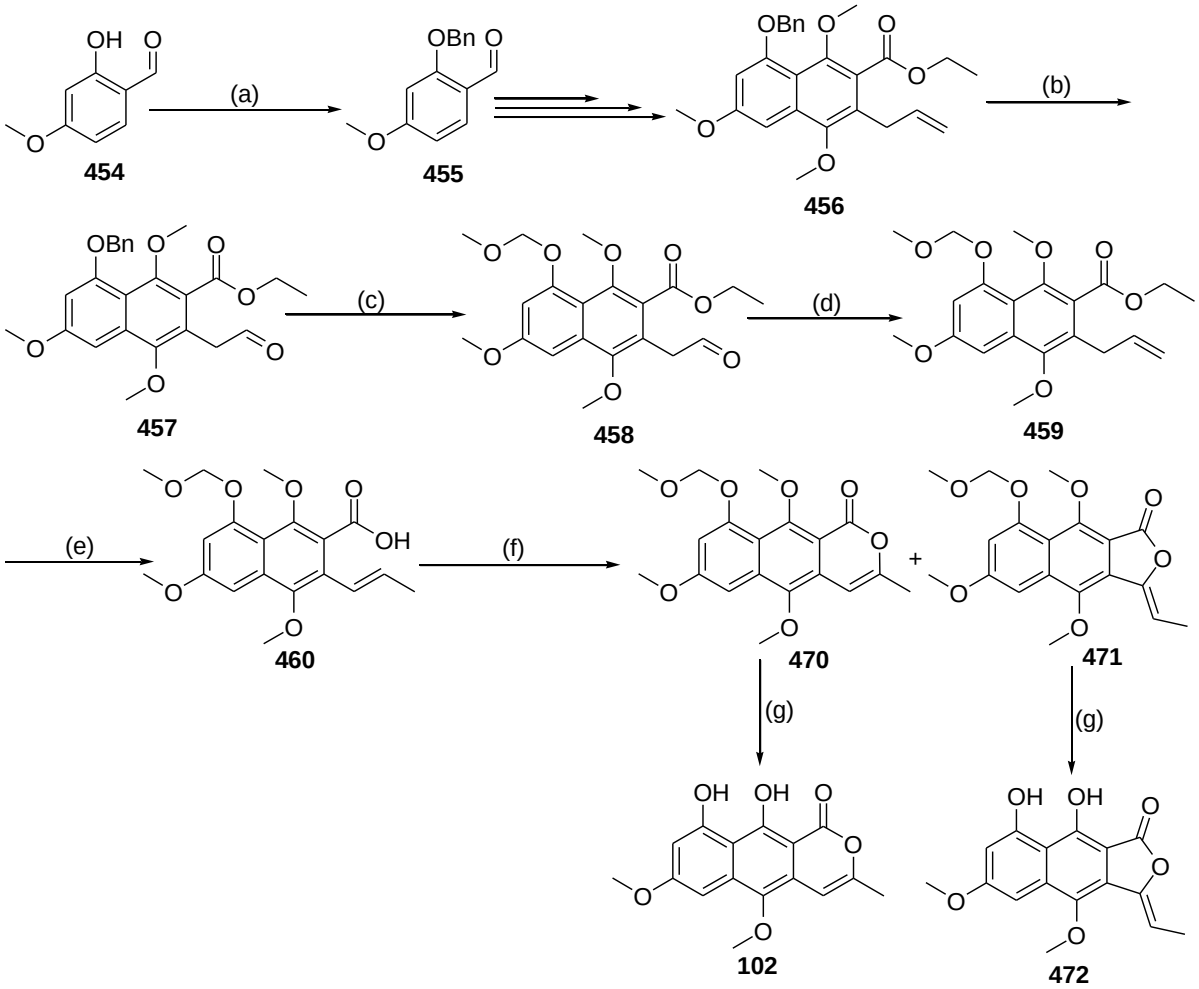
Scheme 6.2: *Reagents and conditions;* (a) BBr_3, CH_2Cl_2, -78 °C → rt, N_2 (g).

In this study we found that boron tribromide mediated demethylation of lactone **103** led to the formation of dehydroherbarin lactone **159** of which the majority of the starting material decomposed whereas boron trichloride mediated demethylation led to isolation of 9-*O*-methylpaepalantine **208** as shown in Scheme **6.3**.



Scheme 6.3: *Reagents and conditions:* (a) BCl_3, CH_2Cl_2, -78 °C → rt, N_2 (g) (b) BBr_3, CH_2Cl_2, -78 °C → rt, N_2 (g).

These results suggested that the methyl group at position 9 of lactone **103** was resistant to demethylation protocols at our disposal. To solve this problem, it would be important to change the protection strategy at this position. We are of the view that if labile protection groups such as MOM or TBDMS were to be used they would not survive the harsh conditions that are employed during the construction of the naphthalene ring system. However, a combination of two different protection protocols could solve this problem as shown in reaction **Scheme 6.4** below.

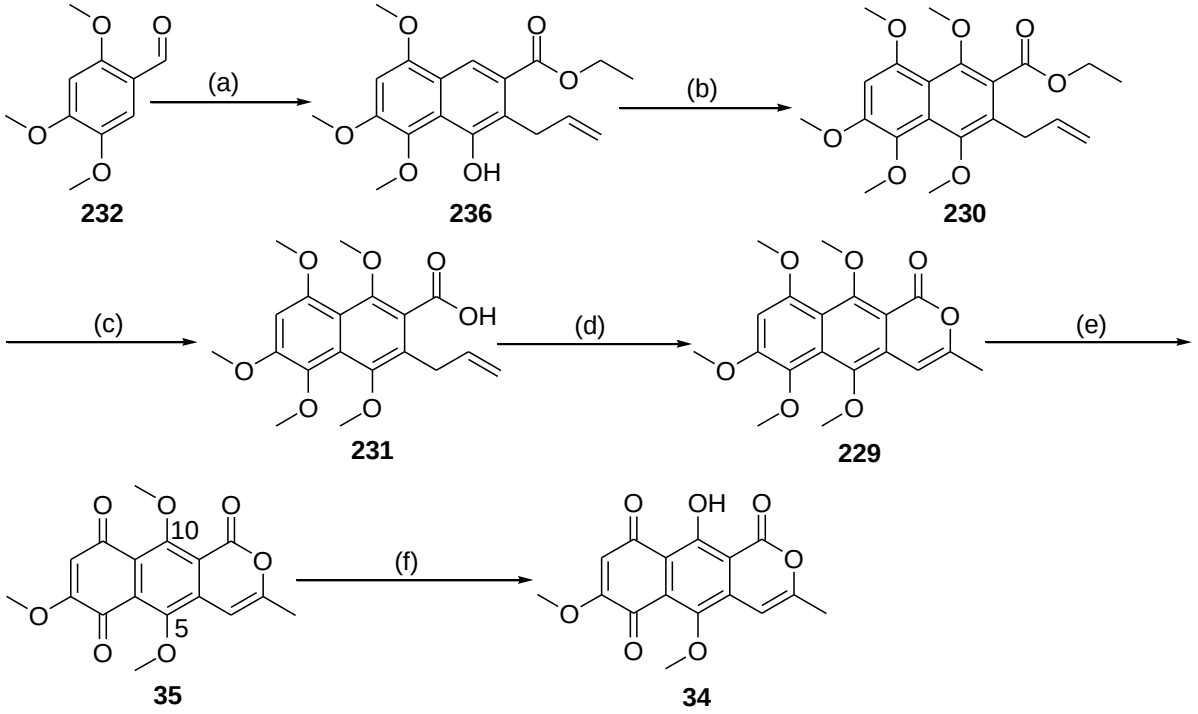


Scheme 6.4: *Reagents and conditions:* (a) BnCl, KI, K_2CO_3, Me_2CO, 18 hrs (b) O_3 (g), CH_2Cl_2, -78 °C (ii) N_2 (g), $(CH_3)_2S$ or cat. OsO_4, $NaIO_4$, H_2O, 1,4-dioxane, rt, 12.5 hrs (c) (i) *10%* Pd/C, H_2 (g), CH_2Cl_2-dioxane, rt, 48 hrs (ii) MOMCl, KI, K_2CO_3, Me_2CO, 18 hrs (d) MTPPBr, Bu^nLi, THF, 0 °C → rt (e) KOH, MeOH/H_2O, reflux, 72 hrs (f) cat. $PdCl_2$, $CuCl_2 \cdot 2H_2O$, DMF/H_2O, O_2 (g), rt, 24 hrs (g) BCl_3, CH_2Cl_2, N_2 (g), -78 °C → rt (the MOM group could also be cleaved by aq. HCl).

Benzylation of the commercially available 2-hydroxy-4-methoxybenzaldehyde **454** could deliver 2-(benzyloxy)-4-methoxybanzaldehyde **455**. Subjecting aldehyde **455** to a series of transformations we have employed in our laboratory could afford ethyl ester **456**. We have previously shown in our laboratory group that a benzyl protection group is stable under these conditions.[119] Ozonolysis of ester **456** could afford aldehyde **457** which could then be subjected to palladium catalysed debenzylation and MOM protection protocols which could potentially afford ethyl ester **458**. Subjecting ester **458** to Wittig reaction conditions could afford naphthalene **459** which could then be subjected to base promoted saponification which

could afford carboxylic acid **460**. MOM protection group is stable under basic conditions.[139c] Alternatively, naphthalene **459** could be subjected to a 3-step reaction protocol of reduction to alcohol followed by PCC oxidation to aldehyde and finally Pinnick oxidation reaction to yield unisomerized carboxylic acid. Wacker oxidation reaction of carboxylic acid **460** and demethylation protocols of the resultant products (lactone **470** and furanone **471**) could deliver paepalantine **102** and its analogue **472**. The suggested protocol for the synthesis of paepalantine **102** and its analogue **472** as depicted in **Scheme 6.4** would be a subject for further research in our laboratories.

The synthesis of 5-methoxy-3,4-dehydroxanthomegnin **34** was accomplished by employing the procedure we developed in the synthesis of dehydroherbarin lactone **159**. The commercially available 2,4,5-trimethoxybenzaldehyde **232** was subjected to Stobbe condensation, naphthalene ring formation and Claisen rearrangement reactions which delivered naphthol **236**. This was followed by the PIFA mediated methoxylation and methylation steps which afforded methylated pentaoxygenated naphthalene **230**. The naphthalene **230** was then subjected to a combination of reduction to alcohol, oxidation of the resultant alcohol to aldehyde and Pinnick oxidation which delivered carboxylic acid **231**. The Wacker oxidation reaction of acid **231** furnished lactone **229** which was then subjected to silver (II) oxide mediated oxidative demethylation protocol yielding pyranonaphthoquione **35**. The last step involved subjecting quinone **35** to boron trichloride mediated demethylation protocol which delivered 5-methyl-3,4-dehydroxanthomegnin **34** in overall percentage yield of 1% as shown in **Scheme 6.5**.



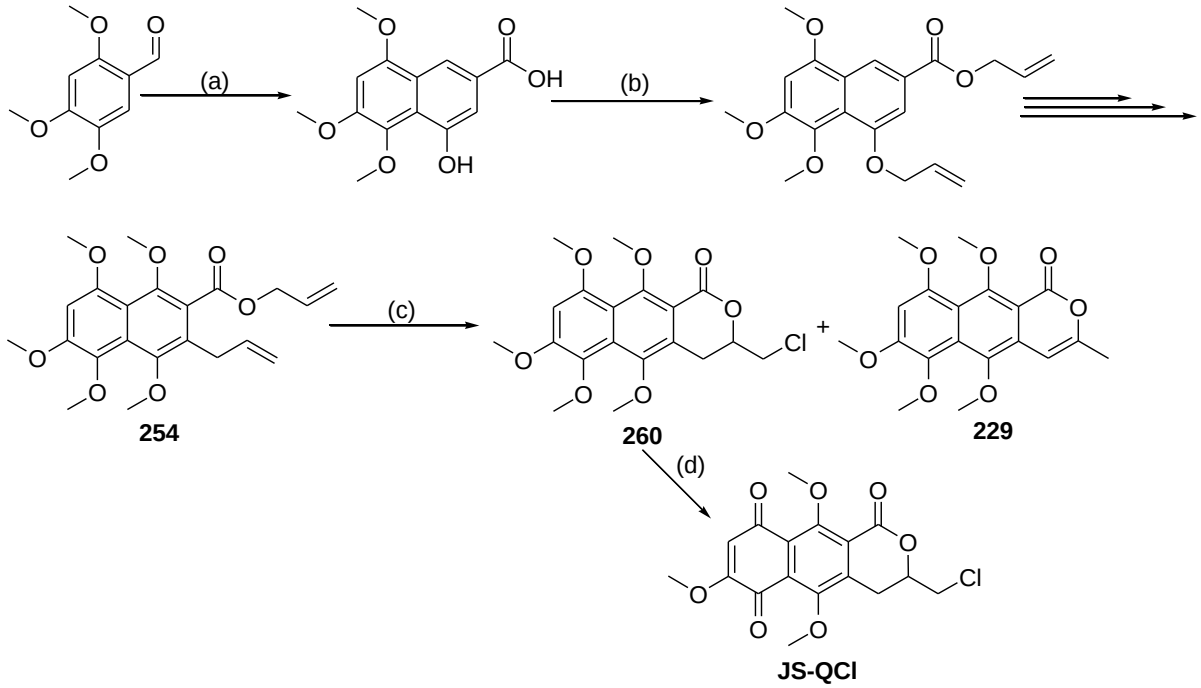
Scheme 6.5: *Reagents and conditions:* (a) (i) diethyl succinate, *t*-BuOH, *t*-BuOK, reflux, 2 hrs (ii) NaOAc-Ac_2O, 130 °C, 12 hrs, 68% (iii) *1%* NaOH in EtOH, rt, 6 hrs (iv) *32%* aq. HCl, 79% (v) allyl bromide, K_2CO_3, Me_2CO, reflux, 16 hrs, 89% (vi) 180 °C, 24 hrs, 71% (b) (i) PIFA, MeOH, rt, 15 min (ii) *t*-BuOK, EtOH, rt, 20 min, 60% (iii) K_2CO_3, Me_2SO_4, Me_2CO, reflux, 18 hrs, 83% (c) (i) $LiAlH_4$, Et_2O, 0 $^oC \rightarrow$ rt, 2 hrs, 80% (ii) PCC, silica, N_2 (g) (iii) NaH_2PO_4, $NaClO_2$, H_2O, *t*-BuOH, 2-methyl-2-butene, 66% (d) cat. $PdCl_2$, $CuCl_2 \cdot 2H_2O$, DMF/H_2O, O_2 (g), rt, 24 hrs, 72% (e) AgO, *55%* aq. HNO_3, 1,4-dioxane, 75% (f) BCl_3, CH_2Cl_2, N_2 (g), -78 °C $\rightarrow$ rt, 20%.

The observed selectivity in demethylation of pyranonaphthoquinone **35** was probably due to the carbonyl group of the lactone ring which enabled better coordination of the boron reagent to the methoxy group at position 10 (two adjacent carbonyl groups) compared to the methoxy at position 5 which had one adjacent carbonyl group.

The low overall percentage yield for the synthesis of 5-methoxy-3,4-dehydroxanthomegnin **34** was due to decomposition during purification of the final quinone product by silica gel column chromatography.

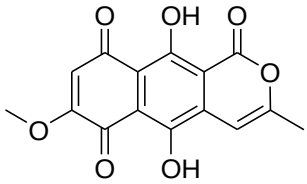
In the course of synthesizing 5-methoxy-3,4-dehydroxanthomegnin **34** we isolated a chlorinated lactone **260** alongside the desired lactone **229** during the ring forming step involving allyl ester **254** as shown in reaction **Scheme 6.6**. The intermediate **260** was

subjected to oxidative demethylation reaction yielding pyranonaphthoquinone **JS-QCl**. We attempted the synthesis of chlorinated analogues of anhydrofusarubin lactone and 5-methyoxy-3,4-dehydroxanthomegnin by subjecting the quinone **JS-QCl** to 4 mole and 2 mole equivalents of boron trichloride, respectively but we did not isolate the intended compounds.



Scheme 6.6: *Reagents and conditions:* (a) (i) diethyl succinate, *t*-BuOH, *t*-BuOK, reflux, 2 hrs (ii) NaOAc-Ac_2O, 130 °C, 12 hrs (iii) NaOH, MeOH/H_2O and *32%* aq. HCl (b) allyl bromide, K_2CO_3, Me_2CO, reflux, 16 hrs (c) cat. $PdCl_2$, $CuCl_2{\cdot}2H_2O$, DMF/H_2O, O_2 (g), rt, 24 hrs (d) AgO, *55%* aq. HNO_3, 1,4-dioxane, rt.

We also attempted the synthesis of anhydrofusarubin lactone **32** (**Figure 6.0**) from intermediate **35** but, despite the crude product showing a prominent peak corresponding to anhydrofusarubin lactone in the MS spectrum, we were unable to isolate the product due to decomposition. We are of the view that purification of the final product using sephadex LH-20 (which unfortunately is very expensive) could deliver anhydrofusarubin lactone **32**. Alternatively, semi-preparative C-18 reverse phase HPLC which was used in the purification of dehydroherbarin lactone could be used in the purification of anhydrofusarubin lactone. The natural product itself was purified from a combination of sephadex LH-20 and preparative TLC.[103]

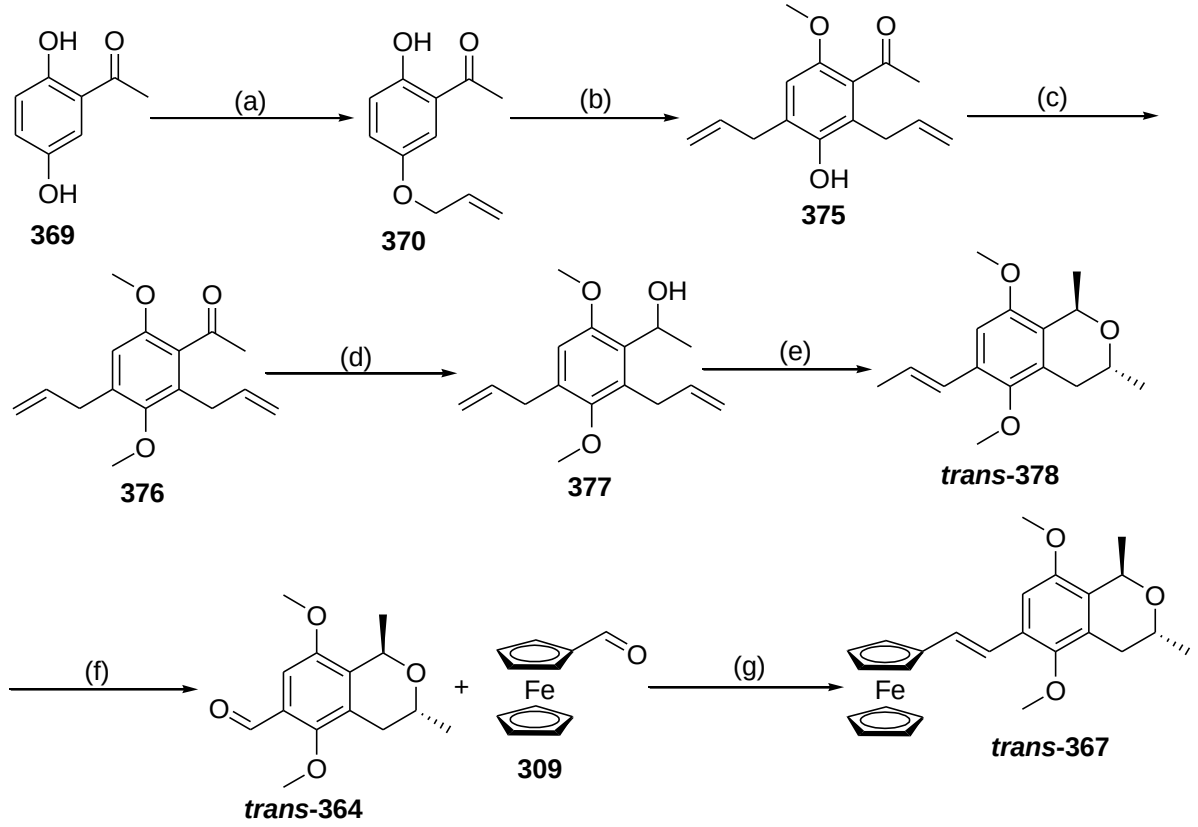


32

Figure 6.0: The molecular structure of anhydrofusarubin lactone **32**.

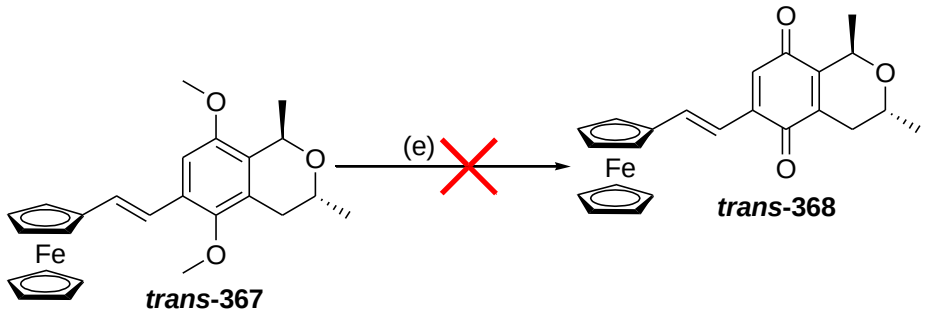
6.1 Synthesis of ferrocenyl 3,4-dihydroisochromene and future work

The second project involved developing a methodology for appending a ferrocene moiety to the 3,4-dihydroisochromene. The synthesis of ferrocenyl 3,4-dihydroisochromene ***trans*-367** was successfully accomplished starting from the commercially available 2,5-dihydroxyacetophenone **369** in 10 steps in an overall yield of 10% as shown in reaction **Scheme 6.7**. The high dilution conditions were employed in the selective synthesis of allyl ether **370** from 2,5-dihydroxyacetophenone **369**. The major steps in this protocol were the Claisen rearrangement reaction which delivered ketone **376** after the methylation of the diallyl phenol **375** and the base mediated ring closure of alcohol **377** which afforded propenyl 3,4-dihydroisochromene ***trans*-378**. Osmium mediated oxidation of the propenyl double bond of compound ***trans*-378** afforded 3,4-dihydroisochromene carbaldehyde ***trans*-364**. This was followed by the McMurray cross-coupling metathesis reaction involving 3,4-dihydroisochromene aldehyde ***trans*-364** and the commercially available ferroaldehyde **309** as a coupling partner which delivered ferrocenyl 3,4-dihydroisochromene ***trans*-367**.



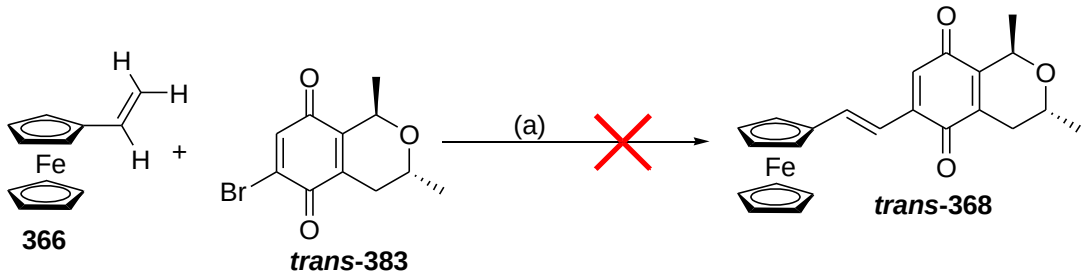
Scheme 6.7: *Reagents and conditions:* (a) allyl bromide, K_2CO_3, Me_2CO, reflux, 18 hrs, 62% (b) Me_2SO_4, K_2CO_3, Me_2CO, reflux, 72 hrs, 82% (c) (i) 170 °C, N_2 (g), 24 hrs (ii) allyl bromide, K_2CO_3, Me_2CO, reflux, N_2 (g), 18 hrs, 74% (iii) 170 °C, N_2 (g), 24 hrs, 71% (iv) Me_2SO_4, K_2CO_3, Me_2CO, reflux, 18 hrs, 87% (d) $LiAlH_4$, THF, N_2 (g), 0 $^oC \rightarrow$ rt, 12 hrs, 71% (e) *t*-BuOK, NMP, 110 °C, 30 min, 63% (f) O_3 (g), CH_2Cl_2, -78 °C then N_2 (g), $(CH_3)_2S$, 68% or; cat. OsO_4, $NaIO_4$, H_2O, 1,4-dioxane, rt, 12.5 hrs, 84% (g) TiCl4, Zn, THF, 14 hrs, 82%.

However, attempts for oxidative demethylation of ferrocenyl 3,4-dihydroisochromene ***trans*-367** to deliver the corresponding ferrocenyl pyranobenzoquinone ***trans*-368** were unsuccessful. The reaction conditions and reagents that were attempted to achieve this transformation are shown in reaction **Scheme 6.8**.



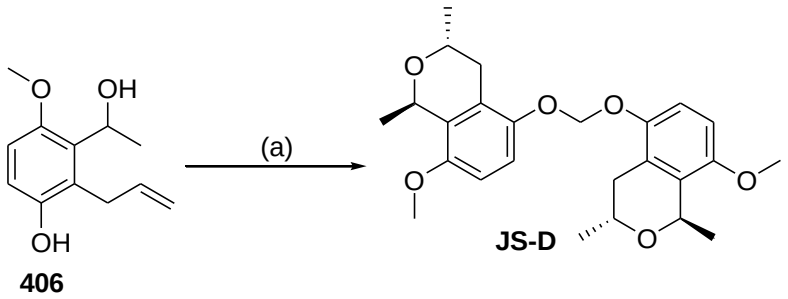
Scheme 6.8: *Reagents and conditions:* AgO, *55%* aq. HNO_3, 1,4-dioxane, rt or PIFA, CH_3CN/H_2O dilute, rt, 45 min; or CAN, CH_3CN/H_2O, rt, 30 min.

In another attempt to achieve the synthesis of ferrocenyl pyranobenzoquinone ***trans*-368**, new methodology was developed starting from the same starting material, 2,5-dihydroxyacetophenone **369**. This methodology relied on coupling a pyranobenzoquinone ***trans*-383** to a vinyl ferrocene **366** as the last step. Attempted Heck-type coupling reaction of brominated quinone ***trans*-383** and vinyl ferrocene **366** failed to deliver the ferrocenyl pyranobenzoquinone ***trans*-368**. The reaction conditions and reagents that were used are shown in the reaction depicted in **Scheme 6.9**.



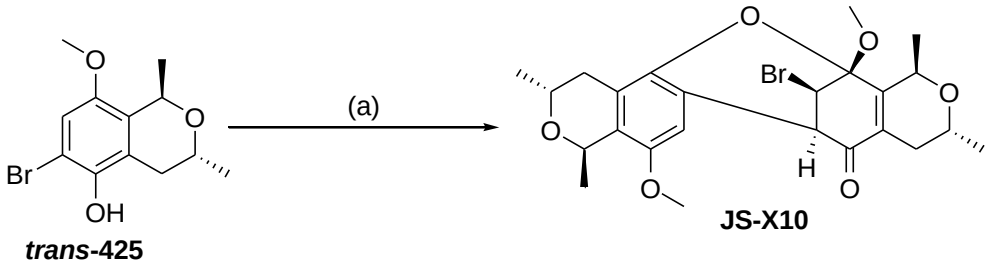
Scheme 6.9: *Reagents and conditions:* cat. $Pd(OAc)_2$, K_2CO_3, THF, PPh_3, reflux, 2 hrs.

A number of unexpected compounds was synthesized of which two dimers, **JS-D** and **JS-X10**, were of biological interest. The base promoted ring closure of phenol **406** led to isolation of **JS-D** (**Scheme 6.10**) as one of the three products that were formed.



Scheme 6.10: *Reagents and conditions:* (a) *t*-BuOK, NMP, 110 °C, 30 min.

Additionally, the attempted silylation of the brominated 3,4-dihydroisochromen-5-ol ***trans*-425** led to the isolation of unsymmetrical dimer **JS-X10** as shown in reaction **Scheme 6.11**.



Scheme 6.11: *Reagents and conditions:* (a) TBDMSCl, imidazole, cat. DMAP, DMF, 72 hrs.

Much as we did not successfully synthesize ferrocenyl pyranobenzoquinone ***trans*-368** using the two methodologies we attempted in this study we are optimistic that we could still accomplish the synthesis of ***trans*-368** by using a different protection strategy. Again, we could take advantage of the first methodology we used in the synthesis of ferrocenyl 3,4-dihydroisochromene ***trans*-367** to synthesize intermediates shown in **Figure 6.1**.

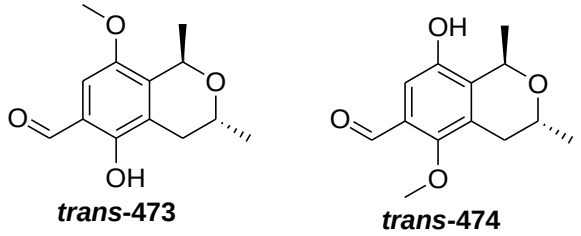
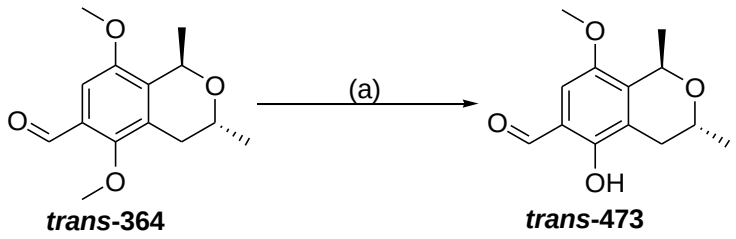


Figure 6.1: The molecular structures of 3,4-dihydroisochromen-5-ol carbaldehyde ***trans*-473** and 3,4-dihydroisochromen-8-ol carbaldehyde ***trans*-474**.

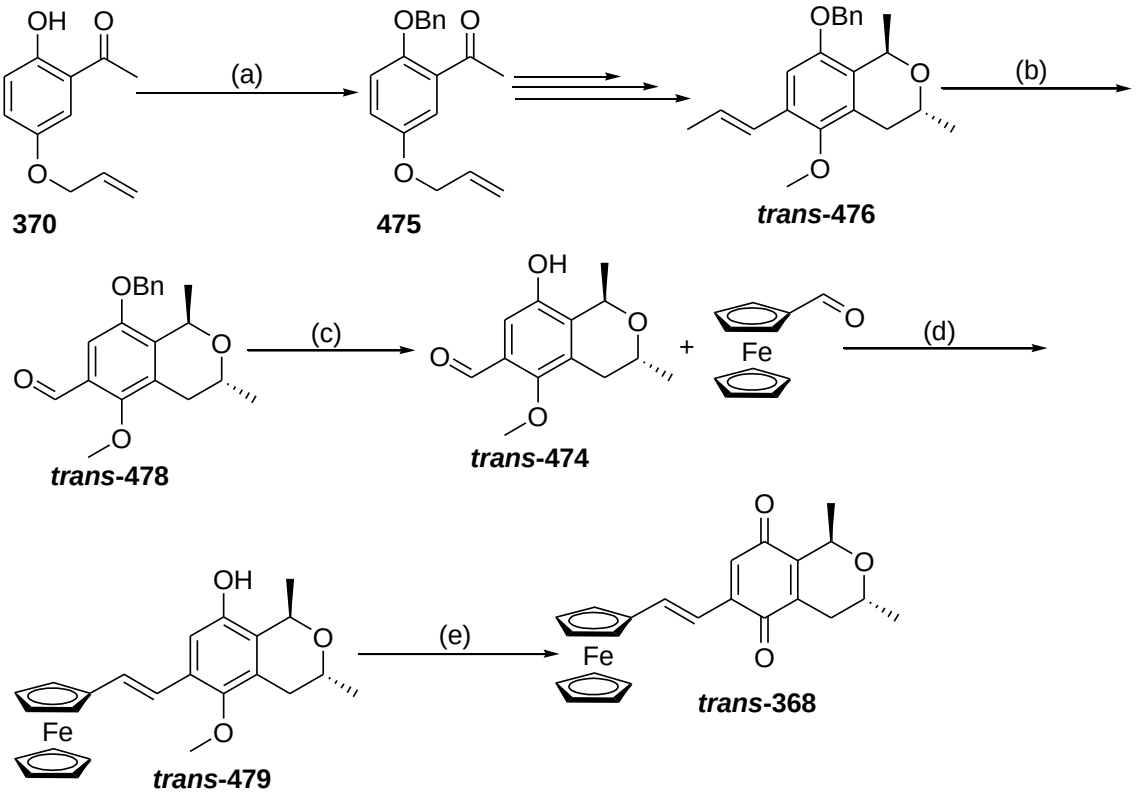
The 3,4-dihydroisochromen-5-ol carbaldehyde ***trans*-473** could be synthesized from boron trichloride mediated demethylation of ***trans*-364** (**Scheme 6.11**) by taking advantage of the coordinating ability of the carbonyl functional group. There are reports of failed demethylations which are mainly ascribed to the carbonyl group being at an oblique angle or orthogonal to the methoxy group which prevents proper coordination of the boron reagent to the methoxy group and if that could be the case with ***trans*-364** then we could use ***trans*-474** as a coupling partner of ferroaldehyde (**Figure 6.1**).



Scheme 6.11: *Reagents and conditions*: BCl_3, CH_2Cl_2, -78 °C → rt.

The synthesis of 3,4-dihydroisochromen-8-ol carbaldehyde ***trans*-474** could involve a different protection strategy from the one that was used in this PhD project. Phenol **370** could be benzylated which could potentially afford allyl ether **475**. Following the same protocol as before, allyl ether **475** could be subjected to a number of transformations which could yield propenyl 3,4-dihydroisochromene ***trans*-476** and subjecting this intermediate to ozonolysis reaction followed by debenzylation could deliver 3,4-dihydroisochromen-8-ol aldehyde ***trans*-474**. The McMurray cross-coupling metathesis reaction of this intermediate could deliver ferrocenyl 3,4-dihydroisochromen-8-ol ***trans*-479** which could easily be oxidised to deliver ferrocenyl pyranobenzoquinone ***trans*-368**. The McMurray cross-coupling metathesis

reaction is tolerant to phenol groups and there could be no need for protection at this stage. The proposed reaction steps are shown in **Scheme 6.12** below.



Scheme 6.12: *Reagents and conditions:* (a) BnCl, KI, K_2CO_3, Me_2CO, 18 hrs (b) O_3 (g), CH_2Cl_2, -78 °C then N_2 (g), $(CH_3)_2S$; or cat. OsO_4, $NaIO_4$, H_2O, 1,4-dioxane, rt, 12.5 hrs (c) TiCl4, Zn, THF, 14 hrs (d) AgO, *55%* aq. HNO_3, 1,4-dioxane or PIFA, CH_3CN/H_2O, dilute, rt, 15 min.

6.2 Preliminary antimalarial screening of selected compounds

In the last part of this PhD studies, 3 compounds namely **JS-X10**, **JS-D** and **JS-QCl** were tested against the Gambian FCR-3 strain of *P. falciparum*. The choice of these compounds was not dictated by any prior studies. The unsymmetrical dimer **JS-X10** showed the best activity with the IC_{50} value of 0.0018 µM which was better than the activity shown by the reference compounds, dihydroartemisinin and quinine which showed activity of 0.0061 µM and 2.81 µM, respectively.

6.3 Future biological screening of pyranonaphthoquinones and ferrocenyl pyranobenzoquinone

The biological testing for anticancer activity of selected compounds synthesized will be carried out as part of the future work. Of special interest will be ferrocenyl 3,4-dihydroisochromenes because studies have shown that ferrocenyl compounds have better anticancer activity compared to their purely organic analogues. The reversible redox property of ferrocene is thought to initiate the formation of quinone methide which is responsible for DNA alkylation leading to arresting of tumor cells. Additionally, there is excess generation of reactive oxygen species in tumor cells and ferrocene moiety has the ability to convert the excess reactive oxygen species into less reactive species thereby preventing normal cells from further damage.

To sum up the work we carried out during this PhD study, we believe that the data generated in this PhD work has significantly contributed to scientific knowledge in the area of pyranonaphthoquinones, especially those compounds with lactone rings containing alkene functionality. Through this work, we did not only successfully synthesize 5-methoxy-3,4-dehydroxanthomegnin **32** for the very first time but we also found out that these compounds are prone to decomposition when subjected to silica gel column chromatography.

We also found out that the methoxy group at position 9 of lactone **137** is very resistant to demethylation protocols and hence lactone **137** did not lead to the synthesis of paepalantine which was in conflict with what was proposed by Mbala in his PhD studies.

One of the best results in this PhD was the unexpected isolation of unsymmetrical dimer **JS-X10**. The preliminary antimalarial studies have shown interesting results and studies in this regard are ongoing in our laboratory. We also aim to synthesizing analogues to this compound which means that this project is self-expanding.

Chapter 7: Experimental procedures

7.0 General Modus Operandi

7.1 Thin layer chromatography, evaporation of solvents and cleaning of glassware

Thin layer chromatography (TLC) was performed on aluminium-backed Macherey-Nagel ALUGRAM Sil G/UV254 plates that are pre-coated with 0.25 mm silica gel 60. The compounds were detected using ultraviolet light and in some cases stained using iodine. Evaporation of solvent under reduced pressure commonly referred to as *in vacuo* was performed on a Büchi Rotavopor R-3 with a Büchi R-3 heating bath. Final drying was carried out using a high vacuum pump at 0.1 mm/Hg at ambient temperature until constant mass was achieved.

All the glass reaction vessels were immersed in a KOH base bath for three days, washed with tap water followed by rinsing with acetone and dried in an oven.

7.2 Purification of solvents and reagents

Solvents utilized for chromatographic techniques (mostly dichloromethane, ethyl acetate and *n*-hexane) were purified by means of conventional distillation processes. The solvents employed in reactions were mostly of absolute grade and those that needed to be purified were first dried over the suitable drying agent, followed by distillation under the atmosphere of nitrogen gas. Acetonitrile and dichloromethane were distilled over calcium hydride, whereas tetrahydrofuran was distilled over sodium with benzophenone as an indicator. All the required chemicals or reagents were obtained from ACE, Merck, Fluka or Sigma-Aldrich and were used without further purification.

7.3 Chromatography procedures

The chromatographic separation of reaction mixtures and purification thereof was mostly performed on silica gel 60 (Macherey-Nagel, particle size 0.063-0.200 mm) and Merck silica gel (particle size 0.035-0.070 mm), commonly referred to as normal and flash silica, respectively. In an appropriately sized column, silica of mass approximately 35 times that of the crude product was packed and the crude product loaded onto the silica surface and

covered with acid washed sand whenever needed. Elution was achieved using the indicated solvent mixtures that were mostly hexane and ethyl acetate based. In some cases, the polarity of the solvent was changed in the course of separation but for the sake of this thesis, the initial solvent systems are reported for simplicity.

An Agilent 3000 instrument was used for semi-preparative HPLC on an Agilent preparative C-18 reverse phase column (21.2 × 20 mm) with a binary solvent system using gradient elution of MeCN/H_2O and a flow rate of 20 mL/min. This was specifically used for separation of dehydroherbarin lactone.

7.4 Spectroscopic methods

7.4.0 NMR spectroscopy

^{1}H NMR spectra were recorded using Bruker Advance-500 and Bruker Advance-300 spectrometers operating at 500 MHz and 300 MHz respectively. All spectra were recorded in deuterated solvents as required with the chemical shift values reported in parts per million (ppm) referenced against 0.03% (v/v) tetramethylsilane (TMS) as an internal standard. Coupling constants, *J*, are reported in Hertz (Hz). The commonly used abbreviations in assignments include but are not limited to: br = broad, s = singlet, d = doublet, t = triplet, q = quartet, m = multiplet, dd = doublet of doublets and dt = doublet of triplets. The subscript ob means observed multiplicity. The ^{13}C NMR spectra were recorded at 75 MHz and 125 MHz and the chemical shifts are reported on the δ scale in parts per million.

All NMR spectroscopic data were processed using the MestReNova software suite licenced to the University of the Witwatersrand.[275] Additional 2D experiments were recorded for compounds where it was deemed necessary.

7.4.1 Infrared spectroscopy

Infrared spectra were recorded on a Bruker Tensor 27 Spectrophotometer and all samples were loaded directly onto a diamond cell. Important functional group absorptions, as per the intended transformation, are reported in terms of wavenumbers (ν/cm^{-1}). IR spectra were

obtained for compounds where it was deemed necessary based on the intended transformation and more so for new compounds.

7.4.2 High resolution mass spectroscopy

High resolution mass spectra were obtained on a Waters-LCT-Premier mass spectrometer carried out at Stellenbosch University, South Africa. The sample was dissolved in methanol to a concentration of 2 ng/μL and introduced by direct infusion. The ionization mode was electrospray positive with a capillary voltage of 2500 V and a desolvation temperature of 250 °C using nitrogen gas at 250 L/hr. The intensity data was recorded on a Bruker APEX II CCD area detector diffractometer with graphite monochromated Mo K3 radiation (50 kV, 30 mA) with temperature of measurement at 173(2) K, using the APEX 2 data collection software. The collection method involved 4-scans of width 0.5 and 512 × 512 bit data frames. The data reduction was achieved by means of the program SAINT+ and face indexed absorption corrections were made using XPRE.

7.5 Melting points

Melting points were recorded using a Stuart SMP10 melting point apparatus. Capillary tubes that were sealed at one end were loaded with small amounts of sample and mounted into the melting point apparatus and observed. The point at which the entire sample uniformly melted was considered as the melting point of the compound and was reported without correction.

7.6 Single crystal x-ray diffraction

The diffraction intensity data collection for suitable crystal and subsequent crystal structure solution and refinement were conducted by Prof A. Lemmerer at Wits School of Chemistry and Material Science. The intensity data were collected on a Bruker APEX II CCD area detector diffractometer with graphite monochromated Mo K α-radiation (50kV, 30mA) using the APEX 2 data collection software. The collection method involved ω-scans of width 0.5° and 512×512 bit data frames. Data reduction was carried out using the program *SAINT+* version 6.02.6 software and *SADABS* was used to make empirical absorption corrections.[276] *SHELXS-97* was used to solve crystal structures by direct methods.[277] After initial isotropic refinements of non-hydrogen atoms, further anisotropic refinements were carried out by full

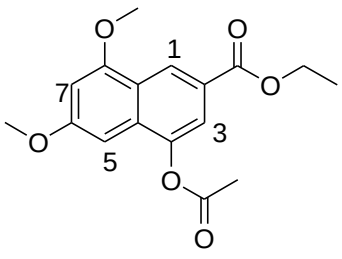
matrix least-squares calculations based on *F2* using *SHELXL-97*.[278] C-bound H atoms were first located in the difference map, then positioned geometrically and allowed to ride on their respective parent atoms, with thermal displacement parameters 1.2 times of the parent C atom. Where possible, the coordinates and isotropic displacement parameters of the O–bound H atoms involved in the hydrogen bonding interactions were allowed to refine freely. The diagrams were generated using *ORTEP-3* and the displacement ellipsoids shown at a 50% probability level.[279]

7.7 Experimental section for the synthesis of dehydroherbarin lactone 159

7.7.0 Synthesis of ethyl 4-acetoxy-6,8-dimethoxynaphthalene-2-carboxylate 170[119]

To a solution of 2,4-dimethoxybenzaldehyde **130** (5.32 g, 32.0 mmol) and diethyl succinate (7.70 g, 44.2 mmol) in *t*-BuOH (80 mL), stirred under N_2 (g), was added *t*-BuOK (4.96 g, 44.2 mmol). The reaction mixture was heated to reflux for 4 hrs after which it was cooled to rt, poured into ice cold H_2O and acidified to pH 4.0 with 32% aqueous HCl. The intermediate was extracted into EtOAc (3 × 100 mL) and the combined organic layers were dried over anhydrous $MgSO_4$, filtered through a pad of Celite® and concentrated *in vacuo*. The resultant thick brown oily residue was transferred into a 500 mL round bottom flask to which anhydrous NaOAc (5.08 g, 61.9 mmol) was added followed by Ac_2O (100 mL) and the mixture was heated to reflux at 130 ^oC for overnight. The solvent was removed *in vacuo* and MeOH was added portion-wise until no effervescence was observed (***warning****: this reaction is extremely exothermic and MeOH should be added slowly and with maximum care*). The MeOH was removed *in vacuo* and the crude product was passed through a short silica gel column. A saturated aqueous solution of sodium hydrogen carbonate (150 mL) was added to the crude product and extracted into EtOAc (3 × 100 mL). The combined organic layers were dried over anhydrous $MgSO_4$, filtered through a Celite® pad and solvent removed *in vacuo*. The residue was then purified by silica gel column chromatography (15% EtOAc/hexane) affording ethyl 4-acetoxy-6,8-dimethoxynaphthalene-2-carboxylate **170** (6.93 g, 68%) as a yellow solid. $\mathbf{R_f}$ = 0.56 (25% EtOAc/hexane);

^{1}H NMR (300 MHz, $CDCl_3$, Me_4Si) δ_H 8.78 (1H, s, H-1), 7.81 (1H, s, H-3), 6.64 (1H, d, *J* = 1.6 Hz, H-5), 6.51 (1H, d, *J* = 1.9 Hz, H-7), 4.42 (2H, q, *J* = 7.3 Hz, $ArCO_2CH_2CH_3$), 3.96



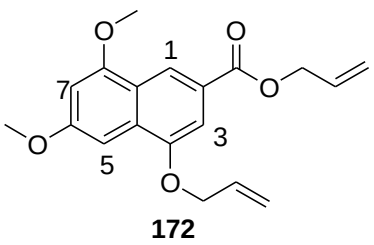
170

(3H, s, ArOCH_3), 3.92 (3H, s, ArOCH_3), 2.46 (3H, s, ArOC(O)CH_3), 1.42 (3H, t, J = 7.3 Hz, $ArCO_2CH_2CH_3$); **^{13}C NMR (75 MHz, $CDCl_3$, Me_4Si)** δ_C 170.1 (ArO*C*(O)CH_3), 166.3 ($ArCO_2CH_2CH_3$), 161.1 (C-6), 157.9 (C-8), 145.4 (C-4), 133.2 (C-4a), 124.4 (C-2), 123.4 (C-1), 122.2 (C-8a) 119.1 (C-3), 98.6 (C-5), 91.7 (C-7), 61.0 ($ArCO_2CH_2CH_3$), 55.8 (ArOCH_3), 55.4 (ArOCH_3), 20.9 (ArOC(O)CH_3), 14.4 ($ArCO_2CH_2CH_3$).

7.7.1 Synthesis of allyl 4-(allyloxy)-6,8-dimethoxynaphthalene-2-carboxylate 172[124]

Ethyl 4-acetoxy-6,8-dimethoxynaphthalene-2-carboxylate **170** (6.32 g, 19.9 mmol) was dissolved in MeOH (150 mL) in a 500 mL round bottom flask to which an aqueous NaOH solution (2.39 g, 59.8 mmol) in H_2O (100 mL) was added portion-wise. The dark-orange reaction mixture was heated to reflux for 6 hrs after which the MeOH was removed *in vacuo*. The aqueous medium was acidified to pH 4.0 with 32% (v/v) aqueous HCl and extracted into EtOAc (3 × 100 mL). The combined organic layers were dried over anhydrous $MgSO_4$, filtered through a Celite® pad and concentrated *in vacuo*. The crude intermediate was transferred into a clean 250 mL round bottom flask to which acetone (150 mL), allyl bromide (7.23 g, 59.8 mmol) and anhydrous K_2CO_3 (8.26 g, 59.8 mmol) were added. The reaction mixture was then heated to reflux for 18 hrs under a N_2 (g) after which it was allowed to cool to rt, filtered through a Celite® pad and the solvent removed *in vacuo*. The residue was purified by silica gel column chromatography (10% EtOAc/hexane) yielding allyl 4-(allyloxy)-6,8-dimethoxynaphthalene-2-carboxylate **172** as a yellow amorphous solid (5.62 g, 86%). $\mathbf{R_f}$ = 0.46 (15% EtOAc/hexane);

^{1}H NMR (300 MHz, $CDCl_3$, Me_4Si) δ_H 8.54 (1H, d, J = 1.6 Hz, H-1), 7.42 (1H, d, J = 1.6 Hz, H-3), 7.15 (1H, d, J = 2.0 Hz, H-5), 6.52 (1H, d, J = 2.0 Hz, H-7), 6.30-5.95 (2H, m, $ArCO_2CH_2CH$=CH_2 and $ArOCH_2CH$=CH_2), 5.59-5.24 (4H, m, $ArCO_2CH_2CH$=CH_2 and $ArOCH_2CH$=CH_2), 4.87 (2H, d, J = 5.6 Hz, $ArCO_2CH_2CH$=CH_2), 4.76 (2H, d, J = 5.1 Hz, $ArOCH_2CH$=CH_2), 3.96 (3H, s, ArOCH_3), 3.94 (3H, s, ArOCH_3); **^{13}C NMR (75 MHz,**

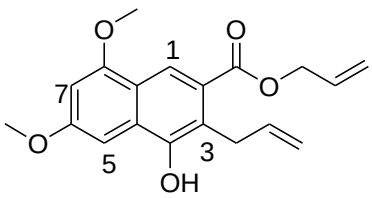


172

$CDCl_3$, Me_4Si) δ_C 166.8 (Ar*C*$O_2CH_2CH=CH_2$), 160.2 (C-6), 157.6 (C-8), 153.1 (C-4), 133.3 ($ArOCH_2$*C*H=CH_2), 132.7 ($ArCO_2CH_2$*C*H=CH_2), 130.0 (C-4a), 124.2 (C-2), 121.6 (C-8a), 118.3 (C-1), 118.05 ($ArOCH_2CH=$*C*H_2), 117.5 ($ArCO_2CH_2CH=$*C*H_2), 105.7 (C-3), 98.6 (C-5), 92.7 (C-7), 69.2 (ArO*C*$H_2CH=CH_2$), 65.6 ($ArCO_2$*C*$H_2CH=CH_2$), 55.8 (ArO*C*H_3), 55.3 (ArO*C*H_3).

7.7.2 Synthesis of allyl 3-allyl-4-hydroxy-6,8-dimethoxynaphthalene-2-carboxylate 152[124]

In a 100 mL round bottom flask equipped with a reflux condenser and a magnetic stirrer bar, was loaded neat allyl 4-(allyloxy)-6,8-dimethoxynaphthalene-2-carboxylate **172** (4.50 g, 13.7 mmol). The reaction vessel was then heated to 180 ^oC for 24 hours under a N_2 (g). The dark viscous residue was allowed to cool to rt and purification by column chromatography (20% EtOAc/hexane) on silica gel furnished allyl 3-allyl-4-hydroxy-6,8-dimethoxynaphthalene-2-carboxylate **152** as a cream white amorphous solid (3.15 g, 70%). $\mathbf{R_f}$ = 0.50 (25% EtOAc/hexane);

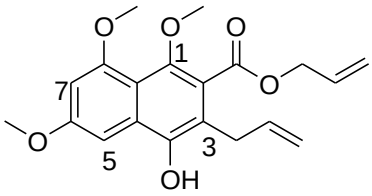


152

^{1}H NMR (300 MHz, $CDCl_3$, Me_4Si) δ_H 8.40 (1H, s, H-1), 7.01 (1H, d, *J* = 1.7 Hz, H-5), 6.45 (1H, d, *J* = 2.0 Hz, H-7), 6.08 (2H, tdd, *J* = 16.8, 11.3, 5.8 Hz, $ArCO_2CH_2CH=CH_2$ and $ArCH_2CH=CH_2$), 5.83 (1H, s, ArO*H*), 5.42 (1H, dd, *J* = 17.2, 1.4 Hz, one of $ArCO_2CH_2CH=CH_2$), 5.28 (1H, dd, *J* = 10.4, 1.0 Hz, one of $ArCO_2CH_2CH=CH_2$), 5.22-5.11 (2H, m, $ArCH_2CH=CH_2$), 4.83 (2H, d, *J* = 5.7 Hz, $COOCH_2CH=CH_2$), 3.96-3.89 (5H, br s, $ArCH_2CH=CH_2$ superimposing with one of the ArOCH_3), 3.88 (3H, s, $ArOCH_3$); **^{13}C NMR (75 MHz, $CDCl_3$, Me_4Si)** δ_C 167.8 (Ar*C*$O_2CH_2CH=CH_2$), 160.1 (C-6 or C-8), 157.2 (C-6 or C-8), 149.6 (C-4), 136.5 ($ArCH_2$*C*H=CH_2), 132.5 ($ArCO_2CH_2$*C*H=CH_2), 128.5 (C-4a), 125.1 (C-2), 120.3 (C-8a), 119.3 (C-3), 118.8 (C-1), 118.2 ($ArCH_2CH=$*C*H_2), 116.0 ($ArCO_2CH_2$*C*H=CH_2), 98.2 (C-5), 92.1 (C-7), 65.6 ($ArCO_2$*C*$H_2CH=CH_2$), 55.6 (ArO*C*H_3), 55.4 (ArO*C*H_3), 31.6 (Ar*C*$H_2CH=CH_2$).

7.7.3 Synthesis of allyl 3-allyl-4-hydroxy-1,6,8-trimethoxynaphthalene-2-carboxylate 153[124]

To a solution of allyl 3-allyl-4-hydroxy-6,8-dimethoxynaphthalene-2-carboxylate **152** (3.10 g, 9.44 mmol) in MeOH (100 mL) was added solid PIFA (4.11 g, 9.55 mmol) and the resultant reaction mixture was stirred for 15 min at rt. A saturated aqueous solution of $NaHCO_3$ was added until effervescence stopped and the MeOH was removed *in vacuo*. The residue was extracted into EtOAc (3 × 100 mL). The combined organic layers were dried over anhydrous $MgSO_4$, filtered through a pad of Celite® and the solvent evaporated *in vacuo*. The residue was then dissolved in EtOH (50 mL) in a 150 mL round bottom flask to which *t*-BuOK (4.24 g, 37.8 mmol) was added with vigorous stirring for 20 min at rt. The reaction was quenched with saturated aqueous solution NH_4Cl (50 mL) and the solvent was concentrated under reduced pressure leaving an aqueous medium which was extracted into EtOAc (3 × 100 mL). The combined organic layers were dried over anhydrous $MgSO_4$, filtered through a bed of Celite® and concentrated *in vacuo*. The residue was purified by silica gel column chromatography (10% EtOAc/hexane) yielding a semi-solid product **153** (1.96 g, 58%). $\mathbf{R_f}$ = 0.46 (25% EtOAc/hexane);

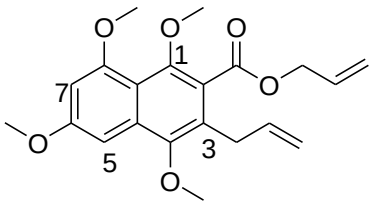


153

^{1}H NMR (300 MHz, $CDCl_3$, Me_4Si) δ_H 9.15 (1H, s, ArO*H*), 7.27 (1H, d, *J* = 2.5 Hz, H-5), 6.75 (1H, d, *J* = 2.5 Hz, H-7), 6.14-5.74 (2H, m, $ArCO_2CH_2CH$=CH_2 and $ArCH_2CH$=CH_2), 5.45 (1H, dd, *J* = 17.2, 1.4 Hz, one of $ArCO_2CH_2CH$=CH_2), 5.33 (1H, dd, *J* = 10.4, 1.1 Hz, one of $ArCO_2CH_2CH$=CH_2), 5.12 (1H, dd, *J* = 17.1, 1.5 Hz, one of $ArCH_2CH$=CH_2), 5.05 (1H, dd, *J* = 10.1, 1.4 Hz, one of $ArCH_2CH$=CH_2), 4.84 (2H, ddd, *J* = 4.9, 3.1, 1.2 Hz, $ArCO_2CH_2CH$=CH_2), 3.90 (3H, s, $ArOCH_3$), 3.88 (3H, s, $ArOCH_3$), 3.22 (2H, d, *J* = 6.4 Hz, $ArCH_2CH$=CH_2), 3.19 (3H, s, $ArOCH_3$); **^{13}C NMR (75 MHz, $CDCl_3$, Me_4Si)** δ_C 168.1 ($ArCO_2CH_2CH$=CH_2), 158.7 (C-6), 157.4 (C-8), 147.6 (C-1), 145.3 (C-4), 136.3 ($ArCO_2CH_2CH$=CH_2), 132.4 ($ArCH_2CH$=CH_2), 131.9 (C-4a), 129.5 (C-3), 124.3 (C-8a), 118.8 ($ArCO_2CH_2CH$=CH_2), 116.8 ($ArCH_2CH$=CH_2), 116.7 (C-2), 99.4 (C-7), 92.9 (C-5), 66.0 ($ArCO_2CH_2CH$=CH_2), 63.9 ($ArOCH_3$), 55.9 ($ArOCH_3$), 55.3 ($ArOCH_3$), 32.6 ($ArCH_2CH$=CH_2).

7.7.4 Synthesis of allyl 3-allyl-1,4,6,8-tetramethoxynaphthalene-2-carboxylate 168[124]

To a 250 mL 2-neck round bottom flask containing allyl 3-allyl-4-hydroxy-1,6,8-trimethoxynaphthalene-2-carboxylate **153** (1.95 g, 5.44 mmol) and anhydrous K_2CO_3 (1.17 g, 8.50 mmol) in acetone (100 mL), was added Me_2SO_4 (0.80 mL, 8.50 mmol) *via* a syringe. The reaction mixture was heated to reflux for 18 hrs after which it was cooled to rt, filtered through a Celite® pad and the solvent was removed *in vacuo*. The residue was then dissolved in EtOAc (100 mL) and successively washed with 25% (v/v) aqueous NH_3 (2 × 75 mL) and H_2O (4 × 100 mL). The combined organic layers were dried over anhydrous $MgSO_4$, filtered through a bed of Celite® and concentrated *in vacuo*. Purification of the crude product by column chromatography (10% EtOAc/hexane) on silica gel furnished the required tetra-oxygenated naphthalene **168** as an off-white solid (1.86 g, 92%). $\mathbf{R_f}$ = 0.54 (25 % EtOAc/hexane);



168

^{1}H NMR (300 MHz, $CDCl_3$, Me_4Si) δ_H 6.98 (1H, d, *J* = 1.8 Hz, H-5), 6.54 (1H, d, *J* = 1.8 Hz, H-7), 6.14-5.84 (2H, m, $ArCO_2CH_2C\mathit{H}=CH_2$ and $ArCH_2C\mathit{H}=CH_2$), 5.43 (1H, d, *J* = 17.2, one of $ArCO_2CH_2CH=C\mathit{H}_2$), 5.28 (1H, d, *J* = 10.4, one of $ArCO_2CH_2CH=C\mathit{H}_2$), 5.13-4.99 (2H, m, $ArCH_2CH=C\mathit{H}_2$), 4.82 (2H, dd, *J* = 5.9, 1.2 Hz, $ArCO_2C\mathit{H}_2CH=CH_2$), 3.96 (3H, s, $ArOC\mathit{H}_3$), 3.93 (3H, s, $ArOC\mathit{H}_3$), 3.86 (3H, s, $ArOC\mathit{H}_3$), 3.84 (3H, s, $ArOC\mathit{H}_3$), 3.56 (2H, dd, *J* = 6.2, 0.9 Hz, $ArC\mathit{H}_2CH=CH_2$); **^{13}C NMR (75 MHz, $CDCl_3$, Me_4Si)** δ_C 167.8 ($ArC O_2CH_2CH=CH_2$), 159.4 (C-6), 158.0 (C-8), 150.6 (C-1 or C-2), 149.3 (C-1 or C-2), 136.3 ($ArCO_2CH_2\mathit{C}H=CH_2$), 132.7 (C-4a), 132.1 ($ArCH_2\mathit{C}H=CH_2$), 126.6 (C-3), 124.8 (C-8a), 118.9 ($ArCO_2CH_2CH=\mathit{C}H_2$), 115.9 ($ArCH_2CH=\mathit{C}H_2$), 115.4 (C-2), 99.3 (C-7), 93.3 (C-5), 66.0 ($ArCO_2\mathit{C}H_2CH=CH_2$), 63.9 ($ArO\mathit{C}H_3$), 61.6 ($ArO\mathit{C}H_3$), 56.1 ($ArO\mathit{C}H_3$), 55.4 ($ArO\mathit{C}H_3$), 31.8 ($ArCH_2CH=CH_2$).

7.7.5 Synthesis of allyl 3-allyl-1,4-dihydro-6,8-dimethoxy-1,4-dioxonaphthalene-2-carboxylate 174

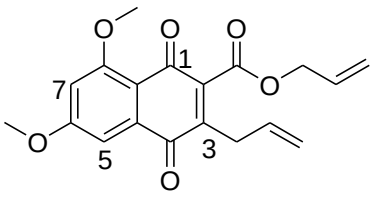
Method one:

Allyl 3-allyl-1,4,6,8-tetramethoxynaphthalene-2-carboxylate **168** (0.900 g, 2.42 mmol) in 1,4-dioxane (50 mL) was charged in a 100 mL round bottom flask equipped with a magnetic stirring bar to which AgO (1.20 g, 9.68 mmol) was added. The reaction mixture was stirred at rt for 10 min after which 55% (v/v) aqueous HNO_3 was added drop-wise until all the AgO dissolved. The resultant reaction mixture was stirred for a further 5 min. A mixture of CH_2Cl_2/H_2O (100 mL, v/v, 1:1) was then added to the reaction mixture and the lower organic layer was separated. The aqueous layer was further extracted into CH_2Cl_2 (2 × 50 mL) and the combined organic layers were dried over anhydrous $MgSO_4$, filtered through a pad of Celite® and concentrated under reduced pressure. The crude product was purified by column chromatography (EtOAc/CH_2Cl_2/hexane 2:1:7) on silica gel which delivered allyl 3-allyl-1,4-dihydro-6,8-dimethoxy-1,4-dioxonaphthalene-2-carboxylate **174** as an orange amorphous solid (0.621 g, 75%).

Method two:

In a 250 mL round bottom flask equipped with a magnetic stirring bar was placed allyl 3-allyl-1,4,6,8-tetramethoxynaphthalene-2-carboxylate **168** (1.80 g, 4.83 mmol) in MeCN (50 mL) and CAN (5.92 g, 10.8 mmol) in H_2O (50 mL) was then added portion-wise. The resultant reaction mixture was stirred at rt for 30 min after which saturated aqueous $NaHCO_3$ (50 mL) was added and the organic layer was extracted into EtOAc (3 × 150 mL). The combined organic layers were then dried over anhydrous $MgSO_4$, filtered through a pad of Celite® and the solvent was removed *in vacuo*. Purification of the crude product by column chromatography (EtOAc/CH_2Cl_2/hexane 2:1:7) on silica gel yielded allyl 3-allyl-1,4-dihydro-6,8-dimethoxy-1,4-dioxonaphthalene-2-carboxylate **174** as an orange amorphous solid (0.992 g, 60%). **R_f** = 0.54 **(**EtOAc/CH_2Cl_2/hexane 3:1:6); **Mp** 89-92 ^oC; **IR ν_{max}(cm^{-1})** 1774 (C=O), 1756 (C=O), 1705 (C=O), 1626 (C=C), 1544 (C=C), 1543 (C=C);

^{1}H NMR (300 MHz, $CDCl_3$, Me_4Si) δ_H 7.25 (1H, d, *J* = 2.4 Hz, H-5), 6.73 (1H, d, *J* = 2.4 Hz, H-7), 6.09-5.70 (2H, m, $ArCO_2CH_2CH$=CH_2 and $ArCH_2CH$=CH_2), 5.44 (1H, dd, *J* =



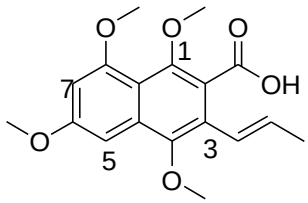
174

17.2, 1.4 Hz, one of $ArCO_2CH_2CH=CH_2$), 5.31 (1H, dd, *J* = 10.4, 1.1 Hz, one of $ArCO_2CH_2CH=CH_2$), 5.17 (1H, dd, *J* = 17.1, 1.4 Hz, one of $ArCH_2CH=CH_2$), 5.09 (1H, dd, *J* = 10.0, 1.3 Hz, one of $ArCH_2CH=CH_2$), 4.83 (2H, dt, *J* = 5.9, 1.2 Hz, $ArCO_2CH_2CH=CH_2$), 3.95 (3H, s, $ArOCH_3$), 3.94 (3H, s, $ArOCH_3$), 3.26 (2H, dt, *J* = 6.6, 1.2 Hz, $ArCH_2CH=CH_2$); **^{13}C NMR (75 MHz, $CDCl_3$, Me_4Si)** δ_C 184.5 (C-4), 179.8 (C-1), 165.0 ($ArCO_2CH_2CH=CH_2$), 164.5 (C-6), 162.1 (C-8), 141.6 (C-3), 141.5 (C-2), 135.5 ($ArCO_2CH_2CH=CH_2$), 132.8 ($ArCH_2CH=CH_2$), 131.3 (C-4a), 119.5 ($ArCO_2CH_2CH=CH_2$), 118.2 ($ArCH_2CH=CH_2$), 113.7 (C-8a), 104.4 (C-7), 103.7 (C-5), 66.4 ($ArCO_2CH_2CH=CH_2$), 56.5 ($ArOCH_3$), 56.0 ($ArOCH_3$), 31.7 ($ArCH_2CH=CH_2$). **HRMS** (*m*/*z*), calculated for $C_{19}H_{19}O_6$: 343.1176, found $(M + H)^+$ 343.1172.

7.7.6 Synthesis of 1,4,6,8-tetramethoxy-3-((*E*)-prop-1-enyl)naphthalene-2-carboxylic acid 175

To a solution of allyl 3-allyl-1,4,6,8-tetramethoxynaphthalene-2-carboxylate **168** (1.50 g, 4.03 mmol), PPh_3 (2.11 g, 8.06 mmol) and morpholine (0.705 mL, 8.06 mmol) in dry THF (50 mL) was added $Pd(OAc)_2$ (90.5 mg, 0.403 mmol). The reaction mixture was stirred for 12 hrs at rt after which it was diluted with diethyl ether (100 mL) and washed with 1 M HCl (2 × 50 mL) followed by H_2O (3 × 100 mL) and brine (2 × 50 mL). The organic layer was dried over anhydrous $MgSO_4$, filtered through a bed of Celite® and concentrated *in vacuo*. The residue was taken up in petroleum ether (150 mL), with a boiling point of between 40-60 ^oC, filtered through a bed of Celite® and the filtrate was concentrated *in vacuo*. After repetition of this process, the residue was purified by silica gel column chromatography (EtOAc/hexane/petroleum ether 1:3:6) affording carboxylic acid **175** (0.750 g, 56%). **R_f** = 0.26 (40% EtOAc/hexane); **Mp** 138-140 ^oC; **IR ν_{max} (cm^{-1})** 3680 (O-H), 1681 (C=O), 1545 (C=C);

^{1}H NMR (300 MHz, MeOD) δ_H 7.05 (1H, d, *J* = 2.3 Hz, H-5), 6.63 (1H, d, *J* = 2.2 Hz, H-7), 6.57 (1H, dq, *J* = 16.1, 1.5 Hz, ArC*H*=CHCH$_3$), 6.41 (1H, dq, *J* = 16.1, 6.3 Hz, ArCH=C*H*CH$_3$), 3.96 (3H, s, ArOC*H*$_3$), 3.92 (3H, s, ArOC*H*$_3$), 3.82 (3H, s, ArOC*H*$_3$), 3.79 (3H, s, ArOC*H*$_3$), 1.93 (3H, dd, *J* = 6.4, 1.4 Hz, ArCH=CHC*H*$_3$); **^{13}C NMR (75 MHz, MeOD)** δ_C 170.7 (Ar*C*O$_2$H), 159.6 (C-6), 157.6 (C-8), 149.1 (C-1 or C-4), 148.6 (C-1 or C-4), 132.4 (Ar*C*H=CHCH$_3$), 131.5 (C-4a), 124.5 (ArCH=*C*HCH$_3$), 124.3 (C-2), 123.7 (C-3), 114.8 (C-8a), 99.2 (C-7), 92.9 (C-5), 62.7 (ArO*C*H$_3$), 59.5 (ArO*C*H$_3$), 55.1 (ArO*C*H$_3$), 54.4 (ArO*C*H$_3$), 18.2 (ArCH=CH*C*H$_3$). **HRMS** (*m*/*z*), calculated for $C_{18}H_{21}O_6$: 333.1333, found $(M + H)^+$ 333.1336.

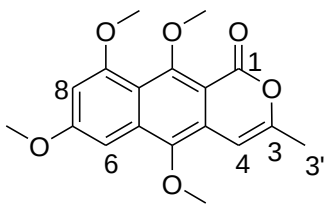


175

7.7.7 Synthesis of 5,7,9,10-tetramethoxy-3-methyl-1*H*-benzo[*g*]isochromen-1-one 103[86]

1,4,6,8-Tetramethoxy-3-((*E*)-prop-1-enyl)naphthalene-2-carboxylic acid **175** (1.00 g, 3.01 mmol) and $CuCl_2.2H_2O$ (0.597 g, 3.50 mmol) were dissolved in DMF/H_2O mixture (2:1, v/v, 100 mL) in a 2-neck round bottom flask to which $PdCl_2$ (53.4 mg, 0.301 mmol) was added under a blanket of O_2 (g). The reaction mixture was vigorously stirred for 24 hrs at rt after which it was filtered through a thick Celite® bed which was washed slowly with CH_2Cl_2 (3 × 50 mL). The combined organic layers were washed with brine (3 × 50 mL) and dried over anhydrous $MgSO_4$, filtered through a pad of Celite® and the solvent was removed *in vacuo*. Purification of the crude residue by column chromatography (EtOAc/CH_2Cl_2/hexane 2:1:7) on silica gel afforded two compounds. The first compound was 5,7,9,10-tetramethoxy-3-methyl-1*H*-benzo[*g*]isochromen-1-one **103** which was obtained as a pale yellow solid (0.467 g, 47%). $\mathbf{R_f}$ = 0.38 (EtOAc/CH_2Cl_2/hexane 3:1:6); **Mp** 154-156 ^oC); **IR ν_{max}(cm^{-1})** 1689 (C=O), 1603 (C=C);

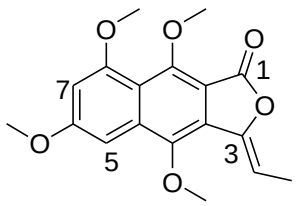
^{1}H NMR (300 MHz, $CDCl_3$, Me_4Si) δ_H 6.98 (1H, d, *J* = 2.3 Hz, H-6), 6.51 (1H, d, *J* = 2.3 Hz, H-8), 6.48 (1H, s, H-4), 3.99 (3H, s, ArOC*H*$_3$), 3.97 (3H, s, ArOC*H*$_3$), 3.96 (3H, s, ArOC*H*$_3$), 3.90 (3H, s, ArOC*H*$_3$), 2.27 (3H, s, H-3'); **^{13}C NMR (75 MHz, $CDCl_3$, Me_4Si)** δ_C 161.4 (C-7), 160.0 (C-1), 159.4 (C-9), 159.3 (C-10), 153.4 (C-3), 143.7 (C-5), 135.5 (C-5a), 126.6 (C-4a), 116.4 (C-9a), 108.6 (C-10a), 99.4



103

(C-8), 97.3 (C-6), 92.2 (C-4), 62.9 (ArO*C*H$_3$), 61.6 (ArO*C*H$_3$), 56.4 (ArO*C*H$_3$), 55.5 (ArO*C*H$_3$), 19.8 (C-3'). **HRMS** (*m*/*z*), calculated for $C_{18}H_{19}O_6$: 331.1176, found $(M + H)^+$ 331.1181.

The second compound was (*Z*)-3-ethylidene-4,6,8,9-tetramethoxynaphtho[2,3,-*c*]furan-1(3*H*)-one **176** which was obtained as a yellow crystalline solid (0.209 g, 21%): $\mathbf{R_f}$ = 0.40 (EtOAc/CH_2Cl_2/hexane 3:1:6); **Mp** 154-156 ^oC; **IR** $\boldsymbol{\nu_{max}}$**(cm^{-1})** 1762 (C=O), 1679 (C=C);



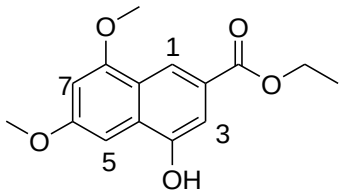
176

^{1}H NMR (300 MHz, CDCl$_3$, Me$_4$Si) δ_H 7.02 (1H, d, *J* = 2.3 Hz, H-5), 6.56 (1H, d, *J* = 2.2 Hz, H-7), 5.92 (1H, q, *J* = 7.3 Hz, ArC=C*H*CH$_3$), 4.06 (3H, s, ArOC*H*$_3$), 3.98 (3H, s, ArOC*H*$_3$), 3.97 (3H, s, ArOC*H*$_3$), 3.91 (3H, s, ArOC*H*$_3$), 2.04 (3H, d, *J* = 7.3 Hz, ArC=CHC*H*$_3$); **^{13}C NMR (75 MHz, CDCl$_3$, Me$_4$Si)** δ_C 164.6 (C-1), 161.3 (C-6), 160.1 (C-8), 155.4 (C-9), 144.5 (C-3), 143.8 (C-4), 137.0 (C-4a), 125.4 (C-3a), 117.5 (C-8a), 111.2 (C-9a), 106.8 (ArC=*C*HCH$_3$), 99.9 (C-7), 93.1 (C-5), 63.4 (ArO*C*H$_3$), 59.9 (ArO*C*H$_3$), 56.3 (ArO*C*H$_3$), 55.5 (ArO*C*H$_3$), 11.7 (ArC=CH*C*H$_3$). **HRMS** (*m*/*z*), calculated for $C_{18}H_{19}O_6$: 331.1176, found $(M + H)^+$ 331.1174.

7.7.8 Synthesis of ethyl 4-hydroxy-6,8-dimethoxynaphthalene-2-carboxylate 198[119]

Ethyl 4-acetoxy-6,8-dimethoxynaphthalene-2-carboxylate **170** (5.00 g, 15.7 mmol) was dissolved in EtOH (50 mL) followed by the portion-wise addition of 1% (w/v) ethanolic solution of KOH (0.926 g, 16.5 mmol) in EtOH (100 mL). The pale orange reaction mixture was stirred for 3 hrs at rt after which H_2O (100 mL) was added. The organic solvent was evaporated under reduced pressure leaving an aqueous residue which was then carefully acidified to pH 5.0 with 32% aqueous HCl. The acidic medium was extracted into EtOAc (3 × 150 mL) and the combined organic layers were dried over anhydrous $MgSO_4$, filtered through a Celite® pad and concentrated *in vacuo*. The residue was purified by silica gel column chromatography (10% EtOAc/hexane) affording ethyl 4-hydroxy-6,8-dimethoxynaphthalene-2-carboxylate **198** as a cream amorphous solid (3.47 g, 88%). $\mathbf{R_f}$ = 0.43 (15% EtOAc/hexane);

^{1}H NMR (300 MHz, Acetone) δ_H 9.13 (1H, s, ArO*H*), 8.41 (1H, d, *J* = 1.5 Hz, H-1), 7.50 (1H, d, *J* = 1.5 Hz, H-3), 7.18 (1H, d, *J* = 2.0 Hz, H-5), 6.65 (1H, d, *J* = 2.0 Hz, H-7), 4.37 (2H, q, *J* = 7.1 Hz, $ArCO_2C\mathit{H}_2CH_3$), 4.04 (3H, s, $ArOC\mathit{H}_3$), 3.95 (3H, s, $ArOC\mathit{H}_3$), 1.39 (3H, t, *J* = 7.1 Hz, $ArCO_2CH_2C\mathit{H}_3$); **^{13}C NMR (75 MHz, Acetone)** δ_C 167.2 ($ArCO_2CH_2CH_3$), 160.9 (C-6), 158.4 (C-8), 153.0 (C-4), 130.0 (C-4a), 125.8 (C-2), 122.7 (C-8a), 117.2 (C-1), 109.2 (C-3), 99.4 (C-7), 93.7 (C-5), 61.2 ($ArCO_2\mathit{C}H_2CH_3$), 56.2 ($ArOCH_3$), 55.8 ($ArOCH_3$), 14.7 ($ArCO_2CH_2\mathit{C}H_3$).

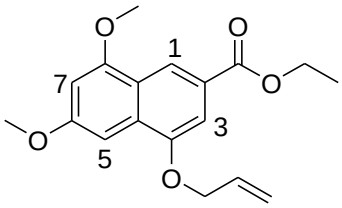


198

7.7.9 Synthesis of ethyl 4-(allyloxy)-6,8-dimethoxynaphthalene-2-carboxylate 131[119]

To a solution of ethyl 4-hydroxy-6,8-dimethoxynaphthalene-2-carboxylate **198** (4.50 g, 16.3 mmol) in acetone (100 mL) was added anhydrous K_2CO_3 (2.70 g, 19.5 mmol) followed by allyl bromide (2.36 g, 19.5 mmol). The reaction mixture was heated to reflux for 24 hrs under a N_2 (g). The mixture was then allowed to cool to rt, filtered through a bed of Celite® and the solvent was removed *in vacuo*. Purification of the residue by column chromatography (10% EtOAc/hexane) on silica gel afforded ethyl 4-(allyloxy)-6,8-dimethoxynaphthalene-2-carboxylate **131** as a yellow amorphous solid (4.43 g, 87%). $\mathbf{R}_f$ = 0.46 (20% EtOAc/hexane);

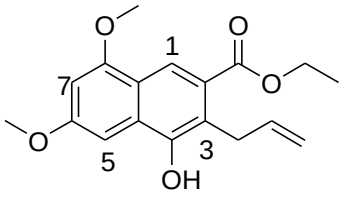
^{1}H NMR (300 MHz, Acetone) δ_H 8.48 (1H, s, H-1), 7.45 (H1, d, *J* = 1.3 Hz, H-3), 7.20 (1H, d, *J* = 2.0 Hz, H-5), 6.67 (1H, d, *J* = 2.2 Hz, H-7), 6.24 (1H, ddt, *J* = 17.2, 10.4, 5.1 Hz, $ArOCH_2C\mathit{H}{=}CH_2$), 5.58 (1H, dd, *J* = 17.3, 1.7 Hz, one of $ArOCH_2CH{=}C\mathit{H}_2$), 5.35 (1H, dd, *J* = 10.6, 1.5 Hz, one of $ArOCH_2CH{=}C\mathit{H}_2$), 4.82 (2H, dt, *J* = 4.9, 1.4 Hz, $ArOC\mathit{H}_2CH{=}CH_2$), 4.40 (2H, q, *J* = 7.1 Hz, $ArCO_2C\mathit{H}_2CH_3$), 4.04 (3H, s, $ArOC\mathit{H}_3$), 3.95 3H, s, $ArOC\mathit{H}_3$), 1.41 (3H, t, *J* = 7.1 Hz, $ArCO_2CH_2C\mathit{H}_3$); **^{13}C NMR (75 MHz, Acetone)** δ_C 167.1 ($ArCO_2CH_2CH_3$), 161.3 (C-6), 158.5 (C-8), 154.1 (C-4), 134.5 ($ArOCH_2\mathit{C}H{=}CH_2$), 130.8 (C-4a), 125.6 (C-2), 122.3 (C-8a), 118.3 (C-1), 117.5 ($ArOCH_2CH{=}\mathit{C}H_2$), 106.3 (C-3), 99.5 (C-7), 93.6 (C-5), 69.8 ($ArOCH_2CH{=}CH_2$), 61.3 ($ArCO_2\mathit{C}H_2CH_3$), 56.3 ($ArOCH_3$), 55.8 ($ArOCH_3$), 14.7 ($ArCO_2CH_2\mathit{C}H_3$).



131

7.7.10 Synthesis of ethyl 3-allyl-4-hydroxy-6,8-dimethoxynaphthalene-2-carboxylate 197[119]

Ethyl 4-(allyloxy)-6,8-dimethoxynaphthalene-2-carboxylate **131** (4.00 g, 12.6 mmol) was loaded neat in a 100 mL round bottom flask equipped with a reflux condenser and a magnetic stirring bar. The flask was then heated to 180 ^{o}C in a silicon oil bath for 24 hrs under a N_2 (g). After 24 hrs, the dark viscous residue was allowed to cool to rt, dissolved in acetone and adsorbed onto normal silica. Purification of the crude product by column chromatography (20% EtOAc/hexane) on silica gel yielded ethyl 3-allyl-4-hydroxy-6,8-dimethoxynaphthalene-2-carboxylate **197** as a yellow amorphous solid (2.75 g, 69%). $\mathbf{R_f}$ = 0.41 (20% EtOAc/hexane);



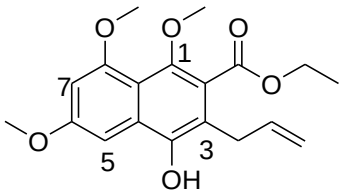
197

^{1}H NMR (500 MHz, $CDCl_3$, Me_4Si) δ_H 8.37 (1H, s, H-1), 7.04 (1H, s, H-5), 6.50 (1H, s, H-7), 6.25–6.04 (1H, m, $ArCH_2CH$=CH_2), 5.65 (1H, s, ArO*H*), 5.23 (1H, dd, *J* = 3.8, 1.6 Hz, one of $ArCH_2CH$=CH_2), 5.18 (1H, dd, *J* = 3.5, 1.6 Hz, one of $ArCH_2CH$=CH_2), 4.38 (2H, q, *J* = 7.1 Hz, $ArCO_2CH_2CH_3$), 3.97 (3H, s, $ArOCH_3$), 3.94 (3H, s, $ArOCH_3$), 3.92 (2H, d, *J* = 6.0 Hz, $ArCH_2CH$=CH_2), 1.42 (3H, t, *J* = 7.1 Hz, $ArCOOCH_2CH_3$); **^{13}C NMR (126 MHz, $CDCl_3$, Me_4Si)** δ_C 168.3 ($ArCO_2CH_2CH_3$), 160.1 (C-6), 157.2 (C-8), 149.7 (C-4), 136.4 ($ArCH_2CH$=CH_2), 128.4 (C-4a), 125.6 (C-2), 120.3 (C-8a), 118.8 (C-3), 118.5 ($ArCH_2CH$=CH_2), 116.2 (C-1), 98.8 (C-7), 92.3 (C-5), 60.8 ($ArCO_2CH_2CH_3$), 55.6 ($ArOCH_3$), 55.4 ($ArOCH_3$), 31.8 ($ArCH_2CH$=CH_2), 14.4 ($ArCO_2CH_2CH_3$).

7.7.11 Synthesis of ethyl 3-allyl-4-hydroxy-1,6,8-trimethoxynaphthalene-2-carboxylate 196

To a solution of ethyl 3-allyl-4-hydroxy-6,8-dimethoxynaphthalene-2-carboxylate **197** (3.50 g, 11.1 mmol) in absolute MeOH (80 mL), was added solid PIFA (5.12 g, 11.9 mmol) and the reaction mixture was stirred for 15 min at rt. After the 15 min had elapsed, saturated aqueous $NaHCO_3$ (73 mL) was added to the reaction mixture portion-wise until effervescence stopped and MeOH was removed *in vacuo* leaving an aqueous medium. The aqueous layer was then extracted into EtOAc (3 × 100 mL) and the combined organic layers were dried over

anhydrous $MgSO_4$, filtered through a Celite® pad and concentrated under reduced pressure. The residue was dissolved in EtOH in a clean 250 mL round bottom flask to which *t*-BuOK (3.32 g, 29.6 mmol) was added and the resultant reaction mixture was vigorously stirred for 20 min at rt. The reaction was quenched with saturated aqueous NH_4Cl (50 mL) and the resultant mixture was concentrated under reduced pressure. The aqueous medium was extracted into EtOAc (3 × 100 mL). The combined organic layers were dried over anhydrous MgSO4, filtered through a Celite® pad and evaporated *in vacuo*. Purification of the residue by column chromatography (20% EtOAc/hexane) on silica gel afforded ethyl 3-allyl-4-hydroxy-1,6,8-trimethoxynaphthalene-2-carboxylate **196** as a pale orange semi-solid (2.31 g, 60%). $\mathbf{R_f}$ = 0.37 (20% EtOAc/hexane);



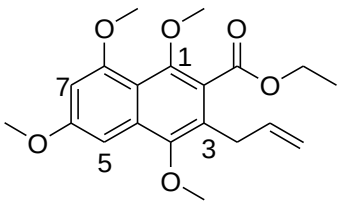
196

^{1}H NMR (300 MHz, $CDCl_3$, Me_4Si) δ_H 7.08 (1H, s, H-5), 6.53 (1H, s, H-7), 6.19-5.89 (1H, m, $ArCH_2CH$=CH_2), 5.56 (1H, s, ArO*H*), 5.25 (2H, d, *J* = 16.9 Hz, $ArCH_2CH$=CH_2), 4.40 (2H, q, *J* = 7.1 Hz, $ArCO_2CH_2CH_3$), 3.87 (9H, two br d, 3 overlapping $ArOCH_3$), 3.43 (2H, br s, $ArCH_2CH$=CH_2), 1.38 (3H, t, *J* = 7.1 Hz, $ArCO_2CH_2CH_3$); **^{13}C NMR (75 MHz, $CDCl_3$, Me_4Si)** δ_C 168.5 ($ArCO_2CH_2CH_3$), 158.8 (C-6), 157.5 (C-8), 147.5 (C-1), 145. 5 (C-4), 135.4 ($ArCH_2CH$=CH_2), 129.4 (C-4a), 124.7 (C-3), 117.2 ($ArCH_2CH$=CH_2), 116.3 (C-8a), 115.2 (C-2), 99.5 (C-7), 92.8 (C-5), 61.3 ($ArCO_2CH_2CH_3$), 58.4 ($ArOCH_3$), 56.0 ($ArOCH_3$), 55.3 ($ArOCH_3$), 32.9 ($ArCH_2CH$=CH_2), 14.3 ($ArCO_2CH_2CH_3$).

7.7.12 Synthesis of ethyl 3-allyl-1,4,6,8-tetramethoxynaphthalene-2-carboxylate 195

A mixture of ethyl 3-allyl-4-hydroxy-1,6,8-trimethoxynaphthalene-2-carboxylate **196** (2.30 g, 6.64 mmol), anhydrous K_2CO_3 (1.17 g, 8.50 mmol) and Me_2SO_4 (0.804 mL, 8.50 mmol) in acetone (100 mL) was heated to reflux for 24 hrs under a N_2 (g). The reaction mixture was then cooled to rt, filtered through a Celite® pad and the solvent removed *in vacuo*. The resultant residue was dissolved in EtOAc (100 mL) and successively washed with 25% (v/v) aqueous NH_3 (2 × 50 mL). The EtOAc layer was then acidified to pH 4 with 32% (v/v) aqueous HCl and the acidic solution was washed with de-ionised H_2O until the aqueous layer was neutral. The organic layer was dried over anhydrous MgSO4, filtered through a bed of

Celite® and concentrated *in vacuo*. Purification of the residue by silica gel column chromatography (10% EtOAc/hexane) yielded ethyl 3-allyl-1,4,6,8-tetramethoxynaphthalene-2-carboxylate **195** as a pale yellow solid (2.13 g, 89%). $\mathbf{R_f}$ = 0.41 (20% EtOAc/hexane);

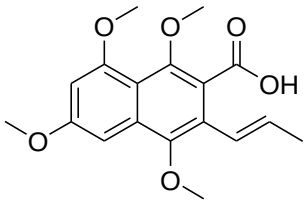


195

^{1}H NMR (300 MHz, $CDCl_3$, Me_4Si) δ_H 6.98 (1H, d, *J* = 2.2 Hz, H-5), 6.53 (1H, d, *J* = 2.2 Hz, H-7), 5.98 (1H, ddt, *J* = 16.4, 10.1, 6.2 Hz, $ArCH_2CH$=CH_2), 5.07 (2H, dd, *J* = 3.7, 1.7 Hz, $ArCH_2CH$=CH_2), 4.39 (2H, q, *J* = 7.1 Hz, $ArCO_2CH_2CH_3$), 3.94 (3H, s, $ArOCH_3$), 3.90 (3H, s, $ArOCH_3$), 3.85 (6H, br s, two overlapping $ArOCH_3$), 3.57 (2H, d, *J* = 6.2 Hz, $ArCH_2CH$=CH_2), 1.38 (3H, t, *J* = 7.1 Hz, $ArCO_2CH_2CH_3$); **^{13}C NMR (75 MHz, $CDCl_3$, Me_4Si)** δ_C 168.0 ($ArCO_2CH_2CH_3$), 159.3 (C-6), 157.9 (C-8), 150.4 (C-1 or C-4), 149.3 (C-1 or C-4), 136.3 ($ArCH_2CH$=CH_2), 132.7 (C-4a), 126.6 (C-3), 125.1 (C-8a), 115.9 ($ArCH_2CH$=CH_2), 115.3 (C-2), 99.2 (C-7), 93.2 (C-5), 63.8 ($ArCO_2CH_2CH_3$), 61.6 ($ArOCH_3$), 61.1 ($ArOCH_3$), 56.1 ($ArOCH_3$), 55.3 ($ArOCH_3$), 31.8 ($ArCH_2CH$=CH_2), 14.3 ($ArCO_2CH_2CH_3$). **HRMS** (*m*/*z*), calculated for $C_{20}H_{25}O_6$: 361.1646 found $(M + H)^+$ 361.1649.

7.7.13 Synthesis of 1,4,6,8-tetramethoxy-3-((*E*)-prop-1-enyl)naphthalene-2-carboxylic acid 175

To a solution of ethyl 3-allyl-1,4,6,8-tetramethoxynaphthalene-2-carboxylate **195** (2.10 g, 5.83 mmol) in MeOH (100 mL) was added an aqueous solution of NaOH (0.933 g, 23.32 mmol) in H_2O (50 mL) and the resultant reaction mixture was heated to reflux for 36 hrs. To this reaction mixture, an aqueous solution of KOH (1.59 g, 28.3 mmol) in H_2O (50 mL) was added portion-wise and the resultant mixture was again heated to reflux for 48 hrs (monitored by TLC). The mixture was then cooled to rt and the solvent was concentrated under reduced pressure. The remaining aqueous medium was carefully acidified to pH 4.0 with 32% (v/v) aqueous HCl and extracted into EtOAc (3 × 150 mL). The combined organic layers were dried over anhydrous $MgSO_4$, filtered through a Celite® bed and concentrated *in vacuo*. The residue was purified by column chromatography (20% EtOAc/hexane) on silica gel. The isolated product was then dissolved in hot solution of



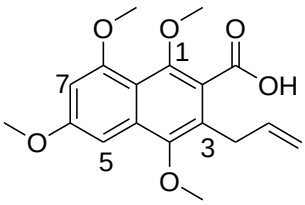
175

20% EtOAc/hexane and allowed to slowly crystallize yielding 1,4,6,8-tetramethoxy-3-((*E*)-prop-1-enyl)naphthalene-2-carboxylic acid **175** as colourless crystals (1.07 g, 55%). $\mathbf{R_f}$ = 0.26 (40 % EtOAc /hexane). The ^{1}H NMR spectrum was similar to the one discussed in **Section 7.7.6**.

7.7.14 Synthesis of 3-allyl-1,4,6,8-tetramethoxynaphthalene-2-carboxylic acid 167

To a solution of ethyl 3-allyl-1,4,6,8-tetramethoxynaphthalene-2-carboxylate **195** (2.10 g, 5.83 mmol) and allyl 3-allyl-1,4,6,8-tetramethoxynaphthalene-2-carboxylate **168** (2.20 g, 5.91 mmol) in dry THF (200 mL), cooled to 0 °C in an ice bath, $LiAlH_4$ (0.569 g, 15.0 mmol) was added portion-wise over a period of 10 min. The reaction mixture was allowed to warm to rt and stirred for a further 4 hrs under a N_2 (g). The mixture was again cooled to 0 °C in an ice bath and cold H_2O was added drop-wise until effervescence stopped. 32% (v/v) aqueous HCl (10 mL) was then added and the resultant mixture was filtered through a thick Celite® bed and the THF was removed *in vacuo*. The aqueous medium was extracted into EtOAc (3 × 100 mL) and the combined organic layers were dried over anhydrous $MgSO_4$, filtered through a Celite® bed and concentrated under reduced pressure. The thick brown residue was carried on without further purification apart from noting the difference in R_f value compared to the starting material. The presumed alcohol intermediate **154** was dissolved in CH_2Cl_2 (200 mL) and silica (2.00 g) was added followed by PCC (4.31 g, 20.0 mmol) in two portions. The reaction mixture was stirred under N_2 (g) for 4 hrs as monitored by TLC. After the starting material was completely consumed, the reaction mixture was filtered through a bed of Celite® in a fume hood and the filtrate was concentrated *in vacuo*. The resultant viscous brown oil (which was presumed to be aldehyde **200**) was taken to the next step without further purification. The crude intermediate **200** was dissolved in 2-methyl-2-butene (113 mL) to which H_2O (150 mL), *t*-BuOH (150 mL), $NaClO_2$ (5.43 g, 60.0 mmol) and NaH_2PO_4 (7.20 g, 60.0 mmol) were added. The biphasic mixture was stirred rapidly for 6 hrs after which the layers were separated and the aqueous layer was further extracted into CH_2Cl_2 (3 × 100 mL). The combined organic layers were dried over anhydrous $MgSO_4$, filtered through a Celite® bed and concentrated *in vacuo*. The residue was purified by column chromatography (25% EtOAc/hexane) on silica gel. The isolated product was re-crystallized from a hot solution (20% EtOAc/hexane) to afford allyl-1,4,6,8-tetramethoxynaphthalene-2-carboxylic acid **167**

as colourless crystals (2.34 g, 60%). $\mathbf{R_f}$ = 0.26 (40% EtOAc/hexane); **Mp** 138-140 ^{o}C; **IR** $\boldsymbol{\nu_{max}}$ **(cm^{-1})** 3680 (O-H), 1681 (C=O), 1545 (C=C);

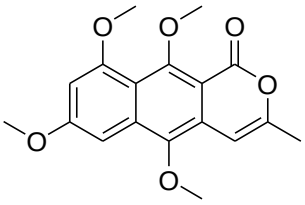


167

^{1}H NMR (300 MHz, $CDCl_3$, Me_4Si) δ_H 10.82 (1H, s, $ArCO_2H$), 7.00 (1H, d, *J* = 2.3 Hz, H-5), 6.55 (1H, d, *J* = 2.3 Hz, H-7), 6.01 (1H, ddt, *J* = 16.3, 10.1, 6.2 Hz, $ArCH_2CH=CH_2$), 5.12 (2H, dd, *J* = 2.8, 1.7 Hz, $ArCH_2CH=CH_2$), 3.97 (3H, s, $ArOCH_3$), 3.94 (3H, s, $ArOCH_3$), 3.91 (3H, s, $ArOCH_3$), 3.87 (3H, s, $ArOCH_3$), 3.69 (2H, d, *J* = 6.2 Hz, $ArCH_2CH=CH_2$); **^{13}C NMR (75 MHz, $CDCl_3$, Me_4Si)** δ_C 172.3 ($ArCO_2H$), 159.7 (C-6), 158.0 (C-8), 150.9 (C-4), 149.5 (C-1), 136.3 ($ArCH_2CH=CH_2$), 133.1 (C-2), 126.9 (C-4a), 123.5 (C-3), 116.1 ($ArCH_2CH=CH_2$), 115.2 (C-8a), 99.5 (C-7), 93.4 (C-5), 64.1 ($ArOCH_3$), 61.6 ($ArOCH_3$), 56.1 ($ArOCH_3$), 55.4 ($ArOCH_3$), 31.6 ($ArCH_2CH=CH_2$). **HRMS** (*m*/*z*), calculated for $C_{18}H_{21}O_6$: 333.1333, found $(M + H)^+$ 333.1332.

7.7.15 Synthesis of 5,7,9,10-tetramethoxy-3-methyl-1*H*-benzo[*g*]isochromen-1-one 103

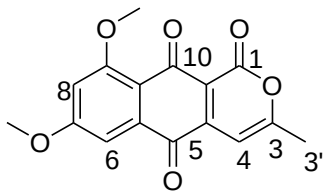
In a 2-neck round bottom flask equipped with a magnetic stirring bar and charged with 3-allyl-1,4,6,8-tetramethoxynaphthalene-2-carboxylic acid **167** (2.00 g, 6.02 mmol) and $CuCl_2.2H_2O$ (1.53 g, 9.00 mmol) in DMF/H_2O mixture (100 mL, v/v, 2:1), was added $PdCl_2$ (0.107 g, 0.602 mmol) under a blanket of O_2 (g) and the mixture was stirred vigorously for 24 hrs at rt. The reaction mixture was then filtered through a thick Celite® pad and the pad was washed with CH_2Cl_2 (3 × 100 mL). The combined organic layers were washed with brine (3 × 100 mL), dried over anhydrous $MgSO_4$, filtered and the solvent was removed *in vacuo*. The residue was adsorbed onto normal silica and purification using flash silica gel column chromatography (EtOAc/hexane/CH_2Cl_2 2:1:7) afforded 5,7,9,10-tetramethoxy-3-methyl-1*H*-benzo[*g*]isochromen-1-one **103** as a cream crystalline solid (1.39 g, 70%). $\mathbf{R_f}$ = 0.54 **(**EtOAc/CH_2Cl_2/hexane 3:2:5). The ^{1}H NMR spectrum was similar to the one discussed in **Section 7.7.7**.



103

7.7.16 Synthesis of 7,9-dimethoxy-3-methyl-1*H*-benzo[*g*]isochromene-1,5,10-trione 159

5,7,9,10-Tetramethoxy-3-methyl-1*H*-benzo[*g*]isochromen-1-one **103** (0.450 g, 1.36 mmol) was dissolved in 1,4-dioxane (40 mL) in a 100 mL round bottom flask in an open vessel at rt. Solid AgO (0.674 g, 5.44 mmol) was then added to the stirred solution and after 10 min of stirring, 25% (v/v) aqueous HNO_3 was added drop-wise until all AgO dissolved. The resultant solution was stirred for a further 5 min after which CH_2Cl_2/H_2O (200 mL, v/v, 1:1) were added and the lower organic layer was extracted. The aqueous residue was further extracted into CH_2Cl_2 (2 × 100 mL) and the combined organic layers were dried over anhydrous $MgSO_4$, filtered through a Celite® bed and concentrated under reduced pressure. The crude product was dissolved in HPLC grade CH_3CN (15 mL) and 250 µL of this solution was injected onto the C-18 reverse-phase column for separation. The quinone was purified using gradient elution (5:5-8:2 CH_3CN/H_2O) and different fractions were collected separately. 5,7,10-Trimethoxy-3-methyl-1*H*-benzo[*g*]isochromene-6,9-dione **159** was obtained as a dark orange amorphous solid (0.229 g, 56%). $\mathbf{R_f}$ = 0.41 (EtOAc/hexane/CH_2Cl_2 2:3:5); **Mp** 176 - 179 °C; **IR ν_{max} (cm^{-1})** 1782 (C=O), 1762 (C=O), 1705 (C=O), 1612 (C=C);



159

^{1}H NMR (500 MHz, $CDCl_3$) δ_H 7.23 (1H, d, *J* = 2.1 Hz, H-6), 6.80 (1H, d, *J* = 2.1 Hz, H-8), 6.69 (1H, s, H-4), 3.96 (3H, s, ArOC*H*$_3$), 3.95 (3H, s, ArOC*H*$_3$), 2.39 (3H, s, H-3'); **^{13}C NMR (126 MHz, $CDCl_3$, Me_4Si)** δ_C 183.1 (C-5 or C-10), 178.1 (C-5 or C-10), 168.9 (C-1), 164.4 (C-7), 162.1 (C-9), 157.3 (C-3), 145.4 (C-4a), 134.9 (C-10a), 116.6 (C-5a), 115.9 (C-9a), 106.1 (C-8), 102.9 (C-6), 98.5 (C-4), 56.6 (ArO*C*H$_3$), 56.0 (ArO*C*H$_3$), 21.1 (C-3'). **HRMS** (*m*/*z*), calculated for $C_{16}H_{13}O_6$: 301.0707, found $(M + H)^+$ 301.0704.

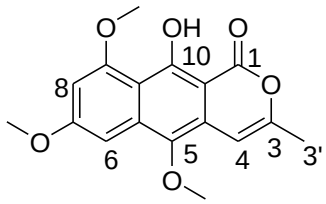
7.7.17 Attempted synthesis of paepalantine 102

7.7.17.0 Method one: Synthesis of 10-hydroxy-5,7,9-trimethoxy-3-methyl-1*H*-benzo[*g*]isochromen-1-one (9-*O*-methylpaepalantine) 208

5,7,9,10-Tetramethoxy-3-methyl-1*H*-benzo[*g*]isochromen-1-one **103** (0.400 g, 1.21 mmol) was dissolved in freshly distilled CH_2Cl_2 (100 mL) in a 2-neck round bottom flask fitted with a rubber septum and cooled to -78 °C under a blanket of N_2 (g). BCl_3 (2.40 mL, 2.40 mmol)

was slowly added to the solution *via* a syringe and the reaction mixture was stirred for a further 40 min at -78 °C. The mixture was then allowed to warm to rt and stirred at this temperature for 2 hrs. After the 2 hrs had elapsed, the mixture was again cooled to -78 °C and BCl_3 (2.40 mL, 2.40 mmol) was slowly added to the solution for the second time using a syringe. The reaction mixture was stirred for a further 40 min at -78 °C. Thereafter, it was allowed to warm to rt and stirred at this temperature for 2 hrs. The reaction was then carefully quenched with ice cold H_2O (50 mL) and extracted into CH_2Cl_2 (3 × 100 mL). The combined organic layers were dried over anhydrous $MgSO_4$, filtered through a Celite® bed and concentrated under reduced pressure. Purification of the residue by column chromatography on silica gel (20% EtOAc/hexane) afforded 9-*O*-methylpaepalantine **208** as a yellow amorphous solid (0.249 g, 65%). $\mathbf{R_f}$ = 0.43 (3:2:5 EtOAc/hexane/CH_2Cl_2); **Mp** 197-199 ^oC; **IR ν_{max} (cm^{-1})** 3580 (O-H), 1701 (C=O), 1620 (C=C);

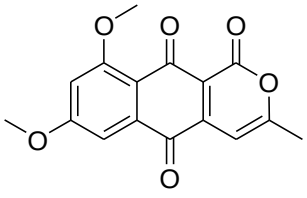
^{1}H NMR (300 MHz, $CDCl_3$, Me_4Si) δ_H 12.79 (1H, s, H-10), 6.86 (1H, d, *J* = 2.0 Hz, H-6), 6.44 (1H, s, H-4), 6.40 (1H, d, *J* = 2.0 Hz, H-8), 3.96 (3H, s, ArOC*H*$_3$), 3.92 (3H, s, ArOC*H*$_3$), 3.81 (3H, s, ArOC*H*$_3$), 2.24 (3H, s, H-3'); **^{13}C NMR (75 MHz, $CDCl_3$, Me_4Si)** δ_C 161.4 (C-7), 160.0 (C-1), 159.4 (C-9), 159.3 (C-10), 153.4 (C-3), 143.7 (C-5), 135.5 (C-5a), 126.6 (C-4a), 116.4 (C-9a), 108.6 (C-10a), 99.4 (C-8), 97.3 (C-6), 92.2 (C-4), 62.9 (ArO*C*H$_3$), 61.6 (ArO*C*H$_3$), 56.4 (ArO*C*H$_3$), 19.8 (C-3'). **HRMS** (*m*/*z*), calculated for $C_{17}H_{17}O_6$: 317.1020 found (M + H)$^+$ 317.1021.



208

7.7.17.1 Method two: Synthesis of 7,9-dimethoxy-3-methyl-1*H*-benzo[*g*]isochromene-1,5,10-trione 159

In a 2-neck round bottom flask fitted with a rubber septum, 5,7,9,10-tetramethoxy-3-methyl-1*H*-benzo[*g*]isochromen-1-one **103** (0.350 g, 1.06 mmol) was dissolved in freshly distilled CH_2Cl_2 (50 mL) and cooled to -78 °C under a blanket of N_2 (g). BBr_3 (2.12 mL, 2.12 mmol) was slowly added to the solution using a syringe and the reaction mixture was stirred for 1 hr at -78 °C. The reaction mixture was then allowed to

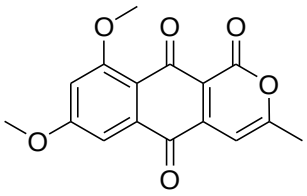


159

warm to 0 ^{o}C and stirred at this temperature for 2 hrs. After this time had elapsed, the reaction mixture was again cooled to -78 °C and BBr_3 (2.12 mL, 2.12 mmol) was slowly added to the solution *via* a syringe for a second time. The reaction mixture was stirred for a further 1 hr at -78 °C. It was then allowed to warm to 0 ^{o}C and stirred for 2 hrs. The reaction was carefully quenched with ice cold H_2O (50 mL) and extracted into CH_2Cl_2 (3 × 40 mL). The combined organic layers were dried over anhydrous $MgSO_4$, filtered through a Celite® bed and concentrated under reduced pressure. The residue was purified by semi-preparative C-18 reverse phase HPLC (H_2O/MeCN) affording 5,7,10-trimethoxy-3-methyl-1*H*-benzo[*g*]isochromene-6,9-dione **159** as a dark-orange amorphous solid (80 mg, 25%). $\mathbf{R_f}$ = 0.43 **(**EtOAc/CH_2Cl_2/hexane 3:2:5). The ^{1}H NMR spectrum was similar to the one discussed in **Section 7.7.16**.

7.7.18 Synthesis of 7,9-dimethoxy-3-methyl-1*H*-benzo[*g*]isochromene-1,5,10-trione 159

To a stirred suspension of 10-hydroxy-5,7,9-trimethoxy-3-methyl-1*H*-benzo[*g*]isochromen-1-one **208** (0.340 g, 1.07 mmol) in CH_3CN/H_2O (20.00 mL, v/v, 2:1) containing a small amount of CH_3OH (2 drops), was added solid PIFA (0.968 g, 2.25 mmol) at room temperature and the mixture was stirred for 35 min. The reaction was quenched with saturated aqueous $NaHCO_3$ (25 mL) and extracted into CH_2Cl_2 (2 × 30 mL). The combined organic layers were dried over anhydrous $MgSO_4$, filtered through a number one sintered glass funnel and the solvent was removed *in vacuo*. The residue was purified by semi-preparative C-18 reverse phase HPLC (as discussed in **Section 7.7.16**) yielding 7,9-dimethoxy-3-methyl-1*H*-benzo[*g*]isochromene-1,5,10-trione (0.260 g, 81%) as a dark orange amorphous solid. $\mathbf{R_f}$ = 0.43 **(**EtOAc/CH_2Cl_2/hexane 3:2:5). The ^{1}H NMR spectrum was similar to the one analysed in **Section 7.7.16**.

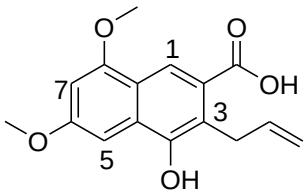


159

7.8 Concise synthesis of 7,9-dimethoxy-3-methyl-1*H*-benzo[*g*]isochromene-1,5,10-trione 159

7.8.0 Synthesis of 3-allyl-4-hydroxy-6,8-dimethoxynaphthalene-2-carboxylic acid 224[124]

To a solution of ethyl 3-allyl-4-hydroxy-6,8-dimethoxynaphthalene-2-carboxylate **197** (5.50 g, 17.4 mmol) in MeOH (100 mL) was added aqueous NaOH solution (2.78 g, 69.6 mmol) in H_2O (75 mL). The dark orange reaction mixture was stirred for 5 hrs at room temperature and then heated to reflux for 12 hrs. The reaction mixture was cooled to rt and the MeOH was removed *in vacuo* leaving an aqueous medium. The aqueous residue was then carefully acidified to pH 4.0 with 32% (v/v) aqueous HCl and extracted into EtOAc (3 × 150 mL). The combined organic layers were dried over anhydrous MgSO4, filtered through a Celite® bed and concentrated *in vacuo*. The crude residue was then purified by silica gel column chromatography (30% EtOAc/hexane) and the product was recrystallized from hot solution (25% EtOAc/hexane) affording 3-allyl-4-hydroxy-6,8-dimethoxynaphthalene-2-carboxylic acid **224** as colourless crystals (4.16 g, 83%). $\mathbf{R_f}$ = 0.21 (40% EtOAc/hexane);



224

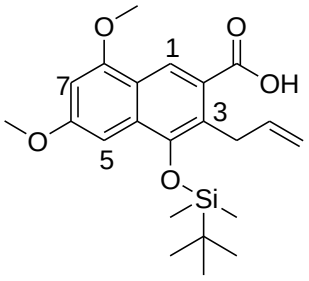
^{1}H NMR (500 MHz, $CDCl_3$, Me_4Si) δ_H 8.61 (1H, s, H-1), 7.05 (1H, s, H-5), 6.51 (1H, s, H-7), 6.22-6.07 (1H, m, $ArCH_2C\mathit{H}{=}CH_2$), 5.22 (2H, d, *J* = 13.2 Hz, $ArCH_2CH{=}C\mathit{H}_2$), 4.01 (2H, d, *J* = 5.3 Hz, $ArC\mathit{H}_2CH{=}CH_2$), 3.98 (3H, s, $ArOC\mathit{H}_3$), 3.95 (3H, s, $ArOC\mathit{H}_3$); **^{13}C NMR (126 MHz, $CDCl_3$, Me_4Si)** δ_C 173.0 ($ArC\mathit{O}_2H$), 160.6 (C-6), 157.5 (C-8), 149.9 (C-4), 136.4 ($ArCH_2\mathit{C}H{=}CH_2$), 129.1 (C-4a), 123.4 (C-2), 120.6 (C-1), 120.3 (C-8a), 119.2 ($ArCH_2CH{=}\mathit{C}H_2$), 116.2 (C-3), 98.4 (C-7), 92.1 (C-5), 55.7 ($ArO\mathit{C}H_3$), 55.5 ($ArO\mathit{C}H_3$), 31.8 ($Ar\mathit{C}H_2CH{=}CH_2$).

7.8.1 Synthesis of 3-allyl-4-(*tert*-butyldimethylsilyloxy)-6,8-dimethoxynaphthalene-2-carboxylic acid 227

3-Allyl-4-hydroxy-6,8-dimethoxynaphthalene-2-carboxylic acid **224** (4.27 g, 14.8 mmol), *tert*-butyldimethylsilyl chloride (3.24 g, 21.5 mmol), imidazole (1.46 g, 21.5 mmol) and DMAP (0.263 g, 2.15 mmol) were dissolved in CH_2Cl_2 (150 mL) in a 250 mL round bottom flask equipped with a magnetic stirring bar and stirred at rt for 24 hrs under a N_2 (g). The mixture was then washed with H_2O (3 × 100 mL), dried over anhydrous $MgSO_4$, filtered

through a Celite® pad and concentrated *in vacuo*. The residue was purified by silica gel column chromatography (20% EtOAc/hexane) yielding 3-allyl-4-(*tert*-butyldimethyl-silyloxy)-6,8-dimethoxynaphthalene-2-carboxylic acid **227** (5.54 g, 93%) as a colourlessr oil. $\mathbf{R_f}$ = 0.32 (20% EtOAc/hexane); **Mp** 129-130 ^{o}C; **IR ν_{max} (cm^{-1})** 3620 (O-H), 1692 (C=O), 1585 (C=C);

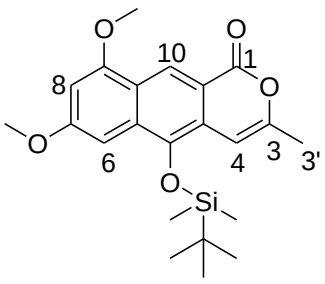
^{1}H NMR (500 MHz, $CDCl_3$, Me_4Si) δ_H 8.67 (1H, s, H-1), 7.00 (1H, s, H-5), 6.51 (1H, s, H-7), 5.99 (1H, ddt, *J* = 10.7, 5.9, 0.9 Hz, $ArCH_2CH{=}CH_2$), 5.05-4.91 (2H, m, $ArCH_2CH{=}CH_2$), 4.03 (2H, d, *J* = 5.2 Hz, $ArCH_2CH{=}CH_2$), 4.00 (3H, s, $ArOCH_3$), 3.96 (3H, s, $ArOCH_3$), 1.16 (9H, s, $ArOSi(CH_3)_2C(CH_3)_3$, 0.26 (6H, s, $ArOSi(CH_3)_2C(CH_3)_3$); **^{13}C NMR (125 MHz, $CDCl_3$, Me_4Si)** δ_C 173.8 ($ArCO_2H$), 160.0 (C-6), 157.5 (C-8), 148.3 (C-4), 137.5 ($ArCH_2CH{=}CH_2$), 132.2 (C-4a), 126.7 (C-2), 124.6 (C-8a), 121.50 (C-1), 120.3 (C-3), 114.9 ($ArCH_2CH{=}CH_2$), 97.8 (C-7), 94.2 (C-5), 55.7 ($ArOCH_3$), 55.5 ($ArOCH_3$), 31.1 ($ArCH_2CH{=}CH_2$), 26.1 ($ArOSi(CH_3)_2C(CH_3)_3$), 18.9 ($ArOSi(CH_3)_2C(CH_3)_3$), -2.9 ($ArOSi(CH_3)_2C(CH_3)_3$). **HRMS** (*m*/*z*), calculated for $C_{22}H_{31}O_5Si$: 403.1935, found $(M + H)^+$ 403.1932.



227

7.8.2 Synthesis of 5-[(*tert*-butyldimethylsilyl)oxy]-7,9-dimethoxy-3-methyl-1*H*-benzo[*g*]isochromen-1-one 228

To a vigorously stirred solution of 3-allyl-4-(*tert*-butyldimethylsilyloxy)-6,8-dimethoxy-naphthalene-2-carboxylic acid **227** (4.25 g, 10.6 mmol) and $CuCl_2.2H_2O$ (2.71 g, 15.9 mmol) in DMF/H_2O (100 mL, 5:2) was added $PdCl_2$ (0.188 g, 1.06 mmol). The stirring was continued for 24 hrs at rt under O_2 (g). The reaction mixture was then filtered through a thick bed of Celite® and the filtrate was extracted into CH_2Cl_2 (3 × 30 mL). The combined organic layers were washed with brine (2 × 60 mL), dried over anhydrous $MgSO_4$, filtered through a Celite® pad and concentrated under reduced pressure. Purification of the residue by column chromatography (15% EtOAc/hexane) on flash silica gel furnished



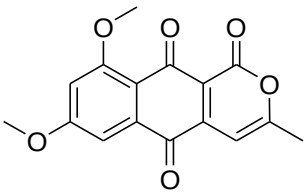
228

5-(*tert*-butyldimethylsilyloxy)-7,9-dimethoxy-3-methyl-1*H*-benzo[*g*]isochromen-1-one **228** as pale yellow crystals (3.10 g, 73%). $\mathbf{R_f}$ = 0.40 **(**EtOAc/CH_2Cl_2/hexane 3:1:6); **Mp** 155-156 ^oC; **IR ν_{max} (cm^{-1})** 1739 (C=O), 1550 (C=C);

^{1}H NMR (300 MHz, $CDCl_3$, Me_4Si) δ_H 8.68 (1H, s, H-10), 6.71 (1H, d, *J* = 1.8 Hz, H-6), 6.29 (1H, s, H-4), 6.25 (1H, d, *J* = 2.1 Hz, H-8), 3.79 (3H, s, $ArOCH_3$), 3.75 (3H, s, $ArOCH_3$), 2.11 (3H, s, H-3'), 0.98 (9H, s, $ArOSi(CH_3)_2C(CH_3)_3$), 0.00 (6H, s, $ArOSi(CH_3)_2C(CH_3)_3$); **^{13}C NMR (75 MHz, $CDCl_3$, Me_4Si)** δ_C 163.4 (C-1), 160.5 (C-7), 157.9 (C-9), 151.4 (C-3), 143.4 (C-5), 132.4 (C-5a), 123.3 (C-9a), 121.9 (C-4a), 119.8 (C-10a), 115.8 (C-2), 99.1 (C-4), 97.9 (C-8), 93.2 (C-6), 55.7 ($ArOCH_3$), 55.4 ($ArOCH_3$), 26.0 ($ArOSi(CH_3)_2C(CH_3)_3$), 19.9 (C-3'), 18.7 ($ArOSi(CH_3)_2C(CH_3)_3$), -3.2 ($ArOSi(CH_3)_2C(CH_3)_3$). **HRMS** (*m*/*z*), calculated for $C_{22}H_{29}O_5Si$: 401.1779, found $(M + H)^+$ 401.1789.

7.8.3 Synthesis of 7,9-dimethoxy-3-methyl-1*H*-benzo[*g*]isochromene-1,5,10-trione 159

To a solution of 5-(*tert*-butyldimethylsilyloxy)-7,9-dimethoxy-3-methyl-1*H*-benzo[*g*]isochromen-1-one **228** (3.00 g, 7.46 mmol) in dry THF (50 mL) was added TBAF (9.00 mL, 9.00 mmol) using a syringe at 0 ^oC and the reaction mixture was allowed to warm to rt and stirred for a further 24 hrs under a N_2 (g). H_2O (100 mL) was added to the mixture and THF was evaporated leaving an aqueous medium which was extracted into CH_2Cl_2 (3 × 100 mL). The combined organic layers were dried over anhydrous $MgSO_4$, filtered through a bed of Celite® and concentrated *in vacuo*. The crude product was dissolved in MeCN (50 mL) and aqueous CAN (8.22 g, 15.0 mmol) in H_2O (50 mL) was added portion-wise. The mixture was then stirred for 30 min after which saturated aqueous $NaHCO_3$ (60 mL) was added and the organic layer was extracted into CH_2Cl_2 (3 × 100 mL). The combined organic layers were dried over anhydrous $MgSO_4$, filtered through a bed of Celite® and the solvent was removed *in vacuo*. The crude product was purified by the semi-preparative C-18 reverse phase HPLC yielding 7,9-dimethoxy-3-methyl-1*H*-benzo[*g*]isochromene-1,5,10-trione **159** as an orange amorphous solid (0.224 g,



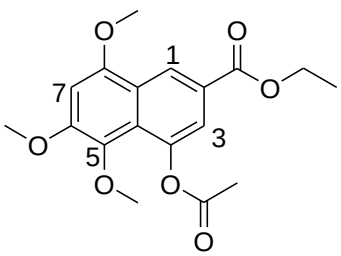
159

10%). $\mathbf{R_f}$ = 0.43 **(**EtOAc/CH_2Cl_2/hexane 3:2:5). The ^{1}H NMR spectrum was similar to the one discussed in **Section 7.7.16**.

7.9 Experimental work pertaining to the synthesis of 5-methoxy-3,4-dehydroxanthomegnin 34

7.9.0 Synthesis of ethyl 4-acetoxy-5,6,8-trimethoxynaphthalene-2-carboxylate 233[124]

To a solution of 2,4,5-trimethoxybenzaldehyde **232** (5.50 g, 28.0 mmol) and diethyl succinate (7.66 g, 44.0 mmol) in *t*-BuOH (80 mL) stirred under N_2 (g) was added *t*-BuOK (4.93 g, 44.0 mmol). The reaction mixture was heated to reflux for 4 hrs after which it was cooled to rt, poured into ice cold H_2O and made acidic to pH 4.0 with 32% aqueous HCl. The intermediate was extracted into EtOAc (3 × 100 mL) and the combined organic layers were dried over anhydrous $MgSO_4$, filtered through a Celite® pad and the filtrate was concentrated *in vacuo*. The resultant oily residue was dissolved in Ac_2O (100 mL) in a clean round bottom flask to which anhydrous NaOAc (5.82 g, 71.0 mmol) was added and the mixture was heated to reflux for overnight. The solvent was removed *in vacuo* to dryness and MeOH was added slowly and portion-wise until no effervescence was observed. Methanol was evaporated *in vacuo* and the solid product was purified using a short silica gel column. A saturated aqueous solution of $NaHCO_3$ (200 mL) was added to the product and the mixture extracted into EtOAc (3 × 100 mL). The combined organic layers were dried over anhydrous $MgSO_4$, filtered through a Celite® bed and the solvent was removed *in vacuo*. The semi-solid residue was purified for the second time by silica gel column chromatography (10% EtOAc/hexane) yielding ethyl 4-acetoxy-5,6,8-trimethoxynaphthalene-2-carboxylate **233** (6.63 g, 68%) as a yellow solid. $\mathbf{R_f}$ = 0.61 (20% EtOAc/hexane).



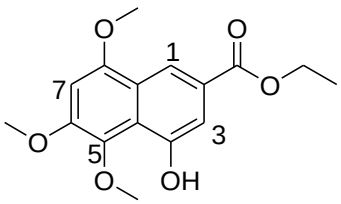
233

^{1}H NMR (300 MHz, $CDCl_3$, Me_4Si) δ_H 8.84 (1H, d, *J* = 1.7 Hz, H-1), 7.68 (1H, d, *J* = 1.7 Hz, H-3), 6.69 (1H, s, H-7), 4.41 (2H, q, *J* = 7.1 Hz, $ArCO_2C\mathit{H}_2CH_3$), 4.01 (3H, s, $ArOC\mathit{H}_3$), 4.00 (3H, s, $ArOC\mathit{H}_3$), 3.82 (3H, s, $ArOC\mathit{H}_3$), 2.38 (3H, s, $ArOC(O)C\mathit{H}_3$), 1.42 (3H, t, *J* = 7.1 Hz, $ArCO_2CH_2C\mathit{H}_3$); **^{13}C NMR (75 MHz, $CDCl_3$, Me_4Si)** δ_C 169.8 ($ArOC(O)CH_3$), 166.1 ($ArCO_2CH_2CH_3$), 154.2 (C-8), 152.4 (C-4), 145.1 (C-6), 135.6 (C-5), 124.8 (C-2 or C-8a),

124.8 (C-2 or C-8a), 124.0 (C-1), 122.1 (C-4a), 120.4 (C-3), 95.6 (C-7), 61.8 ($ArCO_2\mathit{C}H_2CH_3$), 61.1 ($ArO\mathit{C}H_3$), 56.8 ($ArO\mathit{C}H_3$), 56.0 ($ArO\mathit{C}H_3$), 20.7 ($ArOC(O)\mathit{C}H_3$), 14.4 ($ArCO_2CH_2\mathit{C}H_3$).

7.9.1 Synthesis of ethyl 4-hydroxy-5,6,8-trimethoxynaphthalene-2-carboxylate 234[127]

Ethyl 4-acetoxy-5,6,8-trimethoxynaphthalene-2-carboxylate **233** (5.60 g, 16.1 mmol) was dissolved in EtOH (50 mL) followed by the portion-wise addition of 1% (w/v) ethanolic solution of NaOH (0.700 g, 17.5 mmol) in EtOH (70 mL). The orange reaction was stirred for 3 hrs at rt and EtOH was removed *in vacuo*. The aqueous solution was then carefully acidified to pH 4.0 with 32% (v/v) aqueous HCl and extracted into EtOAc (3 × 150 mL). The combined organic layers were dried over anhydrous $MgSO_4$, filtered through a Celite® pad and concentrated *in vacuo*. The crude product was purified by silica gel column chromatography (20% EtOAc/hexane) affording ethyl 4-hydroxy-5,6,8-trimethoxynaphthalene-2-carboxylate **234** as a cream amorphous solid (3.90 g, 79%). $\mathbf{R_f}$ = 0.46 (20% EtOAc/hexane);



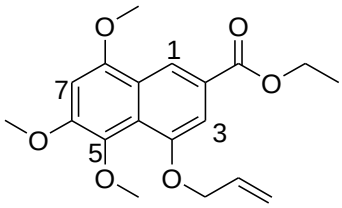
234

^{1}H NMR (300 MHz, $CDCl_3$, Me_4Si) δ_H 9.69 (1H, s, ArO*H*), 8.42 (1H, d, *J* = 1.6 Hz, H-1), 7.44 (1H, d, *J* = 1.6 Hz, H-3), 6.63 (1H, s, H-7), 4.40 (2H, q, *J* = 7.1 Hz, $ArCO_2C\mathit{H}_2CH_3$), 4.01 (6H, br s, superimposed $ArOC\mathit{H}_3$), 4.00 (3H, s, $ArOC\mathit{H}_3$), 1.42 (3H, t, *J* = 7.1 Hz, $ArCO_2CH_2C\mathit{H}_3$); **^{13}C NMR (75 MHz, $CDCl_3$, Me_4Si)** δ_C 166.8 ($Ar\mathit{C}O_2CH_2CH_3$), 154.3 (C-8), 153.2 (C-4), 149.3 (C-6), 136.4 (C-5), 126.6 (C-2), 121.9 (C-8a), 120.5 (C-4a), 116.5 (C-1), 110.4 (C-3), 95.4 (C-7), 62.2 ($ArCO_2\mathit{C}H_2CH_3$), 60.9 ($ArO\mathit{C}H_3$), 57.0 ($ArO\mathit{C}H_3$), 55.9 ($ArO\mathit{C}H_3$), 14.4 ($ArCO_2CH_2\mathit{C}H_3$).

7.9.2 Synthesis of ethyl 4-(allyloxy)-5,6,8-trimethoxynaphthalene-2-carboxylate 235[127]

To a solution of ethyl 4-acetoxy-5,6,8-trimethoxynaphthalene-2-carboxylate **234** (3.80 g, 12.4 mmol) in acetone (100 mL) was added anhydrous K_2CO_3 (2.07 g, 15.0 mmol) followed by allyl bromide (1.81 g, 15.0 mmol). The reaction mixture was heated to reflux for 24 hrs under a N_2 (g). After this time had elapsed, the reaction mixture was allowed to cool to rt, filtered

through a Celite® pad and the solvent evaporated *in vacuo*. The residue was purified by column chromatography (10% EtOAc/hexane) on silica gel yielding ethyl 4-(allyloxy)-5,6,8-trimethoxynaphthalene-2-carboxylate **235** as a yellow amorphous solid (3.82 g, 89%). $\mathbf{R_f}$ = 0.56 (20% EtOAc/hexane);

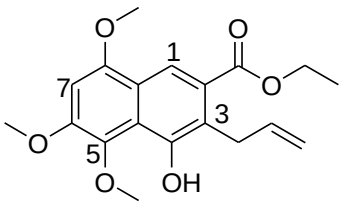


235

^{1}H NMR (300 MHz, $CDCl_3$, Me_4Si) δ_H 8.56 (1H, d, *J* = 1.5 Hz, H-1), 7.43 (1H, d, *J* = 1.4 Hz, H-3), 6.67 (1H, s, H-7), 6.20 (1H, ddt, *J* = 17.1, 10.4, 5.1 Hz, $ArOCH_2CH$=CH_2), 5.60 (1H, dd, *J* = 17.2, 1.6 Hz, one of $ArOCH_2CH$=CH_2), 5.33 (1H, dd, *J* = 10.5, 1.4 Hz, one of $ArOCH_2CH$=CH_2), 4.71 (2H, d, *J* = 5.1 Hz, $ArOCH_2CH$=CH_2), 4.41 (2H, q, *J* = 7.1 Hz, $ArCO_2CH_2CH_3$), 3.98 (3H, s, $ArOCH_3$), 3.96 (3H, s, $ArOCH_3$), 3.82 (3H, s, $ArOCH_3$), 1.43 (3H, t, *J* = 7.1 Hz, $ArCO_2CH_2CH_3$); **^{13}C NMR (75 MHz, $CDCl_3$, Me_4Si)** δ_C 167.1 ($ArCO_2CH_2CH_3$), 153.4 (C-8), 149.3 (C-4), 136.4 (C-6), 126.6 ($ArOCH_2CH$=CH_2), 124.4 (C-5), 121.9 (C-2), 120.5 (C-8a), 116.5 (C-4a), 110.4 (C-1), 107.3 ($ArOCH_2CH$=CH_2), 105.0 (C-3), 99.6 (C-7), 63.9 ($ArOCH_2CH$=CH_2), 61.4 ($ArCO_2CH_2CH_3$), 56.1 ($ArOCH_3$), 55.3 ($ArOCH_3$), 52.1 ($ArOCH_3$), 14.3 ($ArCO_2CH_2CH_3$).

7.9.3 Synthesis of ethyl 3-allyl-4-hydroxy-5,6,8-trimethoxynaphthalene-2-carboxylate 236[127]

Ethyl 4-(allyloxy)-5,6,8-trimethoxynaphthalene-2-carboxylate **235** (4.00 g, 11.5 mmol) was loaded neat into a 100 mL round bottom flask equipped with a reflux condenser and a magnetic stirring bar. The flask was heated to 180 ^oC in silicon oil bath for 24 hrs under a N_2 (g). The dark viscous residue was allowed to cool to 35 ^oC, dissolved in acetone (20 mL) and adsorbed onto silica gel. Purification on normal silica gel column chromatography (10% EtOAc/hexane) yielded ethyl 3-allyl-4-hydroxy-5,6,8-trimethoxynaphthalene-2-carboxylate **236** as a yellow amorphous solid (2.83 g, 71%). $\mathbf{R_f}$ = 0.42 (20% EtOAc/hexane);



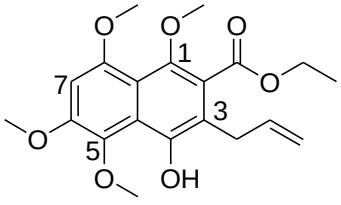
235

^{1}H NMR (300 MHz, $CDCl_3$, Me_4Si) δ_H 10.09 (1H, s, ArO*H*), 8.19 (1H, s, H-1), 6.48 (1H, s, H-7), 6.10 (1H, ddt, *J* = 16.1, 10.1, 6.0 Hz, $ArCH_2CH$=CH_2), 5.04 (2H, dt, *J* = 15.9, 1.9 Hz, $ArCH_2CH$=CH_2), 4.37 (2H, q, *J* = 7.1 Hz, $ArCO_2CH_2CH_3$), 3.98 (3H, s, $ArOCH_3$), 3.92 (3H, s, $ArOCH_3$), 3.91-3.84 (5H, m, One

of the ArOCH_3 superimposed by ArCH_2CH=CH_2), 1.41 (3H, t, *J* = 7.1 Hz, ArCO_2CH_2CH_3); **^{13}C NMR (75 MHz, CDCl$_3$, Me$_4$Si)** δ_C 168.1 (Ar*C*O_2CH_2CH_3), 153.7 (C-8), 151.0 (C-4), 149.1 (C-6), 137.4 (ArCH_2*C*H=CH_2), 135.7 (C-5), 127.7 (C-2), 120.9 (C-8a), 119.9 (C-4a), 119.4 (ArCH_2CH=*C*H_2), 116.4 (C-3), 114.4 (C-1), 94.7 (C-7), 62.1 (ArCO_2*C*H_2CH_3), 60.8 (ArO*C*H_3), 56.8 (ArO*C*H_3), 55.7 (ArO*C*H_3), 30.1 (Ar*C*H_2CH=CH_2), 14.4 (ArCO_2CH_2*C*H_3).

7.9.4 Synthesis of ethyl 3-allyl-4-hydroxy-1,5,6,8-tetramethoxynaphthalene-2-carboxylate 237

To a solution of ethyl 3-allyl-4-hydroxy-5,6,8-trimethoxynaphthalene-2-carboxylate **236** (3.00 g, 8.66 mmol) in absolute MeOH (80 mL) in a 250 mL round bottom flask, PIFA (3.96 g, 9.20 mmol) was added in one portion and the reaction mixture was stirred for 15 min at rt. Saturated aqueous $NaHCO_3$ (50 mL) was added portion-wise until effervescence stopped and the MeOH was removed *in vacuo* to leave an aqueous medium. The aqueous layer was extracted into EtOAc (3 × 100 mL) and the combined organic layers were dried over anhydrous $MgSO_4$, filtered through a Celite® pad and concentrated under reduced pressure. The residue was then treated with a 21% (w/v) ethanolic solution of NaOEt (11.0 mL, 34.0 mmol) with vigorous stirring for 20 min at rt. Saturated aqueous NH_4Cl (50 mL) was added to the reaction and the resultant mixture was evaporated at reduced pressure to leave the aqueous medium which was extracted into EtOAc (3 × 100 mL). The combined organic layers were dried over anhydrous $MgSO_4$, filtered through a Celite® pad and concentrated *in vacuo*. Purification of the residue by column chromatography (20% EtOAc/hexane) on silica gel afforded two compounds. The first compound was ethyl 3-allyl-4-hydroxy-1,5,6,8-tetramethoxynaphthalene-2-carboxylate **237** which was obtained as an orange amorphous solid (1.70 g, 52%). $\mathbf{R_f}$ = 0.54 (20 % EtOAc/hexane);



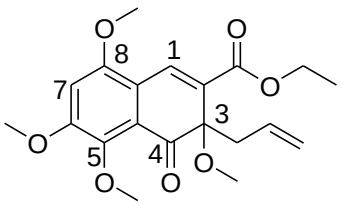
237

^{1}H NMR (300 MHz, CDCl$_3$, Me$_4$Si) δ_H 10.20 (1H, s, ArO*H*), 6.64 (1H, s, H-7), 6.01 (1H, ddt, *J* = 16.4, 10.0, 6.3 Hz, ArCH_2C*H*=CH_2), 5.16-4.96 (2H, m, ArCH_2CH=CH_2), 4.40 (2H, q, *J* = 7.1 Hz, ArCO_2CH_2CH_3), 3.98 (3H, s, ArOCH_3), 3.96 (3H, s, ArOCH_3), 3.96 (3H, s, ArOCH_3), 3.79 (3H, s, ArOCH_3), 3.46 (2H, dt, *J* = 6.3, 1.4 Hz, ArCH_2C*H*=CH_2), 1.39 (3H, t, *J* = 7.1 Hz, ArCO_2CH_2CH_3); **^{13}C**

NMR (75 MHz, $CDCl_3$, Me_4Si) δ_C 168.1 (Ar*C*$O_2CH_2CH_3$), 154.0 (C-8), 148.2 (C-1), 147.1 (C-6), 145.5 (C-4), 136.5 (Ar*C*$H_2CH{=}CH_2$), 135.9 (Ar-C), 126.7 (Ar-C), 120.1 (Ar-C), 118.0 (Ar-C), 115.2 (Ar-C), 115.2 (Ar-C), 96.8 (C-7), 63.8 ($ArCO_2CH_2CH_3$), 62.3 (ArO*C*H_3), 61.1 (ArO*C*H_3), 56.9 (ArO*C*H_3), 56.7 (ArO*C*H_3), 31.5 (Ar*C*$H_2CH{=}CH_2$), 14.3 ($ArCO_2CH_2CH_3$).

The second product was ethyl 3-allyl-3,4-dihydro-3,5,6,8-tetramethoxy-4-oxonaphthalene-2-carboxylate **241** which was obtained as yellow crystals (0.326 g, 10%). $\mathbf{R_f}$ = 0.40 (20 % EtOAc/hexane); **IR** $\boldsymbol{\nu_{max}}$**(cm^{-1})** 1708 (C=O), 1698 (C=C), 1625 (C=C); **Mp** 63-65 ^oC;

^{1}H NMR (300 MHz, $CDCl_3$, Me_4Si) δ_H 8.09 (1H, s, H-1), 6.70 (1H, s, H-7), 5.59 (1H, ddt, *J* = 17.4, 10.1, 7.4 Hz, $ArCH_2CH{=}CH_2$), 5.06-4.85 (2H, m, $ArCH_2CH{=}CH_2$), 4.46-4.24 (2H, m, $ArCO_2CH_2CH_3$), 3.94 (3H, s, ArOCH_3), 3.93 (3H, s, ArOCH_3), 3.84 (3H, s, ArOCH_3), 3.15 (3H, s, OCH_3 attached to *C*-3), 3.00-2.79 (2H, m, $ArCH_2CH{=}CH_2$), 1.37 (3H, t, *J* = 7.1 Hz, $ArCO_2CH_2CH_3$); **^{13}C NMR (75 MHz, $CDCl_3$, Me_4Si)** δ_C 198.3 (C4), 165.5 (Ar*C*$O_2CH_2CH_3$), 156.2 (C-6), 153.3 (C-8), 143.1 (C-5), 132.4 (C-1), 131.3 ($ArCH_2CH{=}CH_2$), 129.1 (C-2), 125.5 (C-4a), 118.9 ($ArCH_2CH{=}CH_2$), 116.0 (C-8a), 101.4 (C-7), 84.9 (C-3), 61.6 (ArO*C*H_3, attached to *C*-5), 60.8 ($ArCO_2CH_2CH_3$), 56.4 (ArO*C*H_3), 56.3 (ArO*C*H_3), 53.7 (O*C*H_3 attached to *C*-3), 43.3 (Ar*C*$H_2CH{=}CH_2$), 14.4 ($ArCO_2CH_2CH_3$). **HRMS** (*m*/*z*), calculated for $C_{20}H_{25}O_7$: 377.1595, found $(M + H)^+$ 377.1591.

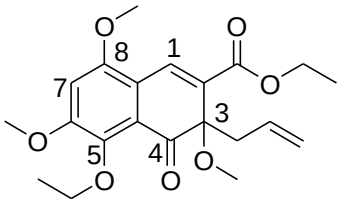


241

7.9.5 Synthesis of ethyl 3-allyl-3-ethoxy-3,4-dihydro-5,6,8-trimethoxy-4-oxonaphthalene-2-carboxylate 242

Ethyl 3-allyl-3,4-dihydro-3,5,6,8-tetramethoxy-4-oxonaphthalene-2-carboxylate **241** (0.500 g, 1.33 mmol) was treated with a 21% (w/v) ethanolic solution of NaOEt (1.72 mL, 5.32 mmol) with vigorous stirring for 30 min at rt. The reaction was washed with saturated aqueous NH_4Cl (50 mL) and the resultant mixture was evaporated at reduced pressure to leave the aqueous medium which was extracted into EtOAc (3 × 100 mL). The combined organic layers were dried over anhydrous $MgSO_4$, filtered through a Celite® pad and concentrated *in vacuo*. Column chromatography (15% EtOAc/hexane) of the residue afforded ethyl 3-allyl-4-hydroxy-1,5,6,8-tetramethoxynaphthalene-2-carboxylate **242** as a semi-solid

(0.332 g, 64%). R_f = 0.46 (20% EtOAc/hexane); **IR ν_{max} (cm^{-1})** 1710 (C=O), 1698 (C=C), 1624 (C=C);



242

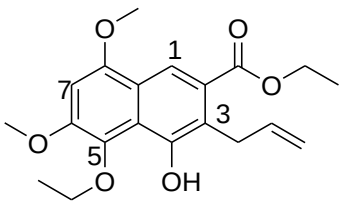
^{1}H NMR (300 MHz, $CDCl_3$, Me_4Si) δ_H 8.10 (1H, s, H-1), 6.70 (1H, s, H-7), 5.58 (1H, ddt, *J* = 17.4, 10.0, 7.4 Hz, $ArCH_2CH$=CH_2), 5.07-4.83 (2H, m, $ArCH_2CH$=CH_2), 4.48-4.23 (2H, m, $ArCO_2CH_2CH_3$), 4.09-3.85 (8H, m, 2 × $ArOCH_3$, $ArOCH_2CH_3$), 3.15 (3H, s, OCH_3 attached to *C*-3), 2.89 (2H, dt, *J* = 4.9, 1.2 Hz, $ArCH_2CH$=CH_2), 1.43 (3H, t, *J* = 7.0 Hz, $ArOCH_2CH_3$), 1.37 (3H, t, *J* = 7.1 Hz, $ArCO_2CH_2CH_3$); **^{13}C NMR (75 MHz, $CDCl_3$, Me_4Si)** δ_C 198.2 (C4), 165.4 ($ArCO_2CH_2CH_3$), 156.5 (C-6), 153.2 (C-8), 142.3 (C-5), 132.4 (C-1), 131.3 ($ArCH_2CH$=CH_2), 128.9 (C-2), 125.6 (C-4a), 118.9 ($ArCH_2CH$=CH_2), 116.0 (C-8a), 101.4 (C-7), 85.0 (C-3), 70.1 ($ArOCH_2CH_3$), 60.7 ($ArCO_2CH_2CH_3$), 56.4 ($ArOCH_3$), 56.3 ($ArOCH_3$), 53.6 (OCH_3 attached to *C*-3), 43.4 ($ArCH_2CH$=CH_2), 15.5 ($ArOCH_2CH_3$), 14.4 ($ArCO_2CH_2CH_3$). **HRMS** (*m*/*z*), calculated for $C_{21}H_{27}O_7$: 391.1751, found $(M + H)^+$ 391.1748.

7.9.6 Synthesis of ethyl 3-allyl-5,8-diethoxy-4-hydroxy-1,6-dimethoxynaphthalene-2-carboxylate 246, ethyl 3-allyl-5-ethoxy-4-hydroxy-6,8-dimethoxynaphthalene-2-carboxylate 245 and ethyl 3-allyl-4-hydroxy-1,5,6,8-tetramethoxynaphthalene-2-carboxylate 237

To a solution of ethyl 3-allyl-4-hydroxy-5,6,8-trimethoxynaphthalene-2-carboxylate **236** (4.50 g, 13.0 mmol) in absolute MeOH (100 mL) in a 250 mL round bottom flask, PIFA (5.81 g, 13.5 mmol) was added and the reaction was stirred for 15 min at rt. Saturated aqueous $NaHCO_3$ (50 mL) was added until effervescence stopped and the MeOH was removed *in vacuo*. The resultant aqueous medium was extracted into EtOAc (2 × 100 mL) and the combined organic layers were dried over anhydrous $MgSO_4$, filtered through a Celite® pad and concentrated under reduced pressure. The residue was then treated with 21% (w/v) ethanolic solution of NaOEt (18.6 mL, 57.5 mmol) with vigorous stirring for 35 min at rt. The reaction was quenched with saturated aqueous NH_4Cl (10 mL) and the resultant mixture was evaporated at reduced pressure to leave the aqueous layer. The aqueous medium

was extracted into EtOAc (3 × 30 mL). The combined organic layers were dried over anhydrous $MgSO_4$, filtered through a Celite® pad and concentrated *in vacuo*. Purification of the residue by column chromatography (20% EtOAc/hexane) on silica gel afforded three naphthols. The first naphthol was ethyl 3-allyl-5-ethoxy-4-hydroxy-6,8-dimethoxynaphthalene-2-carboxylate **245** which was obtained as an oily product (0.890 g, 19%). $\mathbf{R_f}$ = 0.59 (20 % EtOAc/hexane); **IR ν_{max}(cm^{-1})** 3257 (O-H) 1701 (C=O), 1635 (C=C);

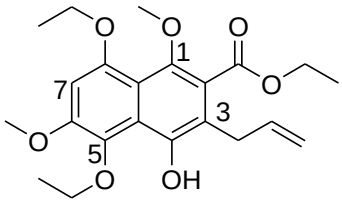
^{1}H NMR (300 MHz, $CDCl_3$, Me_4Si) δ_H 10.25 (1H, s, ArO*H*), 8.20 (1H, s, H-1), 6.57 (1H, s, H-7), 6.09 (1H, ddt, *J* = 16.1, 10.2, 5.9 Hz, $ArCH_2CH$=CH_2), 5.08-4.92 (2H, m, $ArCH_2CH$=CH_2), 4.38 (2H, q, *J* = 7.1 Hz, $ArCO_2CH_2CH_3$), 4.24 (2H, q, *J* = 7.1 Hz, $ArOCH_2CH_3$), 3.97 ($ArOCH_3$, s, 3H), 3.97 ($ArOCH_3$, s, 3H), 3.88 (2H, d, *J* = 5.9 Hz, $ArCH_2CH$=CH_2), 1.45 (3H, t, *J* = 6.4 Hz, $ArOCH_2CH_3$), 1.41 (3H, t, *J* = 6.4 Hz, $ArCO_2CH_2CH_3$); **^{13}C NMR (75 MHz, $CDCl_3$, Me_4Si)** δ_C 168.2 ($ArCO_2CH_2CH_3$), 153.7 (C-8), 151.2 (C-4), 149.1 (C-6), 137.3 ($ArCH_2CH$=CH_2), 134.6 (C-5), 127.9 (C-2), 120.8 (Ar-C), 120.1 (Ar-C), 119.9 (Ar-C), 116.2 ($ArCH_2CH$=CH_2), 114.3 (C-1), 94.9 (C-7), 70.9 ($ArOCH_2CH_3$), 60.8 ($ArCO_2CH_2CH_3$), 57.0 ($ArOCH_3$), 55.8 ($ArOCH_3$), 30.1 ($ArCH_2CH$=CH_2), 15.2 ($ArOCH_2CH_3$), 14.4 ($ArCO_2CH_2CH_3$); **HRMS** (*m*/*z*), calculated for $C_{20}H_{25}O_6$: 361.1646, found $(M + H)^+$ 361.1651.



245

The second naphthol was ethyl 3-allyl-5,8-diethoxy-4-hydroxy-1,6-dimethoxynaphthalene-2-carboxylate **246** which was obtained as a semi-solid (1.17 g, 24%). $\mathbf{R_f}$ = 0.43 (20 % EtOAc/hexane); **IR ν_{max}(cm^{-1})** 3257 (O-H) 1701 (C=O), 1635 (C=C);

^{1}H NMR (300 MHz, $CDCl_3$, Me_4Si) δ_H 10.38 (1H, s, ArO*H*), 6.61 (1H, s, H-7), 6.01 (1H, ddt, *J* = 16.4, 10.0, 6.3 Hz, $ArCH_2CH$=CH_2), 5.14-4.94 (2H, m, $ArCH_2CH$=CH_2), 4.39 (2H, q, *J* = 7.1 Hz, $ArCO_2CH_2CH_3$), 4.21 (2H, q, *J* = 7.1 Hz, $ArOCH_2CH_3$), 4.05-3.86 (8H, m, 2 × $ArOCH_3$, $ArOCH_2CH_3$), 3.46 (2H, d, *J* = 6.3 Hz, $ArCH_2CH$=CH_2), 1.48-1.30 (9H, m, 2 × $ArOCH_2CH_3$, $ArCO_2CH_2CH_3$); **^{13}C NMR (75 MHz, $CDCl_3$, Me_4Si)** δ_C 168.3 ($ArCO_2CH_2CH_3$), 153.9 (C-8), 148.1 (C-1),



246

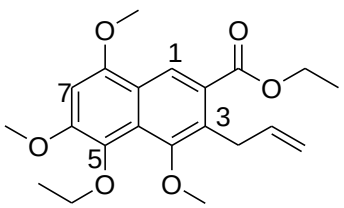
147.2 (C-6), 144.4 (C-4), 136.0 (C-3), 135.4 ($ArCH_2CH=CH_2$), 127.0 (C-5), 120.6 (Ar-C), 117.9 (Ar-C), 115.6 (Ar-C), 115.1 (Ar-C), 96.9 (C-7), 72.1 ($ArOCH_2CH_3$), 71.1 ($ArOCH_2CH_3$), 61.1 ($ArCO_2CH_2CH_3$), 57.0 ($ArOCH_3$), 56.7 ($ArOCH_3$), 31.5 ($ArCH_2CH=CH_2$), 15.5 ($ArOCH_2CH_3$), 15.1 ($ArOCH_2CH_3$), 14.3 ($ArCO_2CH_2CH_3$). **HRMS** (*m*/*z*), calculated for $C_{22}H_{29}O_7$: 405.1908, found $(M + H)^+$ 405.1905.

The third product was ethyl 3-allyl-4-hydroxy-1,5,6,8-tetramethoxynaphthalene-2-carboxylate **237** which was obtained as an orange amorphous solid (0.631 g, 12%). $\mathbf{R_f}$ = 0.54 (20% EtOAc/hexane). The ^{1}H NMR spectrum of this naphthol was similar to the one discussed in **Section 7.9.4**.

7.9.7 Synthesis of ethyl 3-allyl-5-ethoxy-4,6,8-trimethoxynaphthalene-2-carboxylate 247

To a solution of ethyl 3-allyl-5-ethoxy-4-hydroxy-6,8-dimethoxynaphthalene-2-carboxylate **245** (0.780 g, 2.16 mmol) and anhydrous K_2CO_3 (0.415 g, 3.00 mmol) in acetone (100 mL) was added Me_2SO_4 (0.284 mL, 3.00 mmol) *via* a syringe. The mixture was heated to reflux for 24 hrs after which it was cooled to rt, filtered through a Celite® pad and the solvent was removed *in vacuo*. The residue was then dissolved in EtOAc (100 mL) and was successively washed with 25% (v/v) aqueous NH_3 (2 × 50 mL), acidified to pH 4 using 32% (v/v) aqueous HCl followed by washing with H_2O until the aqueous layer was neutral. The organic layer was dried over anhydrous $MgSO_4$, filtered through a bed of Celite® and concentrated *in vacuo*. Purification of the residue by column chromatography (15% EtOAc/hexane) on silica gel delivered ethyl 3-allyl-5-ethoxy-4,6,8-trimethoxynaphthalene-2-carboxylate as a yellow oil (0.582 g, 72%). $\mathbf{R_f}$ = 0.59 (20 % EtOAc/hexane); **IR ν_{max} (cm^{-1})** 1709 (C=O), 1638 (C=C);

^{1}H NMR (300 MHz, $CDCl_3$, Me_4Si) δ_H 8.54 (1H, s, H-1), 6.67 (1H, s, H-7), 6.07 (1H, ddt, *J* = 16.1, 10.3, 5.8 Hz, $ArCH_2CH=CH_2$), 4.98 (1H, dd, *J* = 10.2, 1.7 Hz, $ArCH_2CH=CH_2$), 4.94 (1H, dd, *J* = 17.2, 1.8 Hz, $ArCH_2CH=CH_2$), 4.37 (1H, q, *J* = 7.1 Hz, $ArCO_2CH_2CH_3$), 4.01-3.93 (10H, m, 2 × $ArOCH_3$, $ArOCH_2CH_3$ and $ArCO_2CH_2CH_3$), 3.82 (3H, s, $ArOCH_3$), 1.42 (6H, dt, *J* = 19.2, 7.1 Hz, $ArOCH_2CH_3$ and $ArCO_2CH_2CH_3$); **^{13}C NMR (126 MHz, $CDCl_3$, Me_4Si)** δ_C 168.0

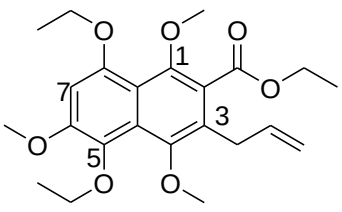


247

(Ar*C*$O_2CH_2CH_3$), 153.5 (C-8), 153.3 (C-4), 152.2 (C-6), 138.4 (ArCH_2*C*H=CH_2), 134.8 (C-5), 130.2 (C-2), 126.9 (Ar-C), 125.6 (Ar-C), 121.9 (Ar-C), 120.8 (Ar-C), 114.7 (Ar-C), 94.8 (C-7), 70.5 (ArOCH_2*C*H_3), 63.0 (ArCO_2CH_2*C*H_3), 60.9 (ArOCH_3), 56.9 (ArOCH_3), 55.8 (ArOCH_3), 30.2 (Ar*C*H_2CH=CH_2), 15.5 (ArOCH_2*C*H_3), 14.4 (ArCO_2CH_2*C*H_3). **HRMS** (*m*/*z*), calculated for $C_{21}H_{27}O_6$: 375.1802, found $(M + H)^+$ 375.1803.

7.9.8 Synthesis of ethyl 3-allyl-5,8-diethoxy-1,4,6-trimethoxynaphthalene-2-carboxylate 252

A solution of ethyl 3-allyl-5,8-diethoxy-4-hydroxy-1,6-dimethoxynaphthalene-2-carboxylate **246** (0.550 g, 1.36 mmol), anhydrous K_2CO_3 (0.359 g, 2.60 mmol) and Me_2SO_4 (0.237 mL, 2.60 mmol) in acetone (100 mL) was heated to reflux for 24 hrs. The reaction mixture was then cooled to rt, filtered through a Celite® pad and solvent removed *in vacuo*. The residue was dissolved in EtOAc (100 mL) and successively washed with 25% (v/v) aqueous NH_3 (2 × 100 mL). The EtOAc solution was then acidified to pH 4 using 32% (v/v) aqueous HCl and was washed with H_2O until the aqueous layer was neutral. The organic layer was dried over anhydrous $MgSO_4$, filtered through a bed of Celite® and concentrated *in vacuo*. The residue was purified by column chromatography (15% EtOAc/hexane) on silica gel yielding ethyl 3-allyl-5,8-diethoxy-1,4,6-trimethoxynaphthalene-2-carboxylate **252** as a yellow oil (0.444 g, 78%). $\mathbf{R_f}$ = 0.55 (20% EtOAc/hexane); **IR ν_{max}(cm^{-1})** 1709 (C=O), 1639 (C=C);



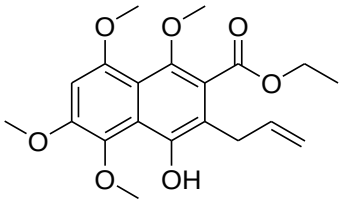
252

^{1}H NMR (500 MHz, $CDCl_3$, Me_4Si) δ_H 6.72 (1H, s, H-7), 5.99 (1H, ddt, *J* = 16.4, 10.1, 6.2 Hz, ArCH_2C*H*=CH_2), 5.04 (2H, ddd, *J* = 13.6, 11.5, 1.4 Hz, ArCH_2CH=CH_2), 4.37 (2H, q, *J* = 7.1 Hz, ArCO_2C$H_2$$CH_3$), 4.03-3.89 (10H, m, 2 × ArOCH_3, 2 × ArOCH_2CH_3), 3.78 (3H, s, ArOCH_3), 3.58 (2H, d, *J* = 6.2 Hz, ArCH_2CH=CH_2), 1.40 (9H, m, 2 × ArOCH_2CH_3, Ar$CO_2CH_2CH_3$); **^{13}C NMR (126 MHz, $CDCl_3$, Me_4Si)** δ_C 168.1 (Ar*C*$O_2CH_2CH_3$), 153.7 (C-8), 151.1 (C-1), 149.2 (C-6), 149.0 (C-3), 136.8 (Ar-C), 135.5 (ArCH_2*C*H=CH_2), 127.4 (Ar-C), 126.5 (Ar-C), 125.8 (Ar-C), 116.3 (Ar-C), 115.6 (Ar-C), 97.1 (C-7), 72.0 (ArOCH_2*C*H_3), 70.4 (ArOCH_2*C*H_3), 62.8 (ArCO_2*C*H_2CH_3), 61.1 (ArOCH_3), 56.8 (ArOCH_3), 56.7 (ArOCH_3),

31.6 (Ar*C*H_2CH=CH_2), 15.5 (ArOCH_2*C*H_3), 15.4 (ArOCH_2*C*H_3), 14.2 (ArCO_2CH_2*C*H_3). **HRMS** (*m*/*z*), calculated for $C_{23}H_{31}O_7$: 419.2064, found $(M + H)^+$ 419.2062.

7.9.9 Synthesis of ethyl 3-allyl-4-hydroxy-1,5,6,8-tetramethoxynaphthalene-2-carboxylate 237

To a solution of ethyl 3-allyl-4-hydroxy-5,6,8-trimethoxynaphthalene-2-carboxylate **236** (4.50 g, 13.0 mmol) in absolute MeOH (100 mL) in a 250 mL round bottom flask, PIFA (5.81 g, 13.5 mmol) was added and the reaction was stirred for 15 min at rt. Saturated aqueous $NaHCO_3$ solution was added to the mixture until effervescence stopped and MeOH was removed *in vacuo* to leave an aqueous medium. This medium was then extracted into EtOAc (3 × 100 mL). The combined organic layers were dried over anhydrous $MgSO_4$, filtered through a Celite® pad and concentrated under reduced pressure. The residue was then dissolved in ethanol (200 mL) and *t*-BuOK (3.41 g, 30.4 mmol) was added with vigorous stirring for 20 min at rt. The reaction was quenched by saturated aqueous solution NH_4Cl (50 mL) and the resultant mixture was evaporated at reduced pressure to leave an aqueous medium. This medium was extracted into EtOAc (3 × 100 mL) and the combined organic layers were dried over anhydrous $MgSO_4$, filtered through a Celite® pad and concentrated *in vacuo*. Purification of the crude product by silica gel column chromatography (15% EtOAc/hexane) delivered ethyl 3-allyl-4-hydroxy-1,5,6,8-tetramethoxynaphthalene-2-carboxylate **237** as an orange amorphous solid (2.94 g, 60%). $\mathbf{R_f}$ = 0.46 (25% EtOAc/hexane). The ^{1}H NMR spectrum of this naphthol was similar to the one discussed in **Section 7.9.4**.

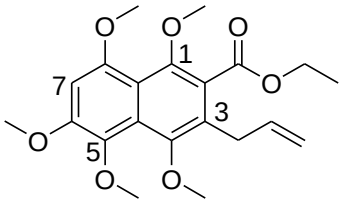


237

7.9.10 Synthesis of ethyl 3-allyl-1,4,5,6,8-pentamethoxynaphthalene-2-carboxylate 230

Me_2SO_4 (1.06 mL, 11.2 mmol) was added to a solution of ethyl 3-allyl-4-hydroxy-1,5,6,8-tetramethoxynaphthalene-2-carboxylate **237** (2.80 g, 7.44 mmol) and anhydrous K_2CO_3 (1.55 g, 11.2 mmol) in acetone (100 mL) in a 250 mL round bottom flask. The mixture was then heated to reflux for 24 hrs after which it was cooled to rt, filtered through a bed of Celite® and the solvent was removed *in vacuo*. The residue was dissolved in EtOAc (100 mL) and successively washed with 25% (v/v) aqueous NH_3 (2 × 100 mL) after which it was acidified

to pH 4 using 32% (v/v) aqueous HCl. The organic layer was then washed with H_2O until the aqueous layer was neutral. It was then dried over anhydrous $MgSO_4$, filtered through a bed of Celite® and concentrated *in vacuo*. Purification of the crude product by silica gel column chromatography (10% EtOAc/hexane) yielded ethyl 3-allyl-1,4,5,6,8-pentamethoxynaphthalene-2-carboxylate **230** as a yellow oil (2.41 g, 83%). $\mathbf{R_f}$ = 0.53 (20 % EtOAc/hexane);



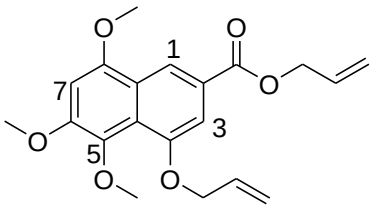
230

^{1}H NMR (300 MHz, $CDCl_3$, Me_4Si) δ_H 6.73 (1H, s, H-7), 5.98 (1H, ddt, *J* = 16.4, 10.1, 6.2 Hz, $ArCH_2CH{=}CH_2$), 5.13-4.98 (2H, m, $ArCH_2CH{=}CH_2$), 4.39 (2H, q, *J* = 7.1 Hz, $ArCO_2CH_2CH_3$), 4.01 (3H, s, $ArOCH_3$), 3.98 (3H, s, $ArOCH_3$), 3.82 (3H, s, $ArOCH_3$), 3.78 (3H, s, $ArOCH_3$), 3.77 (3H, s, $ArOCH_3$), 3.57 (2H, dt, *J* = 6.2, 1.5 Hz, $ArCH_2CH{=}CH_2$), 1.39 (3H, t, *J* = 7.1 Hz, $ArCO_2CH_2CH_3$); **^{13}C NMR (75 MHz, $CDCl_3$, Me_4Si)** δ_C 168.0 ($ArCO_2CH_2CH_3$), 153.7 (C-8), 150.9 (C-1), 150.0 (C-6), 149.2 (C-4), 136.7 ($ArCH_2CH{=}CH_2$), 136.6 (Ar-C), 127.6 (Ar-C), 126.4 (Ar-C), 125.7 (Ar-C), 116.0 (Ar-C), 115.7 (Ar-C), 97.1 (C-7), 63.8 ($ArCO_2CH_2CH_3$), 62.7 ($ArOCH_3$)2, 62.1 ($ArOCH_3$), 61.2 ($ArOCH_3$), 56.9 ($ArOCH_3$), 56.8 ($ArOCH_3$), 31.6 ($ArCH_2CH{=}CH_2$), 14.2 ($ArCO_2CH_2CH_3$). **HRMS** (*m*/*z*), calculated for $C_{21}H_{27}O_7$: 391.1751, found $(M + H)^+$ 391.1750.

7.9.11 Synthesis of allyl 4-(allyloxy)-5,6,8-trimethoxynaphthalene-2-carboxylate 256[124]

Ethyl 4-acetoxy-5,6,8-trimethoxynaphthalene-2-carboxylate **233** (6.00 g, 17.2 mmol) was dissolved in MeOH (100 mL) followed by the portion-wise addition of aqueous NaOH (1.68 g, 40.0 mmol) in H_2O (200 mL). The dark-orange reaction was heated to reflux for 6 hrs at rt after which the MeOH was removed *in vacuo*. The aqueous medium was acidified to pH 4.0 with 32% (v/v) aqueous HCl and then extracted into EtOAc (3 × 150 mL). The combined organic layers were dried over anhydrous $MgSO_4$, filtered through a Celite® pad and concentrated *in vacuo*. The crude product was transferred into a 500 mL round bottom flask charged with acetone (150 mL) to which allyl bromide (4.84 g, 40.0 mmol) and K_2CO_3 (6.08 g, 44.0 mmol) were added. The reaction mixture was then heated to reflux for 24 hrs under a N_2 (g) after which it was allowed to cool to room temperature, filtered through a Celite® pad

and solvent removed *in vacuo*. The residue was purified by column chromatography (10% EtOAc/hexane) on silica gel yielding allyl 4-(allyloxy)-5,6,8-trimethoxynaphthalene-2-carboxylate **256** as a yellow solid (5.18 g, 84%). $\mathbf{R_f}$ = 0.41 (10% EtOAc/hexane);



256

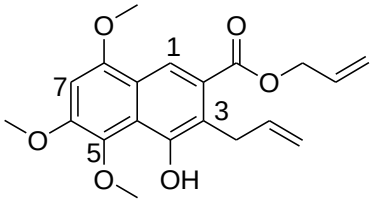
^{1}H NMR (300 MHz, $CDCl_3$, Me_4Si) δ_H 8.54 (1H, d, *J* = 1.3 Hz, H-1), 7.39 (1H, d, *J* = 1.2 Hz, H-3), 6.60 (1H, s, H-7), 6.28-5.97 (2H, m, $ArCO_2CH_2CH$=CH_2 and $ArOCH_2CH$=CH_2), 5.60 (1H, dd, *J* = 17.2, 1.5 Hz, one of $ArCO_2CH_2CH$=CH_2), 5.43 (1H, dd, *J* = 17.2, 1.4 Hz, one of $ArOCH_2CH$=CH_2), 5.37-5.00 (2H, m, one of $ArCO_2CH_2CH$=CH_2 and $ArOCH_2CH$=CH_2), 4.85 (2H, d, *J* = 5.6 Hz, $ArCO_2CH_2CH$=CH_2), 4.68 (2H, d, *J* = 5.1 Hz, $ArOCH_2CH$=CH_2), 3.92 (3H, s, $ArOCH_3$), 3.89 (3H, s, $ArOCH_3$), 3.81 (3H, s, $ArOCH_3$); **^{13}C NMR (75 MHz, $CDCl_3$, Me_4Si)** δ_C 166.5 ($ArCO_2CH_2CH$=CH_2), 154.6 (C-8), 153.6 (C-4), 152.3 (C-6), 137.8 ($ArOCH_2CH$=CH_2), 133.2 ($ArCO_2CH_2CH$=CH_2), 132.6 (C-5), 124.6 (C-2), 124.2 (C-8a), 122.2 (C-4a), 118.8 (C-1), 118.1 ($ArOCH_2CH$=CH_2), 117.6 ($ArCO_2CH_2CH$=CH_2), 107.7 (C-3), 96.1 (C-7), 70.4 ($ArOCH_2CH$=CH2), 65.6 ($ArCO_2CH_2CH$=CH_2), 62.0 ($ArOCH_3$), 57.2 ($ArOCH_3$), 55.9 ($ArOCH_3$).

7.9.12 Synthesis of allyl 3-allyl-4-hydroxy-5,6,8-trimethoxynaphthalene-2-carboxylate 257[124]

Allyl 4-(allyloxy)-5,6,8-trimethoxynaphthalene-2-carboxylate **256** (5.00 g, 14.0 mmol) was loaded neat into a 100 mL round bottom flask equipped with a reflux condenser and a magnetic stirrer bar. The reaction vessel was heated to 180 ^oC for 24 hrs under a N_2 (g). The dark viscous residue was allowed to cool to room temperature and purification by silica gel column chromatography (20% EtOAc/hexane) delivered allyl 3-allyl-4-hydroxy-5,6,8-trimethoxynaphthalene-2-carboxylate **257** as a yellow amorphous solid (3.41 g, 68%). $\mathbf{R_f}$ = 0.43 (20 % EtOAc/hexane);

^{1}H NMR (300 MHz, $CDCl_3$, Me_4Si) δ_H 10.08 (1H, s, ArO*H*), 8.26 (1H, s, H-1), 6.56 (1H, s, H-7), 6.17-5.99 (2H, m, $ArCO_2CH_2CH$=CH_2 and $ArCH_2CH$=CH_2), 5.42 (1H, dd, *J* = 17.2, 1.4 Hz, one of $ArCO_2CH_2CH$=CH_2), 5.28 (1H, dd, *J* = 10.4, 1.1 Hz, one of $ArCO_2CH_2CH$=CH_2), 5.00 (2H, ddd, *J* = 10.9, 9.5, 1.7 Hz, $ArCH_2CH$=CH_2), 4.82 (2H, d, *J* =

5.7 Hz, $ArCO_2CH_2CH=CH_2$), 3.99 (3H, s, $ArOCH_3$), 3.98 (3H, s, $ArOCH_3$), 3.96 (3H, s, $ArOCH_3$), 3.89 (2H, d, J = 6.0 Hz, $ArCH_2CH=CH_2$); **^{13}C NMR (75 MHz, $CDCl_3$, Me_4Si)** δ_C 167.5 ($ArCO_2CH_2CH=CH_2$), 153.7 (C-8), 151.0 (C-4), 149.3 (C-6), 137.4 ($ArCO_2CH_2CH=CH_2$), 135.6 ($ArCO_2CH_2CH=CH_2$), 132.6 (C-5), 127.0 (C-2), 120.9 (C-8a), 119.7 (C-4a), 119.4 (C-3), 118.1 ($ArCH_2CH=CH_2$), 116.7 ($ArCO_2CH_2CH=CH_2$), 114.4 (C-1), 94.5 (C-7), 65.5 ($ArCO_2CH_2CH=CH_2$), 62.1 ($ArOCH_3$), 56.7 ($ArOCH_3$), 55.7 ($ArOCH_3$), 30.0 ($ArCH_2CH=CH_2$).



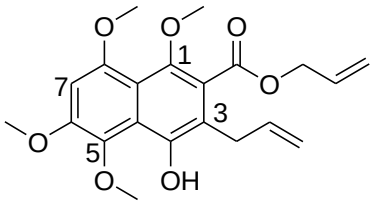
257

7.9.13 Synthesis of allyl 3-allyl-4-hydroxy-1,5,6,8-tetramethoxynaphthalene-2-carboxylate 259[124]

Allyl 3-allyl-4-hydroxy-5,6,8-trimethoxynaphthalene-2-carboxylate **257** (3.40 g, 9.49 mmol) was dissolved in absolute MeOH (90 mL) and PIFA (4.47 g, 10.4 mmol) was added in one portion. The reaction mixture was stirred for 15 min at rt after which a saturated aqueous solution of $NaHCO_3$ was added until effervescence stopped. The MeOH was removed *in vacuo* to leave aqueous medium which was then extracted into EtOAc (3 × 50 mL). The combined organic layers were dried over anhydrous $MgSO_4$, filtered through a pad of Celite® and the solvent was evaporated *in vacuo*. The residue was transferred into a 250 mL round bottom flask charged with EtOH (100 mL) to which *t*-BuOK (3.41 g, 30.4 mmol) was added while vigorously stirring the mixture. The reaction mixture was stirred for a further 20 min at rt after which it was quenched with saturated aqueous solution of NH_4Cl (100 mL). The solvent was concentrated under reduced pressure and the aqueous medium was extracted into EtOAc (3 × 100 mL). The combined organic layers were dried over anhydrous $MgSO_4$, filtered through a bed of Celite® and concentrated *in vacuo*. Purification of the residue on normal silica gel column chromatography (20% EtOAc/hexane) afforded allyl 3-allyl-4-hydroxy-1,5,6,8-tetramethoxynaphthalene-2-carboxylate **259** as a yellow solid (2.17 g, 59%). $\mathbf{R_f}$ = 0.41 (20% EtOAc/hexane);

^{1}H NMR (300 MHz, $CDCl_3$, Me_4Si) δ_H 10.21 (1H, s, ArO*H*), 6.63 (C-7), 6.29-5.84 (2H, m, $ArCO_2CH_2CH=CH_2$ and $ArCH_2CH=CH_2$), 5.43 (1H, dd, J = 17.2, 1.4 Hz, one of

$ArCO_2CH_2CH=CH_2$), 5.28 (1H, dd, *J* = 10.4, 1.2 Hz, one of $ArCO_2CH_2CH=CH_2$), 5.13-4.96 (2H, m, $ArCH_2CH=CH_2$), 4.84 (2H, d, *J* = 5.9 Hz, $ArCO_2CH_2CH=CH_2$), 3.97 (3H, s, $ArOCH_3$), 3.96 (3H, s, $ArOCH_3$), 3.95 (3H, s, $ArOCH_3$), 3.78 (3H, s, $ArOCH_3$), 3.46 (2H, d, *J* = 6.3 Hz, $ArCH_2CH=CH_2$);



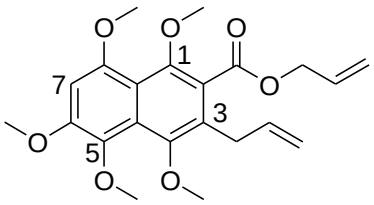
259

^{13}C NMR (75 MHz, $CDCl_3$, Me_4Si) δ_C 167.8 ($ArCO_2CH_2CH=CH_2$), 154.0 (C-8), 148.3 (C-1), 147.1 (C-6), 145.7 (C-4), 136.5 ($ArCH_2CH=CH_2$), 135.9 ($ArCO_2CH_2CH=CH_2$), 132.1 (C-5), 126.3 (C-4a), 120.2 ($ArCH_2CH=CH_2$), 118.8 ($ArCO_2CH_2CH=CH_2$), 118.0 (C-3), 115.2 (C-8a), 115.2 (C-2), 96.8 (C-7), 65.9 ($ArCO_2CH_2CH=CH_2$), 63.9 ($ArOCH_3$), 62.3 ($ArOCH_3$), 56.8 ($ArOCH_3$), 56.7 ($ArOCH_3$), 31.5 ($ArCH_2CH=CH_2$).

7.9.14 Synthesis of allyl 3-allyl-1,4,5,6,8-pentamethoxynaphthalene-2-carboxylate 254[124]

Allyl 3-allyl-4-hydroxy-1,5,6,8-tetramethoxynaphthalene-2-carboxylate **259** (2.00 g, 5.15 mmol), anhydrous K_2CO_3 (1.04 g, 7.50 mmol) and Me_2SO_4 (0.710 mL, 7.50 mmol) were dissolved in acetone (200 mL) in a 500 mL round bottom flask. The reaction mixture was then heated to reflux for 24 hrs after which it was cooled to rt, filtered through a Celite® pad and the solvent was removed *in vacuo*. The residue was then dissolved in EtOAc (150 mL) and successively washed with 25% (v/v) aqueous NH_3 (2 × 50 mL). The organic layer was acidified by 32% (v/v) aqueous HCl after which it was washed with H_2O until the aqueous layer was neutral. It was then dried over anhydrous MgSO4, filtered through a pad of Celite® and concentrated *in vacuo*. The residue was purified by column chromatography (10% EtOAc/hexane) on silica gel yielding allyl 3-allyl-1,4,5,6,8-pentamethoxynaphthalene-2-carboxylate **254** as an off white solid (1.89 g, 91%). $\mathbf{R_f}$ = 0.55 (15% EtOAc/hexane);

^{1}H NMR (500 MHz, $CDCl_3$) δ_H 6.75 (1H, s, H-7), 6.16-5.90 (2H, m, $ArCO_2CH_2CH=CH_2$ and $ArCH_2CH=CH_2$), 5.43 (1H, dd, *J* = 17.2, 1.4 Hz, one of $ArCO_2CH_2CH=CH_2$), 5.27 (1H, dd, *J* = 10.4, 1.1 Hz, one of $ArCO_2CH_2CH=CH_2$), 5.13-5.00 (2H, m, $ArCH_2CH=CH_2$), 4.83 (2H, d, *J* = 5.9 Hz, $ArCO_2CH_2CH=CH_2$), 3.99 (3H, s, $ArOCH_3$), 3.96 (3H, s, $ArOCH_3$), 3.82 (3H, s, $ArOCH_3$), 3.80

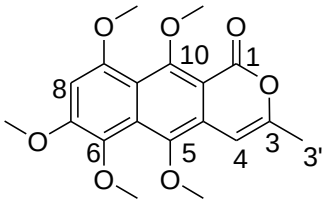


254

(3H, s, ArOC*H*$_3$), 3.79 (3H, s, ArOC*H*$_3$), 3.59 (2H, d, *J* = 6.2 Hz, ArCH$_2$CH=C*H*$_2$); **^{13}C NMR (126 MHz, CDCl$_3$, Me$_4$Si)** δ_C 167.6, 153.7 (C-8), 151.1 (C-1), 150.2 (C-6), 149.2 (C-4), 136.7 (Ar*C*H$_2$CH=CH$_2$), 136.6 (ArCO$_2$CH$_2$*C*H=CH$_2$), 132.1 (C-5), 127.6 (C-4a), 126.4 (C-3), 125.2 (C-8a), 118.8 (ArCO$_2$CH$_2$CH=*C*H$_2$), 115.9 (ArCH$_2$CH=*C*H$_2$), 115.8 (C-2), 97.1 (C-7), 65.9 (ArCO$_2$*C*H$_2$CH=CH$_2$), 63.7 (ArO*C*H$_3$), 62.7 (ArO*C*H$_3$), 62.0 (ArO*C*H$_3$), 56.8 (ArO*C*H$_3$), 56.7 (ArO*C*H$_3$), 31.5 (Ar*C*H$_2$CH=CH$_2$). **HRMS** (*m*/*z*), calculated for $C_{22}H_{27}O_7$: 403.1751, found $(M + H)^+$ 403.1751.

7.9.15 Synthesis of 5,6,7,9,10-pentamethoxy-3-methyl-1*H*-benzo[*g*]isochromen-1-one 229

In a 2-neck round bottom flask equipped with a magnetic stirring bar, allyl 3-allyl-1,4,5,6,8-pentamethoxynaphthalene-2-carboxylate **254** (1.75 g, 4.35 mmol) and $CuCl_2.2H_2O$ (0.890 g, 5.22 mmol) were dissolved in a DMF/H_2O mixture (100 mL, v/v, 2:1). To this solution, $PdCl_2$ (77.1 mg, 0.435 mmol) was added under the blanket of O_2 (g). The reaction mixture was then stirred vigorously for 12 hrs at rt. After this time had elapsed, $CuCl_2.2H_2O$ (1.02 g, 6.00 mmol) and NaCl (0.188 g, 3.22 mmol) were added to the same reaction mixture and stirring continued for a further 36 hrs under the atmosphere of O_2 (g). The reaction mixture was filtered through a thick Celite® pad which was washed with CH_2Cl_2 (2 × 100 mL). The combined organic layers were washed with brine (3 × 100 mL), dried over anhydrous $MgSO_4$, filtered through a pad of Celite® and the solvent was removed *in vacuo*. The residue was purified on flash silica gel column chromatography (EtOAc/hexane) affording two compounds. The first of which was 5,6,7,9,10-pentamethoxy-3-methyl-1*H*-benzo[*g*]isochromen-1-one **229** which was obtained as a pale yellow crystalline solid (0.643 g, 36%). $\mathbf{R_f}$ = 0.43 (EtOAc/CH_2Cl_2/hexane 4:2:4); **Mp** 160-162 ^oC; **IR ν_{max} (cm^{-1})** 1741 (C=O), 1605 (C=C);

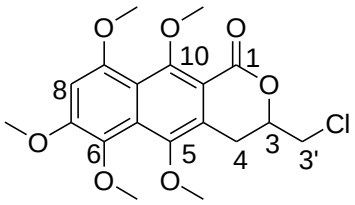


229

^{1}H NMR (300 MHz, CDCl$_3$, Me$_4$Si) δ_H 6.73 (1H, s, H-8), 6.57 (1H, s, H-4), 4.04 (3H, s, ArOC*H*$_3$), 4.02 (3H, s, ArOCH$_3$), 3.95 (3H, s, ArOC*H*$_3$), 3.83 (3H, s, ArOC*H*$_3$), 3.82 (3H, s, ArOC*H*$_3$), 2.26 (3H, s, H-3'); **^{13}C NMR (75 MHz, CDCl$_3$, Me$_4$Si)** δ_C 159.4 (C-1), 156.3 (C-3), 156.2 (Ar-O), 153.2 (Ar-O), 152.9 (Ar-O), 143.6 (Ar-O), 135.8 (Ar-O), 129.0 (C-6a), 127.5 (C-10a), 116.7 (C-4a), 108.9 (C-9a),

97.4 (C-4), 96.9 (C-8), 63.0 (ArO*C*H$_3$), 62.8 (ArO*C*H$_3$), 62.0 (ArO*C*H$_3$), 57.3 (ArO*C*H$_3$), 56.5 (ArO*C*H$_3$), 19.8 (C-3'). **HRMS** (*m*/*z*), calculated for $C_{19}H_{21}O_7$: 361.1282, found $(M + H)^+$ 361.1287.

The second product was 3-(chloromethyl)-3,4-dihydro-5,6,7,9,10-pentamethoxybenzo[*g*]isochromen-1-one **260** which was obtained as a pale yellow semi-solid (0.518 g, 30%). $\mathbf{R_f}$ = 0.45 **(**EtOAc/CH_2Cl_2/hexane 4:2:4); **IR** $\boldsymbol{\nu_{max}}$**(cm^{-1})** 1711 (C=O), 1229 (C-O);



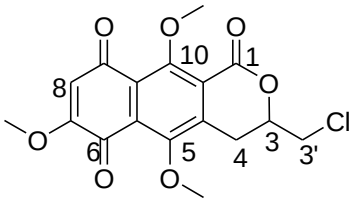
260

^{1}H NMR (300 MHz, $CDCl_3$, Me_4Si) δ_H 6.76 (1H, s, H8), 4.59 (1H, m, H3), 4.04 (3H, s, ArO*C*H$_3$), 4.01 (3H, s, ArO*C*H$_3$), 3.94 (3H, s, ArO*C*H$_3$), 3.88-3.69 (8H, m, 2 × ArO*C*H$_3$, H-3'), 3.53 (1H, dd, *J* = 16.2, 2.8 Hz, H4 *pseudo*-equatorial), 3.00 (1H, dd, *J* = 16.3, 10.8 Hz, H4 *pseudo*-axial); **^{13}C NMR (75 MHz, $CDCl_3$, Me_4Si)** δ_C 161.4 (C-1), 158.6 (Ar-O), 156.0 (Ar-O), 153.1 (Ar-O), 146.6 (Ar-O), 136.2 (Ar-O), 128.8 (C-5a), 126.8 (C-4a), 117.0 (C-9a), 112.5 (C10a), 97.4 (C-8), 76.2 (C-3), 63.4 (ArO*C*H$_3$), 62.1 (ArO*C*H$_3$), 62.1 (ArO*C*H$_3$), 57.3 (ArO*C*H$_3$), 56.5 (ArO*C*H$_3$), 44.9 (C-3'), 26.0 (C-4). **HRMS** (*m*/*z*), calculated for $C_{19}H_{22}ClO_7$: 397.1049, found $(M + H)^+$ 397.1050.

7.9.16 Synthesis of 3-(chloromethyl)-3,4-dihydro-5,7,10-trimethoxybenzobenzo[*g*]-isochromene-1,6,9-trione JS-QCl

To a stirred suspension of 3-(chloromethyl)-3,4-dihydro-5,6,7,9,10-pentamethoxybenzo[*g*]isochromen-1-one **260** (0.470 g, 1.18 mmol) and AgO (0.500 g, 4.04 mmol) in 1,4-dioxane (50 mL) was added 55% (v/v) aqueous HNO_3 drop-wise until all AgO dissolved. The resultant solution was stirred for a further 5 min after which a mixture of CH_2Cl_2/H_2O (100 mL, v/v, 1:1) was added and the lower organic layer was separated. The aqueous layer was further extracted into CH_2Cl_2 (2 × 100 mL) and the combined organic layers were dried over anhydrous $MgSO_4$, filtered through a Celite® bed and concentrated under reduced pressure. The residue was purified by silica gel column chromatography (EtOAc/hexane/CH_2Cl_2, 3:2:5) affording 3-(chloromethyl)-3,4-dihydro-5,7,10-trimethoxy-benzobenzo[*g*]isochromene-1,6,9-trione **JS-QCl** as an orange amorphous solid (0.303 g,

70%). **R_f** = 0.40 **(**EtOAc/CH_2Cl_2/hexane 3:2:5) **Mp** 87-89 ^oC; **IR ν_{max}(cm^{-1})** 1774 (C=O), 1761 (C=O), 1709 (C=O), 1689 (C=C), 1215 (C-O);

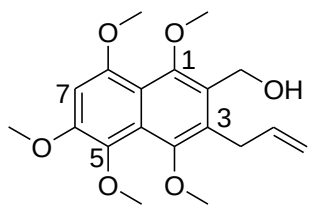


JS-QCl

^{1}H NMR (300 MHz, $CDCl_3$, Me_4Si) δ_H 6.08 (1H, s, H-8), 4.65 (1H, m, H-3), 3.99 (3H, s, ArOCH_3), 3.88 (6H, s, 2 × ArOCH_3), 3.82 (2H, d, *J* = 5.3 Hz, H-3'), 3.45 (1H, dd, *J* = 17.1, 2.8 Hz, H4 *pseudo*-equatorial), 2.98 (1H, dd, *J* = 17.1, 11.4 Hz, H4 *pseudo*-axial); **^{13}C NMR (75 MHz, $CDCl_3$, Me_4Si)** δ_C 182.6 (C-9), 178.9 (C-6), 159.1 (C-1), 157.7 (Ar-O), 152.7 (Ar-O), 141.7 (Ar-O), 128.2 (C-4a), 126.8 (C-10a or C-5a), 125.7 (C-10a or C-5a), 111.8 (C-9a), 111.0 (C-8), 76.1 (C-3), 63.8 (ArO*C*H_3), 62.3 (ArO*C*H_3), 56.5 (ArO*C*H_3), 44.5 (C-3'), 26.0 (C-4); **HRMS** (*m*/*z*), calculated for $C_{17}H_{16}ClO_7$: 367.0579, found $(M + H)^+$ 367.0584.

7.9.17 Synthesis of (2-allyl-1,4,5,7,8-pentamethoxynaphthalene-3-yl)methanol 269[124]

To a solution of allyl 3-allyl-1,4,5,6,8-pentamethoxynaphthalene-2-carboxylate **254** (2.30 g, 5.72 mmol) and ethyl 3-allyl-1,4,5,6,8-pentamethoxynaphthalene-2-carboxylate **230** (2.10 g, 5.38 mmol) in dry THF (100 mL) cooled to 0 °C in an ice bath, $LiAlH_4$ (0.486 g, 12.8 mmol) was added portion-wise over a period of 5 min. The reaction mixture was allowed to warm to rt and stirred for a further 4 hrs under a N_2 (g). After this time had elapsed, the mixture was cooled to 0 °C for a second time and cold H_2O was added portion-wise until the effervescence stopped. The resultant mixture was filtered through a thick Celite® bed and the THF was removed *in vacuo*. The aqueous medium was extracted into EtOAc (3 × 100 mL) and the combined organic layers were dried over anhydrous $MgSO_4$, filtered through a bed of Celite® and concentrated under reduced pressure. Purification of the residue by silica gel column chromatography yielded alcohol **269** (3.09 g, 80%). **R_f** = 0.42 (30% EtOAc/hexane); **Mp** 122-123 °C; **IR ν_{max}(cm^{-1})** 3481 (O-H), 1580 (C=C);



269

^{1}H NMR (300 MHz, $CDCl_3$, Me_4Si) δ_H 6.73 (1H, s, H-7), 6.14 (1H, ddt, *J* = 17.1, 10.5, 5.4 Hz, $ArCH_2CH$=CH_2), 5.06 (1H, ddd, *J* = 17.1, 10.2, 1.7 Hz, one of $ArCH_2CH$=CH_2), 4.95 (1H, ddd, *J* = 15.4, 3.4, 1.6 Hz, one of $ArCH_2CH$=CH_2), 4.81 (2H, s, ArCH_2OH) 4.01 (3H, s, ArOCH_3), 4.00 (3H, s, ArOCH_3), 3.84 (3H, s,

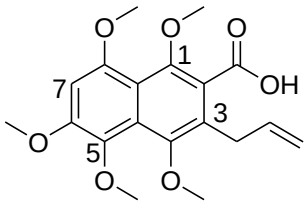
ArOC*H*$_3$), 3.79 (3H, s, ArOC*H*$_3$), 3.78-3.72 (5H, m, ArOC*H*$_3$, and ArC*H*$_2$CH=CH$_2$), 2.46 (1H, br s, ArCH$_2$O*H*); **^{13}C NMR (75 MHz, CDCl$_3$, Me$_4$Si)** δ_C 153.3 (C-8), 151.9 (C-10), 150.3 (C-4), 149.3 (C-6), 138.3 (Ar-C), 136.7 (ArCH$_2$*C*H=CH$_2$), 130.3 (Ar-C), 128.6 (Ar-C), 125.8 (Ar-C), 116.4 (ArCH$_2$CH=*C*H$_2$), 115.3 (Ar-C), 97.1 (C-7), 63.2 (ArO*C*H$_3$), 62.6 (ArO*C*H$_3$), 62.0 (ArO*C*H$_3$), 57.4 (Ar*C*H$_2$OH), 56.9 (ArO*C*H$_3$), 56.8 (ArO*C*H$_3$), 30.4 (Ar*C*H$_2$CH=CH$_2$); **HRMS** (*m*/*z*), calculated for $C_{19}H_{25}O_6$: 349.1646, found $(M + H)^+$ 349.1650.

7.9.18 Synthesis of 3-allyl-1,4,5,6,8-pentamethoxynaphthalene-2-carboxylic acid 231

To a solution of alcohol **269** (3.00 g, 8.61 mmol) in CH_2Cl_2 (150 mL), flash silica (1.50 g) and PCC (3.64 g, 16.9 mmol) were added portion-wise and the reaction mixture was stirred under N_2 (g) for 4 hrs. After the starting material was completely consumed (monitored by TLC), the reaction mixture was filtered through a bed of Celite® in a fume hood and the filtrate was concentrated *in vacuo*. The resultant viscous oil was taken to the next step without further purification apart from noting the difference in R_f value to the starting material. The crude intermediate **270** was dissolved in 2-methyl-2-butene (113 mL) in a 500 mL round bottom flask to which H_2O (187 mL), *t*-BuOH (169 mL), $NaClO_2$ (2.71 g, 30.0 mmol) and NaH_2PO_4 (3.60 g, 30.0 mmol) were added. The biphasic mixture was stirred rapidly for 6 hrs after which the layers were separated and the aqueous layer was further extracted into CH_2Cl_2 (3 × 100 mL). The combined organic layers were dried over $MgSO_4$, filtered through a Celite® bed and concentrated *in vacuo*. The residue was purified by column chromatography (30% EtOAc/hexane) on silica gel and the isolated product was re-crystallized from a hot (20% EtOAc/hexane) mixture affording 3-allyl-1,4,5,6,8-pentamethoxynaphthalene-2-carboxylic acid **231** as colourless crystals (2.06 g, 66%). **R_f** = 0.21 (50% EtOAc/hexane); **Mp** 140-142 ^oC; **IR ν_{max} (cm^{-1})** 3680 (O-H), 1692 (C=O), 1637 (C=C);

^{1}H NMR (300 MHz, CDCl$_3$, Me$_4$Si) δ_H 10.80 (1H, s, ArCO$_2$*H*), 6.76 (1H, s, H-7), 6.04 (1H, ddt, *J* = 16.3, 10.1, 6.2 Hz, ArCH$_2$C*H*=CH$_2$), 5.14 (1H, dd, *J* = 13.8, 1.7 Hz, one of ArCH$_2$C*H*=CH$_2$), 5.10 (1H, dd, *J* = 13.8, 1.6 Hz, one of ArCH$_2$C*H*=CH$_2$), 4.02 (3H, s, ArOC*H*$_3$), 4.00 (3H, s, ArOC*H*$_3$), 3.90 (3H, s, ArOC*H*$_3$), 3.81 (3H, s, ArOC*H*$_3$), 3.80 (3H, s,

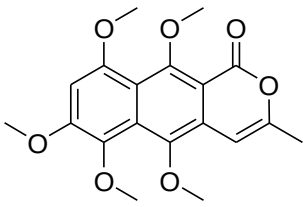
ArOCH_3), 3.70 (2H, d, J = 6.2 Hz, ArCH_2CH=CH_2); **^{13}C NMR (75 MHz, $CDCl_3$, Me_4Si)** δ_C 172.4 (ArCO$_2$H), 153.8 (C-8), 151.3 (C-10), 150.3 (Ar-C), 149.3 (Ar-C), 136.6 (ArCH$_2$$C$H=CH$_2$), 127.6 (Ar-C), 126.6 (Ar-C), 124.3 (Ar-C), 116.0 (ArCH$_2$CH=CH$_2$), 115.8(Ar-C), 97.3 (H7), 63.9 (ArOCH$_3$), 62.7 (ArOCH$_3$), 62.0 (ArOCH$_3$), 56.9 (ArOCH$_3$), 56.8 (ArOCH$_3$), 31.4 (ArCH$_2$CH=CH$_2$). **HRMS** (*m*/*z*), calculated for $C_{19}H_{23}O_7$: 363.1438, found $(M + H)^+$ 363.1440.



231

7.9.19 Synthesis of 5,6,7,9,10-pentamethoxy-3-methyl-1*H*-benzo[*g*]isochromen-1-one 229

To a 250 mL 2-neck round bottom flask equipped with a magnetic stirring bar and charged with 3-allyl-1,4,5,6,8-pentamethoxynaphthalene-2-carboxylic acid **231** (2.00 g, 5.52 mmol) in DMF/H_2O (150 mL, v/v, 2:1) was added $CuCl_2.2H_2O$ (1.77 g, 10.4 mmol). The reaction mixture was vigorously stirred under a blanket of O_2 (g). After 10 min of stirring, $PdCl_2$ (97.9 mg, 0.552 mmol) was added to the reaction mixture and it was further stirred vigorously for 24 hrs at rt. The reaction mixture was then filtered through a thick Celite® bed and the pad was washed with CH_2Cl_2 (3 × 50 mL). The combined organic layers were washed with brine (3 × 50 mL), dried over anhydrous $MgSO_4$, filtered through a number one sintered glass funnel and the solvent was removed *in vacuo*. The residue was adsorbed onto silica and purification by column chromatography (EtOAc/CH_2Cl_2/hexane 3:1:6) afforded 5,6,7,9,10-pentamethoxy-3-methyl-1*H*-benzo[*g*]isochromen-1-one **229** as a cream crystalline solid (1.43 g, 72%). $\mathbf{R_f}$ = 0.43 **(**EtOAc/CH_2Cl_2/hexane 4:2:4). The ^{1}H NMR spectrum was the same the one discussed in **Section 7.9.15**.

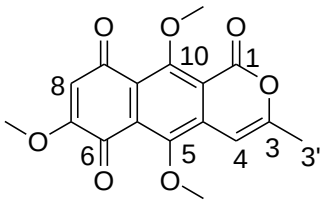


229

7.9.20 Synthesis of 5,7,10-trimethoxy-3-methyl-1*H*-benzo[*g*]isochromene-1,6,9-trione 35

AgO (1.18 g, 9.50 mmol) was added to the stirred solution of 5,6,7,9,10-pentamethoxy-3-methyl-1*H*-benzo[*g*]isochromen-1-one **229** (1.60 g, 4.44 mmol) in 1,4-dioxane (40 mL). The reaction mixture was stirred for 10 min at rt after which 55% (v/v) aqueous HNO_3 was added drop-wise until all AgO dissolved. The resultant solution was stirred for a further 5 min which was followed by addition of CH_2Cl_2 (50 mL) and H_2O (50 mL). The lower organic

layer was separated and the aqueous solution was further extracted into CH_2Cl_2 (2 × 100 mL). The combined organic layers were dried over anhydrous MgSO4, filtered through a Celite® bed and concentrated under reduced pressure. Purification of the residue by silica gel column chromatography (EtOAc/hexane/CH_2Cl_2) afforded 5,7,10-trimethoxy-3-methyl-1*H*-benzo[*g*]isochromene-1,6,9-trione **35** as an orange amorphous solid (1.10 g, 75%). $\mathbf{R_f}$ = 0.40 **(**EtOAc/CH_2Cl_2/hexane 4:2:4); **Mp** 220-222; **IR** $\boldsymbol{\nu_{max}}$**(cm^{-1})** 1788 (C=O), 1762 (C=O), 1712 (C=C), 1693 (C=C), 1606 (C=C);

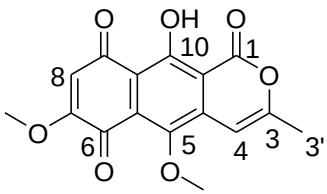


35

^{1}H NMR (300 MHz, $CDCl_3$, Me_4Si) δ_H 6.66 (1H, s, H-8), 6.12 (1H, s, H-4), 4.02 (3H, s, ArOC*H*$_3$), 3.93 (3H, s, ArOC*H*$_3$), 3.88 (3H, s, ArOC*H*$_3$), 2.34 (3H, s, H-3'); **^{13}C NMR (126 MHz, $CDCl_3$, Me_4Si)** δ_C 182.4 (C=O), 178.9 (C=O), 159.3 (Ar-C), 159.1 (Ar-C), 159.0 (Ar-C), 157.4 (Ar-C), 151.0 (Ar-C), 141.2 (Ar-C), 127.7 (Ar-C), 123.4 (Ar-C), 119.4 (Ar-C), 111.6 (C-4), 97.8 (C-8), 63.0 (ArO*C*H$_3$), 62.8 (ArO*C*H$_3$), 56.5 (ArO*C*H$_3$), 20.2 (C-3'); **HRMS** (*m*/*z*), calculated for $C_{17}H_{15}O_7$: 331.0812, found $(M + H)^+$ 331.0814.

7.9.21 Synthesis of 10-hydroxy-5,7-dimethoxy-3-methyl-1*H*-benzo[*g*]isochromene-1,6,9-trione (5-methoxy-3,4-dehydroxanthomegnin) 34[108]

5,7,10-Trimethoxy-3-methyl-1*H*-benzo[*g*]isochromene-1,6,9-trione **35** (0.334 g, 1.01 mmol) was dissolved in a freshly distilled CH_2Cl_2 (50 mL) in a 150 mL 2-neck round bottom flask fitted with a rubber septum. The reaction flask was cooled to -78 °C under a blanket of N_2 (g) and BCl_3 (2.02 mL, 2.02 mmol) was slowly added to the solution using a syringe. The reaction mixture was stirred for a further 40 min at -78 °C and was then allowed to warm to rt. The mixture was stirred at this temperature for 2 hrs after which it was carefully quenched with cold H_2O (100 mL) and the lower layer was separated. The aqueous medium was further extracted into CH_2Cl_2 (2 × 50 mL) and the combined organic layers were dried over anhydrous $MgSO_4$, filtered through a Celite® bed and concentrated under reduced pressure. The residue was purified on deactivated silica gel column chromatography (20% EtOAc/hexane) affording 10-hydroxy-



34

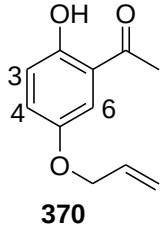
5,7,9-trimethoxy-3-methyl-1*H*-benzo[*g*]isochromen-1-one **34** as a dirty-red solid (51.1 mg, 20%). $\mathbf{R_f}$ = 0.49 **(**EtOAc/CH_2Cl_2/hexane 3:2:5);

^{1}H NMR (500 MHz, $CDCl_3$) δ_H 14.57 (1H, s, O*H* attached to C-10), 6.67 (1H, s, H8), 6.16 (1H, s, H-4), 3.94 (3H, s, ArOCH_3), 3.88 (3H, s, ArOCH_3), 2.37 (3H, s, C-3'); **^{13}C NMR (126 MHz, $CDCl_3$, Me_4Si)** δ_C 189.3 (C-9), 177.9 (C-6), 161.4 (C-1), 161.0 (C-10), 160.7 (C-7), 157.7 (C-3), 148.0 (C-5), 143.5 (C-5a), 125.1 (C-4a), 113.0 (C-10a), 111.2 (C-9a), 109.3 (C-8), 98.3 (C-4), 62.3 (ArO*C*H_3), 56.9 (ArO*C*H_3), 20.4 (C-3').

7.10 Experimental procedures for attempted synthesis of ferrocenyl (±)-*trans*-3,4-dihydro-1,3-dimethyl-6-vinyl-1*H*-isochromene-5,8-dione *trans*-368

7.10.0 Synthesis of 1-(5-allyloxy-2-hydroxyphenyl)ethanone 370[119]

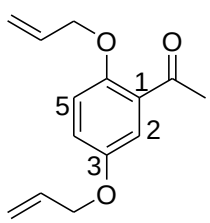
To a vigorously stirred mixture of 1-(2,5-dihydroxyphenyl)ethanone **369** (4.50 g, 29.6 mmol) and K_2CO_3 (4.49 g, 32.5 mmol) in acetone (700 mL) in a 1000 mL 2-neck round bottom flask fitted with a dropping funnel was added allyl bromide (3.93 g, 32.5 mmol) drop-wise for a period of 1 hr. The mixture was heated at reflux under the atmosphere of N_2 (g) for 24 hrs after which it was allowed to cool to rt, filtered through a bed of Celite®, and the filtrate concentrated *in vacuo*. A resultant crude concentrate was purified by column chromatography (10% EtOAc/hexane) on silica gel yielding two allyl ethers. The first allyl ether was 1-(5-allyloxy-2-hydroxyphenyl)ethanone **370** which was obtained as a pale yellow oil (3.53 g, 62%). $\mathbf{R_f}$ = 0.53 (15% EtOAc/hexane);



370

^{1}H NMR (300 MHz, $CDCl_3$, Me_4Si) δ_H 11.86 (1H, s, ArO*H*), 7.22 (1H, d, *J* = 3.0 Hz, H-6), 7.13 (1H, dd, *J* = 9.0, 3.0 Hz, H-4), 6.92 (1H, d, *J* = 9.0 Hz, H-3), 6.13-5.98 (1H, m, ArOCH_2C*H*=CH_2), 5.42 (1H, dq, *J* = 17.3, 3.1, 1.5 Hz, ArOCH_2CH=CH_2), 5.31 (1H, dq, *J* = 10.5, 2.6, 1.3 Hz, ArOCH_2CH=CH_2), 4.52 (2H, dt, *J* = 5.3, 1.4 Hz, ArOCH_2CH=CH_2), 2.61 (3H, s, ArCOCH_3); **^{13}C NMR (75 MHz, $CDCl_3$, Me_4Si)** δ_C 202.4 (Ar*C*OCH_3), 156.8 (C-5), 151.1 (C-2), 133.1 (ArOCH_2*C*H=CH_2), 125.0 (C-6), 121.2 (C-1), 119.1 (C-4), 118.0 (ArOCH_2CH=*C*H_2), 114.9 (C-3), 69.8 (ArO*C*H_2CH=CH_2), 29.7 (ArCO*C*H_3).

The second allyl ether was 1-(2,-*bis*(allyloxy)ethanone **371** which was obtained as a pale yellow semi-solid (0.688 g, 10%). $\mathbf{R_f}$ = 0.53 (15% EtOAc/hexane);



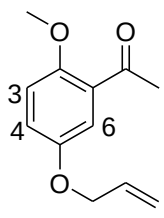
371

^{1}H NMR (300 MHz, $CDCl_3$, Me_4Si) δ_H 7.30 (1H, d, *J* = 3.2 Hz, H-2), 7.02 (1H, dd, *J* = 9.0, 3.2 Hz, H-4), 6.88 (1H, d, *J* = 9.0 Hz, H-5), 6.15-5.94 (2H, m, 2 × $ArOCH_2CH$=CH_2), 5.43 (1H, dd, *J* = 5.4, 1.6 Hz, one of $ArOCH_2CH$=CH_2), 5.38 (1H, dd, *J* = 5.4, 1.6 Hz, one of $ArOCH_2CH$=CH_2), 5.34-5.22 (2H, m, 2 × one of $ArOCH_2CH$=CH_2), 4.58 (2H, dt, *J* = 5.3, 1.4 Hz, $ArOCH_2CH$=CH_2), 4.51 (2H, dt, *J* = 5.3, 1.5 Hz, $ArOCH_2CH$=CH_2), 2.64 (3H, s, $ArC(O)CH_3$).

7.10.1 Synthesis of 1-(5-allyloxy-2-methoxyphenyl)ethanone 372[119]

1-(5-Allyloxy-2-hydroxyphenyl)ethanone **370** (5.28 g, 27.5 mmol) was dissolved in acetone (150 mL) in a 250 mL round bottom flask to which K_2CO_3 (5.53 g, 40.0 mmol) and dimethyl sulfate (3.78 mL, 40.0 mmol) were added. The mixture was heated at reflux under the N_2 (g) for 72 hrs. It was then allowed to cool to rt, filtered through a Celite® bed and the filtrate was concentrated *in vacuo*. The resultant brown oil was re-dissolved in EtOAc (150 mL) in a 500 mL separating funnel and then washed with 25% (v/v) aqueous NH_3 (2 × 50 mL) until no further effervescence was observed. This was followed by washing with a 32% (v/v) aqueous HCl (2 × 40 mL) then H_2O until the aqueous layer was neutral. The organic layer was then dried over anhydrous $MgSO_4$ and filtered through a Celite® bed. The solvent was removed *in vacuo* and the resultant crude residue was purified by silica gel column chromatography (10% EtOAc/hexane) affording 1-(5-allyloxy-2-methoxyphenyl)ethanone **372** (4.65 g, 82%) as a colourless oil. $\mathbf{R_f}$ = 0.49 (15% EtOAc/hexane);

^{1}H NMR (300 MHz, $CDCl_3$, Me_4Si) δ_H 7.30 (1H, d, *J* = 3.2 Hz, H6), 7.01 (1H, dd, *J* = 9.0, 3.2 Hz, H-4), 6.87 (1H, d, *J* = 9.0 Hz, H-3), 6.08-5.92 (1H, m, $ArOCH_2CH$=CH_2), 5.38 (1H, dq, *J* = 17.3, 3.2, 1.6 Hz, $ArOCH_2CH$=CH_2), 5.24 (1H, dq, *J* = 10.5, 2.8, 1.3 Hz, $ArOCH_2CH$=CH_2), 4.47 (2H, dt, *J* = 5.2, 1.5 Hz, $ArOCH_2CH$=CH_2), 3.83 (3H, s, $ArOCH_3$), 2.58 (3H, s, $ArCOCH_3$).



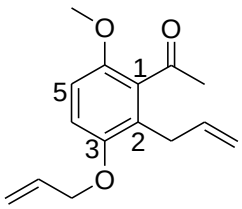
372

^{13}C NMR (75 MHz, $CDCl_3$, Me_4Si) δ_C 199.1 ($ArCOCH_3$), 152.5 (C-5), 151.1

(C-2), 133.2 (ArOCH$_2$*C*H=CH$_2$), 128.8 (C-1), 120.9 (C-4), 117.9 (ArOCH$_2$CH=*C*H$_2$), 117.6 (C-6), 114.6 (C-3), 70.0 (ArO*C*H$_2$CH=CH$_2$), 56.3 (ArO*C*H$_3$), 32.0 (ArCO*C*H$_3$).

7.10.2 Synthesis of 1-(2-allyl-3-(allyloxy)-6-methoxyphenyl)ethanone 373 and 1-(4-allyl-5-(allyloxy)-2-methoxyphenyl)ethanone 374[119]

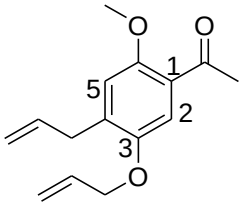
1-(5-Allyloxy-2-methoxyphenyl)ethanone **372** (4.75 g, 23.0 mmol) in a 100 mL round bottom flask was heated at 170 °C in a silicon oil bath under the N_2 (g) for 24 hrs. The resultant dark oil was allowed to cool to rt and purified by column chromatography (EtOAc/hexane 10%) on silica gel affording a mixture of 1-(2-allyl-3-hydroxy-6-methoxyphenyl)ethanone and 1-(4-allyl-5-hydroxy-2-methoxyphenyl)ethanone (4.08 g, 86%). No further analysis was carried out on this intermediate except noting a small difference in R_f values on TLC plate. To a mixture of semi-solid intermediate (4.00 g, 19.4 mmol) and K_2CO_3 (3.54 g, 25.6 mmol) in acetone (100 mL) in a 250 mL round bottom flask, was added allyl bromide (3.10 g, 25.6 mmol). The reaction mixture was then heated to reflux for 24 hours after which it was allowed to cool to room temperature, filtered through a Celite® bed and the filtrate was concentrated *in vacuo*. The resultant residue was purified by column chromatography (10% EtOAc-hexane) on silica gel yielding a pale yellow oil, 1-(2-allyl-3-(allyloxy)-6-methoxyphenyl)ethanone **373** (2.49 g, 51%), as one of the two compounds. $\mathbf{R_f}$ = 0.53 (15% EtOAc/hexane);



373

^{1}H NMR (300 MHz, $CDCl_3$, Me_4Si) δ_H 6.81 (1H, d, *J* = 8.9 Hz, H-4), 6.71 (1H, d, *J* = 8.9 Hz, H-5), 6.12-5.77 (2H, m, ArOCH$_2$C*H*=CH$_2$ and ArCH$_2$C*H*=CH$_2$), 5.39 (1H, dq, *J* = 17.3, 1.6 Hz, one of ArOCH$_2$CH=C*H*$_2$), 5.24 (1H, dq, *J* = 10.1, 1.0 Hz, one of ArOCH$_2$CH=C*H*$_2$), 5.05-4.85 (2H, m, ArCH$_2$CH=C*H*$_2$), 4.48 (2H, dt, *J* = 4.9, 1.6 Hz, ArOC*H*$_2$CH=CH$_2$), 3.75 (3H, s, ArOC*H*$_3$), 3.35 (2H, d, *J* = 6.3 Hz, ArC*H*$_2$CH=CH$_2$), 2.46 (3H, s, ArC(O)C*H*$_3$); **^{13}C NMR (75 MHz, $CDCl_3$, Me_4Si)** δ_C 205.1 (Ar*C*(O)CH$_3$), 150.8 (C-6), 150.0 (C-3), 136.5 (ArCH$_2$*C*H=CH$_2$), 133.5 (ArOCH$_2$*C*H=CH$_2$), 132.9 (C-2), 126.2 (C-4), 116.9 (ArCH$_2$CH=*C*H$_2$), 115.2 (ArOCH$_2$CH=*C*H$_2$), 113.3 (C-1), 109.4 (C-5), 69.8 (ArO*C*H$_2$CH=CH$_2$), 56.0 (ArO*C*H$_3$), 32.5 (Ar*C*H$_2$CH=CH$_2$), 30.9 (ArC(O)*C*H$_3$).

The second product was a double allyl benzene, 1-(4-allyl-5-(allyloxy)-2-methoxyphenyl)ethanone **374**, and was obtained as a yellow semi-solid (1.12 g, 23%). $\mathbf{R_f}$ = 0.53 (15% EtOAc/hexane);

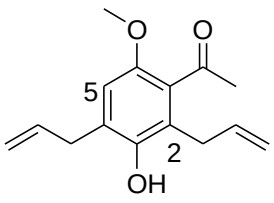


374

^{1}H NMR (300 MHz, $CDCl_3$, Me_4Si) δ_H 7.31 (1H, s, H-2), 6.79 (1H, s, H-5), 6.19-5.88 (2H, m, $ArOCH_2CH$=CH_2 and $ArCH_2CH$=CH_2), 5.41 (1H, dq, *J* = 17.3, 1.7 Hz, one of $ArOCH_2CH$=CH_2), 5.25 (1H, dq, *J* = 10.5, 1.5 Hz, one of $ArOCH_2CH$=CH_2), 5.12 (1H, dq, *J* = 7.6, 1.5 Hz, one of $ArCH_2CH$=CH_2), 5.08 (1H, t, *J* = 1.4 Hz, one of $ArOCH_2CH$=CH_2), 4.53 (2H, dt, *J* = 5.0, 1.6 Hz, $ArOCH_2CH$=CH_2), 3.87 (3H, s, $ArOCH_3$), 3.44 (2H, d, *J* = 6.7 Hz, $ArCH_2CH$=CH_2), 2.60 (3H, s, $ArC(O)CH_3$); **^{13}C NMR (75 MHz, $CDCl_3$, Me_4Si)** δ_C 198.6 ($ArC(O)CH_3$), 153.9 (C-6), 150.1 (C-3), 135.8 ($ArCH_2CH$=CH_2), 135.8 ($ArOCH_2CH$=CH_2), 133.4 (C-4), 125.8 (C-1), 117.0 ($ArCH_2CH$=CH_2), 116.3 ($ArOCH_2CH$=CH_2), 113.8 (C-5), 113.0 (C-2), 69.4 ($ArOCH_2CH$=CH_2), 56.0 ($ArOCH_3$), 34.6 ($ArCH_2CH$=CH_2), 32.0 ($ArC(O)CH_3$).

7.10.3 Synthesis of 1-(2,4-diallyl-3-hydroxy-6-methoxyphenyl)ethanone 375[119]

The mixture of allyl ethers **373** and **374** (4.30 g, 17.5 mmol) was charged in a 100 mL round bottom flask and heated at 170 °C in a silicon oil bath under the N_2 (g) for 24 hrs. The resultant dark oil was allowed to cool to rt and then purified by column chromatography (10% EtOAc/hexane) affording the desired product, 1-(2,4-diallyl-3-hydroxy-6-methoxyphenyl)ethanone **375**, (3.06 g, 71%), as a pale yellow viscous oil. $\mathbf{R_f}$ = 0.39 (15% EtOAc/hexane); **IR ν_{max} (cm^{-1})** 3515 (O-H), 1702 (C=O), 1618 (C=C);

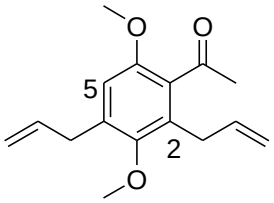


375

^{1}H NMR (300 MHz, $CDCl_3$, Me_4Si) δ_H 6.61 (1H, s, H-5), 6.09-5.84 (2H, m, 2 × $ArCH_2CH$=CH_2), 5.23-5.01 (4H, m, 2 × $ArCH_2CH$=CH_2), 4.90 (1H, s, ArOH), 3.77 (3H, s, $ArOCH_3$), 3.40 (2H, dt, *J* = 6.3, 1.3 Hz, 2 × $ArCH_2CH$=CH_2), 3.32 (2H, dt, *J* = 6.0, 1.6 Hz, 2 × $ArCH_2CH$=CH_2), 2.47 (3H, s, $ArCOCH_3$); **^{13}C NMR (75 MHz, $CDCl_3$, Me_4Si)** δ_C 199.9 ($ArCOCH_3$), 150.2 (C-6), 146.1 (C-3), 136.1 and 135.8 (2 × $ArCH_2CH$=CH_2), 128.8 (C-2), 123.9 (C-4), 117.9 and 117.1 (2 × $ArCH_2CH$=CH_2), 117.6 (C-1), 114.6 (C-5), 56.3 ($ArOCH_3$), 35.9 and 32.7 (2 × $ArOCH_2CH$=CH_2), 29.5 ($ArCOCH_3$).

7.10.4 Synthesis of 1-(2,4-diallyl-3,6-dimethoxyphenyl)ethanone 376[119]

To a mixture of 1-(2,4-diallyl-3-hydroxy-6-methoxyphenyl)ethanone **375** (3.00 g, 12.2 mmol) and K_2CO_3 (0.810 g, 15.9 mmol) in acetone (100 mL) was added dimethyl sulfate (1.50 mL, 15.9 mmol) *via* a syringe. The reaction mixture was then heated to reflux in a silicon oil bath for 24 hrs. After the 24 hrs had elapsed, the mixture was allowed to cool to rt, filtered through Celite® and the filtrate was concentrated on a rotary evaporator. The resultant brown oil was re-dissolved in EtOAc (150 mL) in a 500 mL separating funnel and washed with 25% (v/v) aqueous NH_3 (2 × 100 mL) until no effervescence was observed. This was followed by washing with a 32% (v/v) aqueous HCl (2 × 40 mL) and then H_2O until the aqueous layer was neutral. The organic layer was then dried over anhydrous $MgSO_4$, filtered through a Celite® bed and the solvent was removed *in vacuo*. The resultant oil residue was purified by silica gel column chromatography (10% EtOAc/hexane) yielding 1-(2,4-diallyl-3,6-dimethoxyphenyl)ethanone **376** (2.76 g, 87%) as a pale yellow oil. $\mathbf{R_f}$ = 0.47 (10% EtOAc/hexane); **IR ν_{max} (cm^{-1})** 1715 (C=O), 1602 (C=C);



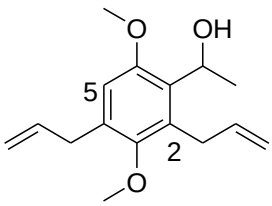
376

^{1}H NMR (300 MHz, $CDCl_3$, Me_4Si) δ_H 6.63 (1H, s, H-5), 6.07–5.80 (2H, m, 2 × $ArCH_2CH$=CH_2), 5.17-4.89 (4H, m, 2 × $ArCH_2CH$=CH_2), 3.78 (3H, s, $ArOCH_3$), 3.68 (3H, s, $ArOCH_3$), 3.42 (4H, 2 overlapping dt, J = 11.6, 1.6 Hz, 2 × $ArCH_2CH$=CH_2), 2.45 (3H, s, $ArCOCH_3$); **^{13}C NMR (75 MHz, $CDCl_3$, Me_4Si)** δ_C 199.3 ($ArCOCH_3$), 153.4 (C-6), 150.1 (C-3), 136.9 and 136.1 (2 × $ArCH_2CH$=CH_2), 134.8 (C-4), 130.8 (C-2), 116.7 and 115.5 (2 × $ArCH_2CH$=CH_2), 115.0 (C-1) 111.3 (C-5), 61.5 and 55.8 (2 × $ArOCH_3$), 34.7 and 32.4 (2 × $ArCH_2CH$=CH_2) and 28.1 ($ArCOCH_3$).

7.10.5 Synthesis of 1-(2,4-diallyl-3,6-dimethoxyphenyl)ethanol 377[119]

In an oven dried 250 mL 2-neck round bottom flask equipped with a magnetic stirring bar was added 1-(2,4-diallyl-3,6-dimethoxyphenyl)ethanone **376** (2.70 g, 10.4 mmol) in dry THF (50.0 mL) stirred at 0 °C under the N_2 (g). $LiAlH_4$ (0.588 g, 15.5 mmol) was added portion-wise and the reaction mixture was allowed to cool to rt and stirred at this temperature for 4 hrs. After the 4 hrs had elapsed, the mixture was cooled to 0 °C for the second time and H_2O (50 mL), followed by a 3.75 M NaOH aqueous solution (5.00 mL) were added. The solution

was filtered through a Celite® bed and the filtrate was concentrated under the reduced pressure. The aqueous medium was extracted into EtOAc (3 × 200 mL) and the combined organic layers were dried over anhydrous $MgSO_4$, filtered using a Celite® pad and concentrated *in vacuo*. The residue was purified by silica gel column chromatography (30% EtOAc/hexane) affording 1-(2,4-diallyl-3,6-dimethoxyphenyl)ethanol **377** (1.94 g, 71%) as a viscous pale yellow oil. $\mathbf{R_f}$ = 0.37 (10% EtOAc/hexane); **IR ν_{max} (cm^{-1})** 3570 (O-H), 1624 (C=C), 1220 (C-O);



377

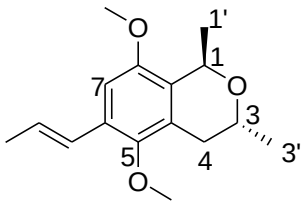
^{1}H NMR (300 MHz, $CDCl_3$, Me_4Si) δ_H 6.66 (1H, s, H-5), 6.05-5.89 (2H, m, 2 × $ArCH_2CH$=CH_2), 5.17-4.90 (5H, m, 2 × $ArCH_2CH$=CH_2 overlapping with $ArCH(OH)CH_3$, 3.85 (3H, s, OCH_3), 3.66 (3H, s, OCH_3), 3.59-3.35 (4H, m, 2 × $ArCH_2CH$=CH_2), 1.52 (3H, d, *J* = 6.7 Hz, $ArCH(OH)CH_3$); **^{13}C NMR (75 MHz, $CDCl_3$, Me_4Si)** δ_C 154.0 (C-3), 150.6 (C-6), 137.1 and 137.0 (2 × $ArCH_2CH$=CH_2), 131.9 (C-2), 130.8 (C-1 or C-4), 130.4 (C-1 or C-4), 116.1 and 115.6 (2 × $ArCH_2CH$=CH_2), 111.3 (C-5), 67.3 ($ArCH(OH)CH_3$), 61.8 ($ArOCH_3$), 55.4 ($ArOCH_3$), 34.2 and 30.4 (2 × $ArCH_2CH$=CH_2), 23.5 ($ArCH(OH)CH_3$);

7.10.6 Synthesis of (±)-*trans*-3,4-dihydro-5,8-dimethoxy-1,3-dimethyl-6-[(*E*)-1-propenyl]-1*H*-isochromene *trans*-378[119]

In a 2-neck 500 mL round bottom flask equipped with a magnetic stirring bar was placed 1-(2,4-diallyl-3,6-dimethoxyphenyl)ethanol **377** (1.90 g, 7.24 mmol) in a freshly distilled anhydrous *N*-methylpyrrolidinone (80 mL) and the solution was heated to 100 °C under the N_2 (g). Sublimed *t*-BuOK (3.21 g, 28.6 mmol) was added in one-portion and stirring was continued for 30 min after which the reaction was carefully quenched with ice cold H_2O (100 mL). The crude product was extracted into CH_2Cl_2 (3 × 100 mL) and the combined organic layers were dried over anhydrous $MgSO_4$, filtered through a Celite® pad and concentrated *in vacuo*. The bulk of the solvent (*N*-methylpyrrolidinone) was distilled off under vacuum and purification of the residue by column chromatography (10% EtOAc/hexane) on silica gel afforded (±)-*trans*-3,4-dihydro-5,8-dimethoxy-1,3-dimethyl-6-[(*E*)-1-propenyl]-1*H*-

isochromene ***trans*-378** (1.20 g, 63%) as colourless crystals. $\mathbf{R_f}$ = 0.33 (20% EtOAc/hexane); **Mp** 93-94 °C; **IR ν_{max} (cm^{-1})** 1577 (C=C), 1222 (C-O);

^{1}H NMR (300 MHz, $CDCl_3$, Me_4Si) δ_H 6.74 (1H, s, H-7), 6.65 (1H, dq, *J* = 15.9, 1.6 Hz, ArC*H*=CHCH$_3$), 6.21 (1H, dq, *J* = 15.7, 6.6 Hz, ArCH=C*H*CH$_3$), 5.06 (1H, q, *J* = 6.5 Hz, H-1), 4.13-3.95 (1H, m, H-3), 3.78 (3H, s, ArOC*H*$_3$), 3.66 (3H, s, ArOC*H*$_3$), 2.83 (1H, dd, *J* = 16.8, 3.2 Hz, H-4 *pseudo*-equatorial), 2.38 (1H, dd, *J* = 16.8, 10.8 Hz, H-4 *pseudo*-axial), 1.91 (3H, dd, *J* = 6.6, 1.6 Hz, ArCH=CHC*H*$_3$), 1.49 (3H, d, *J* = 6.6 Hz, H-1'), 1.33 (3H, d, *J* = 6.1 Hz, H-3'); **^{13}C NMR (75 MHz, $CDCl_3$, Me_4Si)** δ_C 152.2 (C-8), 148.9 (C-5), 129.3 (Ar*C*H=CH$_2$CH$_3$), 128.3 (C-8a), 128.4 (C-4a), 126.7 (ArCH=*C*H$_2$CH$_3$), 126.7 (C-6), 106.5 (C-7), 68.2 (C-1), 62.6 (C-3), 61.2 (ArOCH$_3$), 55.6 (ArOCH$_3$), 31.0 (C-4), 22.3 (C-3'), 20.1 (C-1'), 19.3 ArCH=CH$_2$*C*H$_3$). **HRMS** (*m*/*z*), calculated for $C_{16}H_{23}O_3$: 263.1642, found $(M + H)^+$ 263.1641.



***trans*-378**

7.10.7 Synthesis of (±)-*trans*-3,4-dihydro-5,8-dimethoxy-1,3-dimethyl-1*H*-isochromanene-6-carbaldehyde *trans*-364[119]

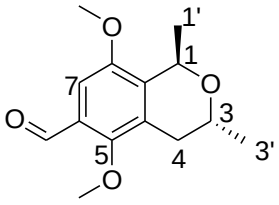
Method one:

(±)-*Trans*-3,4-dihydro-5,8-dimethoxy-1,3-dimethyl-6-[(*E*)-1-propenyl]-1*H*-isochromene ***trans*-378** (1.60 g, 6.10 mmol) was dissolved in dry CH_2Cl_2 (30 mL) in an oven dried 2-neck round bottom flask fitted with a rubber septum to which Sudan(III) indicator (3 drops) was added. The mixture was cooled to -78 °C and ozone was bubbled into the reaction mixture using a syringe connected to the ozone generator until the colour of the solution changed from pink to colourless. N_2 (g) was then passed through the reaction mixture for 10 min after which dimethyl sulfide (1.89 mL, 25.8 mmol) was added to the reaction at -78 °C. The mixture was then warmed to rt and further stirred for 1 hr at this temperature. The solvent was removed *in vacuo* and the resultant residue was purified by silica gel column chromatography (30% EtOAc/hexane) in a fume hood. The product, (±)-*trans*-3,4-dihydro-5,8-dimethoxy-1,3-dimethyl-1*H*-isochroman-6-carbaldehyde ***trans*-364**, (1.04 g, 68%), was isolated as cream-white fluffy needles.

Method two:

To a stirred solution of (±)-*trans*-3,4-dihydro-5,8-dimethoxy-1,3-dimethyl-6-[(*E*)-1-propenyl]-1*H*-isochromene ***trans*-378** (1.40 g, 5.34 mmol) in 1,4-dioxane (40 mL) was added a catalytic amount of osmium(VIII) oxide (0.136 g, 0.534 mmol). After stirring for 30 min, H_2O (10 mL) was added followed by sodium periodate (2.25 g, 10.5 mmol) in small portions over a period of 1 hr and the mixture was stirred for a further 12.5 hrs. The reaction mixture was then acidified with 32% (v/v) aqueous HCl and concentrated under reduced pressure leaving an aqueous residue. The aqueous medium was extracted into CH_2Cl_2 (3 × 50 mL). The combined organic layers were dried over anhydrous $MgSO_4$, filtered through a Celite® pad and evaporated *in vacuo*. The resultant residue was purified by silica gel column chromatography (30% EtOAc/hexane) affording (±)-*trans*-3,4-dihydro-5,8-dimethoxy-1,3-dimethyl-1*H*-isochroman-6-carbaldehyde ***trans*-364** (1.12 g, 84%) as cream-white fluffy needles. $\mathbf{R_f}$ = 0.41 (10% EtOAc/hexane); **Mp** 126-127 °C; **IR ν_{max} (cm^{-1})** 2870 (H-CO), 1692 (C=O);

^{1}H NMR (300 MHz, $CDCl_3$, Me_4Si) δ_H 10.32 (1H, s, ArC*H*O), 7.12 (1H, s, H-7), 5.08 (1H, q, *J* = 6.6 Hz, H-1), 4.18-3.96 (1H, m, H-3), 3.85 (3H, s, ArOCH_3), 3.84 (3H, s, ArOCH_3), 2.88 (1H, dd, *J* = 16.9, 3.2 Hz, H-4 *pseudo*-equatorial), 2.43 (1H, dd, *J* = 16.9, 10.7 Hz, H-4 *pseudo*-axial), 1.51 (3H, d, *J* = 6.7 Hz, H-1'), 1.37 (3H, d, *J* = 6.1 Hz, H-3'); **^{13}C NMR (75 MHz, $CDCl_3$, Me_4Si)** δ_C 189.4 (Ar*C*HO), 155.7 (C-5), 152.1 (C-8), 137.0 (C-8a), 129.3 (C-6), 127.1 (C-4a), 105.0 (C-7), 68.5 (C-1), 63.6 (C-3), 62.3 (ArO*C*H_3), 55.5 (ArO*C*H_3), 30.1 (C-4), 21.8 (C-3'), 19.2 (C-1'). **HRMS** (*m*/*z*), calculated for $C_{14}H_{19}O_4$: 251.2977, found $(M + H)^+$ 251.2980.

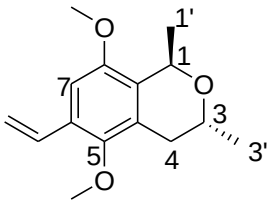


***trans*-364**

7.10.9 Synthesis of (±)-*trans*-3,4-dihydro-5,8-dimethoxy-1,3-dimethyl-6-vinyl-1*H*-isochromene *trans*-365

In a 50 mL 2-neck round bottom flask fitted with a rubber septum, 1.50 M *n*-butyllithium (1.58 mL, 2.37 mmol) was added drop-wise to a suspension of methyltriphenylphosphonium bromide (0.847 g, 2.37 mmol) in dry THF (20 mL) at rt. The resultant orange solution was stirred for a further 30 min before being cooled to 0 °C using an ice-bath. A solution of (±)-

trans-3,4-dihydro-5,8-dimethoxy-1,3-dimethyl-1*H*-isochromene-6-carbaldehyde ***trans*-364**, (0.253 g, 1.01 mmol) in dry THF (10 mL) was added drop-wise at 0 °C to the resulting ylide. The reaction was then warmed to rt and stirred at this temperature for 18 hrs. Upon completion, H_2O (50 mL) was added to the reaction mixture and THF was evaporated at reduced pressure leaving an aqueous medium. The crude product was extracted in EtOAc (3 × 80 mL) and the combined organic layers were dried over anhydrous $MgSO_4$. The mixture was then filtered through a bed of Celite®, solvent removed *in vacuo* and purification of the residue by silica gel column chromatography (5% EtOAc/hexane) yielded (±)-*trans*-3,4-dihydro-5,8-dimethoxy-1,3-dimethyl-6-vinyl-1*H*-isochromene ***trans*-365** as colourless crystals (0.206 g, 82%). $\mathbf{R_f}$ = 0.71 (15% EtOAc/hexane); **Mp** 73-74 °C; **IR ν_{max} (cm^{-1})** 2978 (=CH), 2940 (C-H), 1634 (C=C);



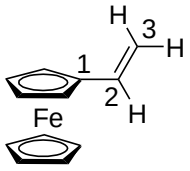
***trans*-365**

^{1}H NMR (300 MHz, $CDCl_3$, Me_4Si) δ_H 6.99 (1H, dd, *J* = 17.7, 11.1 Hz, ArC*H*=CH_2), 6.81 (1H, s, H-7), 5.71 (1H, dd, *J* = 17.7, 1.3 Hz, ArCH=CH_2 *trans*), 5.27 (1H, dd, *J* = 11.1, 1.3 Hz, ArCH=CH_2 *cis*), 5.07 (1H, q, *J* = 6.6 Hz, H-1), 4.11-3.95 (1H, m, H-3), 3.79 (3H, s, ArOCH_3), 3.66 (3H, s, ArOCH_3), 2.83 (1H, dd, *J* = 16.9, 3.3 Hz, H-4 *pseudo*-equatorial), 2.39 (1H, dd, *J* = 16.9, 10.8 Hz, H-4 *pseudo*-axial), 1.49 (3H, d, *J* = 6.6 Hz, H-1'), 1.33 (3H, d, *J* = 6.1 Hz, H-3'); **^{13}C NMR (75 MHz, $CDCl_3$, Me_4Si)** δ_C 151.8 (C-8), 149.2 (C-5), 131.7 (Ar*C*H=CH_2), 129.2 (C-8a), 128.5 (C-4a), 128.2 (C-6), 114.2 (ArCH=*C*H_2), 104.4 (C-7), 68.3 (C-1), 62.4 (C-3), 60.9 (ArO*C*H_3), 55.2 (ArO*C*H_3), 30.6 (C-4), 21.9 (C-3'), 19.6 (C-1'). **HRMS** (*m*/*z*), calculated for $C_{15}H_{21}O_3$: 249.1485, found $(M + H)^+$ 249.1487.

7.10.10 Synthesis of vinyl ferrocene 366[244]

To a suspension of methyltriphenylphosphonium bromide (1.79 g, 5.00 mmol) in dry THF (50 mL) in a 50 mL 2-neck round bottom flask fitted with a rubber septum was added 1.50 M *n*-butyllithium (3.33 mL, 5.00 mmol) drop-wise. The resulting orange solution was stirred for a further 30 min before being cooled to 0 °C in an ice-bath. Ferroaldehyde **309** (0.535 g, 2.50 mmol) in dry THF (5 mL) was added drop-wise to the resulting ylide at 0 °C. The reaction mixture was then warmed to rt and stirred at this temperature for 18 hrs. Upon completion,

the mixture was diluted with diethyl ether (50 mL) and washed with H_2O (50 mL). The organic extract was dried over anhydrous $MgSO_4$, filtered through a bed of Celite® and the solvent removed *in vacuo*. The resulting crude product was purified by silica gel column chromatography (3% EtOAc/hexane) affording vinyl ferrocene **366** as an amorphous orange solid (0.451 g, 85%). $\mathbf{R_f}$ = 0.66 (4% EtOAc/petroleum ether); **Mp** 51-53 ^oC; **IR ν_{max} (cm^{-1})** 1510 (C=C), 1021, 908, 814;



366

^{1}H NMR (300 MHz, $CDCl_3$, Me_4Si) δ_H 6.43 (1H, dd, *J* = 17.5, 10.8 Hz, H-2), 5.32 (1H, d, *J* = 17.5 Hz, one of H-3 in trans position), 5.01 (1H, d, *J* = 10.8 Hz, one of H-3 in *cis* position), 4.34 (2H, br s, Fc-H), 4.19 (2H, br s, Fc-H), 4.09 (5H, br s, Fc-H); **^{13}C NMR (75 MHz, $CDCl_3$, Me_4Si)** δ_C 134.8 (C-2), 111.2 (C-3), 83.7 (C-1), 69.4 (Fc-C), 68.8 (Fc-C), 68.5 (Fc-C), 66.8 (Fc-C).

7.10.11 Synthesis of ferrocenyl 3,4-dihydroisochromene *trans*-367

7.10.11.0 Method one: Grubbs cross-metathesis reaction

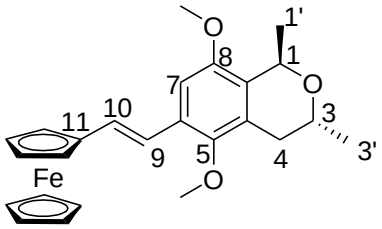
Grubbs (II) catalyst (39.0 mg, 0.050 mmol) was added to vigorously stirred solution of ***trans*-365** (0.571 g, 2.30 mmol) and **366** (0.976 g, 4.60 mmol) in dry degassed CH_2Cl_2 (10 mL). The reaction mixture was then refluxed for 18 hrs and upon completion, the reaction was cooled to rt and the solvent removed *in vacuo*. The residue was purified by silica gel column chromatography (5% EtOAc/hexane) yielding amorphous orange solid ***trans*-367** (0.587 g, 59%). $\mathbf{R_f}$ = 0.53 (6% EtOAc/petroleum ether).

7.10.11.1 Method two: McMurry cross-coupling metathesis reaction

Zinc powder (3.92 g, 60 mmol) was suspended in THF (30 mL) under nitrogen gas in an ice bath and titanium tetrachloride (6.64 g, 35 mmol) was added slowly *via* a syringe. The reaction mixture was removed from the cold bath after complete addition of $TiCl_4$ and was heated to reflux for 1.5 hrs. A second solution of ***trans*-364** (2.50 g, 10 mmol) and **309** (3.21 g, 15 mmol) in THF (25 mL) was added drop-wise to the cooled reaction mixture and reflux was continued for a further 12 hrs. After cooling, the reaction mixture was poured into H_2O (100 mL) and extracted into CH_2Cl_2 (3 × 100 mL). The combined organic layers were again

washed with H_2O (100 mL), dried over anhydrous $MgSO_4$, filtered through a pad of Celite® and the solvent was removed *in vacuo*. The crude product was purified on a silica gel column chromatography (2% EtOAc/petroleum ether) affording ***trans*-367** (3.03 g, 70%). $\mathbf{R_f}$ = 0.53 (6% EtOAc/petroleum ether); **Mp** 78-79 °C; **IR ν_{max} (cm^{-1})** 1631, 1320, 1250, 1000, 902, 823

^{1}H NMR (300 MHz, $CDCl_3$, Me_4Si) δ_H 6.66 (1H, s, H-7), 6.50 (1H, d, *J* = 11.9 Hz, H-10), 6.37 (1H, d, *J* = 11.9 Hz, H-11), 5.05 (1H, q, *J* = 6.5 Hz, H-1), 4.27-3.99 (10H, m, 9H from ferrocene and H-3), 3.77 (3H, s, ArOC*H*$_3$), 3.57 (3H, s, ArOC*H*$_3$), 2.86 (1H, dd, *J* = 16.9, 3.2 Hz, H4 *pseudo*-equatorial), 2.42 (1H, dd, *J* = 17.0, 10.8 Hz, *pseudo*-axial), 1.50 (3H, d, *J* = 6.6 Hz, H-3'), 1.36 (3H, d, *J* = 6.1 Hz, H-1');



***trans*-367**

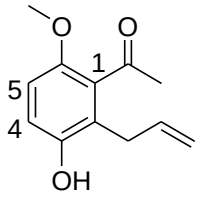
^{13}C NMR (75 MHz, $CDCl_3$, Me_4Si) δ_C 151.9 (C-8), 148.6 (C-5), 128.7 (C-9), 128.3 (C-8a), 128.2 (C-4a), 127.3 (C-10), 120.8 (C-6), 104.1 (C-7), 83.7 (C-11), 69.2 (Fc-C), 69.0 (Fc-C), 68.4 (C-1), 67.1 (Fc-C), 66.8 (Fc-C), 62.5 (C-3), 60.9 (ArO*C*H$_3$), 55.4 (ArO*C*H$_3$), 30.7 (C-4), 22.0 (C-3'), 19.6 (C-1'). **HRMS** (*m*/*z*), calculated for $C_{25}H_{29}FeO_3$: 433.1461, found $(M + H)^+$ 433.1464.

7.11 Route two: Involving Heck-type cross-coupling reaction

7.11.0 Synthesis of 1-(2-allyl-3-hydroxy-6-methoxyphenyl)ethanone 404

1-(5-Allyloxy-2-methoxyphenyl)ethanone **372** (4.83 g, 23.4 mmol) in a 100 mL round bottom flask was heated at 180 °C under the N_2 (g) for 24 hrs. The resultant dark oil was allowed to cool to rt and then purified by silica gel column chromatography (10% EtOAc/hexane) yielding a mixture of 1-(2-allyl-3-hydroxy-6-methoxyphenyl)ethanone **404** and 1-(4-allyl-5-hydroxy-2-methoxyphenyl)ethanone **405** as a yellow semi-solid. This mixture was then re-crystallised from hot solution (50% EtOAc/hexane) affording two products which were physically separated by tweezers. The first product was identified as 1-(2-allyl-3-hydroxy-6-methoxyphenyl)ethanone **404** which was obtained as pale yellow crystals (2.70 g, 56%). $\mathbf{R_f}$ = 0.44 (15% EtOAc/hexane); **IR ν_{max} (cm^{-1})** 3240 (O-H), 1714 (C=O), 1594 (C=C);

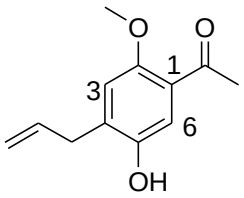
^{1}H NMR (300 MHz, $CDCl_3$, Me_4Si) δ_H 6.81 (1H, d, *J* = 8.8 Hz, H4), 6.68 (1H, d, *J* = 8.8 Hz, H-5), 6.01-5.84 (1H, m, Hz, $ArCH_2CH$=CH_2), 5.40 (1H, s, O*H*), 5.12-4.99 (m, $ArCH_2CH$=CH_2), 3.76 (3H, s, $ArOCH_3$), 3.30 (2H, dt, *J* = 6.0, 1.5 Hz, $ArCH_2CH$=CH_2), 2.48 (3H, s, $ArCOCH_3$); **^{13}C NMR (75 MHz, $CDCl_3$, Me_4Si)** δ_C 206.0 ($ArCOCH_3$), 150.0 (C-6), 148.5 (C-3), 135.9 ($ArCH_2CH$=CH_2), 132.5 (C-2), 123.0 (C-1), 116.9 (C-4), 116.1 ($ArCH_2CH$=CH_2), 110.3 (C-5), 56.1 ($ArOCH_3$), 32.6 ($ArCOCH_3$), 31.2 ($ArCH_2CH$=CH_2). **HRMS** (*m*/*z*), calculated for $C_{12}H_{14}O_3$: 207.1016, found $(M + H)^+$ 207.1021.



404

The second product was 1-(4-allyl-5-hydroxy-2-methoxyphenyl)ethanone **405** (0.965 g, 20%), which was obtained as orange crystals. **R_f** = 0.45 (15% EtOAc/hexane);

^{1}H NMR (300 MHz, $CDCl_3$, Me_4Si) δ_H 7.57 (1H, s, H-6), 7.13 (1H, s, H-3), 6.74 (1H, s, O*H*), 6.12-5.92 (1H, m, $ArCH_2CH$=CH_2), 5.20-5.06 (2H, m, $ArCH_2CH$=CH_2), 3.85 (3H, s, $ArOCH_3$), 3.44 (2H, d, *J* = 6.5 Hz, $ArCH_2CH$=CH_2), 2.63 (3H, s, $ArCOCH_3$); **^{13}C NMR (75 MHz, $CDCl_3$, Me_4Si)** δ_C 200.4 ($ArCOCH_3$), 153.7 (C-2), 148.1 (C-5), 135.7 ($ArCH_2CH$=CH_2), 133.9 (C-4), 125.8 (C-1), 116.6 ($ArCH_2CH$=CH_2), 116.5 (C-3), 113.8 (C-6), 56.0 ($ArOCH_3$), 34.8 ($ArCH_2CH$=CH_2), 32.1 ($ArCOCH_3$). **HRMS** (*m*/*z*), calculated for $C_{12}H_{15}O_3$: 207.1016, found $(M + H)^+$ 207.1013.



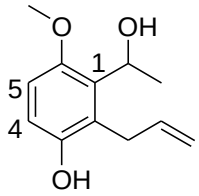
405

7.11.1 Synthesis of 2-allyl-3-(1-hydroxyethyl)-4-methoxyphenol 406

In an oven dried 250 mL 2-neck round bottom flask equipped with a magnetic stirring bar was added 1-(2-allyl-3-hydroxy-6-methoxyphenyl)ethanone **404** (2.60 g, 12.6 mmol) in dry THF (30 mL) and stirred at 0 °C under the N_2 (g). $LiAlH_4$ (0.569 g, 15.0 mmol) was added portion-wise to the reaction mixture and stirred at rt for 4 hrs. The reaction mixture was then cooled to 0 °C for the second time and H_2O (50 mL), followed by 3.75 M NaOH aqueous solution (10 mL) were slowly added to the mixture while stirring. The solution was filtered through a Celite® pad and extracted into EtOAc (3 × 200 mL). The organic layer was dried over anhydrous $MgSO_4$, filtered through a Celite® pad and solvent removed *in vacuo*. The resultant residue was purified by silica gel column chromatography (30% EtOAc/hexane) affording 2-allyl-3-(1-hydroxyethyl)-4-methoxyphenol **406** (2.02 g, 77%) as a viscous pale

yellow oil. $\mathbf{R_f}$ = 0.33 (20% EtOAc/hexane); **IR ν_{max} (cm^{-1})** 3509 (O-H), 3291 (O-H), 2834 (C-H), 1608 (C=C);

^{1}H NMR (300 MHz, $CDCl_3$, Me_4Si) δ_H 6.68 (2H, br s, H-4 and H-5), 6.03-5.86 (1H, m, $ArCH_2CH$=CH_2), 5.61 (1H, s, ArO*H*), 5.13-4.91 (3H, m, $ArCH_2CH$=CH_2 overlapping with

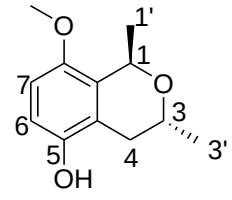


406

Ar*C*H(OH)CH_3), 4.25 (1H, d, *J* = 10.9 Hz, ArCH(O*H*)CH_3), 3.84 (3H, s, $ArOCH_3$), 3.53-3.33 (2H, m, $ArCH_2CH$=CH_2), 1.53 (3H, d, *J* = 6.7 Hz, ArCH(OH)CH_3); **^{13}C NMR (75 MHz, $CDCl_3$, Me_4Si)** δ_C 151.7 (C-6), 148.4 (C3), 135.9 ($ArCH_2CH$=CH_2), 132.3 (C-1 or C-2), 124.0 (C-1 or C-2), 115.6 ($ArCH_2CH$=CH_2), 114.2 (C-4), 110.2 (C-5), 67.4 (Ar*C*H(OH)CH_3), 55.7 ($ArOCH_3$), 30.1 ($ArCH_2CH$=CH_2), 23.7 (ArCH(OH)CH_3). **HRMS** (*m*/*z*), calculated for $C_{12}H_{17}O_3$: 209.1172, found $(M + H)^+$ 209.1171.

7.11.2 Synthesis of (±)-*trans*-3,4-dihydro-8-methoxy-1,3-dimethyl-1*H*-isochromen-5-ol *trans*-409

To a solution of 2-allyl-3-(1-hydroxyethyl)-4-methoxyphenol (2.00 g, 9.60 mmol) in a freshly distilled anhydrous *N*-methylpyrrolidinone (70 mL), stirred vigorously at 100 °C under a N_2 (g) was added sublimed *t*-BuOK (3.25 g, 29.0 mmol). Stirring was continued for a further 30 min after which it was allowed to cool down to 50 ^{o}C and poured into ice cold H_2O (100 mL). The product was extracted into CH_2Cl_2 (3 × 100 mL) and the combined organic layers were dried over $MgSO_4$, filtered through a Celite® pad and concentrated *in vacuo*. The bulk of the solvent (*N*-methylpyrrolidinone) was distilled off under vacuum and purification of the crude product by column chromatography (15% EtOAc/hexane) on silica gel afforded three products. The first product was (±)-*trans*-3,4-dihydro-8-methoxy-1,3-dimethyl-1*H*-isochromen-5-ol ***trans*-409** (0.520 g, 26%) which was obtained as colourless crystals. $\mathbf{R_f}$ = 0.42 (35% EtOAc/hexane);



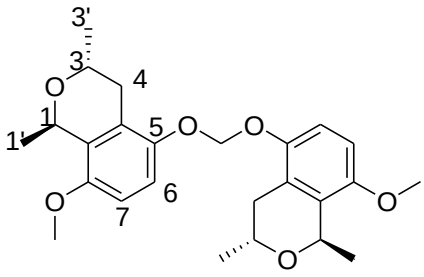
***trans*-409**

IR ν_{max} (cm^{-1}) 3380 (O-H), 1247 (C-O); **Mp** 123-124 ^{o}C; **^{1}H NMR (300 MHz, $CDCl_3$, Me_4Si)** δ_H 6.61 (1H, d, *J* = 8.7 Hz, H-6), 6.52 (1H, d, *J* = 8.7 Hz, H-7), 6.19 (1H, s, O*H*), 5.13 (1H, q, *J* = 6.6 Hz, H-1), 4.29-4.00 (1H, m, H-3), 3.72 (3H, s, OCH_3), 2.74 (1H, dd, *J* = 16.9, 3.4 Hz, H-4

pseudo-equatorial), 2.36 (1H, dd, *J* = 16.8, 10.9 Hz, H-4 *pseudo*-axial), 1.52 (3H, d, *J* = 6.6 Hz, H-1'), 1.34 (3H, d, *J* = 6.1 Hz, H-3'); **^{13}C NMR (75 MHz, $CDCl_3$, Me_4Si)** δ_C 149.2 (C-8), 147.2 (C-5), 128.7 (C-8a), 121.6 (C-4a), 112.4 (C-6), 108.0 (C-7), 68.6 (C-1), 62.7 (C-3), 55.5 (ArO*C*H$_3$), 30.4 (C-4), 21.8 (C-3'), 19.6 (C-1'). **HRMS** (*m*/*z*), calculated for $C_{12}H_{17}O_3$: 209.1172, found $(M + H)^+$ 209.1178.

The second product was *bis*((±)-*trans*-3,4-dihydro-8-methoxy-1,3-dimethyl-1*H*-isochromen-5-yloxy)methane ***trans*-410** (or **JS-D**) which was isolated as colourless crystals (1.40 g, 34%). **R_f** = 0.36 (35% EtOAc/hexane);

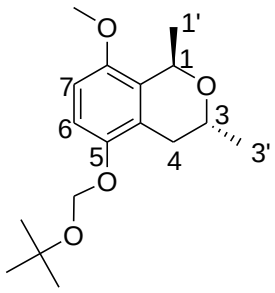
IR ν_{max} (cm^{-1}) 1345 (C-O), 1247 (C-O); **Mp** 106-108 ^oC; **^{1}H NMR (500 MHz, $CDCl_3$, Me_4Si)** δ_H 6.98 (1H, d, *J* = 8.8 Hz, 2 × H-6), 6.63 (1H, d, *J* = 8.9 Hz, 2 × H-7), 5.63 (1H, s, 0.5 × ArOC*H*$_2$OAr), 5.07 (1H, q, *J* = 6.5 Hz, 2 × H-1), 4.07-3.96 (1H, m, 2 × H-3), 3.77 (3H, s, 2 × ArOC*H*$_3$), 2.74 (1H, dd, *J* = 17.1, 3.3 Hz, 2 × H-4 *pseudo*-equatorial), 2.31 (1H, dd, *J* = 17.1, 10.9 Hz, 2 × H-4 *pseudo*-axial), 1.49 (3H, d, *J* = 6.6 Hz, 2 × H-1'), 1.31 (3H, d, *J* = 6.1 Hz, 2 × H-3'); **^{13}C NMR (126 MHz, $CDCl_3$, Me_4Si)** δ_C 150.7 (C-8), 148.4 (C-5), 129.2 (C-8a), 124.8 (C-4a), 112.3 (C-6), 107.5 (C-7), 92.4 (ArO*C*H$_2$OAr), 68.3 (C-1), 62.2 (C-3), 55.4 (ArO*C*H$_3$), 30.6 (C-4), 22.0 (C-3'), 19.5 (C-1'). **HRMS** (*m*/*z*), calculated for $C_{25}H_{33}O_6$: 429.2272, found $(M + H)^+$ 429.2274.



***trans*-410**

The third product was (±)-*trans*-5-(*tert*-butoxymethoxy)-3,4-dihydro-8-methoxy-1,3-dimethyl-1*H*-isochromene ***trans*-411** (0.396 g, 14%) which was isolated as a colourless semi-solid. **R_f** = 0.53 (35% EtOAc/hexane); **IR ν_{max} (cm^{-1})** 1332 (C-O), 1246 (C-O);

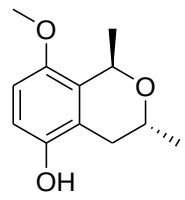
^{1}H NMR (500 MHz, $CDCl_3$, Me_4Si) δ_H 6.98 (1H, d, *J* = 8.8 Hz, H-6), 6.63 (1H, d, *J* = 8.9 Hz, H-7), 5.22 (2H, s, ArOC*H*$_2$OC(CH$_3$)$_3$), 5.06 (1H, q, *J* = 6.5 Hz, 2 × H-1), 4.08-3.98 (1H, m, H-3), 3.79 (3H, s, OC*H*$_3$), 2.74 (1H, dd, *J* = 17.1, 3.3 Hz, H4 *pseudo*-equatorial), 2.31 (1H, dd, *J* = 17.1, 10.9 Hz, H4 *pseudo*-axial), 1.49 (3H, d, *J* = 6.6 Hz, H-1'), 1.31 (3H, d, *J* = 6.1 Hz, H-3'), 1.29 (9H, s, ArOCH$_2$OC(C*H*$_3$)$_3$); **^{13}C NMR (126 MHz, $CDCl_3$, Me_4Si)** δ_C 149.9 (C-8), 148.9 (C-5), 128.9 (C-8a), 124.0 (C-4a), 111.3 (C-6), 107.4 (C-7), 88.4 (ArO*C*H$_2$OC(CH$_3$)$_3$), 75.3 (ArOCH$_2$O*C*(CH$_3$)$_3$), 68.3 (C-1), 62.3 (C-3), 55.4 (ArO*C*H$_3$), 30.7 (C-4), 28.6 (ArOCH$_2$OC(*C*H$_3$)$_3$), 22.0 (C-3'), 19.5 (C-1'). **HRMS** (*m*/*z*), calculated for $C_{17}H_{27}O_4$: 295.1904, found $(M + H)^+$ 295.1909.



***trans*-411**

7.11.3 Hydrolysis of (±)-*trans*-5-(*tert*-butoxymethoxy)-3,4-dihydro-8-methoxy-1,3-dimethyl-1*H*-isochromene *trans*-411

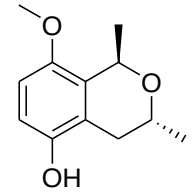
32% Aqueous HCl (1.71 mL, 15.0 mmol) was added to a solution of (±)-*trans*-5-(*tert*-butoxymethoxy)-3,4-dihydro-8-methoxy-1,3-dimethyl-1*H*-isochromene ***trans*-411** (0.400 g, 1.36 mmol) in MeOH/H_2O (40 mL, 4:1) in a 150 mL round bottom flask. The mixture was heated at reflux under a blanket of N_2 (g) for 12 hrs after which it was allowed to cool to rt. The MeOH was evaporated *in vacuo* and the resultant aqueous medium was extracted into EtOAc (3 × 150 mL). The EtOAc extract was washed with H_2O until the aqueous layer was neutral. The organic layer was then dried over MgSO4, filtered through a Celite® pad and the solvent was removed *in vacuo*. The residue was purified by silica gel column chromatography (10% EtOAc/hexane) affording (±)-*trans*-3,4-dihydro-8-methoxy-1,3-dimethyl-1*H*-isochromen-5-ol ***trans*-409** (0.238 g, 84%) as white crystal. $\mathbf{R_f}$ = 0.42 (35% EtOAc/hexane). The ^{1}H NMR spectrum of the product was the same as the one discussed in **Section 7.11.2**.



***trans*-409**

7.11.4 Hydrolysis of *bis*[(±)-*trans*-3,4-dihydro-8-methoxy-1,3-dimethyl-1*H*-isochromen-5-yloxy]methane *trans*-410

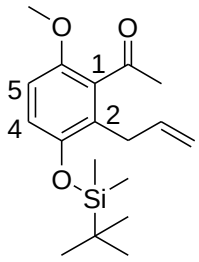
TFA (3.61 mL, 47.1 mmol) was added to a solution of *bis*[(±)-*trans*-3,4-dihydro-8-methoxy-1,3-dimethyl-1*H*-isochromen-5-yloxy]methane ***trans*-410** (1.25 g, 2.92 mmol) in MeOH (100 mL) in a 250 mL round bottom flask. The mixture was heated to reflux for 24 hrs after which it was allowed to cool to rt. H_2O (90 mL) was added to the mixture and MeOH was evaporated *in vacuo*. The resultant acidic medium was dissolved in EtOAc (150 mL) in a 500 mL separating funnel and washed with H_2O until the aqueous layer was neutral. The organic layer was then dried over anhydrous $MgSO_4$, filtered through a Celite® pad and the solvent was removed *in vacuo*. The residue was purified by silica gel column chromatography (10% EtOAc/hexane) affording (±)-*trans*-3,4-dihydro-8-methoxy-1,3-dimethyl-1*H*-isochromen-5-ol ***trans*-409** (2.18 g, 90%) as white crystal. $\mathbf{R_f}$ = 0.42 (35% EtOAc/hexane). The ^{1}H NMR spectrum of the isolated product was the same as the one discussed in **Section 7.11.2**.



***trans*-409**

7.11.5 Synthesis of 1-(2-allyl-3-*tert*-butyldimethylsilyloxy-6-methoxyphenyl)ethanone 422

1-(2-Allyl-3-hydroxy-6-methoxyphenyl)ethanone **404** (6.19 g, 30.0 mmol), *tert*-butyldimethylsilyl chloride (5.43 g, 36.0 mmol), imidazole (2.45 g, 36.0 mmol) and DMAP (0.440 g, 3.60 mmol) were dissolved in dry CH_2Cl_2 (150 mL) and stirred at rt for 24 hrs under a N_2 (g). The mixture was then washed with H_2O (2 × 150 mL), dried over anhydrous $MgSO_4$, filtered through a Celite® pad and concentrated *in vacuo*. Purification of the residue by silica gel column chromatography (10% EtOAc/hexane) delivered 1-(2-allyl-3-*tert*-butyldimethylsilyloxy-6-methoxyphenyl)ethanone **422** (8.94 g, 93%) as colourless crystals. $\mathbf{R_f}$ = 0.61 (49:1 $CHCl_3$/MeOH); **Mp** 61-62 ^oC; **IR ν_{max} (cm^{-1})** 1703 (C=O), 1580 (C=C);



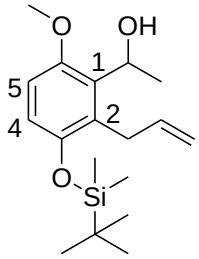
422

^{1}H NMR (300 MHz, $CDCl_3$, Me_4Si) δ_H 6.55 (1H, d, *J* = 8.9 Hz, H-4), 6.45 (1H, d, *J* = 8.9 Hz, H-5), 5.66 (1H, ddt, *J* = 16.3, 10.2, 6.1 Hz, $ArCH_2CH$=CH_2), 4.83-4.61 (2H, m, $ArCH_2CH$=CH_2), 3.54 (3H, s, $ArOCH_3$), 3.11 (2H, d, *J* = 6.1 Hz, $ArCH_2CH$=CH_2), 2.24 (3H,

s, ArCOC*H*$_3$), 0.78 (9H, s, ArOSi(CH$_3$)$_2$C(C*H*$_3$)$_3$), 0.00 (6H, s, ArOSi(C*H*$_3$)$_2$C(CH$_3$)$_3$); **^{13}C NMR (75 MHz, CDCl$_3$, Me$_4$Si)** δ_C 205.3 (Ar*C*(O)CH$_3$), 150.0 (C-6), 147.7 (C-3), 136.4 (ArCH$_2$*C*H=CH$_2$), 133.0 (C-2), 127.4 (C-1), 118.9 (C-4), 115.2 (ArCH$_2$CH=*C*H$_2$), 109.6 (C-5), 56.0 (ArO*C*H$_3$), 32.5 (Ar*C*H$_2$CH=CH$_2$), 30.9 (ArC(O)*C*H$_3$), 25.8 (ArOSi(CH$_3$)$_2$C(*C*H$_3$)$_3$), 18.2 (ArOSi(CH$_3$)$_2$*C*(CH$_3$)$_3$), -4.2 (ArOSi(*C*H$_3$)$_2$C(CH$_3$)$_3$). **HRMS** (*m*/*z*), calculated for $C_{18}H_{29}O_3Si$: 321.1880, found $(M + H)^+$ 321.1880.

7.11.6 Synthesis of 1-(2-allyl-3-[(*tert*-butyldimethylsilyl)oxy]-6-methoxyphenyl)ethanol 423

To a solution of 1-(2-allyl-3-[(*tert*-butyldimethylsilyl)oxy)-6-methoxyphenyl]ethanone **422** (4.33 g, 13.5 mmol) in dry THF (100 mL), stirred at 0 °C under a N_2 (g), was added $LiAlH_4$ (0.615 g, 16.2 mmol) in portion-wise. The reaction mixture was stirred at rt for 12 hrs after which it was once again cooled to 0 °C and cold H_2O (50 mL) followed by a 3.75 M NaOH aqueous solution (10 mL) were added. The slurry was filtered through a Celite® pad which was further washed by EtOAc (3 × 150 mL) and the filtrate was separated using a separating funnel. The organic layer was dried over anhydrous $MgSO_4$, filtered through a bed of Celite® and concentrated *in vacuo*. The residue was purified by silica gel column chromatography (10% EtOAc/hexane) yielding 1-(2-allyl-3-((*tert*-butyldimethylsilyl)oxy)-6-methoxyphenyl)ethanol **423** (3.87 g, 89%) as a viscous pale yellow oil. $\mathbf{R_f}$ = 0.40 (15% EtOAc/hexane); **Mp** 93-94 ^{o}C; **IR ν_{max} (cm^{-1})** 3562 (O-H), 1634 (C=C);



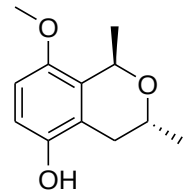
423

^{1}H NMR (300 MHz, CDCl$_3$, Me$_4$Si) δ_H 6.47 (2H, br s, H-4 and H-5), 5.69 (1H, ddt, *J* = 16.0, 10.3, 5.7 Hz, ArCH$_2$C*H*=CH$_2$), 4.94-4.57 (3H, m, ArCH$_2$CH=C*H*$_2$ overlapping with ArC*H*(OH)CH$_3$), 3.81 (1H, d, *J* = 11.1 Hz, ArCH(O*H*)CH$_3$), 3.62 (3H, s, OC*H*$_3$), 3.23 (2H, ddd, *J* = 15.8, 5.3, 1.7 Hz, ArC*H*$_2$CH=CH$_2$), 1.31 (3H, d, *J* = 6.7 Hz, ArCH(OH)C*H*$_3$), 0.79 (9H, s, ArOSi(CH$_3$)$_2$C(C*H*$_3$)$_3$), 0.01 (6H, d, *J* = 5.3 Hz, ArOSi(C*H*$_3$)$_2$C(CH$_3$)$_3$); **^{13}C NMR (75 MHz, CDCl$_3$, Me$_4$Si)** δ_C 151.9 (C-6), 147.8 (C-3), 136.5 (Ar*C*H$_2$*C*H=CH$_2$), 132.9 (C-2 or C-3), 128.0 (C-2 or C-3), 116.5 (ArCH$_2$CH=*C*H$_2$), 115.1 (C-4), 109.6 (C-5), 67.5 (Ar*C*H(OH)CH$_3$), 55.5 (ArO*C*H$_3$), 30.4 (Ar*C*H$_2$CH=CH$_2$), 25.8 (ArOSi(CH$_3$)$_2$C(*C*H$_3$)$_3$), 23.6 (ArC(O)*C*H$_3$), 18.2 (ArOSi(CH$_3$)$_2$*C*(CH$_3$)$_3$), -4.3

(ArOSi(CH_3)$_2$C(CH_3)$_3$). **HRMS** (*m*/*z*), calculated for $C_{18}H_{31}O_3Si$: 323.2037, found $(M + H)^+$ 323.2041.

7.11.7 Synthesis of (±)-*trans*-3,4-dihydro-8-methoxy-1,3-dimethyl-1*H*-isochromen-5-ol *trans*-409

Sublimed *t*-BuOK (2.23 g, 19.9 mmol) was added to a solution of 1-(2-allyl-3-[(*tert*-butyldimethylsilyl)oxy]-6-methoxyphenyl)ethanol **423** (2.14 g, 6.64 mmol) in freshly distilled anhydrous *N*-methylpyrrolidinone (100 mL) stirred at 100 °C under a N_2 (g). Stirring was continued for 30 min after which the reaction mixture was allowed to cool down to 50 °C and then poured into ice cold H_2O (150 mL). The product was extracted into CH_2Cl_2 (3 × 150 mL) and the combined organic layers were dried over anhydrous $MgSO_4$, filtered through a Celite® pad and concentrated *in vacuo*. The bulk of the *N*-methylpyrrolidinone solvent was distilled off under vacuum and purification of the crude product by silica gel column chromatography (20% EtOAc/hexane) afforded (±)-*trans*-3,4-dihydro-8-methoxy-1,3-dimethyl-1*H*-isochromen-5-ol ***trans*-409**, (0.968 g, 70%) as colourless crystals. $\mathbf{R_f}$ = 0.42 (35% EtOAc/hexane). The ^{1}H NMR spectrum confirmed the formation of the isochromen-5-ol ***trans*-409** as discussed in **Section 7.11.2**.

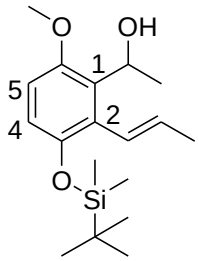


***trans*-409**

7.11.8 Synthesis of 1-(3-[(*tert*-butyldimethylsilyl)oxy]-6-methoxy-2-[(*E*)-prop-1-enyl]phenyl)ethanol 424

To a solution of 1-(2-allyl-3-[(*tert*-butyldimethylsilyl)oxy]-6-methoxyphenyl)ethanol **423** (1.29 g, 4.00 mmol) in a freshly distilled anhydrous *N*-methylpyrrolidinone (50 mL), stirred at 100 °C under N_2 (g), was added sublimed *t*-BuOK (1.37 g, 12.2 mmol). Stirring was continued for 4 min after which a small portion was drawn from the reaction mixture and quenched with ice cold H_2O (50 mL). The crude product was extracted into CH_2Cl_2 (3 × 150 mL) and the combined organic layers were dried over $MgSO_4$, filtered through a Celite® pad and concentrated *in vacuo*. The bulk of the *N*-methylpyrrolidinone solvent was distilled off under vacuum and purification of the crude product by column chromatography (20% EtOAc/hexane) on silica gel yielded (±)-*trans*-3,4-dihydro-8-methoxy-1,3-dimethyl-1*H*-

isochromen-5-ol **424** as a colourless oil. No percentage yield was calculated for this product. $\mathbf{R_f}$ = 0.40 (15% EtOAc/hexane);

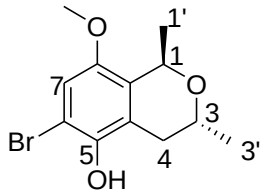


424

^{1}H NMR (300 MHz, $CDCl_3$, Me_4Si) δ_H 6.89 (1H, d, *J* = 8.9 Hz, H-4), 6.83 (1H, d, *J* = 8.9 Hz, H-5), 6.74 (1H, dq, *J* = 11.2, 1.5 Hz, ArC*H*=CHCH$_3$), 6.11 (1H, dq, *J* = 11.2, 6.8 Hz, ArCH=C*H*CH$_3$), 5.55 (1H, q, *J* = 6.5 Hz, ArC*H*(OH)CH$_3$), 5.33 (1H, s, ArCH(O*H*)CH$_3$), 3.86 (3H, s, ArOC*H*$_3$), 1.67 (3H, dd, *J* = 6.8, 1.7 Hz, ArCH=CHC*H*$_3$), 1.44 (3H, d, *J* = 6.6 Hz, ArC(OH)HC*H*$_3$), 0.96 (9H, s, ArOSi(CH$_3$)$_2$C(C*H*$_3$)$_3$), 0.10 (3H, s, 1 × ArOSi(C*H*$_3$)$_2$C(CH$_3$)$_3$), -0.00 (3H, s, 1 × ArOSi(C*H*$_3$)$_2$C(CH$_3$)$_3$); **^{13}C NMR (75 MHz, $CDCl_3$, Me_4Si)** δ_C 149.7 (C-6), 146.4 (C-3), 132.7 (C-2), 129.8 (Ar*C*H=CHCH$_3$), 125.7 (ArCH=*C*HCH$_3$), 122.4 (C-1), 113.0 (C-5), 111.9 (C-4), 64.9 (Ar*C*H(OH)CH$_3$), 56.4 (ArO*C*H$_3$), 26.0 (ArOSi(CH$_3$)$_2$C(*C*H$_3$)$_3$), 23.4 (Ar*C*H(OH)CH$_3$), 18.2 (ArOSi(CH$_3$)$_2$*C*(CH$_3$)$_3$), 14.5 (ArCH=CH*C*H$_3$), -5.0 (1 × (ArOSi(*C*H$_3$)$_2$C(CH$_3$)$_3$), -5.1 (1 × (ArOSi(*C*H$_3$)$_2$C(CH$_3$)$_3$).

7.11.9 Synthesis of (±)-*trans*-(6-bromo-3,4-dihydro-8-methoxy-1,3-dimethyl-1*H*-isochroman-5-ol *trans*-425

Bromine (0.344 mL, 6.71 mmol) was added at rt to a solution of (±)-*trans*-3,4-dihydro-8-methoxy-1,3-dimethyl-1*H*-isochromen-5-ol ***trans*-409** (1.19 g, 5.71 mmol) and NaOAc (0.612 g, 7.46 mmol) in AcOH (130 mL). The resulting yellow solution was stirred for 30 min under N_2 (g). The solvent was removed under vacuum and the residue was poured into an aqueous solution of $NaHCO_3$. The aqueous phase was extracted into EtOAc (3 × 50 mL) and the combined organic layers were washed with brine (100 mL), dried over anhydrous Na_2SO_4 and filtered using a Celite® pad. The filtrate was concentrated *in vacuo* and the residue was purified by silica gel column chromatography (30% EtOAc/hexane) which afforded (±)-*trans*-6-bromo-3,4-dihydro-8-methoxy-1,3-dimethyl-1*H*-isochroman-5-ol ***trans*-425** (0.967 g, 59%) as off white solid. $\mathbf{R_f}$ = 0.34 (20% EtOAc/hexane); **Mp** 110-112 ^{o}C; **IR ν_{max} (cm^{-1})** 3610 (O-H), 1304 (C-O);



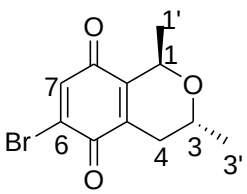
***trans*-425**

^{1}H NMR (300 MHz, $CDCl_3$, Me_4Si) δ_H 6.56 (1H, s, H-7), 5.16 (1H, s, ArO*H*), 5.10 (1H, q, *J* = 6.4 Hz, H-1), 4.19-3.99 (1H, m, H-3), 3.77 (3H, s, OCH_3), 2.81 (1H, dd, *J* = 17.1, 3.4 Hz, H-4 *pseudo*-equatorial), 2.39 (1H, dd, *J* = 17.1, 10.9 Hz, H-4 *pseudo*-axial), 1.54 (3H, d, *J* = 6.6 Hz, H-1'), 1.36 (3H, d, *J* = 6.1 Hz, H-3'); **^{13}C NMR (126 MHz, $CDCl_3$, Me_4Si)** δ_C 149.6 (C-8), 144.2 (C-5), 129.7 (C-8a), 123.1 and 123.0 (C-4a), 119.9 (C-6), 109.0 (C-7), 68.3 (C-1), 62.3 (C-3), 55.6 (ArO*C*H_3), 30.6 (C-4), 22.0 (C-3'), 19.5 (C-1').

7.11.10 Synthesis of (±)-*trans*-6-bromo-3,4-dihydro-1,3-dimethyl-1*H*-isochromene-5,8-dione *trans*-383

(±)-*Trans*-6-bromo-3,4-dihydro-8-methoxy-1,3-dimethyl-1*H*-isochroman-5-ol ***trans*-425** (1.02 g, 3.55 mmol) was dissolved in 1,4-dioxane (50.0 mL) at rt. AgO (1.09 g, 8.77 mmol) was then added to the stirred solution, followed by drop-wise addition of 55% (v/v) aqueous HNO_3 (6.45 mL) and the mixture was stirred for a further 5 min. CH_2Cl_2 (50 mL) and H_2O (50 mL) were added to the reaction mixture and the lower organic layer was separated. The aqueous medium was further extracted into CH_2Cl_2 (2 × 50 mL). The combined organic layers were dried over anhydrous $MgSO_4$, filtered through a Celite® bed and concentrated under reduced pressure. Purification of the residue by silica gel column chromatography (20% EtOAc/hexane) afforded (±)-*trans*-6-bromo-3,4-dihydro-1,3-dimethyl-1*H*-isochromene-5,8-dione ***trans*-383** as an orange amorphous solid (0.703 g, 73%). **R_f** = 0.41 (20% EtOAc/hexane); **Mp** 86-87 ^oC; **IR ν_{max} (cm^{-1})** 1774 (C=O), 1753 (C=O), 1570 (C=C), 1566 (C=C), 1289 (C-O);

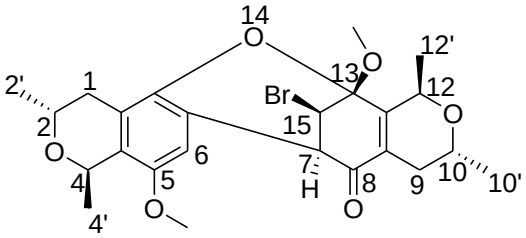
^{1}H NMR (500 MHz, $CDCl_3$, Me_4Si) δ_H 7.22 (1H, s, H-7), 4.83 (1H, q, *J* = 6.7 Hz, H-1), 4.02-3.89 (1H, m, H-3), 2.64 (1H, dd, *J* = 19.2, 3.2 Hz, H-4 *pseudo*-equatorial), 2.18 (1H, ddq, *J* = 19.2, 10.0, 2.2 Hz, H-4 *pseudo*-axial), 1.46 (3H, d, *J* = 6.8 Hz, H-1'), 1.33 (3H, d, *J* = 6.2 Hz, H-3'); **^{13}C NMR (75 MHz, $CDCl_3$, Me_4Si)** δ_C 183.2 (C-8), 178.6 (C-5), 144.7 (C-8a), 139.3 (C-4a), 138.0 (C-7), 136.8 (C-6), 66.9 (C-1), 62.6 (C-3), 30.2 (C-4), 21.3 (C-3'), 19.6 (C-1'). **HRMS** (*m*/*z*), calculated for $C_{11}H_{12}BrO_3$: 270.9964, found $(M + H)^+$ 270.9970.



***trans*-383**

7.11.11 Synthesis of (±)-*trans*-15-bromo-5,13-dimethoxy-2,4,10,12-tetramethyl-4,7,9,10,12,13-hexahydro-1*H*-7,13-methanopyrano[4',3':6,7]oxocino[2,3-*f*]isochromen-8(2*H*)-one JS-X10

A solution of (±)-*trans*-6-bromo-3,4-dihydro-8-methoxy-1,3-dimethyl-1*H*-isochroman-5-ol ***trans*-425** (0.919 g, 3.20 mmol), *tert*-butyldimethylsilyl chloride (0.579 g, 3.84 mmol), imidazole (0.261 g, 3.84 mmol) and DMAP (0.0391 g, 0.320 mmol) in *N*,*N*-dimethylformamide (150 mL) was stirred at rt for 72 hrs under a N_2 (g). The mixture was then diluted with H_2O (100 mL) and stirred for 30 min. The crude product was extracted into ether (3 × 50 mL) and the combined extracts were washed with brine (3 × 50 mL), dried over anhydrous $MgSO_4$, filtered through a pad of Celite® and concentrated *in vacuo*. The residue was purified by column chromatography (10% EtOAc/hexane) on silica gel affording the title compound **JS-X10** (0.474 g, 30%) as colourless crystals. $\mathbf{R_f}$ = 0.31 (30% EtOAc/hexane); **Mp** 185-186 °C; **IR ν_{max} (cm^{-1})** 1763 (C=O), 1642 (C=C), 1330 (C-O), 1236 (C-O);



JS-X10

^{1}H NMR (300 MHz, $CDCl_3$, Me_4Si) δ_H 6.42 (1H, s, H-6), 5.03 (1H, q, *J* = 6.6 Hz, H-4), 4.71 (1H, d, *J* = 3.9 Hz, H-15), 4.66 (1H, q, *J* = 6.8 Hz, H-12), 4.14-3.89 (3H, m, H-2, H-10, H-7), 3.73 (3H, s, ArOC*H*$_3$), 3.53 (3H, s, OC*H*3 attached to C-13), 2.71 (1H, dd, *J* = 17.4, 3.6 Hz, H-1 *pseudo*-equatorial), 2.46 (1H, dd, *J* = 18.3, 4.0 Hz, H-9 *pseudo*-equatorial), 2.29 (1H, dd, *J* = 17.4, 10.9 Hz, H-1 *pseudo*-axial), 1.75 (1H, ddd, *J* = 18.3, 10.6, 1.5 Hz, H-9 *pseudo*-axial), 1.60 (3H, d, *J* = 6.6 Hz, H-12'), 1.48 (3H, d, *J* = 6.6 Hz, H-4'), 1.33 (3H, d, *J* = 6.1 Hz, H-2'), 1.19 (3H, d, *J* = 6.1 Hz, H-10'); **^{13}C NMR (75 MHz, $CDCl_3$, Me_4Si)** δ_C 191.8 (C-8), 150.5 (C-5), 149.5 (C-12a), 143.5 (C-14a), 130.4 (C-4a), 130.0 (C-8a), 123.7 (C-14b), 114.3 (C-6a), 105.8 (C-6), 98.3 (C-13), 68.1 (C-4), 67.7 (C-12), 62.1 (C-10), 61.9 (C-2), 55.6 (ArO*C*H$_3$), 55.3 (C-7), 48.4 (O*C*H$_3$ attached to C-13), 45.1 (C-15), 29.9 (C-1), 29.2 (C-9), 22.0 (C-2'), 21.6 (C-10'), 20.6 (C-12'), 19.3 (C-4'). **HRMS** (*m*/*z*), calculated for $C_{24}H_{30}BrO_6$: 493.1220, found $(M + H)^+$ 493.1226.

7.12 Biological evaluation of selected compounds

The *in vitro P. falciparum* antimalarial activity screening on a Gambian FCR-3 strain (chloroquine and cycloguanil resistant strain) was performed by Prof R. van Zyl at the School of Pharmacy and Pharmacology, University of Witwatersrand, South Africa. The FCR-3 strain of *P. falciparum* was cultured *in vitro* at 37 °C in 3% O_2 (g), 5% CO_2 (g), 92% N_2 (g) and adjusted to a 0.625% parasitaemia/1.25% haematocrit before being incubated along with the compounds for 72 hours. The plates were frozen overnight and, once thawed, incubated in the dark for 1 hour at room temperature with buffered SYBR green I. The fluorescence was read in a microplate reader with excitation and emission wavelength bands centred at 485 and 528 nm, respectively. The percentage inhibition was calculated by taking the untreated and quinine (or dihydroartemisinin) control into account. Dihydroartemisinin (DHA) and quinine were used as the positive controls.

Chapter 8: References

1. (a) Jakupec M. A., Galanski M., Arion V. B., Hartinger C. G. and Keppler B. K., *Dalton Trans.* **2008**, *2*, 183. (b) Dyson P. J. and Sava G., *Dalton Trans.*, **2006**, 1929 and references therein.

2. (a) Wheate N. J. and Collins J. G., *Coord. Chem. Rev.*, **2003**, *241*, 133. (b) Fouda M. F. R., Abd-Elzaher M. M., Abdelsamaia R. A. and Labib A. A., *Appl. Organomet. Chem.*, **2007**, *21*, 613.

3. (a) Kelland L., *Nat. Rev. Cancer*, **2007**, *7*, 573. (b) Stewart D. J., *Crit. Rev. Oncol. Hematol.*, **2007**, *63*, 12. (c) Gust R., Schönenberger H., Klement U. and Range K. J., *Arch. Pharm.*, **1993**, *326*, 967.

4. Gasser G., Ott I. and Metzler-Nolte N., *J. Med. Chem.*, **2011**, *54*, 3.

5. Ravelo Á. G., Estévez-Braun A., Chávez-Orellana H., Pérez-Sacau E. and Mesa-Siverio D., *Curr. Top. Med. Chem.*, **2004**, *4*, 241.

6. Verma, R. P., *Anticancer Agents Med. Chem.*, **2006**, *6*, 489. (a) Medentsev A. G. and Akimenko V. K., *Phytochemistry*, **1998**, *47*, 935.

7. Claes P., Jacobs J., Claessens S. and De Kimpe N., *Tetrahedron*, **2010**, *66*, 7088 and references therein.

8. (a) Lee H., Hong S. -S. and Kim Y. -H., *Bioorg. Med. Chem. Lett.*, **1996**, *6*, 933. (b) Powis G., *Free Rad. Biol. and Med.*, **1989**, *6*, 63.

9. Devienne K. F., Raddi M. S. G., Varanda E. A. and Vilegas W., *Z. Naturforsch.*, **2002**, *57c*, 85.

10. Lagorio S. H., Bianchi D. A., Sutich E. G. and Kaufman T. S., *Eur. J. Med. Chem.*, **2006**, *41*, 1333.

11. (a) Kapoor L. D., *CRC Handbook of Ayurvedic Medicinal Plants*, CRC Press, Boca Raton, **1990**. (b) Schultes R. E. and Raffauf R. F., *The Healing Forest*, Dioscorides Press, Portland, **1990**.

12. Arvigo R. and Balick M., *Rainforest Remedies*, Lotus Press, Twin Lakes, **1993**.

13. Whyte A. C., Gloer J. B., Scott, J. A. and Malloch D., *J. Nat. Prod.*, **1996**, *59*, 765.

14. Hill R. A., *Prog. Chem. Org. Nat. Prods.*, **1986**, *49*, 1 and references cited therein.

15. Qadeer G., PhD Thesis, Quaid-i-Azam University, **2008**.

16. (a) O'Brien P. J., *Chem. Biol. Interactions*, **1991**, *80*, 1. (b) Moore H. W., *Science*, **1977**, *197*, 527. (c) Inbaraj J. J. and Chignell C. F., *Chem. Res. Toxicol.*, **2004**, *17*, 55.

17. (a) Shi M. M., Kugelman A., Iwamoto T., Tian L. and Forman H. J., *J. Bio. Chem.*, **1994**, *269*, 26512. (b) Lind C., Hochstein P. and Ernster L., *Archs Biochem. Biophys.*, **1982**, *216*, 178.

18. Epel B., Niklas J., Sinnecker S., Zimmermann H. and Lubitz W., *J. Phys. Chem. B*, **2006**, *110*, 11549.

19. (a) Klotz L. -O., Hou X., and Jacob C., *Molecules*, **2014**, *19*, 14902. (b) Kappus H. and Sies H., *Experientia*, **1981**, *37*, 1233.

20. (a) Kumagai Y., Shinkai Y., Miura T. and Cho A. K., *Annu. Rev. Pharmacol. Toxicol.*, **2012**, *52*, 221. (b) Buettner G. R., *Arch. Biochem. Biophys.*, **1993**, *300*, 535.

21. (a) Vilamil-Fernandez S., Stoppani A. O. and Dubin M., *Methods Enzymol.*, **2004**, *378*, 67. (b) Lopaczynski W. and Zeisel S. A., *Nutr. Res.*, **2001**, *21*, 295.

22. (a) Brunmark A. and Cadenas E., *Free Radic. Biol. Med.*, **1989**, *7*, 435. (b) Thor H., Smith M. T., Hartzell P., Bellomo G., Jewell S. A. and Orrenius S., *J. Biol. Chem.*, **1982**, *257*, 12419.

23. Lind C., Hochstein P. and Emster L., *Arch. Biochem. Biophys.*, **1982**, *216*, 178.

24. Munday R., Smith B. L. and Munday C. M., *J. Appl. Toxicol.*, **2007**, *27*, 262.

25. Munday R., *Free Rad. Res.*, **2000**, *32*, 245.

26. Lin A. J., Crosby L. A. and Sartorelli A. C., *Cancer Chemother. Rep. Part 2*, **1974**, *4*, 23.

27. Cross B. E. and Zammitt L. J., *J. Chem. Soc., Perkin Trans. 1*, **1973**, 2975.

28. (a) Holenstein J. E., Stoessl A., Kern H. A. and Stothers J. B., *Can. J. Chem.*, **1984**, *62*, 1971. (b) Gatenbeck S. and Bentley R., *Biochem. J.*, **1965**, *94*, 478.

29. Parisot D., Devys M. and Barbier M., *Phytochemitry*, **1985**, *24*, 1977.

30. Arsenault G. P., *Tetrahedron*, **1968**, *24*, 4745.

31. Parisot D., Devys M. and Barbier M., *Phytochemistry*, **1988**, *27*, 3002.

32. Diderot T. N., Silvere N., Etienne T., Mahmud T. H. K. and Arjumand A., in *Advances in Phytomedicine*, Elsevier, Editon edition., **2006**.

33. Hanumaiah T., Marshall D. S., Rao B. K., Rao C. P., Rao G. S. R., Rao J. U. M., Rao K. V. J. and Thomson R. H., *Phytochemistry*, **1985**, *24*, 2373.

34. (a) Thomson R. H., *Science*, **1992**, *10*, 312. (b) Williams D. L. and Ronzio A. R., *J. Org. Chem.*, **1953**, *18*, 489 and references cited therein.

35. ApSimon, J., (editor), *The Total Synthesis of Naturally Occurring Quinones in the Total Synthesis of Natural Products*, John Wiley and Sons, Inc., Canada, **1992**.

36. Bentley R. and Zwitkowits P. M., *J. Am. Chem. Soc.*, **1967**, *89*, 676.

37. Harris T. M., Harris C. M. and Light R. J., *Biochim. Biophys. Acta*, **1966**, *121*, 420.

38. (a) Saunders L. P., Bowman M. J., Mertens J. A., Da Silva N. A. and Hector R. E., *J. Ind. Microbiol. Biotechnol.*, **2015**, *42*, 711. (b) Tang S. Y., Qian S., Akinterinwa O., Frei C. S., Gredell J. A., Cirino P. C., *J. Am. Chem. Soc.*, **2013**, *135*, 10099.

39. Donner C. D., *Tetrahedron*, **2013**, *69*, 3747 and references cited therein.

40. Goel A. and Ram V. J., *Tetrahedron*, **2009**, *65*, 7865.

41. Donner C. D., *Nat. Prod. Rep.*, **2015**, *32*, 578 and references cited therein.

42. (a) Aytemir M. D., Calis U. and Ozalp M., *Arch. Pharm. Med. Chem.*, **2004**, *337*, 281. (b) Fairlamb I. J. S., Marrison L. R., Dickinson J. M., Lu F. J. and Schmidt J. P., *Bioorg. Med. Chem.*, **2004**, *12*, 4285.

43. O'Hagan D., *Nat. Prod. Rep.*, **1992**, 447.

44. Kurosaki F., Kizawa Y. and Nishi A., *Phytochemistry*, **1989**, *218*, 1843.

45. Kurosaki F., Kizawa Y. and Nishi A., *Eur. J. Biochem.*, **1989**, *185*, 85.

46. Hansen C. A. and Frost J. W., *J. Am. Chem. Soc.*, **2002**, *124*, 5926.

47. Richardson M. T., Pohl N. L., Kealey J. T. and Khosla C., *Metab. Eng.*, **1999**, *1*, 180.

48. Suzuki E., Sekizaki H. and Inoue S., *Synth. Commun.*, **1975**, 652.

49. (a) Evans G. E., Leeper F. J., Murphy J. A. and Staunton J., *J. Chem. Soc., Chem. Commun.*, **1979**, 205. (b) Leeper F. J. and Staunton J., *J. Chem. Soc., Perkin Trans. 1*, **1984**, 1053.

50. Drochner D. and Müller M., *Eur. J. Org. Chem.*, **2001**, 211.

51. (a) Blum M. S., Jones T. H., Howard D. F. and Overal W. L., *Comp. Biochem. Physiol*., **1982**, *71B*, 731. (b) Baker T. C., Nishida R. and Roelofs W., *Science*, **1981**, *214*, 1359.

52. Nishikawa H., *J. Agric. Chem. Soc. Jpn.*, **1933**, *9*, 772.

53. (a) Chacón-Morales P., Amaro-Luis J. M. and Bahsas A., *Avances en Química*, **2013**, *8*, 145. (b) Poch G. K. and Gloer J. B., *J. Nat. Prod.*, **1989**, *52*, 257.

54. Kameda K., Aoki H., Tanaka H. and Namiki M., *Agric. Biol. Chem.*, **1973**, *37*, 2137.

55. Cornforth J. W., *Aust. J. Chem.*, **1993**, *46*, 157.

56. Dimitriadis C., Gill M. and Harte M. F., *Tetrahedron: Asymmetry*, **1997**, *8*, 2153.

57. Devys M., Bousquet J. E, Kollmann A. and Barbier M., *Photochemistry*, **1980**, *19*, 2221.

58. Cotterill A. S., Gill M. and Milanovic N. M., *J. Chem. Soc., Perkin Trans. 1*, **1995**, 1215.

59. Stoessl A., *Biochem. Biophys. Res. Comm.*, **1969**, *35*, 186.

60. Eaton M. A. W. and Hutchinson D. H., *Tetrahedron Lett.*, **1971**, *18*, 1337.

61. Saeed A. and Rama N. H., *J. Chem. Soc. Pak.*, **1993**, *15*, 140.

62. Lim D. -S., Yoon S. K., Lee M. -S., Yoon W. H. and Kim C. H., *Korean J. Appl. Microbiol. Biotechnol.*, **1996**, *24*, 664.

63. (a) Asakawa Y., Tada Y. and Hashimoto T., *Phytochemistry*, **1994**, *37*, 233. (b) Deshpande B. S., Ambedkar S. S. and Shewale J. G., *Enzyme. Microb. Technol.*, **1988**, *10*, 455.

64. (a) Lin J., Yoshida S. and Takahashi N., *Agric. Biol. Chem.*, **1971**, *35*, 363. (b) Kiang F. M., Chang S. J. and Wu C. L., *Phytochemistr*y, **1994**, *37*, 1459. (c) Mitscher L. A., Andres W. W. and McCrae W., *Experientia*, **1964**, *20*, 258.

65. Stroech K., PhD Thesis, George-August Univrsity, **2003**.

66. (a) Furutani Y., Naganawa H., Takeuchi T. and Umezawa H., *Agric. Biol. Chem.*, **1977**, *41*, 1179. (b) Furutani Y., Takeuchi T. and Umezawa H., *Agric. Biol. Chem.*, **1977**, *41*, 1587.

67. Lim D. -S., Kwak Y. -S., Lee K. H., Ko S. -H., Yoon W. H., Lee W. -Y. and Kim C. -H., *Chemotherapy*, **2003**, *49*, 146.

68. Saeed A. and Ehsan S., *Chemistry of Heterocyclic Compounds*, **2005**, *41*, 1381 and reference cited therein.

69. Zeeck A., Ruß P., Laatsch H., Loeffler W., Wehrle H., Zähner H., Holst H., *Chem. Ber.*, **1979**, *112*, 957.

70. (a) Chen G., Zhang L., Wang H., Wu H. -H., Lu X., Pei Y. -H., Wu X., Pan B., Hua H. -M. and Bai J., *Rec. Nat. Prod.*, **2013**, *7*, 320. (b) Qiao X., Ye G., Liu C. -F., Zhang Z. -X., Tu Q., Dong J., Li Y. -Q., Guo D. -A. and Ye M., *J. Pharm. Biomed. Anal.*, **2012**, *57*, 133.

71. Yada H., Sate H., Toshima H., Dewra M. and Ichihara A., *Biosci. Biotechnol. Biochem.*, **2001**, *65*, 484.

72. Yang X. -Y., Cai S. -X., Zhang W. -J., Tang X. -L., Shin H. -Y., Lee J. -Y., Gu Q. -Q. and Park H., *Biol. Pharm. Bull.*, **2008**, *31*, 2228.

73. Yamaguchi M., Hasabe K. and Minami T., *Tetrahedron Lett.*, **1986**, *27*, 2401.

74. Blank F., Ng A. S. and Just G., *Can. J. Chem.*, **1966**, *44*, 2873.

75. Bode S. E., Drochner D. and Müller M., *Angew. Chem.*, **2007**, *119*, 6020.

76. Teixeira T. S .P., Freitas R. F., Abrahão O. Jr., Devienne K. F., de Souza, Blaber S. I., Blaber M., Kondo M. Y., Juliano M. A., Juliano L., Puzer L., *Bioorg. Med. Chem. Lett.*, **2011**, *21*, 6112.

77. Elix J. A. and Wardlaw J. H., *Aust. J. Chem.*, **2004**, *57*, 681.

78. Din L. B., Zakaria Z., Samsudin M. W. and Elix J. A., *Sains Malays.*, **2010**, *39*, 901.

79. Grove C. I., Di Maso M. J., Jaipuri F. A., Kim M. B. and Shaw J. T., *Org. Lett.*, **2012**, *14*, 4338.

80. Takahashi S. and Takido M., *J. Pharm. Soc. Jpn.*, **1973**, *93*, 261.

81. (a) Kitanaka S. and Takido M., *J. Pharm. Soc. Jpn.*, **1986**, *106*, 302. (b) Takenaka Y., Nagakura N., Hamada N. and Tanahashi T., *Heterocycles*, **2010**, *81*, 1931.

82. Kim Y. M., Lee C. H., Kim H. G. and Lee H. S., *J. Agric. Food Chem.*, **2004**, *52*, 6096.

83. Carpenter T. A., Evans G. E., Leeper F. J., Staunton J. and Wilkinson M. R., *J. Chem. Soc. Perkin Trans. 1*, **1984**, 1045.

84. Zhang Z. and Yu B., *J. Org. Chem.*, **2003**, *68*, 6309.

85. da Silva M. A., Oliveira A. P. S., Sannomiya M., Sano P. T., Varanda E. A., Vilegas W. and dos Santos L. C., *Chem. Pharm. Bull.*, **2007**, *55*, 1635.

86. Vilegas W., Roque N. F., Salatino A., Giesbrecht A. M. and Davino S., *Phytochemistry*, **1990**, *29*, 2299.

87. Varanda E. A. Raddi M. S. G., Dias F. L., Araujo M. C. P., Gibran S. C. A., Takahashi C. S. and Vilegas W., *Teratogen. Carcinogen. Mutagen.*, **1997**, *17*, 85.

88. Damasceno J. P. L., Rodrigues R. P., Gonçalves R. C. R. and Kitagawa R. R., *Molecules*, **2017**, *22*, 786.

89. Tavares D. C., Varanda E. A., Andrade F. D., Vilegas W. and Takahashi C. S., *J. Ethnopharmaco*., **1999**, *68*, 115.

90. Di Stasi L. C., Camuesco D., Nieto A., Vilegas W., Zarzuelo A. and Galvez J., *Planta Med*., **2004**, *70*, 315.

91. Smoot D. T., Elliott T. B., Verspaget H. W., Jones D., Allen C. R., Vernon K. G., Bremner T., Kidd L. C. R., Kim K. S., Groupman J. D. and Ashktorab H., *Carcinogenesis*, **2000**, *21*, 2091.

92. Coelho R. G., Vilegas W., Devienne K. F. and Raddi M. S. G., *Fitoterapia*, **2000**, *71*, 497.

93. Devienne K. F., Cálgaro-Helena A. F., Dorta D. J., Prado I. M. R., Raddi M. S. G., Vilegas W., Uyemura S. A., Santos A. C. and Curti C., *Phytochemistry*, **2007**, 68, 1075.

94. Santos L. C., Piacente S., Pizza C., Albert K., Dachtler M. and Vilegas W., *J. Nat. Prod.*, **2001**, *64*, 122.

95. Varanda E. A., Varella S. D., Rampazo R. A., Kitagawa R. R., Raddi M. S. G., Vilegas W. and dos Santos L. C., *Toxicology in Vitro*, **2006**, *20*, 664.

96. Fang J. -J., Ye G., Chen W. -L. and Zhao W. -M., *Phytochemistry*, **2008**, *69*, 1279.

97. Cotterill A. S., Donner C.D., Gill M. and White J. M., *Aust. J. Chem.*, **2003**, *56*, 49.

98. Blank F., Day W. C. and Just G.. *J. Invest. Dermatol*., **1963**, *40*, 33 and references cited therein.

99. Durley R. C., MacMillan J., Simpson T. J., Glen A. T. and Turner W. B., *J. Chem. Soc. Perkin Trans. 1*, **1975**, 163.

100. (a) Ito Y., Kawai K. and Nozawa Y., *J. Biochem.*, **1973**, *74*, 805. (b) Akita T., Kawai K., Shimonaka H., Nozawa Y., Ito Y., Nishibe S. and Ogihara Y., *Jpn. J. Med. Mycol.*, **1975**, *16*, 177.

101. Nozawa Y. and Ito Y., *Experientia*, **1970**, *26*, 803.

102. Singh P. D., Johnson J. H., Aklonis C. A., Bush K., Fisher S. M. and O'Sullivan J., *J. Antibiot.*, **1985**, *38*, 706.

103. Parisot D., Devys M., Fèrèzou J. -P. and Barbier M., *Phytochemistry*, **1983**, *22*, 1301.

104. Tatum J. H., Baker R. A. and Berry R. E., *Phytochemistry*, **1989**, *28*, 283.

105. Bruun T. and Lamvik A., *Acta Chem. Scand.*, **1971**, *25*, 483.

106. Maksimov O. B., Gorschkova R. P., Stepanenko L. S., Mischenko N. P. and Krivoschekova O. E., *C. A.*, **1991**, *114*, 78633a.

107. Rycroft D. S., Connolly J. D., Huneck S. and Himmelreich U., *Z. Naturforsch.*, **1995**, *50b*, 1557.

108. Kitagawa R. R., Raddi M. S. G., dos Santos L. C. and Vilegas W., *Chem. Pharm. Bull.*, **2004**, *52*, 1487.

109. Kitagawa R. R., da Fonseca L. M., Ximenes V. F., Khalil N. M., Vilegas W. and Raddi M. S. G., *Phytochemistry*, **2008**, *69*, 2205.

110. Kitagawa R. R., Vilegas W., Carlos I. Z. and Raddi M. S. G., *Rev. Bras. Farmacogn. Braz. J. Pharmacogn.*, **2011**, *21*, 1084.

111. Kitagawa R. R., Bonacorsi C., da Fonseca L. M., Vilegas W. and Raddi M.S.G., *Rev. Bras. Farmacogn.*, **2012**, *22*, 53.

112. (a) Sedmera P., Volc J., Weijer J., Vokoun J. and Musilek V., *Collect. Czech. Chem. Commun.*, **1981**, *46*, 1210. (b) Stack M. E. and Mislivec P. B., *Appl. Environ. Microbiol.*, **1978**, *36*, 552.

113. Stack M. E., Eppley R. M., Dreifuss P. A. and Pohland A. E., *Appl. Environ. Microbiol.*, **1977**, *33*, 351.

114. (a) Wadsworth D., Sperry J. and Brimble M. A., *Synthesis*, **2010**, 2604. (b) Kadkol M. V., Gopalkrishnan K. S. and Narasimhachari N., *J. Antibiot.*, **1971**, *24*, 245.

115. Paranagama P. A., Wijeratne E. M. K., Burns A. M., Marron M. T., Gunatilaka M. K., Arnold A. E. and Gunatilaka A. A. L., *J. Nat. Prod.*, **2007**, *70*, 1700.

116. Singh S. B., Cordingley M. G., Ball R. G., Smith J. L., Dombrowski A. W. and Goetz M. A., *Tetrahedron Lett.*, **1991**, *32*, 5279.

117. Gwaltney J. M. Jr., in *Viral Infection of Man: Epidemiology and Control*, 2nd edition, (editor Evans E. A.), Plenum Publishing Co., New York, **1982**.

118. (a) Donner C. D. and Gill M., *J. Chem. Soc., Perkin Trans. 1*, **2002**, 938. (b) Gill M. and Donner C. D., *Tetrahedron Lett*., **1999**, *40*, 3921.

119. Mmutlane E. M., Michael J. P., Green I. R. and de Koning, C. B., *Org. Biomol. Chem.*, **2004**, *2*, 2461.

120. Stobbe H., *Chem. Ber.*, **1893**, *26*, 2312.

121. Claisen, R. L., *Chem. Ber.*, **1912**, *45*, 3157.

122. (a) Pelly S., PhD Thesis, University of the Witwatersrand, **2009**. (b) Govender S., MSc Thesis, University of the Witwatersrand, **2005**.

123. Sperry J., Sejberg J. J. P., Stiemke F. M. and Brimble M. A., *Org. Biomol. Chem.*, **2009**, *7*, 2599.

124. Pillay A., Rousseau A. L., Fernandes M. A. and de Koning C. B., *Org. Biomol. Chem.*, **2012**, *10*, 7809.

125. Vickery E. H., Pahler L. F. and Eisenbraun E. J., *J. Org. Chem.*, **1979**, *44*, 4444.

126. Mbala B. M., PhD Thesis, Ghent University, **2011**.

127. de Koning C. B., Manzini S. S., Michael J. P., Mmutlane E. M., Tshabidi T. R. and van Otterlo W. A. L., *Tetrahedron*, **2005**, *61*, 555.

128. Lutz R. P., *Chem. Rev.*, **1984**, *84*, 205.

129. Lowell A. N., Fennie M. W. and Kozlowski M. C., *J. Org. Chem.*, **2008**, *73*, 1911.

130. Snyder C.D., Rapoport H., *J. Am. Chem. Soc.*, **1972**, *94*, 227.

131. Jacob P., Callery P. S, Shulgin A. T., Castagnoli N., *J. Org. Chem.*, **1976**, *41*, 3627.

132. (a) Corey E. J. and William J., *J. Org. Chem.*, **1973**, *38*, 3223. (b) Kitamura M., Tanaka S. and Yoshimura M., *J. Org. Chem.*, **2002**, *67*, 4975.

134. (a) Ditrich R. W. and Liebigs K., *Ann. Chem.*, **1990**, 23. (b) Volkmann R. A., Kelbaugh P. R., Nason D. M. and Jasys V. J., *J. Org. Chem.*, **1992**, *57*, 4352.

135. Henry P. M., *J. Am. Chem. Soc.*, **1964**, *86*, 3246. (b) Åkermark B. and Zetterberg K., *J. Am. Chem. Soc.*, **1984**, *106*, 5560. (c) Hegedus L. S., Williams R. E., McGuire M.A. and Hayashi T., *J. Am. Chem. Soc.*, **1980**, *102*, 4973.

136. (a) Keith J. A., Nielsen R. J., Oxgaard J. and Goddard W. A., *J. Am. Chem. Soc*., **2007**, *129*, 12342. (b) Smidt J., Hafner W., Jira R., Sedlmeier S., Sieber R., Rüttinger R. and Kojer H., *Angew. Chem.*, **1959**, *71*, 176.

137. (a) Jhaveri A. S. and Sharma M. M., *Chem. Eng. Sci*., **1967**, *22*, 1. (b) Kovács G., Stirling A., Lledós A. and Ujaque G., *Chem. Eur. J*., **2012**, *18*, 5612.

138. (a) Backvall J. E., Akermark B. and Ljunggren S. O., *J. Am. Chem. Soc.*, **1979**, *101*, 2411. (b) Smith M. B., *March's Advanced Organic Chemistry: Reactions, Mechanisms and Structure*, 5th edition, John Wiley and Sons, New York, **2001**.

139. (a) Guibè F., *Tetrahedron*, **1997**, *53*, 13509. (b) Greene T. W. and Wuts P. G. M., *Protective Groups in Organic Synthesis*, 3rd edition, Wiley: New York, **1999**.

140. Balkrishna S. B., Childers Jr. W. E. and Pinnick H. W., *Tetrahedron*, **1981**, *37*, 2091.

141. https://commons.wikimedia.org/wiki/File:Pinnick_oxidation_mechanism.png. Accessed on January 4, **2018**.

142. Kosak T. M., Conrad H. A., Korich A. L. and Lord R. L., *Eur. J. Org. Chem.*, **2015**, 7460.

143. Tamura Y., Yakura T., Tohma H., Kikuchi K. and Kita Y., *Synth. Commun.*, **1989**, 126.

144. Pillay A., PhD Thesis, University of the Witwatersrand, **2013**.

145. (a) Baldwin J. E., *J. Chem. Soc., Chem. Commun.*, **1976**, 734. (b) Baldwin J. E., Cutting J., Dupont W., Kruse L., Silberman L. and Thomas R. C., *J. Chem. Soc., Chem. Commun.*, **1976**, 736.

146. Ploysuk C., PhD Thesis, Kasetsart University, **2007**.

147. (a) Bèrard D., Jean A. and Canesi S., *Tetrahedron Lett.*, **2007**, *48*, 8238. (b) Guérard K. C., Sabot C., Beaulieu M. -A., Giroux M. -A., S. Canesi, *Tetrahedron*, **2010**, *66*, 5893.

148. Tanura Y., Yakura T., Tohma H., Kikuchi K. and Kita Y., *Syn. Commun.*, **1989**, 126.

149. (a) Nair N. N., *J. Phys. Chem. B*, **2011**, *115*, 2312. (b) Francis J. W. and Henry P. M., *Organometallics*, **1992**, *11*, 2832. (c) Hamed O., Henry P. M. and Thompson C., *J. Org. Chem.*, **1999**, *64*, 7745.

150. Brooks P. R., Wirtz M. C., Vetelino M. G., Rescek D. M., Woodworth G. F., Morgan B. P. and Coe J. W., *J. Org. Chem.*, **1999**, *64*, 9719.

151. Dillon E. and Dame O. F. N., *J. Am. Chem. Soc.*, **1942**, *64*, 1128.

152. Reiter P., *Emerg. Infect. Dis.*, **2000**, *6*, 1.

153. Cox F. E. G., *Parasit. Vectors*, **2010**, *3*, 1.

154. Laveran A., in *The Nobel Prize in Physiology or Medicine*, **1907**. *http://www.nobelprize.org/nobel_prizes/medicine/laureates/1907/laveran-bio.html*. Accessed on November 9, **2017**.

155. Hasitapan K. and Kongkathip N., PhD Thesis, Kasetsart University, **2006**.

156. (a) Volkman S. K., Barry A. E., Lyons E. J., Nielsen K. M., Thomas S. M., Choi M., Thakore S. S., Day K. P., Wirth D. F. and Hartl D. L., *Science*, **2001**, *293*, 482. (b) Dubar F., Khalife J., Brocard J., Dive D. and Biot C., *Molecules*, **2008**, *13*, 2900 and references cited therein.

157. Navarro M., Castro W. and Biot C., *Organometallics*, **2012**, *31*, 5715.

158. (a) Lanfranchi D. A., Cesar-Rodo E., Bertrand B., Huang H. -H., Day L., Johann L., Elhabiri M., Becker, K. Williams D. L. and Davioud-Charve E., *Org. Biomol. Chem.*, **2012**,

10, 6375. (b) Müller T., Johann L., Jannack B., Brückner M., Lanfranchi D. A., Bauer H., Sanchez C., Yardley V., Deregnaucourt C., Schrevel J., Lanzer M., Schirmer R. H. and Davioud-Charvet E., *J. Am. Chem. Soc.*, **2011**, *133*, 11557.

159. Le Bras J., Musset L. and Clain J., *Med. Mal. Infect.*, **2006**, *36*, 401.

160. Yamauchi L. M., Coppi A., Snounou G. and Sinnis P., *Cell. Microbiol.*, **2007**, *9*, 1215.

161. Amino R., Thiberge S., Martin B., Celli S., Shorte S., Frischknecht F. and Menard R., *Nat. Med.*, **2006**, *12*, 220.

162. Doolan D. L., Dobanõ C. and Baird J. K., *Clin. Microbiol. Rev.*, **2009**, *22*, 13.

163. (a) Verhage D. F., Telgt D. S., Bousema J. T., Hermsen C. C., van Gemert G. J., van der Meer J. W. and Sauerwein R. W., *Neth. J. Med.*, **2005**, *63*, 52. (b) Rickman L. S., Jones T. R., Long G. W., Paparello S., Schneider I., Paul C. F., Beaudoin R. L. and Hoffman S. L., *Am. J. Trop. Med. Hyg.*, **1990**, *43*, 441.

164. Belmonte M., Jones T. R., Lu M., Arcilla R., Smalls T., Belmonte A., Rosenbloom J., Carucci D. J. and Sedegah M., *J. Parasitol*., **2003**, *89*, 602.

165. Eichner M., *Malaria life cycle*. *http://www.unituebingen.de/modeling/ModMalariaCycl-een.html*. Accessed on November 14, **2017**.

166. Caraballo H. and King K., *Emerg. Med. Pract*., **2014**, *16*, 1.

167. Doolan D. L., Dobańo C. and Baird J. K., *Clin. Microbiol. Rev.*, **2009**, *22*, 13 and references cited therein.

168. Muregi F. W., *Curr. Drug Discov. Technol.*, **2010**, *7*, 280 and references cited therein.

169. (a) Fotie J., *Agents Med. Chem.*, **2006**, *5*, 357. (b) Fieser L. F., Berliner E., Bondhus F. J., Chang F. C., Dauben W. G., Ettlinger M. G., Fawaz G., Fields M., Heidelberger C.,

Heymann H., Vaughan W.R., Wilson A.G., Wilson E., Wu M. -I., Leffler M. T., Hamlin K. E., Matson E. J., Moore E. E., Moore M. B. and Zaugg H. E., *J. Am. Chem. Soc.*, **1984**, *70*, 3174. (c) Likhitwitayawuid K., Kaewamatawong R., Ruangrungsi N. and Krungkrai J., *Planta Med.*, **1998**, *64*, 237.

170 Croft A. M., *Clin. Evid.*, **2005**, 954.

171. Wendel W. B., *Fed. Proc.*, **1946**, *5*, 406.

172. Williams D. R. and Clark M. P., *Tetrahedron Lett.*, **1998**, *39*, 7629.

173. (a) Hudson A. T., *Parasitol. Today*, **1993**, *9*, 66 and references cited therein. (b) Fry M. and Pudney M., *Biochem. Pharmacol.*, **1992**, *43*, 1545.

174. (a) Looareesuwan S., Chulay J. D., Canfield C. J. and Hutchinson D. B., *Am. J. Trop. Med. Hyg.*, **1999**, *60*, 533. (b) Baggish A. L. and Hill D. R., *Antimicrob. Agents Chemother.*, **2002**, *46*, 1163.

175 (a) Mather M. W.,Darrouzet E., Valkova-Valchanova M., Cooley J. W., McIntosh M. T., Daldal F. and Vaidya A. B., *J. Biol. Chem.*, **2005**, *280*, 27458. (b) Kessl J. J., Lange B. B., Merbitz-Zahradnik T., Zwicker K., Hill P., Meunier B., Palsdottir H., Hunte C., Meshnick S. and Trumpower B. L., *J. Biol. Chem.*, **2003**, *278*, 31312.

176. (a) Hughes W. T., Gray V. L., Gutteridge W. E., Latter V. S. and Pudney M., *Antimicrob. Agents Chemother.*, **1990**, *34*, 225. (b) Kess J. J., Meshnick S. R. and Trumpower B. L., *Trends Parasitol.*, **2007**, *23*, 495 and references cited therein.

177. Kongkathip N., Pradidphol N., Hasitapan K., Grigg R., Kao W. -C., Hunte C., Fisher N., Warman A. J., Biagini G. A., Kongsaeree P., Chuawong P. and Kongkathip B., *J. Med. Chem.*, **2010**, *53*, 1211.

178. Kapadia G. J., Azuine M. A., Balasubramanian V. and Sridhar R., *Pharmacol. Res.*, **2001**, *43*, 363.

179. Carneiro P. F., Pinto M. C. R. F., Marra R. K. F., da Silva F. C., Resende J. A. L. C., de Silva L. F. R., Alves H. G., Barbosa G. S., de Vasconcellos M. C., Lima E. S., Pohlit A. M., Ferreira V. F., *Eur. J. Med. Chem.*, **2016**, *108*, 134.

180. Irvine F. R., *Woody Plants of Ghana*, University Press: Oxford, **1961**.

181. (a) Hoet S., Opperdoes F., Brun R. and Quetin-Leclereq J., *Nat. Prod. Rep.*, **2004**, *21*, 353. (b) Schwikkard S. and van Heerden F. R., *Nat. Prod. Rep.*, **2002**, *19*, 675.

182. Weiss C. R., Moideen S. V. K., Croft S. L. and Houghton P. J., *J. Nat. Prod.*, **2000**, *63*, 1306.

183. Onegi B., Kraft C., Kohler I., Freund M., Jenett-Siems K., Siems K., Beyer G., Melzig M.F., Bienzle U. and Eich E., *Phytochemistry*, **2002**, *60*, 39.

184. (a) De Kimpe N., Van Puyvelde L., Schripsema J., Erkelens J., Verpoortere R., *Magn. Reson. Chem.*, **1993**, *31*, 329. (b) Claessens S., Naidoo D., Mulholland D., Verschaeve L., Staden J. and De Kimpe N., *Synlett.*, **2006**, 621.

185. Van Puyvelde L., Hakizayezu E., Brioen P., De Kimpe N., De Vroey C., Bogaerts J. and Hakizamungu E., *International Congress on Natural Products Research*, July 31 to August 4, **1994**, Halifax: Canada

186. Hari L., De Buyck L. F. and De Pooter H. L., *Phytochemistry*, **1991**, *30*, 1726.

187. Grimshaw J. and Haworth R., *J. Chem. Soc.*, **1956**, 4225.

188. Winter R. W., Cornell K. A., Johnson L. L., lsabelle L. M., Hinrichs D. J. and Riscoe M. K., *Bioorg. Med. Chem. Lett.*, **1995**, *5*, 1927.

189. Hogg T., Nagarajan K., Herzberg S., Chen L., Shen X., Jiang H., Wecke M., Blohmke C., Hilgenfeld R. and Schmidt C. L., *J. Biol. Chem.*, **2006**, *281*, 25425.

190. (a) Togni A., Hayashi T., (Eds.), *Ferrocenes, Homogeneous Catalysis, Organic Synthesis and Materials Science*, VCH, Weinheim, **1995**. (b) Togni A., Halterman R. L., (Eds.), *Metallocenes*, VCH, Weinheim, **1998**. (c) Long N. J., *Metallocenes, An Introduction to Sandwich Complexes*, Blackwell Science, Oxford, **1998**.

191. van Staveren D. R. and Metzler-Nolte N., *Chem. Rev.*, **2004**, *104*, 5931.

192. (a) Wilkinson G., *J. Am. Chem. Soc*., **1952**, *74*, 6146. (b) Fischer E. O. and Pfab W., *Z Naturforsch*., **1952**, *76*, 377.

193. (a) Lin L., Berces A. and Kraatz H. B., *J. Organomet. Chem.*, **1998**, *556*, 11. (b) Barlow S. and Marder R.S., *J. Chem. Soc. Chem. Comm.*, **2000**, 1555.

194 Köpf-Maier P., Köpf H. and Neuse E. W., *Angew. Chem., Int. Ed. Engl.*, **1984**, *23*, 456.

Köpf-Maier P., Köpf H and Neuse E. W., *J. Cancer Res. Clin. Oncol.*, **1984**, *108*, 336.

195. Osella D., Ferrali M., Zanello P., Laschi F., Fontani M., Nervi C. and Cavigiolio G., *Inorg. Chim. Acta*, **2000**, *306*, 42.

196. Yucel B., Sanli B., Soylemez H. and Yilmaz I., *Tetrahedron*, **2011**, *67*, 1406.

197. (a) Gimeno M. C., Goitia H., Laguna A., Luque M. E., Villacampa M. D., Sepúlveda C., Meireles M., *J. Inorg. Biochem.*, **2011**, *105*, 1373. (b) Sun H., Wang Q., Haung R., Li H. and Li Y., *J. Organomet. Chem.*, **2002**, *655*, 182.

198. Damljanović I., Vukićević M., Radulović N., Palić R., Ellmerer E., Ratković Z., Joksović M. D. and Vukićević R. D., *Bioorg. Med. Chem. Lett.*, **2009**, *19*, 1093.

199. Gill G. and Beeching N., *Lecture Notes: Tropical Medicine*, John Wiley, *Vol. 67*, **2011**.

200. Parveen H., Hayat F., Salahuddin A. and Azam A., *Eur. J. Med. Chem.*, **2010**, *45*, 3497.

201. Pejović A., Damljanović I., Stevanović D., Vukićević M., Novaković S. B., Bogdanović G. A., Radulović N. and Vukićević R. D., *Polyhedron*, **2012**, *31*, 789.

202. Biot C., Dessolin J., Ricard I. and Dive D., *J. Organomet. Chem.*, **2004**, *689*, 4678.

203. Guillon J., Moreau S., Mouray E., Sinou V., Forfar I., Fabre S. B., Desplat V., Millet P., Parzy D., Jarry C. and Grellier P., *Bioorg. Med. Chem.*, **2008**, *16*, 9133.

204. Baramee A., Coppin A., Mortuaire M., Pelinski L., Tomavoc S. and Brocard J., *Bioorg. Med. Chem.*, **2006**, *14*, 1294.

205. (a) Dannemann B., McCutchan A., Israelski D., Antoniskis D., Leport C., Luft B., Nussbaum J., Clumeck N., Morlat P., Chiu J., Vilde J. L., Orellana M., Feigal D., Bartok A., Heseltine P., Leedom J., Remington J., and the California Collaboratrive Treatment Group. *Ann. Intern. Med.*, **1992**, *116*, 33. (b) Kovacs J. A. and Masur H., *N. Engl. J. Med.*, **2000**, *342*, 1416. (c) Luft B. J. and Remington J., *Clin. Infect. Dis.*, **1992**, *15*, 211.

206. Quirante J., Dubar F., González A., Lopez C., Cascante M., Cortés R., Forfar I., Pradines B. and Biot C., *J. Organomet. Chem.*, **2011**, *696*, 1011.

207. Boev V. I., Snegur L. V., Babin V. N. and Nekrasov Y. S., *Russ. Chem. Rev.*, **1997**, *66*, 613.

208. Nguyen A., PhD Thesis, de l'Université de Pierre et Marie Curie, **2007**.

209. de Cremoux P., Tran-Perennou C., Elie C., Boudou E., Barbaroux C., Poupon M., De Rycke Y., Asselin B. and Magdelenat H., *Biochem. Pharmacol.*, **2002**, *64*, 507.

210. Gasser G. and Metzler-Nolte N., *Curr. Opinion Chem. Biol.*, **2012**, *16*, 84 and references therein.

211. (a) Morello K. C., Wurz G. T., DeGregorio M. W., *Crit. Rev. Oncol., Hematol*., **2002**, *43*, 63. (b) Wang D. Y., Fulthorpe R., Liss S.N. and Edwards E. A., *Mol Endocrinol*., **2004**, *18*, 402.

212. (a) Jordan V. C., *Nature Reviews Drug Discovery*, **2003**, *2*, 205. (b) Jordan V. C., *Cancer Res.*, **2001**, *61*, 5683.

213. Jordan V. C., Collins M. M. Rowsby L. and Prestwich G., *J. Endocrinol*, **1977**, *75*, 305.

214. (a) Desta Z. Ward B. A., Soukhova N. V. and Flockhart D. A., *J. Pharmacol. Exp. Ther*., **2004**, *310*, 1062. (b) Richard M. A., Hamels D., Pigeon P., Top S., Dansette P. M., Lee H. Z. S., Vessières A., Mansuy D. and Jaouen G., *Chem. Med. Chem.*, **2015**, *10*, 981.

215. https://ipfs.io/ipfs/QmXoypizjW3WknFiJnKLwHCnL72vedxjQkDDP1mXWo6uco/wiki/Afimoxifene.html. Accessed on November 21, **2017**.

216. (a) Bernstein L., Deapen D., Cerhan J. R., Schwartz S. M., Liff J., McGann-Maloney E., Perlman J.A., *J. Natl. Cancer Inst.*, **1999**, *91*, 1654. (b) Hillard E. A., Vessières A. and Jaouen G., *Top Organomet. Chem.*, **2010**, *32*, 81.

217. (a) Top S., Tang J., Vessières. A, Carrez D., Provot C. and Jaouen G., *Chem. Commun.*, **1996**, *8*, 955. (b) Top S., Dauer B., Vaisserman J. and Jaouen G., *J. Organomet. Chem.*, **1997**, *541*, 355.

218. (a) Zhao L. and Brinton R., *J. Med. Chem.*, **2005**, *48*, 3463. (b) Heilmann J. B., Hillard E. A., Plamont M. -A., Pigeon P., Bolte M., Jaouen G. and Vessières A., *J. Organomet. Chem.*, **2008**, *693*, 1716.

219. Jaouen G., Vessières A. and Top S., *Chem. Soc. Rev.*, **2015**, *44*, 8802 and references cited therein.

220. (a) Wlassoff W.A., Albright C.D., Sivashinski M.S., Ivanova A., Appelbaum J.G. and Salganik R.I., *J. Pharm. Pharmacol.*, **2007**, *59*, 1549. (b) Hillard E.A., Vessières A., Thouin L., Jaouen G., Amatore C., *Angew. Chem., Int. Ed.*, **2006**, *45*, 285.

221. Pigeon P., Top S., Zekri O., Hillard E. A., Vessières A., Plamont M. -A., Buriez O., Labbé E., Huché M., Boutamine S., Amatore C. and Jaouen G., *J. Organomet. Chem.*, **2009**, *694*, 895.

222. Loeb R. F., Clarke W. M., Coateney G. R., Coggeshall L. T., Dieuaide F. R., Dochez A. R., Hankansson E. G., Marshall E. K., Marvel S. C., McCoy O. R., Sapero J. J., Serbell W. H., Shannon J. A. and Carden G. A., *J. Am. Med. Assoc.*, **1946**, *130*, 1069.

223. (a) Tilley L., Dixon M. W. A. and Kirk K., *Int. J. Biochem. Cell Biol.*, **2011**, *43*, 839. (b) Egan T. J., Combrinck J. M., Egan J., Hearne G. R., Marques H. M., Ntenteni S., Sewell B. T., Smith P. J., van Taylor D., Schalkwyk D. A. and Walden J. C., *J. Biochem.*, **2002**, *365*, 343.

224. Foley M. and Tilley L., *Pharmacol. Ther.*, **1998**, *79*, 55.

225. (a) Slater A. F. and Cerami A., *Nature*, **1992**, *355*, 167. (b) Egan T. J., Ross D. C. and Adams P. A., *FEBS Lett.*, **1994**, *352*, 54.

226. (a) White N. J., *J. Antimicrob. Chemother.*, **1992**, *30*, 571. (b) Van Est H. G., Skamene G. E. and Schurr E., *Clin. Invest. Med.*, **1993**, *16*, 285.

227. Daher W., Pelinski L., Klieber S., Sadoun F., Meunier V., Bourrié M., Biot C., Guillou F., Fabre G., Brocard J., Fraisse L., Maffrand J. -P., Khalife J. and Dive D., *Drug Metab. Dispos.*, **2006**, *34*, 667.

228. (a) Vander Jagt D. L., Hunsaker L. A. and Campos N. M., *Mol. Biochem. Parasitol.*, **1986**, *18*, 389. (b) Supan C., Mombo-Ngoma G., Dal-Bianco M. P., Ospina Salazar C. L.,

Issifou S., Mazuir F., Filali-Ansary A., Biot C., Ter-Minassian D., Ramharter M., Kremsner P. G. and Lell B., *Antimicrob. Agents Chemother.*, **2012**, *56*, 3165.

229. Biot C., Glorian G., Maciejewski L., Brocard J., Domarle O., Blampain G., Millet P., Georges A. J., Abessolo H. and Dive D., *J. Med. Chem.*, **1997**, *40*, 3715.

230. (a) Chatterjee T., Muhkopadhyay A., Khan K. A., Giri A. K., *Mutagenesis*, **1998**, *13*, 619. (b) Pierrot C., Lafitte S., Dive D., Fraisse L., Brocard J. and Khalife J. *Int. J. Parasitol*, **2005**, *35*, 1601.

231. (a) Henry M., Briolant S., Fontaine A., Mosnier J., Baret E., Amalvict R., Fusaï T., Fraisse L., Rogier C. and Pradines B., *Antimicrob. Agents Chemother.*, **2008**, *52*, 2755. (b) Dubar F., Egan T. J., Pradines B., D. Kuter, Ncokazi K. K., Forge D., Paul J-F, Pierrot C., Kalamou H., Khalife J., Buisine E., Rogier C., Vezin H., Forfar I., Slomianny C., Trivelli X., Kapishnikov S., Leiserowitz L., Dive D. and Biot C., *ACS Chem. Biol.*, **2011**, *6*, 275. (c) Kreidenweiss A., Kremsner P.G., Dietz K. and Mordmüller B., *Am. J. Trop. Med. Hyg.*, **2006**, *75*, 1178.

232. Biot C., Chavain N., Dubar F., Pradines B., Trivelli X., Brocard J., Forfar I. and Dive D., *J. Organomet. Chem.*, **2009**, *694*, 845.

233. Biot C., Taramelli D., Forfar-Bares I., Maciejewski L.A., Boyce M., Nowogrocki G., Brocard J. S., Basilico N., Olliaro P. and Egan T. J., *Mol. Pharm.*, **2005**, *2*, 185.

234. (a) Ré D. B., Nafia I., Nieoullon A. L., Goff L. K. and Had-Aissouni L., *Ann. Fr. Anesth. Reanim.*, **2005**, *24*, 502. (b) Chavain N., Vezin H., Dive D., Touati N., Paul J. F., Buisine E. and C. Biot, *Mol. Pharm.*, **2008**, *5*, 710. (c) Dubar F., Bohic S., Slomianny C., Morin J. C., Thomas P., Kalamou H., Guérardel Y., Cloetens P., Khalife J. and Biot C., *Chem. Commun.*, **2012**, *48*, 910.

235. Dubar F., Bohic S., Dive D., Gürardel Y., Cloetens P., Khalife J. and Biot C., *ACS Med. Chem. Lett.*, **2012**, *3*, 480.

236. (a) Schmid H. and Ebnother A., *Helv. Chim. Acta*, **1951**, *34*, 1041. (b) Eisenhuth W. and Schmid H., *Helv. Chim. Acta*, **1958**, *41*, 2021.

237. Bianchi C. and Ceriotti G., *J. Pharm. Sci.*, **1975**, *64*, 1305.

238. (a) Chen Z., Huang H., Wang C., Li Y. and Ding J., *Zhongcaoyao*, **1981**, *12*, 484. (b) Ding J. and Huang H., *Zhongcaoyao*, **1982**, *13*, 499.

239. (a) Grubbs R. H. and Chang S., *Tetrahedron*, **1998**, *54*, 4413. (b) Blackwell H. E., O'Leary D. J., Chatterjee A. K., Washenfelder R. A., Bussmann D. A. and Grubbs R. H., *J. Am. Chem. Soc.*, **2000**, *122*, 58. (c) Chatterjee A. K., Choi T. -L., Sanders D. P. and Grubbs R. H., *J. Am. Chem. Soc.*, **2003**, *125*, 11360.

240. (a) Wittig G. and Schoollkopf U., *Chem. Ber.*, **1954**, *87*, 1318. (b) Wittig G. and Haag W., *Chem. Ber.*, **1955**, *88*, 1654.

241. (a) McMurry J. E. and Felming M. P., *J. Am. Chem. Soc*., **1974**, *96*, 4708. (b) McMurry J. E., *Chem. Re*v., **1989**, *89*, 1513.

242. Mmutlane E. M., PhD Thesis, University of the Witwatersrand, **2004**.

243. Pelly S. C., Govender S., Fernandes M. A., Schmalz H. -G. and de Koning C. B., *J. Org. Chem.*, **2007**, *72*, 2857.

244. https://www.sigmaaldrich.com/spectra/fnmr/FNMR005446.PDF. Accessed on November 18, **2017**.

245. Hugo V. I., *Cape Technikon Theses and Dissertations. Paper 49*, **1996**.

246. Couladouros E. A. and Strongilos A. T., *Tetrahedron Lett.*, **2000**, *41*, 535.

247. (a) Heck R. E, *Palladium Reagents in Organic Synthesis*, Academic Press, London, **1985**. (b) Heck R. E, Wu G., Tao W. and Reingold . L A., in *Catalysis of Organic Reactions* (Ed. D. W. Blackburen), Marcel Dekker, New York, **1989**.

248. Perez A. L., Lamoureux G. and Zhen-Wu B. Y., *Tetrahedron Lett.*, **2007**, *48*, 3995.

249. Kowalski K., Koceva-Chyła A., Szczupak L., Hikisz P., Bernasińska J., Rajnisz A., Solecka J., Therrien B., *J. Organomet. Chem.*, **2013**, *741*, 153.

250. König B., Zieg H., Bubenitschek P. and Jones P. G., *Chem. Ber.*, **1994**, *127*,1811.

251. Johnson M. M., PhD Thesis, University of the Witwatersrand, **2014**.

252. (a) Baker W. and Lothian O. M., *J. Am. Chem. Soc*., **1936**, 274. (b) Harwood L. M., *J. Chem. Soc*., **1982**, 1120; (c) Harwood L. M., *Chem. Commun.*, **1983**, 530; (d) Harwood L. M., *J. Chem. Soc., Perkin Trans. 1*,**1984**, 2577.

253. Pillay A., Rousseau A. L., Fernandes M. A. and de Koning C. B., *Tetrahedron*, **2012**, *68*, 7116.

254. (a) Giles R. G. F., Green I. R., Hugo V. I., Mitchell P. R. K. and Yorke S. C., *J. Chem. Soc., Perkin Trans. 1*, **1983**, 2309. (b) de Koning C. B., Giles R. G. F. and Green I. R., *J. Chem. Soc., Perkin Trans. 1*, **1991**, 2743. (c) Giles R.G.F., Green I.R, Knight L.S., Lee Son V.R. and Yorke S.C., *J. Chem. Soc., Perkin. Trans. 1*, **1994**, 859.

255. (a) G. L. Closs, *Alkylcarbenes from Methylene Chloride and Alkyllithiums*, **1962**, 809. (b) University of Liverpool, http://www.chemtube3d.com/CarbenesFormation(AlphaElimination).html. Accessed on January 2, **2018**.

256. (a) Brimble M. A. and Brenstrum T. J., *J. Chem. Soc., Perkin Trans. 1*, **2001**, 1612. (b) Deore V., Lohar M. K., Mundada R., Roychowdhury A., Vishwakarma R. and Kumar S.,

Synth. Commun., **2011**, *41*, 177. (c) Hannan R. L., Barber R. B. and Rapoport H., *J. Org. Chem.*, **1979**, 44.

257. (a) Pummerer R., Puttfarcken H. and Schopflocher P., *Chem. Ber.*, **1925**, *58*, 1808. (b) Musso H., *Angew. Chem. Int. Ed., Engl.*, **1963**, *2*, 723 and references cited therein.

258. Saeed A., Altarawneh M. and Dlugogorski B. Z., *Organohal. Comp.*, **2014**, *76*, 345.

259. Rottmann M., McNamara C., Yeung B. K. S., Lee M. C. S., Zou B., Russell B., Seitz P., Plouffe D. M., Dharia N. V., Tan J., Cohen S. B., Spencer K. R., González-Páez G. E., Lakshminarayana S. B. , Goh A., Suwanarusk R., Jegla T., Schmitt E. K., Beck H. -P., Brun R., Nosten F., Renia L., Dartois V., Keller T. H., Fidock D. A., Winzeler E. A., Diagana T. T., *Science*, **2010**, *329*, 1175 and references cited therein.

260. Pradines B., Fusai T., Daries W., Laloge V., Rogier C. and Millet P., *J. Antimicrob. Chemother.*, **2001**, *48*, 179.

261. Pradines B., Mamfoumbi M. M., Parzy D., Medang O. M., Lebeau C. and Mbina M. J. R., *Parasitology*, **1998**, *117*, 541.

262. Chim P., Lim P., Sem R., Nhem S., Maciejewski L. and Fandeur T., *Ann. Trop. Med. Parasitol.*, **2004**, *98*, 419.

263. Okombo J., Kiara S. M., Abdirahman A., Mwai L., Ohuma E., Borrmann S., Nzila A. and Ward S., *J. Antimicrob. Chemother.*, **2013**, *68*, 786 and references cited therein.

264. (a) Peters W., *Ann. Trop. Med. Parasitol.*, **1968**, *62*, 277. (b) Peters W., *Annu. Rev. Pharmacol.*, **1968**, *62*, 488. (c) Peters W. Robinson B. L., *Ann. Trop. Med. Parasitol.*, **1987**, *81*, 459.

265. Petersen E., *J. Travel Med.*, **2003**, *10*, S13.

266. Eastman R. T. and Fidock D. A., *Nat. Rev. Microbiol.*, **2009**, *7*, 864.

267. (a) Kremsner P. G. and Krishna S., *Lancet*, **2004**, *364*, 285 and references cited therein. (b) http://www.who.int/malaria/publications/atoz/9789241549127/en/. Accessed on November 12, **2017**. (c) Ashley E. A. and White N. J., *Curr. Opin. Infect. Dis.*, **2005**, *18*, 531.

268. World Health Organization, Malaria, in *Seventh Programme Report of the Tropical Disease Research (TDR)*. Geneva: World Health Organization.

269. Medicines for Malaria Venture. *Tackling Resistance*. http://www.mmv.org/research-development/tackling-resistance. Accessed on November 18, **2017**.

270. Noedl H., Se Y., Schaecher K., Smith B. L., Socheat D. and Fukuda M. M., *N. Engl. J. Med.*, **2008**, *359*, 2619.

271. (a) Olliaro P., Wells T. N., *Clin. Pharmacol. Ther.*, **2009**, *85*, 584. (b) Wells T. N. C., Alonso P. L., Gutteridge W. E., *Nat. Rev. Drug Discov.*, **2009**, *8*, 879. (c) Ekland E. H. and Fidock D. A., *Int. J. Parasitol*., **2008**, *38*, 743.

272. Delhaes L., Abessolo H., Biot C., Berry L., Delcourt P., Maciejewski L., Camus D. and Dive D., *Parasitol. Res.*, **2001**, *87*, 239.

273. White N. J. and Olliaro P. L., *Parasitol Today*, **1996**, *12*, 399.

274. (a) Pandey A. V., Tekwani B. L., Singh R. L. and Chauhan V. S., *J. Bio. Chem.*, **1999**, *274*, 19383. (b) O'Neill P. M., Barton V. E. and Ward S. A., *Molecules*, **2010**, *15*, 1705. (c) Rudrapal M. and Chetia D., *Drug Design, Develop. Ther.*, **2016**, *10*, 3575.

275. Mestrelab Research. *MestReNova*, 9, **2014**.

276. Bruker AXS Inc. *SAINT+*, Version 6.02 (Includes XPREP and SADABS); Madison, Wisconsin, USA, **2004**.

277. Sheldrick G. M., *Acta Crys. A.*, **2008**, *64*, 112.

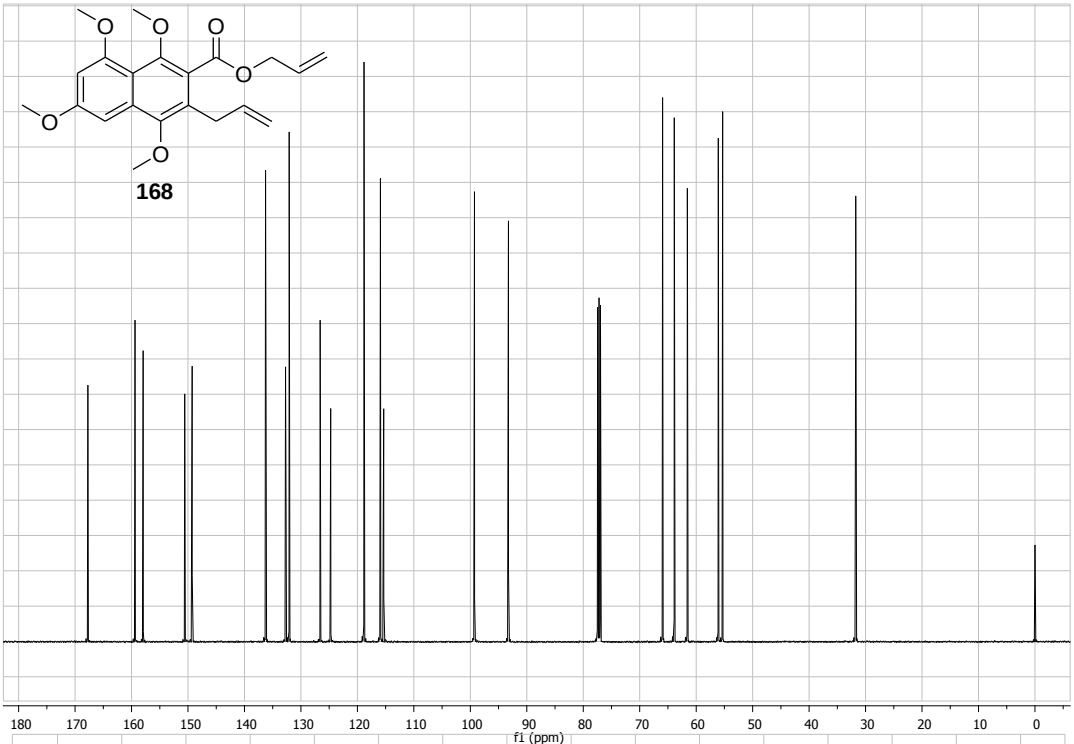
278. Farrugia L., WinGX suite for small-molecule single-crystal crystallography. *J. Appl. Cryst.*, **1999**, *32*, 837.

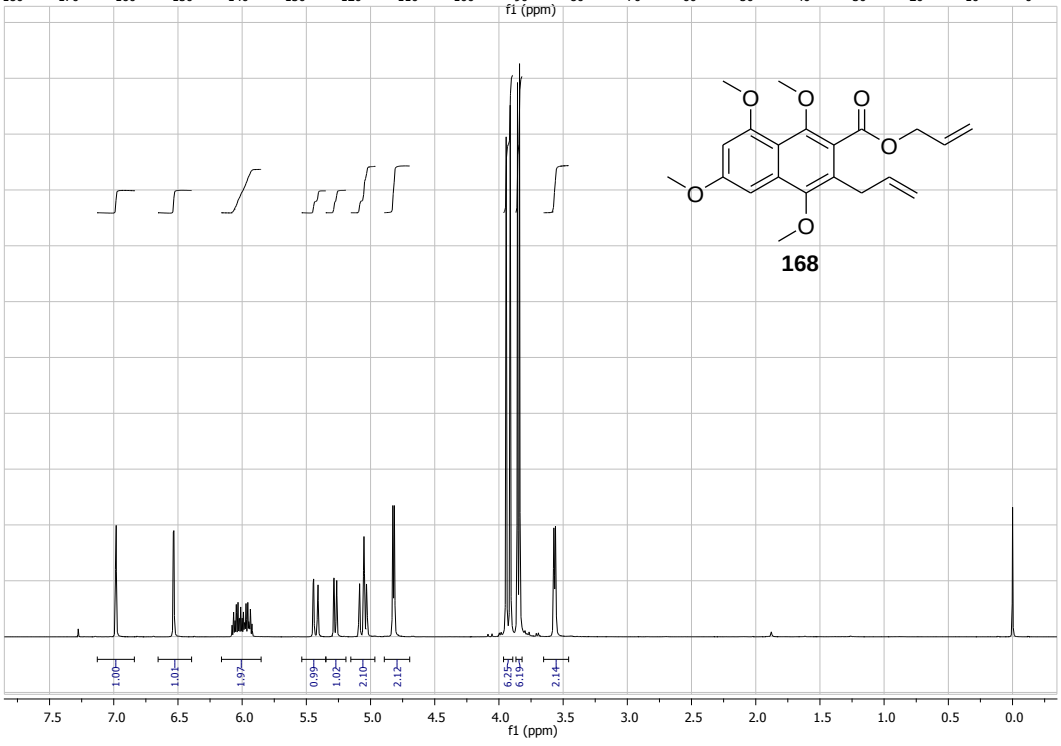
279. Farrugia L., ORTEP-3 for Windows - a version of ORTEP-III with a Graphical User Interface (GUI). *J. Appl. Cryst.*, **1997**, *30*, 565.

Chapter 9: Appendices

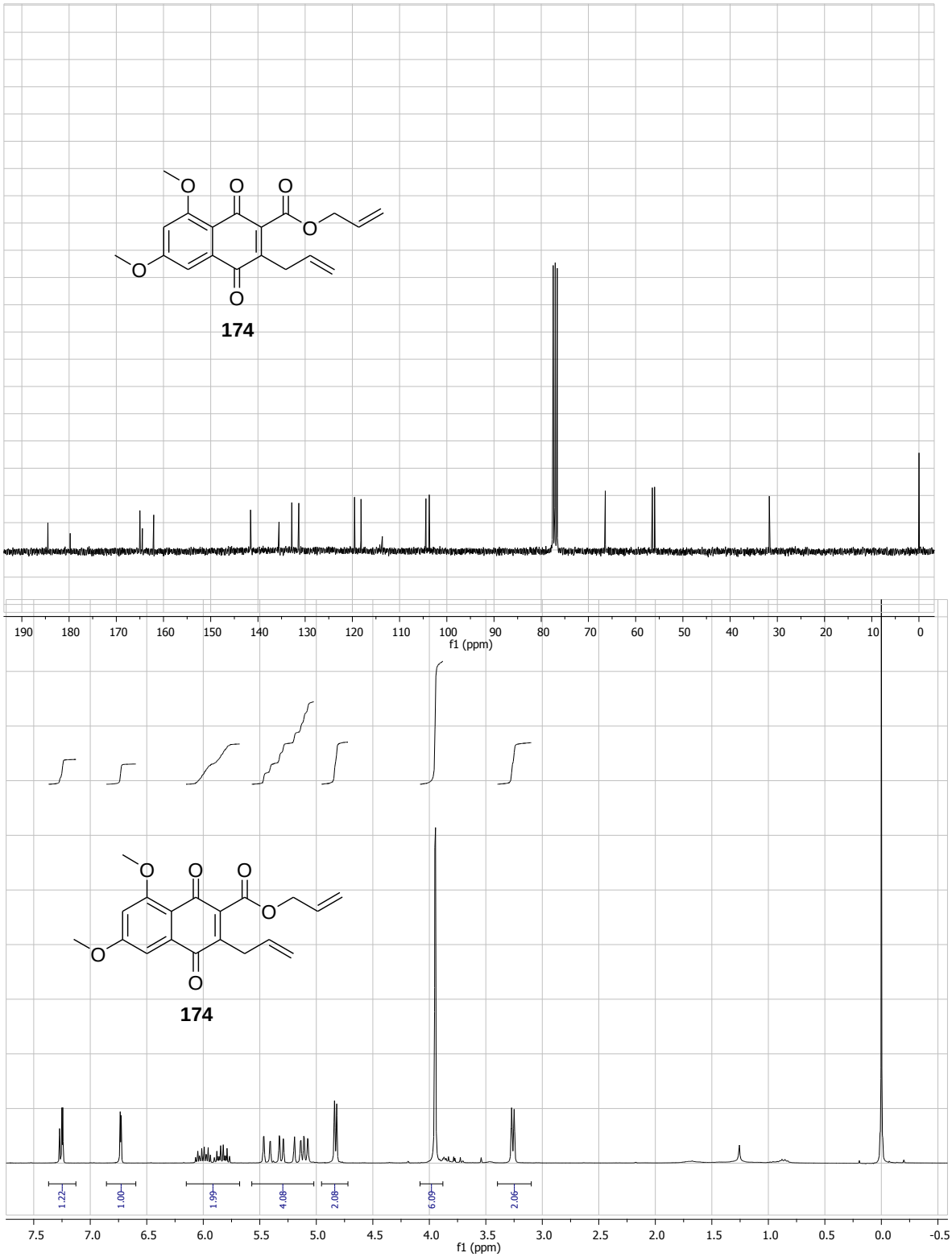
A1 Appendices: 1D NMR spectroscopic data

A1.0 ^{1}H and ^{13}C NMR spectra of allyl ester 168

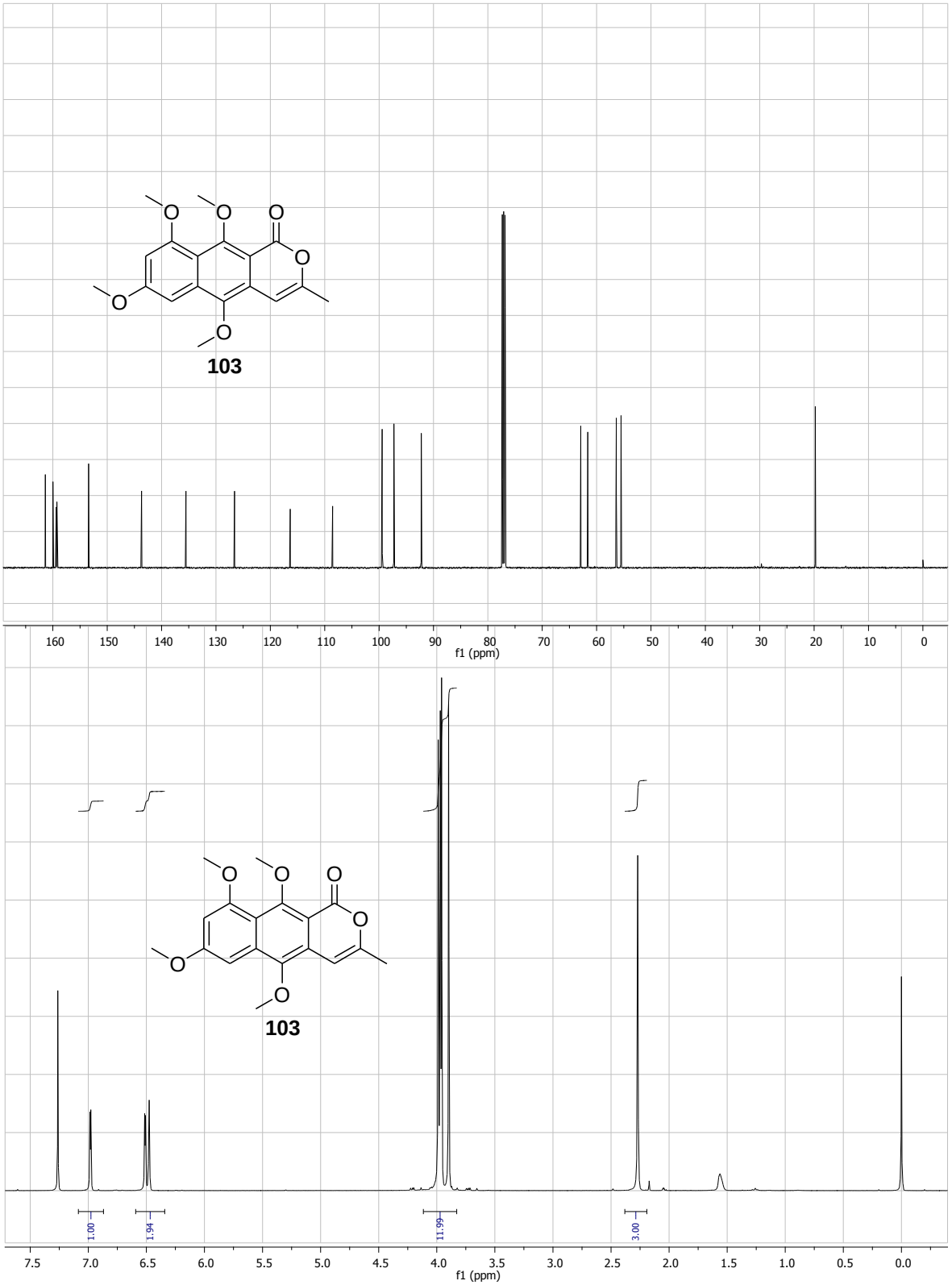




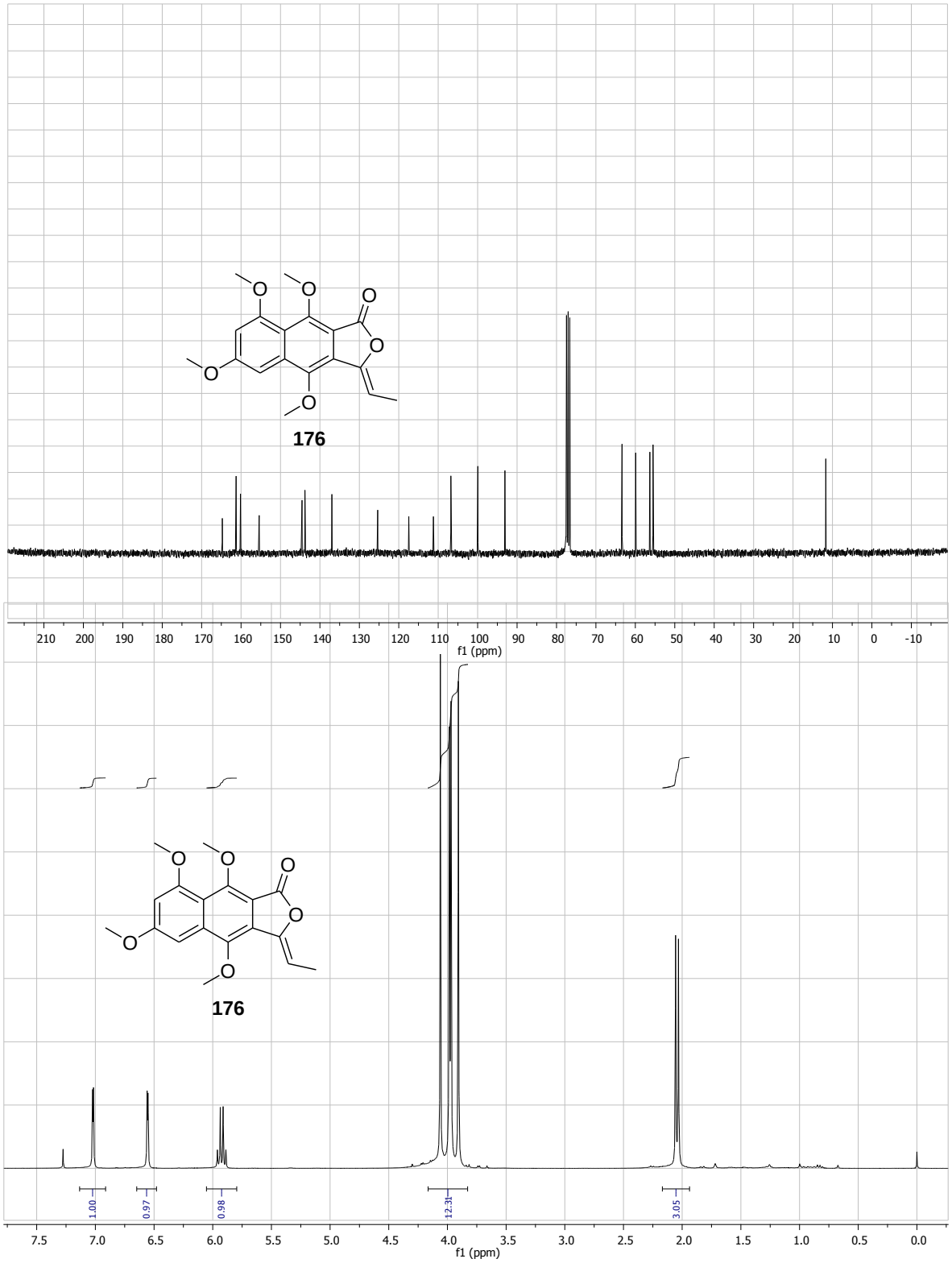
A1.1 ^{1}H and ^{13}C NMR spectra of naphthoquinone 174



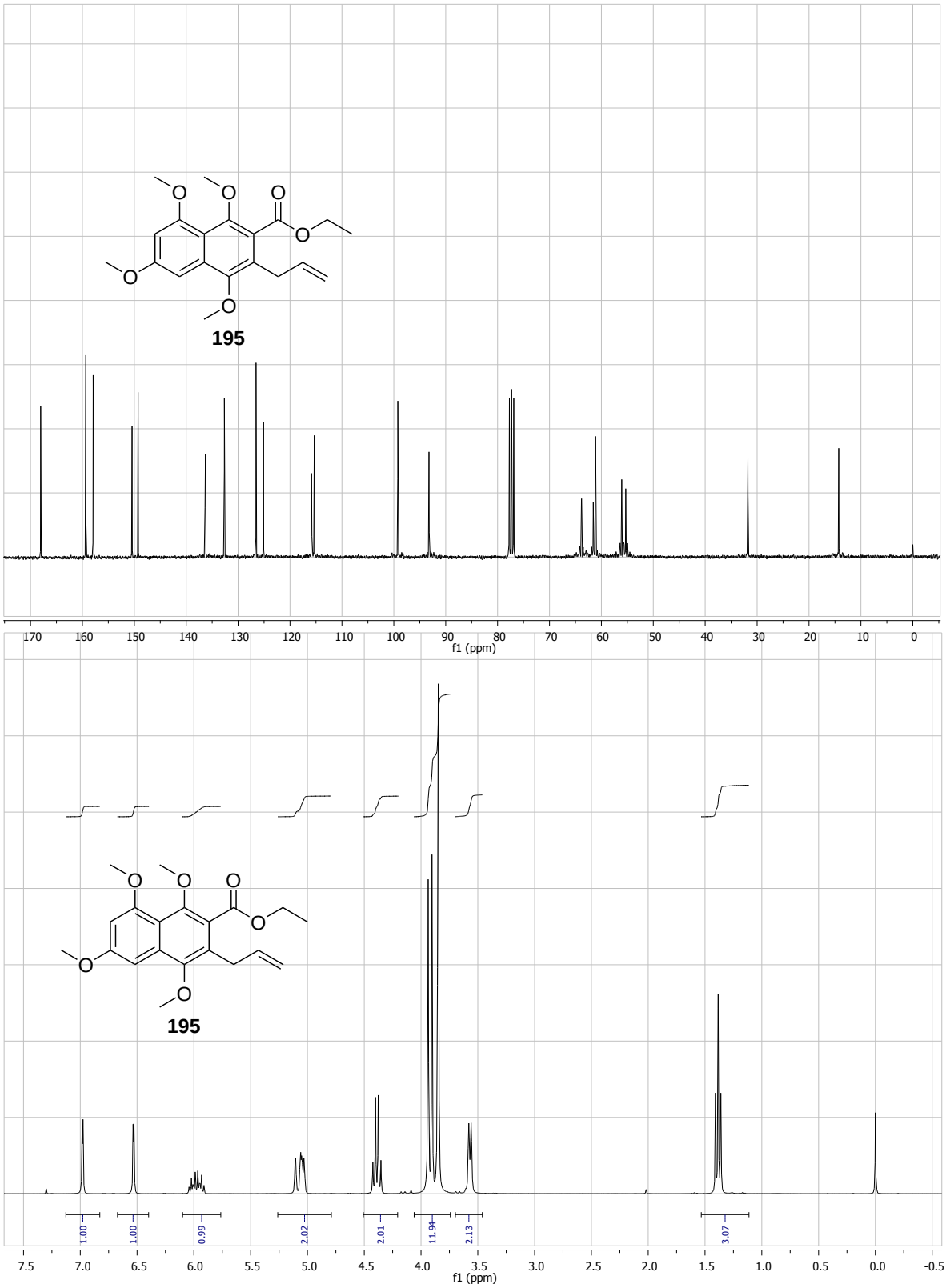
A1.2 ^{1}H and ^{13}C NMR spectra of lactone 103



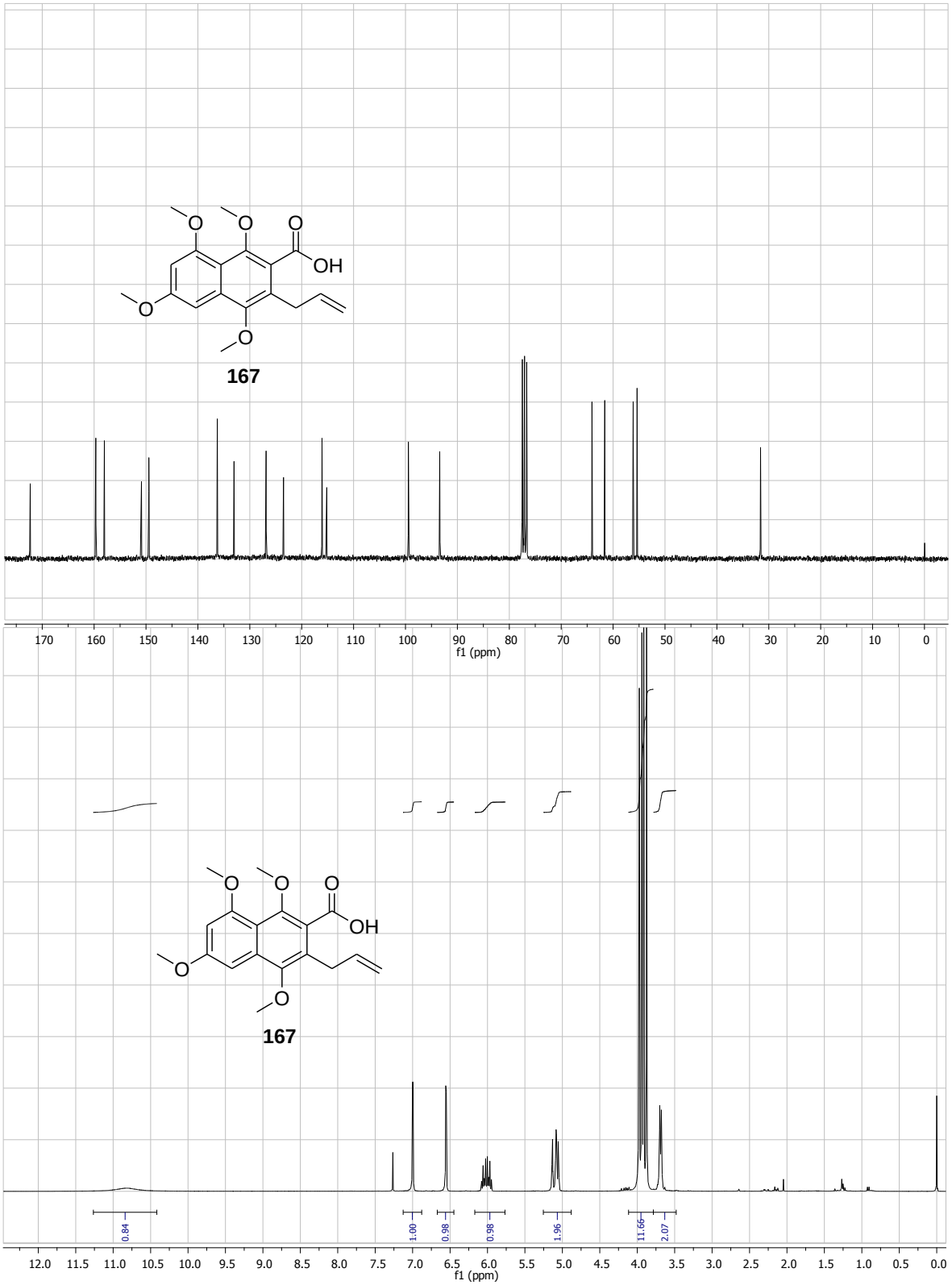
A1.3 ^{1}H and ^{13}C NMR spectra of furanone 176



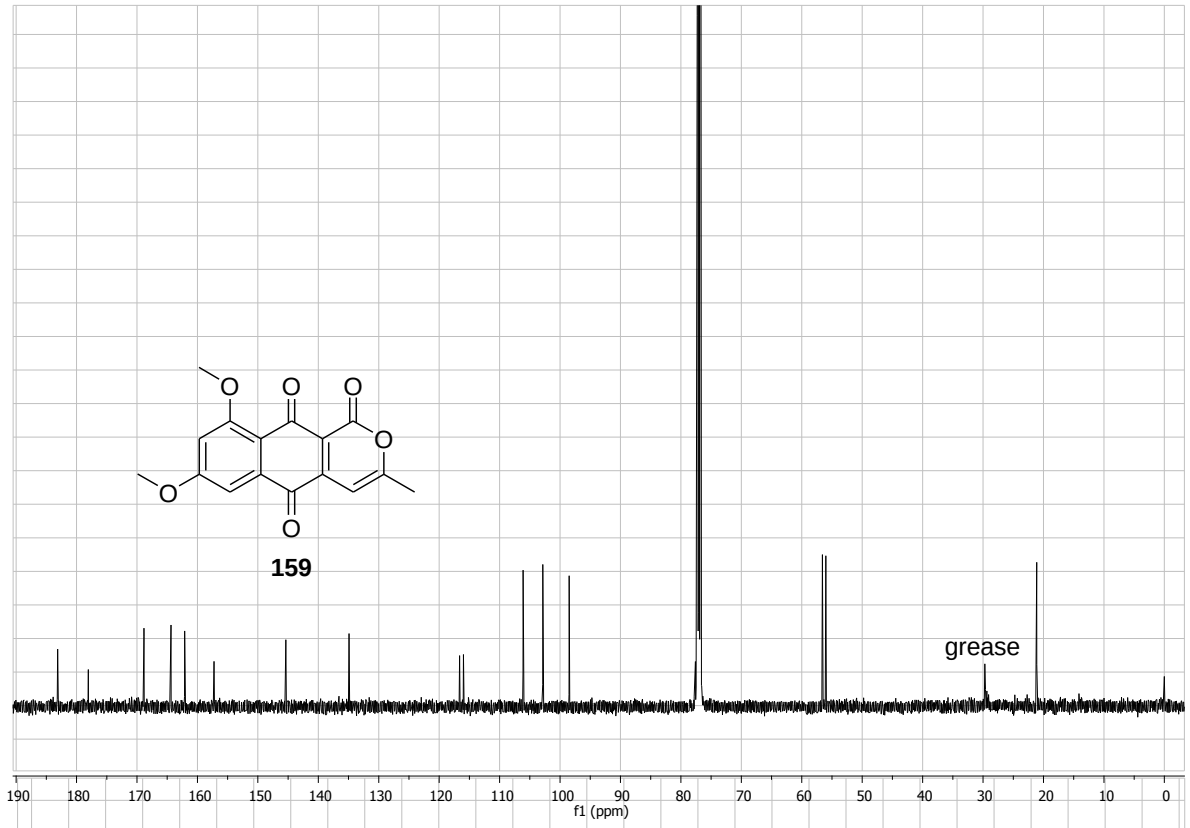
A1.4 ^{1}H and ^{13}C NMR spectra of ethyl ester 195

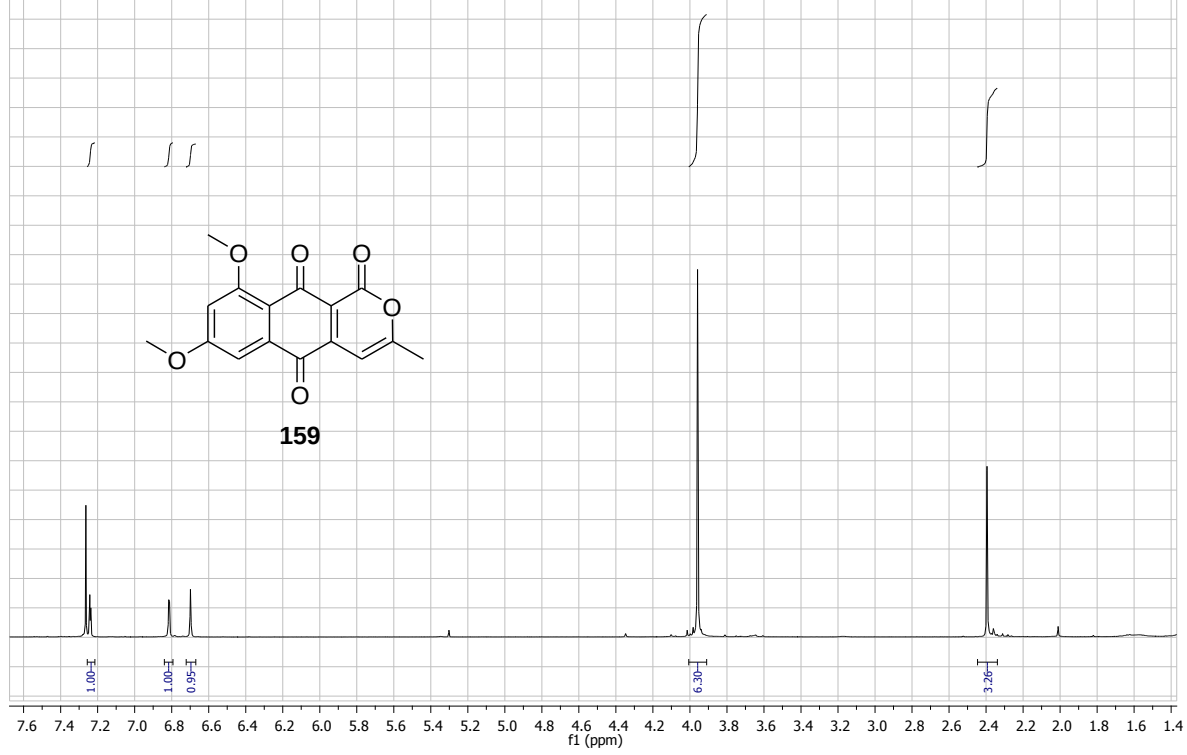


A1.5 ^{1}H and ^{13}C NMR spectra of carboxylic acid 167

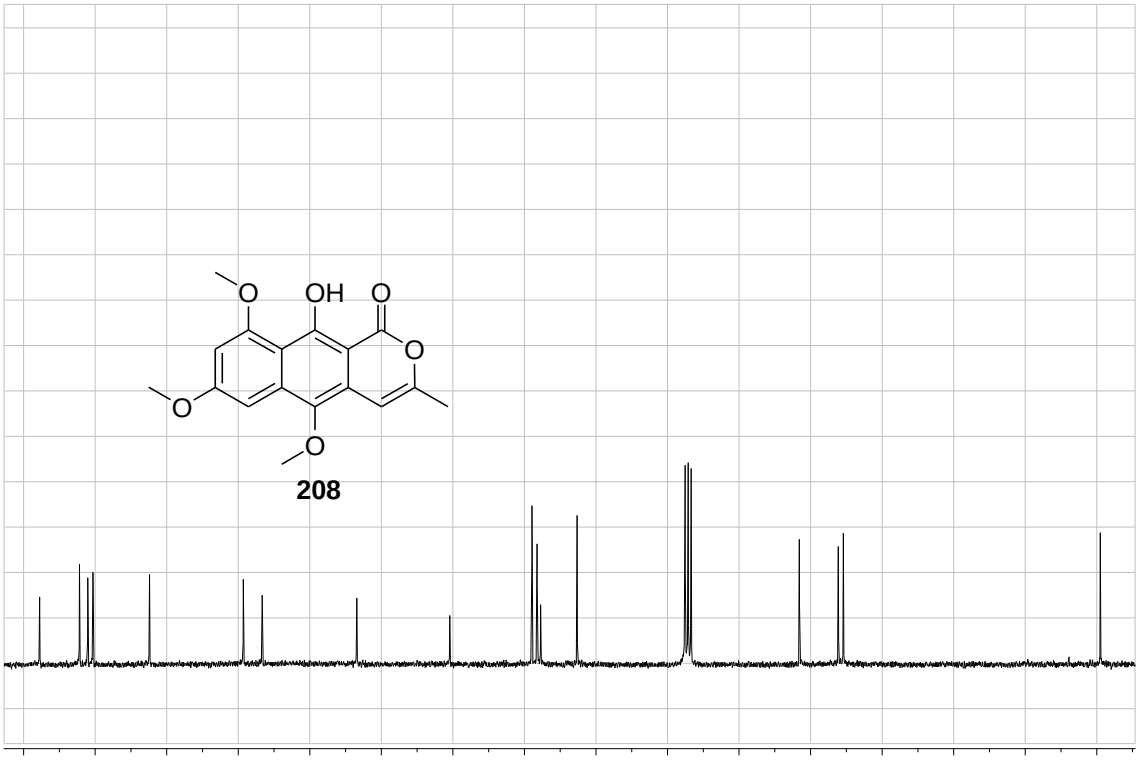


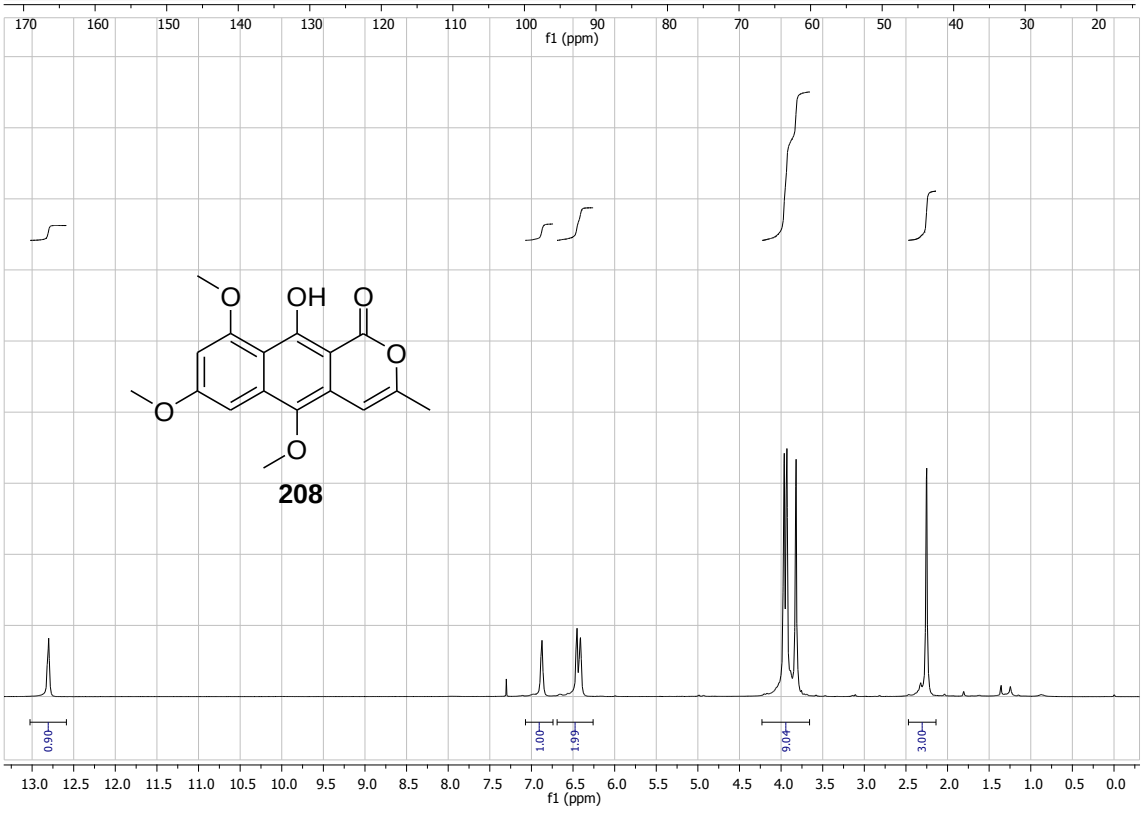
A1.6 ^{1}H and ^{13}C NMR spectra of pyranonaphthoquinone 159



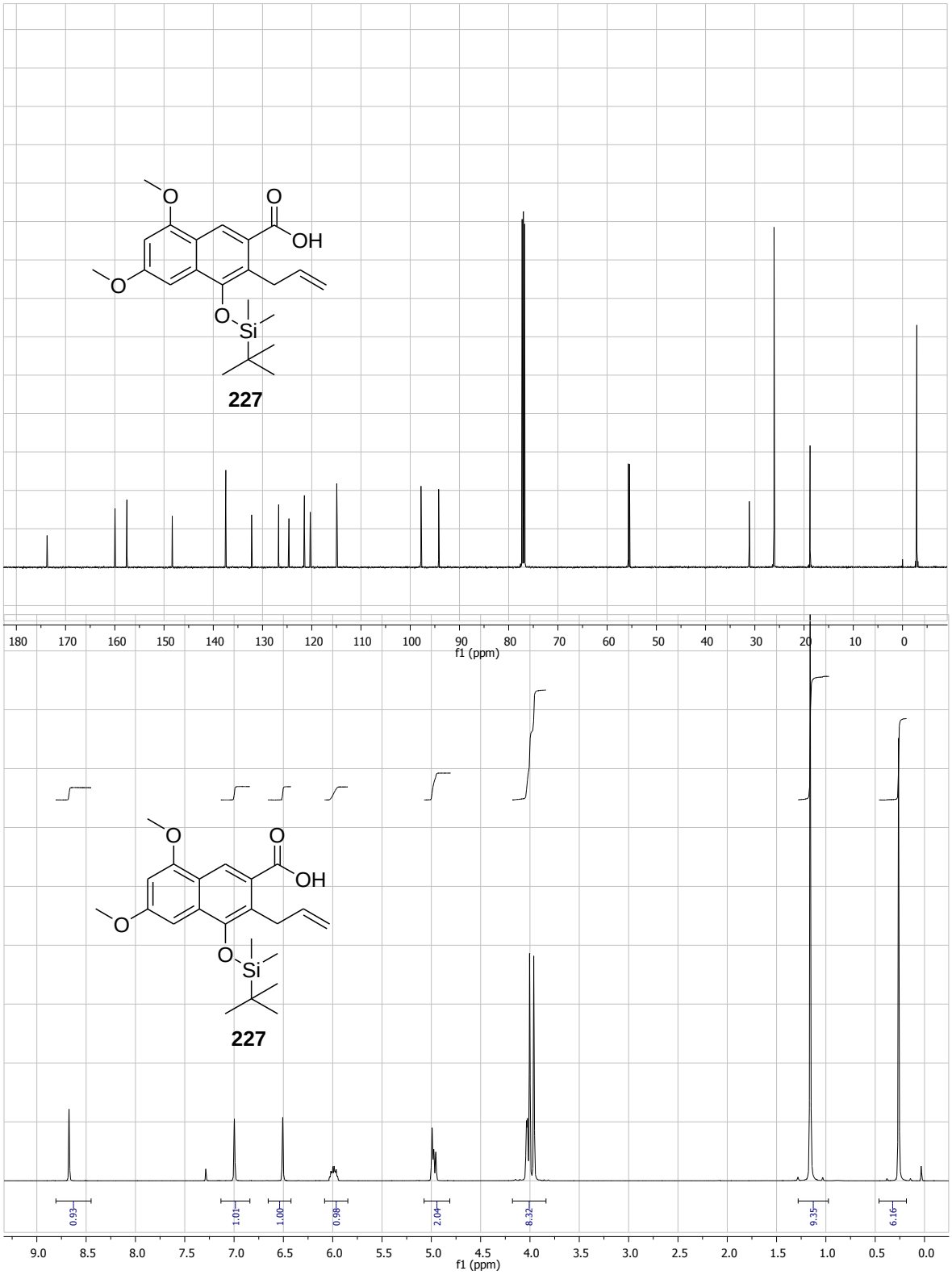


A1.7 ^{1}H and ^{13}C NMR spectra of 9-*O*-methylpaepalantine 208

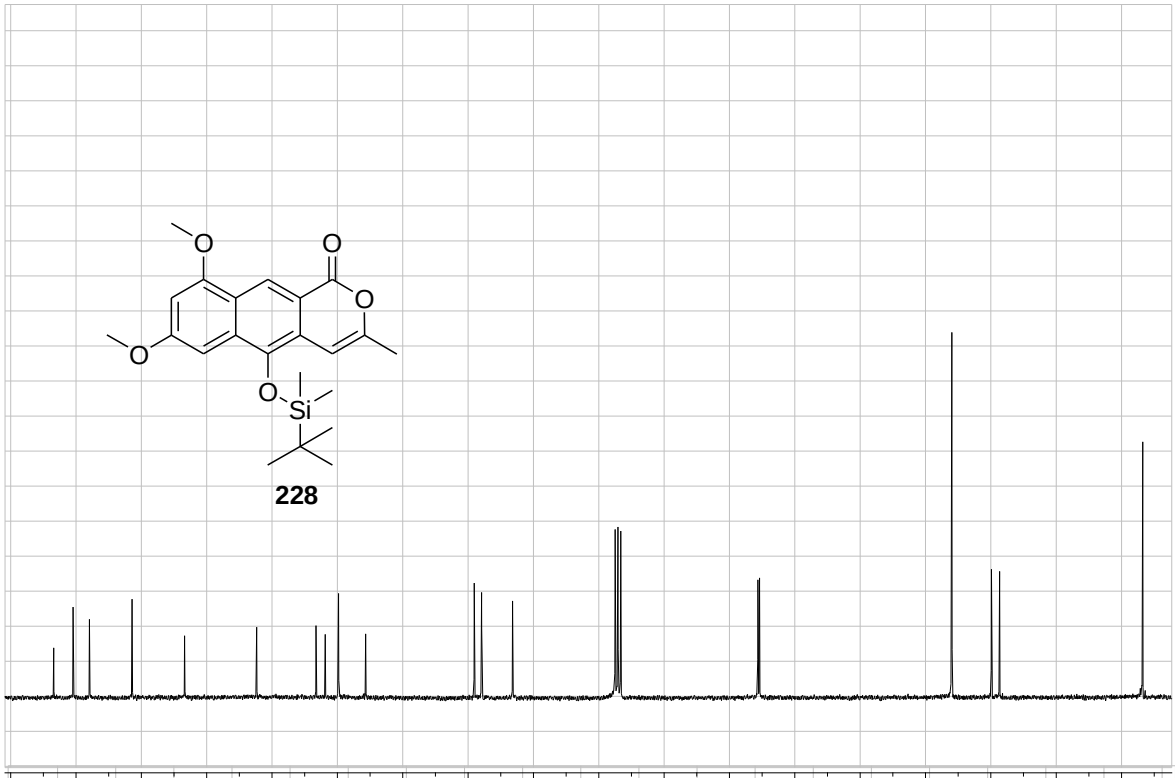


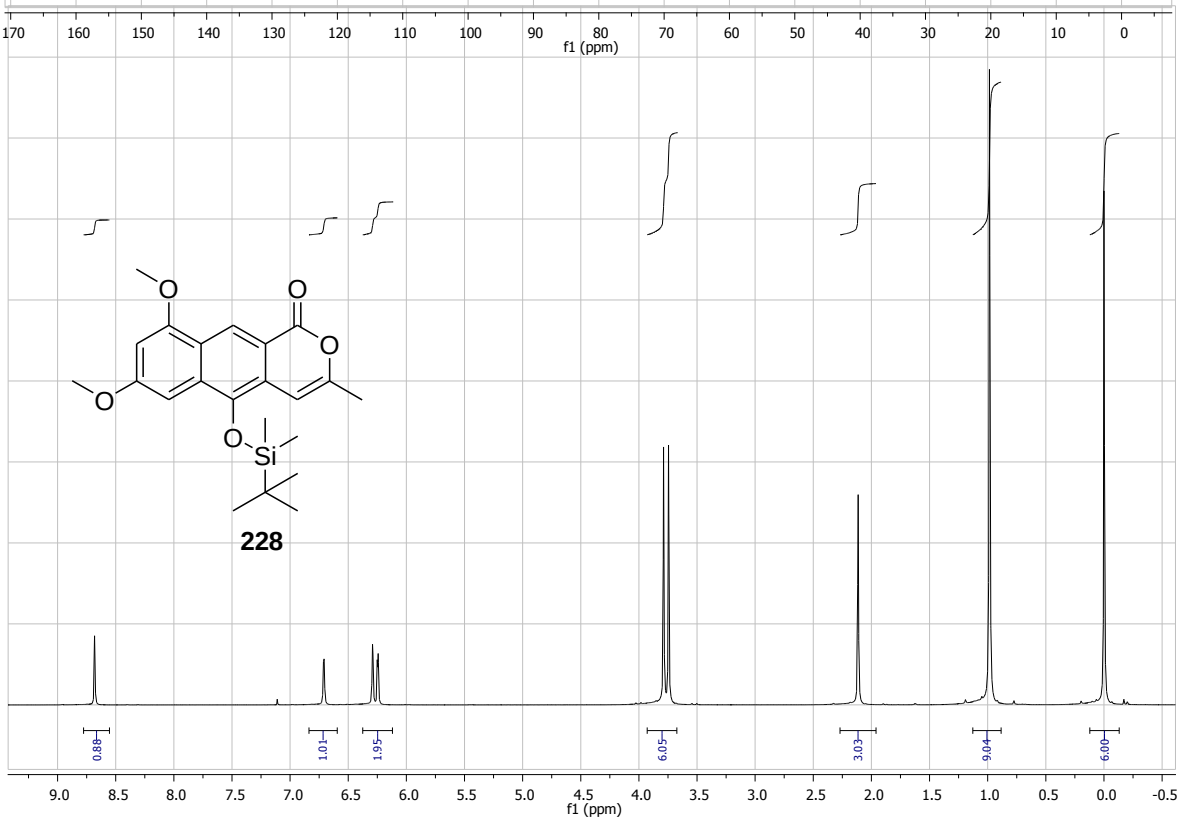


A1.8 ^{1}H and ^{13}C NMR spectra of carboxylic acid 227

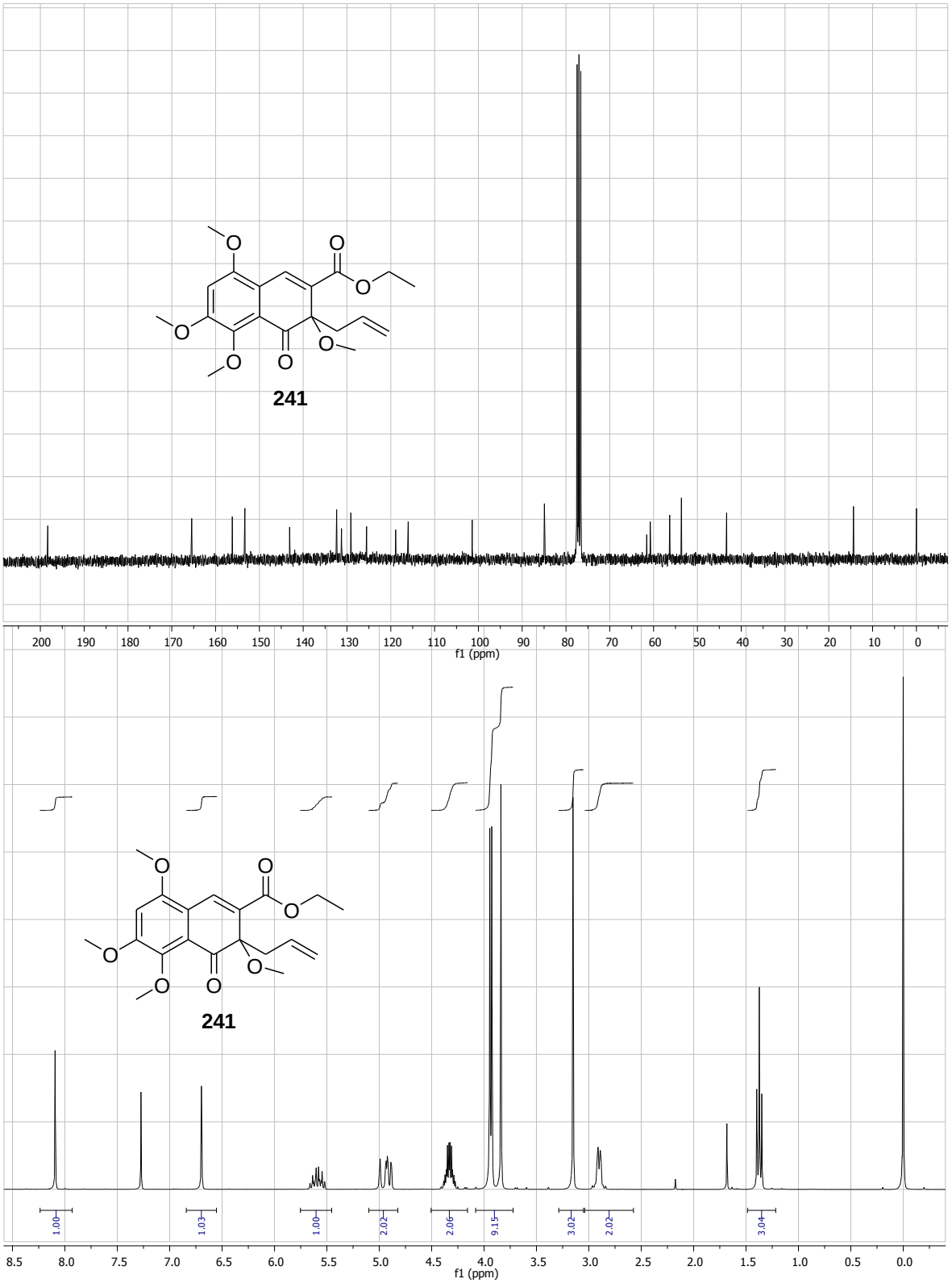


A1.9 ^{1}H and ^{13}C NMR spectra of lactone 228

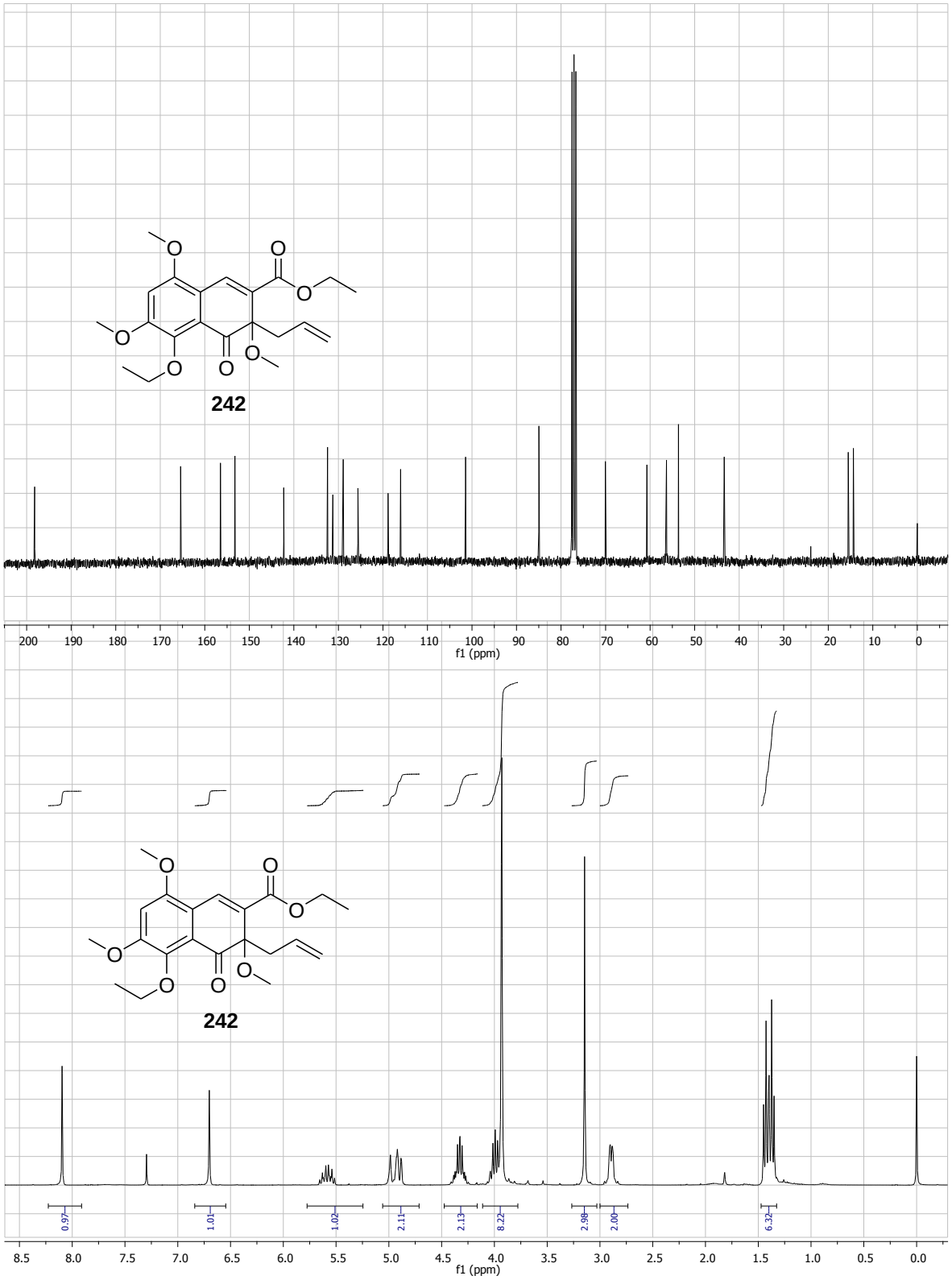




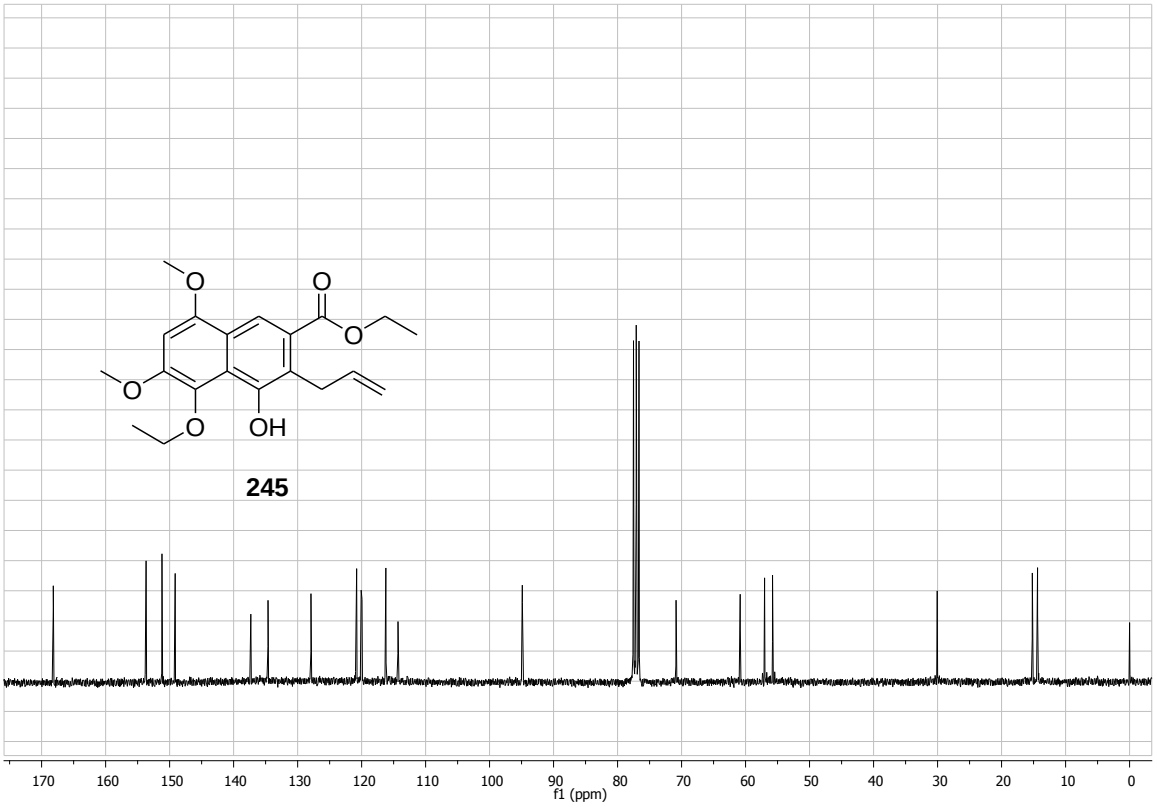
A1.10 ^{1}H and ^{13}C NMR spectra of ethyl ester 241

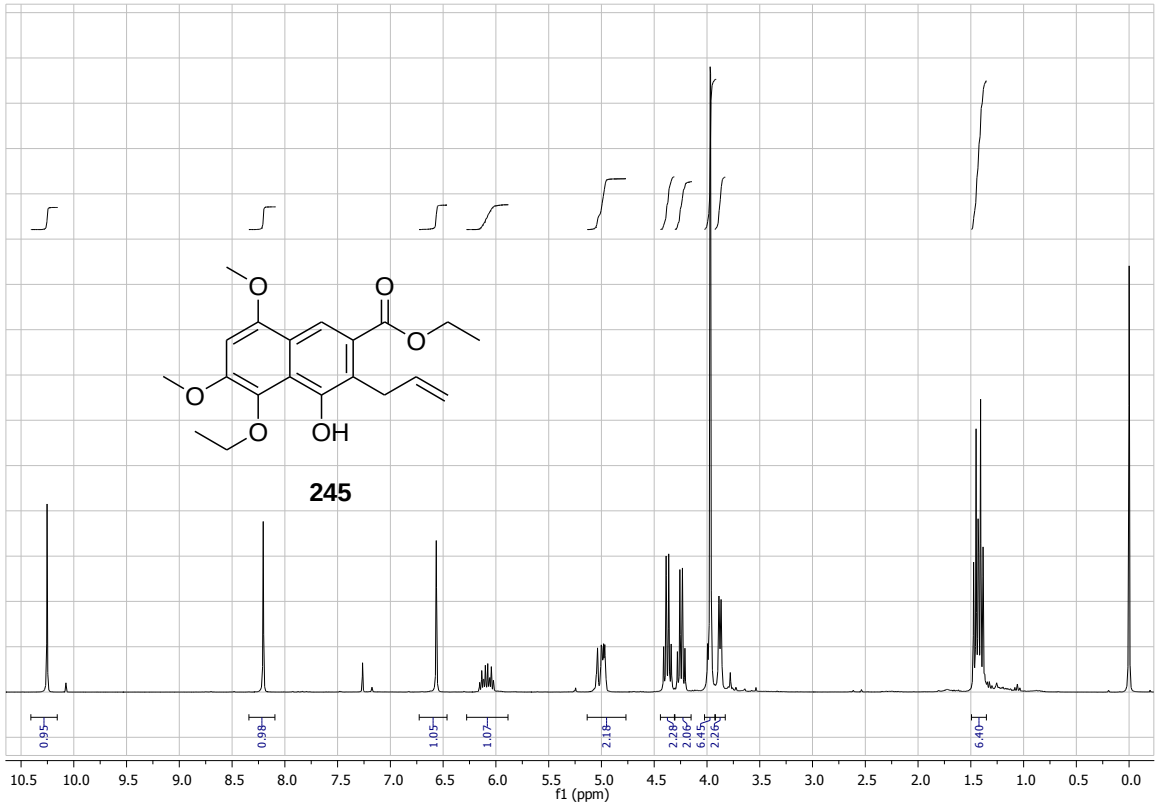


A1.11 ^{1}H and ^{13}C NMR spectra of ethyl ester 242

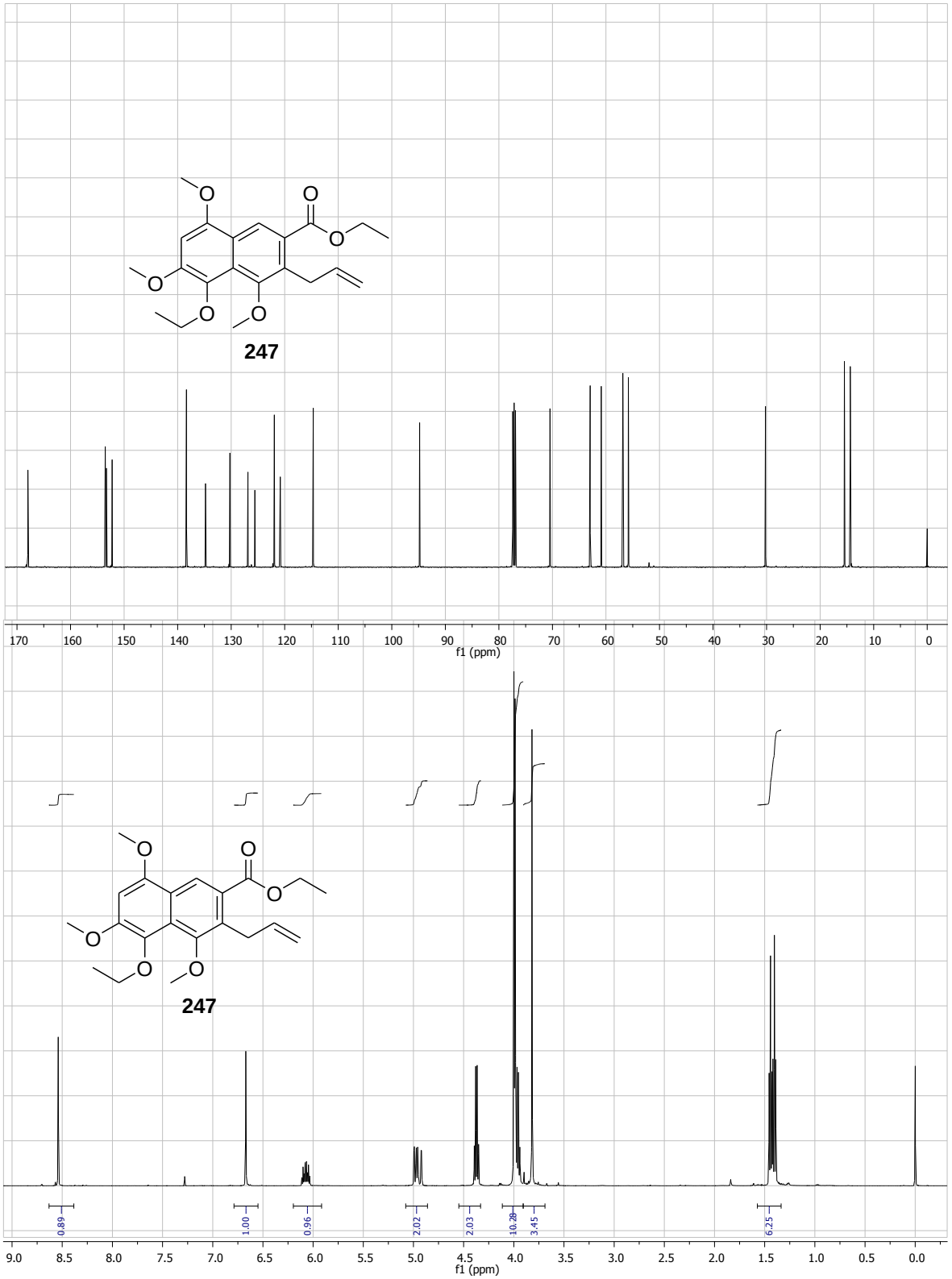


A1.12 ^{1}H and ^{13}C NMR spectra of naphthol 245

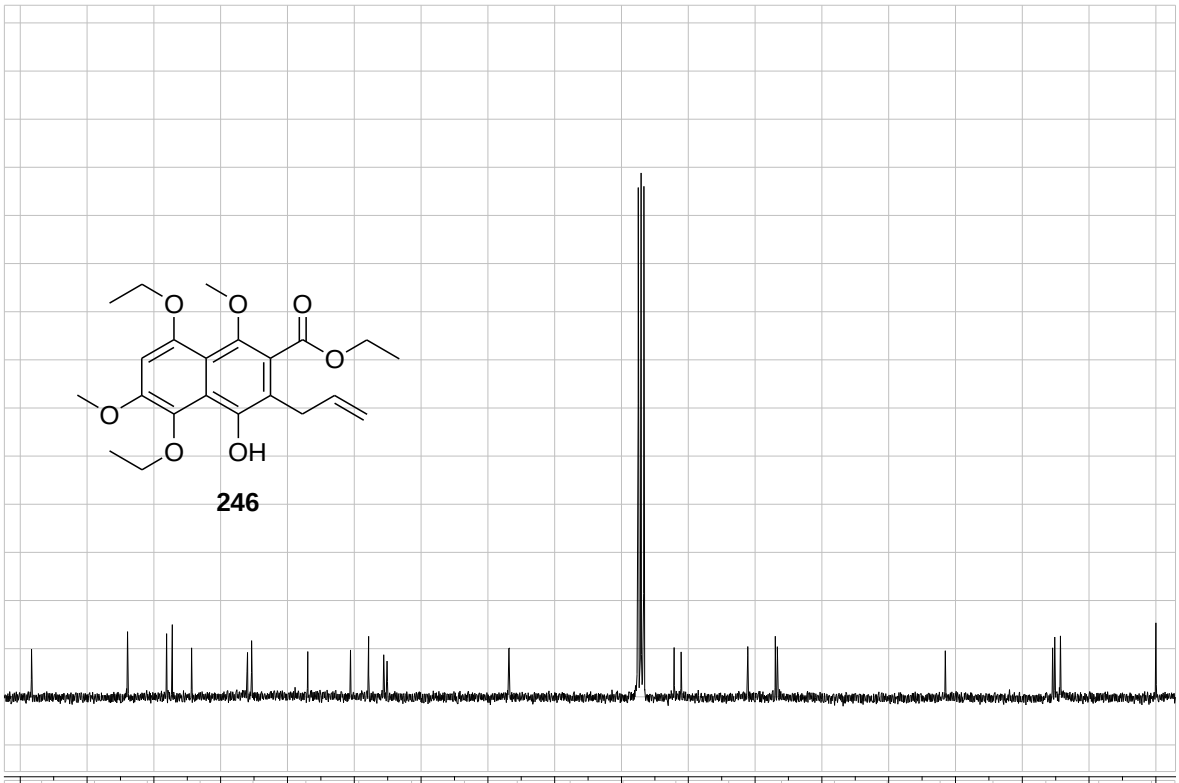


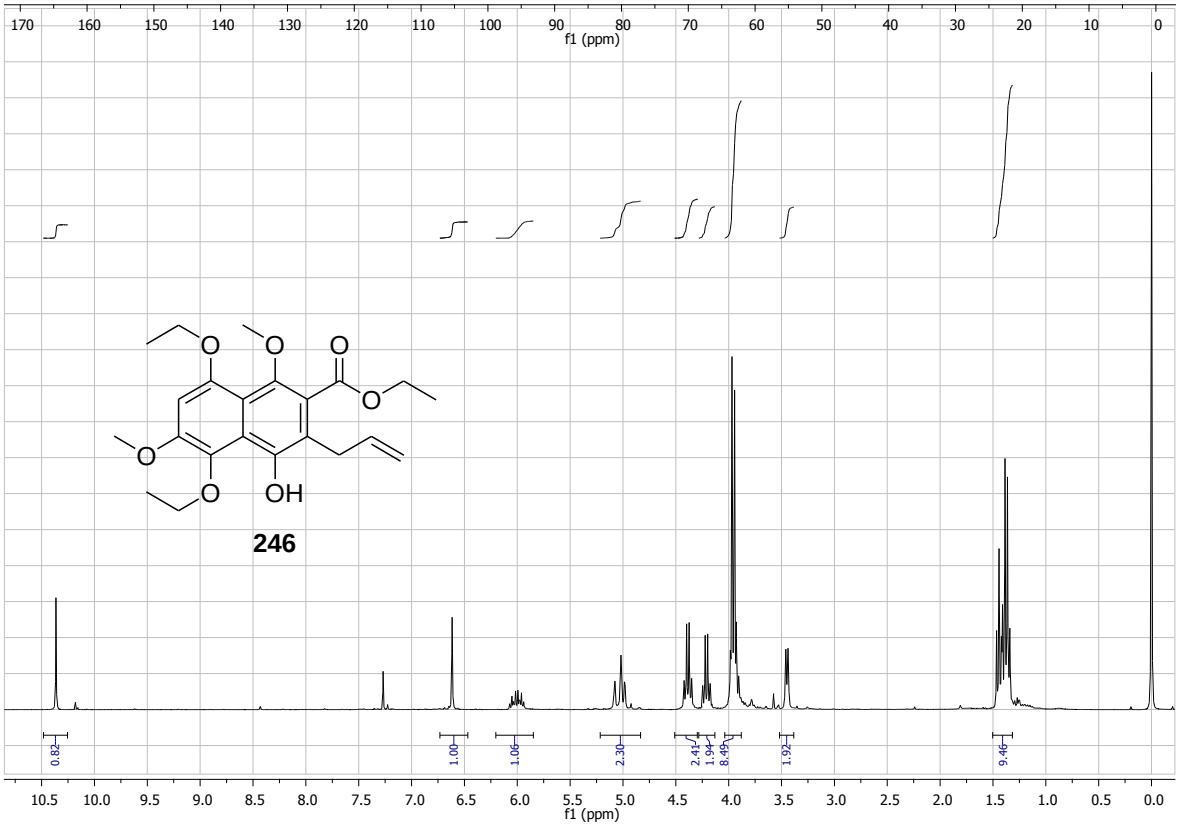


A1.13 ^{1}H and ^{13}C NMR spectra of ethyl ester 247

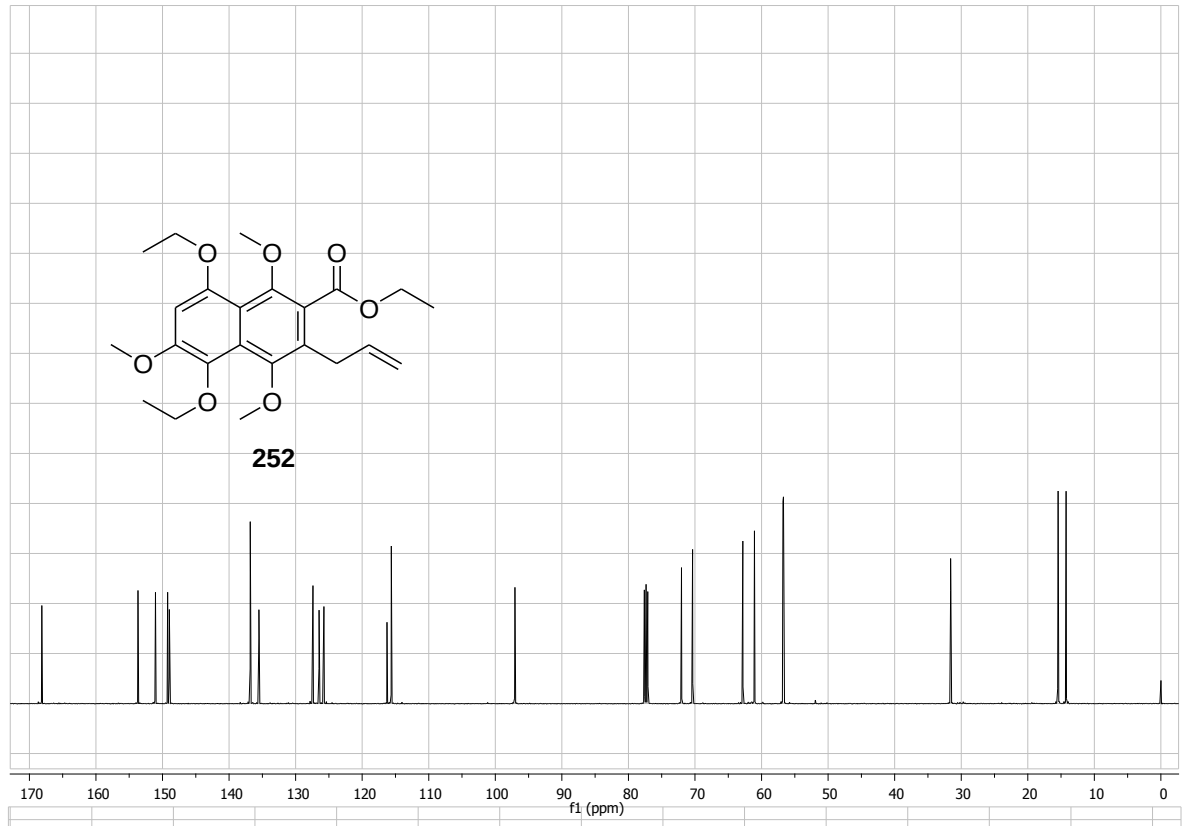


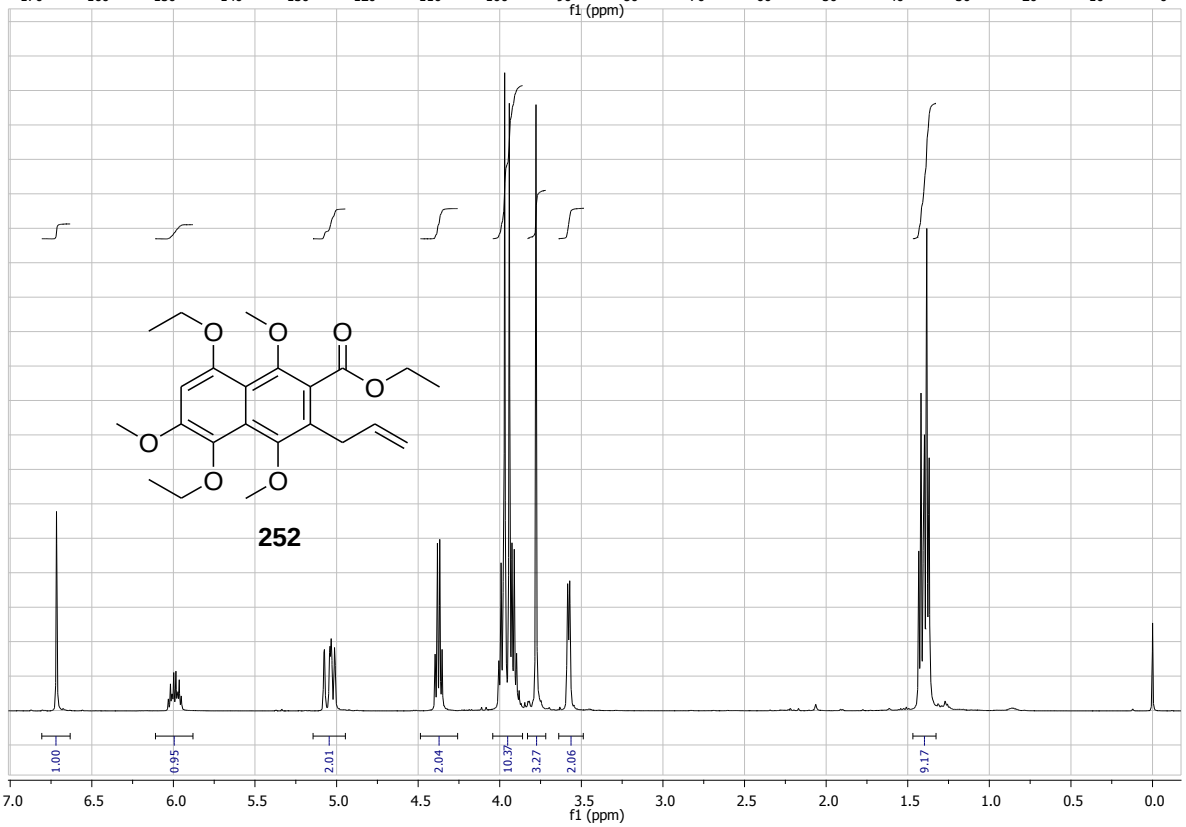
A1.14 ^{1}H and ^{13}C NMR spectra of naphthol 246



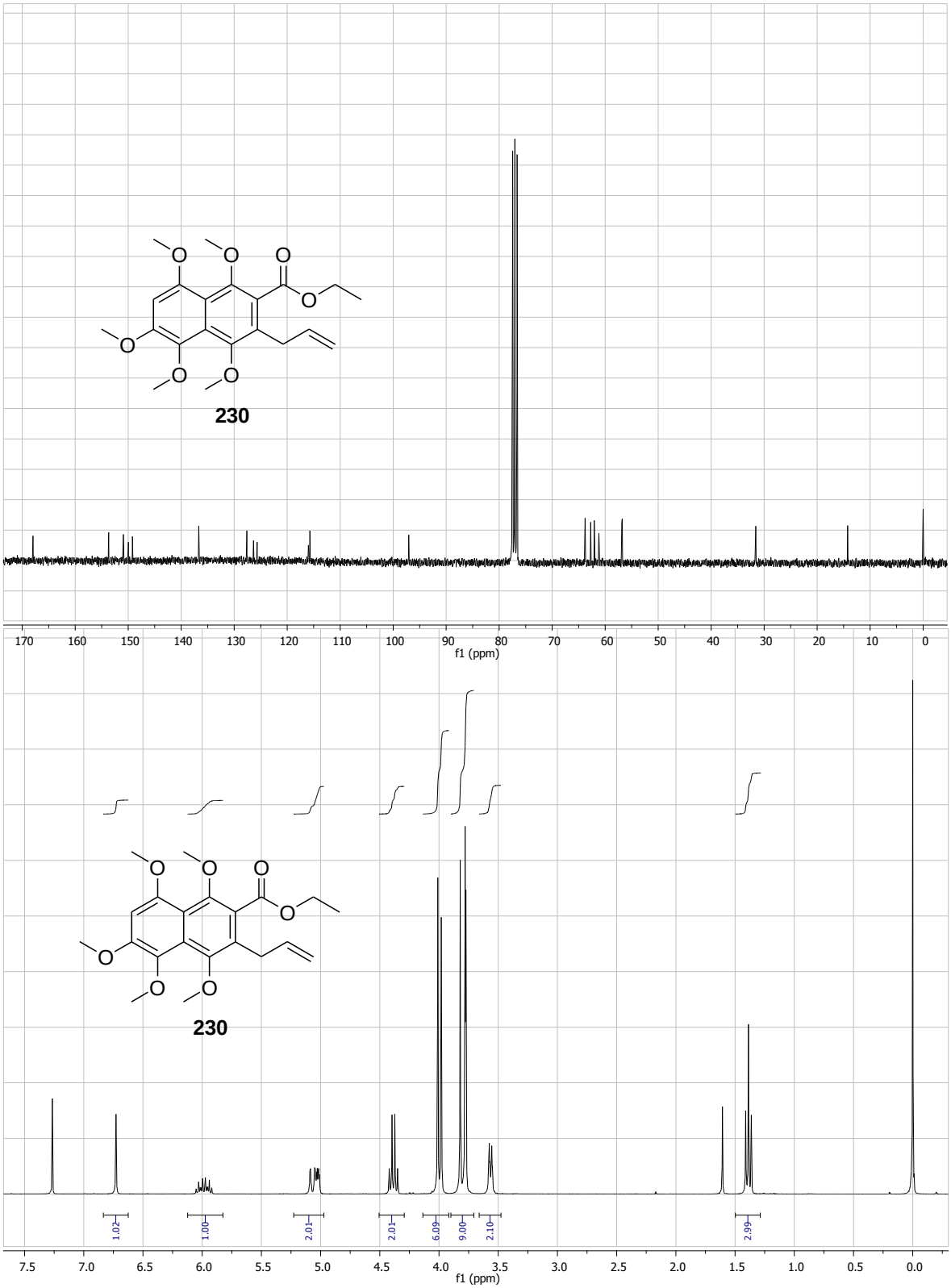


A1.15 ^{1}H and ^{13}C NMR spectra of ethyl ester 252

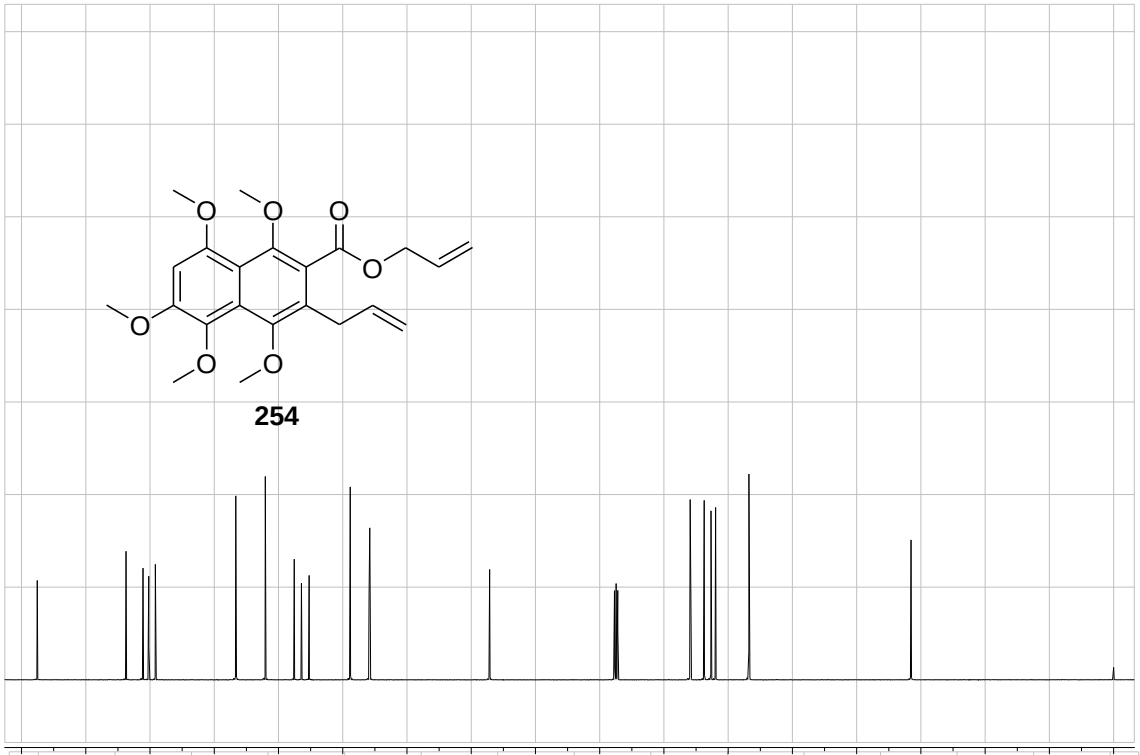


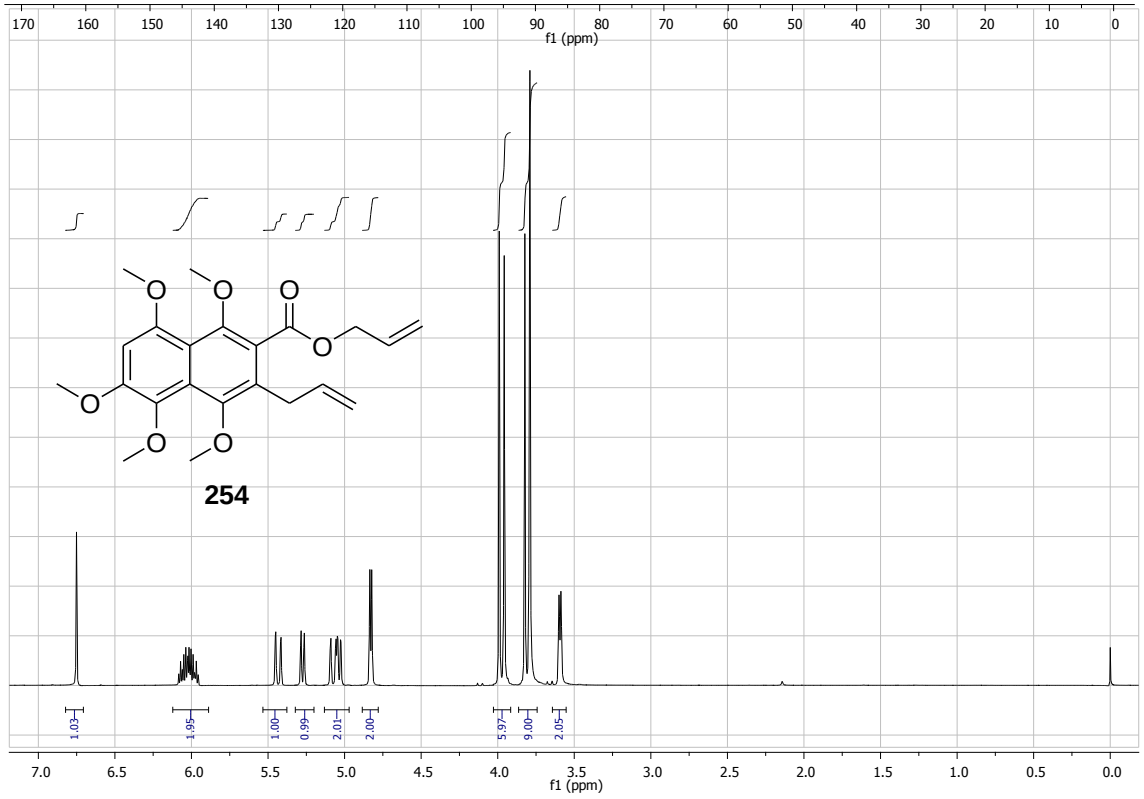


A1.16 ^{1}H and ^{13}C NMR spectra of ethyl ester 230

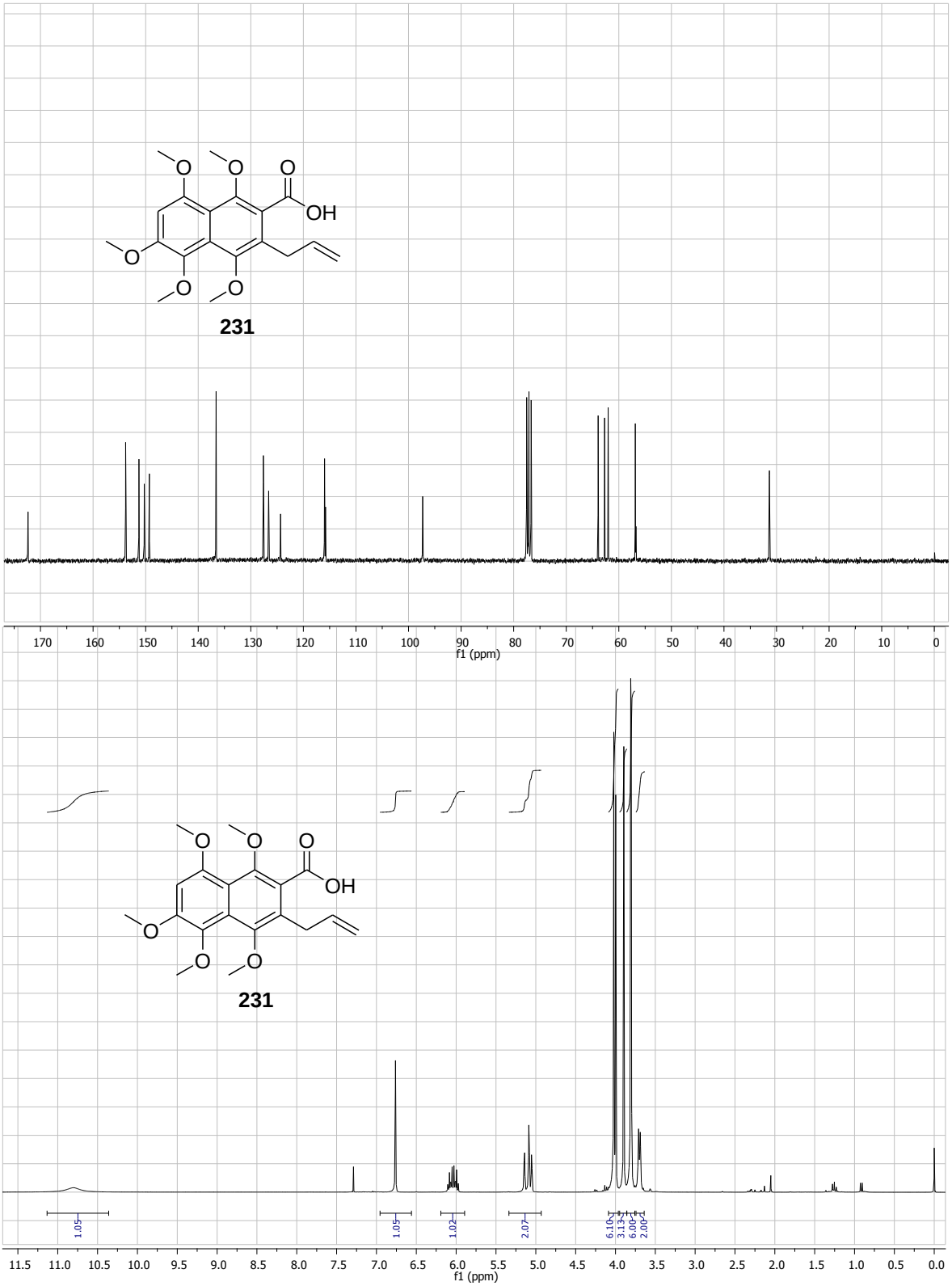


A1.17 ^{1}H and ^{13}C NMR spectra of ethyl ester 254

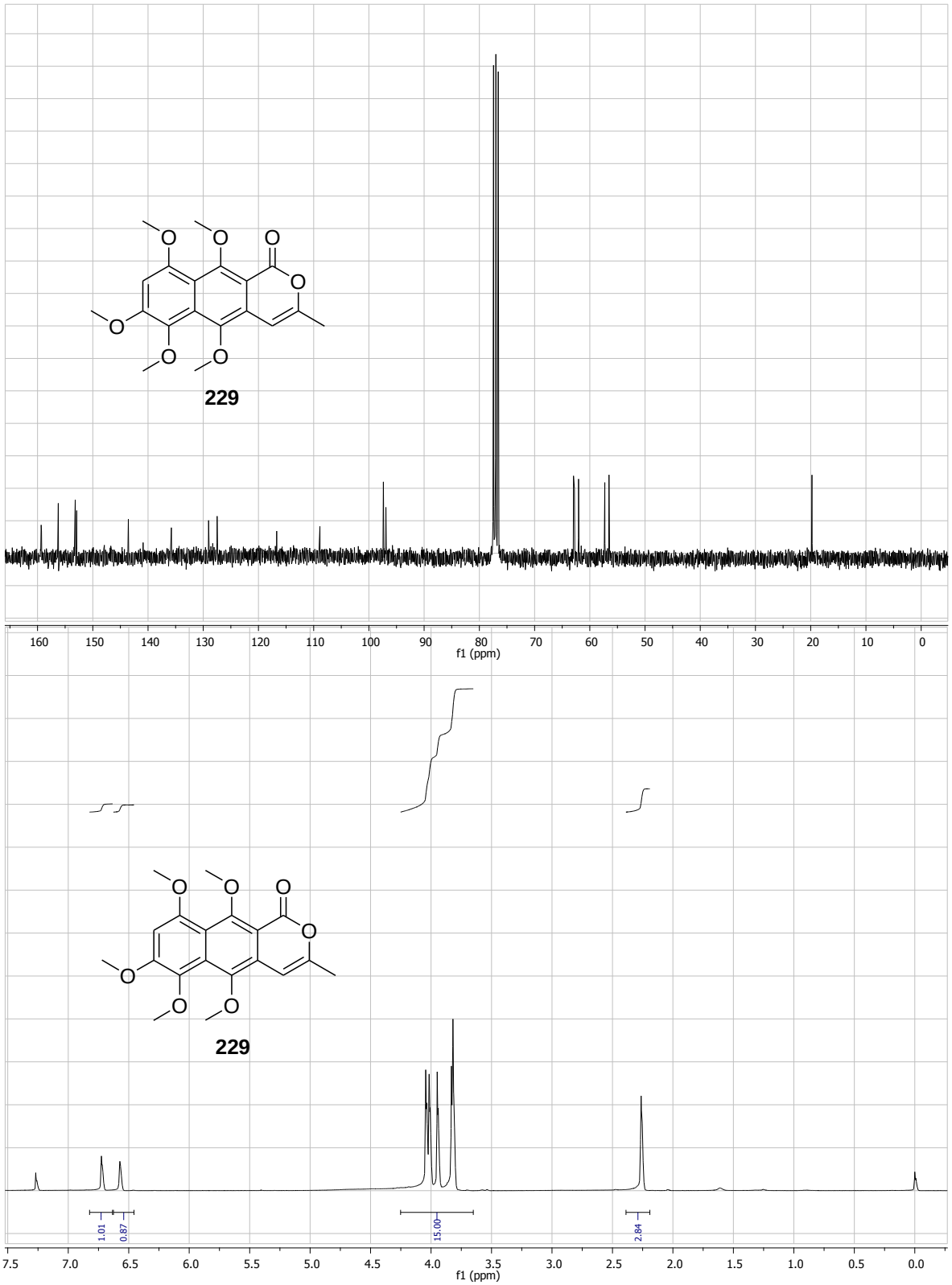




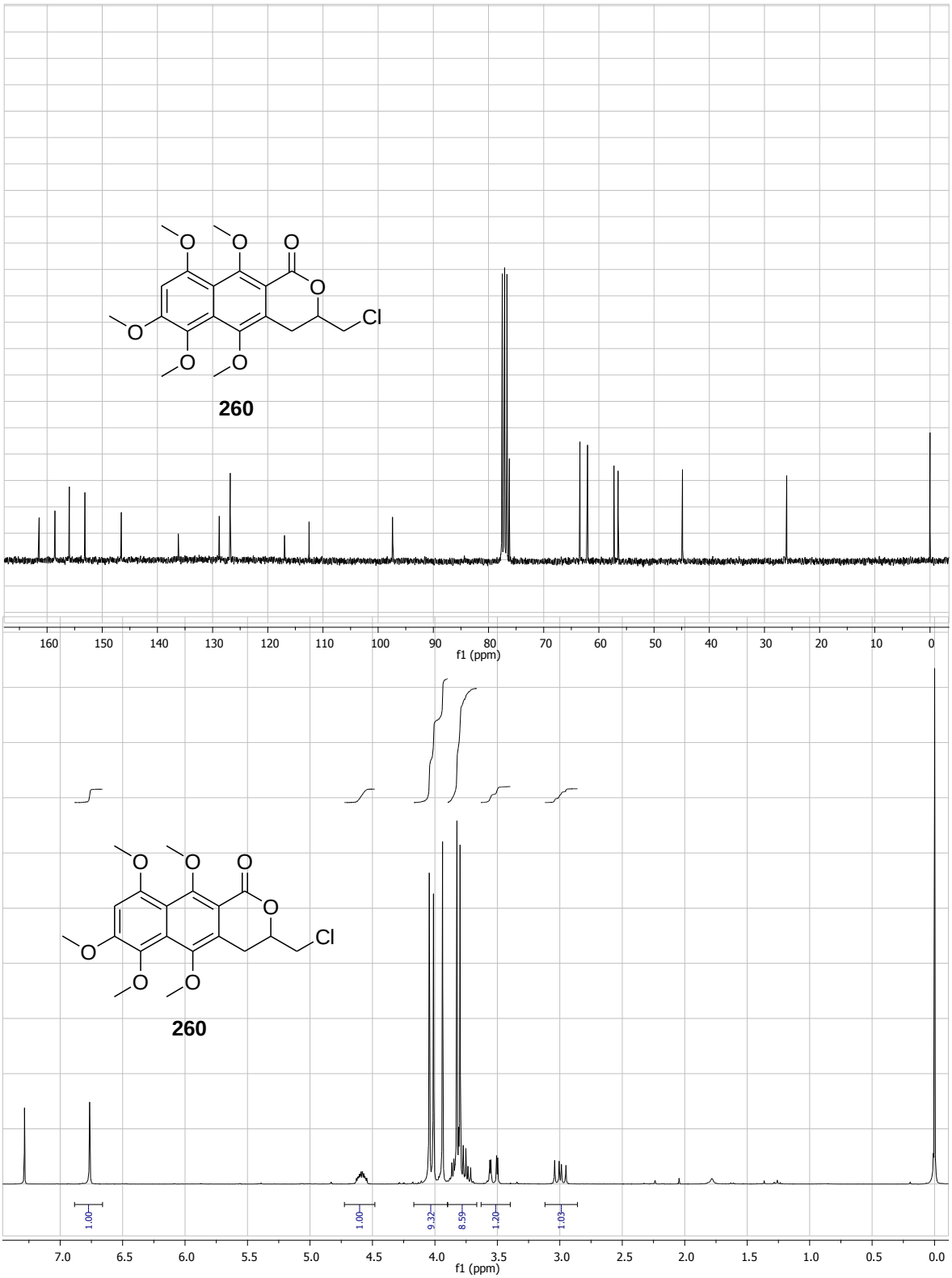
A1.18 ^{1}H and ^{13}C NMR spectra of carboxylic acid 231



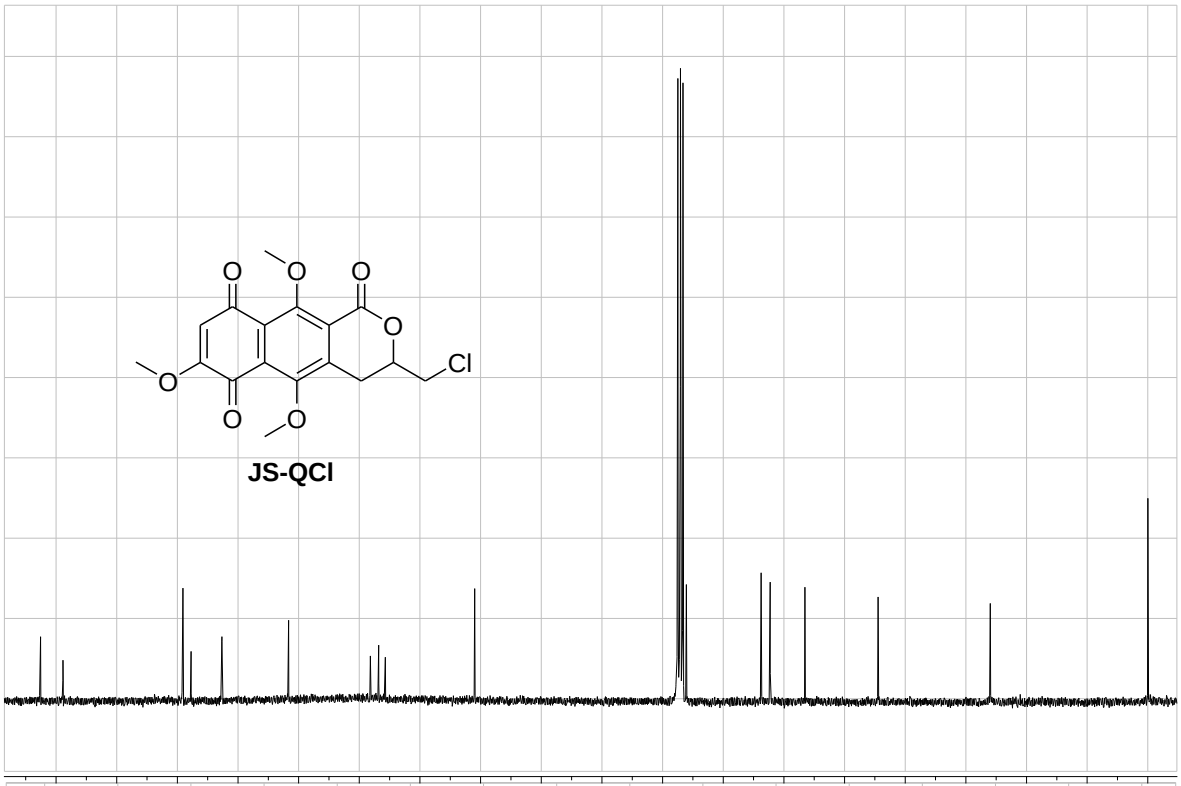
A1.19 ^{1}H and ^{13}C NMR spectra of lactone 229

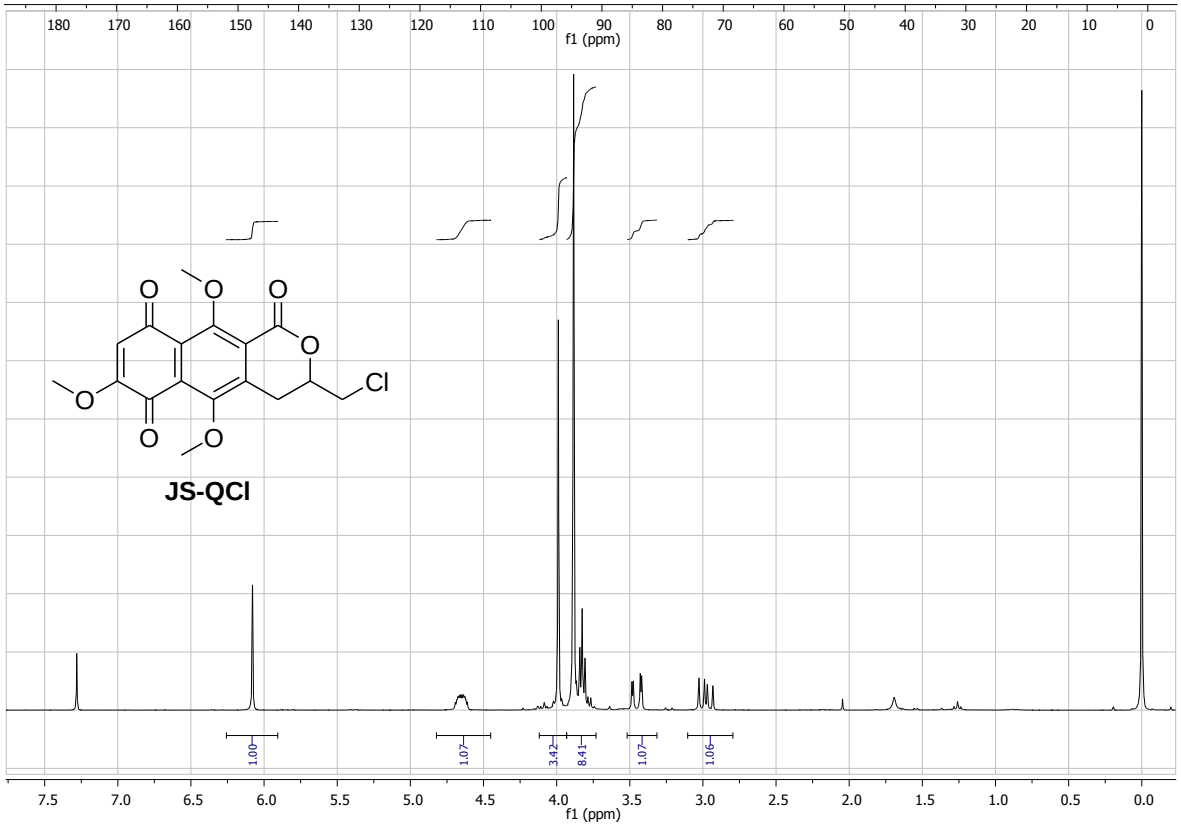


A1.20 ^{1}H and ^{13}C NMR spectra of lactone 260

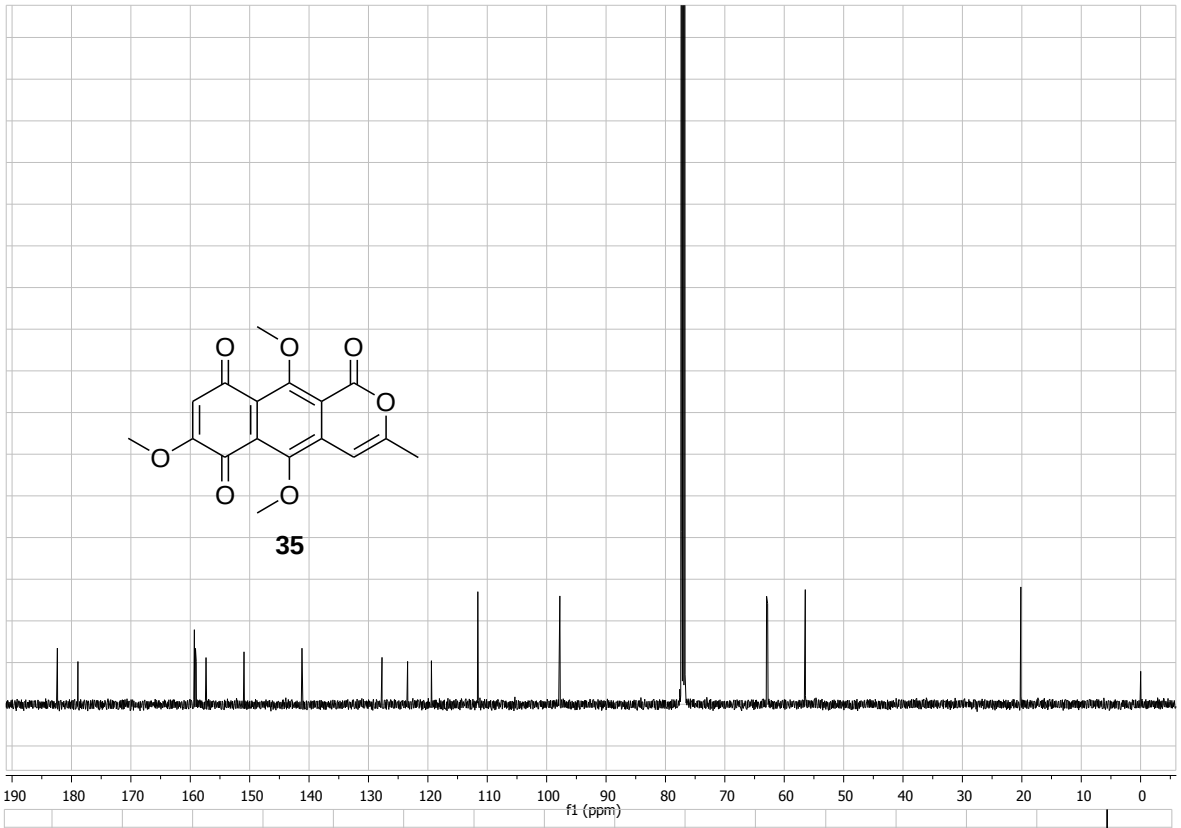


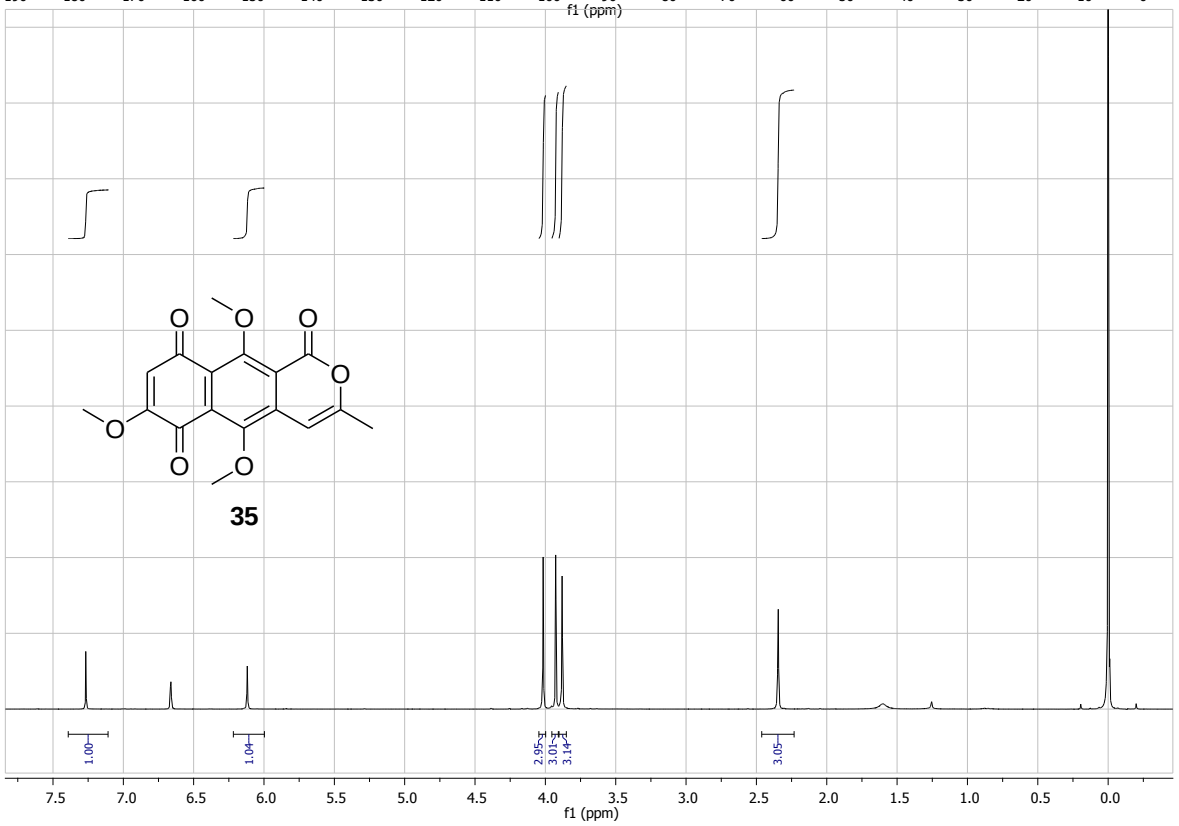
A1.21 ^{1}H and ^{13}C NMR spectra of pyranonaphthoquinone JS-QCl



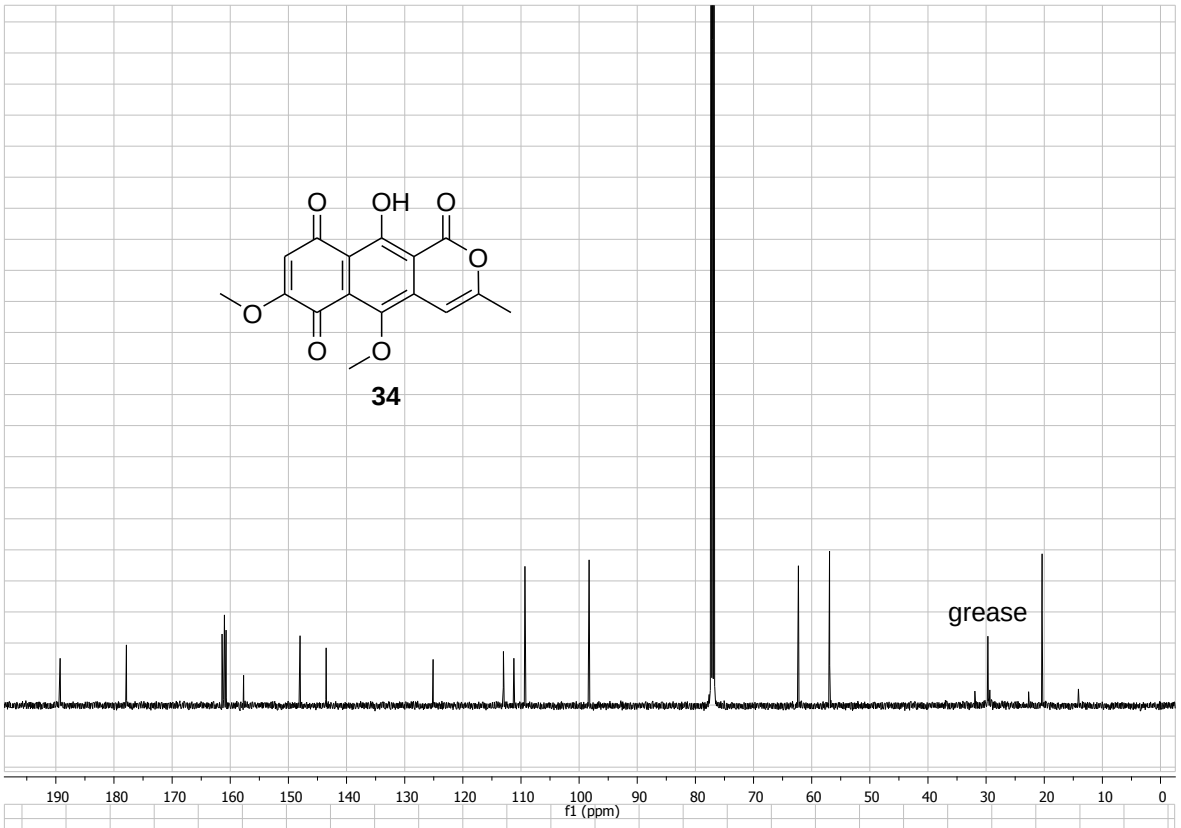


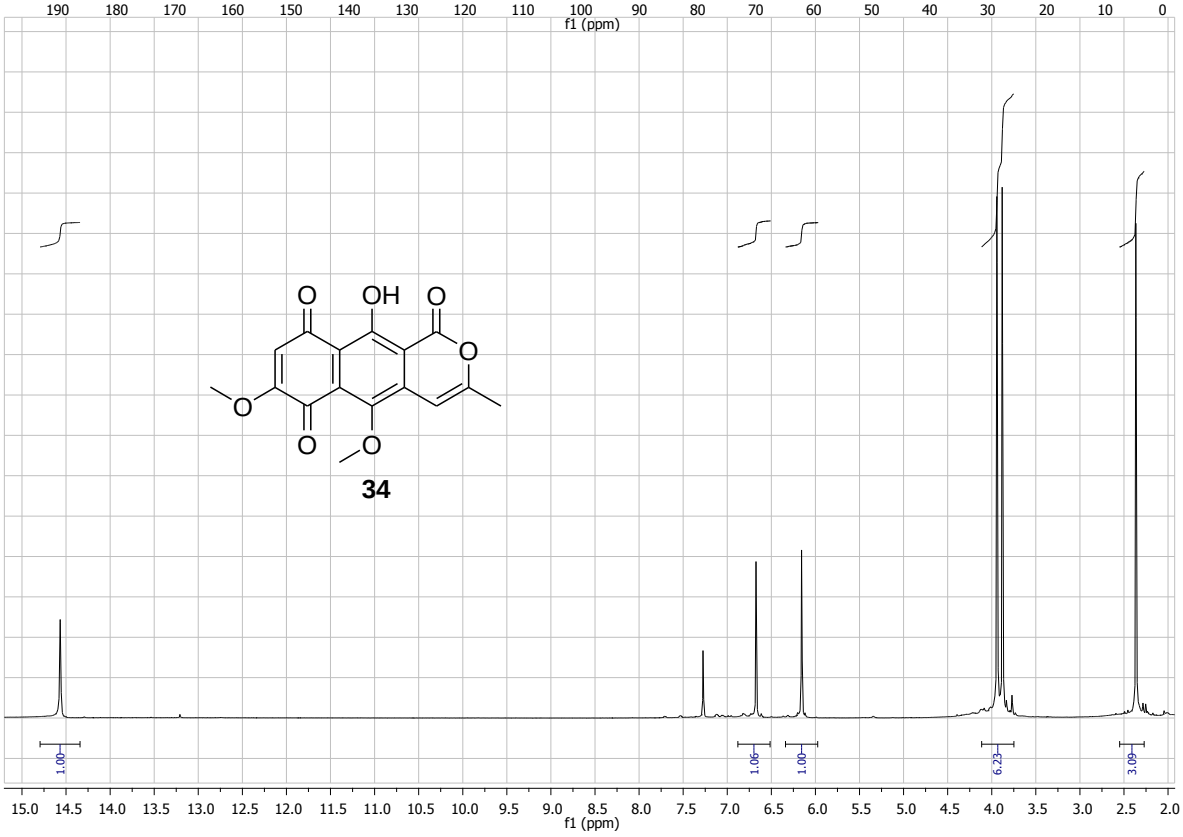
A1.22 ^{1}H and ^{13}C NMR spectra of pyranonaphthoquinone 35



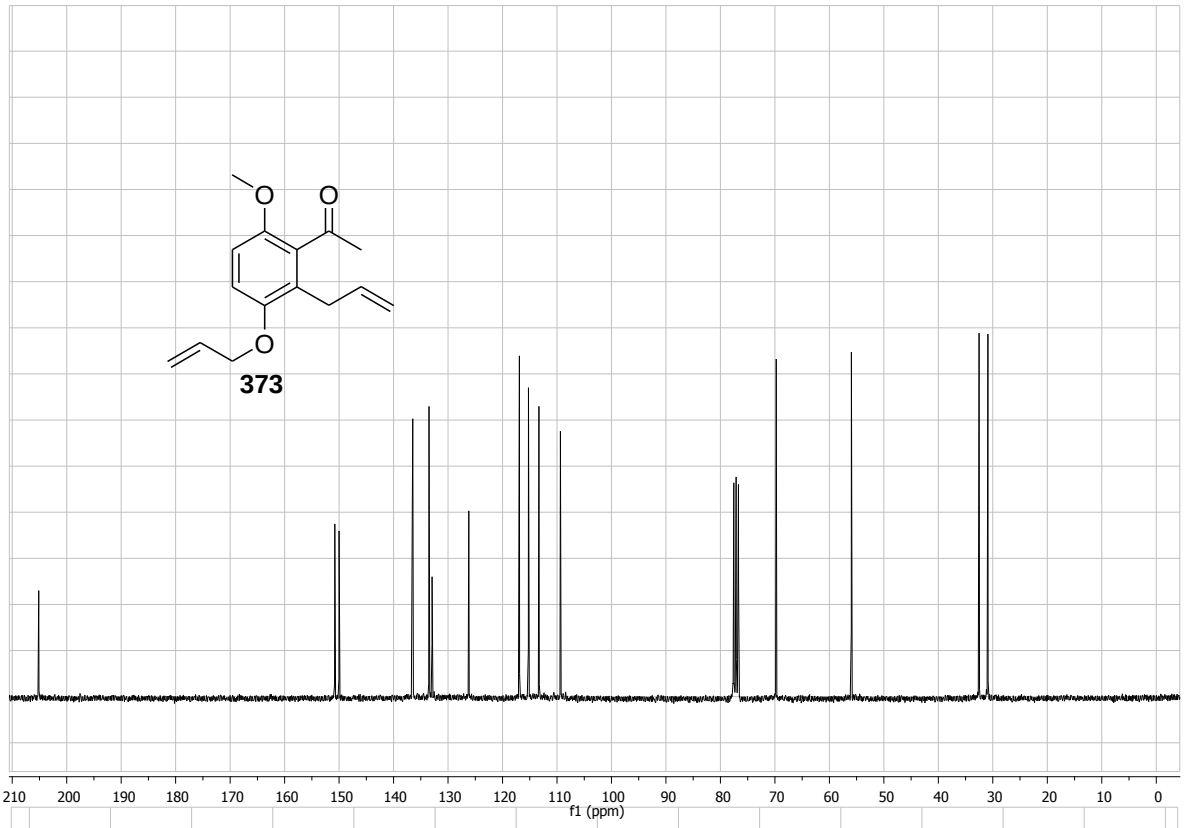


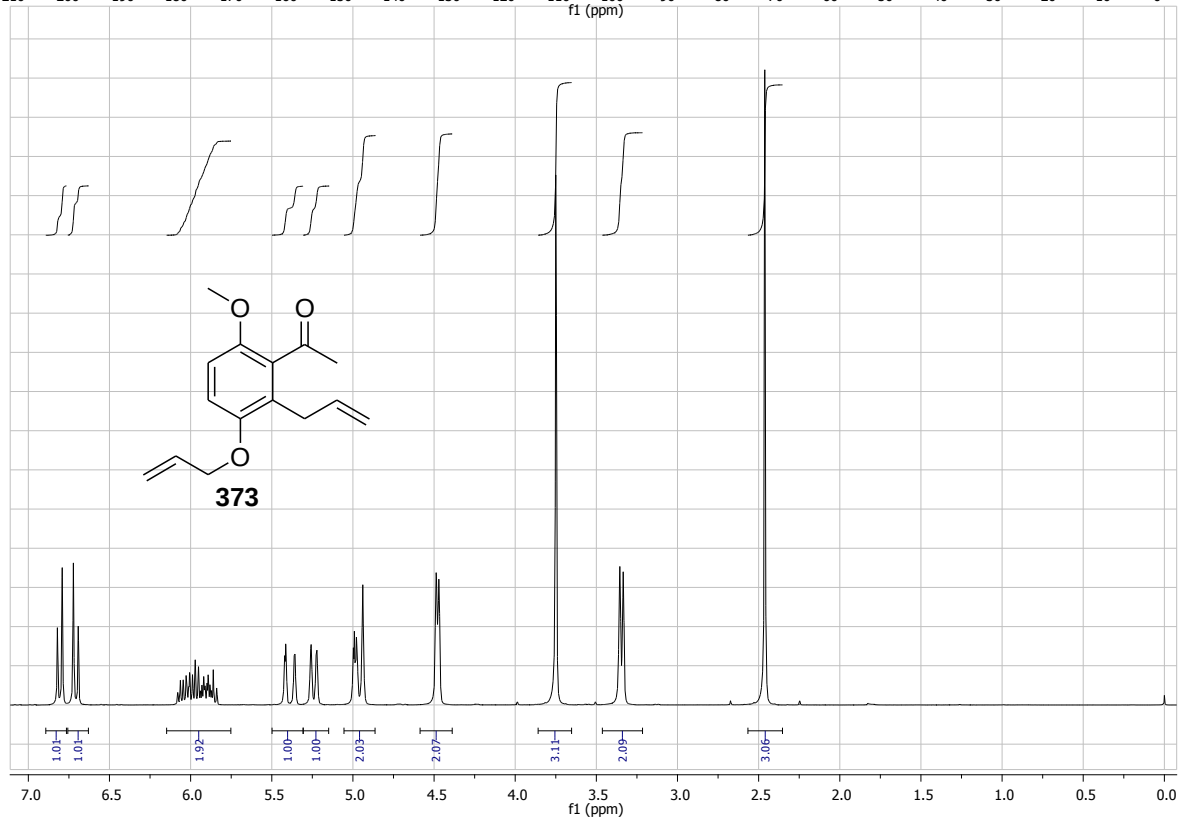
A1.23 ^{1}H and ^{13}C NMR spectra of 5-methoxy-3,4-dehydroxanthomegnin 34



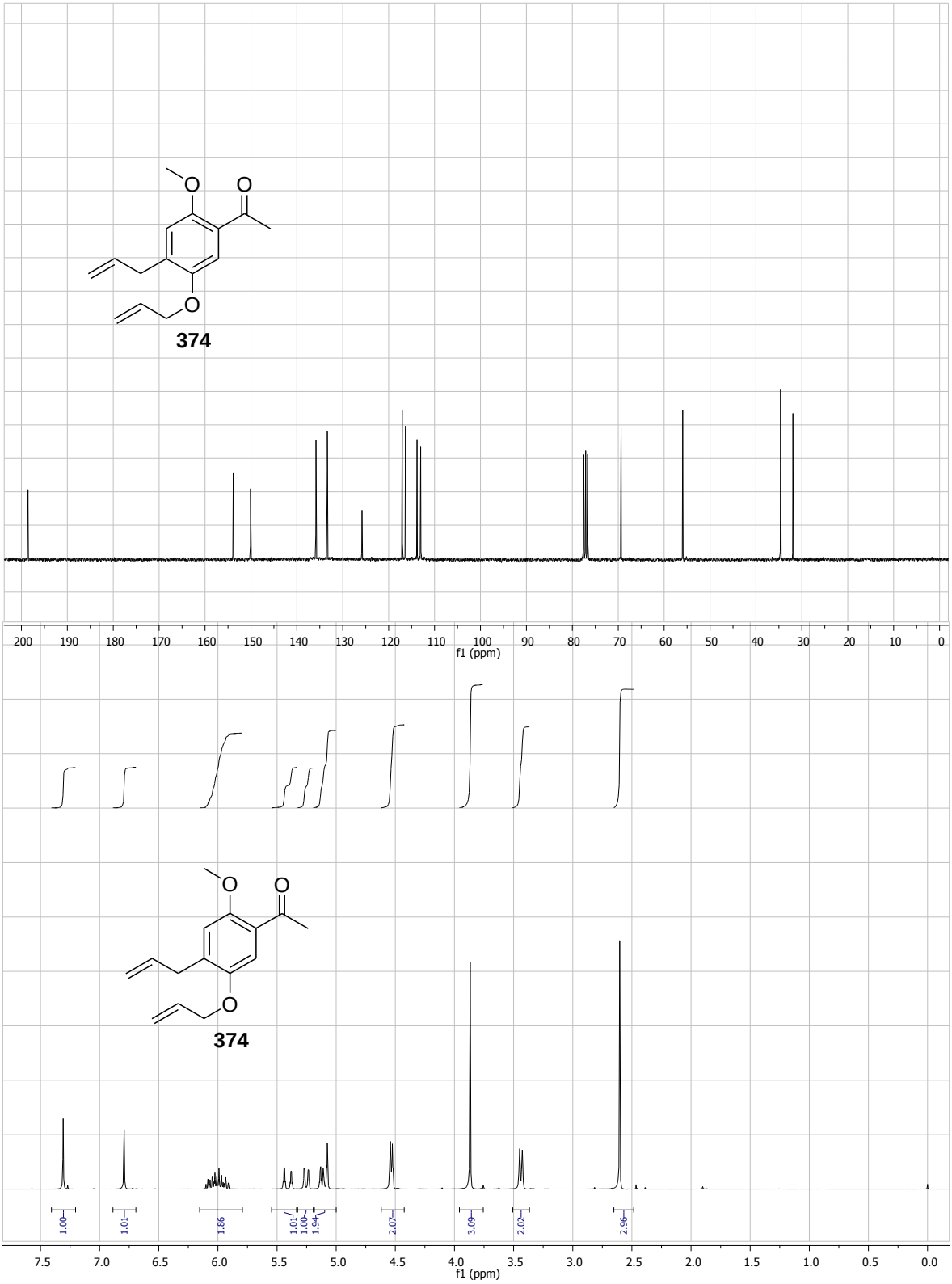


A1.24 ^{1}H and ^{13}C NMR spectra of acetophenone 373

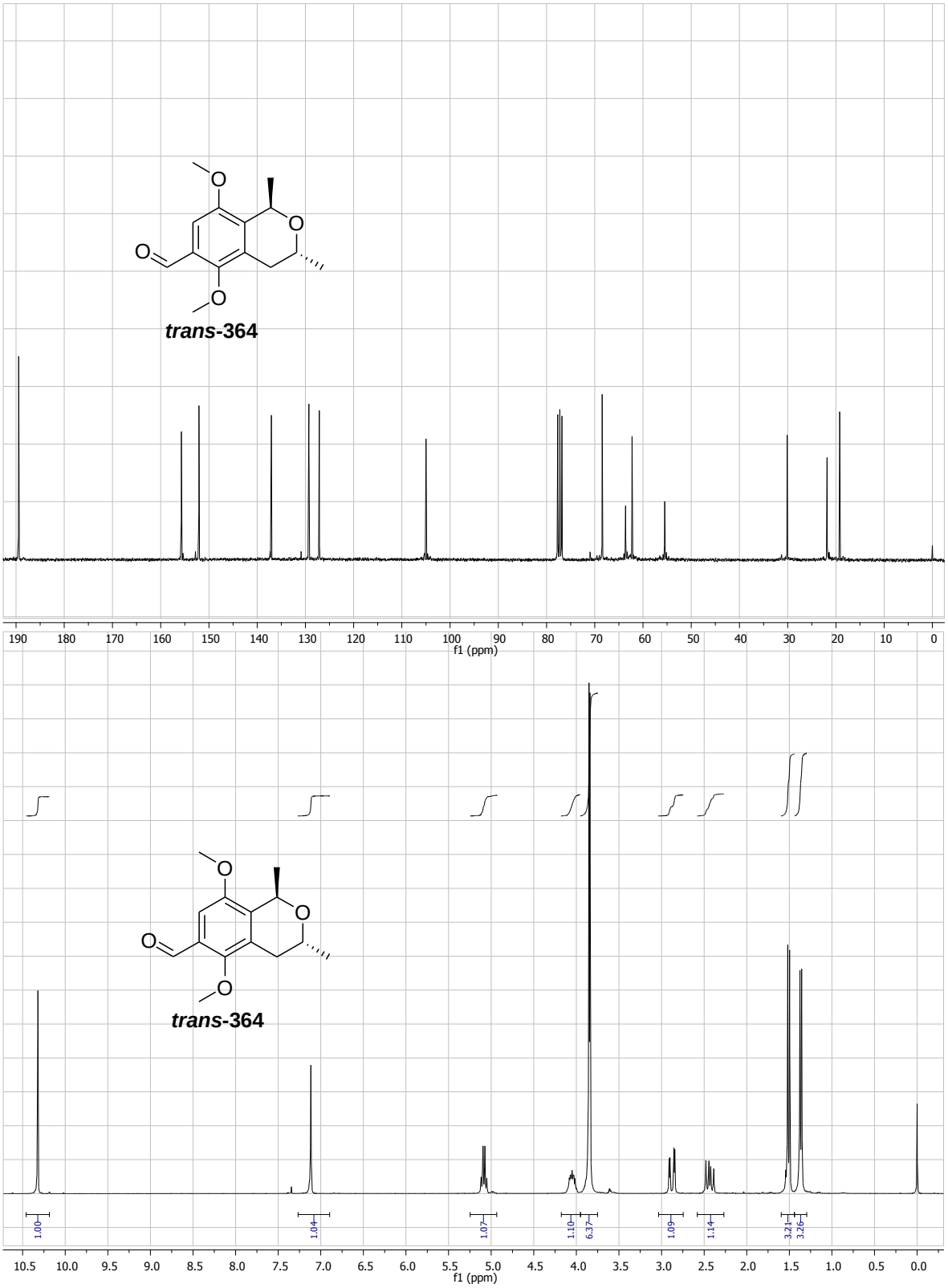




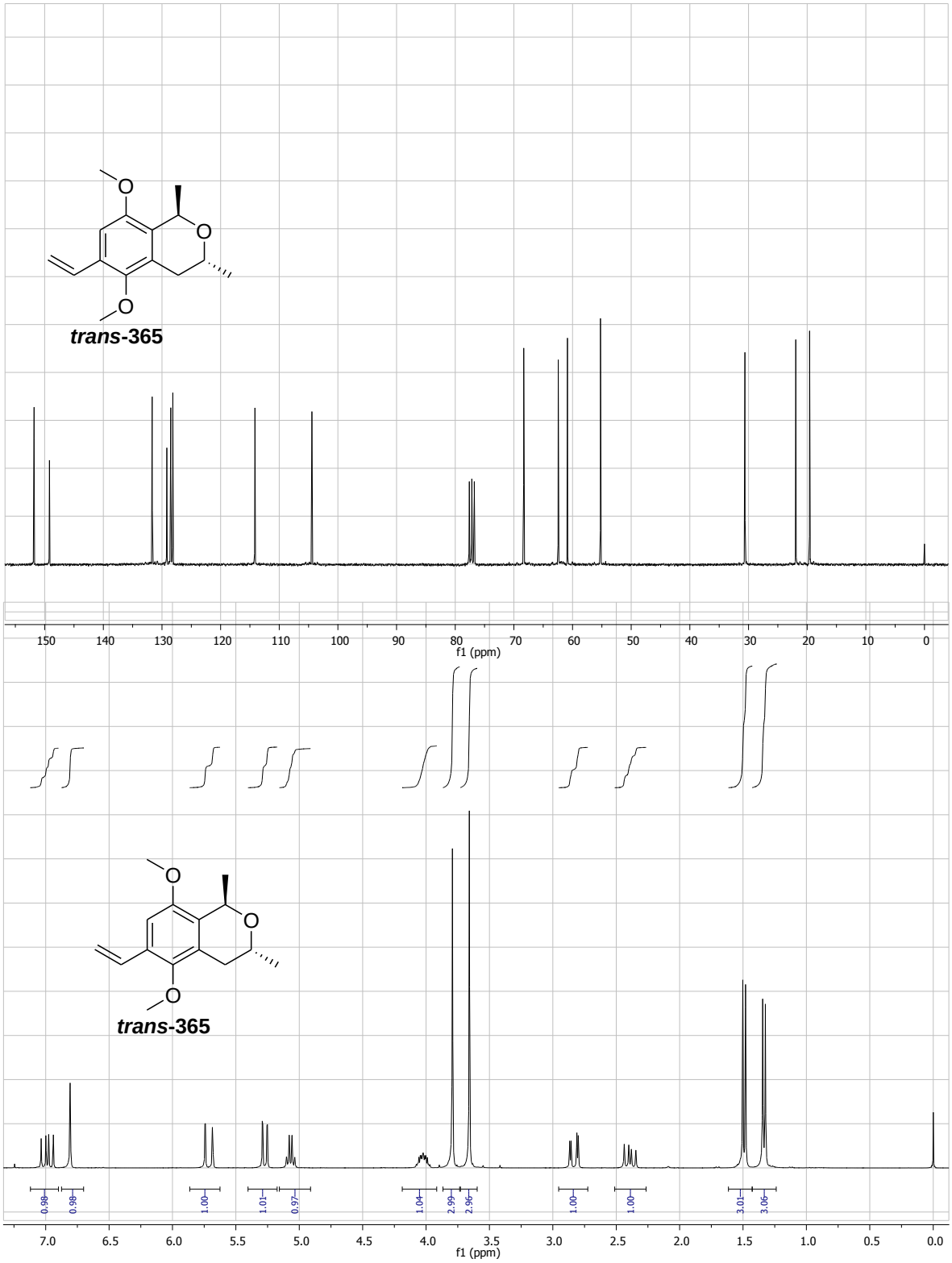
A1.25 ^{1}H and ^{13}C NMR spectra of acetophenone 374



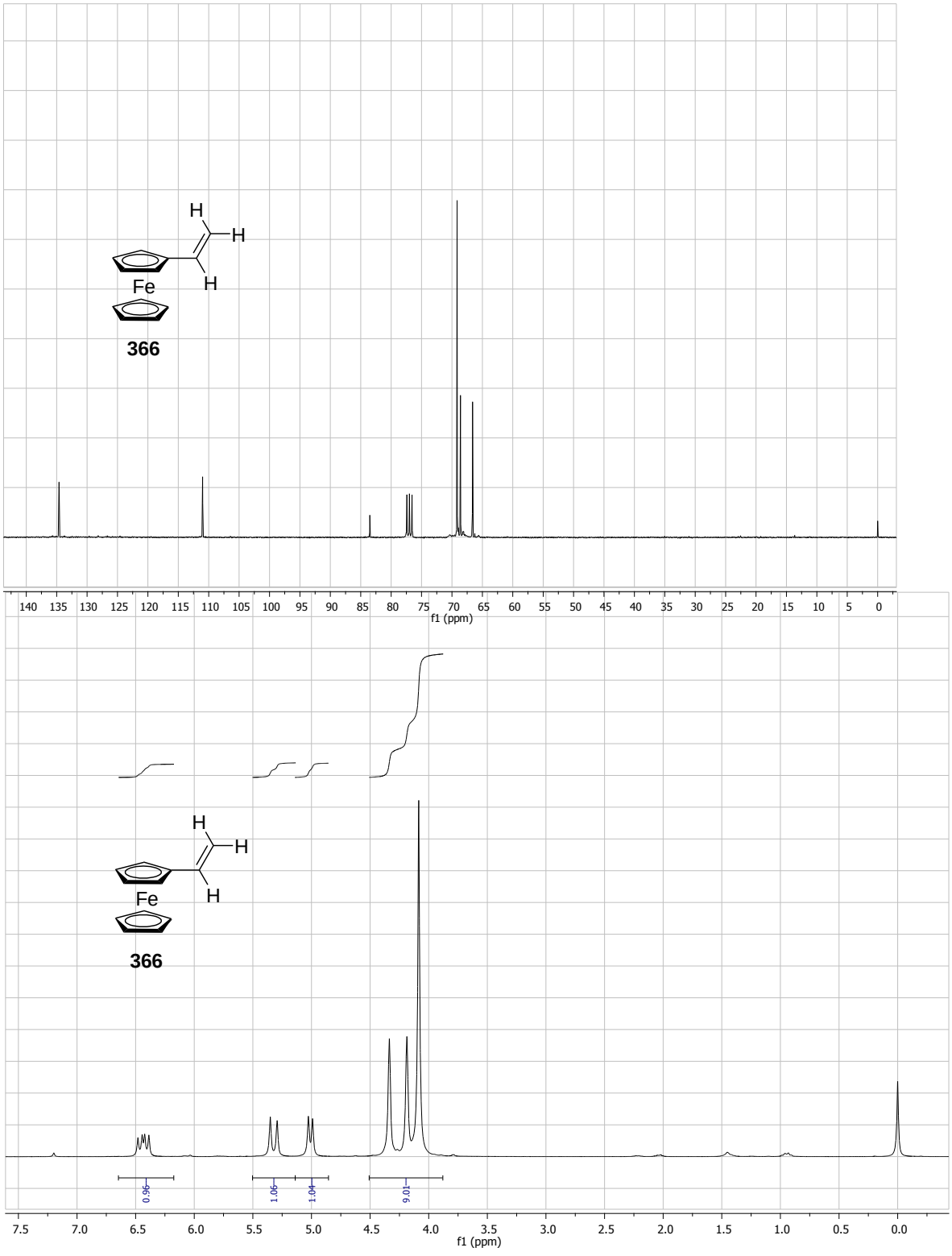
A1.26 ^{1}H and ^{13}C NMR spectra of 3,4-dihydroisochromene carbaldehyde *trans*-364



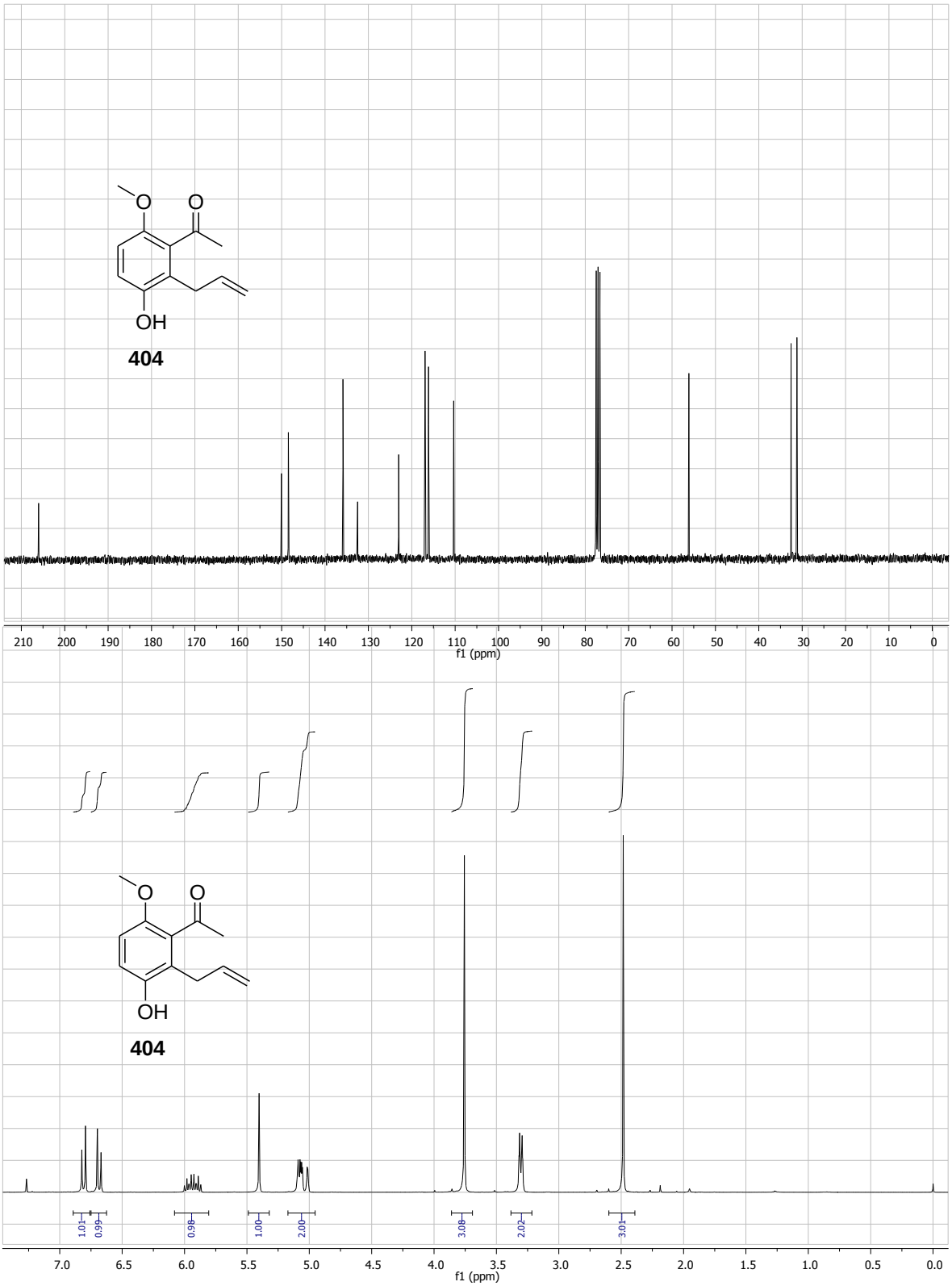
A1.27 ^{1}H and ^{13}C NMR spectra of vinyl 3,4-dihydroisochromene *trans*-365



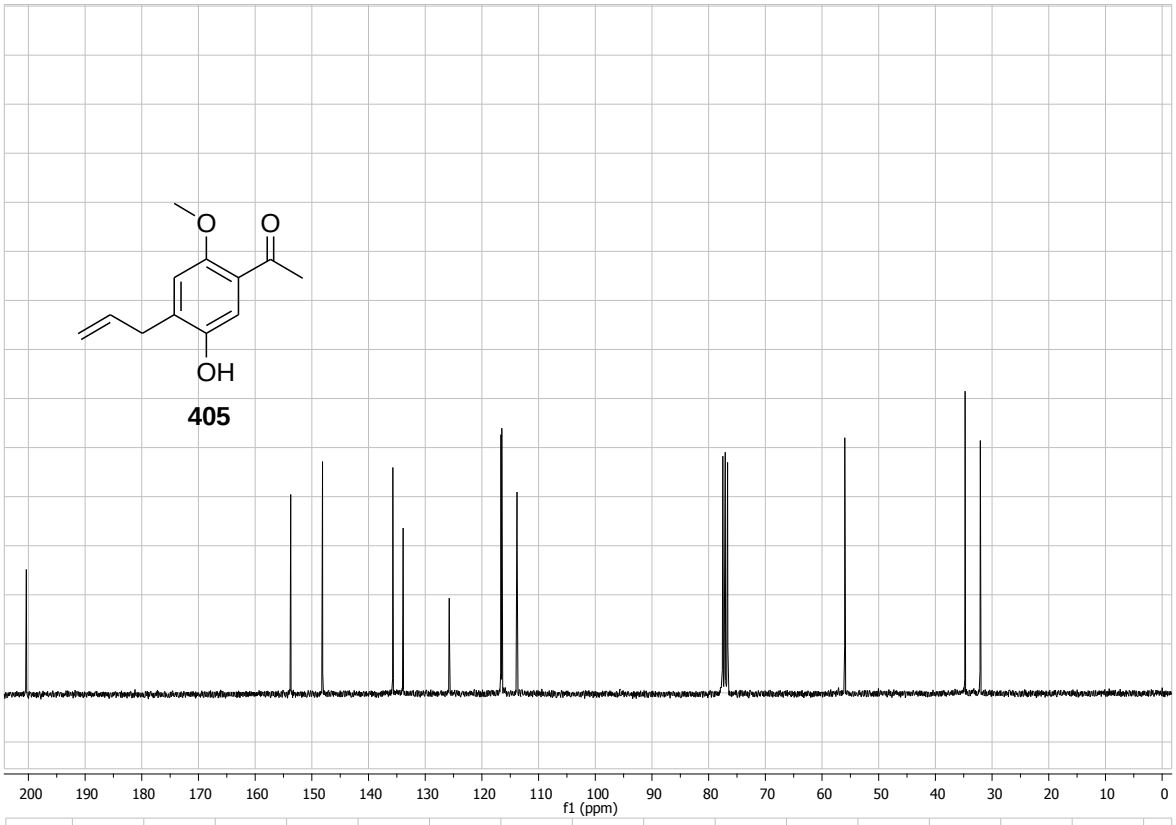
A1.28 ^{1}H and ^{13}C NMR spectra of vinyl ferrocene 366

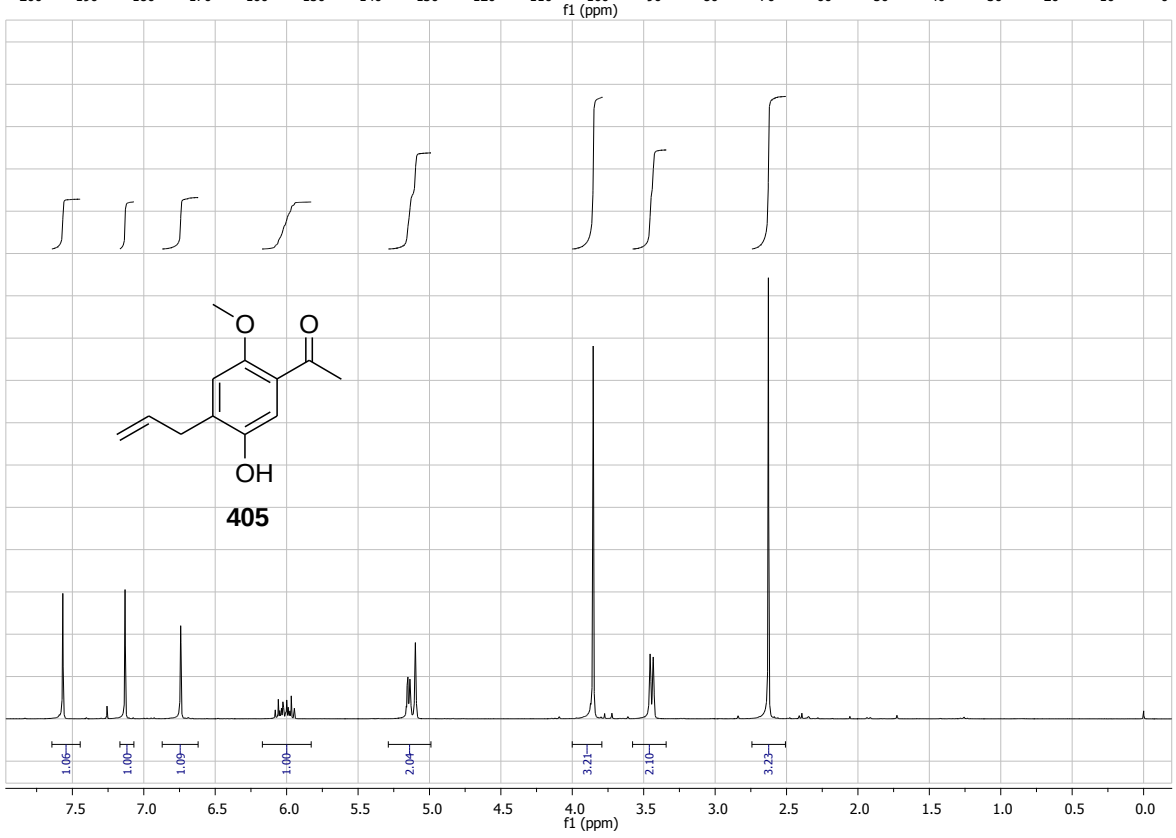


A1.29 ^{1}H and ^{13}C NMR spectra of phenol 404

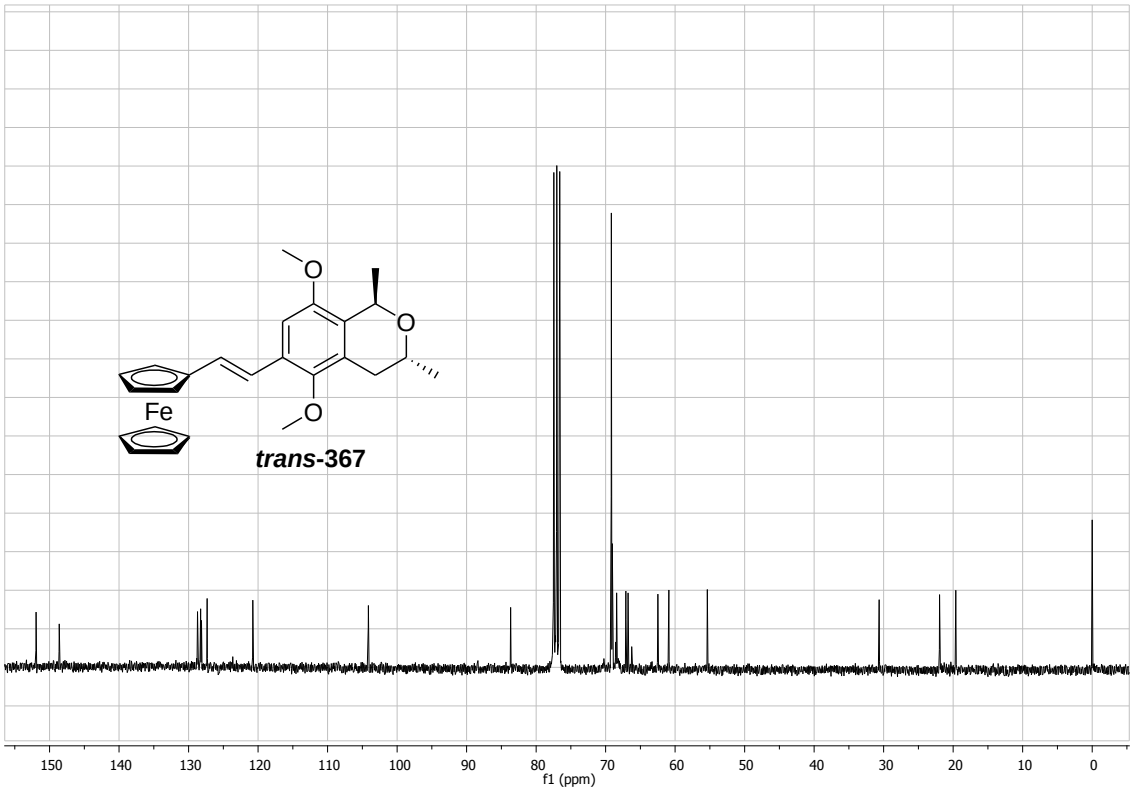


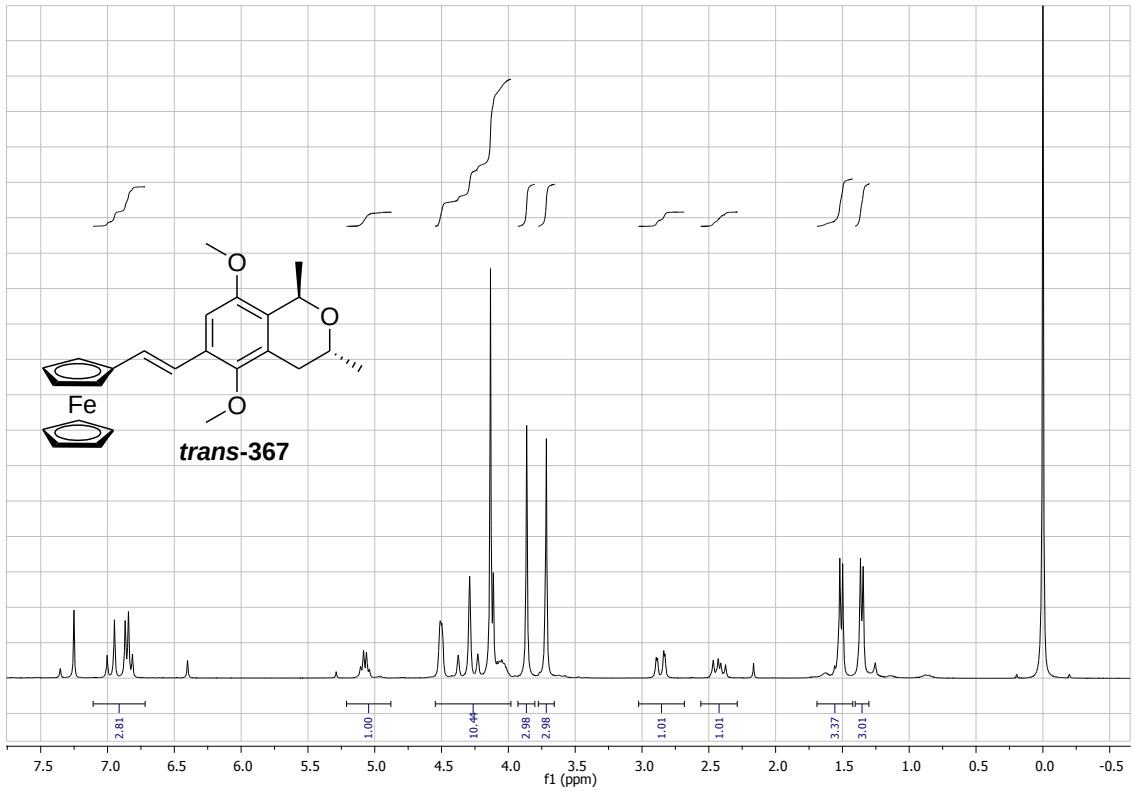
A1.30 ^{1}H and ^{13}C NMR spectra of phenol 405



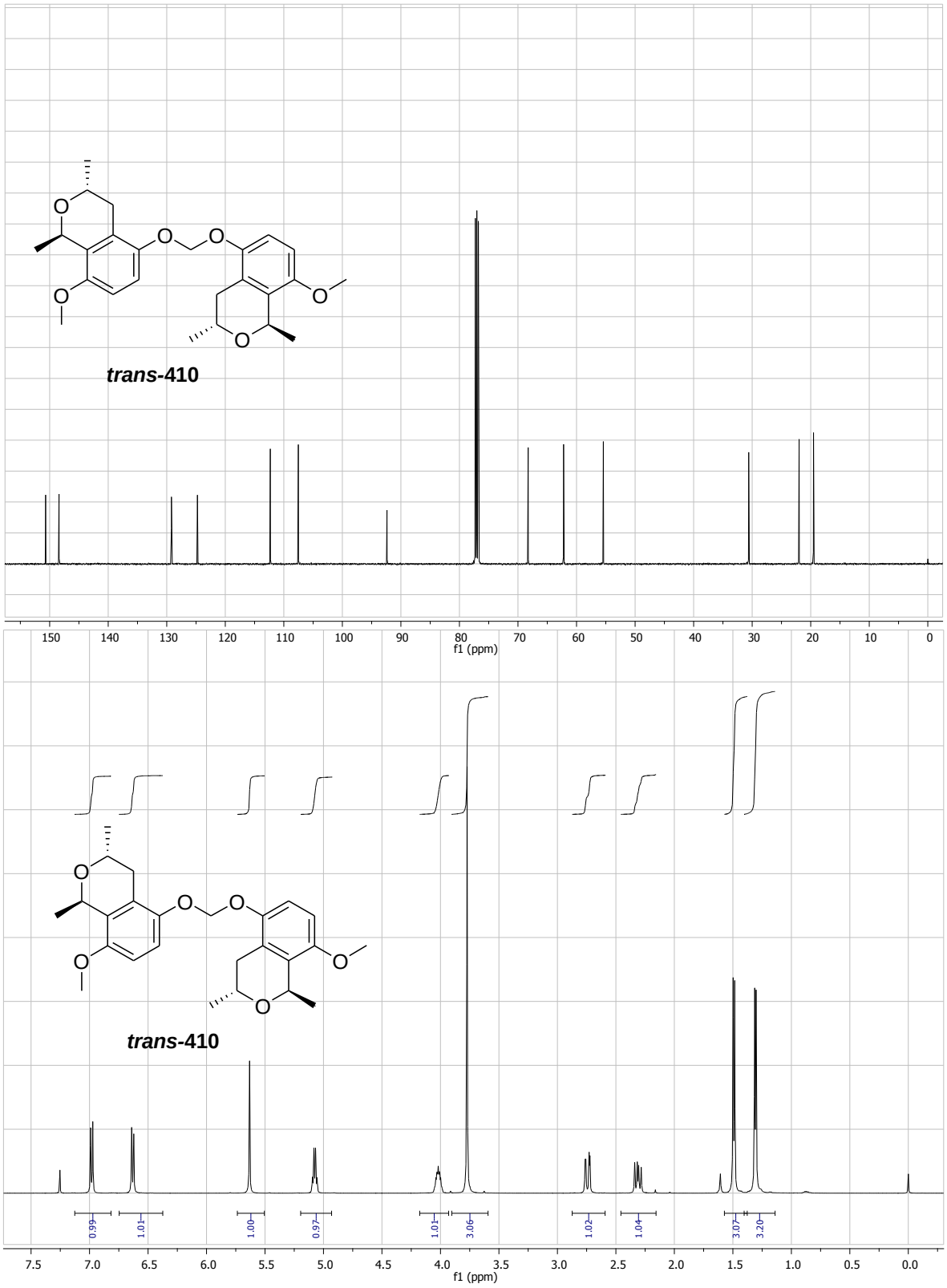


A1.31 ^{1}H and ^{13}C NMR spectra of ferrocenyl 3,4-dihydroisochrome *trans*-367

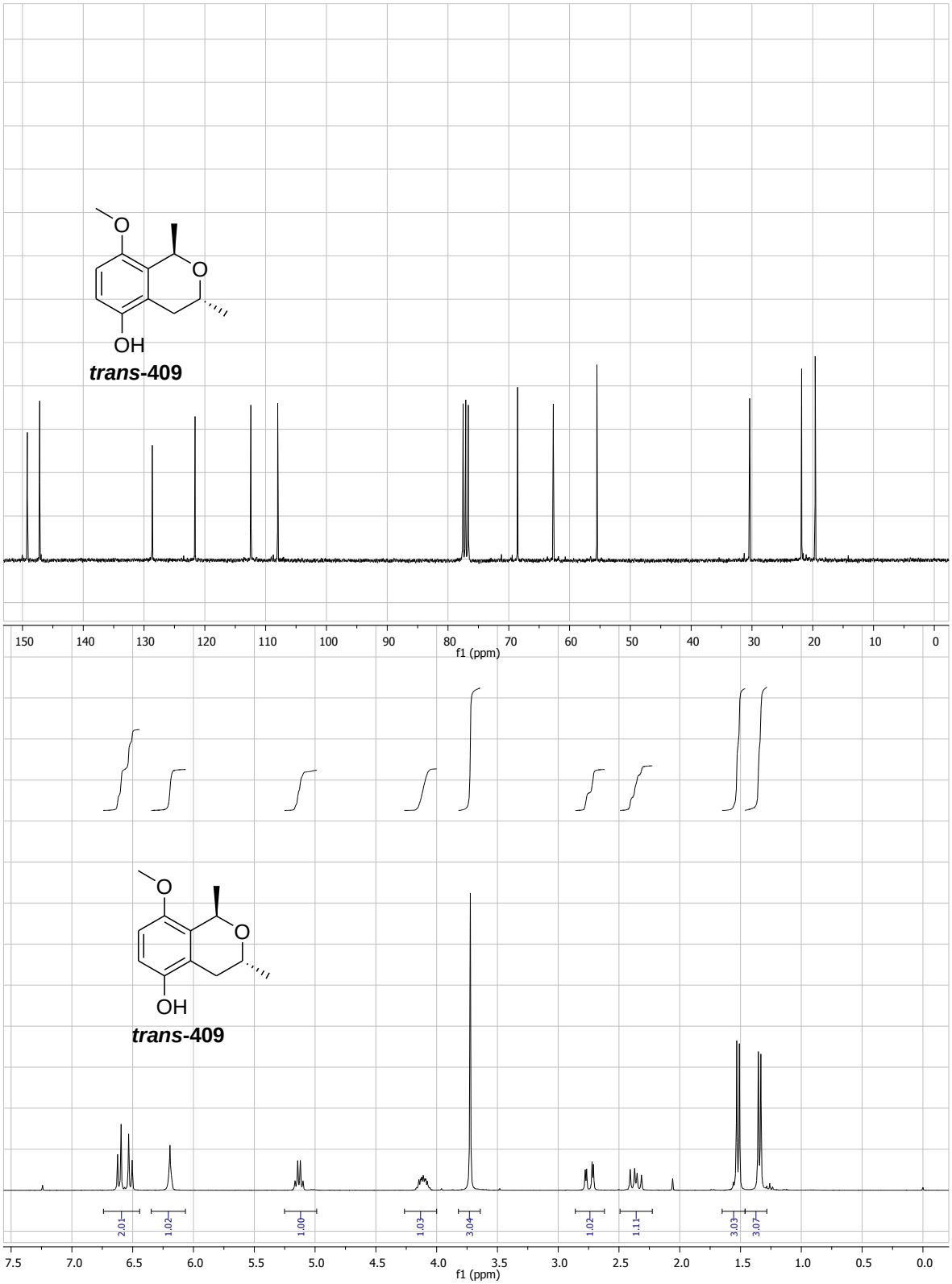




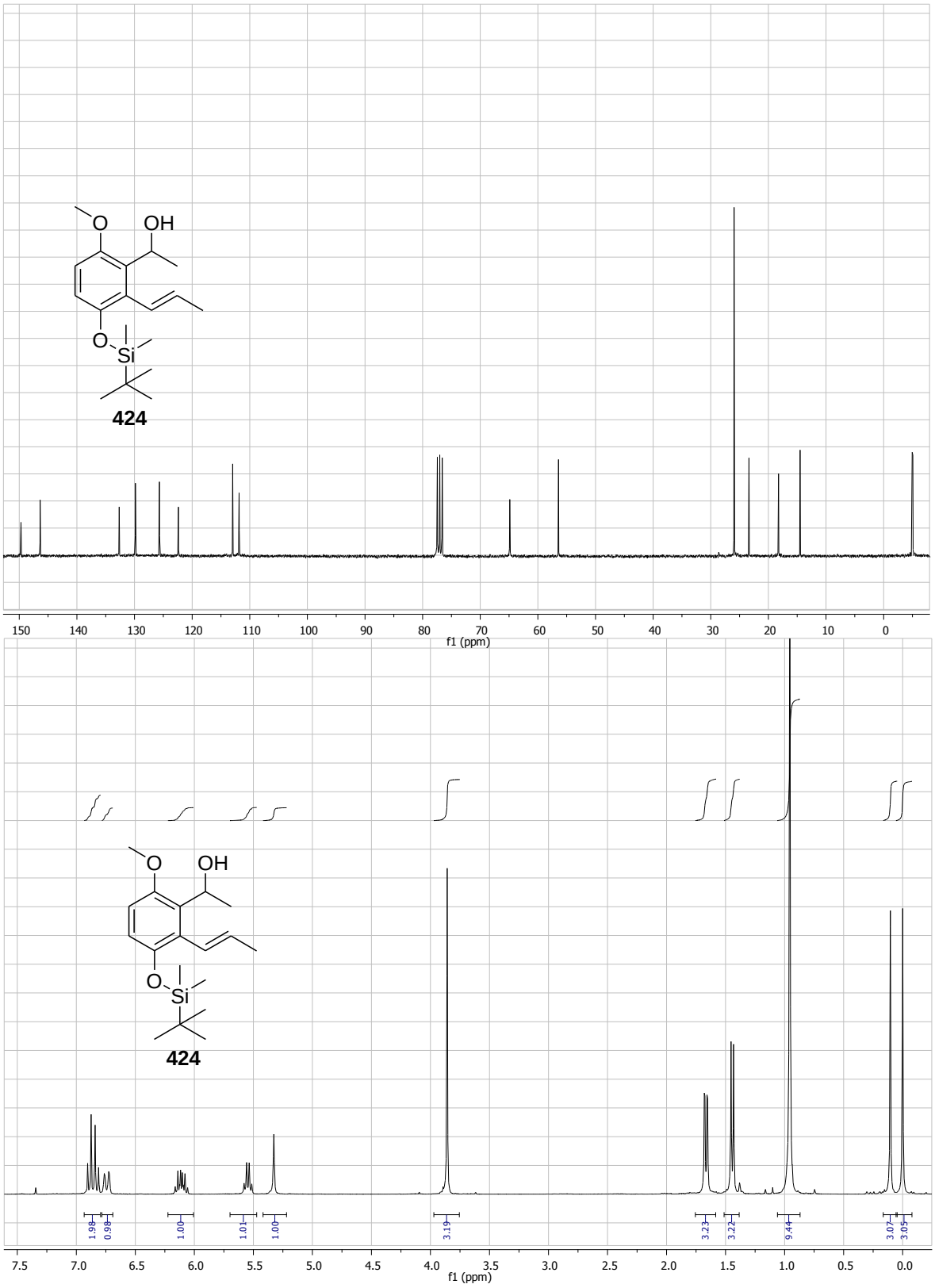
A1.32 ^{1}H and ^{13}C NMR spectra of symmetrical dimer *trans*-410



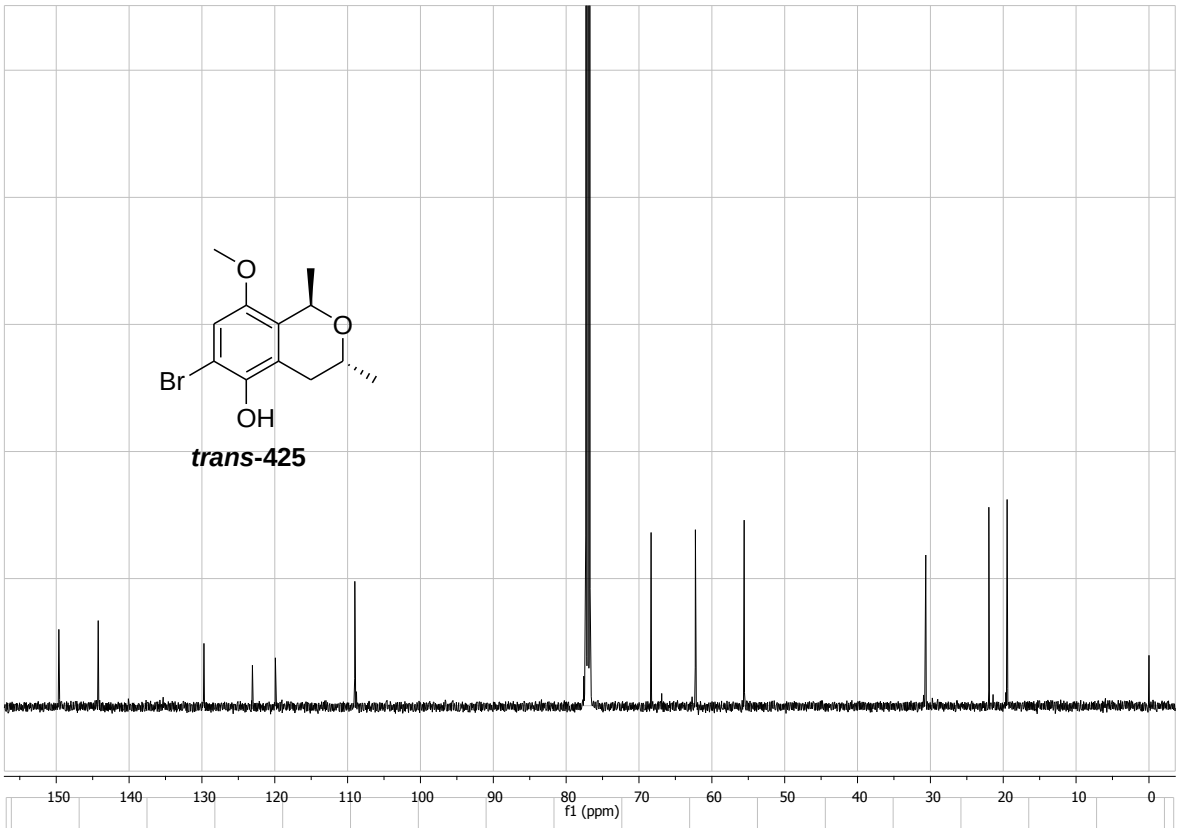
A1.33 ^{1}H and ^{13}C NMR spectra of isochromen-5-ol *trans*-409

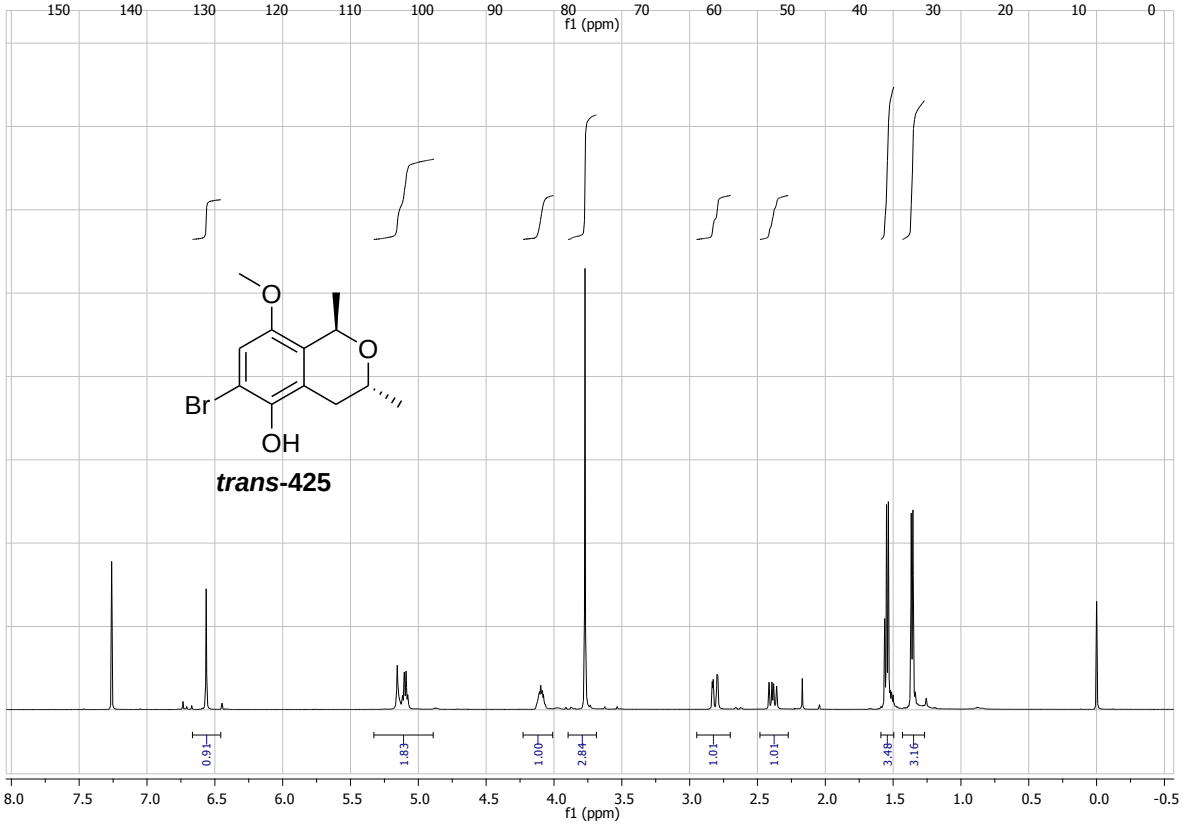


A1.34 ^{1}H and ^{13}C NMR spectra of alcohol 424

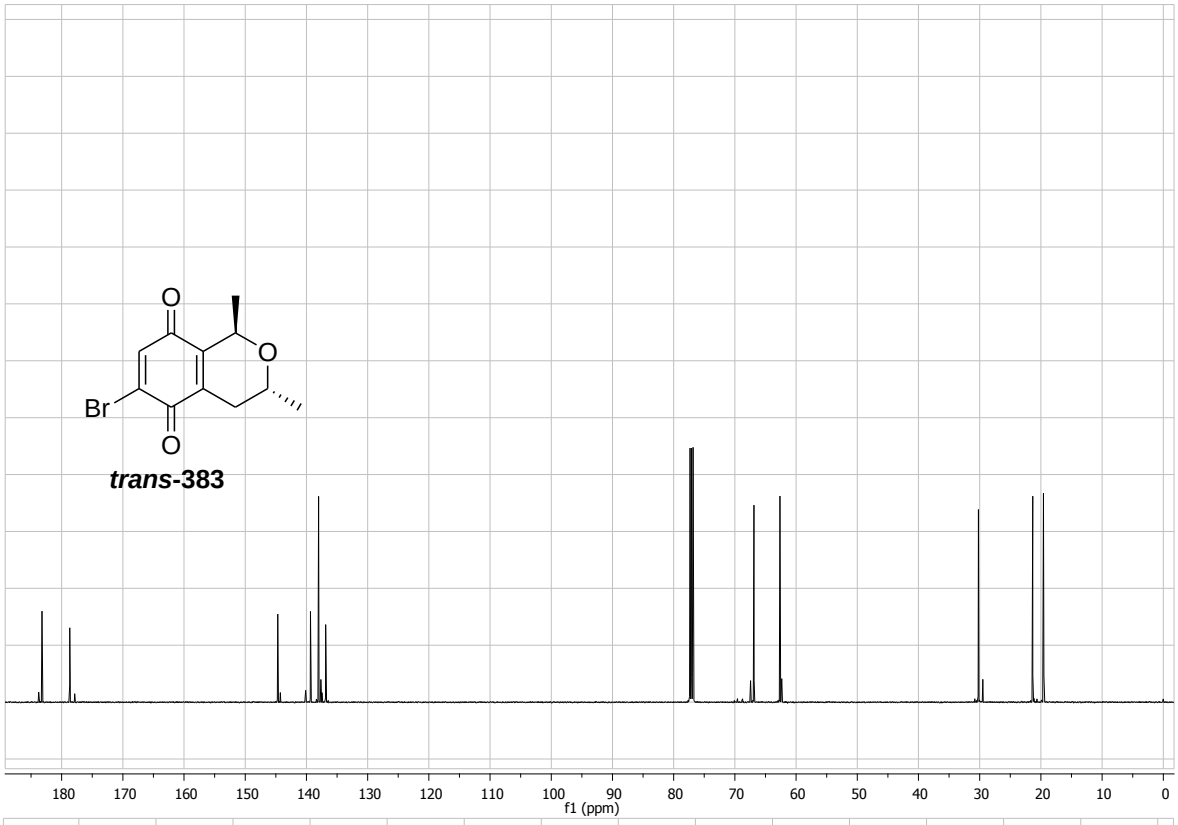


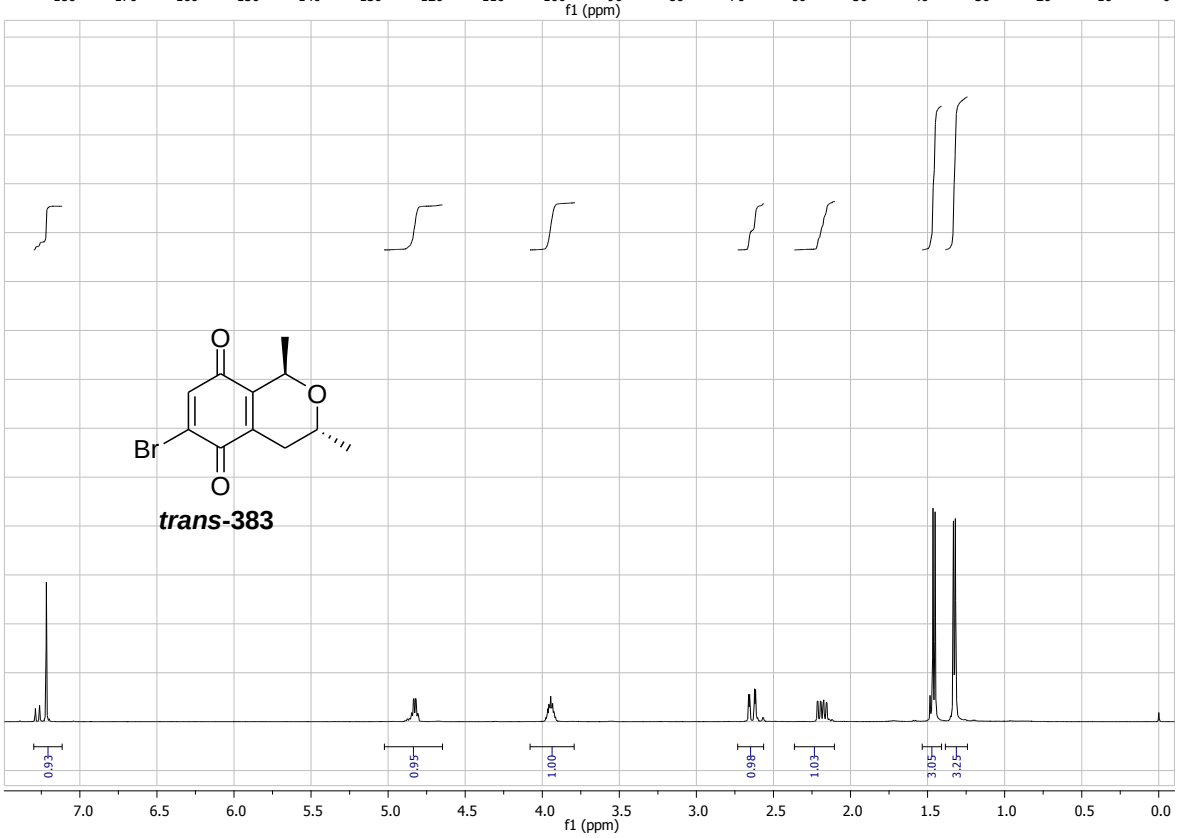
A1.35 ^{1}H and ^{13}C NMR spectra of bromoisochromen-5-ol *trans*-425



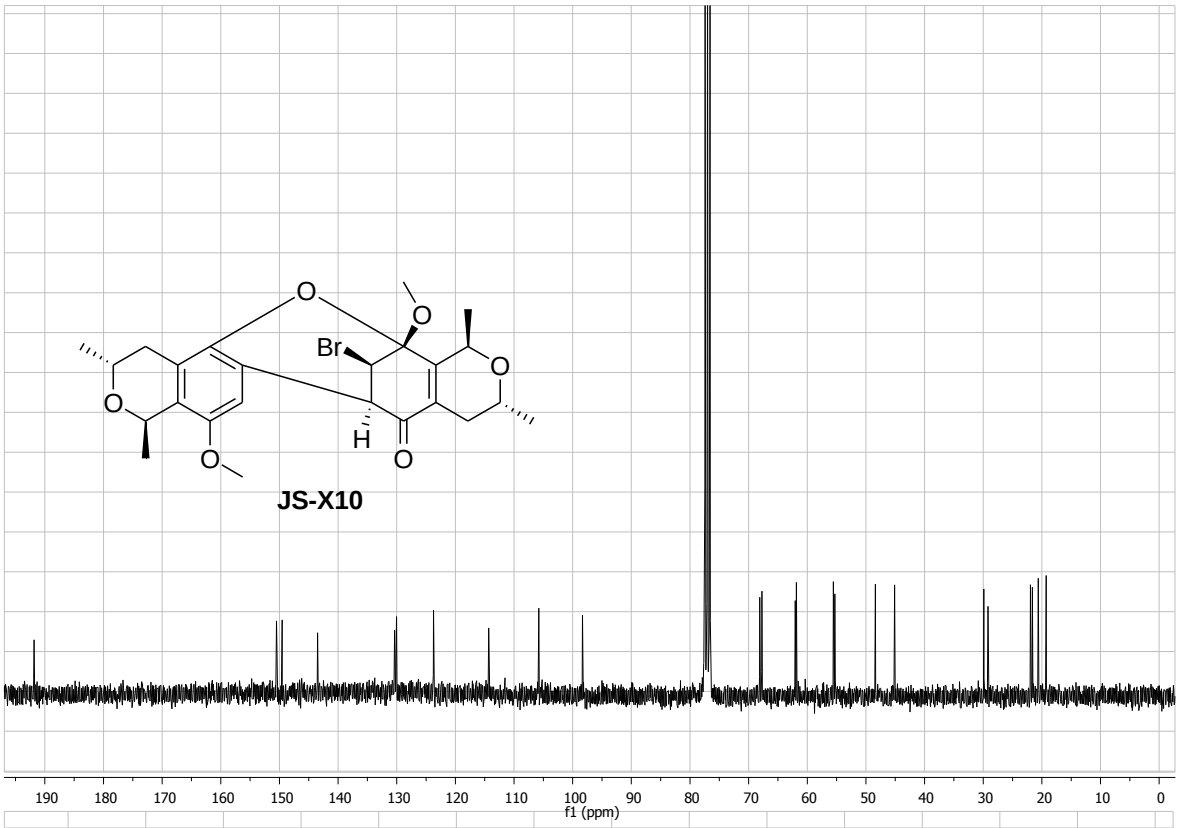


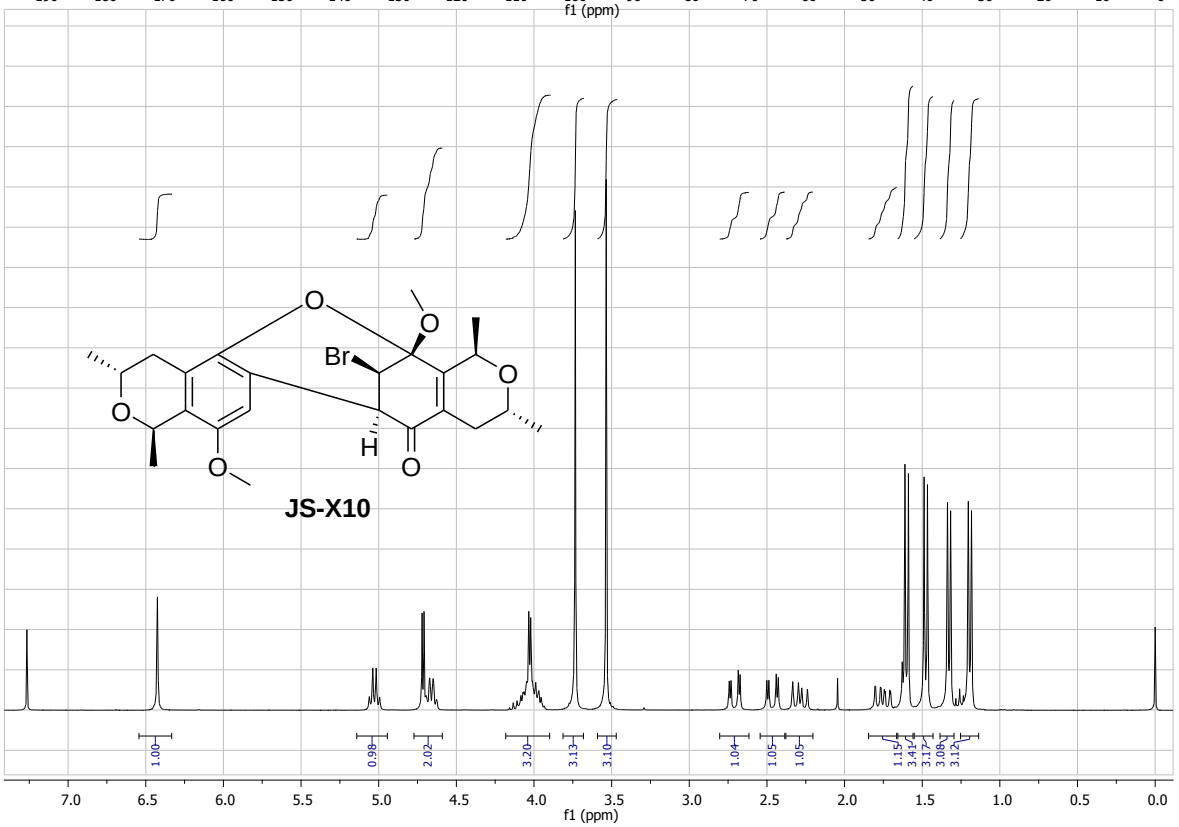
A1.36 ^{1}H and ^{13}C NMR spectra of bromoquinone *trans*-383





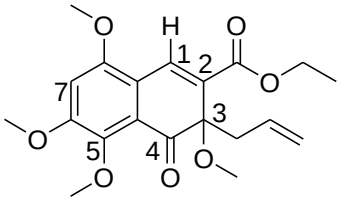
A1.37 ^{1}H and ^{13}C NMR spectra of dimer JS-X10





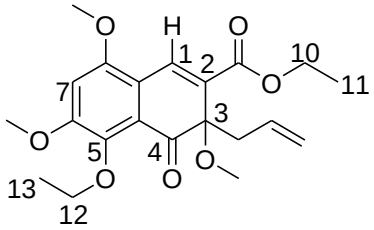
B1 Appendices: Tabulated 2D NMR spectroscopic data

B1.0 2D NMR spectroscopic data for ethyl ester 241



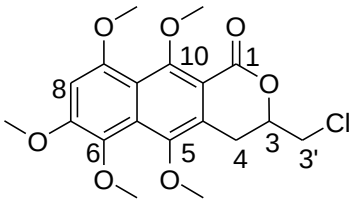
Shift (ppm)	m	Proton	HSQC (ppm)	HMBC (ppm)
8.09	s	H-1	132.4 (C1)	165.5 (Ar*C*$O_2CH_2CH_3$), 153.3 (C-8), 129.1 (C-2), 125.53 (C-4a), 116.0 (C-8a), 84.9 (C-3)
6.70	s	H-7	101.4 (C7)	156.2 (C-6), 153.3 (C-8), 143.1 (C-5), 125.5 (C-4a), 116.0 (C-8a)
5.59	ddt	$ArCH_2CH{=}CH_2$	131.3 ($ArCH_2CH{=}CH_2$)	
5.06-4.85	m	$ArCH_2CH{=}CH_2$	118.9 ($ArCH_2CH{=}CH_2$)	
4.46-4.24	m	$ArCO_2CH_2CH_3$	60.8 ($ArCO_2CH_2CH_3$)	
3.94	s	$ArOCH_3$	56.4 or 56.3 ($ArOCH_3$)	156.2 (C-6)
3.93	s	$ArOCH_3$	56.4 or 56.3 ($ArOCH_3$)	153.3 (C-8)
3.84	s	$ArOCH_3$	61.6 ($ArOCH_3$)	143.1 (C-5)
3.15	s	C(3)-OCH_3	53.7 (C-3)-OCH_3	84.9 (C-3)
2.90	dt	$ArCH_2CH{=}CH_2$	43.3 ($ArCH_2CH{=}CH_2$)	198.3 (C-4), 131.3 ($ArCH_2CH{=}CH_2$), 84.9 (C-3)
1.37	t	$ArCO_2CH_2CH_3$	14.4 ($ArCO_2CH_2CH_3$)	60.8 ($ArCO_2CH_2CH_3$)

B1.1 2D NMR spectroscopic data for ketone 242



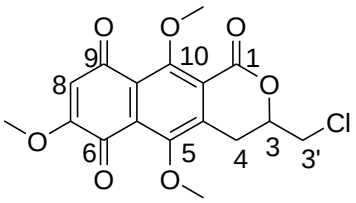
Shift (ppm)	m	Proton	HSQC (ppm)	COSY	HMBC (ppm)
8.10	s	H-1	132.4 (C-1)		165.4 ($ArCO_2CH_2CH_3$), 153.3 (C-8), 142.3 wk (C-5), 128.9 (C-2), 125.6 (C-4a), 116.0 (C-8a), 85.0 (C-3)
6.71	s	H-7	101.4 (C-7)		156.5 (C-6), 153.3 (C-8), 142.3 (C-5), 132.4 (C-1), 125.6 (C-4a), 116.0 (C-8a),
5.59	ddt	$ArCH_2CH=CH_2$	131.3 ($ArCH_2CH=CH_2$)		
5.08-4.76	m	$ArCH_2CH=CH_2$	118.9 ($ArCH_2CH=CH_2$)		
4.55-4.22	m	$ArCO_2CH_2CH_3$	60.7 ($ArCO_2CH_2CH_3$)	$ArCO_2CH_2CH_3$	14.4 ($ArCO_2CH_2CH_3$)
4.13-3.95	m	$ArOCH_2CH_3$	70.1 ($ArOCH_2CH_3$)	$ArOCH_2CH_3$	
3.93	br s	$ArOCH_3$	56.4 and 56.3 ($ArOCH_3$)		153.3 (C-8), 156.5 (C-6)
3.15	s	C(3)-OCH_3	53.6 C(3)-OCH_3		84.98 (C-3)
2.90	dt	$ArCH_2CH=CH_2$	43.4 ($ArCH_2CH=CH_2$)		198.2 (C-4), 128.9 (C-2), 125.6 wk (C-4a), 118.9 ($ArCH_2CH=CH_2$), 85.0 (C-3)
1.43	t	$ArOCH_2CH_3$	15.5 ($ArOCH_2CH_3$)	$ArOCH_2CH_3$	70.1 ($ArOCH_2CH_3$)
1.37	t	$ArCO_2CH_2CH_3$	14.4 ($ArCO_2CH_2CH_3$)	$ArCO_2CH_2CH_3$	60.7 ($ArCO_2CH_2CH_3$)

B1.2 2D NMR spectroscopic data for 3,4-dihydroiscoumarin 260



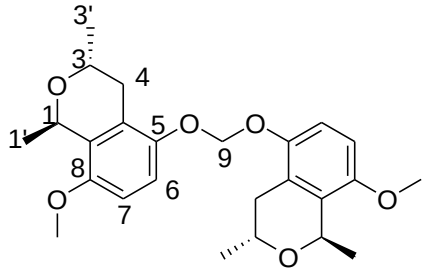
Shift (ppm)	m	Proton	HSQC (ppm)	HMBC (ppm)
6.76	s	H-8	97.4 (C-8)	156.0 (Ar-O), 153.1 (Ar-O), 136.2 (Ar-O), 128.8 (C-5a), 117.0 (C-9a)
4.59	m	H-3	76.2 (C-3)	126.8 (C-4a)
4.04	s	ArOCH_3	56.5 (ArOCH$_3$)	153.1 (Ar-O), 97.4 (C-8)
4.01	s	ArOCH_3	57.3 (ArOCH$_3$)	156.0 (Ar-O), 97.4 (C-8)
3.94	s,	ArOCH_3	63.4 (ArOCH$_3$)	158.6 (Ar-O)
3.88-3.69	m	2 × ArOCH_3, H-3'	62.1 (ArOCH$_3$), 62.1 (ArOCH$_3$), 44.9 (C-3')	146.6 (Ar-O), 136.2 (Ar-O), 76.2 (C-3), 26.0 (C-4)
3.53	dd	H-4	26.0 (C-4)	146.6 (Ar-O), 126.8 (C-4a), 112.5 (C-10a), 76.2 (C-3), 44.9 (C-3')
3.00	dd	H-4	26.0 (C-4)	158.6 (Ar-O), 146.6 (Ar-O), 126.8 (C-4a), 112.5 (C-10a), 76.2 (C-3), 44.9 (C-3')

B1.3 2D NMR spectroscopic data for quinone JS-QCl



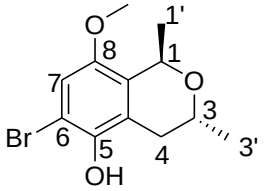
Shift (ppm)	m	Proton	HSQC (ppm)	HMBC (ppm)
6.08	s	H-8	111.0 (C-8)	178.9 (C-6), 182.6 (C-9), 159.1 (C-1), 125.7 (C-10a or C-5a)
4.65	m	H-3	76.1 (C-3)	
3.99	s	ArOCH_3	63.8 (ArOCH$_3$)	157.7 (Ar-O)
3.88	s	2 × ArOCH_3	62.3 (ArOCH$_3$), 56.5 (ArOCH$_3$)	111.0 (C-8), 152.7 (Ar-O), 159.1 (C-1)
3.82	d	H-3'	44.5 (C-3')	25.97 (C-4)
3.45	dd	H-4	26.0 (C-4)	44.5 (C-3'), 76.1 (C-3), 126.8 (C-10a or C-5a), 141.7 (Ar-O), 152.7 (Ar-O)
2.98	dd	H-4	26.0 (C-4)	44.5,(C-3') 128.2(C-4a), 141.7 (Ar-O), 152.7 (Ar-O)

B1.4 2D NMR spectroscopic data for dimer *trans*-410



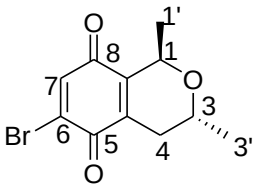
Shift (ppm)	m	Proton	HSQC (ppm)	COSY	HMBC (ppm)
6.98	d	H-6	112.3 (C-6) 150.7 (C-8)	H-7	150.7 (C-8), 148.4 (C-5), 124.8 (C-4a), 129.2 (C-8a) wk, 30.6 (C-4)
6.63	d	H-7	107.5 (C-7) 148.4 (C-5)	H-6	150.7 (C-8), 148.4 (C-5), 124.8 (C-4a) wk, 129.2 (C-8a), 68.3 (C-1)
5.63	s	H-9	92.4 (C-9) 129.2 (C-8a)		148.4 (C-5)
5.07	q	H-1	68.3 (C-4) 124.8 (C-4a)	H-1'	150.7 (C-8), 124.8 (C-4a), 129.2 (C-8a), 62.2 (C-3), 19.5 (C-1')
4.07-3.96	m	H-3	62.2 (C-3)	H-3', H-4	68.3 (C-1), 22.0 (C-3')
3.77	s	ArOC*H*3	55.4 (ArO*C*H3)		150.7 (C-8)
2.74	dd	1 × H-4	30.6 (C-4)		124.8 (C-4a), 129.2 (C-8a), 19.5 (C-1') wk, 148.4 (C-5)
2.31	dd	1 × H-4	30.6 (C-4)		19.5 (C-1'), 22.0 (C-3'), 62.2 (C-3), 107.5 (C-7), 112.3 (C-6), 124.8 (C-4a), 129.2 (C-8a), 150.7 (C-8)
1.49	d	H-1'	19.5 (C-1')		68.3 (C-4), 129.2 (C-8a)
1.31	d	H-3'	22.0 (C-3')		62.2 (C-3), 124.8 (C-4a) wk, 30.6 (C-4)

B1.5 2D NMR spectroscopic data for bromopyran *trans*-383



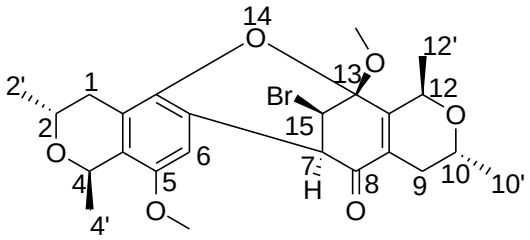
Shift (ppm)	m	Proton	HSQC (ppm)	COSY	HMBC (ppm)
6.56	s	H-7	109.0 (C-7)		149.6 (C-8), 144.2 (C-5), 129.7 (C-8a), 119.9 (C-6), 68.3 (C-1),
5.16	s	OH			144.2 (C-8) wk, 123.1 and 123.0 (C-4a)
5.10	q	H-1	68.3 (C-1)	H-1'	129.7 (C-8a), 123.1 and 123.0 (C-4a), 62.3 (C-3), 19.5 (C-1')
4.19-3.99	m	H-3	62.3 (C-3)	H-4, H-3'	22.0 (C-3') wk
3.77	s	ArOCH_3	55.6 (ArOCH_3)		149.6 (C-8), 109.0 (C-7) wk
2.81	dd	H-4	30.6 (C-4)		144.2 (C-5), 129.7 (C-8a), 123.1 and 123.0 (C-4a)
2.39	dd	H-4	30.6 (C-4)		144.2 (C-5), 129.7 (C-8a), 123.1 and 123.0 (C-4a), 62.3 (C3), 22.0 (C-3')
1.54	d	H-1'	19.5 (C-1')	H-1	129.7 (C-8a), 68.3 (C-1)
1.36	d	H-3'	22.0 (C-3')	H-3	30.6 (C-4), 62.3 (C-3), 123.1 and 123.0 (C-4a)

B1.6 2D NMR spectroscopic data for bromoquinone *trans*-425



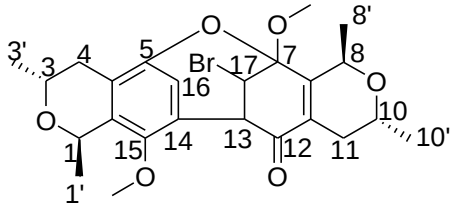
Shift (ppm)	m	Proton	HSQC (ppm)	COSY	HMBC (ppm)
7.22	s	H-7	138.0 (C-7)		178.6 (C-5), 136.8 (C-6), 144.7 (C-8a), 66.9 (C-1)
4.83	q	H-1	66.9 (C-1)	H-1'	183.2 (C-8) wk, 139.3 (C-4a), 144.7 (C-8a), 62.6 (C-3), 19.6 (C-1')
4.02-3.89	m	H-3	62.6 (C-3)	H-3'	66.9 (C1), 21.3 (C3')
2.64	dd	H-4	30.2 (C-4)	H-3	183.2 (C-8) wk, 178.6 (C-5), 139.3 (C-4a), 144.7 (C-8a), 66.9 (C-1), 19.6 (C-1')
2.18	ddd	H-4	30.2 (C-4)	H-3	183.2 (C-8) wk, 139.3 (C-4a), 144.7 (C-8a), 62.6 (C-3), 21.3 (C-3'), 19.6 (C-1')
1.46	d	H-1'	19.6 (C-1')	H-1	144.7 (C-8a), 66.9 (C-1)
1.33	d	H-3'	21.3 (C-3')	H-3	139.3 (C-4a), 62.6 (C-3), 66.9 (C-1), 30.2 (C-4)

B1.7 2D NMR spectroscopic data for dimer JS-X10



Shift (ppm)	m	Proton	HSQC (ppm)	COSY (ppm)	HMBC (ppm)
6.42	s	H-6	105.8 (C-6)	ArOC*H*$_3$, some of H-2, H-10 and H-15	150.5 (C-5), 143.5 (C-14a), 130.4 (C-4a), 114.3 (C-6a), 68.1 (C-4), 55.3 (C-7)
5.03	q	H-4	68.1 (C-4)	H-4'	150.5 (C-5) wk, 130.4 (C-4a), 123.7 (C-14b), 61.9 (C-2), 19.3 (C-4')
4.71	d	H-15	45.1 (C-15)	OCH$_3$, H-7	191.8 (C-8), 149.5 (C-12a), 114.3 (C-6a), 98.3 (C-13), 67.7 (C-12), 55.3 (C-7)
4.66	q	H-12	67.7 (C-12)	H-12'	149.5 (C-12a), 130.0 (C-8a), 62.1 (C-10), 20.6 (C-12')
4.14-3.89	m	H-2, H-10 and H-7	61.9 (C-2), 62.1 (C-10) and 55.3 (C-7)	H-4', H-2', H-15, H-6	191.8 (C-8), 143.5 (C-14a), 130.4 (C-4a), 130.0 (C-8a), 114.3 (C-6a), 105. 8 (C-6), 98.3 (C-13), 45.1 (C-15)
3.73	s	ArOC*H*$_3$	55.6 ArO*C*H$_3$	H-6	150.5 (C-5)
3.53	s	OCH$_3$	48.4 (OCH$_3$)	H-15	98.3 (C-13)
2.71	dd	H-1	29.9 (C-1)		143.5 (C-14a), 123.7 (C-14b), 130.4 (C-4a)
2.46	dd	H-9	29.2 (C-9)		191.8 (C-8), 149.5 (C-12a), 130.0 (C-8a), 20.6 (C-12')
2.29	dd	H-1	29.9 (C-1)		130.4 (C-4a), 123.7 (C-14b), 61.9 (C-2), 22.0 (C-2')
1.75	dd	H-9	29.2 (C-9)		149.5 (C-12a), 130.0 (C-8a), 62.1 (C-10), 21.6 (C-10')
1.60	d	H-12'	20.6 (C-12')	H-12	149.5 (C-12a), 67.7 (C-12)
1.48	d	H-4'	19.3 (C-4')	H-4	130.4 (C-14b) wk, 68.1 (C-4)
1.33	d	H-2'	22.0 (C-2')		123.7 (C-4a) WK, 61.9 (C-2), 29.9 (C-1)
1.19	d	H-10'	21.6 (C-10')		130.0 (C-8a) WK, 62.1 (C-10), 29.2 (C-9)

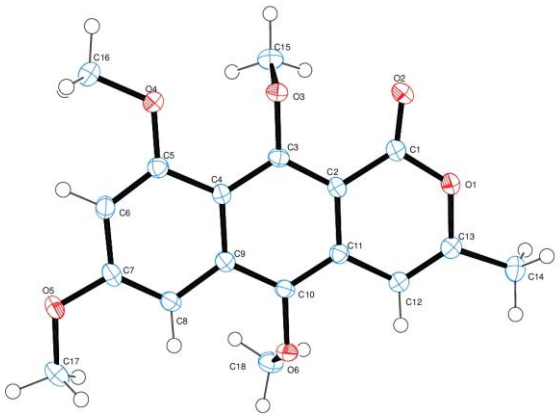
B1.8 2D NMR spectroscopic data for proposed dimer *trans*-429

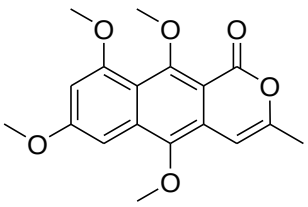


Shift (ppm)	m	Proton	HSQC (ppm)	COSY (ppm)	HMBC (ppm)
6.42	s	H-16	105.8 (C-16)	$ArOCH_3$, some of H-3, H-10 and H-17	150.5 (C-15), 143.5 (C-5), 130.4 (C-15a), 114.3 (C-14), 68.1 (C-1), 55.3 (C-13)
503	q	H-1	68.1 (C-1)	H-1'	150.5 (C-15) wk, 130.0 (C-11a), 123.7 (C-4a), 61.9 (C-3), 19.3 (C-1')
4.71	d	H-17	45.1 (C-17)	OCH_3, H-17, H-13	191.8 (C-12), 149.5 (C-7a), 114.3 (C-14), 98.3 (C-7), 67.7 (C-8), 55.3 (C-13)
4.66	q	H-8	67.7 (C-8)	H-8'	149.5 (C-7a), 130.0 (C-11a), 62.0 (C-10), 20.6 (C-8')
4.14-3.89	m	H-3, H-10 and H-13	61.9 (C-3), 62.1 (C-10) and 55.3 (C-13)	H-1', H-3', H-17, H-16	191.8 (C-12), 143.5 (C-5), 130.4 (C-15a), 130.0 (C-11a), 114.3 (C-14), 105.8 (C-16), 98.3 (C-7), 45.1 (C-17)
3.73	s	$ArOCH_3$	55.6 ($ArOCH_3$)	H-16	150.5 (C-15)
3.53	s	OCH_3	48.4 (OCH_3)	H-17	98.3 (C-7)
2.71	dd	H-4	29.9 (C-4)		143.5 (C-5), 123.7 (C-4a), 130.4 (C-15a)
2.46	dd	H-11	29.2 (C-11)		191.8 (C-12), 149.5 (C-7a), 130.0 (C-11a), 20.6 (C-8')
2.29	dd	H-4	29.9 (C-4)		130.4 (C-15a), 123.7 (C-4a), 61.9 (C-3), 22.0 (C-3')
1.75	dd	H-11	29.2 (C-11)		149.5 (C-7a), 130.0 (C-11a), 62.0 (C-10), 21.6 (C-10')
1.60	d	H-8'	20.6 (C-8')	H-8	149.5 (C7a), 67.7 (C8)
1.48	d	H-1'	19.3 (C-1')	H-1	130.4 (C-15a), 68.1 (C-1)
1.33	d	H-3'	22.0 (C-3')		123.7 (C-4a) wk, 61.9 (C-3), 29.9 (C-4)
1.19	d	H-10'	21.6 (C-10')		130.0 (C-11a) wk, 62.0 (C-10), 29.2 (C-11)

C1 Appendices: Crystallographic data

C1.0 X-ray crystallographic data for 5,7,9,10-tetramethoxy-3-methyl-1*H*-benzo[*g*]isochromen-1-one 103





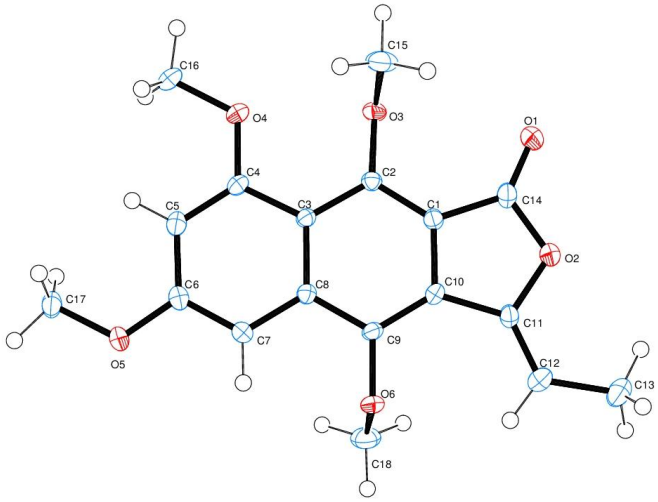
103

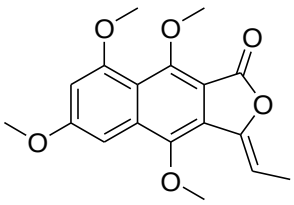
Table C1.0 Crystal data and structure refinement for 14a_js020_p.

Identification code	14a_js020_p	
Empirical formula	$C_{18}H_{18}O_6$	
Formula weight	330.32	
Temperature	173(2) K	
Wavelength	0.71069 Å	
Crystal system	Triclinic	
Space group	P-1	
Unit cell dimensions	a = 7.3600(3) Å	α= 106.474(2)°.
	b = 9.3270(4) Å	β= 106.037(2)°.
	c = 12.3290(5) Å	γ = 94.670(2)°.
Volume	768.21(6) $Å^3$	
Z	2	
Density (calculated)	1.428 Mg/m^3	
Absorption coefficient	0.108 mm^{-1}	
F(000)	348	
Crystal size	0.70 x 0.60 x 0.50 mm^3	
Theta range for data collection	3.40 to 28.00°.	
Index ranges	-9<=h<=9, -12<=k<=12, -16<=l<=16	
Reflections collected	15256	
Independent reflections	3709 [R(int) = 0.0266]	
Completeness to theta = 28.00°	99.7 %	
Absorption correction	Semi-empirical from equivalents	
Max. and min. transmission	0.9482 and 0.9285	

Refinement method	Full-matrix least-squares on F^2
Data / restraints / parameters	3709 / 0 / 222
Goodness-of-fit on F^2	1.040
Final R indices [I>2sigma(I)]	R1 = 0.0418, wR2 = 0.1111
R indices (all data)	R1 = 0.0564, wR2 = 0.1208
Largest diff. peak and hole	0.271 and -0.343 e.$Å^{-3}$

C1.1 X-ray crystallographic data for (*Z*)-3-ethylidene-46,8,9-tetramethoxynaphtho[2,3-*c*]furan-1(3*H*)-one 176





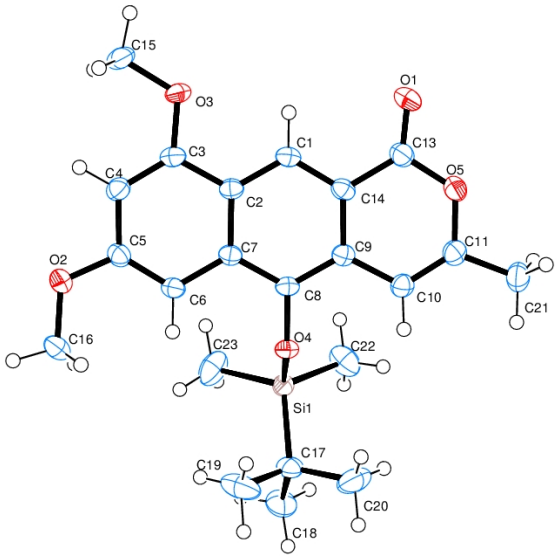
176

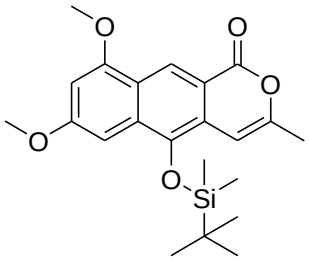
Table C1.1 Crystal data and structure refinement for 13a_cdk_js01paep_p.

Identification code	shelx	
Empirical formula	$C_{18}H_{18}O_6$	
Formula weight	330.32	
Temperature	173(2) K	
Wavelength	0.71073 Å	
Crystal system	Monoclinic	
Space group	P 21/n	
Unit cell dimensions	a = 7.0616(2) Å	α= 90°.
	b = 18.1308(6) Å	β= 91.4520(10)°.
	c = 11.9516(4) Å	γ = 90°.
Volume	1529.70(8) $Å^3$	
Z	4	
Density (calculated)	1.434 Mg/m^3	
Absorption coefficient	0.108 mm^{-1}	
F(000)	696	
Crystal size	0.470 x 0.160 x 0.050 mm^3	
Theta range for data collection	3.097 to 27.999°.	
Index ranges	-9<=h<=9, -23<=k<=23, -15<=l<=15	
Reflections collected	40839	
Independent reflections	3687 [R(int) = 0.0360]	
Completeness to theta = 25.242°	99.5 %	

Refinement method	Full-matrix least-squares on F^2
Data / restraints / parameters	3687 / 0 / 222
Goodness-of-fit on F^2	1.031
Final R indices [I>2sigma(I)]	R1 = 0.0537, wR2 = 0.1419
R indices (all data)	R1 = 0.0661, wR2 = 0.1527
Extinction coefficient	n/a
Largest diff. peak and hole	0.715 and -0.293 e.$Å^{-3}$

C1.2 X-ray crystallographic data for 5-((*tert*-butyldimethylsilyl)oxy)-7,9-dimethoxy-3-methyl-1*H*-benzo[*g*]isochromen-1-one 228





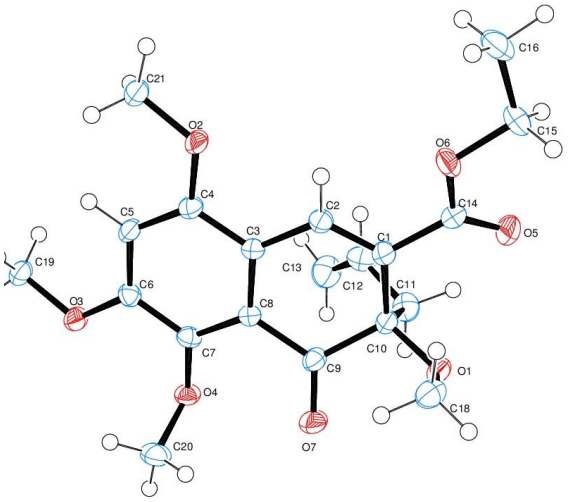
228

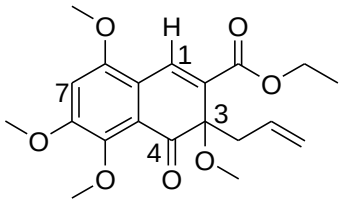
Table C1.2 Crystal data and structure refinement for 15a_js032_p.

Identification code	15a_js032_p	
Empirical formula	$C_{22}H_{28}O_5Si$	
Formula weight	400.53	
Temperature	173(2) K	
Wavelength	0.71073 Å	
Crystal system	Triclinic	
Space group	P-1	
Unit cell dimensions	a = 7.9749(2) Å	α= 84.8910(10)°.
	b = 11.2205(3) Å	β= 72.9250(10)°.
	c = 13.0450(4) Å	γ = 73.1720(10)°.
Volume	1068.05(5) $Å^3$	
Z	2	
Density (calculated)	1.245 Mg/m^3	
Absorption coefficient	0.139 mm^{-1}	
F(000)	428	
Crystal size	0.76 x 0.26 x 0.14 mm^3	
Theta range for data collection	2.90 to 28.00°.	
Index ranges	-10<=h<=10, -14<=k<=14, -17<=l<=17	
Reflections collected	22195	
Independent reflections	5145 [R(int) = 0.0274]	
Completeness to theta = 28.00°	99.6 %	

Absorption correction	Semi-empirical from equivalents
Max. and min. transmission	0.9808 and 0.9021
Refinement method	Full-matrix least-squares on F^2
Data / restraints / parameters	5145 / 0 / 261
Goodness-of-fit on F^2	1.043
Final R indices [I>2sigma(I)]	R1 = 0.0356, wR2 = 0.0956
R indices (all data)	R1 = 0.0427, wR2 = 0.1009
Largest diff. peak and hole	0.284 and -0.225 e.$Å^{-3}$

C1.3 X-ray crystallographic data for ethyl 3-allyl-3,4-dihydro-3,5,6,8-tetramethoxy-4-oxonaphthalene-2-carboxylate 241





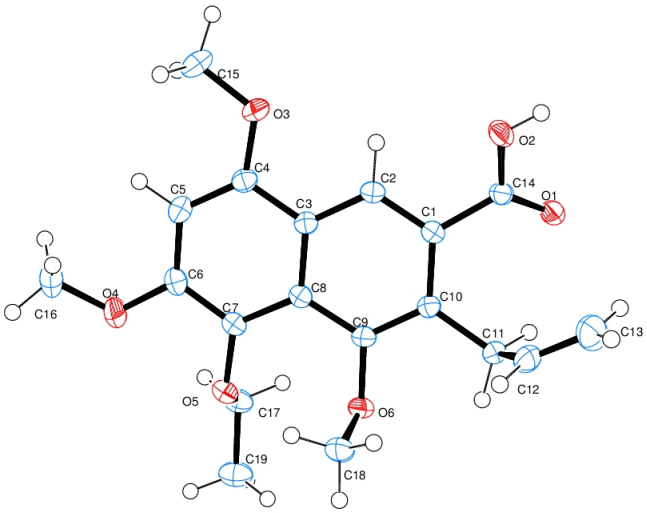
241

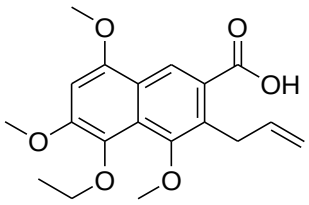
Table C1.3 Crystal data and structure refinement for 14a_js07_p.

Identification code	14a_js07_p	
Empirical formula	$C_{20}H_{24}O_7$	
Formula weight	376.39	
Temperature	173(2) K	
Wavelength	0.71073 Å	
Crystal system	Monoclinic	
Space group	P2(1)/n	
Unit cell dimensions	a = 7.4837(7) Å	α= 90°.
	b = 9.9832(8) Å	β= 98.200(2)°.
	c = 25.142(2) Å	γ = 90°.
Volume	1859.2(3) $Å^3$	
Z	4	
Density (calculated)	1.345 Mg/m^3	
Absorption coefficient	0.102 mm^{-1}	
F(000)	800	
Crystal size	0.54 x 0.37 x 0.22 mm^3	
Theta range for data collection	2.75 to 25.50°.	
Index ranges	-9<=h<=9, -12<=k<=12, -30<=l<=30	
Reflections collected	28028	
Independent reflections	3497 [R(int) = 0.0238]	
Completeness to theta = 25.50°	99.5 %	
Absorption correction	Semi-empirical from equivalents	

Max. and min. transmission	0.9780 and 0.9472
Refinement method	Full-matrix least-squares on F^2
Data / restraints / parameters	3497 / 0 / 250
Goodness-of-fit on F^2	1.164
Final R indices [I>2sigma(I)]	R1 = 0.0899, wR2 = 0.3031
R indices (all data)	R1 = 0.0941, wR2 = 0.3101
Largest diff. peak and hole	0.483 and -0.502 e.$Å^{-3}$

C1.4 X-ray crystallographic data for 3-ethyl 3-allyl-5-ethoxy-4-hydroxy-6,8-dimethoxynaphthalene-2-carboxylate 248





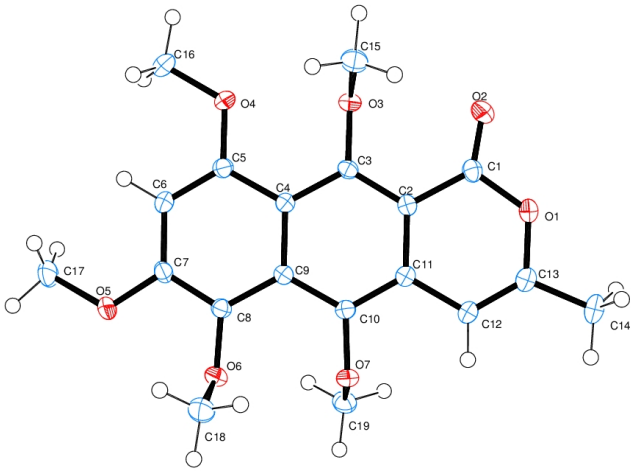
248

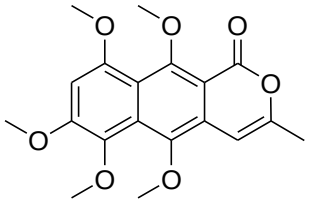
Table C1.4 Crystal data and structure refinement for 14a_js06_p.

Identification code	14a_js06_p	
Empirical formula	$C_{19}H_{22}O_6$	
Formula weight	346.37	
Temperature	173(2) K	
Wavelength	0.71073 Å	
Crystal system	Triclinic	
Space group	P-1	
Unit cell dimensions	a = 8.7947(4) Å	α= 69.238(2)°.
	b = 10.0038(4) Å	β= 67.4880(10)°.
	c = 11.4536(6) Å	γ = 80.9040(10)°.
Volume	870.16(7) $Å^3$	
Z	2	
Density (calculated)	1.322 Mg/m^3	
Absorption coefficient	0.098 mm^{-1}	
F(000)	368	
Crystal size	0.47 x 0.24 x 0.13 mm^3	
Theta range for data collection	3.36 to 28.00°.	
Index ranges	-11<=h<=11, -13<=k<=13, -14<=l<=15	
Reflections collected	18265	
Independent reflections	4187 [R(int) = 0.0186]	
Completeness to theta = 28.00°	99.8 %	
Absorption correction	Semi-empirical from equivalents	

Max. and min. transmission	0.9873 and 0.9553
Refinement method	Full-matrix least-squares on F^2
Data / restraints / parameters	4187 / 0 / 231
Goodness-of-fit on F^2	1.028
Final R indices [I>2sigma(I)]	R1 = 0.0371, wR2 = 0.1067
R indices (all data)	R1 = 0.0424, wR2 = 0.1125
Largest diff. peak and hole	0.340 and -0.223 e.$Å^{-3}$

C1.5 X-ray crystallographic data for 5,6,7,9,10-pentamethoxy-3-methyl-1*H*-benzo[*g*]isochromen-1-one 229





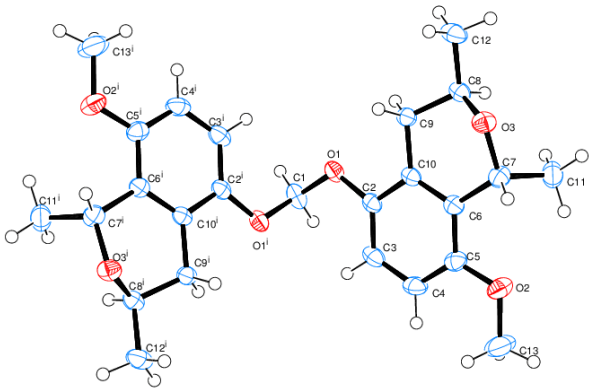
229

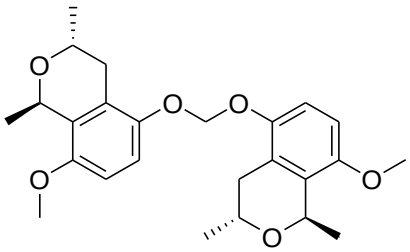
Table C1.5 Crystal data and structure refinement for 14a_js012_p.

Identification code	14a_js012_p	
Empirical formula	$C_{19}H_{20}O_7$	
Formula weight	360.35	
Temperature	173(2) K	
Wavelength	0.71073 Å	
Crystal system	Triclinic	
Space group	P-1	
Unit cell dimensions	a = 7.2651(3) Å	α= 79.4850(10)°.
	b = 9.5241(3) Å	β= 74.548(2)°.
	c = 13.0014(5) Å	γ = 79.6200(10)°.
Volume	844.28(5) $Å^3$	
Z	2	
Density (calculated)	1.417 Mg/m^3	
Absorption coefficient	0.109 mm^{-1}	
F(000)	380	
Crystal size	0.64 x 0.34 x 0.17 mm^3	
Theta range for data collection	3.28 to 28.00°.	
Index ranges	-9<=h<=9, -12<=k<=12, -17<=l<=17	
Reflections collected	22542	
Independent reflections	4075 [R(int) = 0.0227]	
Completeness to theta = 28.00°	99.8 %	
Absorption correction	Semi-empirical from equivalents	
Max. and min. transmission	0.9818 and 0.9337	

Refinement method	Full-matrix least-squares on F^2
Data / restraints / parameters	4075 / 0 / 241
Goodness-of-fit on F^2	1.034
Final R indices [I>2sigma(I)]	R1 = 0.0394, wR2 = 0.1087
R indices (all data)	R1 = 0.0476, wR2 = 0.1162
Largest diff. peak and hole	0.334 and -0.254 e.$Å^{-3}$

C1.6 X-ray crystallographic data for *bis*((±)-*trans*-3,4-dihydro-8-methoxy-1,3-dimethyl-1*H*-isochromen-5-yloxy)methane JS-D or *trans*-410





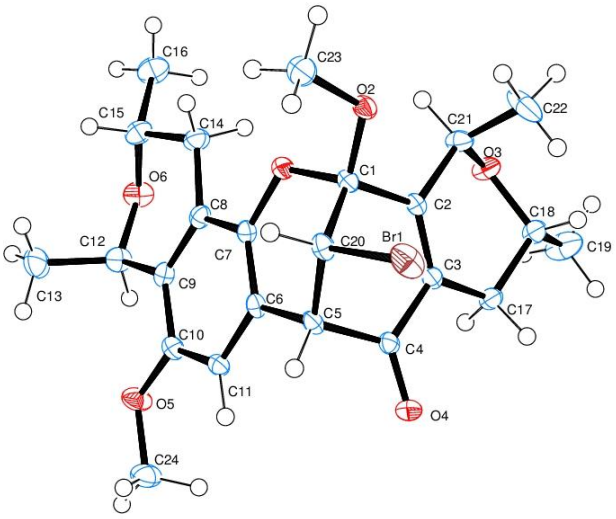
JS-D or ***trans*-410**

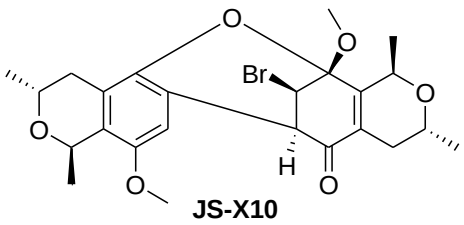
Table C1.6 Crystal data and structure refinement for 14a_js027_p.

Identification code	shelx	
Empirical formula	$C_{25}H_{32}O_6$	
Formula weight	428.50	
Temperature	173(2) K	
Wavelength	0.71073 Å	
Crystal system	Monoclinic	
Space group	P 2/c	
Unit cell dimensions	a = 8.8959(5) Å	α= 90°.
	b = 4.3947(2) Å	β= 94.002(2)°.
	c = 28.3873(15) Å	γ = 90°.
Volume	1107.09(10) $Å^3$	
Z	2	
Density (calculated)	1.285 Mg/m^3	
Absorption coefficient	0.091 mm^{-1}	
F(000)	460	
Crystal size	0.874 x 0.230 x 0.118 mm^3	
Theta range for data collection	3.554 to 27.997°.	
Index ranges	-11<=h<=11, -5<=k<=5, -37<=l<=37	
Reflections collected	24052	
Independent reflections	2666 [R(int) = 0.0333]	
Completeness to theta = 25.242°	99.8 %	
Refinement method	Full-matrix least-squares on F^2	
Data / restraints / parameters	2666 / 0 / 144	

Goodness-of-fit on F^2	1.063
Final R indices [I>2sigma(I)]	R1 = 0.0408, wR2 = 0.1068
R indices (all data)	R1 = 0.0513, wR2 = 0.1145
Extinction coefficient	n/a
Largest diff. peak and hole	0.330 and -0.167 e.$Å^{-3}$

C1.7 X-ray crystallographic data for (±)-*trans*-15-bromo-5,13-dimethoxy-2,4,10,12-tetramethyl-4,7,9,10,12,13-hexahydro-1*H*-7,13-methanopyrano[4',3':6,7]oxocino[2,3-*f*]isochromen-8(2*H*)-one JS-X10





JS-X10

Table C1.7 Crystal data and structure refinement for 15a_js029_a.

Identification code	15a_js029_a	
Empirical formula	$C_{24}H_{29}BrO_6$	
Formula weight	493.38	
Temperature	173(2) K	
Wavelength	0.71073 Å	
Crystal system	Triclinic	
Space group	P-1	
Unit cell dimensions	a = 11.9933(8) Å	α= 66.648(2)°.
	b = 13.4260(9) Å	β= 71.750(2)°.
	c = 16.6443(10) Å	γ = 67.439(2)°.
Volume	2230.9(2) $Å^3$	
Z	4	
Density (calculated)	1.469 Mg/m^3	
Absorption coefficient	1.881 mm^{-1}	
F(000)	1024	
Crystal size	0.49 x 0.47 x 0.07 mm^3	
Theta range for data collection	2.90 to 28.00°.	
Index ranges	-15<=h<=15, -17<=k<=17, -21<=l<=21	
Reflections collected	45699	
Independent reflections	10724 [R(int) = 0.0480]	

Completeness to theta = 28.00°	99.6 %
Absorption correction	Integration
Max. and min. transmission	0.8796 and 0.4593
Refinement method	Full-matrix least-squares on F^2
Data / restraints / parameters	10724 / 0 / 571
Goodness-of-fit on F^2	1.043
Final R indices [I>2sigma(I)]	R1 = 0.0422, wR2 = 0.1117
R indices (all data)	R1 = 0.0526, wR2 = 0.1181
Largest diff. peak and hole	2.305 and -0.634 e.$Å^{-3}$

Table C1.7.0 Atomic coordinates (x 10^4) and equivalent isotropic displacement parameters ($Å^2$x 10^3) for 15a_js029_a. U(eq) is defined as one third of the trace of the orthogonalized U^{ij} tensor.

	x	y	z	U(eq)
C(1)	4801(2)	5009(2)	3292(1)	16(1)
C(2)	4189(2)	4933(2)	2652(1)	14(1)
C(3)	3603(2)	4159(2)	2892(1)	15(1)
C(4)	3593(2)	3278(2)	3780(1)	15(1)
C(5)	4043(2)	3451(2)	4465(1)	16(1)
C(6)	2991(2)	4369(2)	4789(1)	15(1)
C(7)	2973(2)	5490(2)	4388(1)	16(1)
C(8)	1988(2)	6370(2)	4640(2)	17(1)
C(9)	1015(2)	6100(2)	5306(2)	17(1)
C(10)	1020(2)	4955(2)	5711(2)	18(1)
C(11)	1995(2)	4098(2)	5453(1)	17(1)
C(12)	-66(2)	7031(2)	5580(2)	22(1)
C(13)	-61(3)	7105(2)	6475(2)	34(1)
C(14)	1975(2)	7584(2)	4140(2)	22(1)
C(15)	964(2)	8416(2)	4579(2)	23(1)
C(16)	646(3)	9618(2)	3929(2)	30(1)
C(17)	2881(2)	4155(2)	2299(2)	18(1)
C(18)	3029(2)	5018(2)	1373(2)	20(1)
C(19)	1960(3)	5363(2)	932(2)	36(1)
C(20)	5160(2)	3883(2)	4032(2)	18(1)
C(21)	4166(2)	5839(2)	1747(2)	20(1)
C(22)	5340(3)	5553(3)	1072(2)	36(1)
C(23)	6390(2)	5672(2)	3289(2)	28(1)
C(24)	-80(3)	3650(2)	6756(2)	29(1)

O(1)	3907(2)	5834(1)	3718(1)	18(1)
O(2)	5746(2)	5482(1)	2795(1)	19(1)
O(3)	3085(2)	6035(1)	1439(1)	21(1)
O(4)	3181(2)	2496(1)	3974(1)	25(1)
O(5)	-2(2)	4783(2)	6347(1)	26(1)
O(6)	-150(2)	8101(1)	4890(1)	25(1)
Br(1)	6526(1)	2784(1)	3535(1)	28(1)
C(25)	8367(2)	9938(2)	1681(1)	16(1)
C(26)	7141(2)	10031(2)	2321(1)	14(1)
C(27)	6109(2)	10842(2)	2090(1)	16(1)
C(28)	6129(2)	11744(2)	1213(2)	18(1)
C(29)	7296(2)	11536(2)	518(1)	17(1)
C(30)	7258(2)	10636(2)	199(1)	15(1)
C(31)	7854(2)	9504(2)	584(1)	15(1)
C(32)	7824(2)	8644(2)	319(1)	16(1)
C(33)	7176(2)	8941(2)	-342(2)	17(1)
C(34)	6545(2)	10092(2)	-726(2)	18(1)
C(35)	6582(2)	10933(2)	-456(1)	17(1)
C(36)	7132(2)	8036(2)	-645(2)	19(1)
C(37)	7956(2)	8030(2)	-1550(2)	26(1)
C(38)	8445(2)	7422(2)	784(2)	21(1)
C(39)	8526(2)	6621(2)	314(2)	21(1)
C(40)	8724(2)	5400(2)	924(2)	27(1)
C(41)	4869(2)	10863(2)	2679(2)	20(1)
C(42)	4936(2)	9984(2)	3599(2)	19(1)
C(43)	3746(2)	9686(2)	4035(2)	34(1)
C(44)	8428(2)	11060(2)	942(2)	18(1)
C(45)	7089(2)	9093(2)	3208(2)	19(1)
C(46)	7502(3)	9289(3)	3897(2)	30(1)
C(47)	10532(2)	9227(2)	1680(2)	27(1)
C(48)	5240(3)	11429(2)	-1766(2)	28(1)
O(7)	8528(2)	9132(1)	1244(1)	18(1)
O(8)	9293(1)	9436(1)	2177(1)	19(1)
O(9)	5885(2)	8952(1)	3521(1)	20(1)
O(10)	5236(2)	12563(2)	1038(1)	28(1)
O(11)	5910(2)	10289(2)	-1359(1)	26(1)
O(12)	7401(2)	6944(1)	16(1)	22(1)
Br(2)	8501(1)	12133(1)	1433(1)	27(1)

Table C1.7.1 Bond lengths [Å] and angles [°] for 15a_js029_a.

C(1)-O(2)	1.386(3)
C(1)-O(1)	1.454(3)
C(1)-C(2)	1.521(3)
C(1)-C(20)	1.532(3)
C(2)-C(3)	1.337(3)
C(2)-C(21)	1.516(3)
C(3)-C(4)	1.484(3)
C(3)-C(17)	1.505(3)
C(4)-O(4)	1.217(3)
C(4)-C(5)	1.528(3)
C(5)-C(6)	1.520(3)
C(5)-C(20)	1.520(3)
C(5)-H(5)	1.0000
C(6)-C(7)	1.377(3)
C(6)-C(11)	1.403(3)
C(7)-O(1)	1.385(3)
C(7)-C(8)	1.406(3)
C(8)-C(9)	1.386(3)
C(8)-C(14)	1.505(3)
C(9)-C(10)	1.410(3)
C(9)-C(12)	1.514(3)
C(10)-O(5)	1.373(3)
C(10)-C(11)	1.387(3)
C(11)-H(11)	0.9500
C(12)-O(6)	1.430(3)
C(12)-C(13)	1.534(4)
C(12)-H(12)	1.0000
C(13)-H(13A)	0.9800
C(13)-H(13B)	0.9800
C(13)-H(13C)	0.9800
C(14)-C(15)	1.518(3)
C(14)-H(14A)	0.9900
C(14)-H(14B)	0.9900
C(15)-O(6)	1.434(3)
C(15)-C(16)	1.525(3)
C(15)-H(15)	1.0000
C(16)-H(16A)	0.9800

C(16)-H(16B)	0.9800
C(16)-H(16C)	0.9800
C(17)-C(18)	1.522(3)
C(17)-H(17A)	0.9900
C(17)-H(17B)	0.9900
C(18)-O(3)	1.440(3)
C(18)-C(19)	1.504(3)
C(18)-H(18)	1.0000
C(19)-H(19A)	0.9800
C(19)-H(19B)	0.9800
C(19)-H(19C)	0.9800
C(20)-Br(1)	1.952(2)
C(20)-H(20)	1.0000
C(21)-O(3)	1.436(3)
C(21)-C(22)	1.526(4)
C(21)-H(21)	1.0000
C(22)-H(22A)	0.9800
C(22)-H(22B)	0.9800
C(22)-H(22C)	0.9800
C(23)-O(2)	1.434(3)
C(23)-H(23A)	0.9800
C(23)-H(23B)	0.9800
C(23)-H(23C)	0.9800
C(24)-O(5)	1.427(3)
C(24)-H(24A)	0.9800
C(24)-H(24B)	0.9800
C(24)-H(24C)	0.9800
C(25)-O(8)	1.389(3)
C(25)-O(7)	1.453(3)
C(25)-C(26)	1.515(3)
C(25)-C(44)	1.532(3)
C(26)-C(27)	1.341(3)
C(26)-C(45)	1.517(3)
C(27)-C(28)	1.482(3)
C(27)-C(41)	1.500(3)
C(28)-O(10)	1.217(3)
C(28)-C(29)	1.523(3)
C(29)-C(30)	1.519(3)
C(29)-C(44)	1.524(3)

C(29)-H(29)	1.0000
C(30)-C(31)	1.383(3)
C(30)-C(35)	1.403(3)
C(31)-O(7)	1.387(2)
C(31)-C(32)	1.405(3)
C(32)-C(33)	1.387(3)
C(32)-C(38)	1.505(3)
C(33)-C(34)	1.411(3)
C(33)-C(36)	1.512(3)
C(34)-O(11)	1.374(3)
C(34)-C(35)	1.390(3)
C(35)-H(35)	0.9500
C(36)-O(12)	1.430(3)
C(36)-C(37)	1.523(3)
C(36)-H(36)	1.0000
C(37)-H(37A)	0.9800
C(37)-H(37B)	0.9800
C(37)-H(37C)	0.9800
C(38)-C(39)	1.522(3)
C(38)-H(38A)	0.9900
C(38)-H(38B)	0.9900
C(39)-O(12)	1.433(3)
C(39)-C(40)	1.520(3)
C(39)-H(39)	1.0000
C(40)-H(40A)	0.9800
C(40)-H(40B)	0.9800
C(40)-H(40C)	0.9800
C(41)-C(42)	1.521(3)
C(41)-H(41A)	0.9900
C(41)-H(41B)	0.9900
C(42)-O(9)	1.440(3)
C(42)-C(43)	1.510(3)
C(42)-H(42)	1.0000
C(43)-H(43A)	0.9800
C(43)-H(43B)	0.9800
C(43)-H(43C)	0.9800
C(44)-Br(2)	1.956(2)
C(44)-H(44)	1.0000
C(45)-O(9)	1.432(3)

C(45)-C(46)	1.524(3)
C(45)-H(45)	1.0000
C(46)-H(46A)	0.9800
C(46)-H(46B)	0.9800
C(46)-H(46C)	0.9800
C(47)-O(8)	1.436(3)
C(47)-H(47A)	0.9800
C(47)-H(47B)	0.9800
C(47)-H(47C)	0.9800
C(48)-O(11)	1.422(3)
C(48)-H(48A)	0.9800
C(48)-H(48B)	0.9800
C(48)-H(48C)	0.9800

O(2)-C(1)-O(1)	105.36(17)
O(2)-C(1)-C(2)	108.27(17)
O(1)-C(1)-C(2)	107.21(17)
O(2)-C(1)-C(20)	115.41(18)
O(1)-C(1)-C(20)	107.21(17)
C(2)-C(1)-C(20)	112.81(18)
C(3)-C(2)-C(21)	120.26(19)
C(3)-C(2)-C(1)	122.13(19)
C(21)-C(2)-C(1)	117.39(18)
C(2)-C(3)-C(4)	121.2(2)
C(2)-C(3)-C(17)	122.51(19)
C(4)-C(3)-C(17)	116.23(19)
O(4)-C(4)-C(3)	122.0(2)
O(4)-C(4)-C(5)	121.5(2)
C(3)-C(4)-C(5)	116.32(18)
C(6)-C(5)-C(20)	108.39(18)
C(6)-C(5)-C(4)	105.22(17)
C(20)-C(5)-C(4)	110.87(18)
C(6)-C(5)-H(5)	110.7
C(20)-C(5)-H(5)	110.7
C(4)-C(5)-H(5)	110.7
C(7)-C(6)-C(11)	119.4(2)
C(7)-C(6)-C(5)	119.78(19)
C(11)-C(6)-C(5)	120.69(19)
C(6)-C(7)-O(1)	123.1(2)

C(6)-C(7)-C(8)	121.6(2)
O(1)-C(7)-C(8)	115.28(19)
C(9)-C(8)-C(7)	119.0(2)
C(9)-C(8)-C(14)	121.5(2)
C(7)-C(8)-C(14)	119.4(2)
C(8)-C(9)-C(10)	119.7(2)
C(8)-C(9)-C(12)	120.2(2)
C(10)-C(9)-C(12)	120.1(2)
O(5)-C(10)-C(11)	124.4(2)
O(5)-C(10)-C(9)	115.1(2)
C(11)-C(10)-C(9)	120.5(2)
C(10)-C(11)-C(6)	119.7(2)
C(10)-C(11)-H(11)	120.1
C(6)-C(11)-H(11)	120.1
O(6)-C(12)-C(9)	111.19(19)
O(6)-C(12)-C(13)	111.8(2)
C(9)-C(12)-C(13)	112.8(2)
O(6)-C(12)-H(12)	106.9
C(9)-C(12)-H(12)	106.9
C(13)-C(12)-H(12)	106.9
C(12)-C(13)-H(13A)	109.5
C(12)-C(13)-H(13B)	109.5
H(13A)-C(13)-H(13B)	109.5
C(12)-C(13)-H(13C)	109.5
H(13A)-C(13)-H(13C)	109.5
H(13B)-C(13)-H(13C)	109.5
C(8)-C(14)-C(15)	112.7(2)
C(8)-C(14)-H(14A)	109.0
C(15)-C(14)-H(14A)	109.0
C(8)-C(14)-H(14B)	109.0
C(15)-C(14)-H(14B)	109.0
H(14A)-C(14)-H(14B)	107.8
O(6)-C(15)-C(14)	110.33(19)
O(6)-C(15)-C(16)	105.8(2)
C(14)-C(15)-C(16)	112.1(2)
O(6)-C(15)-H(15)	109.5
C(14)-C(15)-H(15)	109.5
C(16)-C(15)-H(15)	109.5
C(15)-C(16)-H(16A)	109.5

C(15)-C(16)-H(16B)	109.5
H(16A)-C(16)-H(16B)	109.5
C(15)-C(16)-H(16C)	109.5
H(16A)-C(16)-H(16C)	109.5
H(16B)-C(16)-H(16C)	109.5
C(3)-C(17)-C(18)	112.81(18)
C(3)-C(17)-H(17A)	109.0
C(18)-C(17)-H(17A)	109.0
C(3)-C(17)-H(17B)	109.0
C(18)-C(17)-H(17B)	109.0
H(17A)-C(17)-H(17B)	107.8
O(3)-C(18)-C(19)	106.94(19)
O(3)-C(18)-C(17)	109.66(18)
C(19)-C(18)-C(17)	112.1(2)
O(3)-C(18)-H(18)	109.4
C(19)-C(18)-H(18)	109.4
C(17)-C(18)-H(18)	109.4
C(18)-C(19)-H(19A)	109.5
C(18)-C(19)-H(19B)	109.5
H(19A)-C(19)-H(19B)	109.5
C(18)-C(19)-H(19C)	109.5
H(19A)-C(19)-H(19C)	109.5
H(19B)-C(19)-H(19C)	109.5
C(5)-C(20)-C(1)	108.35(18)
C(5)-C(20)-Br(1)	110.87(15)
C(1)-C(20)-Br(1)	109.92(15)
C(5)-C(20)-H(20)	109.2
C(1)-C(20)-H(20)	109.2
Br(1)-C(20)-H(20)	109.2
O(3)-C(21)-C(2)	109.68(18)
O(3)-C(21)-C(22)	112.1(2)
C(2)-C(21)-C(22)	112.3(2)
O(3)-C(21)-H(21)	107.5
C(2)-C(21)-H(21)	107.5
C(22)-C(21)-H(21)	107.5
C(21)-C(22)-H(22A)	109.5
C(21)-C(22)-H(22B)	109.5
H(22A)-C(22)-H(22B)	109.5
C(21)-C(22)-H(22C)	109.5

H(22A)-C(22)-H(22C)	109.5
H(22B)-C(22)-H(22C)	109.5
O(2)-C(23)-H(23A)	109.5
O(2)-C(23)-H(23B)	109.5
H(23A)-C(23)-H(23B)	109.5
O(2)-C(23)-H(23C)	109.5
H(23A)-C(23)-H(23C)	109.5
H(23B)-C(23)-H(23C)	109.5
O(5)-C(24)-H(24A)	109.5
O(5)-C(24)-H(24B)	109.5
H(24A)-C(24)-H(24B)	109.5
O(5)-C(24)-H(24C)	109.5
H(24A)-C(24)-H(24C)	109.5
H(24B)-C(24)-H(24C)	109.5
C(7)-O(1)-C(1)	117.55(16)
C(1)-O(2)-C(23)	116.05(18)
C(21)-O(3)-C(18)	112.13(17)
C(10)-O(5)-C(24)	117.91(19)
C(12)-O(6)-C(15)	114.07(18)
O(8)-C(25)-O(7)	105.22(17)
O(8)-C(25)-C(26)	108.20(17)
O(7)-C(25)-C(26)	107.62(17)
O(8)-C(25)-C(44)	115.50(18)
O(7)-C(25)-C(44)	106.66(17)
C(26)-C(25)-C(44)	113.07(18)
C(27)-C(26)-C(25)	122.04(19)
C(27)-C(26)-C(45)	120.3(2)
C(25)-C(26)-C(45)	117.38(18)
C(26)-C(27)-C(28)	121.3(2)
C(26)-C(27)-C(41)	122.41(19)
C(28)-C(27)-C(41)	116.22(19)
O(10)-C(28)-C(27)	122.0(2)
O(10)-C(28)-C(29)	121.8(2)
C(27)-C(28)-C(29)	116.00(19)
C(30)-C(29)-C(28)	106.03(18)
C(30)-C(29)-C(44)	108.13(18)
C(28)-C(29)-C(44)	110.35(18)
C(30)-C(29)-H(29)	110.7
C(28)-C(29)-H(29)	110.7

C(44)-C(29)-H(29)	110.7
C(31)-C(30)-C(35)	119.3(2)
C(31)-C(30)-C(29)	119.83(19)
C(35)-C(30)-C(29)	120.81(19)
C(30)-C(31)-O(7)	123.23(19)
C(30)-C(31)-C(32)	121.62(19)
O(7)-C(31)-C(32)	115.14(18)
C(33)-C(32)-C(31)	119.0(2)
C(33)-C(32)-C(38)	121.4(2)
C(31)-C(32)-C(38)	119.51(19)
C(32)-C(33)-C(34)	119.8(2)
C(32)-C(33)-C(36)	120.3(2)
C(34)-C(33)-C(36)	119.91(19)
O(11)-C(34)-C(35)	124.5(2)
O(11)-C(34)-C(33)	115.01(19)
C(35)-C(34)-C(33)	120.5(2)
C(34)-C(35)-C(30)	119.7(2)
C(34)-C(35)-H(35)	120.1
C(30)-C(35)-H(35)	120.1
O(12)-C(36)-C(33)	111.26(18)
O(12)-C(36)-C(37)	112.18(19)
C(33)-C(36)-C(37)	111.77(19)
O(12)-C(36)-H(36)	107.1
C(33)-C(36)-H(36)	107.1
C(37)-C(36)-H(36)	107.1
C(36)-C(37)-H(37A)	109.5
C(36)-C(37)-H(37B)	109.5
H(37A)-C(37)-H(37B)	109.5
C(36)-C(37)-H(37C)	109.5
H(37A)-C(37)-H(37C)	109.5
H(37B)-C(37)-H(37C)	109.5
C(32)-C(38)-C(39)	112.67(19)
C(32)-C(38)-H(38A)	109.1
C(39)-C(38)-H(38A)	109.1
C(32)-C(38)-H(38B)	109.1
C(39)-C(38)-H(38B)	109.1
H(38A)-C(38)-H(38B)	107.8
O(12)-C(39)-C(40)	106.44(19)
O(12)-C(39)-C(38)	110.32(18)

C(40)-C(39)-C(38)	112.3(2)
O(12)-C(39)-H(39)	109.2
C(40)-C(39)-H(39)	109.2
C(38)-C(39)-H(39)	109.2
C(39)-C(40)-H(40A)	109.5
C(39)-C(40)-H(40B)	109.5
H(40A)-C(40)-H(40B)	109.5
C(39)-C(40)-H(40C)	109.5
H(40A)-C(40)-H(40C)	109.5
H(40B)-C(40)-H(40C)	109.5
C(27)-C(41)-C(42)	113.03(18)
C(27)-C(41)-H(41A)	109.0
C(42)-C(41)-H(41A)	109.0
C(27)-C(41)-H(41B)	109.0
C(42)-C(41)-H(41B)	109.0
H(41A)-C(41)-H(41B)	107.8
O(9)-C(42)-C(43)	107.2(2)
O(9)-C(42)-C(41)	109.54(18)
C(43)-C(42)-C(41)	111.8(2)
O(9)-C(42)-H(42)	109.4
C(43)-C(42)-H(42)	109.4
C(41)-C(42)-H(42)	109.4
C(42)-C(43)-H(43A)	109.5
C(42)-C(43)-H(43B)	109.5
H(43A)-C(43)-H(43B)	109.5
C(42)-C(43)-H(43C)	109.5
H(43A)-C(43)-H(43C)	109.5
H(43B)-C(43)-H(43C)	109.5
C(29)-C(44)-C(25)	108.48(18)
C(29)-C(44)-Br(2)	110.96(15)
C(25)-C(44)-Br(2)	110.13(14)
C(29)-C(44)-H(44)	109.1
C(25)-C(44)-H(44)	109.1
Br(2)-C(44)-H(44)	109.1
O(9)-C(45)-C(26)	110.24(17)
O(9)-C(45)-C(46)	112.06(19)
C(26)-C(45)-C(46)	112.2(2)
O(9)-C(45)-H(45)	107.4
C(26)-C(45)-H(45)	107.4

C(46)-C(45)-H(45)	107.4
C(45)-C(46)-H(46A)	109.5
C(45)-C(46)-H(46B)	109.5
H(46A)-C(46)-H(46B)	109.5
C(45)-C(46)-H(46C)	109.5
H(46A)-C(46)-H(46C)	109.5
H(46B)-C(46)-H(46C)	109.5
O(8)-C(47)-H(47A)	109.5
O(8)-C(47)-H(47B)	109.5
H(47A)-C(47)-H(47B)	109.5
O(8)-C(47)-H(47C)	109.5
H(47A)-C(47)-H(47C)	109.5
H(47B)-C(47)-H(47C)	109.5
O(11)-C(48)-H(48A)	109.5
O(11)-C(48)-H(48B)	109.5
H(48A)-C(48)-H(48B)	109.5
O(11)-C(48)-H(48C)	109.5
H(48A)-C(48)-H(48C)	109.5
H(48B)-C(48)-H(48C)	109.5
C(31)-O(7)-C(25)	117.15(16)
C(25)-O(8)-C(47)	116.11(17)
C(45)-O(9)-C(42)	112.70(17)
C(34)-O(11)-C(48)	117.97(18)
C(36)-O(12)-C(39)	114.22(17)

Symmetry transformations used to generate equivalent atoms:

Table C1.7.2 Anisotropic displacement parameters ($Å^2$x 10^3)for 15a_js029_a. The anisotropic displacement factor exponent takes the form: $-2\pi^2[h^2a^{*2}U^{11} + ... + 2 h k a^* b^* U^{12}]$

	U^{11}	U^{22}	U^{33}	U^{23}	U^{13}	U^{12}
C(1)	16(1)	18(1)	13(1)	-4(1)	-1(1)	-6(1)
C(2)	15(1)	16(1)	11(1)	-3(1)	-2(1)	-4(1)
C(3)	16(1)	14(1)	13(1)	-4(1)	-2(1)	-3(1)
C(4)	16(1)	13(1)	14(1)	-5(1)	1(1)	-3(1)
C(5)	17(1)	14(1)	11(1)	-2(1)	-1(1)	-3(1)
C(6)	15(1)	16(1)	12(1)	-5(1)	-3(1)	-2(1)
C(7)	18(1)	18(1)	13(1)	-5(1)	-4(1)	-6(1)
C(8)	19(1)	16(1)	17(1)	-6(1)	-7(1)	-3(1)
C(9)	18(1)	17(1)	18(1)	-8(1)	-6(1)	-2(1)
C(10)	17(1)	21(1)	15(1)	-6(1)	-1(1)	-6(1)
C(11)	20(1)	16(1)	13(1)	-2(1)	-2(1)	-6(1)
C(12)	18(1)	20(1)	26(1)	-8(1)	-2(1)	-3(1)
C(13)	42(2)	30(1)	25(1)	-14(1)	5(1)	-9(1)
C(14)	24(1)	15(1)	24(1)	-5(1)	-4(1)	-7(1)
C(15)	22(1)	18(1)	29(1)	-8(1)	-7(1)	-4(1)
C(16)	32(1)	18(1)	38(2)	-7(1)	-10(1)	-3(1)
C(17)	21(1)	15(1)	19(1)	-5(1)	-6(1)	-6(1)
C(18)	24(1)	17(1)	19(1)	-3(1)	-9(1)	-6(1)
C(19)	48(2)	29(1)	41(2)	2(1)	-32(1)	-16(1)
C(20)	16(1)	20(1)	15(1)	-6(1)	-2(1)	-2(1)
C(21)	26(1)	19(1)	18(1)	2(1)	-11(1)	-12(1)
C(22)	29(1)	62(2)	15(1)	0(1)	-2(1)	-27(1)
C(23)	29(1)	41(2)	22(1)	-7(1)	-8(1)	-20(1)
C(24)	28(1)	25(1)	29(1)	-8(1)	7(1)	-13(1)
O(1)	20(1)	17(1)	16(1)	-7(1)	1(1)	-7(1)
O(2)	18(1)	26(1)	14(1)	-5(1)	-2(1)	-12(1)
O(3)	26(1)	15(1)	24(1)	0(1)	-15(1)	-6(1)
O(4)	37(1)	17(1)	20(1)	-4(1)	0(1)	-14(1)
O(5)	21(1)	22(1)	26(1)	-7(1)	7(1)	-8(1)
O(6)	19(1)	20(1)	32(1)	-6(1)	-7(1)	-2(1)
Br(1)	19(1)	26(1)	26(1)	-6(1)	1(1)	2(1)

C(25)	18(1)	18(1)	12(1)	-5(1)	-4(1)	-6(1)
C(26)	19(1)	14(1)	11(1)	-4(1)	-3(1)	-6(1)
C(27)	21(1)	14(1)	12(1)	-4(1)	-3(1)	-4(1)
C(28)	24(1)	14(1)	14(1)	-4(1)	-6(1)	-3(1)
C(29)	26(1)	15(1)	11(1)	-2(1)	-4(1)	-8(1)
C(30)	19(1)	15(1)	11(1)	-4(1)	-1(1)	-6(1)
C(31)	16(1)	18(1)	12(1)	-4(1)	-2(1)	-5(1)
C(32)	15(1)	15(1)	16(1)	-5(1)	-3(1)	-4(1)
C(33)	17(1)	19(1)	16(1)	-7(1)	-1(1)	-7(1)
C(34)	21(1)	21(1)	13(1)	-4(1)	-6(1)	-7(1)
C(35)	21(1)	16(1)	14(1)	-4(1)	-4(1)	-4(1)
C(36)	19(1)	19(1)	21(1)	-7(1)	-4(1)	-9(1)
C(37)	32(1)	25(1)	24(1)	-13(1)	-6(1)	-7(1)
C(38)	23(1)	16(1)	23(1)	-6(1)	-9(1)	-2(1)
C(39)	18(1)	18(1)	27(1)	-9(1)	-5(1)	-3(1)
C(40)	30(1)	17(1)	35(1)	-7(1)	-10(1)	-6(1)
C(41)	18(1)	20(1)	17(1)	-4(1)	-3(1)	-1(1)
C(42)	18(1)	19(1)	18(1)	-6(1)	-2(1)	-4(1)
C(43)	22(1)	33(1)	35(2)	-6(1)	4(1)	-10(1)
C(44)	23(1)	19(1)	14(1)	-4(1)	-3(1)	-10(1)
C(45)	17(1)	18(1)	16(1)	1(1)	-3(1)	-4(1)
C(46)	29(1)	44(2)	14(1)	-1(1)	-7(1)	-16(1)
C(47)	16(1)	41(2)	22(1)	-9(1)	-2(1)	-8(1)
C(48)	33(1)	26(1)	26(1)	-6(1)	-17(1)	-4(1)
O(7)	22(1)	16(1)	16(1)	-6(1)	-8(1)	-1(1)
O(8)	16(1)	25(1)	14(1)	-5(1)	-4(1)	-5(1)
O(9)	17(1)	16(1)	22(1)	-2(1)	-1(1)	-5(1)
O(10)	30(1)	20(1)	22(1)	-4(1)	-6(1)	4(1)
O(11)	35(1)	21(1)	26(1)	-5(1)	-19(1)	-4(1)
O(12)	22(1)	19(1)	28(1)	-5(1)	-7(1)	-9(1)
Br(2)	40(1)	25(1)	23(1)	-6(1)	-9(1)	-17(1)

Table C1.7.3 Hydrogen coordinates (x 10^4) and isotropic displacement parameters ($Å^2$x 10^3) for 15a_js029_a.

	x	y	z	U(eq)
H(5)	4232	2731	4971	19
H(11)	1988	3329	5724	20
H(12)	-826	6833	5660	27
H(13A)	689	7270	6431	50
H(13B)	-85	6380	6942	50
H(13C)	-783	7713	6623	50
H(14A)	1863	7779	3525	26
H(14B)	2780	7663	4100	26
H(15)	1225	8418	5093	27
H(16A)	374	9618	3431	45
H(16B)	1374	9885	3700	45
H(16C)	-15	10124	4236	45
H(17A)	2000	4324	2582	21
H(17B)	3155	3387	2241	21
H(18)	3806	4688	993	23
H(19A)	1205	5730	1284	54
H(19B)	1873	4688	892	54
H(19C)	2105	5895	331	54
H(20)	5417	4015	4489	22
H(21)	4104	6560	1827	24
H(22A)	5529	4771	1081	54
H(22B)	6022	5627	1227	54
H(22C)	5222	6077	475	54
H(23A)	5802	6141	3656	42
H(23B)	6988	6065	2875	42
H(23C)	6821	4942	3674	42
H(24A)	18	3328	6294	44
H(24B)	-883	3657	7149	44
H(24C)	572	3186	7105	44
H(29)	7325	12251	11	20
H(35)	6151	11706	-714	21
H(36)	6268	8232	-717	22

H(37A)	8806	7893	-1517	38
H(37B)	7678	8766	-1997	38
H(37C)	7914	7426	-1720	38
H(38A)	7983	7196	1401	25
H(38B)	9285	7346	817	25
H(39)	9218	6657	-212	25
H(40A)	8045	5361	1439	41
H(40B)	9502	5131	1130	41
H(40C)	8755	4919	598	41
H(41A)	4363	10724	2389	24
H(41B)	4454	11629	2746	24
H(42)	5130	10284	3985	23
H(43A)	3573	9363	3669	51
H(43B)	3074	10374	4091	51
H(43C)	3820	9129	4628	51
H(44)	9182	10911	479	22
H(45)	7674	8370	3104	23
H(46A)	7081	10070	3908	45
H(46B)	8393	9164	3738	45
H(46C)	7298	8757	4486	45
H(47A)	10631	8813	1280	41
H(47B)	11106	8773	2093	41
H(47C)	10703	9953	1329	41
H(48A)	4662	11753	-1305	41
H(48B)	4784	11441	-2168	41
H(48C)	5813	11878	-2106	41

Table C1.7.4 Torsion angles [°] for 15a_js029_a.

O(2)-C(1)-C(2)-C(3)	153.6(2)
O(1)-C(1)-C(2)-C(3)	-93.1(2)
C(20)-C(1)-C(2)-C(3)	24.7(3)
O(2)-C(1)-C(2)-C(21)	-31.8(3)
O(1)-C(1)-C(2)-C(21)	81.5(2)
C(20)-C(1)-C(2)-C(21)	-160.73(19)
C(21)-C(2)-C(3)-C(4)	-178.8(2)
C(1)-C(2)-C(3)-C(4)	-4.3(3)
C(21)-C(2)-C(3)-C(17)	-1.2(3)
C(1)-C(2)-C(3)-C(17)	173.3(2)

C(2)-C(3)-C(4)-O(4)	-171.9(2)
C(17)-C(3)-C(4)-O(4)	10.3(3)
C(2)-C(3)-C(4)-C(5)	12.4(3)
C(17)-C(3)-C(4)-C(5)	-165.33(18)
O(4)-C(4)-C(5)-C(6)	-99.3(2)
C(3)-C(4)-C(5)-C(6)	76.4(2)
O(4)-C(4)-C(5)-C(20)	143.8(2)
C(3)-C(4)-C(5)-C(20)	-40.6(2)
C(20)-C(5)-C(6)-C(7)	25.0(3)
C(4)-C(5)-C(6)-C(7)	-93.6(2)
C(20)-C(5)-C(6)-C(11)	-159.16(19)
C(4)-C(5)-C(6)-C(11)	82.2(2)
C(11)-C(6)-C(7)-O(1)	-178.92(19)
C(5)-C(6)-C(7)-O(1)	-3.0(3)
C(11)-C(6)-C(7)-C(8)	1.1(3)
C(5)-C(6)-C(7)-C(8)	177.03(19)
C(6)-C(7)-C(8)-C(9)	-0.1(3)
O(1)-C(7)-C(8)-C(9)	-179.99(18)
C(6)-C(7)-C(8)-C(14)	-176.0(2)
O(1)-C(7)-C(8)-C(14)	4.0(3)
C(7)-C(8)-C(9)-C(10)	-0.7(3)
C(14)-C(8)-C(9)-C(10)	175.2(2)
C(7)-C(8)-C(9)-C(12)	-179.0(2)
C(14)-C(8)-C(9)-C(12)	-3.2(3)
C(8)-C(9)-C(10)-O(5)	-178.5(2)
C(12)-C(9)-C(10)-O(5)	-0.1(3)
C(8)-C(9)-C(10)-C(11)	0.4(3)
C(12)-C(9)-C(10)-C(11)	178.7(2)
O(5)-C(10)-C(11)-C(6)	179.4(2)
C(9)-C(10)-C(11)-C(6)	0.7(3)
C(7)-C(6)-C(11)-C(10)	-1.5(3)
C(5)-C(6)-C(11)-C(10)	-177.3(2)
C(8)-C(9)-C(12)-O(6)	21.7(3)
C(10)-C(9)-C(12)-O(6)	-156.7(2)
C(8)-C(9)-C(12)-C(13)	-104.9(3)
C(10)-C(9)-C(12)-C(13)	76.8(3)
C(9)-C(8)-C(14)-C(15)	13.0(3)
C(7)-C(8)-C(14)-C(15)	-171.2(2)
C(8)-C(14)-C(15)-O(6)	-41.3(3)

C(8)-C(14)-C(15)-C(16)	-159.0(2)
C(2)-C(3)-C(17)-C(18)	7.2(3)
C(4)-C(3)-C(17)-C(18)	-175.08(19)
C(3)-C(17)-C(18)-O(3)	-37.4(3)
C(3)-C(17)-C(18)-C(19)	-156.0(2)
C(6)-C(5)-C(20)-C(1)	-55.9(2)
C(4)-C(5)-C(20)-C(1)	59.1(2)
C(6)-C(5)-C(20)-Br(1)	-176.62(14)
C(4)-C(5)-C(20)-Br(1)	-61.6(2)
O(2)-C(1)-C(20)-C(5)	-176.35(18)
O(1)-C(1)-C(20)-C(5)	66.6(2)
C(2)-C(1)-C(20)-C(5)	-51.2(2)
O(2)-C(1)-C(20)-Br(1)	-55.1(2)
O(1)-C(1)-C(20)-Br(1)	-172.06(13)
C(2)-C(1)-C(20)-Br(1)	70.1(2)
C(3)-C(2)-C(21)-O(3)	25.5(3)
C(1)-C(2)-C(21)-O(3)	-149.21(19)
C(3)-C(2)-C(21)-C(22)	-99.9(3)
C(1)-C(2)-C(21)-C(22)	85.4(3)
C(6)-C(7)-O(1)-C(1)	13.8(3)
C(8)-C(7)-O(1)-C(1)	-166.30(18)
O(2)-C(1)-O(1)-C(7)	-168.13(16)
C(2)-C(1)-O(1)-C(7)	76.7(2)
C(20)-C(1)-O(1)-C(7)	-44.7(2)
O(1)-C(1)-O(2)-C(23)	62.5(2)
C(2)-C(1)-O(2)-C(23)	176.96(19)
C(20)-C(1)-O(2)-C(23)	-55.5(3)
C(2)-C(21)-O(3)-C(18)	-58.5(2)
C(22)-C(21)-O(3)-C(18)	67.0(3)
C(19)-C(18)-O(3)-C(21)	-172.6(2)
C(17)-C(18)-O(3)-C(21)	65.7(2)
C(11)-C(10)-O(5)-C(24)	-1.5(3)
C(9)-C(10)-O(5)-C(24)	177.3(2)
C(9)-C(12)-O(6)-C(15)	-53.2(3)
C(13)-C(12)-O(6)-C(15)	73.9(3)
C(14)-C(15)-O(6)-C(12)	64.4(3)
C(16)-C(15)-O(6)-C(12)	-174.1(2)
O(8)-C(25)-C(26)-C(27)	152.4(2)
O(7)-C(25)-C(26)-C(27)	-94.4(2)

C(44)-C(25)-C(26)-C(27)	23.2(3)
O(8)-C(25)-C(26)-C(45)	-34.1(2)
O(7)-C(25)-C(26)-C(45)	79.2(2)
C(44)-C(25)-C(26)-C(45)	-163.32(18)
C(25)-C(26)-C(27)-C(28)	-4.4(3)
C(45)-C(26)-C(27)-C(28)	-177.74(19)
C(25)-C(26)-C(27)-C(41)	172.9(2)
C(45)-C(26)-C(27)-C(41)	-0.4(3)
C(26)-C(27)-C(28)-O(10)	-170.4(2)
C(41)-C(27)-C(28)-O(10)	12.1(3)
C(26)-C(27)-C(28)-C(29)	14.5(3)
C(41)-C(27)-C(28)-C(29)	-162.98(19)
O(10)-C(28)-C(29)-C(30)	-101.0(2)
C(27)-C(28)-C(29)-C(30)	74.1(2)
O(10)-C(28)-C(29)-C(44)	142.1(2)
C(27)-C(28)-C(29)-C(44)	-42.8(3)
C(28)-C(29)-C(30)-C(31)	-94.9(2)
C(44)-C(29)-C(30)-C(31)	23.5(3)
C(28)-C(29)-C(30)-C(35)	82.4(2)
C(44)-C(29)-C(30)-C(35)	-159.3(2)
C(35)-C(30)-C(31)-O(7)	-179.1(2)
C(29)-C(30)-C(31)-O(7)	-1.8(3)
C(35)-C(30)-C(31)-C(32)	1.6(3)
C(29)-C(30)-C(31)-C(32)	178.9(2)
C(30)-C(31)-C(32)-C(33)	-0.2(3)
O(7)-C(31)-C(32)-C(33)	-179.58(19)
C(30)-C(31)-C(32)-C(38)	-177.6(2)
O(7)-C(31)-C(32)-C(38)	3.0(3)
C(31)-C(32)-C(33)-C(34)	-1.0(3)
C(38)-C(32)-C(33)-C(34)	176.3(2)
C(31)-C(32)-C(33)-C(36)	179.7(2)
C(38)-C(32)-C(33)-C(36)	-3.0(3)
C(32)-C(33)-C(34)-O(11)	-178.5(2)
C(36)-C(33)-C(34)-O(11)	0.8(3)
C(32)-C(33)-C(34)-C(35)	0.9(3)
C(36)-C(33)-C(34)-C(35)	-179.8(2)
O(11)-C(34)-C(35)-C(30)	179.8(2)
C(33)-C(34)-C(35)-C(30)	0.4(3)
C(31)-C(30)-C(35)-C(34)	-1.7(3)

C(29)-C(30)-C(35)-C(34)	-179.0(2)
C(32)-C(33)-C(36)-O(12)	21.3(3)
C(34)-C(33)-C(36)-O(12)	-158.0(2)
C(32)-C(33)-C(36)-C(37)	-105.0(2)
C(34)-C(33)-C(36)-C(37)	75.7(3)
C(33)-C(32)-C(38)-C(39)	13.0(3)
C(31)-C(32)-C(38)-C(39)	-169.7(2)
C(32)-C(38)-C(39)-O(12)	-41.3(3)
C(32)-C(38)-C(39)-C(40)	-159.9(2)
C(26)-C(27)-C(41)-C(42)	8.1(3)
C(28)-C(27)-C(41)-C(42)	-174.48(19)
C(27)-C(41)-C(42)-O(9)	-38.3(3)
C(27)-C(41)-C(42)-C(43)	-157.0(2)
C(30)-C(29)-C(44)-C(25)	-55.7(2)
C(28)-C(29)-C(44)-C(25)	59.8(2)
C(30)-C(29)-C(44)-Br(2)	-176.82(14)
C(28)-C(29)-C(44)-Br(2)	-61.3(2)
O(8)-C(25)-C(44)-C(29)	-175.53(18)
O(7)-C(25)-C(44)-C(29)	68.0(2)
C(26)-C(25)-C(44)-C(29)	-50.1(2)
O(8)-C(25)-C(44)-Br(2)	-53.9(2)
O(7)-C(25)-C(44)-Br(2)	-170.43(13)
C(26)-C(25)-C(44)-Br(2)	71.5(2)
C(27)-C(26)-C(45)-O(9)	23.4(3)
C(25)-C(26)-C(45)-O(9)	-150.28(18)
C(27)-C(26)-C(45)-C(46)	-102.3(2)
C(25)-C(26)-C(45)-C(46)	84.1(2)
C(30)-C(31)-O(7)-C(25)	14.1(3)
C(32)-C(31)-O(7)-C(25)	-166.59(19)
O(8)-C(25)-O(7)-C(31)	-169.19(17)
C(26)-C(25)-O(7)-C(31)	75.6(2)
C(44)-C(25)-O(7)-C(31)	-46.0(2)
O(7)-C(25)-O(8)-C(47)	62.3(2)
C(26)-C(25)-O(8)-C(47)	177.09(19)
C(44)-C(25)-O(8)-C(47)	-55.0(3)
C(26)-C(45)-O(9)-C(42)	-56.6(2)
C(46)-C(45)-O(9)-C(42)	69.1(2)
C(43)-C(42)-O(9)-C(45)	-173.3(2)
C(41)-C(42)-O(9)-C(45)	65.2(2)

C(35)-C(34)-O(11)-C(48)	-0.1(4)
C(33)-C(34)-O(11)-C(48)	179.3(2)
C(33)-C(36)-O(12)-C(39)	-52.8(2)
C(37)-C(36)-O(12)-C(39)	73.2(2)
C(40)-C(39)-O(12)-C(36)	-173.67(19)
C(38)-C(39)-O(12)-C(36)	64.2(3)

Symmetry transformations used to generate equivalent atoms:

Table C1.7.4 Hydrogen bonds for 15a_js029_a [Å and °].

D-H...A	d(D-H)	d(H...A)	d(D...A)	<(DHA)